Synthetic, electrochemical, spectroscopic and computational aspects of ferrocene derivatives coordinated to subphthalocyanines

A dissertation submitted in fulfilment of the requirements for the degree

Philosophiae Doctor

in the

Department of Chemistry
Faculty of Natural and Agricultural Sciences

at the

University of the Free State

by

Petrus Johannes Swarts

Supervisor
Prof. J. Conradie

February 2020

Declaration

It is hereby declared that the thesis submitted for the degree Philosophiae Doctor (Chemistry) at the University of the Free State is the independent work of the undersigned and has not previously been submitted to/at another university or faculty. Copyright of this thesis is hereby ceded in favor of the University of the Free State.

_____ _____

Petrus Johannes Swarts Date

Department of Chemistry

Faculty of Natural and Agricultural Sciences

University of the Free State

South Africa

Language and style used in this thesis are in accordance with the requirements of indicated journals, unless otherwise stated.

Abstract

A series of six ferrocene derivatives, namely the ferrocenylcarboxylic acid dyads ($Fc(CH_2)_nCO_2H$ (n = 0 – 3), $Fc(CH)_2CO_2H$ and $FcCO(CH_2)_2CO_2H$) were synthesized and coordinated to subphthalocyanines (SubPcs) in the axial position to form seven novel $(Fc(CH_2)_nCO_2BSubPc(H)_{12}$ (n = 1 – 3), $FcCO(CH_2)_2CO_2BSubPc(H)_{12}$, (Fc-CH=CH-COO)$BSubPc(H)_{12}$ and Y-$BSubPc(F)_{12}$ with Y = (Fc-CH_2-CH_2-COO) or (Fc-CH=CH-COO)) and one known ($Fc(CH_2)_nCO_2BSubPc(H)_{12}$) ferrocenylcarboxylic acid subphthalocyanines dyads. In addition a novel subphthalocyanine $HOBSubPc(C_{12}H_{25})_6(H)_6$ with a hydroxy group in the axial position and alkyl ligands ($C_{12}H_{25}$) on the non-peripheral positions, as well as the known $ClBSubPc(F)_{12}$ and the mother compound $ClBSubPc(H)_{12}$ were synthesized.

UV/vis analysis of the SubPcs revealed that both the donor ($C_{12}H_{25}$) non-peripheral substituents and the acceptor (F) ring substituents shifted the Q band of SubPcs toward longer wavelengths compared to the unsubstituted ClBSubPc. However, the different ferrocenylcarboxylic acid dyads in the axial position did not have any influence on the position of the Q band of the SubPcs.

An electrochemical study of the SubPcs showed that peripheral substitution generally has a smaller influence (ca 0.1 V shift) on the shift of the oxidation and reduction potential of a SubPc than non-peripheral substitution (ca 0.3 V shift). It was found that the novel SubPc $HOBSubPc(C_{12}H_{25})_6(H)_6$ had the lowest macrocycle-based oxidation potential and that novel SubPc $Fc(CH_2)_3CO_2BSubPc(H)_{12}$ has the lowest first ring-based reduction potential reported for SubPcs to date. The experimental conditions used for the electrochemical study made it possible for the first time to obtain chemically reversible ring-based oxidation with peak current ratios approaching 1 and peak current separation $\Delta E_p < 0.086$ V for SubPcs.

The cyclic voltammetry data of the seven new ferrocenylsubphthalocyanine dyads, in agreement with the character of DFT calculated molecular orbitals, showed that Fe group of the ferrocenyl-containing axial ligand is involved in the first reversible oxidation process, followed by a second ring based oxidation. All reductions are localised on the subphthalocyanine ligand. The fluorine ring substituents of the electron-withdrawing SubPcs Y-BSubPc$(F)_{12}$, caused the ferrocenyl oxidation to shift with *ca.* 0.1 V more positive compared to electron-rich Y-BSubPc$(H)_{12}$. Furthermore, the CV data revealed that the formal reduction potential of Fe(II/III) of the axial ferrocenyl moiety of the eight ferrocenylcarboxylic acid-containing SubPc dyads followed the same trend than the free ferrocenylcarboxylic acid dyads, but shifted to a lower oxidation potential compared to free ferrocenylcarboxylic acid dyads. The carboxylic group in the free ferrocenylcarboxylic acid dyads is directly connected to ferrocenyl, or by an ethene group, or by an alkyl chain of varying length. The length of the alkyl chain separating the two groups affected the formal reduction potential of Fe of the ferrocenyl group. The formal reduction potential of Fe was also affected by the electron-withdrawing carbonyl group. The extent of the effect depended on whether the carbonyl group was directly bound to a ferrocenyl moiety or isolated by an sp^3 hybridised carbon atom backbone (-CH_2-CH_2- with no π-communication) or a non-isolated sp^2 hybridised carbon atom backbone (-CH=CH- with π-communication between Fc and the carbonyl group possible). Density functional theory (DFT) calculations gave further insight into the redox properties of the novel dyads. A linear relationship between the formal reduction potential of these ferrocenyl carboxylic acid derivatives and DFT calculated HOMO (highest occupied molecular orbital) energies were obtained.

The DFT study also provided linear relationships between the first oxidation potential and HOMO energies, as well as between the first reduction potential and LUMO (lowest

unoccupied molecular orbital) energies for a series of non-ferrocene-containing SubPcs with peripheral and non-peripheral substituents = H, F or ($C_{12}H_{25}$) and axial substituent = Cl or an alkoxy group. The neutral ferrocenylcarboxylic acid subphthalocyanines dyads have LUMOs and HOMOs of mainly π-ring and iron-d character respectively, confirming ring-based reduction and Fe(II) to Fe(III) oxidation. Optimisation of the cation (oxidised) species was essential to verify the locus of the second ring-based oxidation, since the frontier orbitals rearranged upon oxidation.

Key Words: Subphthalocyanines, Ferrocenylcarboxylic acids; Ferrocenysubphthalocyanines; Electrochemistry, Chemical reversibility; Density functional theory (DFT); ADF; Molecular orbitals; Linear correlations.

Acknowledgements

First and foremost, thanks must go to our Lord, for always being with me, guiding me, giving me strength and insight throughout this project.

I would like to thank my family, friends and colleagues for their support, friendship and guidance throughout this period of my studies. Special thanks must be made to the following people:

My supervisor, Prof. Dr J. Conradie, for her excellent guidance, leadership and kindness throughout this study. It has been a privilege to be your student. Thank you for allowing me to be able to work with an excellent research group and learn from one of the best.

To my immediate family, a special thanks to my wife (Elzahn Swarts) thank you for all the love, support and encouragement through the course of this study. I would not have been able to come this far had it not been for you. To my father (Jannie Swarts), for all your wisdom and advice through my entire student career, my mother (Tessa Swarts), for all your grace, love and kindness and my brother (Christo Swarts), for your encouragement and love. Your love, guidance and support over the years are the reason I am here today. If not for you, I would not have had this opportunity.

To the Physical Chemistry group, thank you *ALL* for your support and guidance throughout this study, and for always helping me whenever I needed it. Also, thank you for all the laughter and fun throughout my time with the group.

I would like to acknowledge the Chemistry department at the UFS for the available facilities.

A special thank you to the National Research Foundation and the University of the Free State for financial support.

To the High-Performance Computing facility of the UFS, the CHPC of South Africa for computer time.

Table of Contents

Chapter 1
Introduction

This research is concerned with ferrocenylcarboxylic acid dyads, subphthalocyanines (SubPcs) and a combination of the ferrocenylcarboxylic acid dyads and SubPcs.

Ferrocene was a serendipitous discovery made in 1951, the first recognised sandwich compound [1]. The discovery opened an entirely new research area. Ferrocene has been extensively researched, and numerous cyclopentadienyl derivatives with various metals have been studied leading to good reviews in organic and inorganic chemistry [2–6]. As ferrocene is an aromatic compound with reactivity more than million times that of benzene, it undergoes many reactions characteristic of aromatic compounds [7]. Functional groups can easily be introduced to the electron-donating ferrocene. The reversible electrochemical behaviour of the Fe(II/III) redox couple in ferrocene-containing compounds allows for electrochemical and reactivity studies of the functionalised ferrocene derivatives. Ferrocene-containing compounds thrive and are primarily stimulated by their successful applications including asymmetric catalysis [8,9], non-linear optics [10] and especially electrochemistry due to the ideal redox behaviour of the Fe(II/III) couple [11,12].

Subphthalocyanines such as ClBSubPc$(H)_{12}$ has been used in research for almost 50 years [13] due to their diverse applications including light-emitting diodes [14], dye-sensitized solar cells [15], and photodynamic therapy [16]. The uses of SubPcs can be modified by substituting the axial ligand as well as by functionalising the ring substituents [17]. Four ferrocenylsubphthalocyanine dyads with a direct ferrocene-boron or substituted ferrocene-boron bond have been reported till date [18], with potential application in light-harvesting elements [18].

Phthalocyanines (Pc) are macrocycles which are structurally related to the naturally occurring porphyrins (Por). Natural occurring porphyrins form the active centres of various natural molecules such as chlorophyll, haemoglobin and myoglobin. Phthalocyanines do not occur in nature; the synthetically available phthalocyanines are more robust and stable than most porphyrins and thus have a wider application range. Phthalocyanines and porphyrins have been studied for their use in photodynamic therapy where they produce singlet oxygen to kill cancer cells.[19] Subphthalocyanines (SubPcs) are closely related to Pcs and as a result, can be used for similar studies. Researchers continuously strive to improve the effectiveness of photodynamic therapy (PDT) and to expand it to different types of cancer therapy.[20] Clinical trials are underway to evaluate the use of PDT for various cancers such as skin, prostate, cervical and brain cancer.[21,22] Both subphthalocyanines[16] and ferrocene[2,3] have been studied as possible antineoplastic (anticancer) agents. With the combination of subphthalocyanines and ferrocene moieties, antineoplastic studies will hopefully advance the effectiveness of photodynamic therapy. Subphthalocyanines is also useful in various other high technology areas sensors [23,24], light-emitting devices [25,26], supramolecular systems [27] and low bandgap molecular solar cells [28].

The goal of this study was the i) synthesis and characterisation of ferrocenylcarboxylic acid dyads, subphthalocyanines and a combination of the ferrocenyl acid dyads and SubPcs, ii) electrochemical analysis of all dyads to determine the redox activity of compounds, iii) UV/vis analysis of novel SubPc dyads and iv) density functional theory (DFT) studies to get further insight into redox activity and properties of all the complexes. The results are presented in article form in chapters 2 – 5.

Chapter 2 presents the synthesis, characterisation and DFT calculations of a series of six ferrocenylcarboxylic acid dyads ($Fc(CH_2)_nCO_2H$ (n = 0 – 3), $Fc(CH)_2CO_2H$ and

$FcCO(CH_2)_2CO_2H$). The effect of the following on the value of the formal reduction potential of the Fe(II/III) redox couple in series of this six ferrocenylcarboxylic acid dyads is explored: (a) the solvent acetonitrile (CH_3CN) versus a non-coordinating solvent dichloromethane (DCM), (b) the carbonyl group, (c) isolated and non-isolated carboxylic groups, (d) different alkyl chain lengths between Fc and the CO moieties and (e) the amount of substituents on Fc.

Chapter 3 presents the synthesis, characterisation, electrochemistry and DFT calculations of a series of three subphthalocyanines, novel ($HOBSubPc(C_{12}H_{25})_6(H)_6$), ($ClBSubPc(F)_{12}$) and the mother SubPc ($ClBSubPc(H)_{12}$). The effect of electron-donating ($C_{12}H_{25}$) and electron-withdrawing (F) ring substituents on the redox properties and the UV/vis absorption spectrum maxima of the SubPcs are presented. The redox results were further validated by comparison with 16 related subphthalocyanines from literature.

Chapter 4 presents the synthesis, characterisation, electrochemistry and DFT calculations of a series of four novel subphthalocyanines $Y\text{-}BSubPc(X)_{12}$ with X = H or F, Y = ($Fc\text{-}CH_2\text{-}CH_2\text{-}COO$) or (Fc-CH=CH-COO). Specifically, the effect (a) of the electron-withdrawing F ring-substituents on the redox potentials of the SubPcs and (b) of the presence or absence of π-communication on the redox potentials of SubPcs and the $iron^{II/III}$ oxidation potential, were explored.

Chapter 5 presents the synthesis, characterisation, electrochemistry and DFT calculations of a series of three novel and two known subphthalocyanines $Fc(CH_2)_nCO_2BSubPc(H)_{12}$ (n = 0 – 3) and $FcCO(CH_2)_2CO_2BSubPc(H)_{12}$. The effect of the varying alkyl chain lengths n and the CO groups on the redox properties of the SubPc and the Fe(II/III) redox couple of the ferrocene

moiety is presented. It was found that the novel SubPc, $Fc(CH_2)_3CO_2BSubPc(H)_{12}$, exhibited the lowest first macrocycle-based reduction potential reported for SubPcs till date [18,29,30].

References

(1) Dagani, R. Fifty Years of Ferrocene Chemistry. *Chem. Eng. News* **2001**, *79* (49), 37–38. https://doi.org/10.1021/cen-v079n049.p037.

(2) Fouda, M. F. R.; Abd-Elzaher, M. M.; Abdelsamaia, R. A.; Labib, A. A. On the Medicinal Chemistry of Ferrocene. *Appl. Organomet. Chem.* **2007**, *21* (8), 613–625. https://doi.org/10.1002/aoc.1202.

(3) Ornelas, C. Application of Ferrocene and Its Derivatives in Cancer Research. *New J. Chem.* **2011**, *35* (10), 1973. https://doi.org/10.1039/c1nj20172g.

(4) Daeneke, T.; Kwon, T.-H.; Holmes, A. B.; Duffy, N. W.; Bach, U.; Spiccia, L. High-Efficiency Dye-Sensitized Solar Cells with Ferrocene-Based Electrolytes. *Nat. Chem.* **2011**, *3* (3), 211–215. https://doi.org/10.1038/nchem.966.

(5) Gómez Arrayás, R.; Adrio, J.; Carretero, J. C. Recent Applications of Chiral Ferrocene Ligands in Asymmetric Catalysis. *Angew. Chemie Int. Ed.* **2006**, *45* (46), 7674–7715. https://doi.org/10.1002/anie.200602482.

(6) Astruc, D. Why Is Ferrocene so Exceptional? *Eur. J. Inorg. Chem.* **2017**, *2017* (1), 6–29. https://doi.org/10.1002/ejic.201600983.

(7) Rosenblum, N. *Chemistry of The Iron Group Metallocenes: Ferrocene, Ruthenocene, Osmocene*; John Wiley & Sons, Ed.; John Wiley & Sons: New York, 1965.

(8) Feyrer, A.; Breher, F. Palladium Complexes of Ferrocene-Based Phosphine Ligands as Redox-Switchable Catalysts in Buchwald–Hartwig Cross-Coupling Reactions. *Inorg. Chem. Front.* **2017**, *4* (7), 1125–1134. https://doi.org/10.1039/C7QI00125H.

(9) Zain-ul-Abdin, Z.-A.; Wang, L.; Yu, H.; Saleem, M.; Akram, M.; Abbasi, N. M.;

Khalid, H.; Sun, R.; Chen, Y. Ferrocene-Based Polyethyleneimines for Burning Rate Catalysts. *New J. Chem.* **2016**, *40* (4), 3155–3163. https://doi.org/10.1039/C5NJ03171K.

(10) Wang, W.-Y.; Ma, N.-N.; Wang, L.; Zhu, C.-L.; Fang, X.-Y.; Qiu, Y.-Q. Effect of π-Conjugate Units on the Ferrocene-Based Complexes: Switchable Second Order Nonlinear Optics Controlled by Redox Stimuli. *Dye. Pigment.* **2016**, *126*, 29–37. https://doi.org/10.1016/j.dyepig.2015.11.006.

(11) Hu, B.; Zhang, X.; Tian, B.; Qi, Y.; Lai, X.; Jin, L. Synthesis, Electrochemical and Spectroelectrochemical Properties of Carbazole Derivatives with Ferrocene Groups. *J. Electroanal. Chem.* **2017**, *788*, 29–37. https://doi.org/10.1016/j.jelechem.2017.01.046.

(12) Tsierkezos, N. G. Cyclic Voltammetric Studies of Ferrocene in Nonaqueous Solvents in the Temperature Range from 248.15 to 298.15 K. *J. Solution Chem.* **2007**, *36* (3), 289–302. https://doi.org/10.1007/s10953-006-9119-9.

(13) A, M.; A, O. Phthalocyaninartige Bor-Komplexe. *Monatshefte fur Chemie* **1972**, *103*, 150–155.

(14) Ma, Z.; Liu, S.; Hu, S.; Yu, J. Highly Efficient Tandem Organic Light-Emitting Diodes Based on SubPc:C60 Bulk Heterojunction as Charge Generation Layer. *J. Lumin.* **2016**, *169*, 29–34. https://doi.org/10.1016/j.jlumin.2015.08.040.

(15) Ince, M.; Medina, A.; Yum, J. H.; Yella, A.; Claessens, C. G.; Martínez-Díaz, M. V.; Grätzel, M.; Nazeeruddin, M. K.; Torres, T. Peripherally and Axially Carboxylic Acid Substituted Subphthalocyanines for Dye-Sensitized Solar Cells. *Chem. - A Eur. J.* **2014**, *20* (7), 2016–2021. https://doi.org/10.1002/chem.201303639.

(16) van de Winckel, E.; Mascaraque, M.; Zamarrón, A.; Juarranz de la Fuente, Á.; Torres, T.; de la Escosura, A. Dual Role of Subphthalocyanine Dyes for Optical Imaging and Therapy of Cancer. *Adv. Funct. Mater.* **2018**, *28* (24).

https://doi.org/10.1002/adfm.201705938.

(17) Claessens, C. G.; González-Rodríguez, D.; Rodríguez-Morgade, M. S.; Medina, A.; Torres, T. Subphthalocyanines, Subporphyrazines, and Subporphyrins: Singular Nonplanar Aromatic Systems. *Chemical Reviews*. February 26, 2014, pp 2192–2277. https://doi.org/10.1021/cr400088w.

(18) Solntsev, P. V.; Spurgin, K. L.; Sabin, J. R.; Heikal, A. A.; Nemykin, V. N. Photoinduced Charge Transfer in Short-Distance Ferrocenylsubphthalocyanine Dyads. *Inorg. Chem.* **2012**, *51* (12), 6537–6547. https://doi.org/10.1021/ic3000608.

(19) Bonnett, R. Photosensitizers of the Porphyrin and Phthalocyanine Series for Photodynamic Therapy. *Chem. Soc. Rev.* **1995**, *24* (1), 19. https://doi.org/10.1039/cs9952400019.

(20) Felsher, D. W. Cancer Revoked: Oncogenes as Therapeutic Targets. *Nat. Rev. Cancer* **2003**, *3* (5), 375–380. https://doi.org/10.1038/nrc1070.

(21) Xu, H.; Jiang, X.-J.; Chan, E. Y. M.; Fong, W.-P.; Ng, D. K. P. Synthesis, Photophysical Properties and in Vitro Photodynamic Activity of Axially Substituted Subphthalocyanines. *Org. Biomol. Chem.* **2007**, *5* (24), 3987. https://doi.org/10.1039/b712788j.

(22) Yurt, F.; Sarı, F. A.; Ince, M.; Colak, S. G.; Er, O.; Soylu, H. M.; Kurt, C. C.; Avci, C. B.; Gunduz, C.; Ocakoglu, K. Photodynamic Therapy and Nuclear Imaging Activities of SubPhthalocyanine Integrated TiO2 Nanoparticles. *J. Photochem. Photobiol. A Chem.* **2018**, *367*, 45–55. https://doi.org/10.1016/j.jphotochem.2018.08.004.

(23) Ros-Lis, J. V.; Martínez-Máñez, R.; Soto, J. Subphthalocyanines as Fluoro-Chromogenic Probes for Anions and Their Application to the Highly Selective and Sensitive Cyanide Detection. *Chem. Commun.* **2005**, No. 42, 5260. https://doi.org/10.1039/b510710e.

(24) Palomares, E.; Martínez-Díaz, M. V.; Torres, T.; Coronado, E. A Highly Sensitive Hybrid Colorimetric and Fluorometric Molecular Probe for Cyanide Sensing Based on a Subphthalocyanine Dye. *Adv. Funct. Mater.* **2006**, *16* (9), 1166–1170. https://doi.org/10.1002/adfm.200500517.

(25) Morse, G. E.; Castrucci, J. S.; Helander, M. G.; Lu, Z.-H.; Bender, T. P. Phthalimido-Boronsubphthalocyanines: New Derivatives of Boronsubphthalocyanine with Bipolar Electrochemistry and Functionality in OLEDs. *ACS Appl. Mater. Interfaces* **2011**, *3* (9), 3538–3544. https://doi.org/10.1021/am200758w.

(26) Morse, G. E.; Helander, M. G.; Maka, J. F.; Lu, Z.-H.; Bender, T. P. Fluorinated Phenoxy Boron Subphthalocyanines in Organic Light-Emitting Diodes. *ACS Appl. Mater. Interfaces* **2010**, *2* (7), 1934–1944. https://doi.org/10.1021/am1002603.

(27) Claessens, C. G.; Sánchez-Molina, I.; Torres, T. Self-Sorting among the Diastereoisomers of a M 3 L 2 Subphthalocyanine Capsule. *Supramol. Chem.* **2009**, *21* (1–2), 44–47. https://doi.org/10.1080/10610270802478263.

(28) Claessens, C. G.; Vicente-Arana, M. J.; Torres, T. Post-Assembly Error-Checking in Subphthalocyanine Based M3L2 Metallosupramolecular Capsules. *Chem. Commun.* **2008**, No. 47, 6378. https://doi.org/10.1039/b815898c.

(29) Maligaspe, E.; Hauwiller, M. R.; Zatsikha, Y. V.; Hinke, J. A.; Solntsev, P. V.; Blank, D. A.; Nemykin, V. N. Redox and Photoinduced Electron-Transfer Properties in Short Distance Organoboryl Ferrocene-Subphthalocyanine Dyads. *Inorg. Chem.* **2014**, *53* (17), 9336–9347. https://doi.org/10.1021/ic5014544.

(30) Sampson, K. L.; Josey, D. S.; Li, Y.; Virdo, J. D.; Lu, Z. H.; Bender, T. P. Ability to Fine-Tune the Electronic Properties and Open-Circuit Voltage of Phenoxy-Boron Subphthalocyanines through Meta-Fluorination of the Axial Substituent. *J. Phys. Chem. C* **2018**, *122* (2), 1091–1102. https://doi.org/10.1021/acs.jpcc.7b11157.

Chapter 2

Solvent and Substituent Effect on Electrochemistry of Ferrocenylcarboxylic Acid Dyads

Submitted to: Journal of Electroanalytical Chemistry

Manuscript number: JELECHEM-D-19-02346

Redox data of ferrocenyl carboxylic acid dyads in DCM and ACN.

To be submitted to: Data in brief (DIB)

Supporting information also included.

Author Contributions:

Pieter J. Swarts

1. All experimental synthesis of compounds
2. Electrochemical studies and interpretation
3. Characterisation:
    a. ^{1}H NMR and ^{13}C NMR
    b. FTIR
    c. DFT calculations
4. Writing of publication manuscript draft and revised publications under the supervision of Prof. Jeanet Conradie

Above mentioned work was done under the supervision of Prof. Jeanet Conradie.

Synopsis TOC

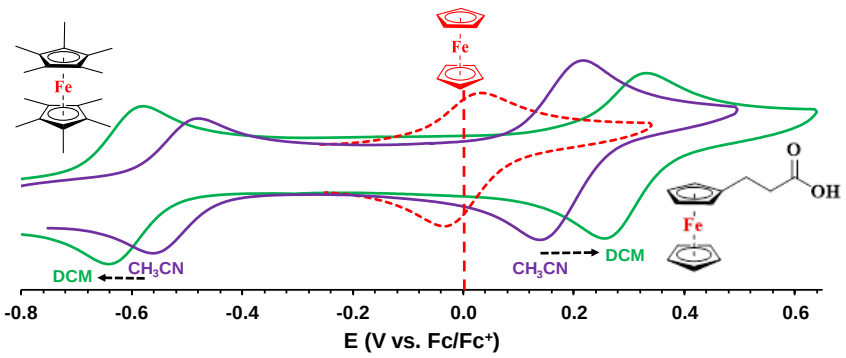

Solvent and Substituent Effect on Electrochemistry of Ferrocenylcarboxylic Acid Dyads

Pieter J. Swarts and Jeanet Conradie*

Department of Chemistry, University of the Free State, P.O. Box 339, Bloemfontein, 9300, South Africa

Corresponding author: Jeanet Conradie, email conradj@ufs.ac.za

0000-0002-8120-6830 (J Conradie)

0000-0003-0157-8763 (PJ Swarts)

Synopsis TOC

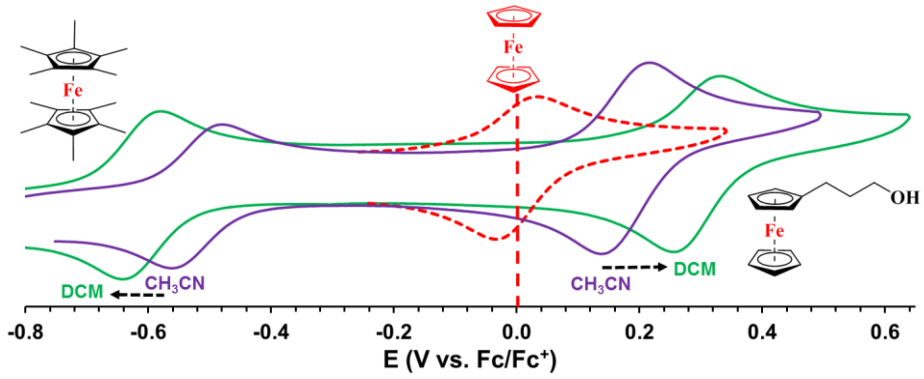

Synopsis Text

The effect of dichloromethane *versus* acetonitrile as the solvent on the iron(III)/(II) reduction potential of ferrocenium-containing dyads.

Keywords

Ferrocene; redox potentials; DFT; electron-withdrawing; carboxy-substituent

Highlights

Reduction potentials of ferrocenyl acid dyads in dichloromethane and acetonitrile

Isolated *vs.* non-isolated carboxy substituents on ferrocenyl acid dyads

DFT molecular view of ferrocenyl acid dyads oxidation

Effect of alkyl chain length connecting ferrocenyl and carboxylic moieties on redox potentials

Abstract

The redox properties of six ferrocenyl carboxylic acid dyads (**1** – **6**) in dichloromethane and acetonitrile are compared. The formal reduction potential of Fe of the ferrocenyl group in these carboxylic acid dyads occur *ca.* 0.1 V more positive in DCM than in CH_3CN. The carboxylic group is directly connected to ferrocenyl, or by an ethene group, or by an alkyl chain of varying length. The length of the alkyl chain separating the two groups affected the formal reduction potential of Fe of the ferrocenyl group. The formal reduction potential was also affected by the electron-withdrawing carbonyl group. The extent of the effect depended on whether the carbonyl group was directly bound to a ferrocenyl moiety or, isolated by an sp^3 hybridized carbon atom backbone ($-CH_2-CH_2-$) or a non-isolated sp^2 hybridized carbon atom backbone (-CH=CH-). The results obtained were further validated by density functional theory (DFT) calculations on ferrocenyl carboxylic acids (**1** – **6**) as well as selected substituted ferrocenyl compounds from literature. A linear relationship between the

formal reduction potential of these ferrocenyl carboxylic acid derivatives and DFT calculated HOMO energies were obtained.

Introduction

Ferrocene was a serendipitous discovery made in 1951, the first recognised sandwich compound [1]. The discovery opened an entirely new research area. Ferrocene has been extensively researched, and numerous cyclopentadienyl derivatives with various metals have been studied giving good reviews in organic and inorganic chemistry [2–5]. As ferrocene is an aromatic compound with reactivity more than million times that of benzene, it undergoes many reactions characteristic of aromatic compounds [6]. Functional groups can easily be introduced to the electron-donating ferrocene. The reversible electrochemical behaviour of the $Fe^{II/III}$ redox couple in ferrocene-containing compounds allows for electrochemical and reactivity studies of the functionalised ferrocene derivatives [7]. Ferrocene-containing compounds thrive and are primarily stimulated by their successful applications including asymmetric catalysis [7–9], non-linear optics [7] and especially electrochemistry due to the ideal redox behaviour of the $Fe^{II/III}$ couple [7,10]. The electrochemical behaviour of four carboxy-substituted ferrocene molecules has been studied in CH_3CN [11]. It was found that separating the ferrocene moiety from the electron-withdrawing carbonyl group via varying alkyl chain lengths affected the redox potential of ferrocenes $Fe^{II/III}$ couple [12]. Here we present the synthesis, characterization and a comprehensive electrochemical study of six carboxy-substituted ferrocene molecules $FcCO_2H$ **(1)**, $FcCH_2CO_2H$ **(2)**, $Fc(CH)_2CO_2H$ **(3)**, $Fc(CH_2)_2CO_2H$ **(4)**, $Fc(CH_2)_3CO_2H$ **(5)** and $FcCO(CH_2)_2CO_2H$ **(6)**, see **Figure 1**. The goal of the study is to explore the effect on the value of the $Fe^{II/III}$ redox couple of (i) the solvent acetonitrile (CH_3CN) versus a non-coordinating solvent dichloromethane (DCM) [13], (ii) the carbonyl group, (iii) isolated and non-isolated carboxylic

groups, (iv) different alkyl chain lengths between Fc and the CO moieties and (v) the amount of substituents on Fc.

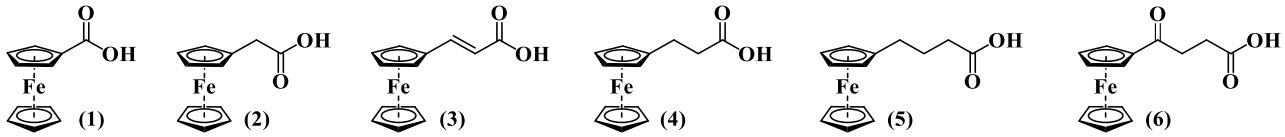

Figure 1 Structures of $FcCO_2H$ **(1)**, $FcCH_2CO_2H$ **(2)**, $Fc(CH)_2CO_2H$ **(3)**, $Fc(CH_2)_2CO_2H$ **(4)**, $Fc(CH_2)_3CO_2H$ **(5)** and $FcCO(CH_2)_2CO_2H$ **(6)**.

Experimental Section

Reagents and Materials

Solid reagents (Sigma-Aldrich, Strem and Merck) were used as received. Liquid reagents (Sigma-Aldrich and Merck) were used without any further purification unless specified otherwise. Solvents were distilled, and water was double distilled. Organic solvents used in this study were dried according to published methods [14]. Melting points are uncorrected and were determined with an Olympus BX 51 microscope equipped with a Linkam THMS 600 hot stage.

Spectroscopy Measurements

^{1}H and ^{13}C NMR spectroscopic analysis were performed for all compounds in the study. ^{1}H NMR spectra were recorded at 600.28 MHz at 25°C on a 600 MHz AVANCE II NMR spectrometer while ^{13}C NMR spectra were recorded at 150.95 MHz at 25°C. Hydrogen and carbon chemical shifts are relative to hydrogen and carbon in $CDCl_3$ at 7.24 ppm and 77.16 ppm, respectively. The following

abbreviations are used to describe peak patterns: s = singlet, d = doublet, dd = doublet of doublets, t = triplet, q = quartet and m = multiplet. Solid-state Fourier Transform infrared measurements were performed on a Thermo Scientific Nicolet iS50 Attenuated Total Reflectance Fourier transform infrared spectroscopy (ATR-FTIR) spectrometer using the iS50 ATR option running OMNIC software (Version 9.2).

Synthesis of ferrocene precursors

The following derivatives were required as substrates for the ferrocenyl carboxylic acid derivatives. They were synthesised using literature methods: 2-chlorobenzoyl ferrocene [15], ferrocenyl acetonitrile [16], ferrocenecarboxaldehyde [17] and *β*-ferrocenoylpropionic acid [18] (see the supporting information for the reaction procedures and characterisation data).

Synthesis of carboxy-substituted ferrocenes (1 – 6)

$FcCO_2H$ **(1)**, $FcCH_2CO_2H$ **(2)**, $Fc(CH)_2CO_2H$ **(3)**, $Fc(CH_2)_2CO_2H$ **(4)**, $Fc(CH_2)_3CO_2H$ **(5)** and $FcCO(CH_2)_2CO_2H$ **(6)** were synthesised using slight modifications to literature methods [12] to improve yields and to simplify the reaction setup. The reaction schemes for the synthesis of the ferrocenyl carboxylic acid derivatives, **(1 - 6)**, are given in **Scheme 1**. The ^{1}H and ^{13}C NMR of each in the supporting information.

Preparation of $FcCO_2H$ (1), [12]**:** 2-Chlorobenzoyl ferrocene (1.75 g, 0.005 mol) was added to a mixture of potassium tertiary butoxide (13 g, 0.115 mol) and water (0.61 cm^3, 0.034 mol) in dimethoxyethane (0.1 dm^3) under an argon atmosphere. The mixture produced a yellow slurry which was refluxed for 24 hours. After cooling the mixture, ice water (0.3 dm^3) was added, and the resulting solution was washed with ether (3 x 0.1 dm^3). The aqueous phases were combined and acidified with concentrated hydrochloric acid. The residue was collected by filtration, washed thoroughly with water and air-dried, yielding 1.01 g (80 %) of as light-yellow crystals. m.p.: 156 – 162 °C. NMR: δ_H (600.28 MHz, $CDCl_3$, 25 °C): δ 4.84 (2 H, pt, 2 x CH_2: Substituted-Cp), 4.45 (2 H, pt, 2 x CH_2: Substituted-Cp), 4.24 (5 H, s, Unsubstituted-Cp). ^{13}C NMR: δ_C (150.95 MHz, $CDCl_3$, 25 °C): δ 168.24 (1C, C=O), 70.23 (1C, C-CO_2H), 69.72 (5C, Unsubstituted-Cp), 68.42 (2C, Substituted-Cp), 66.24 (2C, Substituted-Cp).

Preparation of $FcCH_2CO_2H$ (2), [12]**:** To a solution of potassium hydroxide (1 g, 0.018 mol) in water (10 cm^3), a suspension of the ferrocene acetonitrile (0.2 g, 0.00074 mol) in ethanol (5 cm^3) was added and refluxed for 5 hours until the evolution of ammonia had ceased. Most (> 95 %) of the ethanol was removed under reduced pressure. The residual suspension was dissolved in water (50 cm^3), extracted with ether (2 x 50 cm^3) and filtered. The solution was acidified with 2 M HCl and the precipitate filtered, washed and air-dried to yield 0.110 g (51 %) as a white powder. m.p.: 159 – 165 °C. NMR: δ_H (600.28 MHz, $CDCl_3$, 25 °C): δ 4.21 (2 H, pt, 2 x CH_2: Substituted-Cp), 4.13 (5 H, s, Unsubstituted-Cp), 3.73 (2 H, pt, 2 x CH_2: Substituted-Cp), 3.38 (2H, s, CH_2). ^{13}C NMR: δ_C (150.95 MHz, $CDCl_3$, 25 °C): δ 172.34 (1C, C=O), 82.44 (1C, C-CO_2H), 69.19 (5C, Unsubstituted-Cp), 68.31 (2C, Substituted-Cp), 67.97 (2C, Substituted-Cp), 39.84 (1C, CH_2).

Preparation of $Fc(CH)_2CO_2H$ (3), [19]**:** Ferrocenecarboxaldehyde (1.5 g, 0.006 mol), malonic acid (1.785 g, 0.017 mol) and piperidine (0.56 cm^3) were dissolved in pyridine and heated in an oil bath

at 110 °C for 2 hours under an argon atmosphere. The cooled solution was diluted with water and extracted with chloroform. The chloroform extracts were washed with 1 M HCl (2 x 100 cm^3) and water (2 x 100 cm^3) before the acrylic acid was extracted with ice-cooled 2 M NaOH (200 cm^3). While effectively cooling the solution with ice, the water phase was acidified with 1 M HCl and the precipitate filtered, washed with water and air-dried to yield 1.58 g (90 %) as a yellow powder. m.p.: 132 – 138 °C. NMR: δ_H (600.28 MHz, $CDCl_3$, 25 °C): δ 7.64 (1H, d, CH_2), 6.01 (1H, d, CH_2), 4.50 (2 H, pt, 2 x CH_2: Substituted-Cp), 4.42 (2 H, pt, 2 x CH_2: Substituted-Cp), 4.15 (5 H, s, Unsubstituted-Cp). ^{13}C NMR: δ_C (150.95 MHz, $CDCl_3$, 25 °C): δ 172.29 (1C, C=O), 148.76 (1C,CH=CH), 113.73 (1C,CH=CH), 78.26 (1C, C-CO_2H), 71.44 (2C, Substituted-Cp), 69.92 (5C, Unsubstituted-Cp), 69.05 (2C, Substituted-Cp).

Preparation of $Fc(CH_2)_2CO_2H$ (4), [12]**:** 3-Ferrocenylacrylic acid (0.250 g, 0.00082 mol), H_2/Pd (5% Pd on Carbon), (0.030 g) was suspended in absolute ethanol (50 cm^3). The suspension was stirred under a 10-bar hydrogen atmosphere for 20 hours before the reaction mixture was filtered through 2 cm of silica gel. Equal volumes of water and ice were added to the yellow ethanolic mixture. The solution was extracted with diethyl ether (2 x 250 cm^3) the combined ether extracts were thoroughly washed with water to remove the excess ethanol. The solution was dried over $MgSO_4$ and evaporated under reduced pressure to yield 0.177 g (71%) an off-white powder. m.p.: 124 – 138 °C. NMR: δ_H (600.28 MHz, $CDCl_3$, 25 °C): δ 4.12 (5 H, s, Unsubstituted-Cp), 4.09 (2 H, pt, 2 x CH_2: Substituted-Cp), 4.07 (2 H, pt, 2 x CH_2: Substituted-Cp), 2.66 (2H, d, CH_2), 2.59 (2H, d, CH_2). ^{13}C NMR: δ_C (150.95 MHz, $CDCl_3$, 25 °C): δ 179.37 (1C, C=O), 87.49 (1C, C-CO_2H), 68.89 (5C, Unsubstituted-Cp), 68.23 (2C, Substituted-Cp), 67.75 (2C, Substituted-Cp), 35.53 (2C, CH2-CH_2).

Preparation of $Fc(CH_2)_3CO_2H$ (5), [12]**:** Ferrocenyl-methyl-butyrate (0.150 g, 0.00045 mol) was dissolved in ethanol (25 cm^3) followed by the addition of sodium hydroxide solution (25 cm^3, 2 M).

The solution was stirred for 1 hour at room temperature followed by the addition of ice (25 m^3) and washed with cold diethyl ether (3 x 50 cm^3). While cooling the solution by adding fresh ice chunks, the water phase was acidified with 1 M HCl and the precipitate filtered, washed and air-dried to liberate 0.132 g (93 %) as an off-white powder. m.p.: 120 – 124 °C. NMR: δ_H (600.28 MHz, $CDCl_3$, 25 °C): δ 4.12 (5 H, s, Unsubstituted-Cp), 4.09 (2 H, pt, 2 x CH_2: Substituted-Cp), 4.07 (2 H, pt, 2 x CH_2: Substituted-Cp), 2.38 (2H, d, CH_2), 1.84 (2H, d, CH_2), 0.86 (2H, m, CH_2). ^{13}C NMR: δ_C (150.95 MHz, $CDCl_3$, 25 °C): δ 179.42 (1C, C=O), 82.44 (1C, C-CO_2H), 68.31 (2C, Substituted-Cp), 67.48 (5C, Unsubstituted-Cp), 66.24 (2C, Substituted-Cp), 33.45 (2C, CH_2-CH_2-CH_2), 28.88 (1C, CH_2-CH_2-CH_2).

Preparation of $FcCO(CH_2)_2CO_2H$ (6), [10]**:** Succinic anhydride (0.250 g, 0.00215 mol) dissolved in dichloromethane (25 cm^3) was added to a mixture of ferrocene (0.250 g, 0.0215 mol) and aluminium chloride (0.76 g, 0.0056 mol) in dichloromethane (25 cm^3) under a nitrogen atmosphere. The reaction mixture was refluxed for 24 hours. After cooling, ice-cold water (40 cm^3) was added and the aqueous layer extracted twice with dichloromethane. The combined dichloromethane extracts were thoroughly washed with water. The organic phase was then extracted twice with equal amounts of 2 M NaOH. While cooling the solution with ice, the water phase was acidified with 1 M HCl and the precipitate filtered, washed with water and air-dried to liberate 1.1 g (74 %) as orange crystals. m.p.: 134 – 148 °C. NMR: δ_H (600.28 MHz, $CDCl_3$, 25 °C): δ 4.80 (2 H, pt, 2 x CH_2: Substituted-Cp), 4.51 (2 H, pt, 2 x CH_2: Substituted-Cp), 4.22 (5 H, s, Unsubstituted-Cp), 3.07 (2H, d, CH_2), 2.75 (2H, d, CH_2), 0.86 (2H, m, CH_2). ^{13}C NMR: δ_C (150.95 MHz, $CDCl_3$, 25 °C): δ 202.54 (1C, C=O), 171.21 (1C, CO_2H), 80.38 (1C, C-CO_2H), 72.55 (2C, Substituted-Cp), 70.14 (5C, Unsubstituted-Cp), 69.41 (2C, Substituted-Cp), 34.23 (2C, CH_2-CH_2).

Cyclic Voltammetry

All the electrochemical experiments were performed in an M Bruan Lab Master SP glove box under a high purity argon atmosphere (H_2O and O_2 < 10 ppm). Cyclic voltammetry (CV) measurements were performed utilising a Princeton Applied Research PARSTAT 2273 potentiostat, running Powersuite software (Version 2.58). A three-electrode cell was used. A glassy carbon electrode with a surface area 3.14 x 10^{-6} m^2 was chosen as working electrode, platinum wires were chosen as auxiliary and reference electrodes. The glassy carbon working electrode was polished and prepared before every experiment on a Buhler polishing mat first with 1-micron and then with ¼-micron diamond paste, rinsed with H_2O, acetone and dichloromethane (DCM), and dried before each experiment. Electrochemical analysis of the complexes was performed in DCM (anhydrous, ≥ 99.8%, contains 40-150 ppm amylene as a stabiliser) and CH_3CN (anhydrous, ≥ 99.8%) at room temperature. Solutions were made in 0.001 dm^3 spectrochemical grade anhydrous DCM or CH_3CN containing *ca.* 0.0005 M of analyte, 0.0005 mol dm^{-3} of internal reference (decamethylferrocene, DmFc) and 0.1 mol dm^{-3} of supporting electrolyte tetrabutylammonium tetrakispentafluorophenylborate, $[N(^nBu)_4][B(C_6F_5)_4]$ in DCM, or tetrabutylammonium hexafluorophosphate, $TBAPF_6$, $[N(^nBu)_4][PF_6]$ in CH_3CN. Experimental potential data was collected *vs.* the Pt wire reference electrode but is reported *vs.* the redox couple of ferrocene, Fc/Fc^+ at 0 V. $E^{0`}$(DmFc) = - 0.610 V *vs.* Fc/Fc^+ at 0 V in DCM/$[N(^nBu)_4][B(C_6F_5)_4]$ and at -0.520 *vs.* Fc/Fc^+ at 0 V in $CH_3CN/[N(^nBu)_4][PF_6]$. Scan rates were between 0.05 and 5.00 Vs^{-1}. Electrochemical reversibility (or Nernstian behaviour) of redox processes is indicated by a peak current ratio (i_{pc}/i_{pa} for oxidation and i_{pa}/i_{pc} for reduction) of 1 [20,21] and peak current separation $\Delta E = |E_{pa} - E_{pc}| = 0.059$ V for a one-electron transfer process [13]. In this experiment, due to experimental cell imperfections and ohmic drop effects, ΔE_p slightly larger than 0.059 V was obtained, even for the known 1 e^- transfer processes of ferrocene, Fc^+/Fc

(0.082 V in CH_3CN and 0.072 V in DCM) and decamethylferrocene, $DmFc^+$/DmFc (0.079 V in CH_3CN, 0.060 V in DCM) couples [22–24].

DFT calculations

Density functional theory (DFT) calculations were performed on the neutral molecules using the B3LYP [25–27] functional, as implemented in the Gaussian 16 package [28], and the triple-ζ basis set 6-311G(d,p). DFT calculations on neutral molecules were also performed using the OLYP [26,29] functional as implemented in the ADF package [30] with the all-electron Slater-type TZP (Triple ζ polarised) basis set. All calculations were performed in the gas phase and DCM (ε=8.9) and CH_3CN (ε=37.5) as solvents. The implicit solvent Polarizable Continuum Model (PCM) [28] that uses the integral equation formalism variant (IEFPCM) [31] was used for solvent calculations in Gaussian. For calculations using ADF [32], the COSMO (Conductor like Screening Model) model of solvation [33–35] with the Esurf type of cavity [36], was used.

Results and Discussion

Synthesis

Ferrocenyl carboxylic acids (**1** – **6**) were synthesised in multigram quantities using slightly modified methods than previously published [7,10,13], to improve yields and to simplify the reaction setup. The reactions are shown in **Scheme 1**, with detailed synthetic methods and characterisation in the experimental section. Special care was taken to work under strict Schleck conditions to avoid a drastic decrease in yield.

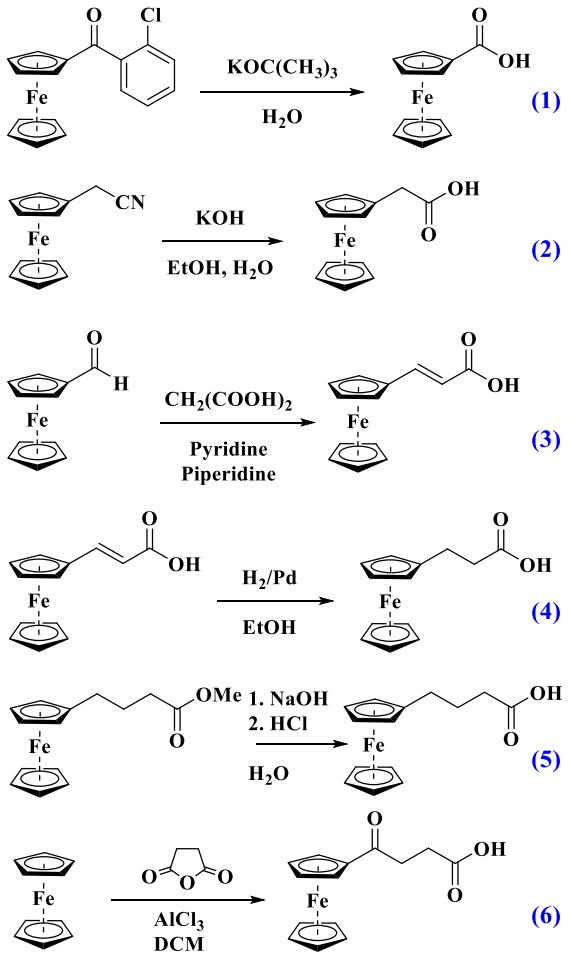

Scheme 1. Reaction scheme of $FcCO_2H$ **(1)**, $FcCH_2CO_2H$ **(2)**, $Fc(CH)_2CO_2H$ **(3)**, $Fc(CH_2)_2CO_2H$ **(4)**, $Fc(CH_2)_3CO_2H$ **(5)** and $FcCO(CH_2)_2CO_2H$ **(6)**.

Cyclic Voltammetry

The CV's of the acids (**1** - **6**) performed at 25°C in CH_3CN and DCM as the solvent, at a scan rate of 0.100 V s^{-1}, are shown in **Figure 2** (**6**) and **Figure 3** (**1** - **6**), with electrochemically relevant data summarised in **Table 1**. The CV's at different scan rates varying from 0.050 – 5.00 V s^{-1}, with data tables are provided in the Supplementary Information. The formal reduction potentials of each of the ferrocenyl acid derivatives (**1**) - (**6**) were found to be independent of scan rate.

Effect of the solvent

The redox properties of ferrocenyl carboxylic acids were examined using cyclic voltammetry (CV's) in CH_3CN and DCM as solvent. **Figure 2** compares the CV's of (**6**) in CH_3CN and DCM as solvent at a scan rate of 0.100 V s^{-1}, using DmFc as the internal standard. The formal reduction potential of the ferrocenyl group of (**6**) occur *ca*. 0.1 V more positive in DCM than in CH_3CN as the solvent, while the formal reduction potential of DmFc occurs *ca*. 0.09 V more negative in DCM than in CH_3CN as the solvent. Similarly, the formal redox potential of the ferrocenyl group of (**1** - **5**), all occur *ca*. 0.1 V more positive in DCM than in CH_3CN as solvent (**Figure 3**, **Table 1**). The observation that positive (negative) redox potentials *vs.* Fc/Fc^+ shift more positive (negative) in DCM than in CH_3CN as solvent, agree with published CV's of Fischer tungsten carbene complexes, where it was found that the peak reduction potential of the irreversible tungsten-based oxidation process in DCM is 0.05–0.25 V higher (more positive) than the peak reduction potential in CH_3CN, while the carbene ligand-based reduction process in DCM is observed at a potential 0.05–0.43 V lower (more negative) than in CH_3CN [37]. Comparing the electrochemical data obtained in DCM/$[N(^nBu)_4][B(C_6F_5)_4]$ and $CH_3CN/[N(^nBu)_4][B(PF)_6]$, both sets of experiments gave reversible chemical results with peak current ratios of 1. CV's obtained in DCM, however, have slightly smaller peak current-voltage separations ΔE_p, ranging from 0.067 to 0.079 V in DCM, and from 0.072 to 0.082 V CH_3CN. Previously reported electrochemical studies on ferrocenyl carboxylic acids (**1**), (**2**), (**4**) and (**5**), were performed in CH_3CN as solvent and $LiClO_4$ as electrolyte [12], with larger ΔE_p values, ranging from 0.096 to 0.110 V CH_3CN, see the results summarised in **Table 1**. The solvent DCM (of low polarity) minimises solvent−compound interactions, while the chosen supporting electrolyte, $[N(^nBu)_4][B(C_6F_5)_4]$, reduces nucleophilic attack by the electrolyte anion [38–41], providing better

conditions for anodic electrochemical studies of multi-ferrocenyl compounds [13,37]. The $Fe^{II/III}$ redox potential of (**1**), (**2**), (**4**) and (**5**) obtained in CH_3CN in this study, compare well with previously published data [12] within 0.005 - 0.024 V.

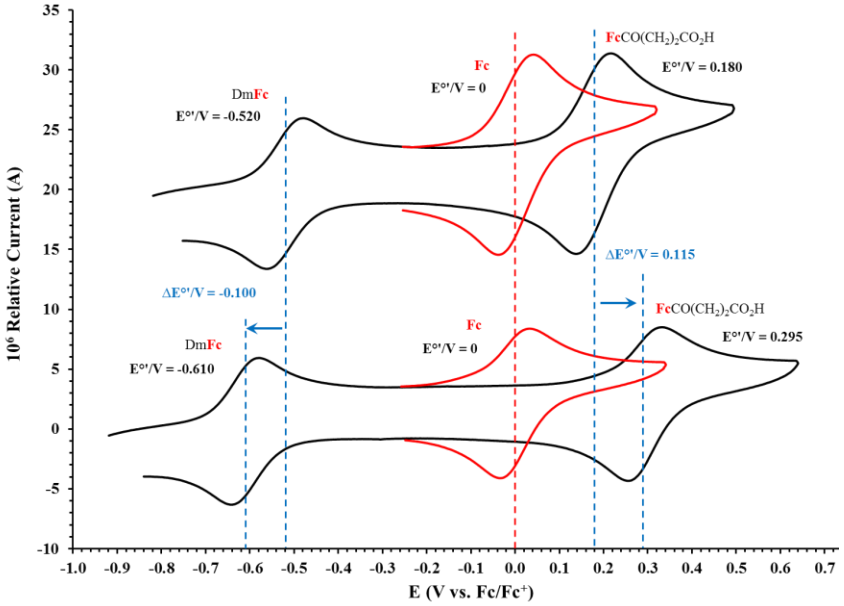

Figure 2. CV of 0.0005 M ferrocenyl carboxylic acid (**6**) in DCM as solvent (bottom) and CH_3CN as solvent (top) at a scan rate of 0.100 V s^{-1}. Scans initiated in the positive direction from *ca.* -0.9 V *vs.* Fc/Fc^+.

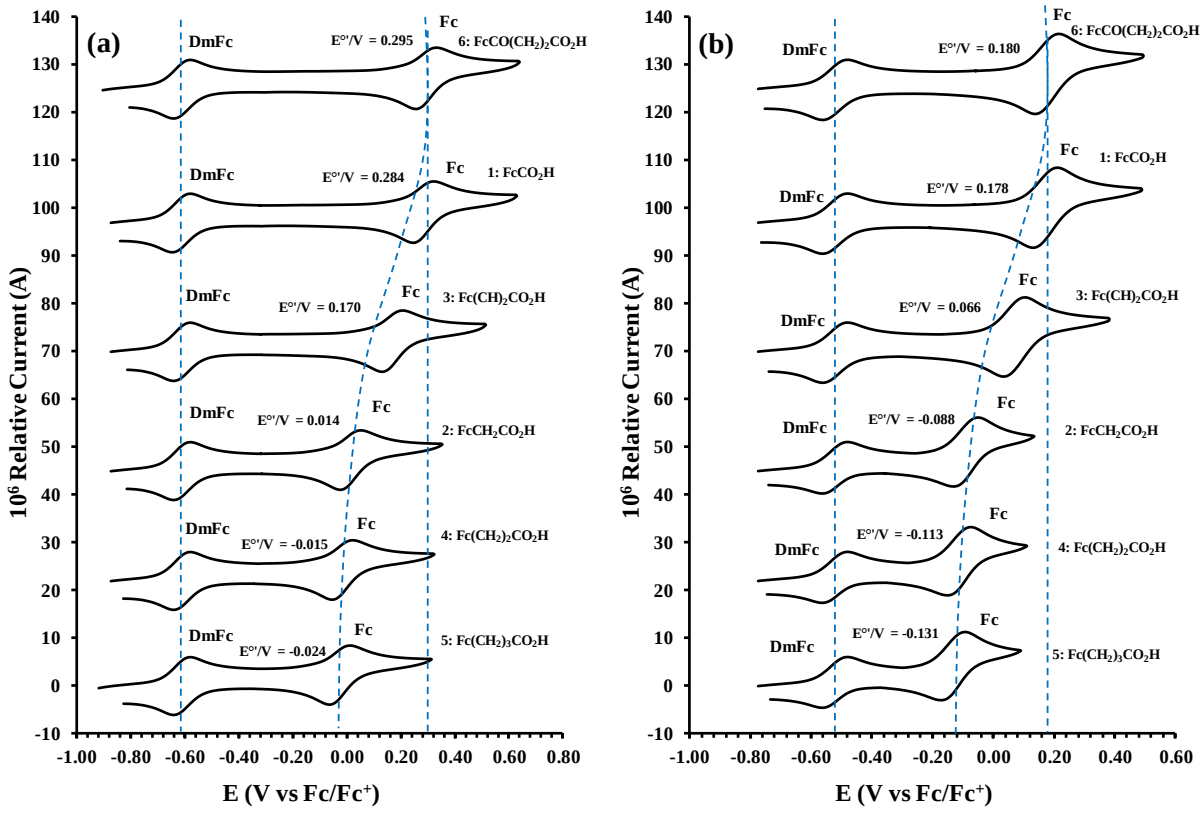

Figure 3. Stacked CV's of 0.0005 M ferrocenyl carboxylic acids (**1** – **6**) in **(a)** DCM **(b)** CH_3CN as solvent at a scan rate of 0.100 V s^{-1}. Scans initiated in the positive direction from *ca.* -0.9 V *vs.* Fc/Fc^+.

Influence of carbonyl group

The CV's in **Figure 3** shows that the carbonyl group has an electron-withdrawing effect on the formal reduction potential of the ferrocene group. The formal reduction potential E°'of Fe in **(1)** and **(6)**, both with a carbonyl group directly attached to Fc, is *ca.* 0.2 (CH_3CN) and 0.3 V (DCM) more positive than the formal reduction potential of free ferrocene at 0 V. Ferrocene acid **(6)** has two carbonyl groups, the first directly bound to the ferrocene group and the second bridged by two additional CH_2 groups. The effect of the carbonyl group directly attached to the ferrocene group is the main reason for the formal reduction potential shift. The much smaller effect of the second

carbonyl group on E°'of Fe in **(6)** is observed where E°'of Fe in **(6)** is insignificantly slightly higher than E°'of Fe in **(1)** by 0.011 V in DCM and 0.002 V in CH_3CN.

Effect of the non-isolated carboxylic group

The carboxylic acid group (-COOH in **(3)**) is connected to the ferrocenyl group Fc via a -C(H)=C(H)- double bond, allowing for good communication between -COOH and Fc *via* π-orbitals (also see the computational section below, for a molecular orbital view of the communication *via* π-orbitals). In **(4)** the -COOH group is connected to Fc *via* a $–C(H_2)-C(H_2)-$ single bond, hampering communication between -COOH and Fe in **(4)**. We will thus refer to **(4)** as having an isolated -COOH group and to **(3)** as having a non-isolated -COOH group. The effect of isolated **(4)** and non-isolated **(3)** -COOH groups on the formal reduction potential of Fc is shown in the CV's, see **Figure 4**. The formal reduction potential E°' of the ferrocene group of **(3)** that is not isolated from the electron-withdrawing effect of the carbonyl group, is at 0.066 V (CH_3CN) and 0.170 V (DCM) *vs.* Fc/Fc^+, while E°'of the ferrocene group of **(4)** that is more isolated from the electron-withdrawing effect of the carbonyl group, is lower, at -0.113 V (CH_3CN) and -0.015 V (DCM) *vs.* Fc/Fc^+, 0.179 V (CH_3CN) and 0.185 V (DCM) more negative than E°' of **(3)**, see **Figure 4**. The electron-withdrawing -COOH group withdraws electron density from Fe in **(3)**, making Fc of **(3)** more difficult to be oxidized at a higher potential, namely 0.066 V (CH_3CN) and 0.170 V (DCM) more positive than the reduction potential of free ferrocene at 0 V. The electron-withdrawing -COOH group withdraws less electron density from Fe in **(4)**, than in **(3)**, due to the weaker communication between -COOH and Fc in **(4)** *via* the $–C(H_2)-C(H_2)-$ single bond than the -C(H)=C(H)- double bond in **(3)**.

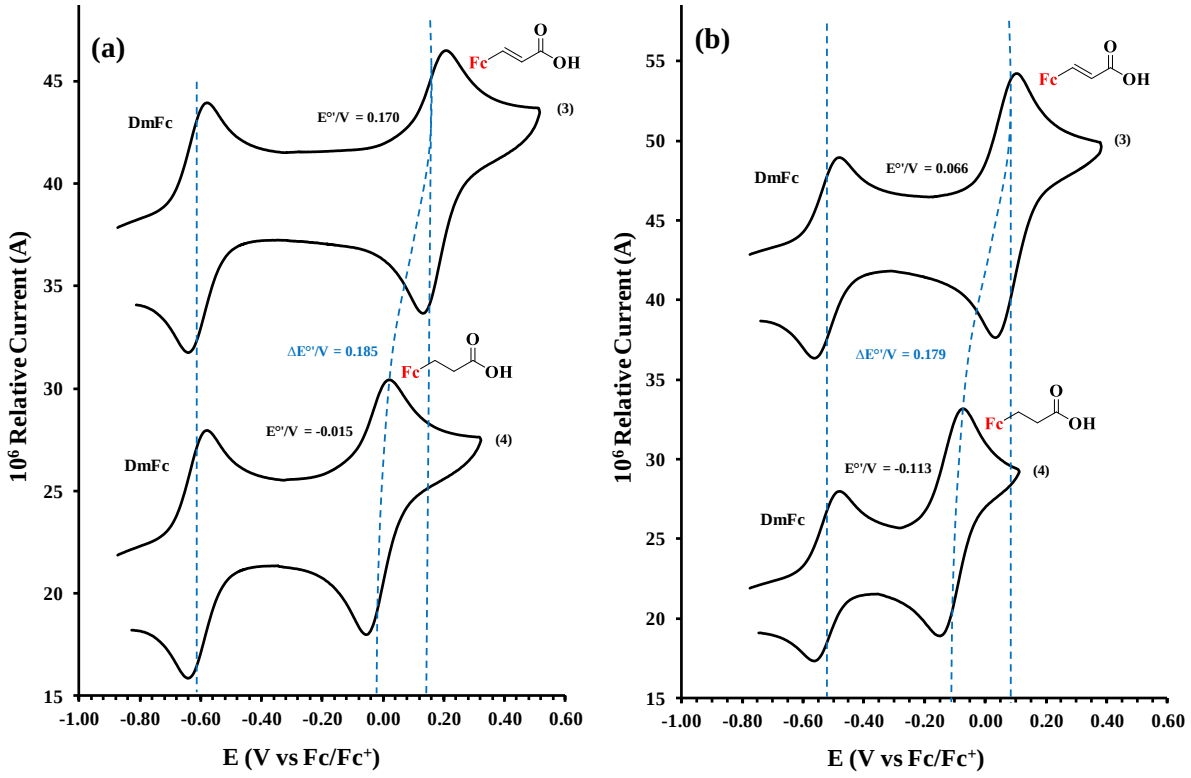

Figure 4. CV's of 0.0005 M ferrocenyl carboxylic acids (**3**) and (**4**) in DCM as the solvent for **(a)** and CH_3CN for **(b)** at a scan rate of 0.100 V s^{-1}.

Effect of chain length

The ferrocenecarboxylic acids **(1)**, **(2)**, **(4)** and **(5)** are of the form $Fc(CH_2)_nCO_2H$ (n = 0 **(1)**, 1 **(2)**, 2 **(4)** and 3 **(5)**) with an increasing number of CH_2 spacers separating the ferrocenyl group from the carbonyl group. **Figure 3** shows how the shift of the formal reduction potential E°' of the ferrocene group in relation to the proximity of the carbonyl group to the ferrocene group in the acid derivative. The carbonyl group is electron-withdrawing and in DCM the formal reduction potential E°' of the ferrocene group of **(1)** is at 0.284 V compared to free ferrocene at 0 V. With one isolating CH_2 group between ferrocene and the carbonyl group the formal reduction potential shift decreases significantly by 0.270 V to 0.014 V (DCM). In acid **(4)** and **(5)** with the carbonyl group isolated by two and three

CH_2 groups respectively, with E°' of the ferrocene group decreases to -0.015 V (**(4)** DCM) and -0.024 V (**(5)** DCM) respectively. The formal reduction potentials of Fc in each of the ferrocenyl acid derivatives **(1)**, **(2)**, **(4)** and **(5)** became exponentially smaller (less positive) with an increase in (CH_2)-chain length, see **Figure 5,** becoming constant after *ca.* n = 4. This is since the longer the $(CH_2)_n$ chain lengths, the more successfully the electron-withdrawing properties of the carbonyl group is isolated from the electron-donating ferrocene group. This trend was observed in both DCM and CH_3CN as solvents. Similar behaviour was observed for E°' of the ferrocene group of $Fc(CH_2)_nSH$ and $Fc(CH_2)_nOH$ [43], also containing CH_2 spacers separating the ferrocenyl group from the electron-withdrawing SH and OH group respectively.

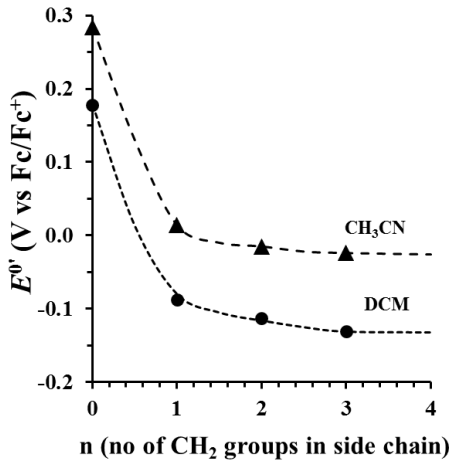

Figure 5. Relation between $E^{0`}$ and the number of CH_2 groups in the side chain of Fc–(CH_2)n–COOH for $FcCO_2H$ **(1)**, $FcCH_2CO_2H$ **(2)**, $Fc(CH_2)_2CO_2H$ **(4)** and $Fc(CH_2)_3CO_2H$ **(5)**.

Effect of number of substituent groups

The formal reduction potential E°' of the Fe in **(1 - 6)** in CH_3CN as solvent varies over a range of 0.31 V between 0.180 and -0.131 V, all around E°' of Fc at 0 V. E°' of the Fe in **(1)**, **(3)** and **(6)** is higher, and E°' of the Fe in **(2)**, **(4)** and **(5)** is lower than E°' of Fc at 0 V. Each of **(1 - 6)** has one

substituent group on Fc. The formal reduction potential E°' of DmFc with ten CH_3 substituents on Fc, is much lower, namely -0.480 in CH_3CN. E°' (in CH_3CN) of the Fe in $Fe(CpMe_4)(CpMe_4)$, $Fe(Cp)(CpMe_5)$ and Fe(CpMe)(CpMe) with 8, 5 and 2 CH_3 substituents on Fc, is -0.346 [44], -0.300 V [45] and -0.057 [46] *vs.* Fc/Fc^+ respectively (**Table 2**). There is a linear relationship between E°' of the Fe in $Fe(CpMe_{n1})(CpMe_{n2})$ and the total number (n1+n2) of CH_3 substituents, see **Figure 6**. The electron-donating property of the CH_3 groups directly bonded to Fc is thus additive.

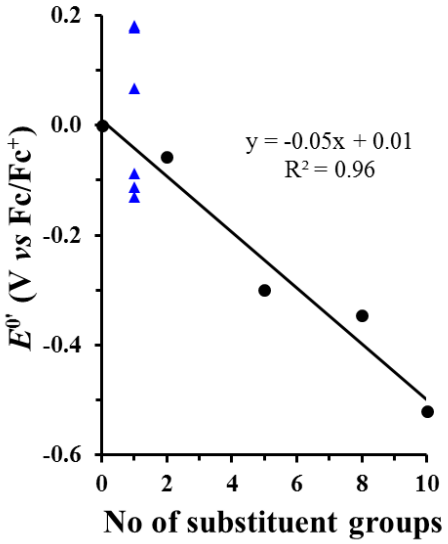

Figure 6. The relation between $E^{0`}$ and the number of CH_3 substituent groups on ferrocene (black dots). Data for complexes (**1** – **6**) with one substituent group on Fc, shown with blue triangles. Data in **Table 2**.

Table 1. Cyclic voltammetry data of ferrocenyl carboxylic acids (**1** – **6**) in DCM and CH_3CN containing 0.1 mol dm^{-3} $[N(^nBu)_4][B(C_6F_5)_4]$ as supporting electrolyte at a scan rate of 0.100 V s^{-1} at 25°C.

		DCM			**CH_3CN**			**$\Delta E^{o'}$ (DCM-CH_3CN)**	**Ref.**
		i_{pa} (µA), i_{pc}/i_{pa}	**E_{pa} (V)**	**$E^{o'}$ (V), ΔE_p (V)**	**i_{pa} (µA), i_{pc}/i_{pa}**	**E_{pa} (V)**	**$E^{o'}$ (V), ΔE_p (V)**		
Ferrocene	DmFc	3.68, 0.99	-0.573	-0.610, 0.074	3.74, 0.99	-0.480	-0.520, 0.079	-0.090	this work
	Fc	3.81, 0.99	0.036	0, 0.072	3.92, 0.99	0.040	0, 0.080	0	this work
$FcCO_2H$	DmFc[a]	3.47, 0.99	-0.580	-0.610, 0.060	3.21, 0.99	-0.480	-0.520, 0.080	-0.090	this work
1	Fc	3.60, 0.99	0.321	0.284, 0.074	3.86, 0.99	0.218	0.178, 0.080	0.106	this work
						0.202	0.154, 0.095		[12] [b]
$FcCH_2CO_2H$	DmFc[a]	3.65, 0.99	-0.580	-0.610, 0.060	3.35, 0.99	-0.481	-0.520, 0.078	-0.090	this work
2	Fc	3.79, 0.99	0.047	0.014, 0.067	3.57, 0.99	-0.047	-0.088, 0.082	0.102	this work
						-0.026	-0.076, 0.100		[12] [b]
$Fc(CH)_2CO_2H$	DmFc[a]	3.25, 0.99	-0.579	-0.610, 0.061	3.82, 0.99	-0.480	-0.520, 0.080	-0.090	this work
3	Fc	3.36, 0.99	0.210	0.170, 0.079	3.93, 0.99	0.105	0.066, 0.078	0.104	this work
$Fc(CH_2)_2CO_2H$	DmFc[a]	3.74, 0.99	-0.579	-0.610, 0.060	3.58, 0.99	-0.482	-0.520, 0.076	-0.090	this work
4	Fc	3.87, 0.99	0.020	-0.015, 0.070	3.74, 0.99	-0.077	-0.113, 0.072	0.098	this work
						-0.056	-0.106, 0.100		[12] [b]
$Fc(CH_2)_3CO_2H$	DmFc[a]	3.89, 0.99	-0.579	-0.610, 0.061	3.64, 0.99	-0.482	-0.520, 0.075	-0.090	this work
5	Fc	3.98, 0.99	0.011	-0.024, 0.070	3.83, 0.99	-0.092	-0.131, 0.078	0.107	this work
						-0.071	-0.126, 0.110		[12] [b]
$FcCO(CH_2)_2CO_2H$	DmFc[a]	3.51, 0.99	-0.580	-0.610, 0.060	3.13, 0.99	-0.480	-0.520, 0.080	-0.090	this work
6	Fc	3.66, 0.99	0.330	0.295, 0.070	3.52, 0.99	0.220	0.180, 0.080	0.115	this work

[a.] Internal standard decamethylferrocene, DmFc

[b.] Reported *vs.* SCE [12]; to convert to potential *vs.* Fc^+/Fc for comparative reasons, a correction value of 0.416 V was used, obtained from E°' (Fc/Fc^+) = 0.66(5) V *vs.* SHE in $[n(Bu_4)N][PF_6]/CH_3CN$ [47], and thus E°' (Fc/Fc^+) = (0.66 - 0.2444) = 0.416 V *vs.* SCE (SCE = 0.2444 V *vs.* SHE.)

Table 2. Experimental formal reduction potentials obtained in DCM and CH_3CN (*vs.* Fc/Fc^+) and the DFT calculated HOMO energies of ferrocenecarboxylic acids (**1** – **6**) as well as substituted ferrocenyl compounds from literature.

	Experimental			**Calculated B3LYP**		**Calculated OLYP**		
	No of sub-stituent groups	***E*°′ *vs.* Fc/Fc$^+$ in DCM**	***E*°′ *vs.* Fc/Fc$^+$ in CH_3CN**	**E_{HOMO} eV in DCM solution**	**E_{HOMO} eV in CH_3CN solution**	**E_{HOMO} eV in DCM solution**	**E_{HOMO} eV in CH_3CN solution**	**Ref.**
Ferrocene	0	0	0	-5.48	-5.49	-4.07	-4.07	this work
Decamethylferrocene	10	-0.610	-0.520	-4.88	-4.90	-3.47	-3.46	this work
$FcCO_2H$ – **(1)**	1	0.284	0.177	-5.79	-5.80	-4.46	-4.16	this work
$Fc(CH_2)_2CO_2H$ – **(2)**	1	0.010	-0.088	-5.51	-5.52	-4.15	-4.37	this work
$Fc(CH)_2CO_2H$ – **(3)**	1	0.170	0.066	-5.70	-5.70	-4.39	-4.13	this work
$Fc(CH_2)_2CO_2H$ – **(4)**	1	-0.019	-0.113	-5.48	-5.48	-4.14	-4.07	this work
$Fc(CH_2)_3CO_2H$ – **(5)**	1	-0.025	-0.131	-5.42	-5.44	-4.06	-4.46	this work
$FcCO(CH_2)_2CO_2H$ - **(6)**	1	0.295	0.180	-5.78	-5.79	-4.48	-4.36	this work
$Fe(CpMe_4)CpMe_4)$	8	-	-0.346	-	-5.01	-	-3.54	[44]
$Fe(Cp)(CpMe_5)$	5	-	-0.300	-	-5.13	-	-3.77	[45]
Fe(CpMe)(CpMe)	2	-	-0.057	-	-5.36	-	-3.94	[46]

Computational Analysis

The ferrocenecarboxylic acids (**1** – **6**), ferrocene and the substituted ferrocenes, $Fe(CpMe_5)(CpMe_5)$ (DmFc), $Fe(CpMe_4)(CpMe_4)$, $Fe(Cp)(CpMe_5)$ and Fe(CpMe)(CpMe) were optimized using DFT. On a molecular level, the highest occupied molecular orbital (HOMO) of these molecules, provide information of where the electrons are removed during the oxidation process of these molecules. As expected, the HOMOs of all these molecules are of mainly iron-d character, involving Fe(II) to Fe(III) oxidation, see **Figure 7**. The HOMO of (**3**) clearly shows the communication between the carbonyl group and ferrocenyl along π bonds in (**3**), that is absent in the HOMO of (**4**).

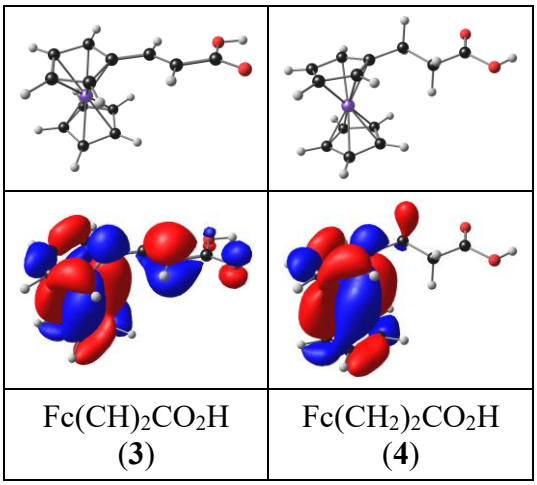

Figure 7. B3LYP/6-311G(d,p) optimised structures (top) and HOMOs (bottom) of ferrocenyl carboxylic acids (**3**) and (**4**). Colour code (online version): Fe (purple), O (red), C (dark grey), H (white). Contour used for the HOMO plots is 0.015 e $Å^{-1}$.

Furthermore, the ease of oxidation (energy in eV to remove an electron from the HOMO), is related to the energy of the HOMO; less energy (lower oxidation potential) is needed to remove an electron from a higher energy HOMO than from lower energy, more stable, HOMO. Thus, HOMO energies

and formal reduction potentials are inversely proportional. The relationship between the experimental formal reduction potential $E°'$ of Fe in these molecules *vs.* DFT calculated HOMO energies are shown in **Figure 8**, with the data summarised in **Table 2**. The relationships result in the following linear mathematical relationships using experimental formal reduction potential $E°'$ data, and DFT calculated HOMO energies, using B3LYP/6-311G(d,p) or OLYP/TZP, calculated in the experimental solvent (gas phase DFT results provided in the Supplementary Information):

$E°'_{exp,DCM} = - 0.872\ E_{HOMO,DCM} - 3.61$ $(R^2 = 0.98)$

$E°'_{exp,CH3CN} = - 0.617\ E_{HOMO,CH3CN} - 2.59$ $(R^2 = 0.91)$

$E°'_{exp,DCM} = - 0.977\ E_{HOMO,DCM} - 5.37$ $(R^2 = 0.99)$

$E°'_{exp,CH3CN} = - 0.669\ E_{HOMO,CH3CN} - 3.72$ $(R^2 = 0.93)$

Since the HOMO energies are inversely proportional to the experimental formal reduction potentials, their relationship results in a graph with a negative slope. The relationships in **Figure 8** can be used to predict the formal reduction potential of related substituted ferrocenes.

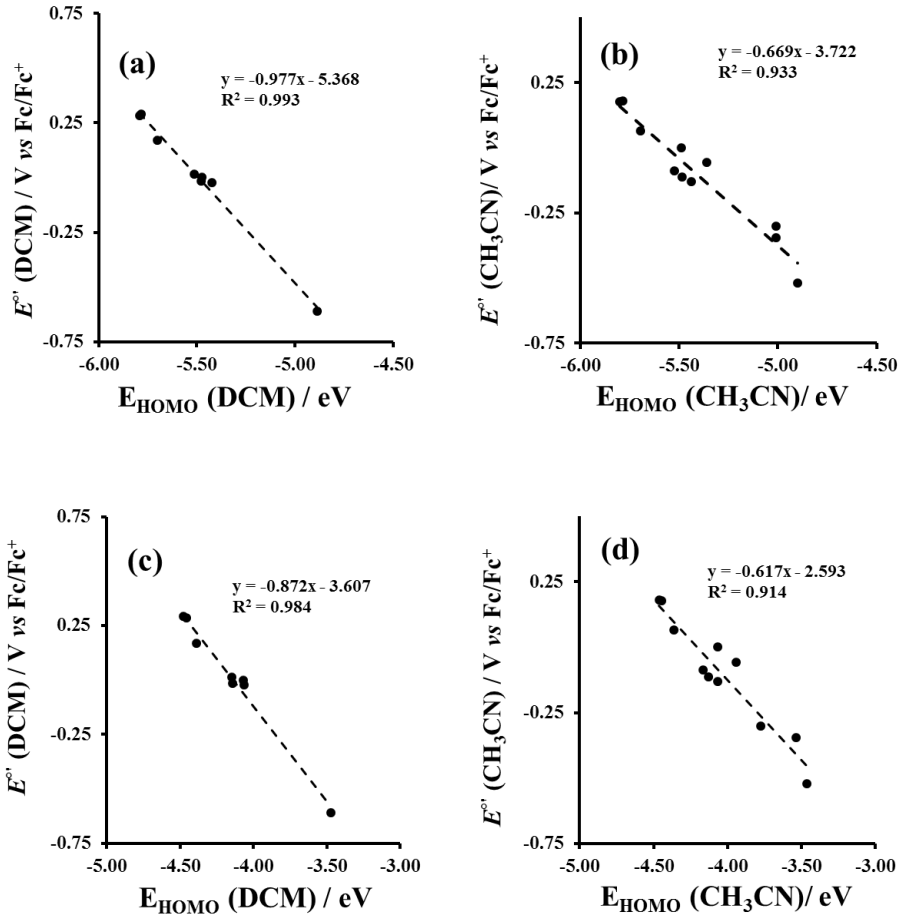

Figure 8 Linear relationships of calculated E_{HOMO} *vs.* experimental $E°'$ using **(a)** B3LYP/6-311G(d,p) E_{HOMO} calculated in DCM *vs.* $E°'$ in DCM, **(b)** B3LYP/6-311G(d,p) E_{HOMO} calculated in CH_3CN *vs.* $E°'$ in CH_3CN, **(c)** OLYP/TZP E_{HOMO} calculated in DCM *vs.* $E°'$ in DCM, and **(d)** OLYP/TZP E_{HOMO} calculated in CH_3CN *vs.* $E°'$ in CH_3CN. Data in **Table 2**

Conclusions

The experimental formal reduction potential of Fe in the six ferrocenyl carboxylic acid dyads (**1** – **6**) is *ca* 0.1 V higher in dichloromethane than in acetonitrile. The electron-withdrawing effect of the carboxy group on the reduction potential of the ferrocenyl group became exponentially smaller as the length of the alkyl chain separating the two groups increases. The formal reduction potential of Fe is also affected by the electron-withdrawing carbonyl group depending on whether the carbonyl group

is directly bonded to ferrocenyl or is isolated from ferrocenyl by an sp^3 hybridised carbon atom backbone or by an sp^2 hybridised carbon atom backbone. The DFT calculated HOMO energies are inversely proportional to the experimental formal reduction potential.

Supplementary Information

The synthesis and characterisation, additional graphs, tables, and optimised coordinates are provided in the Supporting information.

Author Information

Name: Jeanet Conradie, Tel: +27-(51)-4012194, Fax: +27-4017295, email: *conradj@ufs.ac.za*

Notes

The authors declare no competing financial interest.

Acknowledgements

This work has received support the South African National Research Foundation (Grant numbers 113327 and 96111) and the Central Research Fund of the University of the Free State, Bloemfontein. The High-Performance Computing facility of the UFS, the CHPC of South Africa and the Norwegian Supercomputing Program (UNINETT Sigma2, Grant No. NN9684K) are acknowledged for computer time.

References

[1] R. Dagani, Fifty Years of Ferrocene Chemistry, Chem. Eng. News. 79 (2001) 37–38. doi:10.1021/cen-v079n049.p037.

[2] K.L. Bublitz, D. E.Rinehart, Inorganic Reactions, 17th ed., Eiley: New York, 1969.

[3] J. Deeming, In Comprehensive Organometallic Chemistry, 4th ed., Oxford, 1982.

[4] W.. Watts, In Comprhensive Organometallic Chemistry, 8th ed., Oxford, 1982.

[5] A.N. Nesmeyanov, N.S. Kochetkova, Applications of Ferrocene and Its Derivatives, Russ. Chem. Rev. 5 (1974) 710–715. doi:10.1143/JJAP.33.5533.

[6] N. Rosenblum, Chemistry of The Iron Group Metallocenes: Ferrocene, Ruthenocene, Osmocene, John Wiley & Sons, New York, 1965.

[7] P.T.N. Nonjola, U. Siegert, J.C. Swarts, Synthesis, Electrochemistry and Cytotoxicity of Ferrocene-Containing Amides, Amines and Amino-Hydrochlorides, J. Inorg. Organomet. Polym. Mater. 25 (2015) 376–385. doi:10.1007/s10904-015-0195-4.

[8] J. Conradie, G.J. Lamprecht, A. Roodt, J.C. Swarts, Kinetic study of the oxidative addition reaction between methyl iodide and [Rh(FcCOCHCOCF3)(CO)(PPh3)]: Structure of [Rh(FcCOCHCOCF3)(CO)(PPh3)(CH3)(I)], Polyhedron. 26 (2007) 5075–5087. doi:10.1016/j.poly.2007.07.004.

[9] Q. Shen, S. Shekhar, J.P. Stambuli, J.F. Hartwig, Highly reactive, general, and long-lived catalysts for coupling heteroaryl and aryl chlorides with primary nitrogen nucleophiles,

Angew. Chemie - Int. Ed. 44 (2005) 1371–1375. doi:10.1002/anie.200462629.

[10] W.L. Davis, R.F. Shago, E.H.G. Langner, J.C. Swarts, Synthesis and electrochemical properties of a series of ferrocene-containing alcohols, Polyhedron. 24 (2005) 1611–1616. doi:10.1016/j.poly.2005.04.022.

[11] D.J. Bauer, L. St Vincent, C.H. Kempe, A.W. Downe, C.W. Johnson, J.W. Jolyner, R.P. Perry, B.G. Benns, B.A. Gingers, C.H. Bayley, N.F. Blom, E.W. Neuse, H.G. Thomas, Electrochemical characterization of some ferrocenylcarboxylic acids, Transit. Met. Chem. 12 (1987) 974.

[12] N.F. Blom, E.W. Neuse, H.G. Thomas, Electrochemical characterization of some ferrocenylcarboxylic acids, Transit. Met. Chem. 12 (1987) 301–306. doi:10.1007/BF01024018.

[13] H.J. Gericke, N.I. Barnard, E. Erasmus, J.C. Swarts, M.J. Cook, M.A.S. Aquino, Solvent and electrolyte effects in enhancing the identification of intramolecular electronic communication in a multi redox-active diruthenium tetraferrocenoate complex, a triple-sandwiched dicadmium phthalocyanine and a ruthenocene-containing β-diketone, Inorganica Chim. Acta. 363 (2010) 2222–2232. doi:10.1016/j.ica.2010.03.031.

[14] D.B.G. Williams, M. Lawton, Drying of organic solvents: Quantitative evaluation of the efficiency of several desiccants, J. Org. Chem. 75 (2010) 8351–8354. doi:10.1021/jo101589h.

[15] S.C. by Perry Reeves, C.J. by J Mrowca, M.M. Borecki, W.A. Sheppard, Carboxylation of Aromatic Compounds: Ferrocenecarboxylic acid, Org. Synth. Coll. 6 (1988). doi:10.15227/orgsyn.056.0028.

[16] D. Lednicer, J.K. Lindsay, C.R. Hauser, Reaction of the Methiodide of N,N-Dimethylaminomethylferrocene with Potassium Cyanide to Form Ferroeylacetonitrile, J. Org. Chem. 23 (1958) 653–655. doi:10.1021/jo01099a001.

[17] P.J. Graham, R. V. Lindsey, G.W. Parshall, M.L. Peterson, G.M. Whitman, Some Acyl Ferrocenes and their Reactions, J. Am. Chem. Soc. 79 (1957) 3416–3420. doi:10.1021/ja01570a027.

[18] K.J.R. Jr., R.J.C. Jr., P.E. Sokol, Organic Chemistry of Ferrocene. II. The Preparation of Ferrocenyl Aliphatic, J. Am. Chem. Soc. 79 (2005) 3420–3424. doi:10.1021/ja01570a028.

[19] G.D. Broadhead, J.M. Osgerby, P.L. Pauson, Broadhead, Osgerby, and Pauson : 127. Ferrocene Derivatives. Part V. * Perrocenealdehyde.., J. Chem. Soc. (1958) 650–656.

[20] N. Elgrishi, K.J. Rountree, B.D. McCarthy, E.S. Rountree, T.T. Eisenhart, J.L. Dempsey, A Practical Beginner's Guide to Cyclic Voltammetry, J. Chem. Educ. 95 (2018) 197–206. doi:10.1021/acs.jchemed.7b00361.

[21] P.T. Kissinger, W.R. Heineman, Cyclic voltammetry, J. Chem. Educ. 60 (1983) 702–706. doi:10.1021/ed060p702.

[22] R.L. Blake, M.H. Kim, M. Strassfeld, Diagnosis of Reversible, Quasi-Reversible, and Irreversible Electrode Processes with Differential Pulse Polarography, Anal. Chem. 53 (1981) 852–856. doi:10.1021/ac00229a026.

[23] M. V. Mirkin, A.J. Bard, Simple Analysis of Quasi-Reversible Steady-State Voltammograms, Anal. Chem. 64 (1992) 2293–2302. doi:10.1021/ac00043a020.

[24] J.C. Myland, K.B. Oldham, Quasireversible cyclic voltammetry of a surface confined redox

system: A mathematical treatment, Electrochem. Commun. 7 (2005) 282–287. doi:10.1016/j.elecom.2005.01.005.

[25] L.S. Kassel, The limiting high temperature rotational partition function of nonrigid molecules: I. General theory. II. CH4, C2H6, C3H8, CH(CH3)3, C(CH 3)4 and CH3(CH2)2CH 3. III. Benzene and its eleven methyl derivatives, J. Chem. Phys. 4 (1936) 276–282. doi:10.1063/1.1749835.

[26] C. Lee, W. Yang, R.G. Parr, Development of the Colle-Salvetti correlation-energy formula into a functional of the electron density, Phys. Rev. B. 37 (1988) 785–789. doi:10.1103/PhysRevB.37.785.

[27] B.K. Somani, S. Griffin, Ureteroscopy for paediatric calculi: The twin-surgeon model, J. Pediatr. Urol. 14 (2018) 73–74. doi:10.1016/j.jpurol.2017.10.004.

[28] A. V Marenich, C.J. Cramer, D.G. Truhlar, Universal Solvation Model Based on Solute Electron Density and on a Continuum Model of the Solvent Defined by the Bulk Dielectric Constant and Atomic Surface Tensions, J. Phys. Chem. B. 113 (2009) 6378–6396.

[29] N.C. Handy, A.J. Cohen, Left-right correlation energy, Mol. Phys. 99 (2001) 403–412. doi:10.1080/00268970010018431.

[30] G. te Velde, F.M. Bickelhaupt, E.J. Baerends, C. Fonseca Guerra, S.J.A. van Gisbergen, J.G. Snijders, T. Ziegler, Chemistry with ADF, J. Comput. Chem. 22 (2001) 931–967. doi:10.1002/jcc.1056.

[31] R.E. Skyner, J.L. Mcdonagh, C.R. Groom, T. Van Mourik, A review of methods for the calculation of solution free energies and the modelling of systems in solution, Phys. Chem.

Chem. Phys. 17 (2015) 6174–6191. doi:10.1039/C5CP00288E.

[32] C.C. Pye, T. Ziegler, An implementation of the conductor-like screening model of solvation within the Amsterdam density functional package, Theor. Chem. Accounts Theory, Comput. Model. (Theoretica Chim. Acta). 101 (1999) 396–408. doi:10.1007/s002140050457.

[33] A. Klamt, G. Schüürmann, COSMO: a new approach to dielectric screening in solvents with explicit expressions for the screening energy and its gradient, J. Chem. Soc., Perkin Trans. 2. (1993) 799–805. doi:10.1039/P29930000799.

[34] A. Klamt, V. Jonas, Treatment of the outlying charge in continuum solvation models, J. Chem. Phys. 105 (1996) 9972–9981. doi:10.1063/1.472829.

[35] A. Klamt, Conductor-like Screening Model for Real Solvents: A New Approach to the Quantitative Calculation of Solvation Phenomena, J. Phys. Chem. 99 (1995) 2224–2235. doi:10.1021/j100007a062.

[36] J.L. Pascual-ahuir, E. Silla, I. Tuñon, GEPOL: An improved description of molecular surfaces. III. A new algorithm for the computation of a solvent-excluding surface, J. Comput. Chem. 15 (1994) 1127–1138. doi:10.1002/jcc.540151009.

[37] M. Landman, B.E. Buitendach, M.M. Conradie, R. Fraser, P.H. van Rooyen, J. Conradie, Fischer mono- and biscarbene complexes of tungsten with mono- and dimeric heteroaromatic substituents, J. Electroanal. Chem. 739 (2015) 202–210. doi:10.1016/j.jelechem.2014.12.019.

[38] B.E. Buitendach, E. Erasmus, J.W. Niemantsverdriet, J.C. Swarts, Can Electrochemical Measurements Be Used to Predict X-ray Photoelectron Spectroscopic Data? the Case of Ferrocenyl-β-Diketonato Complexes of Manganese(III), Inorg. Chem. 57 (2018) 6606–6616.

doi:10.1021/acs.inorgchem.8b00745.

[39] D. Chong, J. Slote, W.E. Geiger, The role of solvent in the stepwise electrochemical oxidation of nickelocene to the nickelocenium dication, J. Electroanal. Chem. 630 (2009) 28–34. doi:10.1016/j.jelechem.2009.02.009.

[40] A. Nafady, T.T. Chin, W.E. Geiger, Manipulating the electrolyte medium to favor either one-electron or two-electron oxidation pathways for (fulvalendiyl)dirhodium complexes, Organometallics. 25 (2006) 1654–1663. doi:10.1021/om051101e.

[41] F. Barrière, R.U. Kirss, W.E. Geiger, Anodic electrochemistry of multiferrocenyl phosphine and phosphine chalcogenide complexes in weakly nucleophilic electrolytes, Organometallics. 24 (2005) 48–52. doi:10.1021/om040123i.

[42] W.E. Geiger, Use of Weakly Coordinating Anions to Develop an Integrated Approach to the Tuning of ΔE1/2 Values by Medium Effects, J. Am. Chem. Soc. 128 (2006) 3980–3989. doi:10.1021/ja058171x.

[43] J.P. Lewtak, M. Landman, I. Fernández, J.C. Swarts, A DFT-Elucidated Comparison of the Solution-Phase and SAM Electrochemical Properties of Short-Chain Mercaptoalkylferrocenes: Synthetic and Spectroscopic Aspects, and the Structure of Fc–CH 2 CH 2 –S–S–CH 2 CH 2 –Fc, Inorg. Chem. 55 (2016) 2584–2596. doi:10.1021/acs.inorgchem.5b02936.

[44] J.A. Davies, C.M. Hockensmith, V.Y. Kukushkin, Y.N. Kukushkin, Synthetic Coordination Chemistry: Principles and Practice, WORLD SCIENTIFIC, 1996. doi:10.1142/2588.

[45] I. Noviandri, K.N. Brown, D.S. Fleming, P.T. Gulyas, P.A. Lay, A.F. Masters, L. Phillips, The

Decamethylferrocenium/Decamethylferrocene Redox Couple: A Superior Redox Standard to the Ferrocenium/Ferrocene Redox Couple for Studying Solvent Effects on the Thermodynamics of Electron Transfer, J. Phys. Chem. B. 103 (1999) 6713–6722.

[46] A.M. Makal, D. Plażuk, J. Zakrzewski, B. Misterkiewicz, K. Woźniak, Experimental Charge Density Analysis of Symmetrically Substituted Ferrocene Derivatives, Inorg. Chem. 49 (2010) 4046–4059. doi:10.1021/ic9019958.

[47] A.J.L. Pombeiro, Electron-donor/acceptor properties of carbynes, carbenes, vinylidenes, allenylidenes and alkynyls as measured by electrochemical ligand parameters, J. Organomet. Chem. 690 (2005) 6021–6040. doi:10.1016/j.jorganchem.2005.07.111.

Data in brief (DIB)

Supporting information for publication: **Solvent and Substituent Effect on Electrochemistry of Ferrocenylcarboxylic Acid Dyads**

Redox data of ferrocenyl carboxylic acid dyads in DCM and ACN.

Pieter J. Swarts and Jeanet Conradie

Department of Chemistry, PO Box 339, University of the Free State, Bloemfontein, 9300, South Africa

Corresponding author(s)
conradj@ufs.ac.za

Abstract
Redox data obtained from cyclic voltammetry experiments of the $Fe^{II/III}$ oxidation of six ferrocenyl carboxylic acid dyads are presented in this data in brief article. Data is obtained from the cyclic voltammograms at scan rates of two orders of magnitude (0.05 – 5.00 Vs^{-1}) using (i) acetonitrile as solvent and tetrabutylammonium hexafluorophosphate as supporting electrolyte and (ii) dichloromethane as solvent and tetrabutylammonium tetrakispentafluorophenylborate, as the supporting electrolyte. Data is reported *versus* the $Fe^{II/III}$ redox couple of ferrocene. The experimental redox potential data of the $Fe^{II/III}$ oxidation of the ferrocenyl group of the six ferrocenyl carboxylic acid dyads are ca 0.10 V lower in acetonitrile than in dichloromethane as solvent.

Keywords

Ferrocenyl acids; cyclic voltammetry; oxidation

Specifications Table

Subject	Chemistry
Specific subject area	Electrochemistry
Type of data	Table Image Graph Figure
How data were acquired	Princeton Applied Research PARSTAT 2273 potentiostat running Powersuite software (Version 2.58).

Data format	Raw Analysed
Parameters for data collection	Samples were used as synthesised. All the electrochemical experiments were performed in an M Bruan Lab Master SP glove box under a high purity argon atmosphere (H_2O and O_2 < 10 ppm).
Description of data collection	All electrochemical experiments were done in a 2 ml electrochemical cell containing three-electrodes (a glassy carbon working electrode, a Pt auxiliary electrode and a Pt pseudo reference electrode), connected to a Princeton Applied Research PARSTAT 2273 electrochemical analyser. Data obtained were exported to excel for analysis and diagram preparation.
Data source location	Institution: University of the Free State City/Town/Region: Bloemfontein Country: South Africa
Data accessibility	With the article
Related research article	P.J. Swarts, J. Conradie, *Solvent and substituent effect on Electrochemistry of ferrocenyl carboxylic acid dyads*" submitted to Journal of Electroanalytical Chemistry.

Value of the Data

- This data provide cyclic voltammograms and detailed electrochemical data for six ferrocenyl carboxylic acids in both dichloromethane and acetonitrile for scan rates over two orders of magnitude (0.05 – 5.00 Vs^{-1}).
- This data illustrate the influence of the solvent used in cyclic voltammetry experiments, on the formal redox potential of Fe of the ferrocenyl group for ferrocenyl carboxylic acids.
- This data illustrate the influence of the solvent on the peak current-voltage separations, ΔE_p, of the Fe oxidation peak of ferrocenyl carboxylic acids.
- This data illustrate the influence of electron-withdrawing carbonyl group on the iron's oxidation potential, depending on how close the carbonyl group is to the iron.
- Accurate redox potential data of these ferrocenyl (Fc) carboxylic acid dyads are important, since these dyads are used as ligands in organometallic complexes.

Data

This article presents redox data of six ferrocene-containing carboxylic acids, 1 – 6, reported versus the redox couple ferrocene (Fc) at 0, using decamethyleferrocene (DmFc) as internal standard, see Figure 1 for the series of complexes of this data study. The cyclic voltammograms obtained in dichloromethane (DCM) and acetonitrile (ACN) for compound 1 – 6 with DmFc as internal standard are shown in Figure 2-Figure 13. The cyclic voltammograms of DmFc and ferrocene in DCM and ACN are shown in Figure 14 and Figure 15. Electrochemical data obtained from the cyclic voltammograms at scan rates 0.05 Vs^{-1} – 5.00 Vs^{-1} are tabulated in Table 1 – Table 12 (0.10 Vs^{-1} scans from [1]. Presented data is related to the research article "Solvent and substituent effect on Electrochemistry of ferrocenyl carboxylic acid dyads" submitted to Journal of Electroanalytical Chemistry [1]. Redox data of ferrocene-containing compounds are important for application in asymmetric catalysis [2–4], energy transfer processes[5], biological applications [6], as additives in high burning rate composite rocket propellants [7], non-linear optics [4], etc.

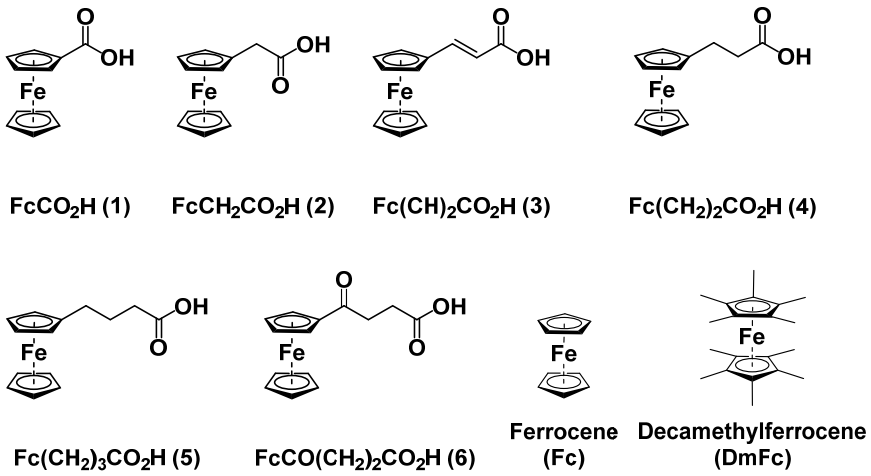

Figure 1. Structure of compounds in this study used for cyclic voltammetry.

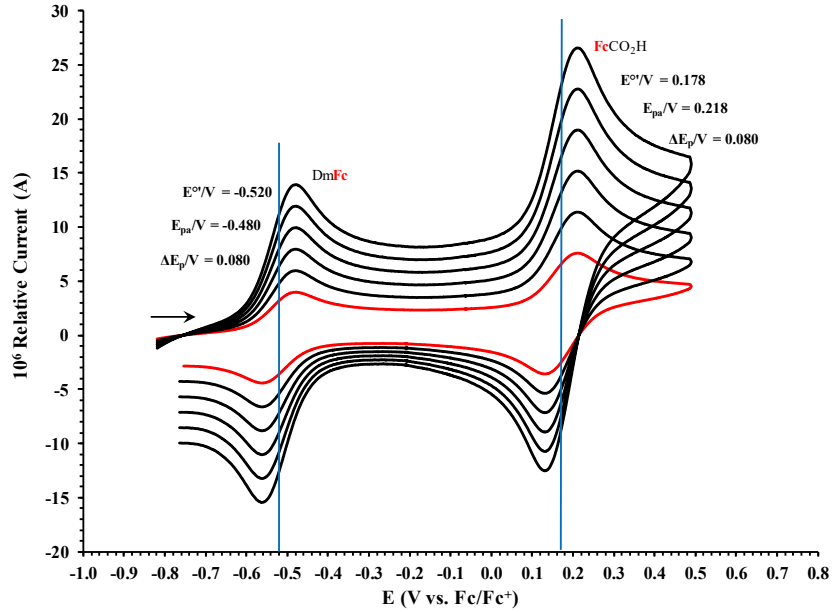

Figure 2. Cyclic voltammograms in ACN of $FcCO_2H$ at scan rates 0.050 (smallest peak currents), 0.100, 0.200, 0.300, 0.400 and 0.500 (largest peak currents). All scans initiated in a positive direction. Data for the peak oxidation potential (E_{pa}), the formal reduction potential ($E^{0'}$) and the peak current separation ΔE_p of the $Fe^{II/III}$ oxidation of DmFc (internal standard, left) and the indicated ferrocene-containing carboxylic acid (right) are indicated in V.

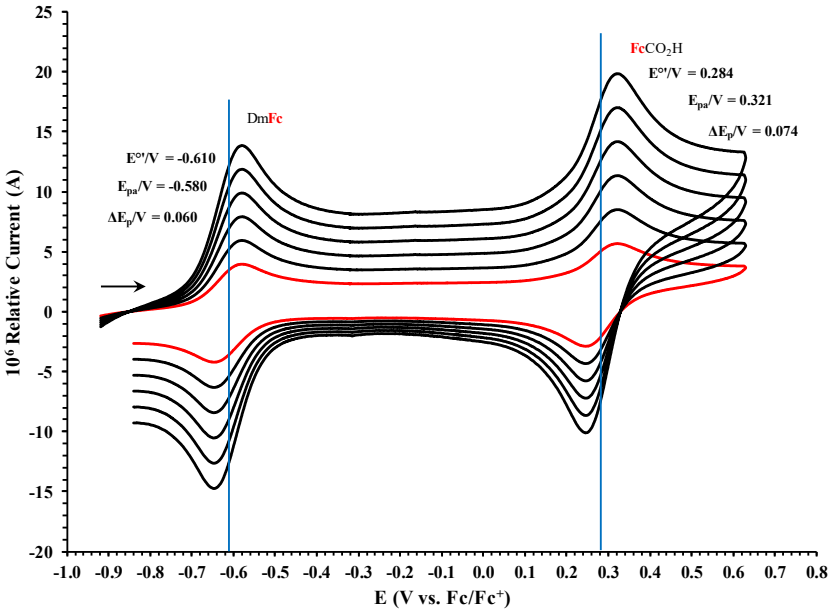

Figure 3. Cyclic voltammograms in DCM of $FcCO_2H$ at scan rates 0.050 (smallest peak currents), 0.100, 0.200, 0.300, 0.400 and 0.500 (largest peak currents). All scans initiated in a positive direction. Data for the peak oxidation potential (E_{pa}), the formal reduction potential ($E^{0'}$) and the peak current separation ΔE_p of the $Fe^{II/III}$ oxidation of DmFc (internal standard, left) and the indicated ferrocene-containing carboxylic acid (right) are indicated in V.

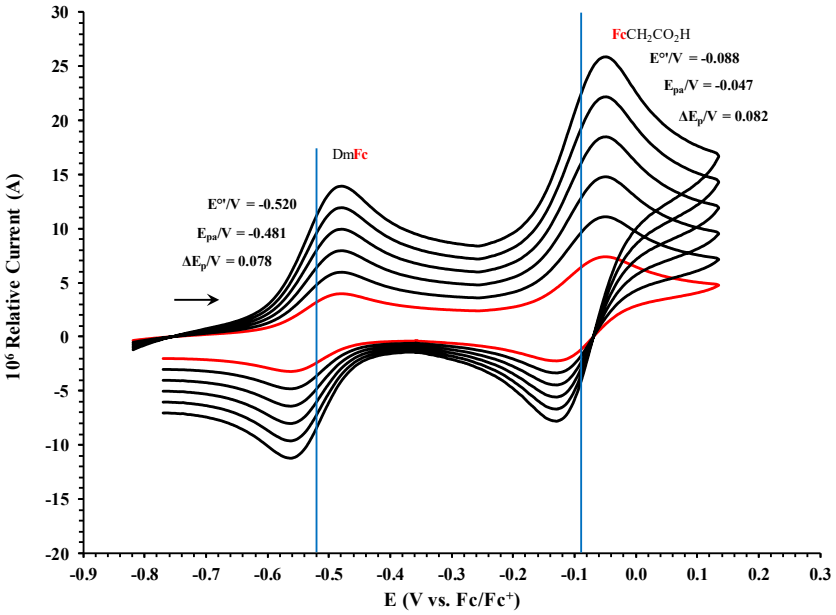

Figure 4. Cyclic voltammograms in ACN of $FcCH_2CO_2H$ at scan rates 0.050 (smallest peak currents), 0.100, 0.200, 0.300, 0.400 and 0.500 (largest peak currents). All scans initiated in a positive direction. Data for the peak oxidation potential (E_{pa}), the formal reduction potential ($E^{0'}$) and the peak current separation ΔE_p of the $Fe^{II/III}$ oxidation of DmFc (internal standard, left) and the indicated ferrocene-containing carboxylic acid (right) are indicated in V.

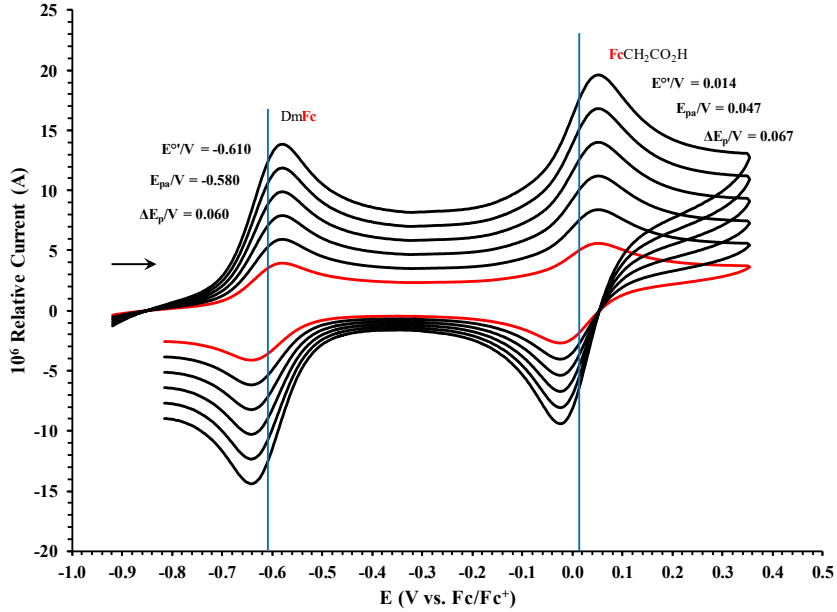

Figure 5. Cyclic voltammograms in DCM of $FcCH_2CO_2H$ at scan rates 0.050 (smallest peak currents), 0.100, 0.200, 0.300, 0.400 and 0.500 (largest peak currents). All scans initiated in a positive direction. Data for the peak oxidation potential (E_{pa}), the formal reduction potential ($E^{0'}$) and the peak current separation ΔE_p of the $Fe^{II/III}$ oxidation of DmFc (internal standard, left) and the indicated ferrocene-containing carboxylic acid (right) are indicated in V.

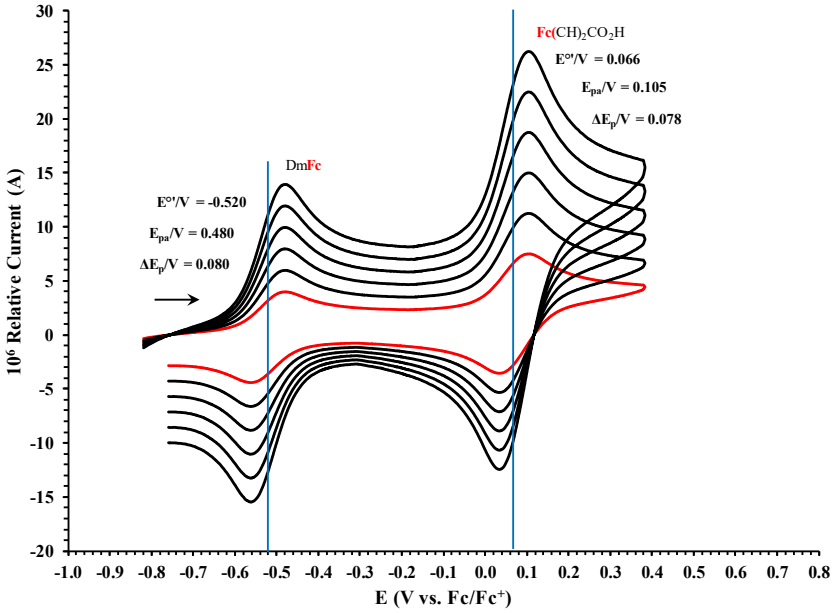

Figure 6. Cyclic voltammograms in ACN of $Fc(CH)_2CO_2H$ at scan rates 0.050 (smallest peak currents), 0.100, 0.200, 0.300, 0.400 and 0.500 (largest peak currents). All scans initiated in a positive direction. Data for the peak oxidation potential (E_{pa}), the formal reduction potential ($E^{0'}$) and the peak current separation ΔE_p of the $Fe^{II/III}$ oxidation of DmFc (internal standard, left) and the indicated ferrocene-containing carboxylic acid (right) are indicated in V.

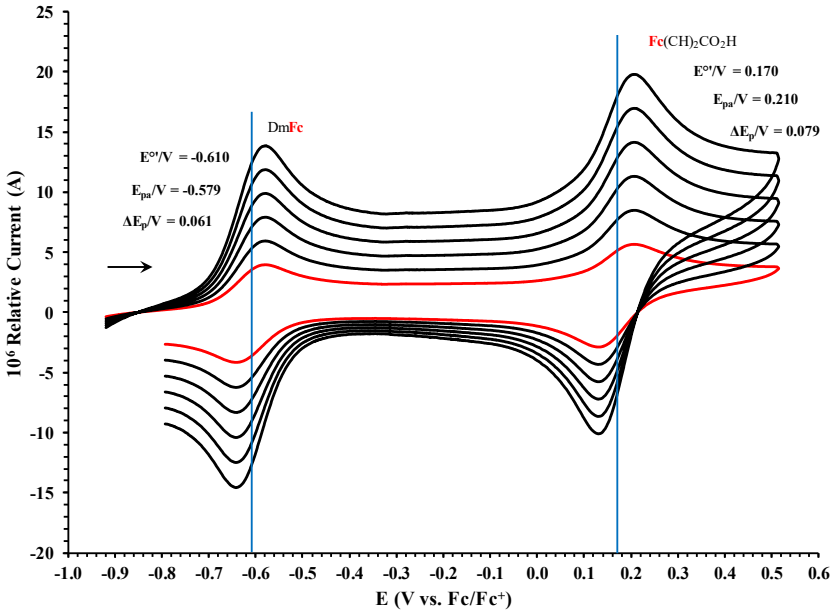

Figure 7. Cyclic voltammograms in DCM of $Fc(CH)_2CO_2H$ at scan rates 0.050 (smallest peak currents), 0.100, 0.200, 0.300, 0.400 and 0.500 (largest peak currents). All scans initiated in a positive direction. Data for the peak oxidation potential (E_{pa}), the formal reduction potential ($E^{0'}$) and the peak current separation ΔE_p of the $Fe^{II/III}$ oxidation of DmFc (internal standard, left) and the indicated ferrocene-containing carboxylic acid (right) are indicated in V.

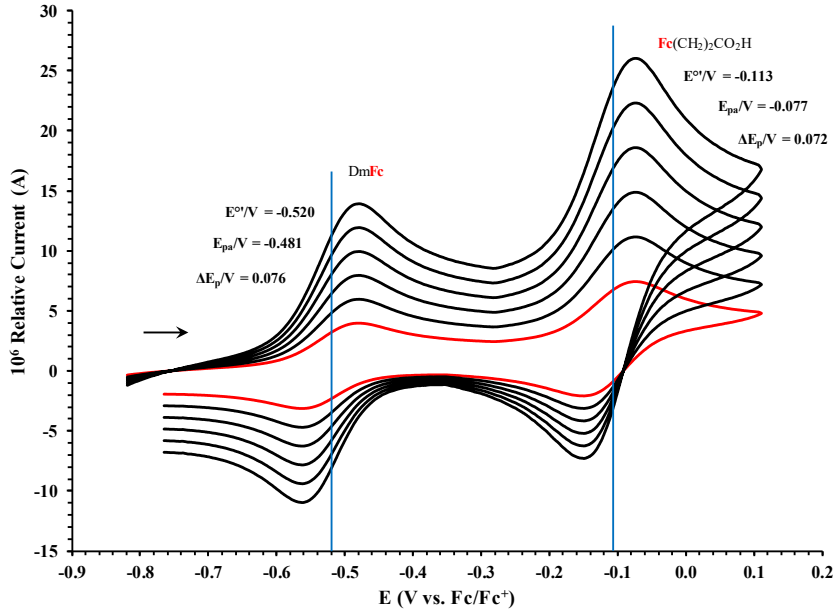

Figure 8. Cyclic voltammograms in ACN of $Fc(CH_2)_2CO_2H$ at scan rates 0.050 (smallest peak currents), 0.100, 0.200, 0.300, 0.400 and 0.500 (largest peak currents). All scans initiated in a positive direction. Data for the peak oxidation potential (E_{pa}), the formal reduction potential ($E^{0'}$) and the peak current separation ΔE_p of the $Fe^{II/III}$ oxidation of DmFc (internal standard, left) and the indicated ferrocene-containing carboxylic acid (right) are indicated in V.

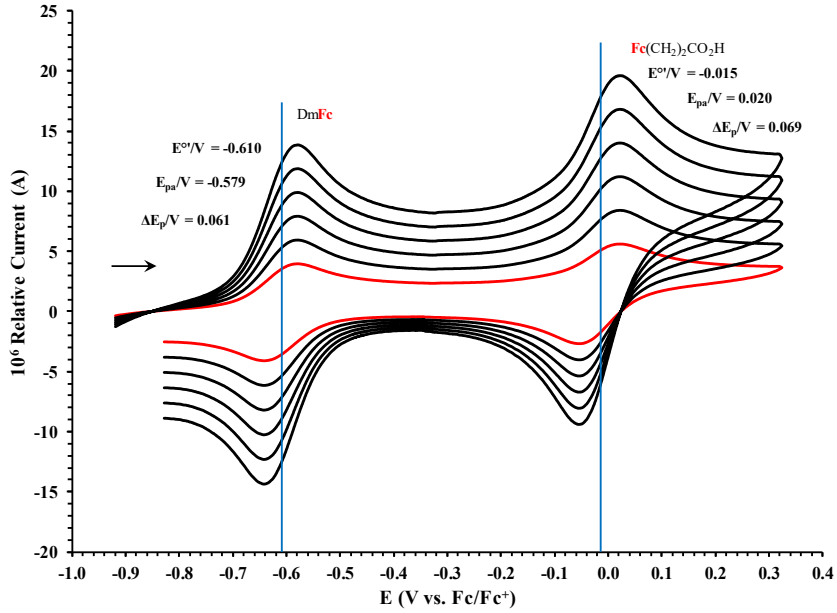

Figure 9. Cyclic voltammograms in DCM of $Fc(CH_2)_2CO_2H$ at scan rates 0.050 (smallest peak currents), 0.100, 0.200, 0.300, 0.400 and 0.500 (largest peak currents). All scans initiated in a positive direction. Data for the peak oxidation potential (E_{pa}), the formal reduction potential ($E^{0'}$) and the peak current separation ΔE_p of the $Fe^{II/III}$ oxidation of DmFc (internal standard, left) and the indicated ferrocene-containing carboxylic acid (right) are indicated in V.

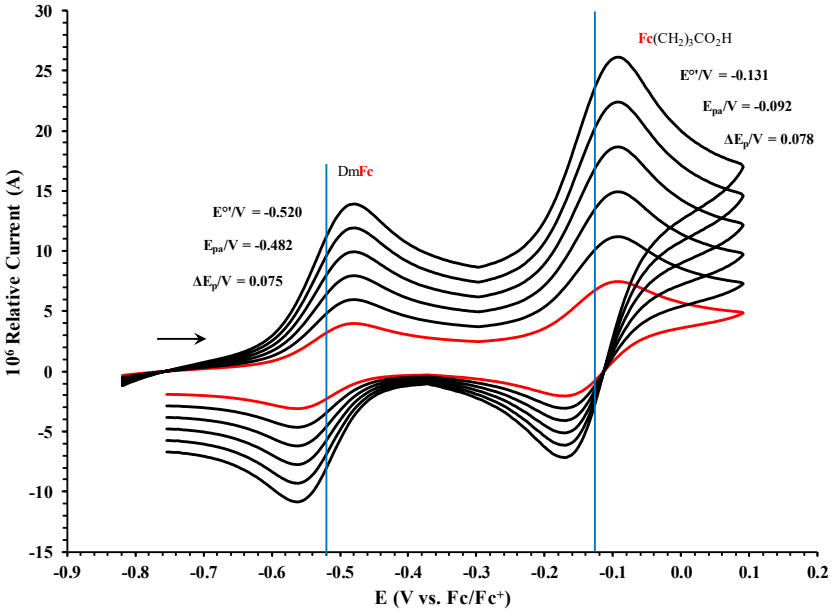

Figure 10. Cyclic voltammograms in ACN of $Fc(CH_2)_3CO_2H$ at scan rates 0.050 (smallest peak currents), 0.100, 0.200, 0.300, 0.400 and 0.500 (largest peak currents). All scans initiated in a positive direction. Data for the peak oxidation potential (E_{pa}), the formal reduction potential ($E^{0'}$) and the peak current separation ΔE_p of the $Fe^{II/III}$ oxidation of DmFc (internal standard, left) and the indicated ferrocene-containing carboxylic acid (right) are indicated in V.

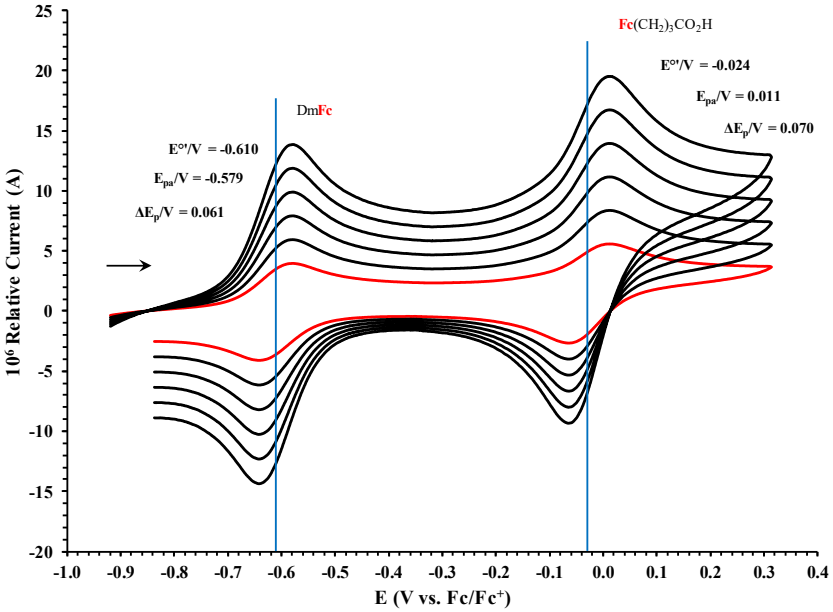

Figure 11. Cyclic voltammograms in DCM of $Fc(CH_2)_3CO_2H$ at scan rates 0.050 (smallest peak currents), 0.100, 0.200, 0.300, 0.400 and 0.500 (largest peak currents). All scans initiated in a positive direction. Data for the peak oxidation potential (E_{pa}), the formal reduction potential ($E^{0'}$) and the peak current separation ΔE_p of the $Fe^{II/III}$ oxidation of DmFc (internal standard, left) and the indicated ferrocene-containing carboxylic acid (right) are indicated in V.

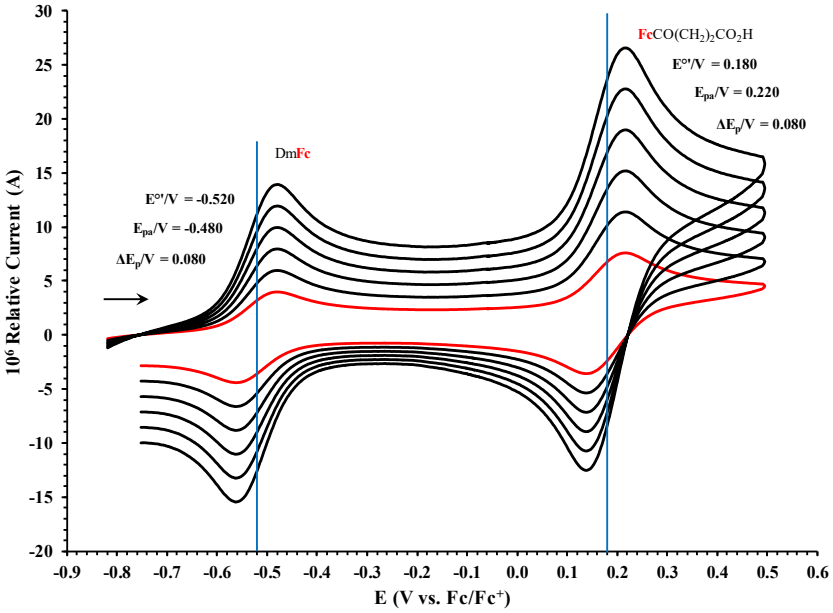

Figure 12. Cyclic voltammograms in ACN of $FcCO(CH_2)_2CO_2H$ at scan rates 0.050 (smallest peak currents), 0.100, 0.200, 0.300, 0.400 and 0.500 (largest peak currents). All scans initiated in a positive direction. Data for the peak oxidation potential (E_{pa}), the formal reduction potential ($E^{0`}$) and the peak current separation ΔE_p of the $Fe^{II/III}$ oxidation of DmFc (internal standard, left) and the indicated ferrocene-containing carboxylic acid (right) are indicated in V.

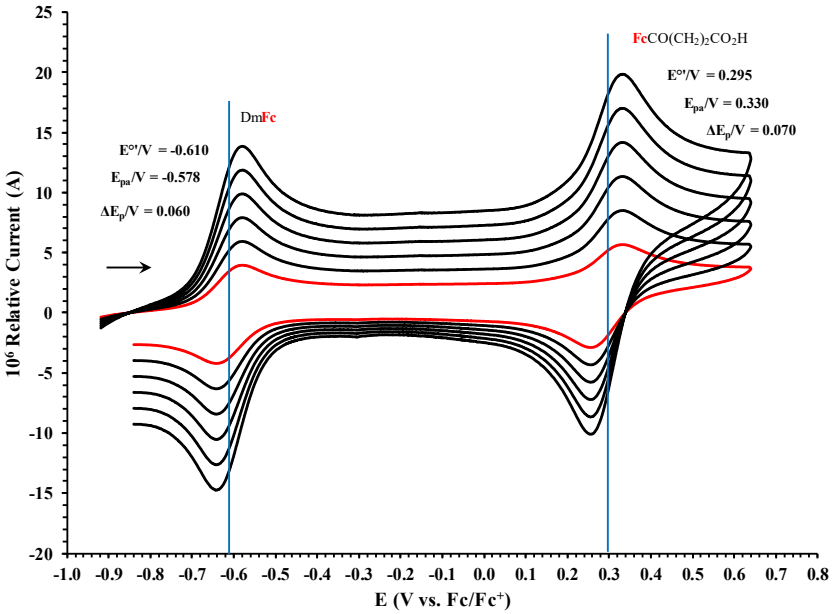

Figure 13. Cyclic voltammograms in DCM of $FcCO(CH_2)_2CO_2H$ at scan rates 0.050 (smallest peak currents), 0.100, 0.200, 0.300, 0.400 and 0.500 (largest peak currents). All scans initiated in a positive direction. Data for the peak oxidation potential (E_{pa}), the formal reduction potential ($E^{0`}$) and the peak current separation ΔE_p of the $Fe^{II/III}$ oxidation of DmFc (internal standard, left) and the indicated ferrocene-containing carboxylic acid (right) are indicated in V.

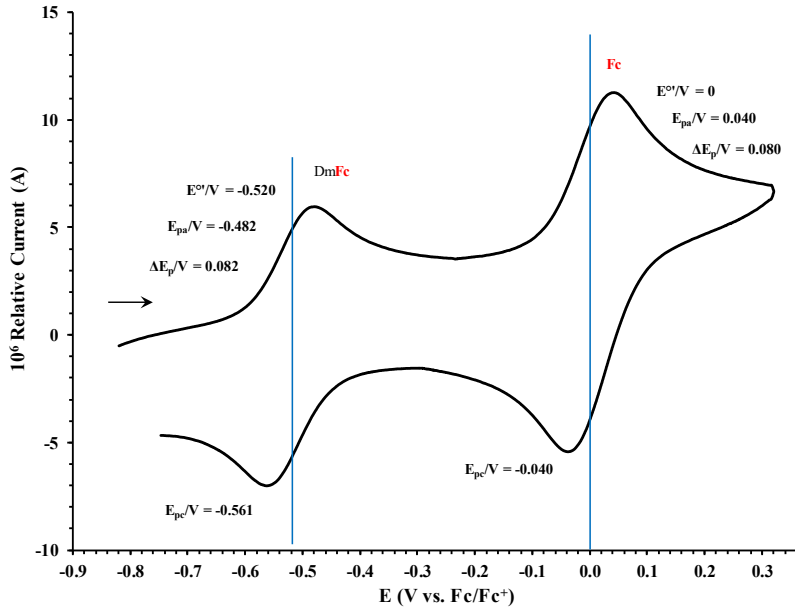

Figure 14. Cyclic voltammograms in ACN of decamethylferrocene and ferrocene at scan rate 0.100 Vs^{-1}. The scan is initiated in a positive direction. Data for the peak oxidation potential (E_{pa}), the formal reduction potential ($E^{0'}$) and the peak current separation ΔE_p of the $Fe^{II/III}$ oxidation of DmFc (internal standard, left) and Fc (right) is indicated in V.

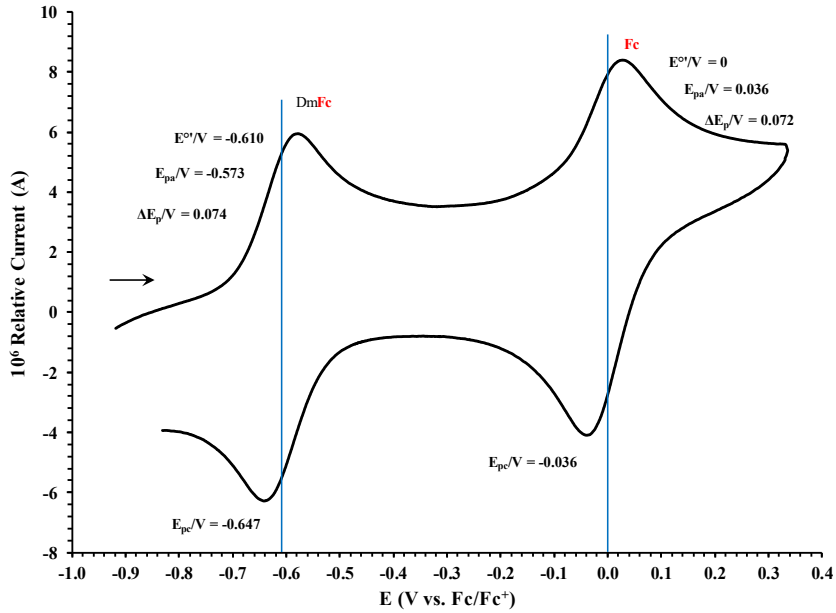

Figure 15. Cyclic voltammograms in DCM decamethylferrocene and ferrocene at scan rate 0.100 Vs^{-1}. The scan is initiated in a positive direction. Data for the peak oxidation potential (E_{pa}), the formal reduction potential ($E^{0'}$) and the peak current separation ΔE_p of the $Fe^{II/III}$ oxidation of DmFc (internal standard, left) and Fc (right) is indicated in V.

Table 1. Electrochemical data (potential in V *vs* Fc/Fc^+) in ACN for *c.a.* 0.0005 mol dm^{-3} of $FcCO_2H$ at indicated scan rates (ν in V/s).

ν (V/s)	E_{pa} / V	ΔE_p / V	$E^{o'}$ / V	i_{pa} / μA	i_{pc}/i_{pa}
DmFc					
0.100	**-0.480**	**0.080**	**-0.520**	**3.21**	**0.99**
$FcCO_2H$					
0.050	0.217	0.078	0.178	2.16	0.99
0.100	**0.218**	**0.080**	**0.178**	**3.86**	**0.99**
0.200	0.218	0.080	0.178	5.54	0.99
0.300	0.218	0.080	0.178	6.59	0.99
0.400	0.219	0.082	0.178	8.01	0.99
0.500	0.219	0.082	0.178	9.04	0.99
5.000	0.219	-	-	-	-

Table 2. Electrochemical data (potential in V *vs* Fc/Fc^+) in DCM for *c.a.* 0.0005 mol dm^{-3} of $FcCO_2H$ at indicated scan rates (ν in V/s).

ν (V/s)	E_{pa} / V	ΔE_p / V	$E^{o'}$ / V	i_{pa} / μA	i_{pc}/i_{pa}
DmFc					
0.100	**-0.580**	**0.060**	**-0.610**	**3.47**	**0.99**
$FcCO_2H$					
0.050	0.320	0.072	0.284	2.33	0.99
0.100	**0.321**	**0.074**	**0.284**	**3.60**	**0.99**
0.200	0.321	0.074	0.284	5.62	0.99
0.300	0.321	0.074	0.284	6.80	0.99
0.400	0.322	0.076	0.284	8.16	0.99
0.500	0.322	0.076	0.284	9.14	0.99
5.000	0.323	-	-	-	-

Table 3. Electrochemical data (potential in V *vs* Fc/Fc^+) in ACN for *c.a.* 0.0005 mol dm^{-3} of $FcCH_2CO_2H$ at indicated scan rates (ν in V/s).

ν (V/s)	E_{pa} / V	ΔE_p / V	$E^{o'}$ / V	i_{pa} / μA	i_{pc}/i_{pa}
DmFc					
0.100	**-0.481**	**0.078**	**-0.520**	**3.35**	**0.99**
$FcCH_2CO_2H$					
0.050	-0.048	0.080	-0.088	2.31	0.99
0.100	**-0.047**	**0.082**	**-0.088**	**3.57**	**0.99**
0.200	-0.047	0.083	-0.088	4.29	0.99
0.300	-0.046	0.084	-0.088	6.45	0.99
0.400	-0.046	0.085	-0.088	8.15	0.99

0.500	-0.045	0.086	-0.088	10.22	0.99
5.000	-0.045	-	-	-	-

Table 4. Electrochemical data (potential in V *vs* Fc/Fc^+) in DCM for *c.a.* 0.0005 mol dm^{-3} of $FcCH_2CO_2H$ at indicated scan rates (ν in V/s).

ν (V/s)	E_{pa} / V	ΔE_p / V	$E^{o'}$ / V	i_{pa} / μA	i_{pc}/i_{pa}
DmFc					
0.100	**-0.580**	**0.060**	**-0.610**	**3.65**	**0.99**
$FcCH_2CO_2H$					
0.050	0.046	0.065	0.014	2.21	0.99
0.100	**0.047**	**0.067**	**0.014**	**3.78**	**0.99**
0.200	0.047	0.068	0.014	4.35	0.99
0.300	0.047	0.068	0.014	6.25	0.99
0.400	0.047	0.069	0.014	8.24	0.99
0.500	0.048	0.070	0.014	10.51	0.99
5.000	0.049	-	-	-	-

Table 5. Electrochemical data (potential in V *vs* Fc/Fc^+) in ACN for *c.a.* 0.0005 mol dm^{-3} of $Fc(CH)_2CO_2H$ at indicated scan rates (ν in V/s).

ν (V/s)	E_{pa} / V	ΔE_p / V	$E^{o'}$ / V	i_{pa} / μA	i_{pc}/i_{pa}
DmFc					
0.100	**-0.480**	**0.080**	**-0.520**	**3.82**	**0.99**
$Fc(CH)_2CO_2H$					
0.050	0.104	0.076	0.066	2.01	0.99
0.100	**0.105**	**0.078**	**0.066**	**3.93**	**0.99**
0.200	0.105	0.078	0.066	4.84	0.99
0.300	0.105	0.078	0.066	6.48	0.99
0.400	0.106	0.080	0.066	7.85	0.99
0.500	0.106	0.080	0.066	8.84	0.99
5.000	0.107	-	-	-	-

Table 6. Electrochemical data (potential in V *vs* Fc/Fc^+) in DCM for *c.a.* 0.0005 mol dm^{-3} of $Fc(CH)_2CO_2H$ at indicated scan rates (ν in V/s).

ν (V/s)	E_{pa} / V	ΔE_p / V	$E^{o'}$ / V	i_{pa} / μA	i_{pc}/i_{pa}
DmFc					
0.100	**-0.579**	**0.061**	**-0.610**	**3.25**	**0.99**
$Fc(CH)_2CO_2H$					
0.050	0.209	0.078	0.170	1.98	0.99
0.100	**0.210**	**0.079**	**0.170**	**3.36**	**0.99**

0.200	0.210	0.079	0.170	4.91	0.99
0.300	0.210	0.079	0.170	6.54	0.99
0.400	0.211	0.080	0.170	7.94	0.99
0.500	0.211	0.080	0.170	8.94	0.99
5.000	0.212	-	-	-	-

Table 7. Electrochemical data (potential in V *vs* Fc/Fc^+) in ACN for *c.a.* 0.0005 mol dm^{-3} of $Fc(CH_2)_2CO_2H$ at indicated scan rates (ν in V/s).

ν (V/s)	E_{pa} / V	ΔE_p / V	$E^{o'}$ / V	i_{pa} / μA	i_{pc}/i_{pa}
DmFc					
0.100	**-0.482**	**0.076**	**-0.520**	**3.58**	**0.99**
$Fc(CH_2)_2CO_2H$					
0.050	-0.078	0.070	-0.113	2.22	0.99
0.100	**-0.077**	**0.072**	**-0.113**	**3.74**	**0.99**
0.200	-0.077	0.073	-0.113	4.84	0.99
0.300	-0.076	0.074	-0.113	6.48	0.99
0.400	-0.076	0.075	-0.113	8.39	0.99
0.500	-0.075	0.076	-0.113	9.55	0.99
5.000	-0.074	-	-	-	-

Table 8. Electrochemical data (potential in V *vs* Fc/Fc^+) in DCM for *c.a.* 0.0005 mol dm^{-3} of $Fc(CH_2)_2CO_2H$ at indicated scan rates (ν in V/s).

ν (V/s)	E_{pa} / V	ΔE_p / V	$E^{o'}$ / V	i_{pa} / μA	i_{pc}/i_{pa}
DmFc					
0.100	**-0.579**	**0.060**	**-0.610**	**3.74**	**0.99**
$Fc(CH_2)_2CO_2H$					
0.050	0.019	0.068	-0.015	2.12	0.99
0.100	**0.020**	**0.070**	**-0.015**	**3.87**	**0.99**
0.200	0.020	0.070	-0.015	5.11	0.99
0.300	0.020	0.070	-0.015	6.73	0.99
0.400	0.021	0.072	-0.015	8.01	0.99
0.500	0.021	0.072	-0.015	9.11	0.99
5.000	0.022	-	-	-	-

Table 9. Electrochemical data (potential in V *vs* Fc/Fc^+) in ACN for *c.a.* 0.0005 mol dm^{-3} of $Fc(CH_2)_3CO_2H$ at indicated scan rates (ν in V/s).

ν (V/s)	E_{pa} / V	ΔE_p / V	$E^{o'}$ / V	i_{pa} / μA	i_{pc}/i_{pa}
DmFc					
0.100	**-0.482**	**0.075**	**-0.520**	**3.64**	**0.99**

$Fc(CH_2)_3CO_2H$					
0.050	-0.091	0.077	-0.131	2.52	0.99
0.100	**-0.092**	**0.078**	**-0.131**	**3.83**	**0.99**
0.200	-0.092	0.079	-0.131	5.15	0.99
0.300	-0.092	0.080	-0.131	6.95	0.99
0.400	-0.093	0.081	-0.131	8.35	0.99
0.500	-0.093	0.082	-0.131	9.69	0.99
5.000	-0.094	-	-	-	-

Table 10. Electrochemical data (potential in V *vs* Fc/Fc^+) in DCM for *c.a.* 0.0005 mol dm^{-3} of $Fc(CH_2)_3CO_2H$ at indicated scan rates (ν in V/s).

ν (V/s)	E_{pa} / V	ΔE_p / V	$E^{o'}$ / V	i_{pa} / µA	i_{pc}/i_{pa}
DmFc					
0.100	**-0.579**	**-0.061**	**-0.610**	**3.89**	**0.99**
$Fc(CH_2)_3CO_2H$					
0.050	0.010	0.068	-0.024	2.39	0.99
0.100	**0.011**	**0.070**	**-0.024**	**3.98**	**0.99**
0.200	0.011	0.070	-0.024	5.26	0.99
0.300	0.012	0.072	-0.024	6.82	0.99
0.400	0.012	0.072	-0.024	8.23	0.99
0.500	0.013	0.074	-0.024	9.46	0.99
5.000	0.014	-	-	-	-

Table 11. Electrochemical data (potential in V *vs* Fc/Fc^+) in ACN for *c.a.* 0.0005 mol dm^{-3} of $FcCO(CH_2)_2CO_2H$ at indicated scan rates (ν in V/s).

ν (V/s)	E_{pa} / V	ΔE_p / V	$E^{o'}$ / V	i_{pa} / µA	i_{pc}/i_{pa}
DmFc					
0.100	**-0.480**	**0.080**	**-0.520**	**3.13**	**0.99**
$FcCO(CH_2)_2CO_2H$					
0.050	0.219	0.078	0.180	2.31	0.99
0.100	**0.220**	**0.080**	**0.180**	**3.52**	**0.99**
0.200	0.220	0.080	0.180	5.29	0.99
0.300	0.220	0.080	0.180	6.85	0.99
0.400	0.221	0.082	0.180	8.66	0.99
0.500	0.221	0.082	0.180	9.85	0.99
5.000	0.222	-	-	-	-

Table 12. Electrochemical data (potential in V *vs* Fc/Fc^+) in DCM for *c.a.* 0.0005 mol dm^{-3} of $FcCO(CH_2)_2CO_2H$ at indicated scan rates (ν in V/s).

ν (V/s)	E_{pa} / V	ΔE_p / V	$E^{o'}$ / V	i_{pa} / µA	i_{pc}/i_{pa}
DmFc					
0.100	**-0.580**	**0.060**	**-0.610**	**3.51**	**0.99**
$FcCO(CH_2)_2CO_2H$					
0.050	0.329	0.068	0.295	2.42	0.99
0.100	**0.330**	**0.070**	**0.295**	**3.67**	**0.99**
0.200	0.330	0.070	0.295	5.22	0.99
0.300	0.331	0.072	0.295	6.99	0.99
0.400	0.331	0.072	0.295	8.31	0.99
0.500	0.332	0.074	0.295	9.55	0.99
5.000	0.335	-	-	-	-

Experimental Design, Materials, and Methods

Electrochemical studies through cyclic voltammetry (CV) experiments were performed in an M Bruan Lab Master SP glove box under a high purity argon atmosphere (H_2O and O_2 < 10 ppm), utilising a Princeton Applied Research PARSTAT 2273 potentiostat running Powersuite software (Version 2.58). The cyclic voltammetry experimental setup consists of a cell with three electrodes, namely (i) a glassy carbon electrode as working electrode, (ii) a platinum wire auxiliary and (ii) a platinum wire as pseudo reference electrode. The glassy carbon working electrode was polished and prepared before every experiment on a Buhler polishing mat first with 1-micron and then with ¼-micron diamond paste, rinsed with H_2O, acetone and DCM, and dried before each experiment. The electrochemical analysis is performed in dichloromethane (DCM, anhydrous, ≥ 99.8%, contains 40-150 ppm amylene as a stabilizer) and in acetonitrile (ACN, anhydrous, 99.8%) as solvents, at RT. Solutions were made in 0.001 dm^3 spectrochemical grade anhydrous DCM or ACN containing ca. 0.0005 M of analyte, 0.0005 mol dm^{-3} of internal reference (decamethylferrocene, DmFc) and 0.1 mol dm^{-3} of supporting electrolyte tetrabutylammonium tetrakispentafluorophenylborate, $[N(^nBu)_4][B(C_6F_5)_4]$ in DCM, or tetrabutylammonium hexafluorophosphate, $TBAPF_6$, $[N(^nBu)_4][PF_6]$ in ACN. Experimental potential data was measured *vs.* the redox couple of decamethylferrocene DmFc as internal standard and reported vs. the redox couple of ferrocene, Fc, as suggested by IUPAC [8]. Experimental potential data was collected vs. the Pt wire reference electrode but is reported vs the redox couple of ferrocene, Fc, at 0 V. E°`(DmFc) = - 0.610 V vs. Fc/Fc^+ at 0 V in DCM/$[N(nBu)_4][B(C_6F_5)_4]$ and -0.520 vs. Fc/Fc^+ at 0 V in ACN/$[N(nBu)_4][PF_6]$. Scan rates were between 0.05 and 5.00 Vs^{-1}.

Acknowledgements

This work has received support from the South African National Research Foundation (Grant numbers 113327 and 96111) and the Central Research Fund of the University of the Free State, Bloemfontein, South Africa.

Conflict of interest statement

The authors declare that they have no known competing financial interests or personal relationships which have, or could be perceived to have, influenced the work reported in this article.

References

[1] P.J. Swarts, J. Conradie, Solvent and Substituent effect on Electrochemistry of ferrocenyl carboxylic acid dyads, Electroanal. Chem. (2019).

[2] J. Conradie, G.J. Lamprecht, A. Roodt, J.C. Swarts, Kinetic study of the oxidative addition reaction between methyl iodide and [Rh(FcCOCHCOCF3)(CO)(PPh3)]: Structure of [Rh(FcCOCHCOCF3)(CO)(PPh3)(CH3)(I)], Polyhedron. 26 (2007) 5075–5087. doi:10.1016/j.poly.2007.07.004.

[3] Q. Shen, S. Shekhar, J.P. Stambuli, J.F. Hartwig, Highly reactive, general, and long-lived catalysts for coupling heteroaryl and aryl chlorides with primary nitrogen nucleophiles, Angew. Chemie - Int. Ed. 44 (2005) 1371–1375. doi:10.1002/anie.200462629.

[4] P.T.N. Nonjola, U. Siegert, J.C. Swarts, Synthesis, Electrochemistry and Cytotoxicity of Ferrocene-Containing Amides, Amines and Amino-Hydrochlorides, J. Inorg. Organomet. Polym. Mater. 25 (2015) 376–385. doi:10.1007/s10904-015-0195-4.

[5] F. Spänig, C. Kovacs, F. Hauke, K. Ohkubo, S. Fukuzumi, D.M. Guldi, A. Hirsch, Tuning charge transfer energetics in reaction center mimics via T h-functionalization of fullerenes, J. Am. Chem. Soc. 131 (2009) 8180–8195. doi:10.1021/ja900675t.

[6] S.C. by Perry Reeves, C.J. by J Mrowca, M.M. Borecki, W.A. Sheppard, Carboxylation of Aromatic Compounds: Ferrocenecarboxylic acid, Org. Synth. Coll. 6 (1988). doi:10.15227/orgsyn.056.0028.

[7] P.J. Swarts, M. Immelman, G.J. Lamprecht, S.E. Greyling, J.C. Swarts, Ferrocene derivatives as high burning rate catalysts in composite propellants, South African J. Chem. 50 (1997) 208–216.

[8] G. Gritzner, J. Kuta, Recommendations on reporting electrode potentials in nonaqueous solvents (Recommendations 1983), Pure Appl. Chem. 56 (1984) 461–466. doi:10.1351/pac198456040461.

Supporting Information

Additional supporting information for publication: **Solvent and Substituent Effect on Electrochemistry of Ferrocenylcarboxylic Acid Dyads**

Solvent effect on Electrochemistry and Computational Chemistry on ferrocenylcarboxylic acid dyads

*Pieter J. Swarts and Jeanet Conradie**

Department of Chemistry, University of the Free State, P.O. Box 339, Bloemfontein, 9300, South Africa

Supporting Information

Contents

1 Synthesis

The synthetic methods reported below were modified to improve yields and simplify reaction setup.

Below is the reaction schemes for ferrocenylcarboxylic acid derivatives, **1** – **6**, Scheme 1.

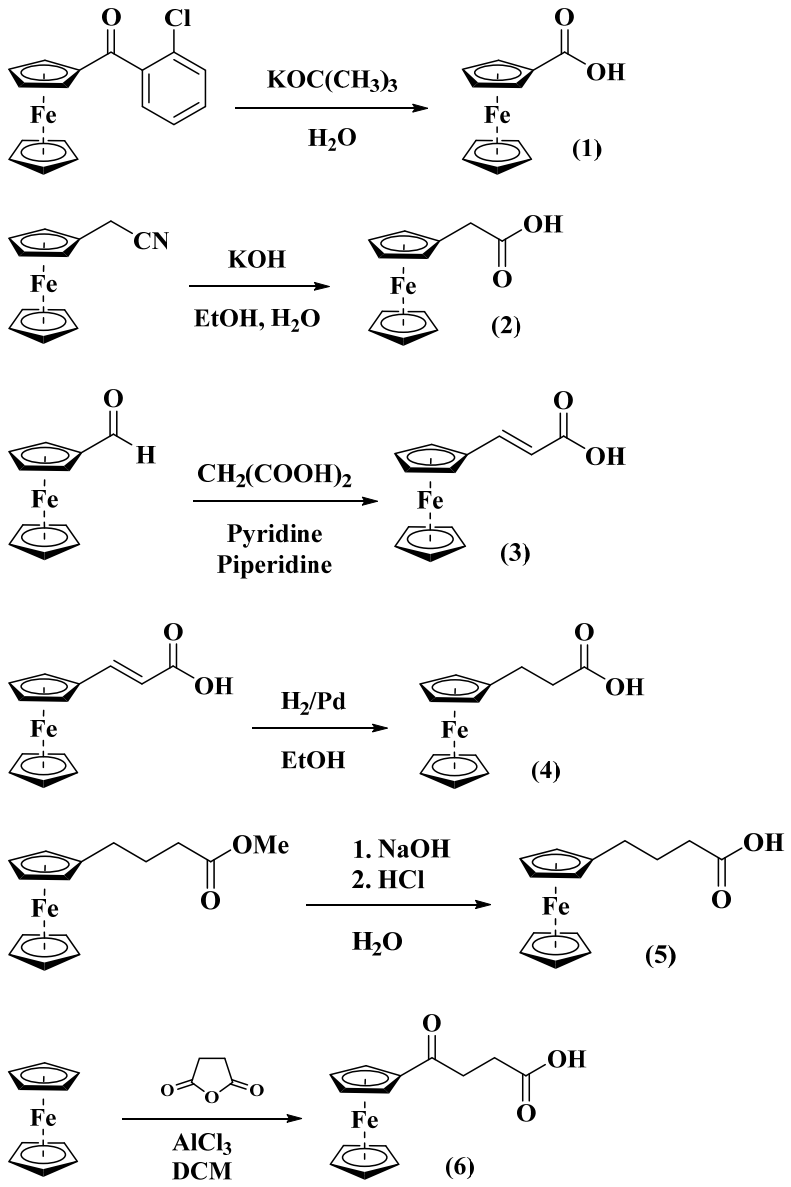

Scheme 1. Reaction scheme of $FcCO_2H$ **(1)**, $FcCH_2CO_2H$ **(2)**, $Fc(CH)_2CO_2H$ **(3)**, $Fc(CH_2)_2CO_2H$ **(4)**, $Fc(CH_2)_3CO_2H$ **(5)** and $FcCO(CH_2)_2CO_2H$ **(6)**.

Synthesis of ferrocene derivatives

Preparation of 2-chlorobenzoyl ferrocene [1]**:** Ferrocene (2 g, 8.62 mmol) and 2-chlorobenzoyl chloride (1.5 g, 9 mmol) were added to dichloromethane (40 cm^3) while stirring under an argon atmosphere. After the solution was chilled in an ice bath thoroughly, solid anhydrous aluminium chloride (1.72 g, 12.9 mmol) was added in small portions at a rate so that the reaction mixture temperature did not exceed 5 °C. Stirring continued for 60 minutes in an ice bath. After stirring for 16 hours at room temperature, the reaction mixture was cooled in ice. Ice water (80 cm^3) was added cautiously and the resulting mixture stirred vigorously for 30 minutes before the aqueous layer was extracted with dichloromethane (3 x 200 cm^3). The organic extracts were combined and washed with an equal volume of water, then with 10 % aqueous NaOH (140 cm^3), dried over $MgSO_4$ and the solvent removed under reduced pressure to yield 2.03 g (64%) as dark yellow crystals.

Preparation of ferrocenyl acetonitrile [2]**:** A solution of *N*,*N*,*N*-Trimethylaminomethyl ferrocene iodide (500 mg, 1.162 mmol) and potassium cyanide 965 mg, 10 mmol) in water (10 cm^3) was refluxed for 3 hours. The solution was cooled to room temperature and the light-yellow precipitate extracted with ether (3 x 20 cm^3). The ether extracts were combined, washed with water, dried over $MgSO_4$ and the solvent removed under reduced pressure on a rotary evaporator to yield 220 mg (70 %) as a brown-yellow powder.

Preparation of ferrocenecarboxaldehyde [3]**:** To ice-cold argon-degassed *N*-methylformanilide (16.60 cm^3, 0.1344 mol, 50 eq.), phosphorus(V) oxychloride (10 cm^3, 0.1075 mol, 40 eq.) was added at a rate that ensured the solution was kept cold. The solution was then stirred for one hour after which ferrocene (500 mg, 2.687 mmol) in 10 cm^3 dry toluene was added. The reaction mixture was then heated to 115 °C to reflux for two hours and was cooled in an ice bath. Sodium acetate (6.61 g, 80.625 mmol, 30 eq.) in 50 cm^3 of water was added slowly and the reaction mixture stirred at room

temperature for 16 hours before the separated organic layer was washed with 1 M HCl, distilled water, a saturated solution of sodium carbonate and again with distilled water. Anhydrous $MgSO_4$ was used to dry the organic layer. After filtration, the filtrate was distilled off under reduced pressure. The crude product was purified by column chromatography, using hexane:diethyl ether (3:4) (R_f: 0.62) as eluent to give 412 mg (82%).

Preparation of *β*-ferrocenoylpropionic acid [4]**:** Zinc granules (10 g) were cut to pieces smaller than 5 mm^3. This was washed with HCl (2 M) for 5 minutes followed by running water for 5 minutes. The washed zinc granules were then added to $HgCl_2$ (0.8 g) dissolved in a mixture of concentrated HCl (0.5 cm^3) and water (11 cm^3). The mixture was shaken for 10 minutes before the liquid was decanted. The amalgam was then washed with water, methanol, HCl (2 M) and again with water. Methyl 3-ferrocenoyl propanoate (240 mg, 0.7 mmol) was added to a mixture containing concentrated hydrochloric acid (1.875 cm^3), water (12.5 cm^3), methanol (7.5 cm^3) and zinc amalgam (2.5g) under nitrogen for 5 days. During this time the reaction was topped up with conc. HCl (0.75 cm^3) and methanol to the original level every 12 hours. The product was extracted by dichloromethane (3 x 50 cm^3) and the dichloromethane layer washed with water. The dichloromethane layer was dried over $MgSO_4$ and the solvent removed under reduced pressure to yield 171 mg (74 %) as a yellow oil.

Synthesis of ferrocene derivatives

Preparation of $FcCO_2H$ (1), [5]**:** 2-Chlorobenzoyl ferrocene (1.75 g, 0.005 mol) was added to a mixture of potassium tertiary butoxide (13 g, 0.115 mol) and water (0.61 cm^3, 0.034 mol) in dimethoxyethane (0.1 dm^3) under an argon atmosphere. This produced a yellow slurry which was refluxed for 24 hours. After cooling the mixture, ice water (0.3 dm^3) was added and the resulting solution was washed with ether (3 x 0.1 dm^3). The aqueous phases were combined and acidified with concentrated hydrochloric acid. The residue was collected by filtration, washed thoroughly with

water and air dried, yielding 1.01 g (80 %) of as light-yellow crystals. m.p.: 156 – 162 °C. ^{1}H NMR: δ_H (600.28 MHz, $CDCl_3$, 25 °C): δ 4.72 (5 H, s, Unsubstituted-Cp), 4.63 (2 H, pt, 2 x CH_2: Substituted-Cp), 4.59 (2 H, pt, 2 x CH_2: Substituted-Cp). ^{13}C NMR: δ_C (150.95 MHz, $CDCl_3$, 25 °C): δ 174.36 (1C, C=O), 72.64 (5C, Unsubstituted-Cp), 69.32 (2C, Substituted-Cp), 67.97 (2C, Substituted-Cp).

Preparation of $FcCH_2CO_2H$ (2), [5]**:** To a solution of potassium hydroxide (1 g, 0.018 mol) in water (10 cm^3), a suspension of the ferrocene acetonitrile (0.2 g, 0.74 mmol) in ethanol (5 cm^3) was added and refluxed for 5 hours until the evolution of ammonia had ceased. Most (> 95 %) of the ethanol was removed under reduced pressure. The residual suspension was dissolved in water (50 cm^3), extracted with ether (2 x 50 cm^3) and filtered. The solution was acidified with 2 M HCl and the precipitate filtered, washed and air dried to yield 110 mg (51 %) as a white powder. m.p.: 159 – 165 °C. ^{1}H NMR: δ_H (600.28 MHz, $CDCl_3$, 25 °C): δ 4.11 (5 H, s, Unsubstituted-Cp), 4.09 (2 H, pt, 2 x CH_2: Substituted-Cp), 4.06 (2 H, pt, 2 x CH_2: Substituted-Cp), 1.69 (2H, s, CH_2). ^{13}C NMR: δ_C (150.95 MHz, $CDCl_3$, 25 °C): δ 179.46 (1C, C=O), 69.84 (5C, Unsubstituted-Cp), 67.48 (2C, Substituted-Cp), 66.32 (2C, Substituted-Cp), 24.14 (1C, CH_2).

Preparation of $Fc(CH)_2CO_2H$ (3), [6]**:** Ferrocenecarboxaldehyde (1.5 g, 0.006 mol), malonic acid (1.785 g, 0.017 mol) and piperidine (0.56 cm^3) were dissolved in pyridine and heated in an oil bath at 110 °C for 2 hours under an argon atmosphere. The cooled solution was diluted with water and extracted with chloroform. The chloroform extracts were washed with 1 M HCl (2 x 100 cm^3) and water (2 x 100 cm^3) before the acrylic acid was extracted with ice cooled 2 M NaOH (200 cm^3). While effectively cooling the solution with ice the water phase was acidified with 1 M HCl and the precipitate filtered, washed with water and air dried to yield 1.58 g (90 %) as a yellow powder. m.p.: 132 – 138 °C. ^{1}H NMR: δ_H (600.28 MHz, $CDCl_3$, 25 °C): δ 7.69 (1H, s, CH=CH), 6.03 (1H, s, CH=CH), 4.51 (2 H, pt, 2 x CH_2: Substituted-Cp), 4.43 (2 H, pt, 2 x CH_2: Substituted-Cp), 4.16 (5 H, s, Unsubstituted-Cp). ^{13}C NMR: δ_C (150.95 MHz, $CDCl_3$, 25 °C): δ 168.37 (1C, C=O), 124.14 (1C,

CH), 118.25 (1C, CH), 72.21 (5C, Unsubstituted-Cp), 69.14 (2C, Substituted-Cp), 67.24 (2C, Substituted-Cp).

Preparation of $Fc(CH_2)_2CO_2H$ (4), [5]**:** 3-Ferrocenylacrylic acid (250 mg, 0.82 mmol) and H_2/Pd (30 mg) was suspended in absolute ethanol (50 cm^3). The suspension was stirred under a 10-bar hydrogen atmosphere for 20 hours before the reaction mixture was filtered through 2 cm of silica gel. Equal volumes of water and ice were added to the yellow ethanolic mixture. The solution was extracted with diethyl ether (2 x 250 cm^3) the combined ether extracts were thoroughly washed with water to remove the excess ethanol. The solution was dried over $MgSO_4$ and evaporated under reduced pressure to yield 0.177 g (71%) an off-white powder.

m.p.: 124 – 138 °C. ^{1}H NMR: δ_H (600.28 MHz, $CDCl_3$, 25 °C): δ 4.12 (5 H, s, Unsubstituted-Cp) , 4.09 (2 H, pt, 2 x CH_2: Substituted-Cp), 4.07 (2 H, pt, 2 x CH_2: Substituted-Cp), 2.66 (2H, s, CH_2-CH_2), 2.59 (2H, s, CH_2-CH_2). ^{13}C NMR: δ_C (150.95 MHz, $CDCl_3$, 25 °C): δ 179.24 (1C, C=O), 68.76 (5C, Unsubstituted-Cp), 68.11 (2C, Substituted-Cp), 67.69 (2C, Substituted-Cp), 35.40 (1C, CH_2-CH_2), 34.63 (1C, CH_2-CH_2).

Preparation of $Fc(CH_2)_3CO_2H$ (5), [5]**:** The ester (150 mg, 0.45 mmol) was dissolved in ethanol (25 cm^3) followed by the addition of sodium hydroxide solution (25 cm^3, 2 M). The solution was stirred for 1 hour at room temperature followed by the addition of ice (25 m^3) and washed with cold diethyl ether (3 x 50 cm^3). While cooling the solution by adding fresh ice chunks, the water phase was acidified with 1 M HCl and the precipitate filtered, washed and air dried to liberate 132 mg (93 %) as an off-white powder. m.p.: 120 – 124 °C. ^{1}H NMR: δ_H (600.28 MHz, $CDCl_3$, 25 °C): δ 4.17 (5 H, s, Unsubstituted-Cp) , 4.12 (2 H, pt, 2 x CH_2: Substituted-Cp), 4.09 (2 H, pt, 2 x CH_2: Substituted-Cp), 2.66 (2H, d, CH_2-CH_2-CH_2), 2.59 (2H, dd, CH_2-CH_2-CH_2), 2.46 (2H, d, CH_2-CH_2-CH_2). ^{13}C NMR: δ_C (150.95 MHz, $CDCl_3$, 25 °C): δ 179.24 (1C, C=O), 68.76 (5C, Unsubstituted-Cp), 68.11

(2C, Substituted-Cp), 67.69 (2C, Substituted-Cp), 35.40 (1C, CH_2-CH_2-CH_2), 24.63 (1C, CH_2-CH_2-CH_2), 22.18 (1C, CH_2-CH_2-CH_2).

Preparation of $FcCO(CH_2)_2CO_2H$ (6), [7]**:** Succinic anhydride (250 mg, 2.15 mmol) dissolved in dichloromethane (25 cm^3) was added to a mixture of ferrocene (250 mg, 2.15 mmol) and aluminium chloride (0.76 g, 5.6 mmol) in dichloromethane (25 cm^3) under a nitrogen atmosphere. The reaction mixture was refluxed for 24 hours. After cooling, ice cold water (40 cm^3) was added and the aqueous layer extracted twice with dichloromethane. The combined dichloromethane extracts were thoroughly washed with water. The organic phase was then extracted twice with equal amounts of 2 M NaOH. While cooling the solution with ice the water phase was acidified with 1 M HCl and the precipitate filtered, washed with water and air dried to liberate 1.1 g (74 %) as orange crystals. m.p.: 134 – 148 °C. ^{1}H NMR: δ_H (600.28 MHz, $CDCl_3$, 25 °C): δ 4.63 (5 H, s, Unsubstituted-Cp) , 4.24 (2 H, pt, 2 x CH_2: Substituted-Cp), 4.17 (2 H, pt, 2 x CH_2: Substituted-Cp), 2.97 (2H, d, CH_2-CH_2), 2,82 (2H, d, CH_2-CH_2). ^{13}C NMR: δ_C (150.95 MHz, $CDCl_3$, 25 °C): δ 182.31, 179.24 (2C, C=O), 74.63 (5C, Unsubstituted-Cp), 71.84 (2C, Substituted-Cp), 69.17 (2C, Substituted-Cp), 39.62 (1C, CH_2-CH_2), 37.41 (1C, CH_2-CH_2).

2 Electrochemistry

2.1 $FcCO_2H$ – DCM as Solvent

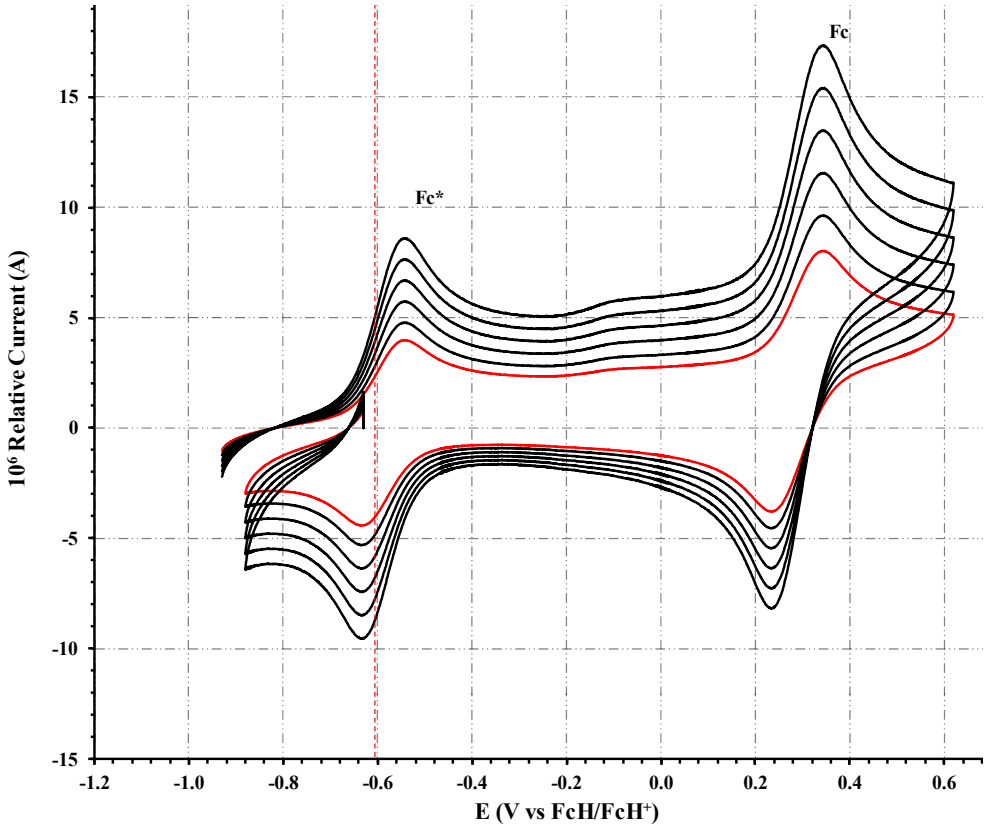

2.2 $FcCO_2H$ – CH_3CN as Solvent

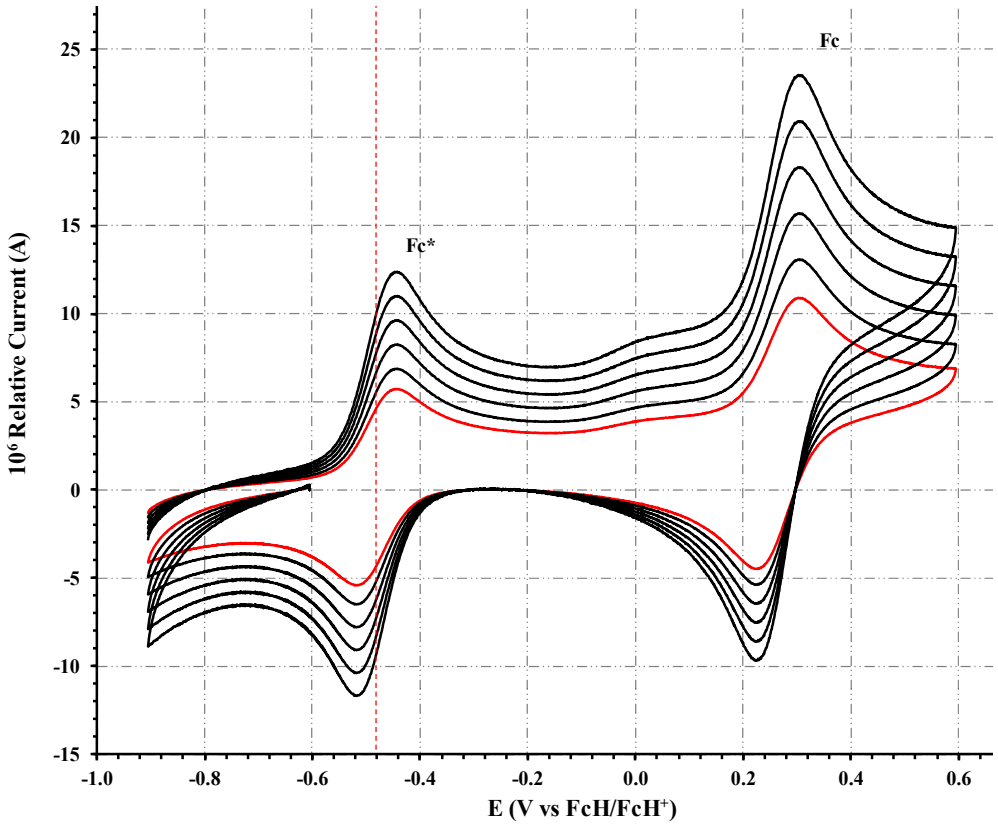

2.3 $FcCH_2CO_2H$ – DCM as Solvent

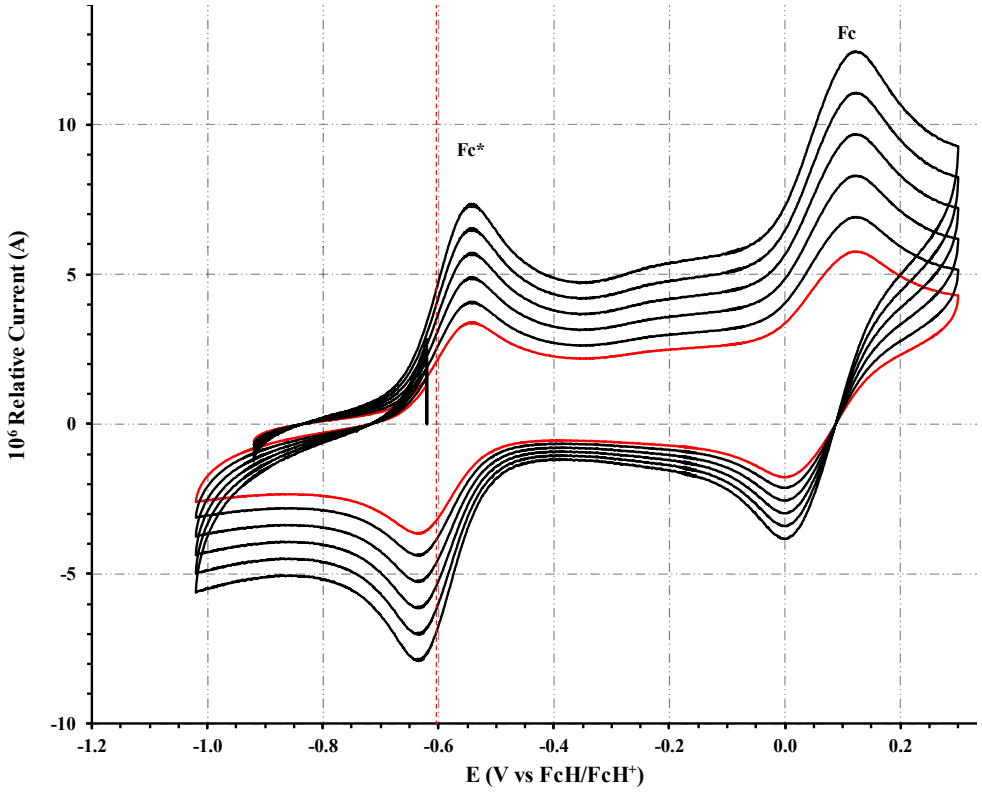

2.4 $FcCH_2CO_2H$ – CH_3CN as Solvent

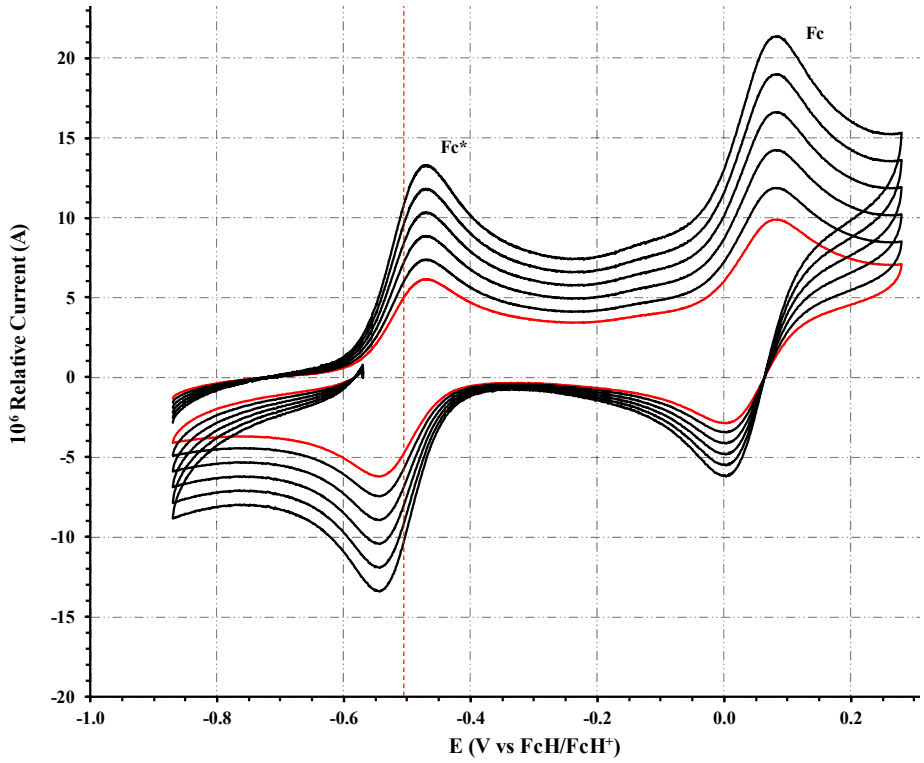

2.5 $Fc(CH)_2CO_2H$ – DCM as Solvent

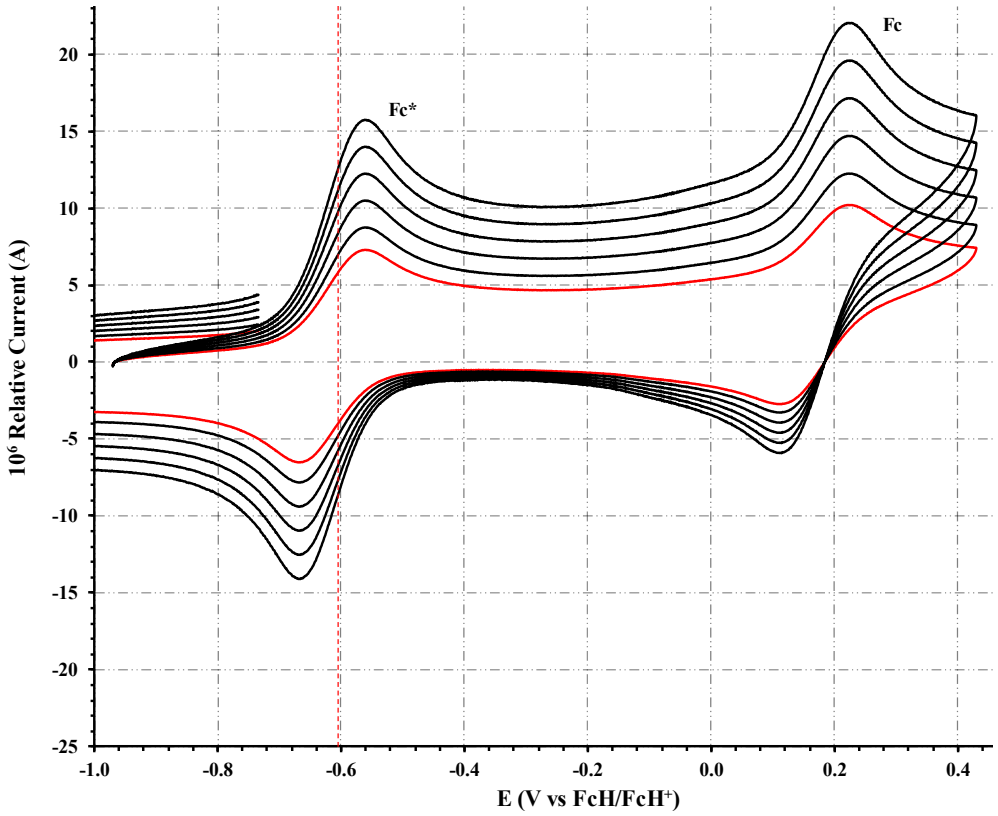

2.6 $Fc(CH)_2CO_2H$ – CH_3CN as Solvent

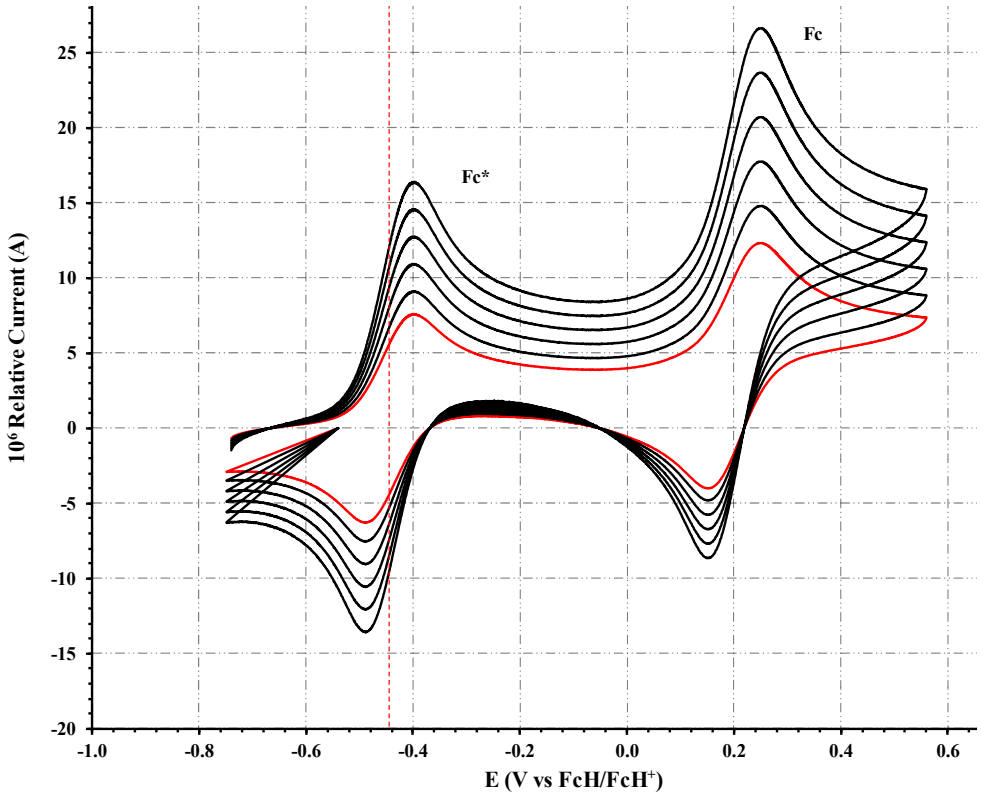

2.7 $Fc(CH_2)_2CO_2H$ – DCM as Solvent

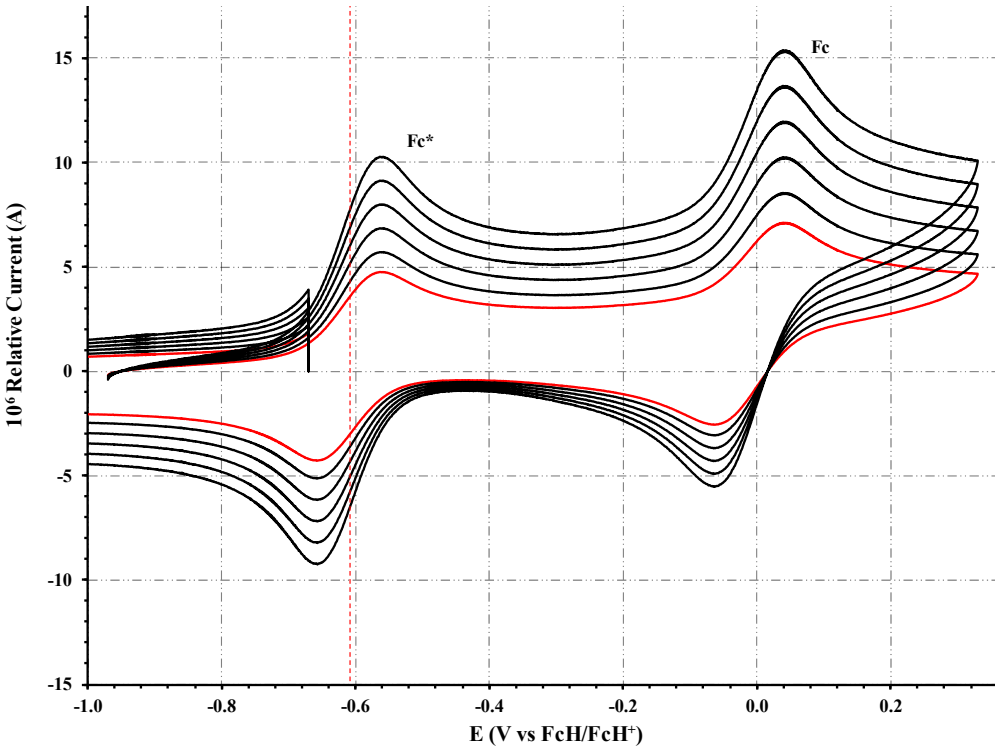

2.8 $Fc(CH_2)_2CO_2H$ – CH_3CN as Solvent

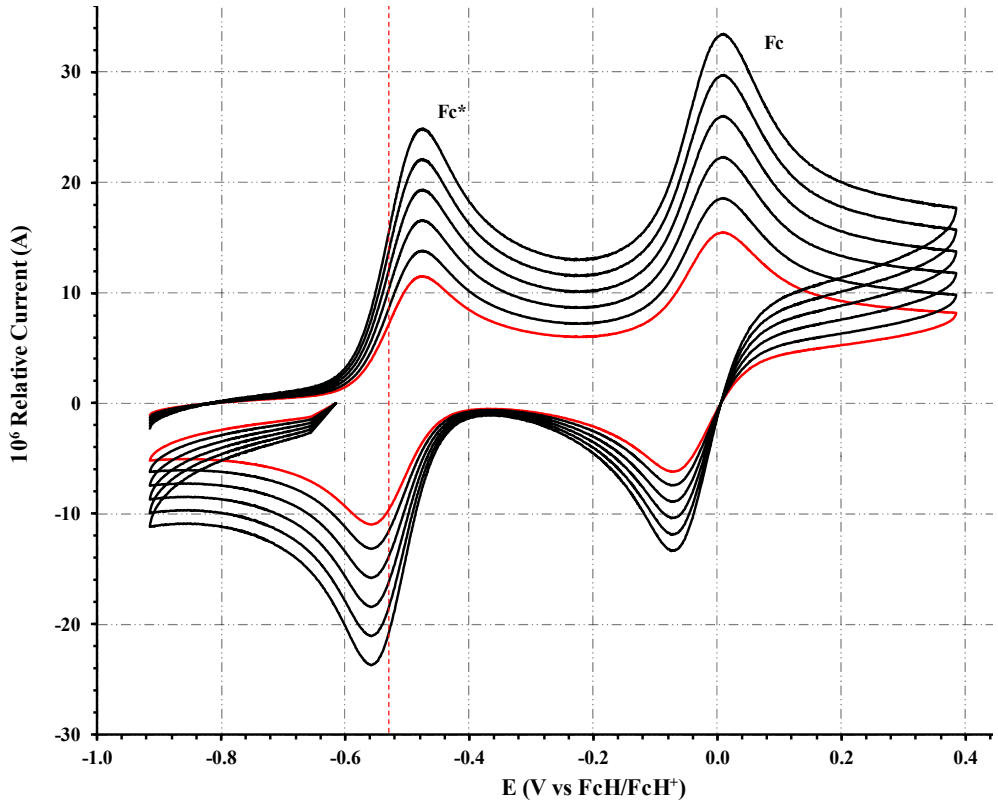

2.9 $Fc(CH_2)_3CO_2H$ – DCM as Solvent

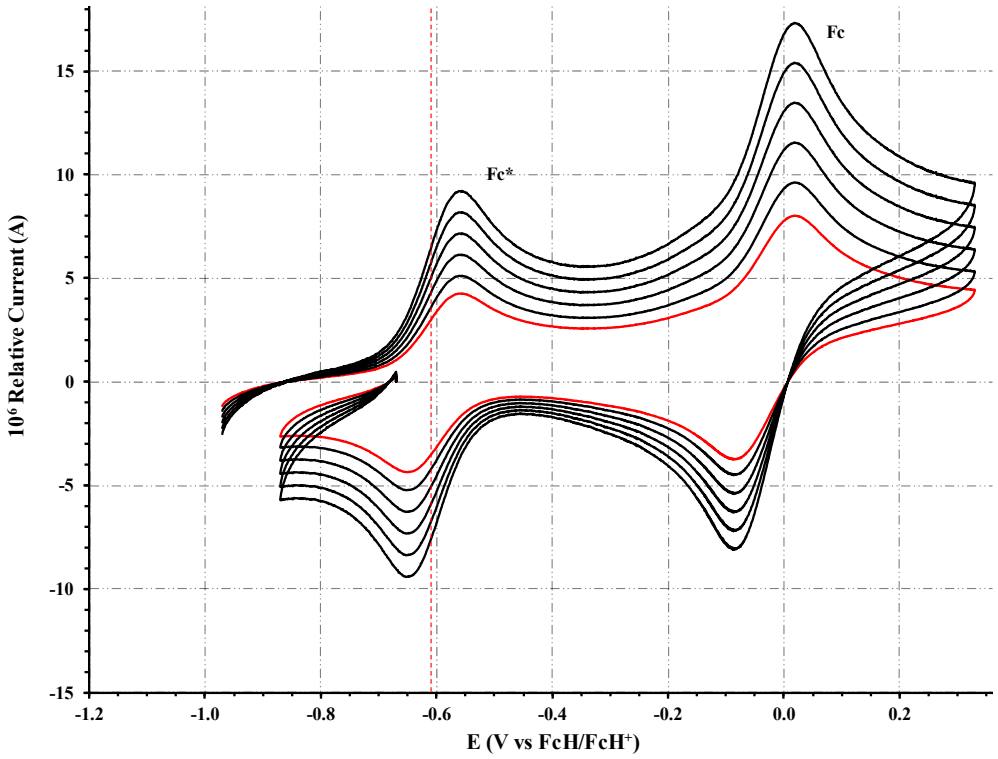

2.10 $Fc(CH_2)_3CO_2H$ – CH_3CN as Solvent

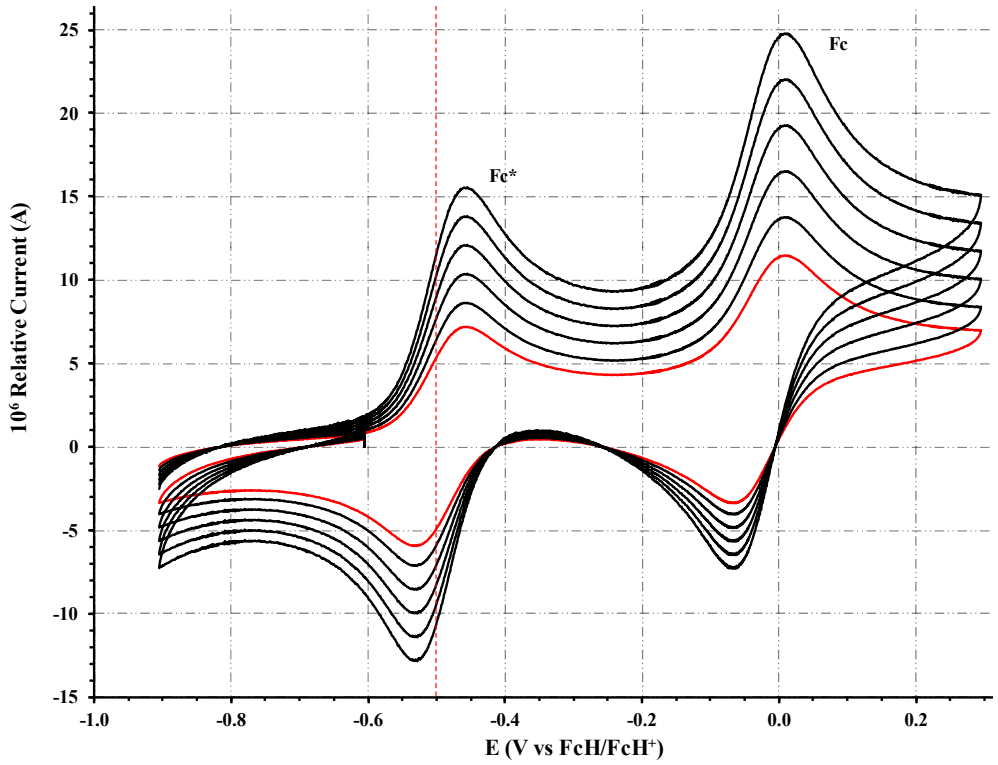

2.11 $FcCO(CH_2)_2CO_2H$ – DCM as Solvent

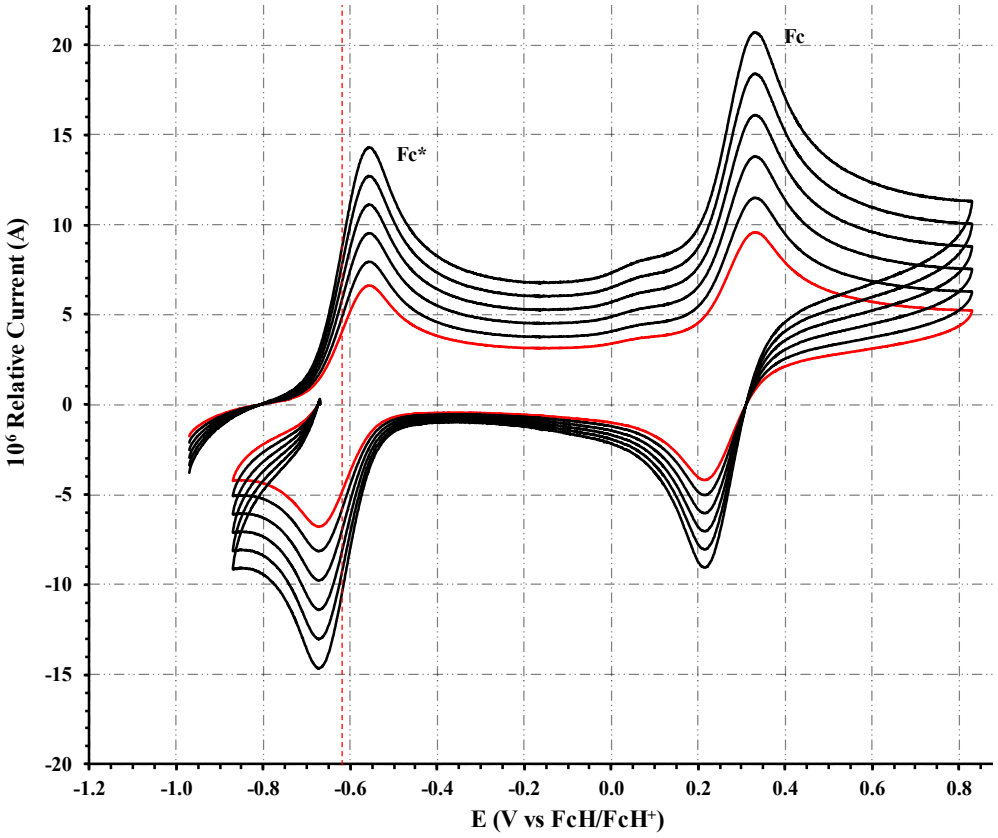

2.12 $FcCO(CH_2)_2CO_2H$ – CH_3CN as Solvent

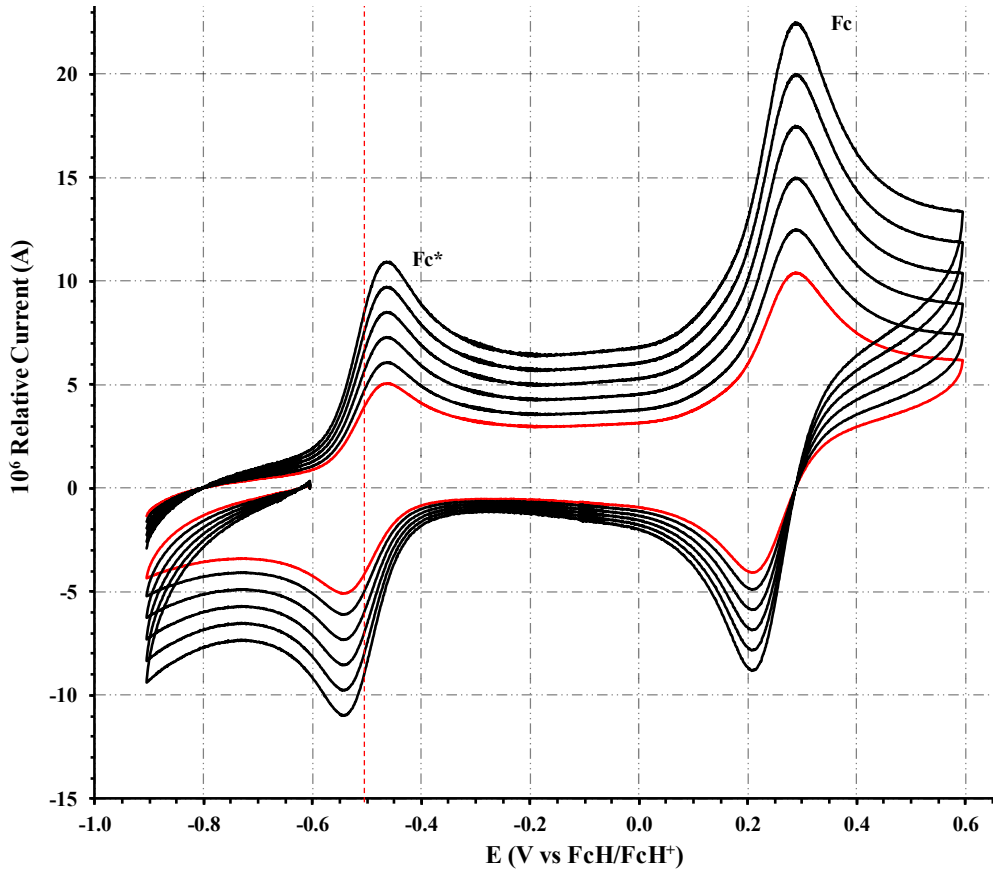

		DCM			ACN		
		i_p (μA)[a], peak current ratio [b]	E_p (V)[c]	$E^{o'}$ (V), ΔE_p (V)	i_p (μA)[a], peak current ratio [b]	E_p (V)[c]	$E^{o'}$ (V), ΔE_p (V)
$FcCO_2H$ - 1	Fc*	3.478, 0.995	-0.575	-0.610, 0.071	3.212, 0.992	-0.478	-0.520, 0.082
	Fc	3.595, 0.997	0.327	0.288, 0.078	3.861, 0.998	0.218	0.178, 0.087
$FcCH_2CO_2H$ - 2	Fc*	3.653, 0.996	-0.576	-0.610, 0.069	3.347, 0.995	-0.479	-0.520, 0.081
	Fc	3.788, 0.994	0.098	0.061, 0.075	3.572, 0.993	0.021	0.042, 0.088
$Fc(CH)_2CO_2H$ - 3	Fc*	3.247, 0.993	-0.574	-0.610, 0.073	3.815, 0.997	-0.478	-0.520, 0.083
	Fc	3.359, 0.992	0.224	0.184, 0.079	3.927, 0.995	0.111	0.066, 0.090
$Fc(CH_2)_2CO_2H$ - 4	Fc*	3.735, 0.993	-0.575	-0.610, 0.072	3.581, 0.992	-0.477	-0.520, 0.084
	Fc	3.872, 0.994	0.039	0.001, 0.078	3.743, 0.991	-0.153	-0.045, 0.091
$Fc(CH_2)_3CO_2H$ - 5	Fc*	3.885, 0.991	-0.576	-0.610, 0.070	3.637, 0.994	-0.478	-0.520, 0.082
	Fc	3.979, 0.992	0.013	-0.025, 0.076	3.834, 0.997	-0.002	-0.041, 0.089
$FcCO(CH_2)_2CO_2H$ - 6	Fc*	3.512, 0.994	-0.575	-0.610, 0.071	3.128, 0.991	-0.479	-0.520, 0.080
	Fc	3.658, 0.992	0.330	0.291, 0.078	3.518, 0.989	0.223	0.181, 0.086

3 Diffusion Coefficient

3.1 $FcCO_2H$

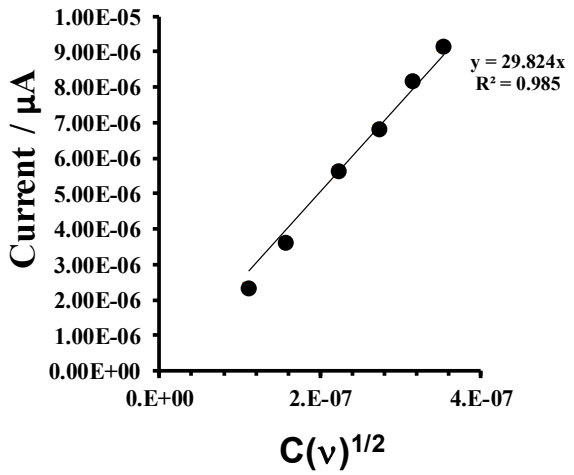

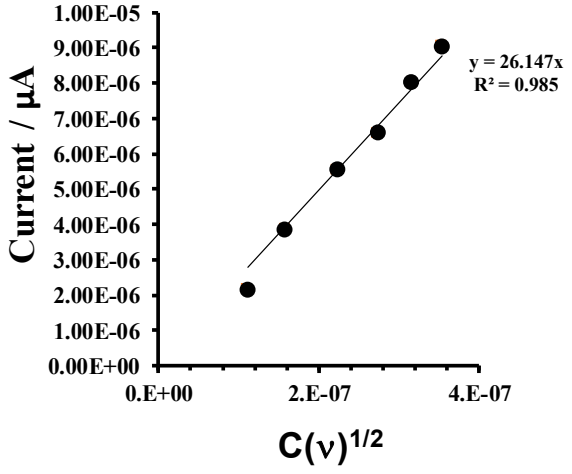

DCM - D slope with zero intercept: 1.25 $X10^{-5}$

DCM - D slope without zero intercept: 2.85 $X10^{-6}$

CH_3CN - D slope with zero intercept: 1.04 $X10^{-5}$

CH_3CN - D slope without zero intercept: 1.57 $X10^{-6}$

3.2 $FcCH_2CO_2H$

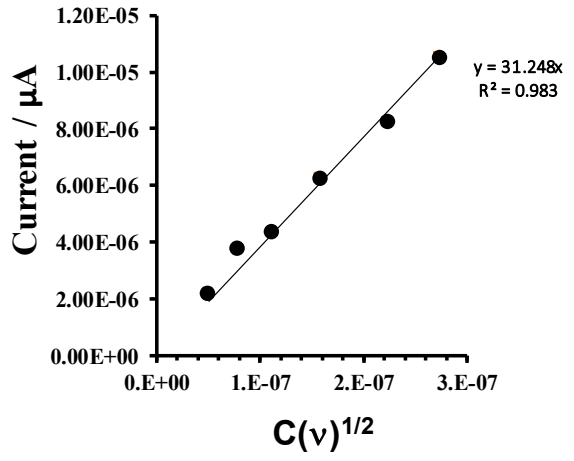

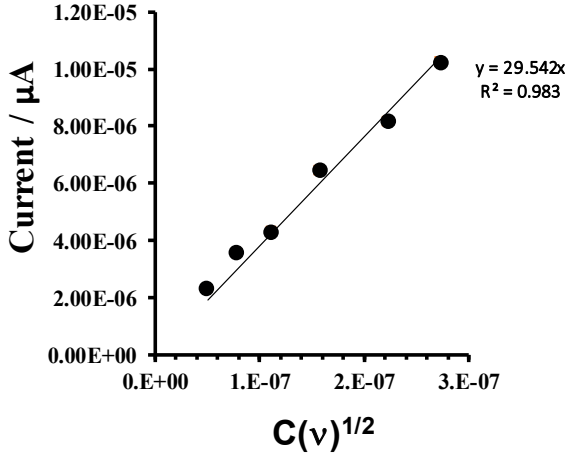

DCM - D slope with zero intercept: 1.37 $X10^{-5}$

DCM - D slope without zero intercept: 4.89 $X10^{-6}$

CH_3CN - D slope with zero intercept: 1.22 $X10^{-5}$

CH_3CN - D slope without zero intercept: 2.74 $X10^{-6}$

3.3 $Fc(CH)_2CO_2H$

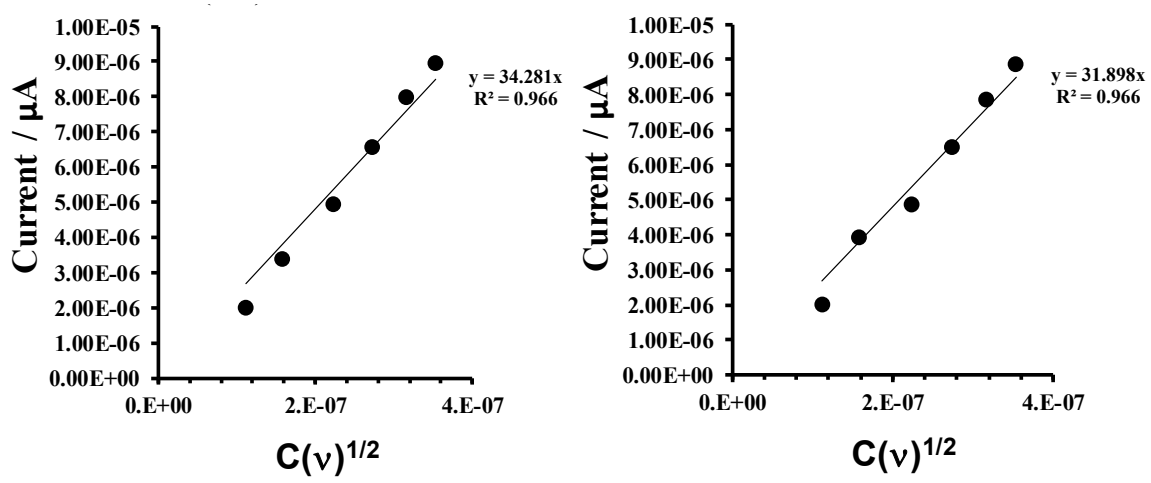

DCM - D slope with zero intercept: 1.65 $X10^{-5}$

DCM - D slope without zero intercept: 4.91 $X10^{-6}$

CH_3CN - D slope with zero intercept: 1.43 $X10^{-5}$

CH_3CN - D slope without zero intercept: 3.74 $X10^{-6}$

3.4 $Fc(CH_2)_2CO_2H$

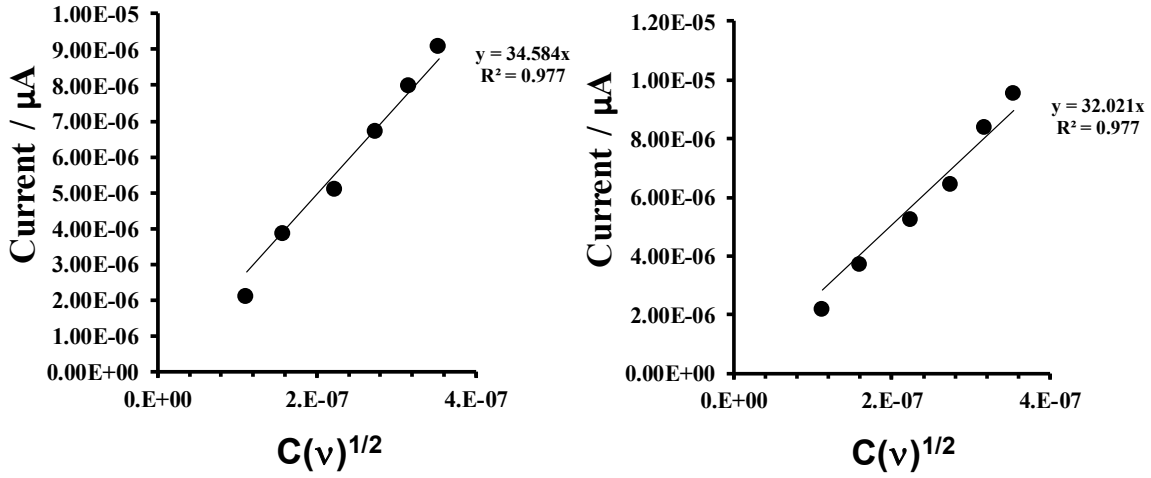

DCM - D slope with zero intercept: 1.68 $X10^{-5}$

DCM - D slope without zero intercept: 5.07 $X10^{-6}$

CH_3CN - D slope with zero intercept: 1.44 $X10^{-5}$

CH_3CN - D slope without zero intercept: 3.79 $X10^{-6}$

3.5 $Fc(CH_2)_3CO_2H$

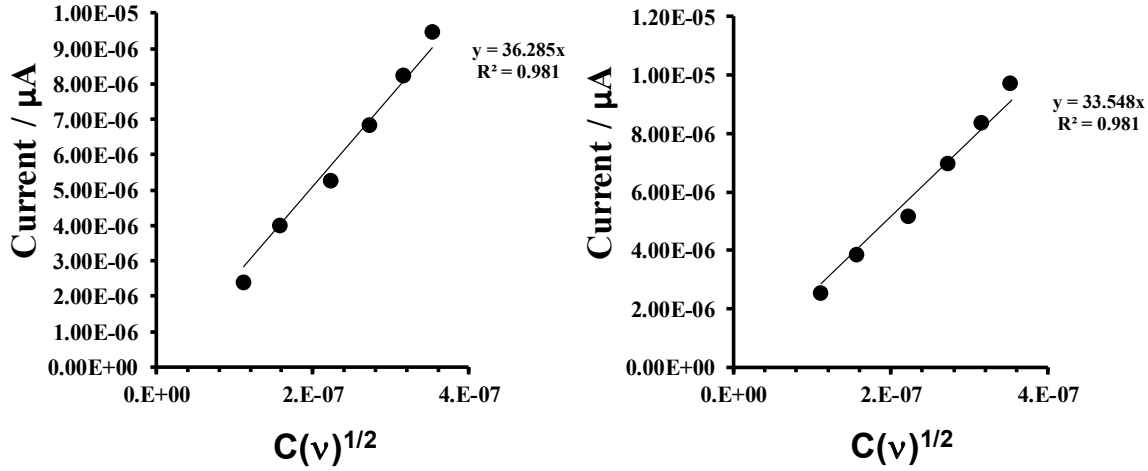

DCM - D slope with zero intercept: 1.85 $X10^{-5}$

DCM - D slope without zero intercept: 6.01 $X10^{-6}$

CH_3CN - D slope with zero intercept: 1.58 $X10^{-5}$

CH_3CN - D slope without zero intercept: 4.53 $X10^{-6}$

3.6 $FcCO(CH_2)_2CO_2H$

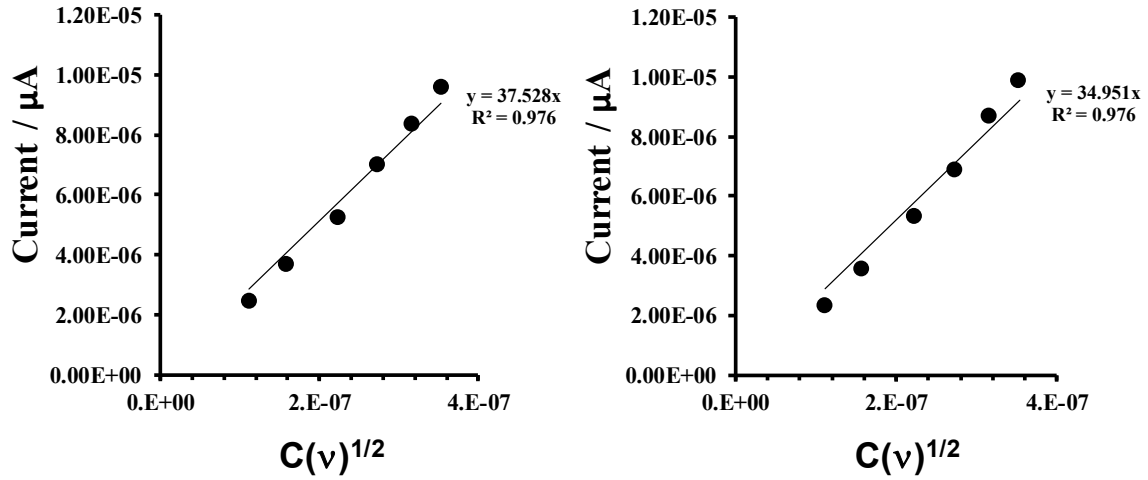

DCM - D slope with zero intercept: 1.97 $X10^{-5}$

DCM - D slope without zero intercept: 6.76 $X10^{-6}$

CH_3CN - D slope with zero intercept: 1.71 $X10^{-5}$

CH_3CN - D slope without zero intercept: 5.26 $X10^{-6}$

4 DFT HOMO

HOMO of optimized of $FcCO_2H$ **(1)**, $FcCH_2CO_2H$ **(2)**, $Fc(CH)_2CO_2H$ **(3)**, $Fc(CH_2)_2CO_2H$ **(4)**, $Fc(CH_2)_3CO_2H$ **(5)** and $FcCO(CH_2)_2CO_2H$ **(6)** with calculations performed on the neutral molecules using the B3LYP functional.

4.1 $FcCO_2H$ in DCM as solvent

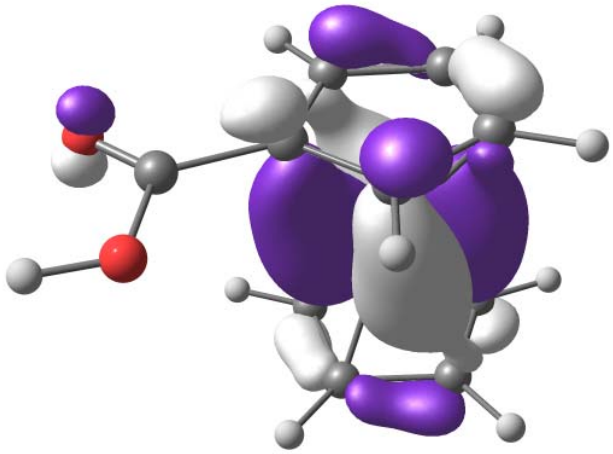

4.2 $FcCH_2CO_2H$ in DCM as solvent

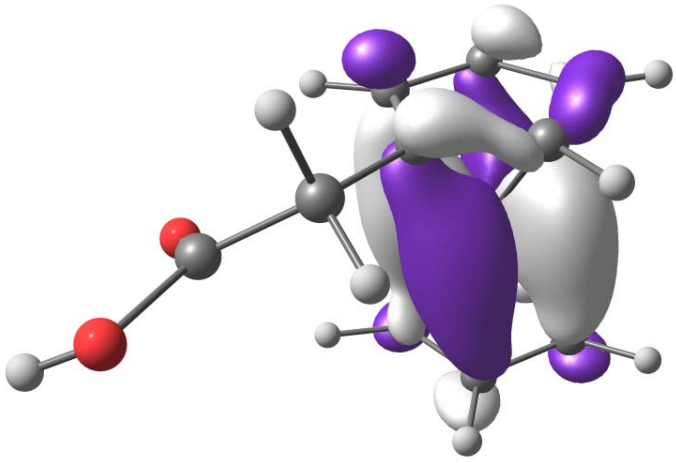

4.3 $Fc(CH)_2CO_2H$ in DCM as solvent

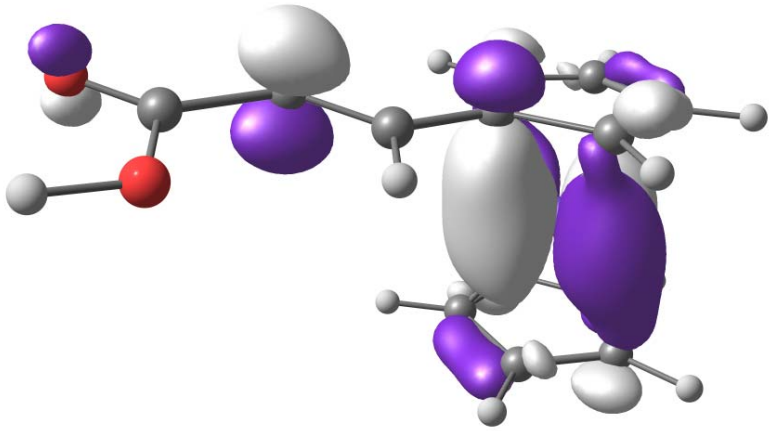

4.4 $Fc(CH_2)_2CO_2H$ in DCM as solvent

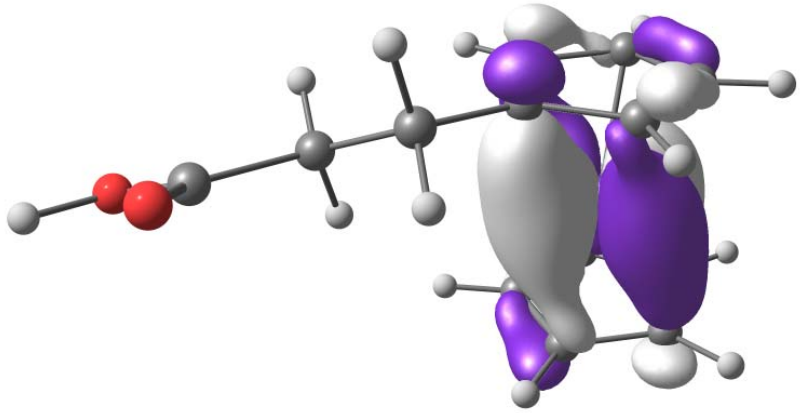

4.5 $Fc(CH_2)_3CO_2H$ in DCM as solvent

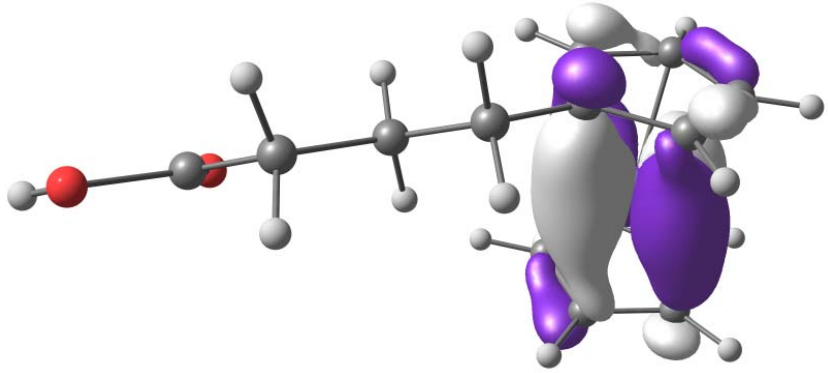

4.6 $FcCO(CH_2)_2CO_2H$ in DCM as solvent

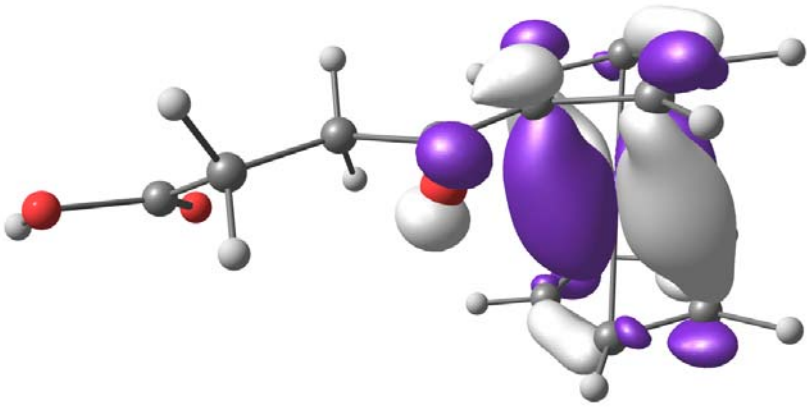

5 DFT data

Table S1. Experimental oxidation potentials in DCM and CH_3CN (*vs.* FcH/FcH^+) and DFT calculated HOMO energies of ferrocenecarboxylic acids (**1** – **6**) as well as related ferrocenyl compounds from literature (where alkyl chain lengths substituted on the ferrocene group increases) for both Gaussian and ADF.

			Gaussian			ADF			
	Oxidation *vs.* FcH/FcH^+ in DCM	**Oxidation *vs.* FcH/FcH^+ in CH_3CN**	**$E_{(HOMO)}$ eV in Gas phase**	**$E_{(HOMO)}$ eV in DCM solution**	**$E_{(HOMO)}$ eV in CH_3CN solution**	**$E_{(HOMO)}$ eV in Gas phase**	**$E_{(HOMO)}$ eV in DCM solution**	**$E_{(HOMO)}$ eV in CH_3CN solution**	**Ref.**
Ferrocene	0.011	0.012	-5.40	-5.48	-4.07	-4.11	-4.17	-4.07	T.W
Decamethylferrocene	-0.575	-0.478	-4.88	-4.89	-3.46	-3.61	-3.64	-3.46	T.W
$FcCO_2H$ – **(1)**	0.327	0.218	-5.77	-5.76	-4.16	-4.51	-4.57	-4.16	T.W
$Fc(CH_2)_2CO_2H$ – **(2)**	0.098	0.021	-5.36	-5.51	-4.37	-4.24	-4.31	-4.37	T.W
$Fc(CH)_2CO_2H$ – **(3)**	0.224	0.111	-5.75	-5.70	-4.13	-4.58	-4.64	-4.13	T.W
$Fc(CH_2)_2CO_2H$ – **(4)**	0.039	-0.153	-5.46	-5.48	-4.07	-4.27	-4.38	-4.07	T.W
$Fc(CH_2)_3CO_2H$ – **(5)**	0.013	-0.002	-5.36	-5.42	-4.46	-4.16	-4.27	-4.46	T.W
$FcCO(CH_2)_2CO_2H$ - **(6)**	0.330	0.223	-5.76	-5.78	-5.61	-4.27	-4.33	-4.36	T.W
$FcCH_2OH$	-	0.016	-5.27	-	-5.44	-4.07	-	-4.09	[7]
$Fc(CH_2)_2OH$	-	-0.046	-5.40	-	-5.46	-4.87	-	-4.06	[7]
$Fc(CH_2)_3OH$	-	-0.052	-5.32	-	-5.43	-4.06	-	-4.01	[7]
$Fc(CH_2)_4OH$	-	-0.054	-5.35	-	-5.41	-4.09	-	-4.02	[7]
$Fc(CpMe_4)CpMe_4)$	-	-0.346	-4.95	-	-5.01	-3.61	-	-3.54	[21]
$Fc(Cp)(CpMe_5)$	-	-0.300	-5.13	-	-5.20	-3.83	-	-3.77	[21]
[4][3]Fcp	-	-0.163	-5.24	-	-5.10	-3.96	-	-3.93	[21]
[4][4][3]Fcp	-	-0.246	-5.05	-	-5.13	-3.76	-	-3.68	[21]
[4][4][4]Fcp	-	-0.262	-5.02	-	-5.24	-3.72	-	-3.65	[22]
[4][4]Fcp	-	-0.169	-5.17	-	-5.26	-3.91	-	-3.85	[22]

6 References

[1] S.C. by Perry Reeves, C.J. by J Mrowca, M.M. Borecki, W.A. Sheppard, Carboxylation of Aromatic Compounds: Ferrocenecarboxylic acid, Org. Synth. Coll. 6 (1988). doi:10.15227/orgsyn.056.0028.

[2] D. Lednicer, J.K. Lindsay, C.R. Hauser, Reaction of the Methiodide of N,N-Dimethylaminomethylferrocene with Potassium Cyanide to Form Ferroeylacetonitrile, J. Org. Chem. 23 (1958) 653–655. doi:10.1021/jo01099a001.

[3] P.J. Graham, R. V. Lindsey, G.W. Parshall, M.L. Peterson, G.M. Whitman, Some Acyl Ferrocenes and their Reactions, J. Am. Chem. Soc. 79 (1957) 3416–3420. doi:10.1021/ja01570a027.

[4] K.J.R. Jr., R.J.C. Jr., P.E. Sokol, Organic Chemistry of Ferrocene. II. The Preparation of Ferrocenyl Aliphatic, J. Am. Chem. Soc. 79 (2005) 3420–3424. doi:10.1021/ja01570a028.

[5] N.F. Blom, E.W. Neuse, H.G. Thomas, Electrochemical characterization of some ferrocenylcarboxylic acids, Transit. Met. Chem. 12 (1987) 301–306. doi:10.1007/BF01024018.

[6] G.D. Broadhead, J.M. Osgerby, P.L. Pauson, Broadhead, Osgerby, and Pauson : 127. Ferrocene Derivatives. Part V. * Perrocenealdehyde.., J. Chem. Soc. (1958) 650–656.

[7] W.L. Davis, R.F. Shago, E.H.G. Langner, J.C. Swarts, Synthesis and electrochemical properties of a series of ferrocene-containing alcohols, Polyhedron. 24 (2005) 1611–1616. doi:10.1016/j.poly.2005.04.022.

[8] J.C. Swarts, E.H.G. Langner, N. Krokeide-Hove, M.J. Cook, Synthesis and electrochemical characterisation of some long chain 1,4,8,11,15,18,22,25-octa-alkylated metal-free and zinc phthalocyanines possessing discotic liquid crystalline properties, J. Mater. Chem. 11 (2001) 434–443. doi:10.1039/b006123i.

[9] P. Sullivan, A. Duraud, L. Hancox, N. Beaumont, G. Mirri, J.H.R. Tucker, R.A. Hatton, M. Shipman, T.S. Jones, Halogenated boron subphthalocyanines as light harvesting electron acceptors in organic photovoltaics, Adv. Energy Mater. 1 (2011) 352–355. doi:10.1002/aenm.201100036.

[10] K. Kasuga, T. Idehara, M. Handa, Y. Ueda, T. Fujiwara, K. Isa, Structure and Properties of Alkoxo-SubPc, Bull. Chem. Soc. Jpn. 69 (1996) 2559–2563.

[11] R. Potz, M. Go, H. Hu, U. Cornelissen, A. Tutaû, È. Aza-bru, Synthese und strukturelle

Charakterisierung von Borsubphthalocyaninaten Synthesis and Structural Characterization of Boron Subphthalocyaninates, 626 (2000) 588–596. doi:10.1002/(SICI)1521-3749(200002)626:2<588::AID-ZAAC588>3.0.CO;2-B.

[12] D. González-rodríguez, T. Torres, D.M. Guldi, J. Rivera, M. Ángeles, Subphthalocyanines : New Tuneable Tectons for Intramolecular Electron and Energy Transfer Processes, J. Am. Chem. Soc. 126 (2004) 6301–6313.

[13] G.E. Morse, M.G. Helander, J.F. Maka, Z.H. Lu, T.P. Bender, Fluorinated phenoxy boron subphthalocyanines in organic light-emitting diodes, ACS Appl. Mater. Interfaces. 2 (2010) 1934–1944. doi:10.1021/am1002603.

Chapter 3

Electrochemical behaviour of chloro- and hydroxy-subphthalocyanines

Published at: Electrochimica Acta 329 (2020) 135165

DOI: https://doi.org/10.1016/j.electacta.2019.135165

Oxidation and reduction data of subphthalocyanines

Published at: Data in brief (DIB)

DOI: https://doi.org/10.1016/j.dib.2019.105039

Supporting information also included.

Author Contributions:

Pieter J. Swarts

1. Synthesis of compounds of compounds
2. Electrochemical studies and interpretation
3. Characterisation:
    a. ^{1}H NMR, ^{11}B NMR, ^{13}C NMR and ^{19}F NMR
    b. FTIR
    c. UV/vis
    d. DFT calculations
4. Writing of publication manuscript draft and revised publications under the supervision of Prof. Jeanet Conradie

Above mentioned work was done under the supervision of Prof. Jeanet Conradie.

Synopsis TOC

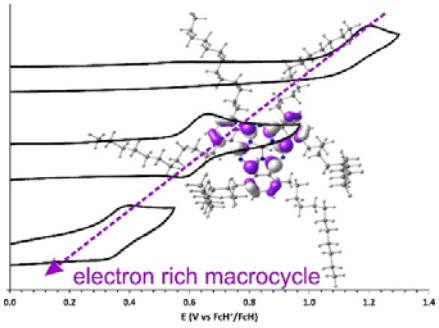

Electrochimica Acta 329 (2020) 135165

Contents lists available at ScienceDirect

Electrochimica Acta

journal homepage: www.elsevier.com/locate/electacta

Electrochemical behaviour of chloro- and hydroxy-subphthalocyanines

Pieter J. Swarts, Jeanet Conradie*

Department of Chemistry, University of the Free State, P.O. Box 339, Bloemfontein, 9300, South Africa

ARTICLE INFO

Article history:
Received 26 June 2019
Received in revised form
28 October 2019
Accepted 28 October 2019
Available online 5 November 2019

Keywords:
Subphthalocyanines
Redox potential
DFT
Non-peripheral
Electron-donating

ABSTRACT

A novel subphthalocyanine (HO)BSubPc($C_{12}H_{25}$)$_6$(H)$_6$, **3**, with a hydroxy group in the axial position and alkyl ligands ($C_{12}H_{25}$) on the non-peripheral positions as well as two other subphthalocyanines, ClBSubPc(H)$_{12}$, **2**, and ClBSubPc(F)$_{12}$, **1**, have been synthesized and characterized. The redox properties of subphthalocyanines **1**–**3** was investigated using cyclic voltammetry (CV), both in dichloromethane (at 25 °C) and dichloroethane (at 60 °C) as solvent and compared to previous studies. The electrochemical experimental conditions used made it possible for the first time to experimentally observe electrochemically quasi reversible oxidation for subphthalocyanines. It was found that the novel subphthalocyanine **3** exhibits the lowest macrocycle-based oxidation potential reported for SubPcs till date. The results obtained were further validated by DFT calculations on subphthalocyanines **1**–**3** as well as related subphthalocyanines from literature. Linear relationships between the redox potentials (oxidation and reduction vs Fc^+/Fc) of these subphthalocyanines and various solvent phase B3LYP calculated energies were obtained.

1. Introduction

Phthalocyanines (Pcs) are intensely coloured 18 π-electron aromatic macrocyclic compounds that have four isoindoline units linked by nitrogen atoms (Fig. 1). They play a variety of roles in various high technology areas such as semiconductor devices [1], liquid crystals [2], sensors [3], catalysts [4,5], non-linear optics [6], photovoltaic solar cells [7], antiviral research [8] and photodynamic therapy [9,10]. They are versatile chemicals by virtue of their stability, photophysical, photochemical, redox and coordination properties. Subphthalocyanines (SubPcs) are 14 π-electron aromatic macrocyclic compounds that only have three isoindoline units. These contracted porphyrinoid species are conically shaped around a boron atom with a halogen or alkoxy axial group. While the planar phthalocyanines are generally difficult to handle due to their strong ability to aggregate, the conically shaped subphthalocyanines are less prone to aggregation. The first known SubPc, the purple ClBSubPc(H)$_{12}$, compound 2 in Fig. 1, was accidentally discovered in 1972 by Meller and Ossko during the attempted synthesis of boronPc [11]. The physical and electronic properties of ClBSubPc(H)$_{12}$ can be modified by varying the chloro-axial ligand or by functionalizing the various positions R and R' (Fig. 1) [12]. Till date no SubPc without a boron or with another metal than boron have been synthesized [12]. SubPcs are used in multiple different fields. These include dyes [13,14], dye-sensitized solar cells [15], optical recording [13], light-emitting diodes [16] and photodynamic therapy [17]. This study was designed to explore by means of cyclic voltammetry, the difference in the electronic properties of SubPcs containing electron-donating substituents (SubPc **3** in Fig. 1) and SubPcs containing electron-withdrawing substituents (SubPc **1** in Fig. 1), in comparison to the standard SubPc **2**. Since it was found that substituents on the non-peripheral positions R′ of Pcs (Fig. 1) have a greater influence on the redox potential of Pcs than substituents on the peripheral positions R [18,19], the synthesis, characterization and redox properties of the first SubPc containing alkyl substituents on the non-peripheral positions R' (Complex 3 in Fig. 1) are presented here.

2. Experimental

2.1. General

Reagents and Materials. Solid reagents (Sigma-Aldrich, Strem and Merck) were used as received. Liquid reagents (Sigma-Aldrich

* Corresponding author.
E-mail address: conradj@ufs.ac.za (J. Conradie).

https://doi.org/10.1016/j.electacta.2019.135165
0013-4686/

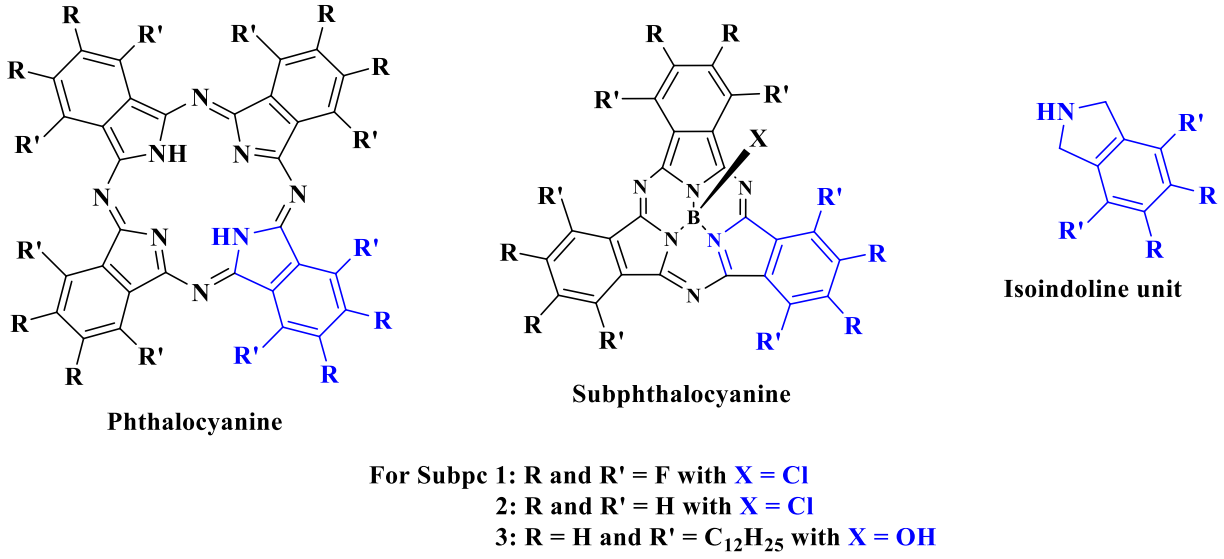

Fig. 1. Structure of phthalocyanines (Pcs, left) and subphthalocyanines (SubPcs, middle), containing four and three isoindoline units (right) respectively. Complexes of this study are ClBSubPc(F)$_{12}$, **1**, ClBSubPc(H)$_{12}$, **2** and (HO)BSubPc($C_{12}H_{25}$)$_6$(H)$_6$, **3**.

and Merck) were used without any further purification unless specified otherwise. Solvents were distilled and water was double distilled. Organic solvents used in this study were dried according to published methods [20]. Melting points are uncorrected and were determined with an Olympus BX 51 microscope equipped with a Linkam THMS 600 hot stage.

2.2. Synthesis of chloro- and hydroxy-boron-subphthalocyanines *1*–*3*

The ClBSubPc(F)$_{12}$ **1** [21] and ClBSubPc(H)$_{12}$ **2** [21] were synthesized using slight modifications to literature methods (see the supporting information for the reaction scheme, reaction procedures and characterization data). Compounds **1**–**3** were characterized by NMR, ATR-FTIR, UV/vis, elemental analysis and m.p.

Spectroscopy Measurements. ^{1}H, ^{11}B and ^{13}C NMR spectroscopic analysis were performed for all compounds in the study and ^{19}F for SubPc **1**. ^{1}H, ^{13}C and ^{19}F NMR spectra were recorded at 25 °C on a 600 MHz AVANCE II NMR spectrometer at 600.28 MHz, 150.95 MHz and 564.33 MHz respectively. ^{11}B NMR spectra were recorded at 25 °C on a 400 MHz AVANCE III NMR spectrometer at 128.38 MHz. Hydrogen and carbon chemical shifts are relative to hydrogen and carbon in $CDCl_3$ at 7.24 ppm and 77.16 ppm respectively. The following abbreviations are used to describe peak patterns: s = singlet, d = doublet, t = triplet, q = quartet and m = multiplet. Solid state Fourier transform infrared measurements were performed on a Thermo Scientific Nicolet iS50 Attenuated Total Reflectance Fourier transform infrared (ATR-FTIR) spectrometer using the iS50 ATR option running OMNIC software (Version 9.2). UV/vis spectra were recorded on a Varian Cary 5000 UV–Vis–NIR Spectrophotometer. The pathlength of the cuvette used for the UV/vis spectra was 1 cm, while the Beer-Lambert data was obtained with a cuvette of pathlength 1 cm for SubPc **1** and **2** and 1 mm for SubPc **3**.

Preparation of (HO)BSubPc($C_{12}H_{25}$)$_6$(H)$_6$, 3. BCl_3 (0.015 dm^3, 1 M solution in p-xylene, 1.5 eq.) was added to dry phthalonitrile (1 g, 0.0022 mol) under an argon atmosphere (H_2O: 0.3 ppm and O_2: 9.8 ppm) at room temperature. The reaction mixture was stirred under reflux (132 °C) for 30 min. The solvent was evaporated and the solid was extracted with toluene (0.4 dm^3). The solution was evaporated, and the resultant purple solid was thoroughly washed with methanol (0.2 dm^3) and hexane (0.2 dm^3). Pure (HO)BSubPc($C_{12}H_{25}$)$_6$(H)$_6$ was obtained as a purple solid, yield: 23% (0.23 g). m.p.: 42 °C, UV–vis: λ_{max} 590 nm, ε = 184 499 dm^3 mol^{-1} cm^{-1} in THF. ^{1}H NMR: δ_H (600.28 MHz, $CDCl_3$): δ 7.43 (6H, q, peripheral H_6), 2.82 (12H, m, 6 x CH_2), 1.63 (12H, m, 6 x CH_2), 1.23 (108H, m, 54 x CH_2) and 0.86 (18H, t, 6 x CH_3). ^{11}B NMR: δ_B (128.38 MHz, $CDCl_3$): δ −18.43 (1B). ^{13}C NMR: δ_C (150.95 MHz, $CDCl_3$, 25 °C): δ 148.17 (6C, C=N: inner core carbons), 136.64 (6C, C=C: isoindoline unit), 126.82 (6C, non-peripheral C_6), 108.34 (6C, peripheral C_6), 35.83 (6C, non-peripheral C_6), 32.77 (6C, non-peripheral C_6), 30.69 (36C, non-peripheral C_{36}), 23.41 (6C, non-peripheral C_6) and 14.27 (6C, non-peripheral C_6). IR: υ/cm^{-1}: 3673–2700 (H–O, stretch), 2900–2800 (C–H, alkyl chain) and 1479 (C=C, stretch). Elemental analysis calculated for $C_{96}H_{157}BN_6O$ (element, %): C, 81.08; H, 11.13; N, 5.91; O, 1.12, obtained: C, 81.14; H, 10.98; N, 5.94; O, 1.11.

2.3. Cyclic voltammetry

All the electrochemical experiments were performed in an M Bruan Lab Master SP glove box under a high purity argon atmosphere (H_2O and O_2 < 10 ppm). Cyclic voltammetry (CV) measurements were performed utilizing a Princeton Applied Research PARSTAT 2273 potentiostat running Powersuite software (Version 2.58). A three-electrode cell was used. A glassy carbon electrode with a surface area 3.14 × 10^{-6} m^2 was chosen as working electrode, platinum wires were chosen as auxiliary and pseudo reference electrodes. It was observed that electrode deposition occurs at negative potentials, therefore in this study the glassy carbon working electrode was polished and prepared before every scan experiment on a Buhler polishing mat first with 1-μm and then with ¼-micron diamond paste, rinsed with H_2O, acetone and DCM, and dried. Electrochemical analysis of the complexes was performed in both dichloromethane (DCM, anhydrous, ≥ 99.8%, contains 40–150 ppm amylene as stabilizer) at RT and dichloroethane (DCE, anhydrous, 99.8%) at 60 °C, as solvents. A double wall glass electrochemical cell was used with the outer part connected to a water bath, to control the temperature of the electrochemical experiment. The temperature of the solution was checked with a

thermostat. During the experimental setup a mark was made on the cell, indicating the appropriate volume level of solvent. During the experiment the level of solvent was carefully monitored to not drop below this mark. The setup was a closed system and as a result it was hardly ever required to top up with solvent. Electrochemical experiments were performed at a temperature well below the boiling point of the solvent (for example at 60 °C for DCE with a boiling point of is 83.47 °C), to minimize solvent evaporation. Data obtained from CV's in DCE as solvent at RT and at 60 °C were identical, but better resolution of the CV curves and better solubility of SubPc **3** were obtained at 60 °C. For DCM as solvent, solutions were made in 0.001 dm^3 spectrochemical grade anhydrous DCM containing ca. 0.0005 M (SubPcs **1** and **2**) or 0.004 mol dm^{-3} (SubPc **3**) of analyte, 0.0005 mol dm^{-3} of internal standard (decamethylferrocene, DmFc) and 0.1 mol dm^{-3} of supporting electrolyte tetrabutylammonium tetrakispentafluorophenylborate $[N(^nBu)_4][B(C_6F_5)_4]$. For DCE as solvent, solutions were made in 0.001 dm^3 spectrochemical grade anhydrous DCE containing ca. 0.0005 M (SubPcs **1** and **2**) or 0.002 mol dm^{-3} (SubPc **3**) of analyte, 0.0005 mol dm^{-3} of internal standard DmFc and 0.2 mol dm^{-3} of supporting electrolyte $[N(^nBu)_4][B(C_6F_5)_4]$. The supporting electrolyte $[N(^nBu)_4][B(C_6F_5)_4]$ was synthesized as described in literature [22] and dried in vacuo at P < 0.01 mm Hg for 3 days at 90 °C. Experimental potential data was collected vs the Pt wire pseudo reference electrode but is reported vs the redox couple of ferrocene, Fc^+/Fc at 0 V. To achieve this, data was manipulated on a spreadsheet to readjust the potential of the internal standard $DmFc^+/DmFc$ redox couple to −0.610 V in DCM (−0.597 V in DCE), since the $DmFc^+/DmFc$ redox couple is at −0.610 V in DCM (−0.597 V in DCE) vs Fc^+/Fc at 0 V. Scan rates were between 0.05 and 5.00 V s^{-1}. The formal reduction potential is determined by $E^{\circ\prime} = (E_{pa} - E_{pc})/2$ for an electrochemically reversible (and quasi reversible) process where E_{pa} (E_{pc}) = anodic (cathodic) peak potential and i_{pa} (i_{pc}) = anodic (cathodic) peak current. In this study E_{pa} of the first oxidation process of the SubPcs is also denoted by E_{ox}, while the E_{pc} of the first reduction process of the SubPcs is denoted by E_{red}. Electrochemical reversibility (or Nernstian behaviour) of redox processes is indicated by a peak current ratio (i_{pc}/i_{pa} for oxidation and i_{pa}/i_{pc} for reduction) of 1 [23,24] and peak current separation ΔE_p is 0.059 V for a one electron transfer process [22]. In this experiment, due to experimental cell imperfections and ohmic drop effects, ΔE_p slightly larger than 0.059 V was obtained, even for the known 1 e^- transfer processes of the Fc^+/Fc (0.078 V in DCM, 0.074 V in DCE) and $DmFc^+/DmFc$ (0.079 V in DCM, 0.078 V in DCE) couples and will be referred to as quasi reversible electrochemical behaviour [25–27].

2.4. DFT calculations

Density functional theory (DFT) calculations were performed on the neutral molecules using the B3LYP functional, as implemented in the Gaussian 16 package [28], using the triple-ζ basis set 6-311G(d,p). All calculations were performed in DCM and DCE as solvent, using the IEF-PCM model (polarizable continuum model (PCM) [29] which solved the non-homogeneous Poisson equation by applying the integral equation formalism variant) [30]. The energy of the highest occupied molecular orbital (E_{HOMO}) and the lowest unoccupied molecular orbital (E_{LUMO}) were obtained from the output files from the DFT calculations. Electronic chemical potential (μ, the partial derivative of the energy of the system with respect to the number of electrons at a constant external potential) and the global electrophilicity index (ω, a measure of the electrophilic power of atoms and molecules. i.e. a measure of the energy lowering of a species due to maximal electron flow between donor and acceptor) were calculated with the following formulas [31–35]:

Electron affinity EA(compound) = - E_{LUMO}

Ionization potential IP(compound) = - E_{HOMO}

$$\mu = -(IP + EA)/2$$

$$\omega = \mu^2/(2\,(IP + EA))$$

3. Results and discussion

3.1. Synthesis

The synthesis of subphthalocyanines has always been complex due to the difficult purification process. By slightly modifying the synthetic method that was proposed by Torres and his co-workers [21], it was possible to improve the reported yields of SubPc **1** and **2**. The success of the synthesis is drastically increased when working under strict Schlenk conditions. When the reactions were performed in a glovebox with H_2O < 0.5 ppm and O_2 < 10 ppm, it was possible to improve the yields of SubPc **1** from 74% [21] and of SubPc **2** from 82% [21] to > 90% for both **1** and **2**. It is known that ClBSubPcs readily hydrolyses to from (HO)BSubPcs [12,36]. SubPc **3** was initially intended to also have a chloride in the axial position, however, even though we worked under extreme dry conditions the B–Cl bond was too labile and as a result $ClBSubPc(C_{12}H_{25})_6(H)_6$ could not be isolated. This is due to the electron-donating ligands in the non-peripheral positions enhancing the reactivity of the chloride. As a result, the chloride was substituted by a hydroxy group that was present in the system. The axial (OH) ligand of **3** was confirmed by elemental analysis as well as the O–H stretching vibration shown in FTIR (see supporting information). The yields of SubPc **3** was also much lower in comparison to SubPcs **1** and **2**; this could be due to the long alkyl chains on the phthalonitrile substrate hindering the cyclisation of the SubPc. The UV–Vis spectra of SubPcs **1**–**3** exhibited the expected two main transitions, the Soret band between 250 and 350 nm, and the Q-band between 450 and 600 nm, see Fig. 2. It was reported that both donor and acceptor peripheral substituents shifted the Q band of SubPcs toward longer wavelengths compared to the unsubstituted ClBSubPc, due to extension of the π conjugation of the macrocycle [12]. The same trend was observed here, namely the Q-band of both SubPc **1** (573 nm) and SubPc **3** (590 nm) are red shifted compared to SubPc **2** (564 nm). Both SubPc **1** and **2** have stronger Q-bands than Soret-band while SubPc **3** has a stronger Soret-band than Q-bands. The extinction coefficient at the Q band maximum, $\mathcal{E}$ = 184 499 $dm^3\,mol^{-1}\,cm^{-1}$, of **3** is in the same range as was found for phthalocyanines with long alkyl chains on the non peripheral position (ca 200 000 $dm^3\,mol^{-1}\,cm^{-1}$) [37]. Related to their general high solubility in organic solvents, SubPcs **1**–**3** showed no aggregation in the concentration range of 0.01–0.10 ($\times 10^{-3}$ M) and followed the Beer-Lambert law, see Fig. 2 (d).

3.2. Cyclic voltammetry

The CV's of SubPc **1**–**3** in dichloromethane (DCM) and dichloroethane (DCE) at a scan rate of 0.100 V s^{-1} are shown in Fig. 3 with electrochemically relevant data summarized in Table 1. Selected previously reported electrochemical data on related SubPcs (with R and R' = H, F or Cl and X = Cl, F, Br or alkoxy group) are summarized in Table 2. All three SubPc **1**–**3** show a single oxidation peak and one or more reduction peaks. It is generally known that the first oxidation and the first reduction of SubPcs are both centred at the

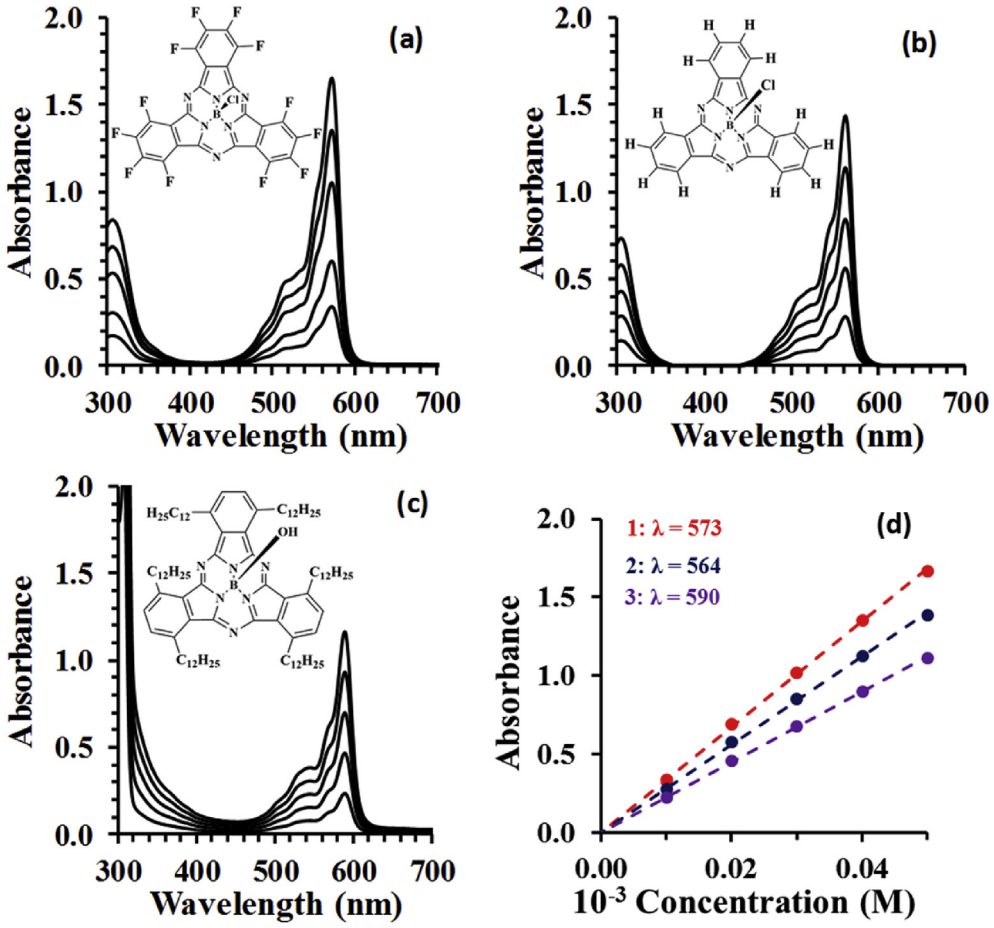

Fig. 2. (a)–(c) The UV–vis spectra of SubPc 1–3 at concentrations 0.01, 0.02, 0.03, 0.04, 0.05 ($\times 10^{-3}$ M), obtained with a cuvette of pathlength 1 cm. (d) The Beer-Lambert correlation between the absorbance A and concentration of ClBSubPc(F)$_{12}$, 1 ($\varepsilon = 236441$ dm^3 mol^{-1} cm^{-1}); ClBSubPc(H)$_{12}$, 2 ($\varepsilon = 210338$ dm^3 mol^{-1} cm^{-1}) (obtained with a cuvette of pathlength 1 cm) and (HO)BSubPc($C_{12}H_{25}$)$_6$(H)$_6$, 3 ($\varepsilon = 184499$ dm^3 mol^{-1} cm^{-1}) (obtained with a cuvette of pathlength 1 mm, corrected to match 1 cm pathlength) at the indicated wavelength in nm. Beer-Lambert graph up to 0.10 ($\times 10^{-3}$ M) is given in the supporting information.

macrocyclic ligand [38]. This agrees with the character of the highest occupied molecular orbital (HOMO for oxidation) and lowest unoccupied molecular orbital (LUMO for reduction) which will be discussed in the next section. The oxidised species of SubPcs are generally unstable on the cyclic voltammetry time scale and all published results showed irreversible SubPc oxidation behaviour [38,39], while the first reduction is sometimes reported to be electrochemically reversible [12].

In this study, for the first time, electrochemically quasi reversible oxidation, with peak separation $\Delta E_p = 0.074$ V and peak current ratio of 0.99 (scan rate of 0.100 V s^{-1}) are observed for SubPc **2** in DCE as solvent, see wave I in Fig. 3. Published CVs for SubPc **2** (Table 2), all showing irreversible oxidation behaviour, were performed utilizing DMF/TBAP [38] or DCM/TBAP (TBAP = tetra-*n*-butylammoniumhexafluorophosphate) [39] as solvent/electrolyte combination, while quasi reversible oxidation behaviour was obtained here utilizing anhydrous DCE as solvent and [N(^{n}Bu)$_4$][B(C_6F_5)$_4$] as supporting electrolyte. The solvents DCM and DCE used in this study, minimizes solvent–compound interactions, while the chosen supporting electrolyte, [N(^{n}Bu)$_4$][B(C_6F_5)$_4$], minimizes ionic interactions of the type (cations)n$^{+}\cdots{}^{-}$[B(C_6F_5)$_4$ [22]. Solvents such as DMF and THF are known to have the capability to interact with analytes to form analyte-DMF or analyte-THF conjugates especially under oxidative conditions when + charges are produced [22,40–44]. The [N(^{n}Bu)$_4$][B(C_6F_5)$_4$] as supporting electrolyte used in this study gave quasi reversible oxidation in DCM with peak separation $\Delta E_p = 0.086$ V and peak current ratio of 0.99 (scan rate of 0.100 V s^{-1}) for SubPc **2**, see Fig. 3. The CVs obtained for SubPc **2** in DCE and in DCM both show one oxidation and two reduction peaks, but at different potentials (Fig. 3 and Table 1). It must be noted that redox potentials are solvent and electrolyte concentration dependant [45]. Electrochemistry performed in DCE however, show better CV curves (Fig. 3) and a smaller peak separation for the first ring oxidation for SubPc **2** ($\Delta E_p = 0.074$ and 0.086 V at a scan rate of 0.100 V s^{-1} in DCE and DCM respectively). The first ring-reduction of **2** is irreversible in DCM ($E_{red} = -1.519$ V), but quasi reversible in DCE ($E_{red} = -1.501$ V with $\Delta E_p = 0.116$ V), peak II in Fig. 3. The first reduction is followed by a second irreversible reduction at −2.050 V (DCM)/−1.980 V (DCE) vs Fc$^+$/Fc, peak III in Fig. 3. The first oxidation (E_{ox}) and first reduction (E_{red}) potential in DCM of 0.674 and −1.519 V vs Fc$^+$/Fc respectively and in DCE of 0.795 and −1.501 V vs Fc$^+$/Fc respectively, obtained for SubPc **2** in this study, compare well with the peak potentials of previously reported electrochemical irreversible results, see Table 2. The reaction scheme for the redox signals of SubPc **2** in DCE as solvent in Fig. 3 is given in Scheme 1.

The first ring oxidation of **1** (wave I in Fig. 3) is irreversible in DCM at all scan rates, while first ring-oxidation of **1** in DCE (wave I in Fig. 3) is electrochemically quasi reversible, at slow scan rates, $\Delta E_p = 0.081$ V and peak current ratio of 0.99 (DCE at a scan rate of

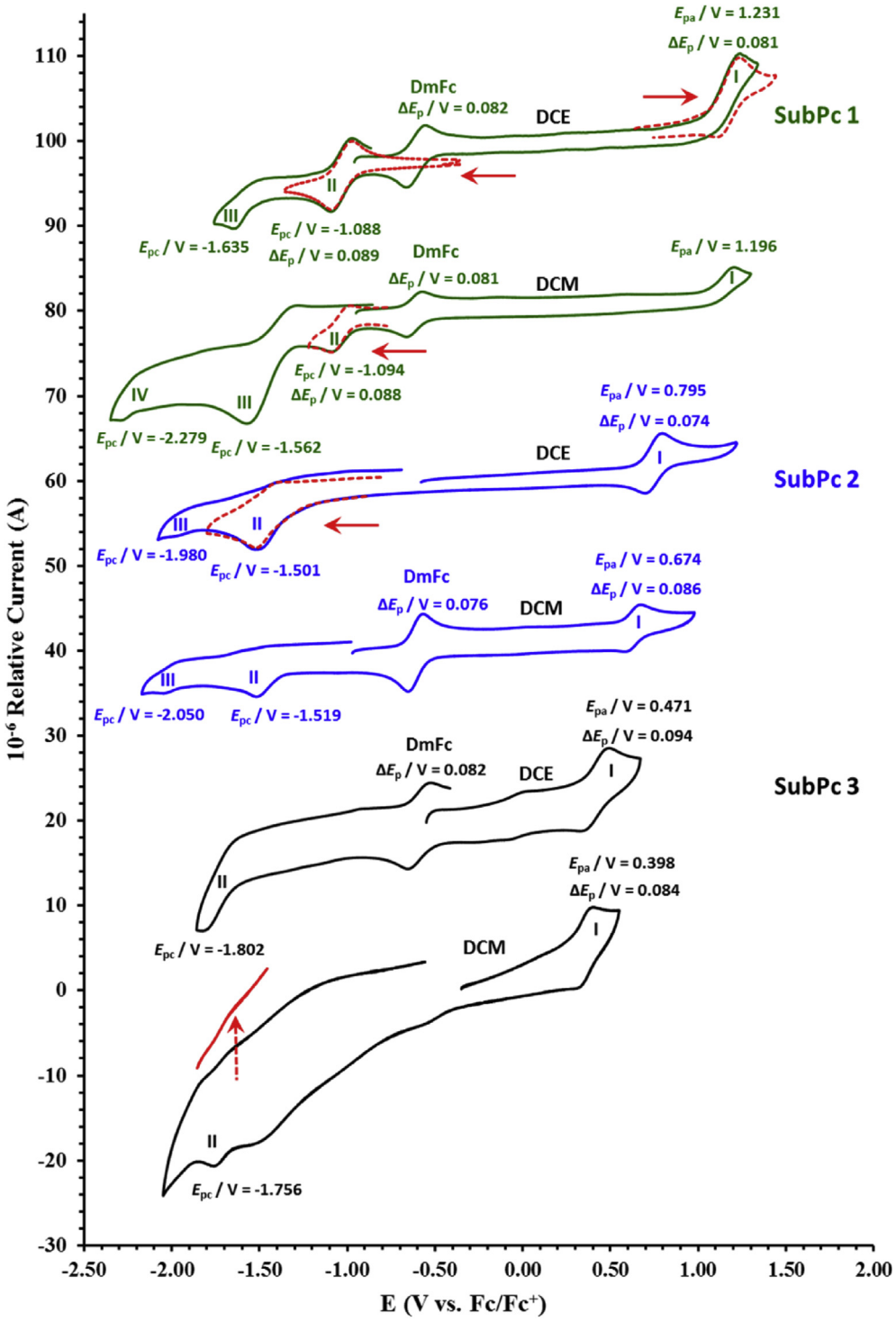

Fig. 3. CV's of SubPc **1** (green), **2** (blue) and **3** (black) at 0.100 V s^{-1} in the in DCM (at 25 °C) and DCE (at 60 °C) with $[N(^nBu)_4][B(C_6F_5)_4]$ as supporting electrolyte. Concentration of **1** and **2** = 0.0005 mol dm^{-3} and of **3** = 0.004 (DCM) or 0.002 (DCE) mol dm^{-3}. The full scans were initiated in the positive direction and the scan fragments in the direction indicated by a red arrow. (For interpretation of the references to colour in this figure legend, the reader is referred to the Web version of this article.)

0.100 V s^{-1}). The first ring reduction of **1** (wave II) is electrochemically quasi reversible (wave II with $\Delta E_p = 0.089$ V) for SubPc **1**. The resolution of the re-oxidation of wave II in DCM as solvent is lost when the next reduction, indicated with III, is allowed to take place before the scan direction is reversed, see Fig. 3. A third irreversible reduction wave IV at −2.279 V vs Fc^+/Fc in DCM as solvent can be observed because of the strong electron-withdrawing F substituents that shift the wave into the DCM solvent window but could not be observed with DCE as solvent. The observed oxidation at $E_{ox} = 1.196$ V (DCM)/1.231 V (DCE) vs Fc^+/Fc and the reduction in DCM at $E_{red} = -1.094$ V vs Fc^+/Fc ($E^{o'} = -1.050$ V with $\Delta E = 0.088$ V) and in DCE at $E_{red} = -1.088$ V vs Fc^+/Fc ($E^{o'} = -1.044$ V with $\Delta E = 0.089$ V) for SubPc **1** in this study, are in agreement with reported results for SubPc **1** in THF [46] and CH_3CN [47], see Table 2.

Table 1
Cyclic voltammetry data of SubPcs 1–3 at a scan rate of 0.100 V s^{-1} in DCM (at 25 °C) and DCE (at 60 °C) with $[N(^nBu)_4][B(C_6F_5)_4]$ as supporting electrolyte.

		DCM			DCE		
		i_p (μA)[a], peak current ratio[b]	E_p (V)[c]	$E^{o\prime}$ (V), ΔE_p (V)	i_p (μA)[a], peak current ratio[b]	E_p (V)[c]	$E^{o\prime}$ (V), ΔE_p (V)
SubPc **1**	$DmFc^+$/DmFc	3.48, 0.99	−0.571	−0.610, 0.081	3.78, 0.99	−0.556	−0.597, 0.082
	Wave: I	3.21, -[d]	1.196	-[d], -[d]	3.75, 0.99	1.231	1.190, 0.081
	Wave: II	3.22, 0.97	−1.094	−1.050, 0.088	3.80, 0.99	−1.088	−1.044, 0.089
	Wave: III	-[d], -[d]	−1.562	-[d], -[d]	3.65, -[d]	−1.635	-[d], -[d]
	Wave: IV	-[d], -[d]	−2.279	-[d], -[d]	-[e], -[e]	-[e], -[e]	-[e], -[e]
SubPc **2**	$DmFc^+$/DmFc	3.89, 0.99	−0.559	−0.610, 0.076	3.80, 0.99	−0.556	−0.597, 0.070
	Wave: I	3.08, 0.99	0.674	0.628, 0.086	3.75, 0.99	0.795	0.758, 0.074
	Wave: II	3.63, -[d]	−1.519	-[d], -[d]	3.95, -[d]	−1.501	−1.487, 0.116
	Wave: III	-[d], -[d]	−2.050	-[d], -[d]	-[d], -[d]	−1.980	-[d], -[d]
SubPc **3**	$DmFc^+$/DmFc	3.14, 0.99	−0.571	−0.610, 0.079	3.54, 0.94	−0.552	−0.597, 0.082
	Wave: I	3.46, -[d]	0.398	0.356, 0.084	3.98, 0.92	0.471	0.426, 0.094
	Wave: II	-[d], -[d]	−1.756	-[d], -[d]	-[d], -[d]	−1.802	-[d], -[d]

[a] i_p is peak anodic peak for oxidation (i_{pa}) and peak cathodic peak for reduction (i_{pc}).
[b] Peak current ratio = i_{pc}/i_{pa} for oxidation and i_{pa}/i_{pc} for reduction.
[c] E_p is peak anodic peak for oxidation (E_{ox}) and peak cathodic peak for reduction (E_{red}).
[d] Could not be determined.
[e] Not observed in solvent window possible for DCE.

Table 2
Experimental electrochemical data of synthesized SubPcs **1**–**3** complexes from this study, as well as additional data obtained from literature, for **1**, **2** and related SubPcs, in the indicated solvents, reported vs the indicated reference.

	Solvent	Internal Reference	1st Reduction E_{red}[a]	1st Oxidation E_{ox}[b]	E_{ox} - E_{red}	Ref
$ClBSubPc(F)_{12}$ - **1**	DCM	Fc^+/Fc	−1.094	1.196	2.29	tw[c]
	DCE	Fc^+/Fc	−1.088	1.231	2.32	tw[c]
$ClBSubPc(F)_{12}$	THF	Fc^+/Fc	−0.923	1.001	1.92	[46]
$ClBSubPc(F)_{12}$	CH_3CN	SCE	−0.43	-[d]	–	[47]
$ClBSubPc(H)_{12}$ - **2**	DCM	Fc^+/Fc	−1.519	0.674	2.19	tw[c]
	DCE	Fc^+/Fc	−1.501	0.795	2.30	tw[c]
$ClBSubPc(H)_{12}$	DCM	Fc^+/Fc	−1.47	0.53	2.00	[53]
$ClBSubPc(H)_{12}$	DMF	Fc^+/Fc	−1.698	0.655	2.35	[38]
$ClBSubPc(H)_{12}$	DCM	Fc^+/Fc	-[e]	0.64	–	[51]
$ClBSubPc(H)_{12}$	DCM	Ag/AgCl	-[e]	0.584	–	[36]
$ClBSubPc(H)_{12}$	DCM	Ag/AgCl	−1.05	1.04	2.09	[39]
$ClBSubPc(H)_{12}$	DCM	Ag/AgCl	-[e]	0.82	–	[54]
$(HO)BSubPc(C_{12}H_{25})_6(H)_6$ - **3**	DCM	Fc^+/Fc	−1.756	0.398	2.15	tw[c]
	DCE	Fc^+/Fc	−1.802	0.471	2.27	tw[c]
$FBSubPc(H)_{12}$	DCM	Ag/AgCl	-[e]	0.532	–	[36]
$ClBSubPc(Cl)_6(H)_6$	DCM	Fc^+/Fc	-[e]	0.85	–	[51]
$ClBSubPc(Cl)_{12}$	CH_3CN	-[f]	−0.97	1.15	2.12	[55]
$ClBSubPc(F)_3(H)_9$	DCM	Fc^+/Fc	−1.43	0.73	2.16	[51]
$ClBSubPc(F)_6(H)_6$	DCM	Fc^+/Fc	−0.30	0.84	2.18	[51]
$ClBSubPc(I)_3(H)_9$	DCM	Ag/AgCl	−0.92	1.13	2.05	[39]
$ClBSubPc(NO_2)_3$	DCM	Ag/AgCl	−0.57	1.34	1.91	[39]
$ClBSubPc(tBu)_3$	DCM	Ag/AgCl	−1.11	0.98	2.09	[39]
$ClBSubPc(tBu)_3$	CH_3CN	Ag/AgCl	−0.51	0.25	0.76	[54]
$(EtO)BSubPc(H)_{12}$	DCM	SCE	−1.11	1.06	2.17	[48]
$(MeO)BSubPc(H)_{12}$	DCM	Fc^+/Fc	−1.59	0.56	2.15	[49]
$(PhO)BSubPc(F)_{12}$	THF	Fc^+/Fc	−1.088	1.057	2.15	[56]
$(PhO)BSubPc(F)_{12}$	DCM	$DmFc^+$/DmFc[g]	−0.571	-[d]	–	[52]
$(F_5C_6O)BSubPc(F)_{12}$	DCM	$DmFc^+$/DmFc[g]	−0.523	-[d]	–	[52]
$(F_5C_6O)BSubPc(H)_{12}$	DCM	$DMFc^+$/DmFc[g]	−0.889	-[d]	–	[52]

[a] E_{red} = peak reduction potential since most reported first reduction peaks for SubPcs are irreversible.
[b] E_{ox} = peak oxidation potential since all reported first oxidation peaks for SubPcs are irreversible.
[c] This work.
[d] No reported oxidation value.
[e] No reported reduction values.
[f] No reported internal reference.
[g] $E^{o\prime}(Fc^+/Fc) = -0.610$ V vs Fc^+/Fc in DCM, measured in this work.

With the electron-withdrawing fluoride ring substituents in both the peripheral and the non-peripheral positions of SubPc **1**, the oxidation wave I shifted with 0.52 V from 0.674 to 1.196 V in DCM and with 0.44 V from 0.795 to 1.231 V in DCE in comparison with SubPc **2**. The first reduction wave shifted with 0.43 V in DCM and with 0.41 V in DCE as solvent. The reaction scheme for the redox signals of SubPc **1** in DCE as solvent in Fig. 3 is given in Scheme 1.

The ring oxidation process (wave I in Fig. 3) for SubPc **3** also shows quasi electrochemical reversibility with $\Delta E = 0.084$ V and 0.094 V (at 0.100 V s^{-1}) in DCM and DCE respectively. The quasi

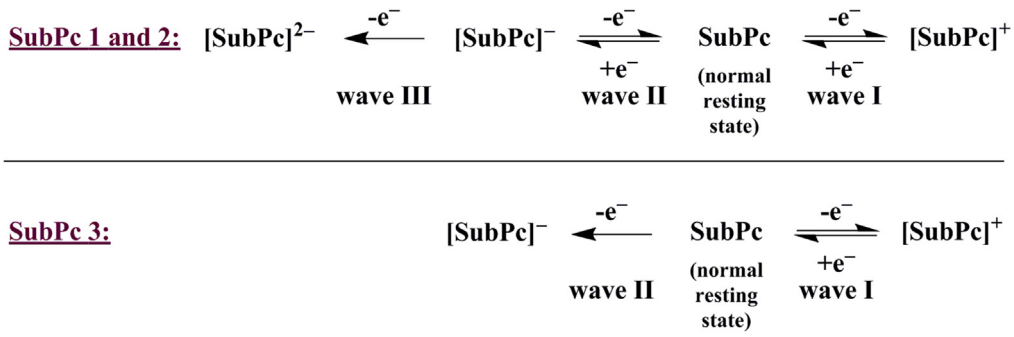

Scheme 1. The reaction scheme for the redox signals of SubPc 1–3 in DCE as solvent, see Fig. 3.

electrochemical reversibility of the oxidation process can be attributed to the stabilization of the macrocycle brought by the electron-donation of the non-peripheral and axial substituents. The use of DCE as solvent over DCM for SubPc **3** is especially clear from the much better resolution and definition of the CV curve of the first ring reduction wave obtained for SubPc **3**.

The effect of the electron-donating ligands ($C_{12}H_{25}$) on the non-peripheral positions of SubPc **3** is observable, on both the position of the oxidation and reduction waves. In DCM as solvent, the first oxidation (wave **I**) potential exhibits a shift of 0.28 V to a less positive potential 0.398 V vs Fc^+/Fc, compared to SubPc **2** at 0.674 V vs Fc^+/Fc. The oxidation potential of 0.398 V vs Fc^+/Fc of SubPc **3** is the lowest oxidation potential reported for SubPc's in DCM till date [12]. Thus, the novel SubPc **3** of this study contains the most electron-rich macrocycle of all reported SubPcs till date. SubPc **3** only has one electrochemically irreversible reduction wave, wave II, shifted to a more negative potential than was observed for SubPc **1** and **2**. In DCM a very small re-oxidation at −1.67 V peak, coupled to the reduction at −1.756 V is visible, see Fig. 3, the enlarged wave in red. The reaction scheme for the redox signals of SubPc **3** in DCE as solvent in Fig. 3 is given in Scheme 1.

Comparing the electrochemical data obtained in DCM this study with available related published data in DCM referenced vs Fc^+/Fc (Table 3), it is observed that axial or peripheral substitution has a less influence on the oxidation potential of a SubPc than non-peripheral substitution:

(i) In comparing complex SubPc (**2**, $E_{ox} = 0.674$ V) with (EtO)BSubPc$(H)_{12}$ (**6**, $E_{ox} = 0.53$ V vs Fc^+/Fc [48]) and (MeO)BSubPc$(H)_{12}$ (**7**, $E_{ox} = 0.56$ V vs Fc^+/Fc [49]), it is observed that substitution of the electron-withdrawing axial chloride ligand with an electron-donating alkoxy group, shifts the first oxidation potential of the SubPc with ca 0.13 V to less positive potentials. The same trend is observed in comparing ClBSubPc$(F)_{12}$ (**1**, $E_{ox} = 1.196$ V) with (PhO)BSubPc$(F)_{12}$ (**8a**, $E_{ox} = 1.057$ V vs Fc^+/Fc [50]). It is expected that stronger electron-donating groups lead to less positive oxidation potentials.

(ii) In comparing complexes ClBSubPc (**2**, $E_{ox} = 0.674$ V) with ClBSubPc$(F)_3(H)_9$ (**4**, $E_{ox} = 0.73$ V [51]) and ClBSubPc$(F)_6(H)_6$ (**5**, $E_{ox} = 0.84$ V [51]), it is observed that substitution of a peripheral substituent, by a more electron-withdrawing substituent, leads to an increase of the first oxidation potential of the SubPc of ca 0.1 V to a more positive value. It is expected that electron-withdrawing substituents lead to a more positive oxidation potential.

Table 3
Experimental first oxidation (E_{ox}) and first reduction (E_{red}) potentials (vs Fc^+/Fc) and DFT calculated HOMO and LUMO energies of SubPcs **1**–**3** and related SubPcs (with peripheral and non-peripheral substituents = H or F and axial substituent Cl or alkoxy group). Calculated global electrophilicity index (ω) and the calculated electro chemical potentials (μ) are also given.

	1st oxidation[a]	1st reduction[b]	E(HOMO) eV	E(LUMO) eV	ω	μ	Ref
	E in DCM vs Fc^+/Fc		Calculated DCM				
ClBSubPc$(F)_{12}$–**1**	1.196	−1.094	−6.104	−3.494	3.417	−4.288	tw[c]
ClBSubPc$(H)_{12}$–**2**	0.674	−1.519	−5.633	−2.943	2.965	−3.917	tw[c]
(HO)BSubPc$(C_{12}H_{25})_6(H)_6$ - **3**	0.398	−1.756	−5.210	−2.623	3.603	−4.414	tw[c]
ClBSubPc$(F)_3(H)_9$–**4**	0.73	−1.43	−5.766	−3.062	3.765	−4.538	[51]
ClBSubPc$(F)_6(H)_6$–**5**	0.84	−1.34	−5.906	−3.171	3.104	−4.108	[51]
(EtO)BSubPc$(H)_{12}$–**6**	0.53	−1.64	−5.467	−2.749	3.111	−4.112	[48]
(MeO)BSubPc$(H)_{12}$–**7**	0.56	−1.59	−5.471	−2.753	4.235	−4.711	[49]
(PhO)BSubPc$(F)_{12}$ – **8a**	1.057[b]	−1.088[d]	−6.021	−3.401	4.235	−4.711	[56]
(PhO)BSubPc$(F)_{12}$ – **8b**	–	−1.181[e]	−6.021	−3.401	4.344	−4.742	[52]
(F_5C_6O)BSubPc$(F)_{12}$ - **9**	–	−1.133[e]	−6.036	−3.448	3.331	−4.218	[52]
(F_5C_6O)BSubPc$(H)_{12}$ - **10**	–	−1.499[e]	−5.553	−2.883	3.417	−4.288	[52]
	E in DCE vs Fc^+/Fc		**Calculated DCE**				
ClBSubPc$(F)_{12}$–**1**	1.231	−1.088	−6.098	−3.494	4.417	−4.796	tw[c]
ClBSubPc$(H)_{12}$–**2**	0.795	−1.501	−5.635	−2.946	3.423	−4.290	tw[c]
(HO)BSubPc$(C_{12}H_{25})_6(H)_6$ - **3**	0.471	−1.802	−5.214	−2.628	2.973	−3.921	tw[c]

[a] First reduction is peak oxidation potential since all reported first oxidation peaks for SubPcs are irreversible.
[b] First reduction is peak reduction potential since most reported first reduction peaks for SubPcs are irreversible.
[c] This work.
[d] Experimental value in THF.
[e] Values reported versus $DmFc^+$/DmFc. To convert to potential vs Fc^+/Fc for comparative reasons, $E^{0'}(DmFc^+/DmFc) = -0.610$ V vs Fc^+/Fc in DCM has been used, the value measured in this work.

(iii) Substitution of a non-peripheral substituent, by a more electron-withdrawing substituent, has a much more profound influence on the oxidation potential. For example, when comparing ClBSubPc(F)$_6$(H)$_6$ (**5**, $E_{ox} = 0.84$ V [51]) with ClBSubPc(F)$_{12}$ (**1**, $E_{ox} = 1.196$ V), a shift of more than 0.35 V to a more positive oxidation potential is observed.

(iv) Substitution of a non-peripheral substituent, by a more electron-donating substituent, as when comparing SubPc (**2**, $E_{ox} = 0.674$ V) with the novel (HO)BSubPc(C$_{12}$H$_{25}$)$_6$(H)$_6$ (**3**, $E_{ox} = 0.398$ V, DCM) of this study, led to a decrease of the first oxidation potential of the SubPc of more than *ca.* 0.28 V to a smaller potential value.

(v) Similar trends are observed for the first reduction potential of above-mentioned examples, see Table 3. This is expected, since the electrochemical HOMO-LUMO gap = E_{ox} - E_{red} is relatively constant at ca. 2.1 V (Table 2). Another example is substitution of H in the axial OPh ligand in (PhO)BSubPc(F)$_{12}$ (**8b**, $E_{red} = -1.181$ V vs Fc$^+$/Fc), to get OC$_6$F$_5$, in F$_5$C$_6$OBSubPc(F)$_{12}$ (**9**, $E_{red} = -1.133$ V vs Fc$^+$/Fc), shifts the first reduction potential with only 0.05 V to a more positive value. However, substitution of both peripheral and non-peripheral H in (F$_5$C$_6$O)BSubPc(H)$_{12}$ (**10**, $E_{red} = -1.449$ V vs Fc$^+$/Fc), by the more electron-withdrawing F to get (F$_5$C$_6$O)BSubPc(F)$_{12}$ (**9**, $E_{red} = -1.133$ V vs Fc$^+$/Fc), a shift of more than 0.3 V to a more positive reduction potential is observed [52] (Table 3).

3.3. Computational analyses

SubPcs **1**–**3** and related SubPcs **4**–**10** (with peripheral and non-peripheral substituents = H or F and axial substituent Cl or alkoxy group) of which the oxidation and/or reduction potential vs Fc$^+$/Fc is known, were optimized by DFT methods. The character of the HOMO (LUMO) generally indicate the locus of oxidation (reduction) of a complex [57]. Fig. 6 shows the HOMO and LUMO for the novel SubPc **3** of this study, confirming that both the first oxidation and the first reduction of SubPcs **1**–**3** are centred at the macrocyclic ligand. (See the supplementary information for HOMO and LUMO

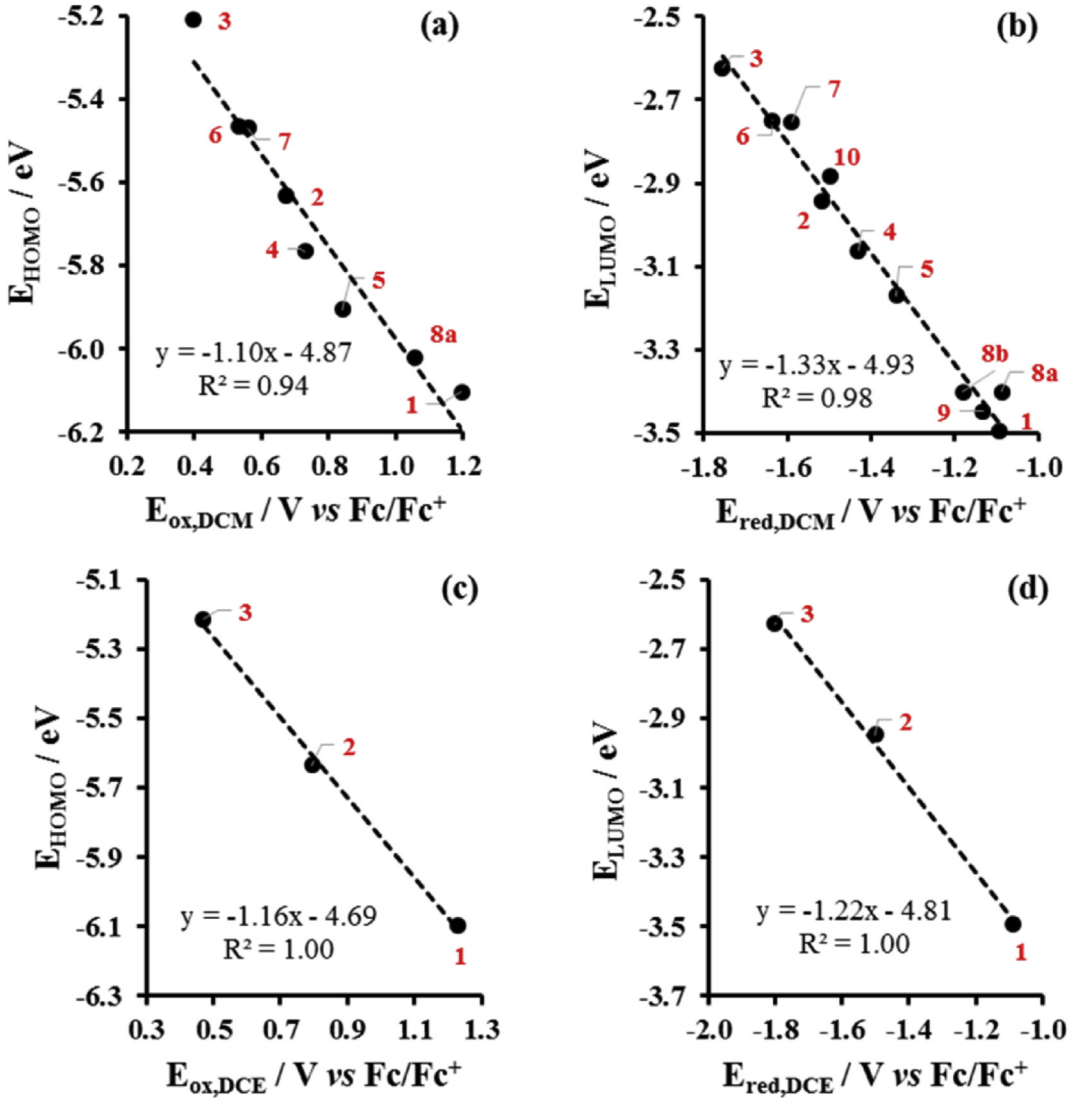

Fig. 4. Relationships obtained between experimental redox potential (vs Fc$^+$/Fc) and B3LYP/6-311G(d,p) DFT calculated frontier orbital energies in DCM (top) or DCE (bottom), of SubPcs 1–3 as well as related SubPcs 4–10 from literature (with peripheral and non-peripheral substituents = H or F and axial substituent Cl or alkoxy group). (a) Calculated HOMO energies *vs* E_{ox} in DCM, (b) calculated LUMO energies vs E_{red} in DCM, (c) calculated HOMO energies vs E_{ox} in DCE and (d) calculated LUMO energies vs E_{red} in DCE. Compound numbers and data from Table 3.

figures of SubPcs **1** and **2**). The oxidation potential of a molecule is generally related to its ionization potential (IP), since the oxidation potential is the energy needed to move an electron from the HOMO of the solution species into the electrode, while the IP is the amount of energy required to remove a HOMO electron from an isolated gaseous molecule to form a cation. Thus, HOMO energies, IP and oxidation potentials are related [57]. Similarly LUMO energies, electron affinities and reduction potentials are related [57]. DFT calculated energies of the SubPcs **1**–**10** are reported in Table 3. The relationship between the experimental E_{ox} vs HOMO energies, as well as experimental E_{red} vs LUMO energies, are shown in Fig. 4 (a) and (b) for experimental E obtained in DCM as solvent and in Fig. 4 (c) and (d) for experimental E obtained in DCE as solvent. The relationships result in the following linear mathematical relationships using experimental data obtained in DCM as solvent:

$$E_{HOMO} = -1.10\,E_{ox,DCM} - 4.87 \qquad (R^2 = 0.94)$$

DFT calculations in DCM as solvent

$$E_{LUMO} = -1.33\,E_{red,DCM} - 4.93 \qquad (R^2 = 0.98)$$

DFT calculations in DCM as solvent

The relationships result in the following linear mathematical relationships using the experimental data obtained in this study in DCE as solvent:

$$E_{HOMO} = -1.16\,E_{ox,DCE} - 4.69 \qquad (R^2 = 1.00)$$

DFT calculations in DCE as solvent

$$E_{LUMO} = -1.22\,E_{red,DCE} - 4.81 \qquad (R^2 = 1.00)$$

DFT calculations in DCE as solvent

The HOMO and LUMO energies are inversely proportional to the experimental oxidation and reduction potential respectively, both resulting in a graph with a negative slope. More energy is needed to remove an electron from a lower energy, more stable, HOMO, resulting in higher oxidation potential. A lower energy, more stable, LUMO can accept an electron more easily, resulting in a reduced

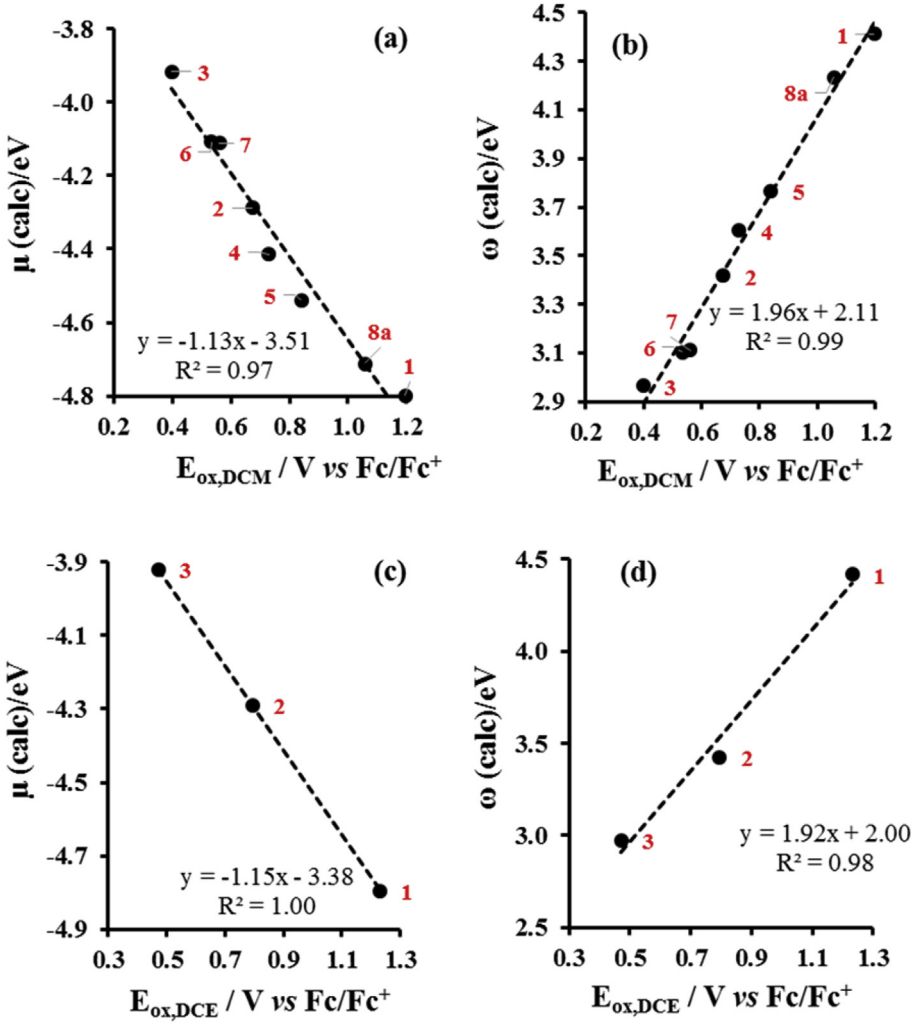

Fig. 5. Relationships obtained between experimental redox potential (vs Fc^+/Fc) and B3LYP/6-311G(d,p) DFT calculated energies in DCM (top) or DCE (bottom), of SubPcs 1–3 as well as related SubPcs 4–10 from literature (with peripheral and non-peripheral substituents = H or F and axial substituent Cl or alkoxy group). (a) DCM calculated global electrophilicity index (ω) vs E_{ox} in DCM, (b) DCM calculated electro chemical potential (μ) vs E_{ox} in DCM (c) DCE calculated global electrophilicity index (ω) vs E_{ox} in DCE and (d) DCE calculated electro chemical potential (μ) vs E_{ox} in DCE. Compound numbers and data from Table 3.

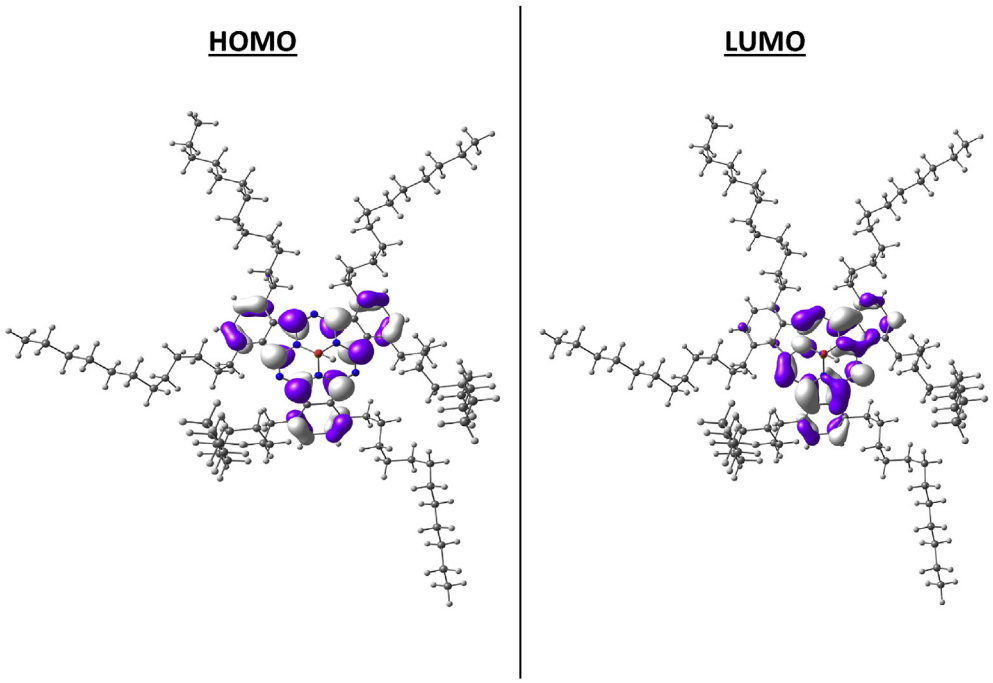

Fig. 6. HOMO and LUMO of the optimized geometry of SubPc 3.

species at a higher potential.

The electrophilicity index (ω), which is a measure of the electrophilic power of atoms and molecules and the electronic chemical potential (μ) of the SubPcs can be calculated from the HOMO and LUMO energies [31–33]. The relationship between the experimental oxidation potential of the SubPcs and the electrophilicity index and the electronic chemical potential are shown in Fig. 5 and given by.

$$\mu = -1.13\ E_{ox,DCM} - 3.51 \qquad (R^2 = 0.97)$$

DFT calculations in DCM as solvent

$$\omega = 1.96\ E_{ox,DCM} + 2.11 \qquad (R^2 = 0.99)$$

DFT calculations in DCM as solvent

$$\mu = -1.15\ E_{ox,DCE} - 3.38 \qquad (R2^{=1.00})$$

DFT calculations in DCE as solvent

$$\omega = 1.92\ E_{ox,DCE} + 2.00 \qquad (R^2 = 0.98)$$

DFT calculations in DCE as solvent

The linear relationships obtained from the graphs in Figs. 4 and 5 are a measure of the reliability of the results obtained in this study compared to previously published results. The equations also enable the calculation of electrophilicity index, electronic chemical potential, HOMO and LUMO energies from experimental redox potentials (and *vice versa*).

4. Conclusions

The experimental conditions used to perform cyclic voltammetry experiments, namely when using DCE solvent that minimizes solvent–compound interactions, and $[N(^nBu)_4][B(C_6F_5)_4]$ as supporting electrolyte, that minimizes ionic interactions between cationic species and the electrolyte, made it possible for the first time to experimentally observe electrochemically quasi reversible oxidation for SubPc **1** ($ClBSubPc(F)_{12}$), SubPc **2** ($ClBSubPc(H)_{12}$) and SubPc **3**, $(HO)BSubPc(C_{12}H_{25})_6(H)_6$. The novel SubPc **3**, $(HO)BSubPc(C_{12}H_{25})_6(H)_6$, contains the most electron-rich macrocycle of all reported SubPcs till date with an oxidation potential in DCM of 0.398 V vs Fc^+/Fc. The electrochemical data reported for SubPc **1** ($ClBSubPc(F)_{12}$), containing electron-withdrawing substituents on the peripheral and non-peripheral positions), SubPc **2** ($ClBSubPc(H)_{12}$) and SubPc **3** ($(HO)BSubPc(C_{12}H_{25})_6(H)_6$), containing electron-donating substituents on the non-peripheral positions), together with previously reported data in DCM as solvent, show that axial or peripheral substitution has a less influence (ca 0.1 V shift) on the shift of the oxidation and reduction potential of a SubPc than non-peripheral substitution (ca 0.3 V shift). Linear relationships obtained between the first oxidation potential and HOMO energies, as well as between the first reduction potential and LUMO energies for a series of related SubPcs (with peripheral and non-peripheral substituents = H or F and axial substituent Cl or alkoxy group) can be used to calculate HOMO and LUMO energies from experimental first oxidation and the first reduction potential of related SubPcs (and *vice versa*).

Declaration of competing interest

The author declares that there is no known competing financial interests or personal relationships that could have appeared to influence the work reported in this paper.

Acknowledgements

This work has received support the South African National Research Foundation (Grant numbers 113327 and 96111) and the Central Research Fund of the University of the Free State, Bloemfontein. The High-Performance Computing facility of the UFS, the CHPC of South Africa and the Norwegian Supercomputing Program (UNINETT Sigma2, Grant No. NN9684K) are acknowledged for

computer time.

Appendix A. Supplementary data

Supplementary data to this article can be found online at https://doi.org/10.1016/j.electacta.2019.135165.

References

[1] F. Yakuphanoglu, M. Kandaz, M.N. Yaraşir, F.B. Şenkal, Electrical transport and optical properties of an organic semiconductor based on phthalocyanine, Phys. B Condens. Matter 393 (2007) 235–238, https://doi.org/10.1016/j.physb.2007.01.007.

[2] F. Yilmaz, D. Atilla, V. Ahsen, Synthesis and liquid-crystalline behaviour of Ni(II) and Zn(II) phthalocyanines with peripheral monoazacrown ethers, Polyhedron 23 (2004) 1931–1937, https://doi.org/10.1016/j.poly.2004.04.031.

[3] N. Padma, A. Joshi, A. Singh, S.K. Deshpande, D.K. Aswal, S.K. Gupta, J.V. Yakhmi, NO2 sensors with room temperature operation and long term stability using copper phthalocyanine thin films, Sens. Actuators B Chem. 143 (2009) 246–252, https://doi.org/10.1016/j.snb.2009.07.044.

[4] J. Haber, R. Iwanejko, J. Połtowicz, P. Battioni, D. Mansuy, Pernitrated metalloporphyrins as catalysts in oxidation with magnesium monoperoxophthalate, J. Mol. Catal. A Chem. 152 (2002) 111–115, https://doi.org/10.1016/s1381-1169(99)00269-1.

[5] S. ichi Yamazaki, N. Fujiwara, K. Yasuda, A catalyst that uses a rhodium phthalocyanin for oxalic acid oxidation and its application to an oxalic acid sensor, Electrochim. Acta 55 (2010) 753–758, https://doi.org/10.1016/j.electacta.2009.09.028.

[6] H.A. Abdeldayem, D.O. Frazier, B.G. Penn, D.D. Smith, C.E. Banks, Non-linear optothermal properties of metal-free phthalocyanine, Thin Solid Films 350 (1999) 245–248, https://doi.org/10.1016/S0040-6090(98)01432-1.

[7] Y. Yoshida, M. Nakamura, S. Tanaka, I. Hiromitsu, Y. Fujita, K. Yoshino, Photovoltaic properties and inner electric field of ZnO/Zn-phthalocyanine hybrid solar cells, Synth. Met. 156 (2006) 1213–1217, https://doi.org/10.1016/j.synthmet.2006.09.001.

[8] A.N. Vzorov, L.G. Marzilli, R.W. Compans, D.W. Dixon, Prevention of HIV-1 infection by phthalocyanines, Antivir. Res. 59 (2003) 99–109, https://doi.org/10.1016/S0166-3542(03)00035-4.

[9] F. Giuntini, Y. Raoul, D. Dei, M. Municchi, G. Chiti, C. Fabris, P. Colautti, G. Jori, G. Roncucci, Synthesis of tetrasubstituted Zn(II)-phthalocyanines carrying four carboranyl-units as potential BNCT and PDT agents, Tetrahedron Lett. 46 (2005) 2979–2982, https://doi.org/10.1016/j.tetlet.2005.03.030.

[10] Y. Zorlu, F. Dumoulin, D. Bouchu, V. Ahsen, D. Lafont, Monoglycoconjugated water-soluble phthalocyanines. Design and synthesis of potential selectively targeting PDT photosensitisers, Tetrahedron Lett. 51 (2010) 6615–6618, https://doi.org/10.1016/j.tetlet.2010.10.044.

[11] A. Meller, A. Ossko, Phthalocyaninartige bor-komplexe, Monatshefte Fur Chemie 155 (1972) 150–151.

[12] C.G. Claessens, D. González-Rodríguez, M.S. Rodríguez-Morgade, A. Medina, T. Torres, Subphthalocyanines, subporphyrazines, and subporphyrins: singular nonplanar aromatic system, Chem. Rev. 114 (2014) 2192–2277, https://doi.org/10.1021/cr400088w.

[13] Y. Wang, D. Gu, F. Gan, Optical recording properties of a novel subphthalocyanine thin film, Phys. Status Solidi Appl. Res. 186 (2001) 71–77, https://doi.org/10.1002/1521-396X(200107)186:1<71::AID-PSSA71>3.0.CO;2-G.

[14] W.F. Cao, H.Y. Tu, J. Wang, H. Tian, Y. Wang, D. Gu, F. Gan, Synthesis and optical properties of axially bromo-substituted subphthalocyanines, Dyes Pigments 54 (2002) 213–219, https://doi.org/10.1016/S0143-7208(02)00038-4.

[15] M. Ince, A. Medina, J.H. Yum, A. Yella, C.G. Claessens, M.V. Martínez-Díaz, M. Grätzel, M.K. Nazeeruddin, T. Torres, Peripherally and axially carboxylic acid substituted subphthalocyanines for dye-sensitized solar cells, Chem. Eur J. 20 (2014) 2016–2021, https://doi.org/10.1002/chem.201303639.

[16] Z. Ma, S. Liu, S. Hu, J. Yu, Highly efficient tandem organic light-emitting diodes based on SubPc:C60 bulk heterojunction as charge generation layer, J. Lumin. 169 (2016) 29–34, https://doi.org/10.1016/j.jlumin.2015.08.040.

[17] E. van de Winckel, M. Mascaraque, A. Zamarrón, Á. Juarranz de la Fuente, T. Torres, A. de la Escosura, Dual role of subphthalocyanine dyes for optical imaging and therapy of cancer, Adv. Funct. Mater. 28 (2018) 1–10, https://doi.org/10.1002/adfm.201705938.

[18] E. Fourie, J.C. Swarts, I. Chambrier, M.J. Cook, Electrochemical and spectroscopic detection of self-association of octa-alkyl phthalocyaninato cadmium compounds into dimeric species, Dalton Trans. (2009) 1145–1154, https://doi.org/10.1039/b811455b.

[19] R. Li, X. Zhang, P. Zhu, D.K.P. Ng, N. Kobayashi, J. Jiang, Electron-donating or -withdrawing nature of substituents revealed by the electrochemistry of metal-free phthalocyanines, Inorg. Chem. 45 (2006) 2327–2334, https://doi.org/10.1021/ic051931k.

[20] D.B.G. Williams, M. Lawton, Drying of organic solvents: quantitative evaluation of the efficiency of several desiccants, J. Org. Chem. 75 (2010) 8351–8354, https://doi.org/10.1021/jo101589h.

[21] C.G. Claessens, D. González-Rodríguez, B. Del Rey, T. Torres, G. Mark, H.P. Schuchmann, C. Von Sonntag, J.G. MacDonald, R.S. Nohr, Highly efficient synthesis of chloro- and phenoxy-substituted subphthalocyanines, Eur. J. Org. Chem. (2003) 2547–2551, https://doi.org/10.1002/ejoc.200300169.

[22] H.J. Gericke, N.I. Barnard, E. Erasmus, J.C. Swarts, M.J. Cook, M.A.S. Aquino, Solvent and electrolyte effects in enhancing the identification of intramolecular electronic communication in a multi redox-active diruthenium tetraferrocenoate complex, a triple-sandwiched dicadmium phthalocyanine and a ruthenocene-containing β-diketone, Inorg. Chim. Acta 363 (2010) 2222–2232, https://doi.org/10.1016/j.ica.2010.03.031.

[23] N. Elgrishi, K.J. Rountree, B.D. McCarthy, E.S. Rountree, T.T. Eisenhart, J.L. Dempsey, A practical beginner's guide to cyclic voltammetry, J. Chem. Educ. 95 (2018) 197–206, https://doi.org/10.1021/acs.jchemed.7b00361.

[24] P.T. Kissinger, W.R. Heineman, Cyclic voltammetry, J. Chem. Educ. 60 (1983) 702–706, https://doi.org/10.1021/ed060p702.

[25] R.L. Blrke, M.H. Kim, M. Strassfeld, Diagnosis of reversible, quasi-reversible, and irreversible electrode processes with differential pulse polarography, Anal. Chem. 53 (1981) 852–856, https://doi.org/10.1021/ac00229a026.

[26] M.V. Mirkin, A.J. Bard, Simple analysis of quasi-reversible steady-state voltammograms, Anal. Chem. 64 (1992) 2293–2302, https://doi.org/10.1021/ac00043a020.

[27] J.C. Myland, K.B. Oldham, Quasireversible cyclic voltammetry of a surface confined redox system: a mathematical treatment, Electrochem. Commun. 7 (2005) 282–287, https://doi.org/10.1016/j.elecom.2005.01.005.

[28] M.J. Frisch, G.W. Trucks, H.B. Schlegel, G.E. Scuseria, M.A. Robb, J.R. Cheeseman, G. Scalmani, V. Barone, G.A. Petersson, H. Nakatsuji, X. Li, M. Caricato, A.V. Marenich, J. Bloino, B.G. Janesko, R. Gomperts, B. Mennucci, H.P. Hratchian, J.V. Ortiz, A.F. Izmaylov, J.L. Sonnenberg, D. Williams-Young, F. Ding, F. Lipparini, F. Egidi, J. Goings, B. Peng, A. Petrone, T. Henderson, D. Ranasinghe, V.G. Zakrzewski, J. Gao, N. Rega, G. Zheng, W. Liang, M. Hada, M. Ehara, K. Toyota, R. Fukuda, J. Hasegawa, M. Ishida, T. Nakajima, Y. Honda, O. Kitao, H. Nakai, T. Vreven, K. Throssell, J.A. Montgomery, J.E. Peralta, F. Ogliaro, M.J. Bearpark, J.J. Heyd, E.N. Brothers, K.N. Kudin, V.N. Staroverov, T.A. Keith, R. Kobayashi, J. Normand, K. Raghavachari, A.P. Rendell, J.C. Burant, S.S. Iyengar, J. Tomasi, M. Cossi, J.M. Millam, M. Klene, C. Adamo, R. Cammi, J.W. Ochterski, R.L. Martin, K. Morokuma, O. Farkas, J.B. Foresman, D.J. Fox, Gaussian 16, Revision B.01, 2016, p. 2016.

[29] A.V. Marenich, C.J. Cramer, D.G. Truhlar, Universal solvation model based on solute electron density and on a continuum model of the solvent defined by the bulk dielectric constant and atomic surface tensions, J. Phys. Chem. B 113 (2009) 6378–6396.

[30] R.E. Skyner, J.L. Mcdonagh, C.R. Groom, T. Van Mourik, A review of methods for the calculation of solution free energies and the modelling of systems in solution, Phys. Chem. Chem. Phys. 17 (2015) 6174–6191, https://doi.org/10.1039/C5CP00288E.

[31] R.S. Mulliken, A new electroaffinity scale; Together with data on valence states and on valence ionization potentials and electron affinities, J. Chem. Phys. 2 (1934) 782–793, https://doi.org/10.1063/1.1749394.

[32] F. De Proft, W. Langenaeker, P. Geerlings, Ab initio determination of substituent constants in a density functional theory formalism: calculation of intrinsic group electronegativity, hardness, and softness, J. Phys. Chem. 97 (1993) 1826–1831, https://doi.org/10.1021/j100111a018.

[33] R.G. Parr, L.V. Szentpály, S. Liu, Electrophilicity index, J. Am. Chem. Soc. 121 (1999) 1922–1924, https://doi.org/10.1021/ja983494x.

[34] T. Koopmans, Über die Zuordnung von Wellenfunktionen und Eigenwerten zu den Einzelnen Elektronen Eines Atoms, Physica 1 (2004) 104–113, https://doi.org/10.1016/s0031-8914(34)90011-2.

[35] S. Hamel, P. Duffy, M.E. Casida, D.R. Salahub, Kohn-Sham orbitals and orbital energies: fictitious constructs but good approximations all the same, J. Electron. Spectrosc. Relat. Phenom. 123 (2002) 345–363, https://doi.org/10.1016/S0368-2048(02)00032-4.

[36] M.V. Fulford, D. Jaidka, A.S. Paton, G.E. Morse, E.R.L. Brisson, A.J. Lough, T.P. Bender, Crystal structures, reaction rates, and selected physical properties of halo-boronsubphthalocyanines (Halo = Fluoride, chloride, and bromide), J. Chem. Eng. Data 57 (2012) 2756–2765, https://doi.org/10.1021/je3005112.

[37] J.C. Swarts, E.H.G. Langner, N. Krokeide-Hove, M.J. Cook, Synthesis and electrochemical characterisation of some long chain 1,4,8,11,15,18,22,25-octa-alkylated metal-free and zinc phthalocyanines possessing discotic liquid crystalline properties, J. Mater. Chem. 11 (2001) 434–443, https://doi.org/10.1039/b006123i.

[38] P.V. Solntsev, K.L. Spurgin, J.R. Sabin, A.A. Heikal, V.N. Nemykin, Photoinduced charge transfer in short-distance ferrocenylsubphthalocyanine dyads, Inorg. Chem. 51 (2012) 6537–6547, https://doi.org/10.1021/ic3000608.

[39] B. Del Rey, U. Keller, T. Torres, G. Rojo, F. Agulló-López, S. Nonell, C. Martí, S. Brasselet, I. Ledoux, J. Zyss, Synthesis and nonlinear optical, photophysical, and electrochemical properties of subphthalocyanines, J. Am. Chem. Soc. 120 (1998) 12808–12817, https://doi.org/10.1021/ja980508q.

[40] B.E. Buitendach, E. Erasmus, J.W. Niemantsverdriet, J.C. Swarts, Can electrochemical measurements Be used to predict X-ray photoelectron spectroscopic data? The case of ferrocenyl-β-diketonato complexes of manganese(III), Inorg. Chem. 57 (2018) 6606–6616, https://doi.org/10.1021/acs.inorgchem.8b00745.

[41] D. Chong, J. Slote, W.E. Geiger, The role of solvent in the stepwise electrochemical oxidation of nickelocene to the nickelocenium dication, J. Electroanal. Chem. 630 (2009) 28–34, https://doi.org/10.1016/

j.jelechem.2009.02.009.
[42] A. Nafady, T.T. Chin, W.E. Geiger, Manipulating the electrolyte medium to favor either one-electron or two-electron oxidation pathways for (fulvalendiyl)dirhodium complexes, Organometallics 25 (2006) 1654–1663, https://doi.org/10.1021/om051101e.
[43] F. Barrière, R.U. Kirss, W.E. Geiger, Anodic electrochemistry of multiferrocenyl phosphine and phosphine chalcogenide complexes in weakly nucleophilic electrolytes, Organometallics 24 (2005) 48–52, https://doi.org/10.1021/om040123i.
[44] W.E. Geiger, Use of weakly coordinating anions to develop an integrated approach to the tuning of ΔE1/2 values by medium effects, J. Am. Chem. Soc. 128 (2006) 3980–3989, https://doi.org/10.1021/ja058171x.
[45] D. Bao, B. Millare, W. Xia, B.G. Steyer, A.A. Gerasimenko, A. Ferreira, A. Contreras, V.I. Vullev, Electrochemical oxidation of ferrocene: a strong dependence on the concentration of the supporting electrolyte for nonpolar solvents, J. Phys. Chem. A 113 (2009) 1259–1267, https://doi.org/10.1021/jp809105f.
[46] R.S. Iglesias, C.G. Claessens, G.M.A. Rahman, M.A. Herranz, D.M. Guldi, T. Torres, Subphthalocyanine fused dimers-C60 dyads: synthesis, characterization, and theoretical study, Tetrahedron 63 (2007) 12396–12404, https://doi.org/10.1016/j.tet.2007.09.051.
[47] R.A. Kipp, J.A. Simon, M. Beggs, H.E. Ensley, R.H. Schmehl, Photophysical and photochemical investigation of a dodecafluorosubphthalocyanine derivative, J. Phys. Chem. A 102 (1998) 5659–5664, https://doi.org/10.1021/jp980383b.
[48] K. Kasuga, T. Idehara, M. Handa, Y. Ueda, T. Fujiwara, K. Isa, Structure and properties of alkoxo-SubPc, Bull. Chem. Soc. Jpn. 69 (1996) 2559–2563, https://doi.org/10.1246/bcsj.69.2559.
[49] R. Potz, M. Go, H. Hu, U. Cornelissen, A. Tutaû, È. Aza-bru, Synthese und strukturelle Charakterisierung von Borsubphthalocyaninaten Synth. Struct. Char. Boron Subphthalocyaninates 626 (2000) 588–596, https://doi.org/10.1002/(SICI)1521-3749(200002)626:2<588::AID-ZAAC588>3.0.CO;2-B.
[50] D. Gonzalez-Rodríguez, T. Torres, M.M. Olmstead, J. Rivera, M.Á. Herranz, L. Echegoyen, C.A. Castellanos, D.M. Guldi, Photoinduced charge-transfer states in subphthalocyanine-ferrocene dyads, J. Am. Chem. Soc. 128 (2006) 10680–10681, https://doi.org/10.1021/ja0632409.
[51] P. Sullivan, A. Duraud, L. Hancox, N. Beaumont, G. Mirri, J.H.R. Tucker, R.A. Hatton, M. Shipman, T.S. Jones, Halogenated boron subphthalocyanines as light harvesting electron acceptors in organic photovoltaics, Adv. Energy Mater. 1 (2011) 352–355, https://doi.org/10.1002/aenm.201100036.
[52] G.E. Morse, M.G. Helander, J.F. Maka, Z.H. Lu, T.P. Bender, Fluorinated phenoxy boron subphthalocyanines in organic light-emitting diodes, ACS Appl. Mater. Interfaces 2 (2010) 1934–1944, https://doi.org/10.1021/am1002603.
[53] F. Camerel, G. Ulrich, P. Retailleau, R. Ziessel, Ethynyl-boron subphthalocyanines displaying efficient cascade energy transfer and large Stokes shifts, Angew. Chem. Int. Ed. 47 (2008) 8876–8880, https://doi.org/10.1002/anie.200803131.
[54] E. Ohno-Okumura, K. Sakamoto, T. Kato, T. Hatano, K. Fukui, T. Karatsu, A. Kitamura, T. Urano, Synthesis of subphthalocyanine derivatives and their characterization, Dyes Pigments 53 (2002) 57–65, https://doi.org/10.1016/S0143-7208(01)00102-4.
[55] J.V. Ros-Lis, R. Martínez-Máñez, J. Soto, Subphthalocyanines as fluorochromogenic probes for anions and their application to the highly selective and sensitive cyanide detection, Chem. Commun. (2005) 5260–5262, https://doi.org/10.1039/b510710e.
[56] D. González-Rodríguez, T. Torres, D.M. Guldi, J. Rivera, M.Á. Herranz, L. Echegoyen, Subphthalocyanines : new tuneable tectons for intramolecular electron and energy transfer processes, J. Am. Chem. Soc. 126 (2004) 6301–6313, https://doi.org/10.1021/ja039883v.
[57] J. Conradie, A Frontier orbital energy approach to redox potentials, J. Phys. Conf. Ser. 633 (2015), 012045, https://doi.org/10.1088/1742-6596/633/1/012045.

Data in brief 28 (2020) 105039

Contents lists available at ScienceDirect

Data in brief

journal homepage: www.elsevier.com/locate/dib

Data Article

Oxidation and reduction data of subphthalocyanines

Pieter J. Swarts, Jeanet Conradie*

Department of Chemistry, PO Box 339, University of the Free State, Bloemfontein, 9300, South Africa

ARTICLE INFO

Article history:
Received 11 November 2019
Accepted 13 December 2019
Available online 24 December 2019

Keywords:
Subphthalocyanines
Cyclic voltammetry
Oxidation
Reduction

ABSTRACT

The data presented in this paper are related to the research article entitled "*Electrochemical behaviour of chloro- and hydroxy-subphthalocyanines*" [1]. This paper presents detailed oxidation and reduction potential data, obtained from cyclic voltammograms of three subphthalocyanines (SubPcs), in both dichloromethane (DCM) and dichloroethane (DCE) as solvent. The first SubPc is the unsubstituted boron-subphthalocyanine, (ClB)SubPc(H)$_{12}$, as reference SubPc, the second SubPc is (ClB)SubPc(F)$_{12}$, containing an electron-poor macro-cycle and (HOB)SubPc($C_{12}H_{25}$)$_6$(H)$_6$, containing an electron-rich macro-cycle. The oxidation and reduction potential of (ClB)SubPc(F)$_{12}$ in DCM is ca. 0.5 V more positive than that of the reference ClBSubPc(H)$_{12}$, while oxidation and reduction potential of (HOB)SubPc($C_{12}H_{25}$)$_6$(H)$_6$ in DCM is ca. 0.45 V more negative than that of the reference (ClB)SubPc(H)$_{12}$.

1. Data description

The oxidation and reduction potential data of the unsubstituted boron-subphthalocyanine, (ClB)SubPc(H)$_{12}$, **1**, as reference SubPc, (ClB)SubPc(F)$_{12}$, **2**, containing an electron-poor macro-cycle and (HOB)SubPc($C_{12}H_{25}$)$_6$(H)$_6$, **3**, containing an electron-rich macro-cycle, is presented here. Fig. 1 shows

* Corresponding author.
E-mail address: conradj@ufs.ac.za (J. Conradie).

https://doi.org/10.1016/j.dib.2019.105039

Specifications Table

Subject	Chemistry
Specific subject area	Electrochemistry
Type of data	Table Image Graph Figure
How data were acquired	Princeton Applied Research PARSTAT 2273 potentiostat running Powersuite software (Version 2.58).
Data format	Raw Analyzed
Parameters for data collection	Samples was used as synthesized. All the electrochemical experiments were performed in an M Bruan Lab Master SP glove box under a high purity argon atmosphere (H_2O and O_2 < 10 ppm).
Description of data collection	All electrochemical experiments were done in a 2 ml electrochemical cell containing three-electrodes (a glassy carbon working electrode, a Pt auxiliary electrode and a Pt pseudo reference electrode), connected to a Princeton Applied Research PARSTAT 2273 electrochemical analyzer. Data obtained were exported to excel for analysis and diagram preparation.
Data source location	Institution: University of the Free State City/Town/Region: Bloemfontein Country: South Africa
Data accessibility	With the article
Related research article	P.J. Swarts, J. Conradie, Electrochemical behaviour of chloro- and hydroxy-subphthalocyanines, Electrochimica Acta https://doi.org/10.1016/j.electacta.2019.135165

Value of the Data

- This data provides cyclic voltammograms and detailed electrochemical data for three subphthalocyanines for scan rates over two orders of magnitude (0.05–5.0 Vs^{-1}).
- This data illustrates the influence of the solvent on the resolution of the cyclic voltammograms for three subphthalocyanines.
- This data illustrates the influence of the solvent on the value of the redox potentials for three subphthalocyanines.
- This data illustrates the influence of electron donating and electron withdrawing substituents on the redox potential of the subphthalocyanine.
- This data illustrates that electrochemical quasi reversible oxidation can be obtained when electrochemical experiments are performed in a high purity argon atmosphere, while using DCM or DCE as the solvent and $[N(^nBu)_4][B(C_6F_5)_4]$ as supporting electrolyte.

the structures of the SubPcs **1**–**3**. Cyclic voltammograms and redox data obtained in dichloromethane (DCM) as solvent are given in Figs. 2–7 and Tables 1–3 respectively. Cyclic voltammograms and redox data obtained in dichloroethane (DCE) as solvent are given in Figs. 8–13 and Tables 4–6 respectively. The 0.10 Vs^{-1} scans and data are from the research article related to this article "*Electrochemical behaviour of chloro- and hydroxy-subphthalocyanines*" [1]. The CV scan indicated in red in selected graphs are done at 5.00 V s^{-1}. The oxidation and reduction potential data obtained here, compare well with available published data on obtained under different experimental conditions (namely different solvents, scan rates and supporting electrolytes) for SubPc **1** [2–7] and SubPc **2** [8]. No detail electrochemical data is available for SubPc **3**. Data presented in this study for **1** and **3** in DCM, and **1**–**3** in DCE show electrochemical quasi reversible oxidation. No electrochemical quasi reversible oxidation with peak current ratios = 1 and peak current separation <0.09 V, is reported till date for SubPcs [3,4].

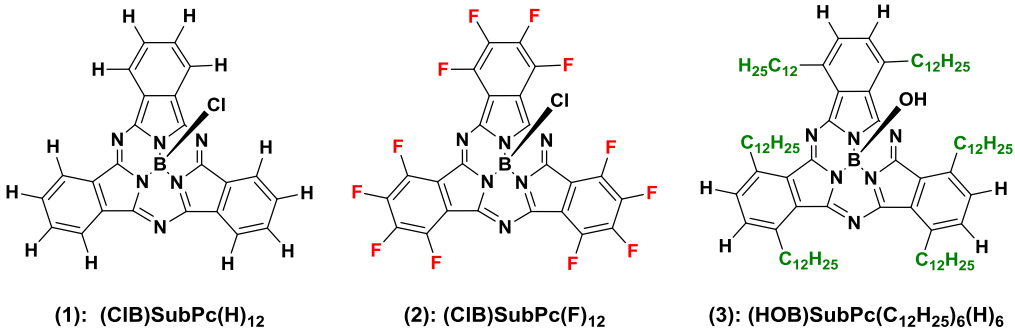

Fig. 1. Structure of the SubPcs 1–3.

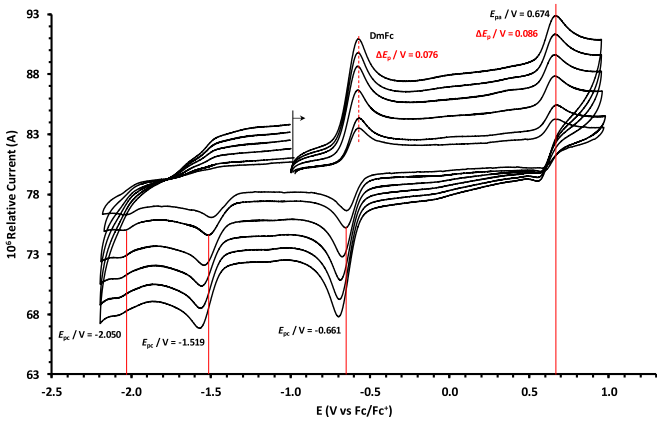

Fig. 2. Cyclic voltammograms in DCM of (ClB)SubPc(H)$_{12}$, 1, at scan rates 0.050 (smallest peak currents), 0.100, 0.200, 0.300, 0.400 and 0.500 (largest peak currents). All scans initiated in the positive direction. Wave I is the oxidation and waves II and III are reduction of (ClB)SubPc(H)$_{12}$. Data of 0.100 V s^{-1} shown on graph.

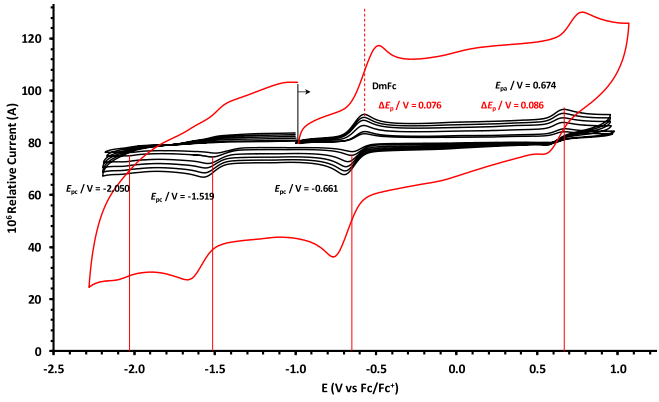

Fig. 3. Cyclic voltammograms in DCM of (ClB)SubPc(H)$_{12}$, 1, scan rates 0.050 (smallest peak currents), 0.100, 0.200, 0.300, 0.400, 0.500 and 5.000 Vs^{-1} (largest peak currents shown in red). All scans initiated in the positive direction. Wave I is the oxidation and waves II and III are reduction of (ClB)SubPc(H)$_{12}$. Data of 0.100 V s^{-1} shown on graph.

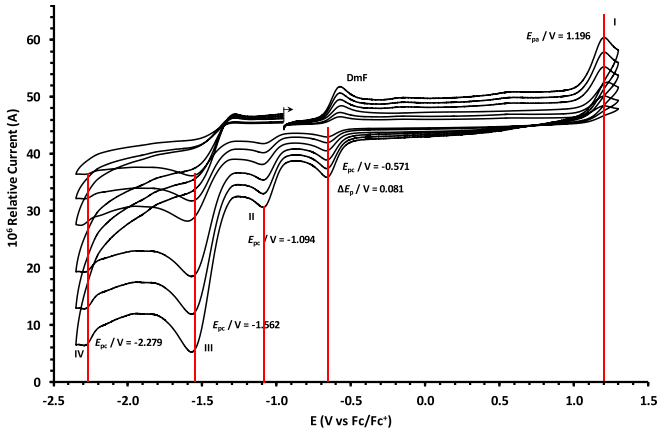

Fig. 4. Cyclic voltammograms in DCM of (ClB)SubPc(F)$_{12}$, 2, at scan rates 0.050 (smallest peak currents), 0.100, 0.200, 0.300, 0.400 and 0.500 (largest peak currents). All scans initiated in the positive direction. Wave I is the oxidation and waves II, III and IV are reduction of (ClB)SubPc(F)$_{12}$. Data of 0.100 V s^{-1} shown on graph.

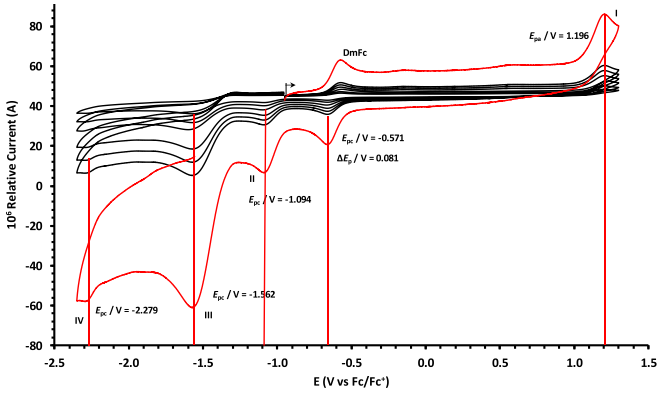

Fig. 5. Cyclic voltammograms in DCM of (ClB)SubPc(F)$_{12}$, 2, at scan rates 0.050 (smallest peak currents), 0.100, 0.200, 0.300, 0.400, 0.500 and 5.000 Vs^{-1} (largest peak currents shown in red). All scans initiated in the positive direction. Wave I is the oxidation and waves II, III and IV are reduction of (ClB)SubPc(F)$_{12}$. Data of 0.100 V s^{-1} shown on graph.

2. Experimental design, materials, and methods

Electrochemical studies by means of cyclic voltammetry (CV) experiments were performed in an M Bruan Lab Master SP glove box under a high purity argon atmosphere (H_2O and O_2 < 10 ppm), utilizing a Princeton Applied Research PARSTAT 2273 potentiostat running Powersuite software (Version 2.58).

The cyclic voltammetry experimental setup consists of a cell with three electrodes, namely (i) a glassy carbon electrode as working electrode, (ii) a platinum wire auxiliary and (ii) a platinum wire as pseudo reference electrode. The glassy carbon working electrode was polished and prepared before every experiment on a Buhler polishing mat first with 1-micron and then with ¼-micron diamond paste, rinsed with H_2O, acetone and DCM, and dried before each experiment.

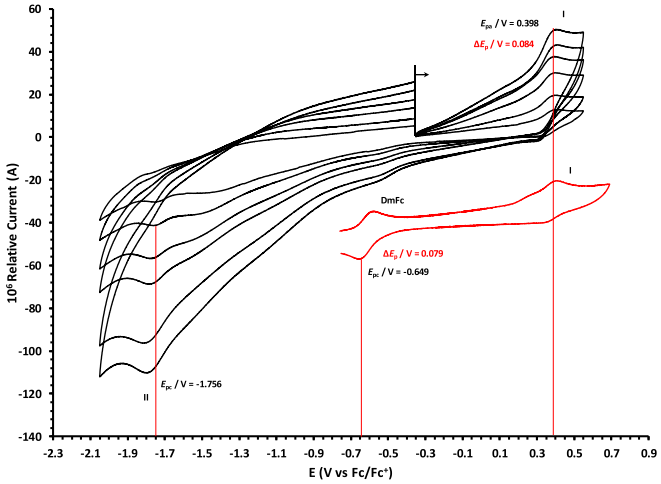

Fig. 6. Cyclic voltammograms in DCM of (HOB)SubPc($C_{12}H_{25}$)$_6$(H)$_6$, 3, at scan rates 0.050 (smallest peak currents), 0.100, 0.200, 0.300, 0.400 and 0.500 (largest peak currents). All scans initiated in the positive direction. Wave I is the oxidation and wave II is the reduction of (HOB)SubPc($C_{12}H_{25}$)$_6$(H)$_6$. Data of 0.100 V s^{-1} shown on graph.

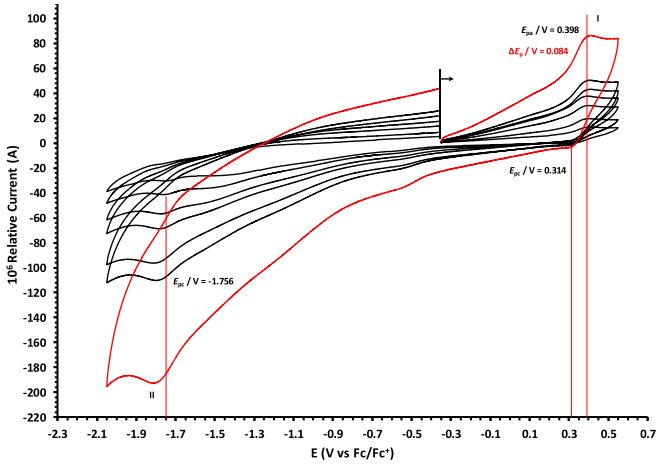

Fig. 7. Cyclic voltammograms in DCM of (HOB)SubPc($C_{12}H_{25}$)$_6$(H)$_6$, 3, at scan rates 0.050 (smallest peak currents), 0.100, 0.200, 0.300, 0.400, 0.500 and 5.000 Vs^{-1} (largest peak currents shown in red). All scans initiated in the positive direction. Wave I is the oxidation and wave II is the reduction of (HOB)SubPc($C_{12}H_{25}$)$_6$(H)$_6$. Data of 0.100 V s^{-1} shown on graph.

Electrochemical analysis in dichloromethane (DCM, anhydrous, $\geq$ 99.8%, contains 40–150 ppm amylene as stabilizer) as solvent was at RT and in dichloroethane (DCE, anhydrous, 99.8%) at 60 °C. The analyte solutions in DCM as solvent were: 0.0005 M for (ClB)SubPc(H)$_{12}$, 1, 0.0005 M for (ClB)SubPc(F)$_{12}$, 2, and 0.004 mol dm^{-3} for (SubPc 3). The analyte solutions in DCE as solvent were: 0.0005 M for (ClB)SubPc(H)$_{12}$, 1, 0.0005 M for (ClB)SubPc(F)$_{12}$, 2, and 0.004 mol dm^{-3} for (SubPc 3). The

Table 1
Electrochemical data (potential in V *vs* Fc/Fc^{+}) in DCM for *c.a.* 0.0005 mol dm^{-3} of (ClB)SubPc$(H)_{12}$, 1, at indicated scan rates (v in V/s).

v (V/s)	E_{pa}/V	ΔE_p/V	$E^{o\prime}$/V	i_{pa}/μA	i_{pc}/i_{pa}
Wave: I					
0.050	0.673	0.084	0.627	2.02	0.99
0.100	**0.674**	**0.086**	**0.628**	**3.08**	**0.99**
0.200	0.679	0.089	0.628	4.84	0.99
0.300	0.680	0.092	0.628	6.13	0.99
0.400	0.687	0.095	0.629	7.49	0.99
0.500	0.692	0.099	0.629	8.25	0.99
5.000	0.707	–	–	–	–
Wave: II					
0.050	−1.516	–	–	2.11	–
0.100	**−1.519**	-	-	**3.08**	-
0.200	−1.532	–	–	4.35	–
0.300	−1.544	–	–	6.15	–
0.400	−1.566	–	–	7.49	–
0.500	−1.574	–	–	8.34	–
5.000	−1.592	–	–	–	–
Wave: III					
0.050	−2.050	–	–	–	–
0.100	**−2.050**	-	-	-	-
0.200	−2.051	–	–	–	–
0.300	−2.051	–	–	–	–
0.400	−2.051	–	–	–	–
0.500	−2.051	–	–	–	–
5.000	−2.055	–	–	–	–

Data for 0.100 V/s shown in bold font.

Table 2
Electrochemical data (potential in V *vs* Fc/Fc^{+}) in DCM for *c.a.* 0.0005 mol dm^{-3} of (ClB)SubPc$(F)_{12}$, 2, at indicated scan rates.

v (V/s)	E_{pa}/V	ΔE_p/V	$E^{o\prime}$/V	i_{pa}/μA	i_{pc}/i_{pa}
Wave: I					
0.050	1.196	–	–	1.99	–
0.100	**1.196**	-	-	**3.21**	-
0.200	1.196	–	–	4.98	–
0.300	1.197	–	–	6.21	–
0.400	1.197	–	–	8.11	–
0.500	1.197	–	–	9.00	–
5.000	1.207	–	–	–	–
Wave: II					
0.050	−1.093	–	–	1.95	–
0.100	**−1.094**	**0.088**	**−1.050**	**3.22**	**0.97**
0.200	−1.098	–	–	4.58	–
0.300	−1.101	–	–	6.15	–
0.400	−1.108	–	–	8.78	–
0.500	−1.110	–	–	9.25	–
5.000	−1.119	–	–	–	–
Wave: III					
0.050	−1.560	–	–	–	–
0.100	**−1.562**	-	-	-	-
0.200	−1.564	–	–	–	–
0.300	−1.567	–	–	–	–
0.400	−1.568	–	–	–	–
0.500	−1.570	–	–	–	–
5.000	−1.581	–	–	–	–
Wave: IV					
0.050	−2.276	–	–	–	–
0.100	**−2.279**	-	-	-	-
0.200	−2.284	–	–	–	–
0.300	−2.288	–	–	–	–
0.400	−2.290	–	–	–	–
0.500	−2.292	–	–	–	–
5.000	−2.311	–	–	–	–

Data for 0.100 V/s shown in bold font.

Table 3
Electrochemical data (potential in V *vs* Fc/Fc^{+}) in DCM for *c.a.* 0.002 mol dm^{-3} of (HOB)SubPc$(C_{12}H_{25})_6(H)_6$, 3, at indicated scan rates.

ν (V/s)	E_{pa}/V	ΔE_p/V	$E^{o\prime}$/V	i_{pa}/μA	i_{pc}/i_{pa}
Wave: I					
0.050	0.398	0.082	0.355	2.22	–
0.100	**0.398**	**0.084**	**0.356**	**3.46**	-
0.200	0.399	0.086	0.356	4.98	–
0.300	0.401	0.088	0.356	6.23	–
0.400	0.402	0.090	0.358	8.01	–
0.500	0.402	0.092	0.359	9.11	–
5.000	0.405	–	–	–	–
Wave: II					
0.050	−1.752	–	–	–	–
0.100	**−1.756**	-	-	-	-
0.200	−1.762	–	–	–	–
0.300	−1.769	–	–	–	–
0.400	−1.772	–	–	–	–
0.500	−1.780	–	–	–	–
5.000	−1.792	–	–	–	–

Data for 0.100 V/s shown in bold font.

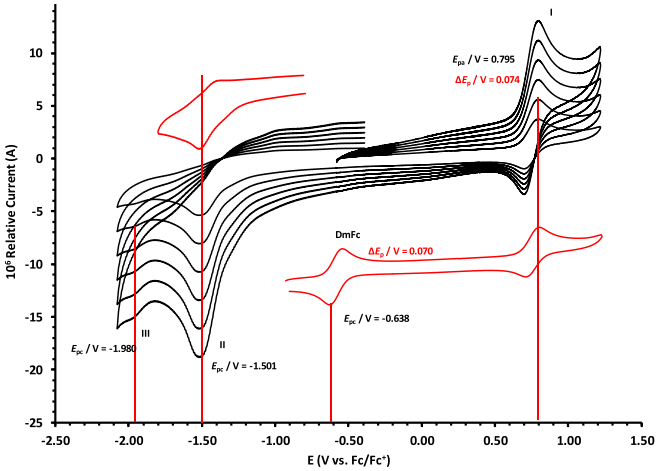

Fig. 8. Cyclic voltammograms in DCE of (ClB)SubPc$(H)_{12}$, 1, at scan rates 0.050 (smallest peak currents), 0.100, 0.200, 0.300, 0.400 and 0.500 (largest peak currents). All scans initiated in the positive direction. Wave I is the oxidation and waves II and III are reduction of (ClB)SubPc$(H)_{12}$. Data of 0.100 V s^{-1} shown on graph.

supporting electrolyte 0.1 mol dm^{-3} (in DCM) or 0.2 mol dm^{-3} (in DCE) tetrabutylammonium tetrakispentafluorophenylborate $[N(^{n}Bu)_4][B(C_6F_5)_4]$ [9].

Experimental potential data was measured vs. the redox couple of decamethyl ferrocene DmFc as internal standard and reported vs. the redox couple of ferrocene Fc, as suggested by IUPAC [10]. Under our experimental conditions E(DmFc/DmFc+ = − 0.610 V Fc/Fc^{+} (DCM) and −0.597 V Fc/Fc^{+} (DCE) (see Figs. 14 and 15). Scan rates were done over two orders of magnitude, namely between 0.05 and 5.00 Vs^{-1}.

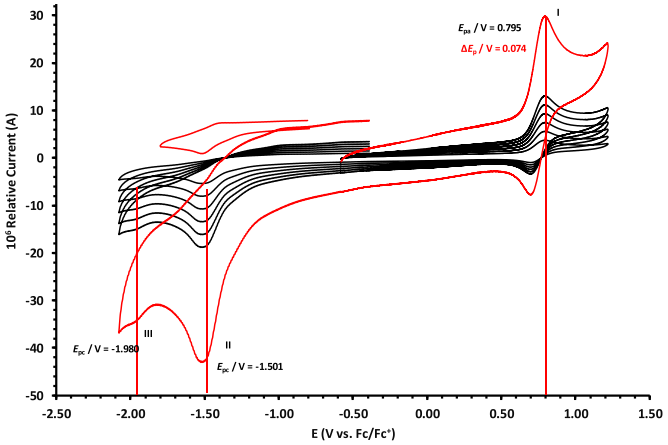

Fig. 9. Cyclic voltammograms in DCE of (ClB)SubPc(H)$_{12}$, 1, scan rates 0.050 (smallest peak currents), 0.100, 0.200, 0.300, 0.400, 0.500 and 5.000 Vs^{-1} (largest peak currents shown in red). All scans initiated in the positive direction. Wave I is the oxidation and waves II and III are reduction of (ClB)SubPc(H)$_{12}$. Data of 0.100 V s^{-1} shown on graph.

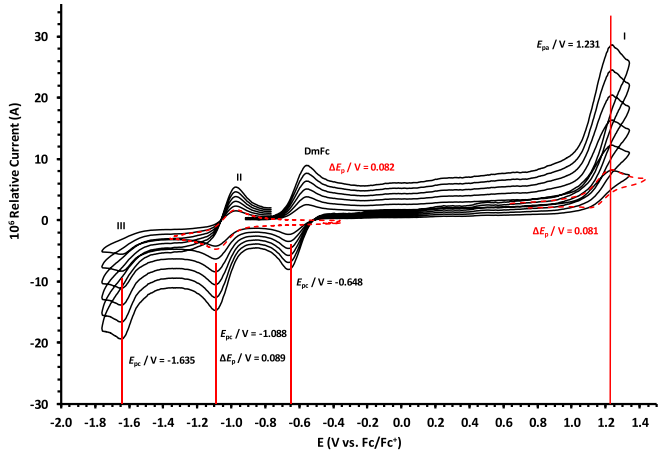

Fig. 10. Cyclic voltammograms in DCE of (ClB)SubPc(F)$_{12}$, 2, at scan rates 0.050 (smallest peak currents), 0.100, 0.200, 0.300, 0.400 and 0.500 (largest peak currents). All scans initiated in the positive direction. Wave I is the oxidation and waves II and III are reduction of (ClB)SubPc(F)$_{12}$. Data of 0.100 V s^{-1} shown on graph. Dotted lines are 0.050 V s^{-1}.

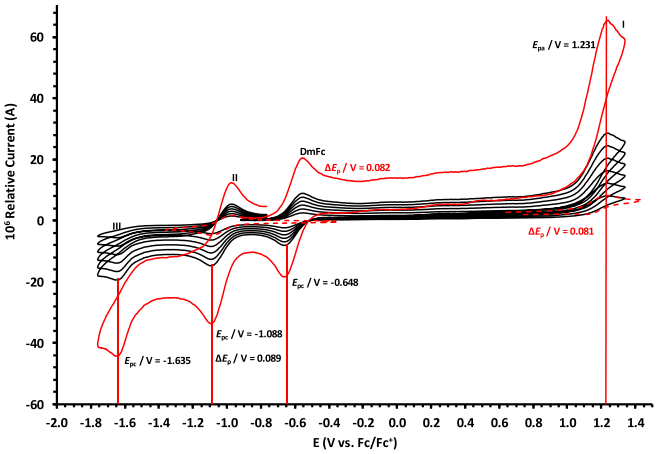

Fig. 11. Cyclic voltammograms in DCE of (ClB)SubPc(F)$_{12}$, 2, at scan rates 0.050 (smallest peak currents), 0.100, 0.200, 0.300, 0.400, 0.500 and 5.000 Vs^{-1} (largest peak currents shown in red). All scans initiated in the positive direction. Wave I is the oxidation and waves II and III are reduction of (ClB)SubPc(F)$_{12}$. Data of 0.100 V s^{-1} shown on graph. Dotted lines are 0.050 V s^{-1}.

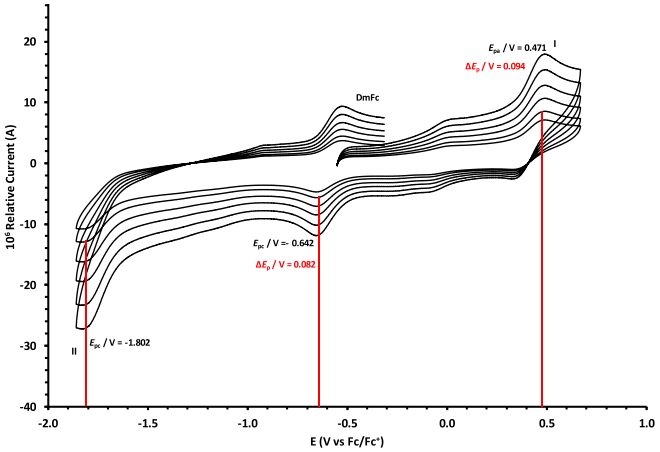

Fig. 12. Cyclic voltammograms in DCE of (HOB)SubPc($C_{12}H_{25}$)$_6$(H)$_6$, 3, at scan rates 0.050 (smallest peak currents), 0.100, 0.200, 0.300, 0.400 and 0.500 (largest peak currents). All scans initiated in the positive direction. Wave I is the oxidation and wave II is the reduction of (HOB)SubPc($C_{12}H_{25}$)$_6$(H)$_6$. Data of 0.100 V s^{-1} shown on graph.

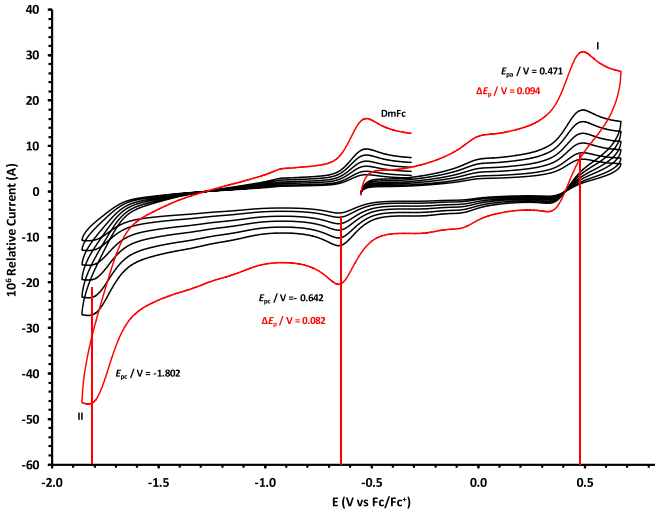

Fig. 13. Cyclic voltammograms in DCE of (HOB)SubPc($C_{12}H_{25}$)$_6$(H)$_6$, 3, at scan rates 0.050 (smallest peak currents), 0.100, 0.200, 0.300, 0.400, 0.500 and 5.000 Vs^{-1} (largest peak currents shown in red). All scans initiated in the positive direction. Wave I is the oxidation and wave II is the reduction of (HOB)SubPc($C_{12}H_{25}$)$_6$(H)$_6$. Data of 0.100 V s^{-1} shown on graph.

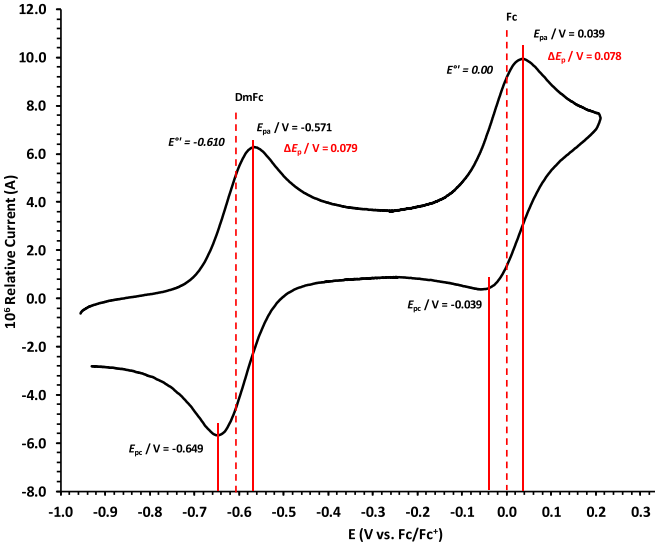

Fig. 14. Cyclic voltammograms in DCM of Decamethylferrocene at scan rate 0.100 Vs^{-1}. All scans initiated in the positive direction. Data of 0.100 V s^{-1} shown on graph.

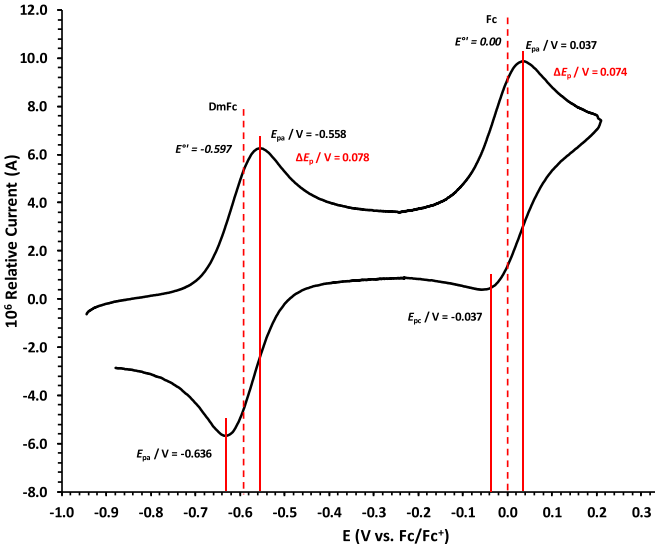

Fig. 15. Cyclic voltammograms in DCE of Decamethylferrocene at scan rate 0.100 Vs^{-1}. All scans initiated in the positive direction. Data of 0.100 V s^{-1} shown on graph.

Table 4
Electrochemical data (potential in V *vs* Fc/Fc^{+}) in DCE for *c.a.* 0.0005 mol dm^{-3} of (ClB)SubPc$(H)_{12}$, 1, at indicated scan rates (v in V/s).

v (V/s)	E_{pa}/V	ΔE_p/V	$E^{o\prime}$/V	i_{pa}/μA	i_{pc}/i_{pa}
Wave: I					
0.050	0.795	0.072	0.757	2.14	0.99
0.100	**0.795**	**0.074**	**0.758**	**3.75**	**0.99**
0.200	0.796	0.076	0.758	4.95	0.99
0.300	0.796	0.078	0.759	6.11	0.99
0.400	0.797	0.081	0.759	7.95	0.99
0.500	0.798	0.082	0.759	8.95	0.99
5.000	0.808	–	–	–	–
Wave: II					
0.050	−1.501	–	–	2.36	–
0.100	**−1.501**	-	-	**3.75**	-
0.200	−1.502	–	–	4.92	–
0.300	−1.502	–	–	6.44	–
0.400	−1.503	–	–	7.98	–
0.500	−1.504	–	–	10.62	–
5.000	−1.505	–	–	–	–
Wave: III					
0.050	−1.980	–	–	–	–
0.100	**−1.980**	-	-	-	-
0.200	−1.980	–	–	–	–
0.300	−1.980	–	–	–	–
0.400	−1.980	–	–	–	–
0.500	−1.980	–	–	–	–
5.000	−1.980	–	–	–	–

Data for 0.100 V/s shown in bold font.

Table 5
Electrochemical data (potential in V *vs* Fc/Fc^{+}) in DCE for *c.a.* 0.0005 mol dm^{-3} of (ClB)SubPc$(F)_{12}$, 2, at indicated scan rates.

v (V/s)	E_{pa}/V	ΔE_p/V	$E^{o\prime}$/V	i_{pa}/μA	i_{pc}/i_{pa}
Wave: I					
0.050	1.230	0.080	1.190	2.18	0.99
0.100	**1.231**	**0.081**	**1.190**	**3.75**	**0.99**
0.200	1.232	0.083	1.191	5.24	0.99
0.300	1.233	0.084	1.191	6.29	0.99
0.400	1.234	0.085	1.191	8.65	0.99
0.500	1.235	0.087	1.191	9.54	0.99
5.000	–	–	–	–	–
Wave: II					
0.050	−1.087	0.088	−1.043	2.90	0.99
0.100	**−1.088**	**0.089**	**−1.044**	**3.80**	**0.99**
0.200	−1.089	0.091	−1.044	5.25	0.99
0.300	−1.092	0.093	−1.045	7.32	0.99
0.400	−1.092	0.094	−1.045	8.55	0.99
0.500	−1.094	0.096	−1.046	10.60	0.99
5.000	–	–	–	–	–
Wave: III					
0.050	−1.634	–	–	2.89	–
0.100	**−1.635**	–	–	**3.65**	–
0.200	−1.636	–	–	5.43	–
0.300	−1.637	–	–	7.38	–
0.400	−1.639	–	–	8.74	–
0.500	−1.641	–	–	10.12	–
5.000	–	–	–	–	–

Data for 0.100 V/s shown in bold font.

Table 6
Electrochemical data (potential in V *vs* Fc/Fc^{+}) in DCE for *c.a.* 0.002 mol dm^{-3} of (HOB)SubPc$(C_{12}H_{25})_6(H)_6$, 3, at indicated scan rates.

v (V/s)	E_{pa}/V	ΔE_p/V	$E^{o\prime}$/V	i_{pa}/μA	i_{pc}/i_{pa}
Wave: I					
0.050	0.471	0.093	0.424	2.34	0.92
0.100	**0.471**	**0.094**	**0.426**	**3.98**	**0.94**
0.200	0.471	0.095	0.426	4.95	0.95
0.300	0.472	0.095	0.427	6.12	0.95
0.400	0.472	0.096	0.428	7.42	0.96
0.500	0.482	0.097	0.428	7.95	0.96
5.000	0.493	–	–	–	–
Wave: II					
0.050	−1.801	–	–	–	–
0.100	**−1.804**	–	–	–	–
0.200	−1.811	–	–	–	–
0.300	−1.815	–	–	–	–
0.400	−1.821	–	–	–	–
0.500	−1.834	–	–	–	–
5.000	−1.844	–	–	–	–

Data for 0.100 V/s shown in bold font.

Acknowledgments

This work has received support from the South African National Research Foundation (Grant numbers 113327 and 96111) and the Central Research Fund of the University of the Free State, Bloemfontein, South Africa.

Conflict of Interest

The authors declare that they have no known competing financial interests or personal relationships that could have appeared to influence the work reported in this paper.

References

[1] P.J. Swarts, J. Conradie, Electrochemical behaviour of chloro- and hydroxy- subphthalocyanines, Electrochim. Acta (2020) 135165, https://doi.org/10.1016/j.electacta.2019.135165.
[2] M.V. Fulford, D. Jaidka, A.S. Paton, G.E. Morse, E.R.L. Brisson, A.J. Lough, T.P. Bender, Crystal structures, reaction rates, and selected physical properties of halo-boronsubphthalocyanines (Halo = Fluoride, chloride, and bromide), J. Chem. Eng. Data 57 (2012) 2756–2765, https://doi.org/10.1021/je3005112.
[3] P.V. Solntsev, K.L. Spurgin, J.R. Sabin, A.A. Heikal, V.N. Nemykin, Photoinduced charge transfer in short-distance ferrocenylsubphthalocyanine dyads, Inorg. Chem. 51 (2012) 6537–6547, https://doi.org/10.1021/ic3000608.
[4] B. Del Rey, U. Keller, T. Torres, G. Rojo, F. Agulló-López, S. Nonell, C. Martí, S. Brasselet, I. Ledoux, J. Zyss, Synthesis and nonlinear optical, photophysical, and electrochemical properties of subphthalocyanines, J. Am. Chem. Soc. 120 (1998) 12808–12817, https://doi.org/10.1021/ja980508q.
[5] P. Sullivan, A. Duraud, L. Hancox, N. Beaumont, G. Mirri, J.H.R. Tucker, R.A. Hatton, M. Shipman, T.S. Jones, Halogenated boron subphthalocyanines as light harvesting electron acceptors in organic photovoltaics, Adv. Energy Mater. 1 (2011) 352–355, https://doi.org/10.1002/aenm.201100036.
[6] F. Camerel, G. Ulrich, P. Retailleau, R. Ziessel, Ethynyl-boron subphthalocyanines displaying efficient cascade energy transfer and large Stokes shifts, Angew. Chem. Int. Ed. 47 (2008) 8876–8880, https://doi.org/10.1002/anie.200803131.
[7] E. Ohno-Okumura, K. Sakamoto, T. Kato, T. Hatano, K. Fukui, T. Karatsu, A. Kitamura, T. Urano, Synthesis of subphthalocyanine derivatives and their characterization, Dyes Pigments 53 (2002) 57–65, https://doi.org/10.1016/S0143-7208(01)00102-4.
[8] R.A. Kipp, J.A. Simon, M. Beggs, H.E. Ensley, R.H. Schmehl, Photophysical and photochemical investigation of a dodecafluorosubphthalocyanine derivative, J. Phys. Chem. A 102 (1998) 5659–5664, https://doi.org/10.1021/jp980383b.
[9] H.J. Gericke, N.I. Barnard, E. Erasmus, J.C. Swarts, M.J. Cook, M.A.S. Aquino, Solvent and electrolyte effects in enhancing the identification of intramolecular electronic communication in a multi redox-active diruthenium tetraferrocenoate complex, a triple-sandwiched dicadmium phthalocyanine and a ruthenocene-containing β-diketone, Inorg. Chim. Acta 363 (2010) 2222–2232, https://doi.org/10.1016/j.ica.2010.03.031.
[10] G. Gritzner, J. Kuta, Recommendations on reporting electrode potentials in nonaqueous solvents, Pure Appl. Chem. 56 (1984) 461–466, https://doi.org/10.1351/pac198456040461.

Electrochemical behaviour of chloro- and hydroxy- subphthalocyanines

*Pieter J. Swarts and Jeanet Conradie**

Department of Chemistry, University of the Free State, P.O. Box 339, Bloemfontein, 9300, South Africa

Supporting Information

1 Synthesis

The synthetic methods reported below were modified to improve yields and simplify reaction setup. Below is the reaction scheme for SubPcs **1** – **3**, **Scheme 1**.

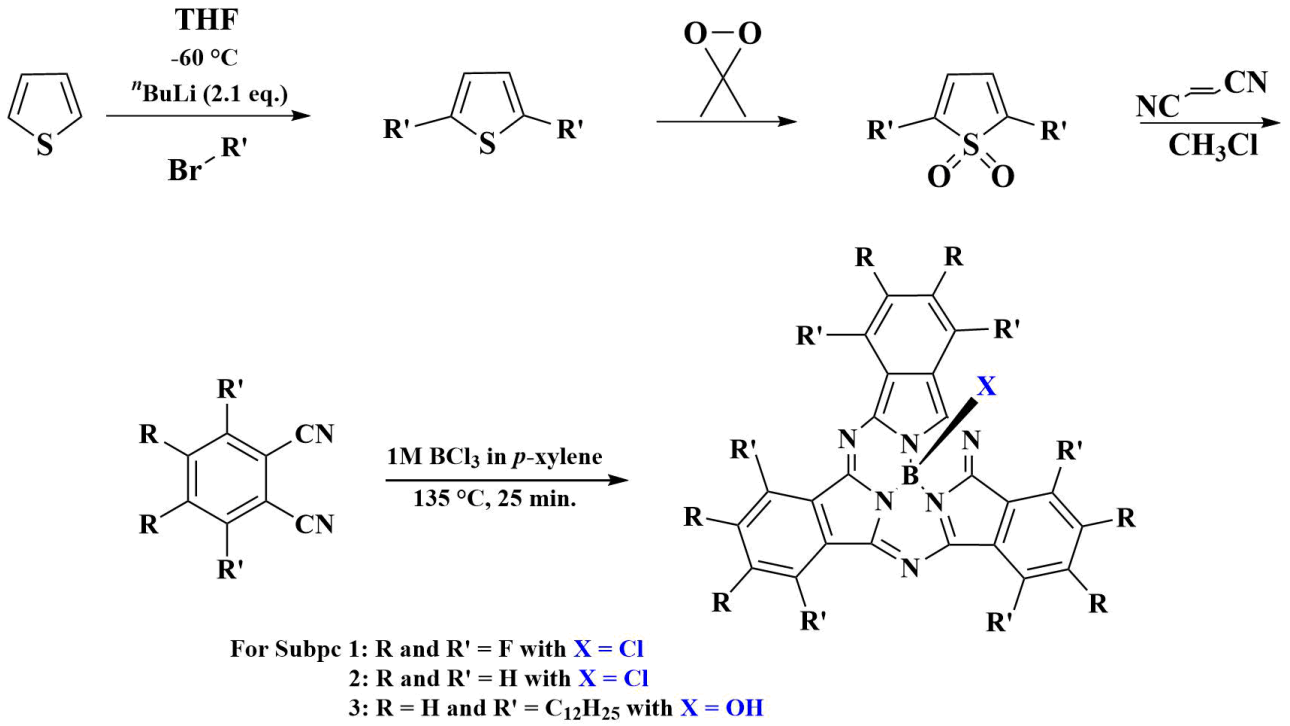

Scheme 1. Reaction scheme of SubPcs, ClBSubPc(F)$_{12}$, **1**, ClBSubPc(H)$_{12}$, **2**, and (HO)BSubPc(C$_{12}$H$_{25}$)$_6$(H)$_6$, **3**.

Preparation of 2,5-didodecylthiophene [1]**:** To a solution of thiophene (0.5 g, 0.0005 dm^3, 0.0059 mol) in anhydrous THF (dried over sodium; 0.01 dm^3), pre-cooled to -60°C in an isopropanol bath, was added under argon over 30 min *n*-butyllithium in hexanes (0.0063 dm^3 of a 2.0 mol dm^{-3} solution, 0.0125 mol, 2.1 eq.). After the addition was completed the reaction mixture was allowed to spontaneously heat up to room temperature, while stirring continued for 18 hours at room temperature. The dilithiated species that formed during this time was not isolated but treated *in situ* at -60°C under argon over 30 minutes with 1-bromododecane (2.96 g, 0.0028 cm^3, 0.012 mol, 2 eq.). The stirred reaction mixture was then allowed to warm to room temperature. After 18 hours it was poured onto ice, the product extracted with diethyl ether (3 x 0.07 dm^3) and the organic extracts were washed with H_2O (2 x 0.07 dm^3) before it was dried with ($MgSO_4$) and filtered. Removal of solvents was followed by recrystallization of the residue from warm ethanol and gave pure 2,5-

dodecylthiophene (yield: 0.47 g, 94 %) as an off-white low-melting wax after solvent evaporation, m.p.: 56°C. ^{1}H NMR: δ_H (600.28 MHz, $CDCl_3$, 25 °C): δ 6.53 (2 H, s, C_4H_2), 2.71 (4 H, t, 2 x CH_2), 1.62 (4 H, m, 2 x CH_2), 1.24 (36 H, m, 18 x CH_2), 0.86 (6 H, t, 2 x CH_3). Elemental analysis calculated for $C_{28}H_{52}S$ (element, %): C, 79.92; H, 12.46; S, 7.62 obtained: C, 80.03; H, 12.78.

Preparation of 2,5-didodecylthiophene-1,1-dioxide [1]**:** To a 1 dm^3 2-neck flask, equipped with an efficient stirrer, a large condenser (acetone cooled to – 40 °C with an electronic cold finger) and charged with H_2O (0.4 dm^3), acetone (0.3 dm^3) and $NaHCO_3$ (200 g, 2.3 mol, 140 eq.) was added a solution of 2,5-dodecylthiophene (10 g, 0.017 mol) in dichloromethane (0.3 dm^3). The resulting heterogeneous mixture was cooled in an ice bath before solid oxone (350 g, 11 mol ,66 eq.) was carefully added over 30 min under efficient stirring. Stirring continued at 0°C for 16 hours before water (2 dm^3) was added to dissolve most inorganics. The aqueous filtered layer, and all remaining solids were extracted with chloroform, the combined organic phases washed with water (0.2 – 0.3 dm^3) and dried ($MgSO_4$) before solvent removal and recrystallization of the residue from warm ethanol gave pure off-white 2,5-didodecylthiophene-1,1-dioxide (yield: 9.12 g, 91 %). m.p.: 88°C. ^{1}H NMR: δ_H (600.28 MHz, $CDCl_3$): δ 6.24 (2 H, s, C_4H_2), 2.44 (4 H, t, 2 x CH_2), 1.63 (4 H, m, 2 x CH_2), 1.35 (4 H, m, 2 x CH_2), 1.24 (36 H, m, 18 x CH_2) and 0.86 (6 H, t, 2 x CH_3). Elemental analysis calculated for $C_{28}H_{52}O_2S$ (element, %): C, 74.28; H, 11.58; O, 7.07; S, 7.08 obtained: C, 74.88; H, 11.98; O, 7.37.

Preparation of 3,6-didodecylphthalonitrile [1]**:** A minimum amount of chloroform (*ca.* 0.2 cm^3) was used to dissolve 2,5-didodecylthiophene-1,1-dioxide (2 g, 0.004 mol) and fumaronitrile (0.345 g, 0.004 mmol, 1 eq.). The stirred solution was sealed in a high-pressure glass vessel and heated to 160°C. After 24 hours the contents of the reactor vessel were dissolved in chloroform and the solvent evaporated under reduced pressure at 90°C. The oily residue was kept under reduced pressure until it no longer liberated gas anymore (*ca.* 1 hour). The remaining residue was chromatographed over silica

with toluene as eluent. The second eluted band afforded after solvent removal and recrystallization from ethanol 3,6-dodecylphthalonitrile (yield: 1.82 g, 91 %). MP: 82°C. ^{1}H NMR: δ_H (600.28 MHz, $CDCl_3$): δ 7.43 (2 H, s, C_4H_2), 2.82 (4 H, t, 2 x CH_2), 1.63 (4 H, m, 2 x CH_2), 1.35 (4 H, m, 2 x CH_2), 1.23 (36 H, m, 18 x CH_2) and 0.86 (6 H, t, 2 x CH_3). Elemental analysis calculated for $C_{32}H_{52}N_2$ (element, %): C, 82.70; H, 11.28; N, 6.03 obtained C, 83.09; H, 11.68; N, 6.73.

Preparation of ClBSubPc(F)$_{12}$, 1: BCl_3 (6 cm^3,1 M solution in p-xylene, 1.5 eq.) was added to dry phthalonitrile (0.4 g, 1.9 mmol) in a glove box (H_2O: < 0.5 ppm and O_2: < 10 ppm) at room temperature in a high-pressure glass tube. The reaction mixture was stirred under reflux (137°C) for 30 minutes. The solvent was evaporated and the solid was extracted with toluene (0.1 dm^3). The solution was evaporated, and the resultant purple solid was purified by means of silica gel column chromatography using hexane: ethyl acetate (3:1, v:v, R_f: 0.68). Pure ClBSubPc(F)$_{12}$ was obtained as a purple solid, yield: 92 % (0.368 g). m.p.: 355 – 360°C. ^{11}B NMR: δ_B (128.38 MHz, $CDCl_3$): δ -14.89 (1B). ^{13}C NMR: δ_C (150.95 MHz, $CDCl_3$, 25 °C): δ 149.23 (6C, C=N: inner core carbons), 144.92 (6C, C=C: iminoisoindoline unit), 140.75 (6C, non-peripheral C_6), 108.33 (6C, peripheral C_6). ^{19}F NMR: δ_C (564.33 MHz, $CDCl_3$, 25 °C): δ -136.27 (6H, q, non-peripheral H_6) and -146.81 (6H, q, peripheral H_6). IR: υ/cm^{-1}: 1479 (C=C, Stretch). Elemental analysis calculated for $C_{24}BClF_{12}N_6$ (element, %): C, 44.59; F, 35.26; N, 13.00, obtained: C, 46.99; F, 34.89; N, 12.74.

Preparation of ClBSubPc(H)$_{12}$, 2: BCl_3 (15 cm^3,1 M solution in p-xylene, 1.5 eq.) was added to dry phthalonitrile (1 g, 0.008 mol) in a glove box (H_2O: < 0.5 ppm and O_2: < 10 ppm) at room temperature in a high-pressure glass tube. The reaction mixture was stirred under reflux (137°C) for 30 minutes. The solvent was evaporated and the solid was extracted with toluene (0.4 dm^3). The solution was evaporated, and the resultant purple solid was thoroughly washed with methanol (0.2 dm^3) and hexane (0.2 dm^3). Pure ClBSubPc(H)$_{12}$ was obtained as a purple solid, yield: 94 % (0.94 g). m.p.: 375 –

380°C. ^{1}H NMR: δ_H (600.28 MHz, $CDCl_3$): δ 8.88 (6H, m, non-peripheral H_6) and 7.94 (6H, q, peripheral H_6). ^{11}B NMR: δ_B (128.38 MHz, $CDCl_3$): δ -16.22 (1B). ^{13}C NMR: δ_C (150.95 MHz, $CDCl_3$, 25 °C): δ 149.68 (6C, C=N: inner core carbons), 125.68 (6C, C=C: iminoisoindoline unit), 122.01 (6C, non-peripheral C_6), 119.84 (6C, peripheral C_6). IR: υ/cm^{-1}: 1451 (C=C, Stretch). Elemental analysis calculated for $C_{24}H_{12}BClN_6$ (element, %): C, 66.94; H, 2.81; N, 19.51, obtained: C, 66.42; H, 2.68; N, 18.31.

2 NMR

2.1 ^{1}H NMR: 2,5-didodecylthiophene

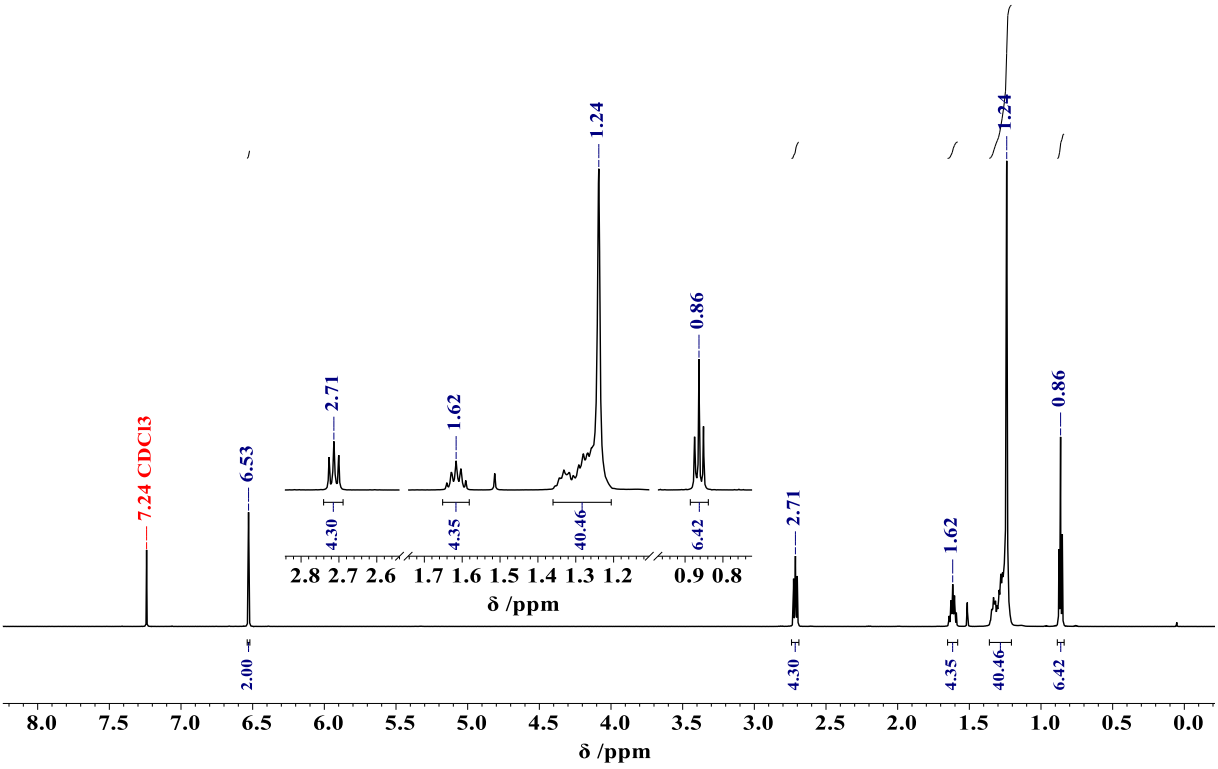

2.2 ^{1}H NMR: 2,5-didodecylthiophene-1,1-dioxide

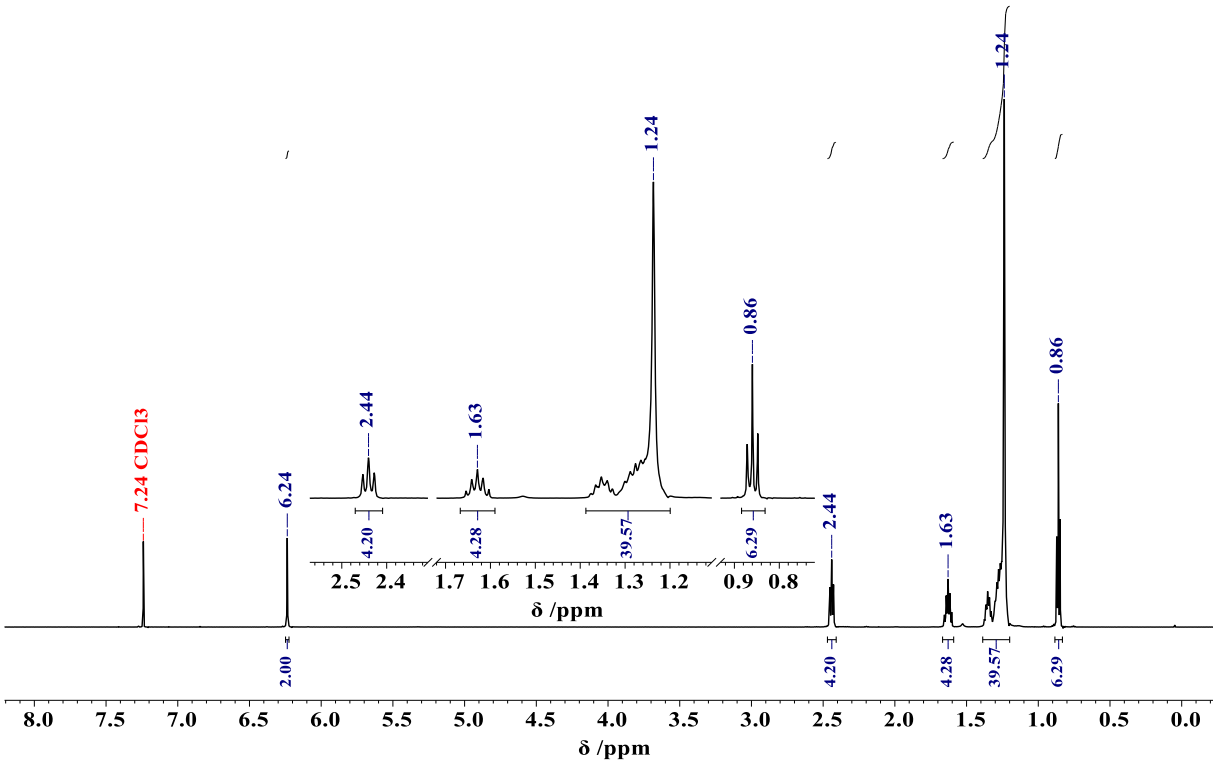

2.3 ^{1}H NMR: 3,6-didodecylphthalonitrile

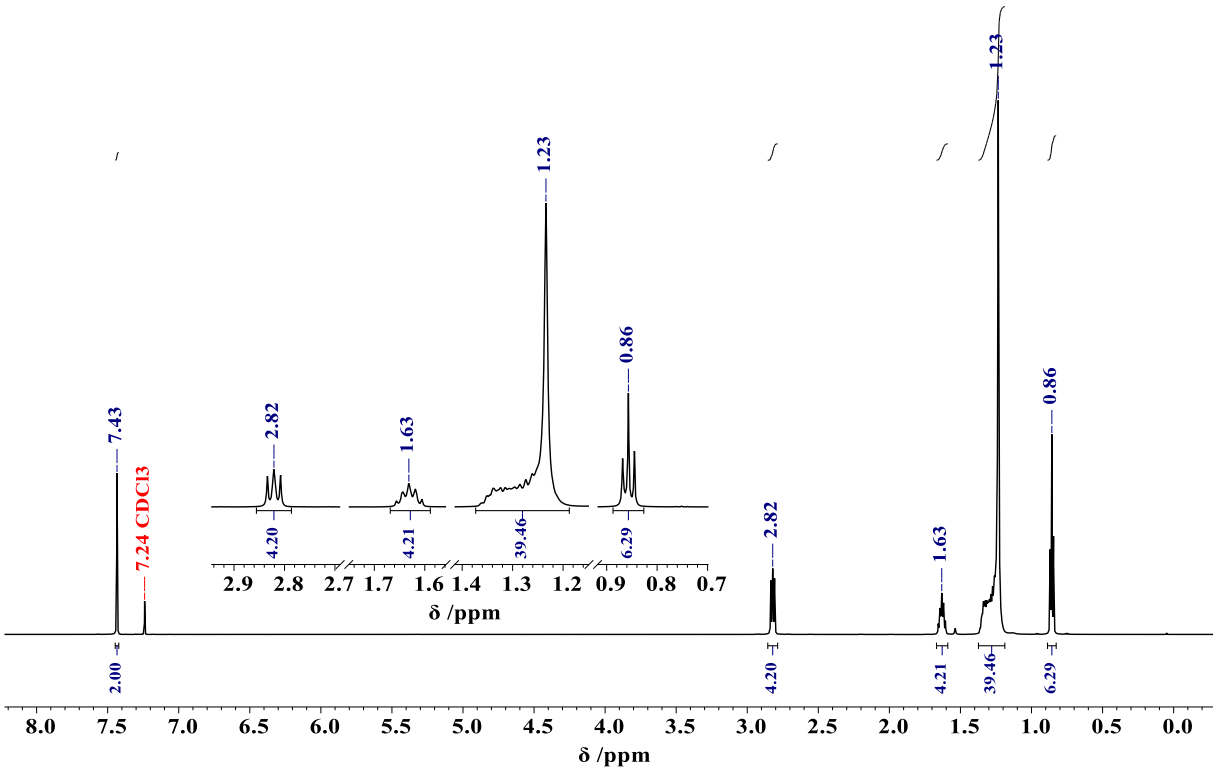

2.4 ^{11}B NMR: ClBubPc(F)$_{12}$

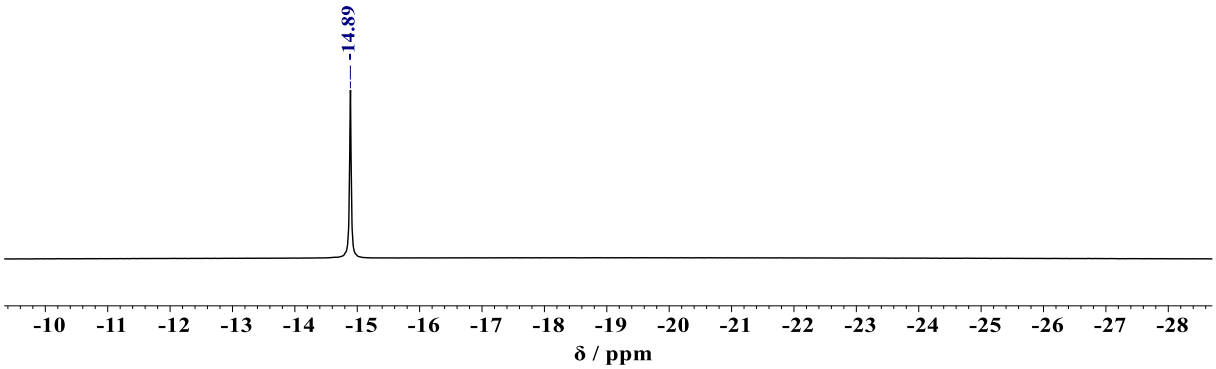

2.5 ^{13}C NMR ClBSubPc(F)$_{12}$

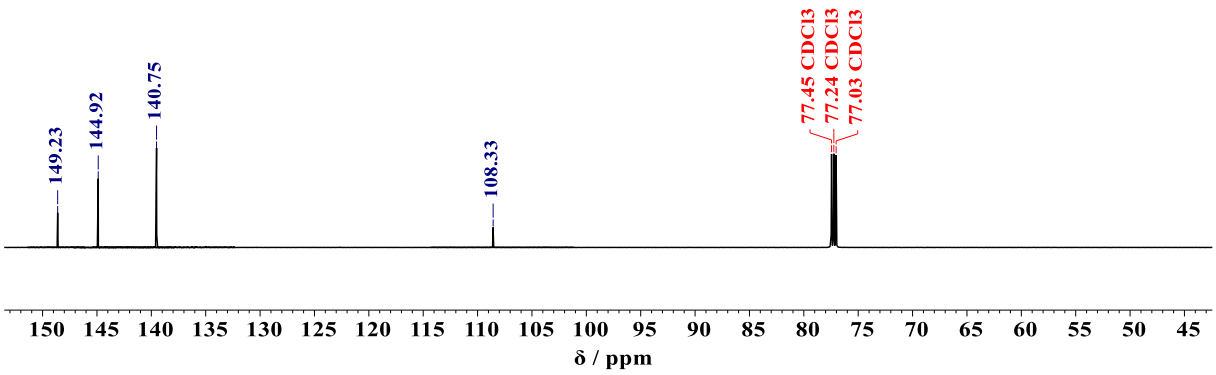

2.6 ^{19}F NMR: ClBSubPc(F)$_{12}$

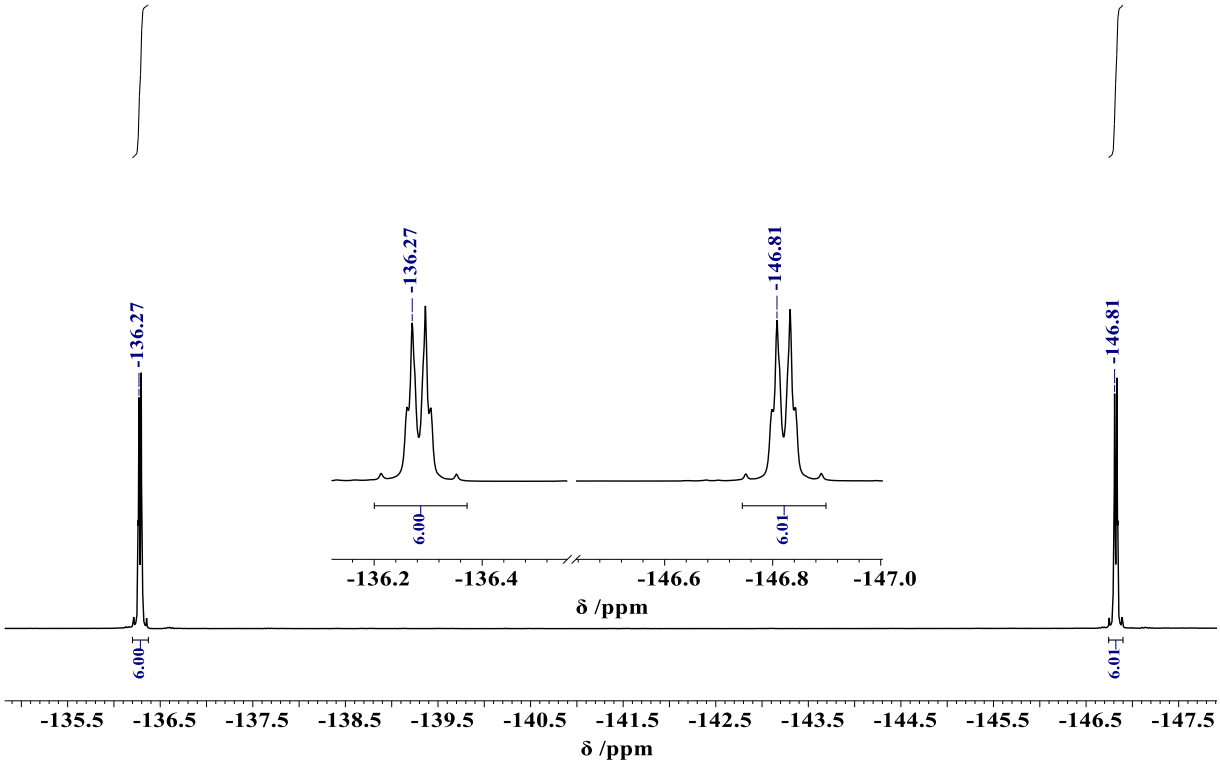

2.7 ^{1}H NMR: ClBSubPc(H)$_{12}$

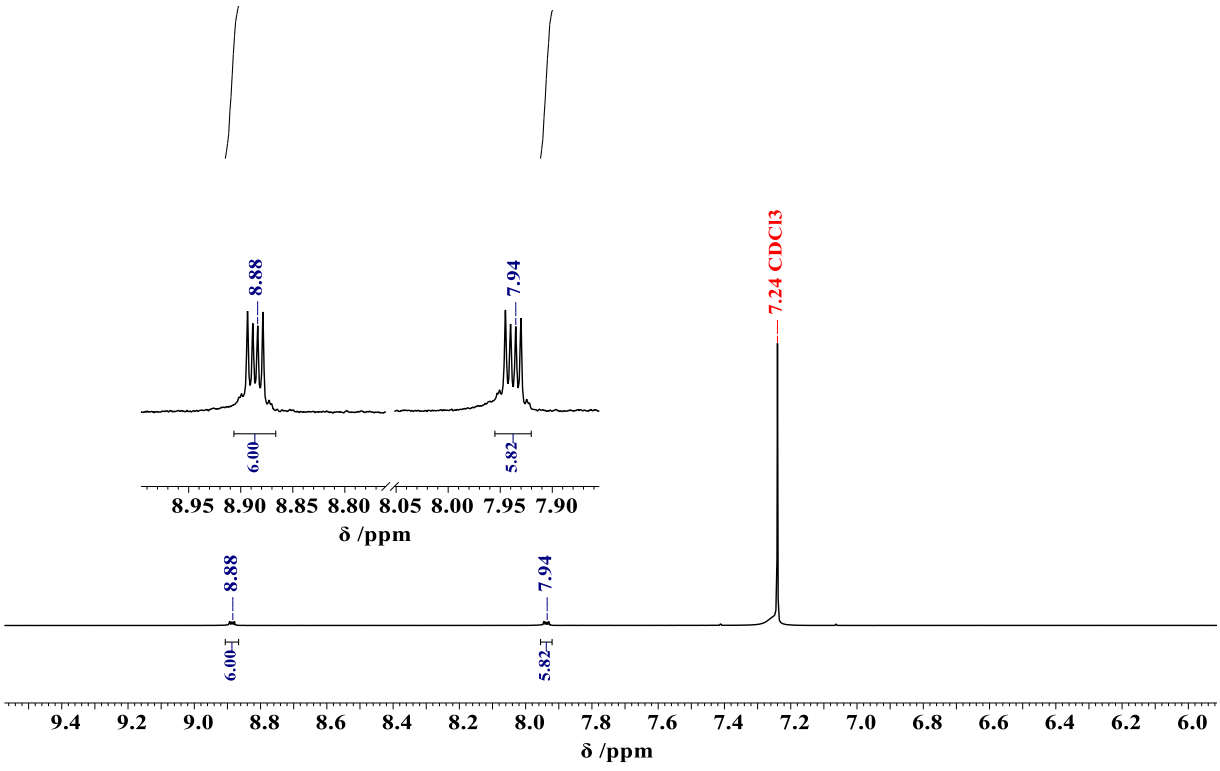

2.8 ^{11}B NMR: ClBSubPc(H)$_{12}$

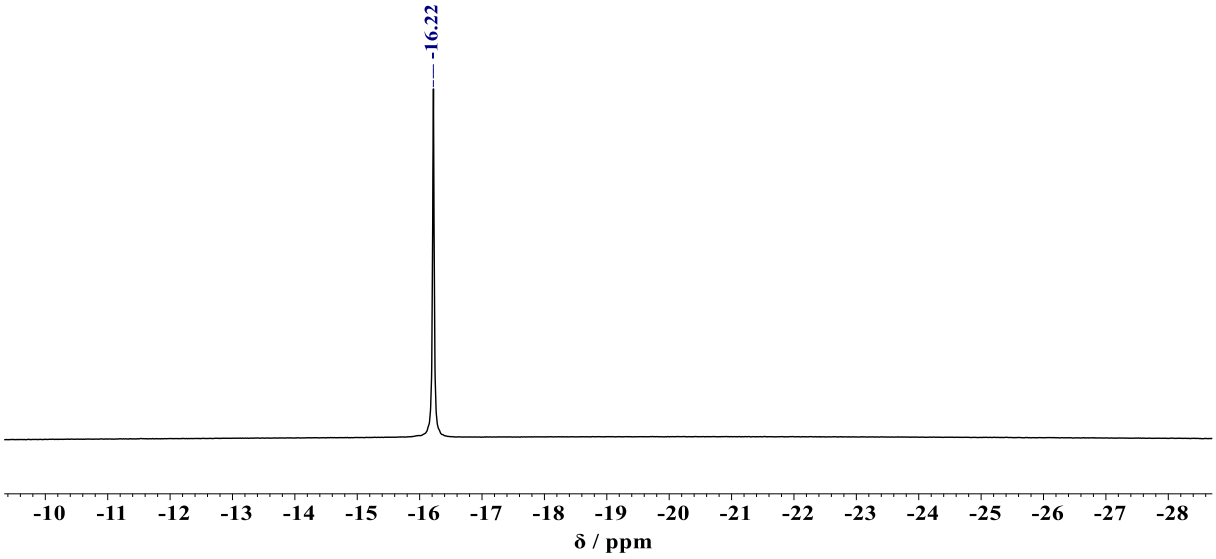

2.9 ^{13}C NMR: ClBSubPc(H)$_{12}$

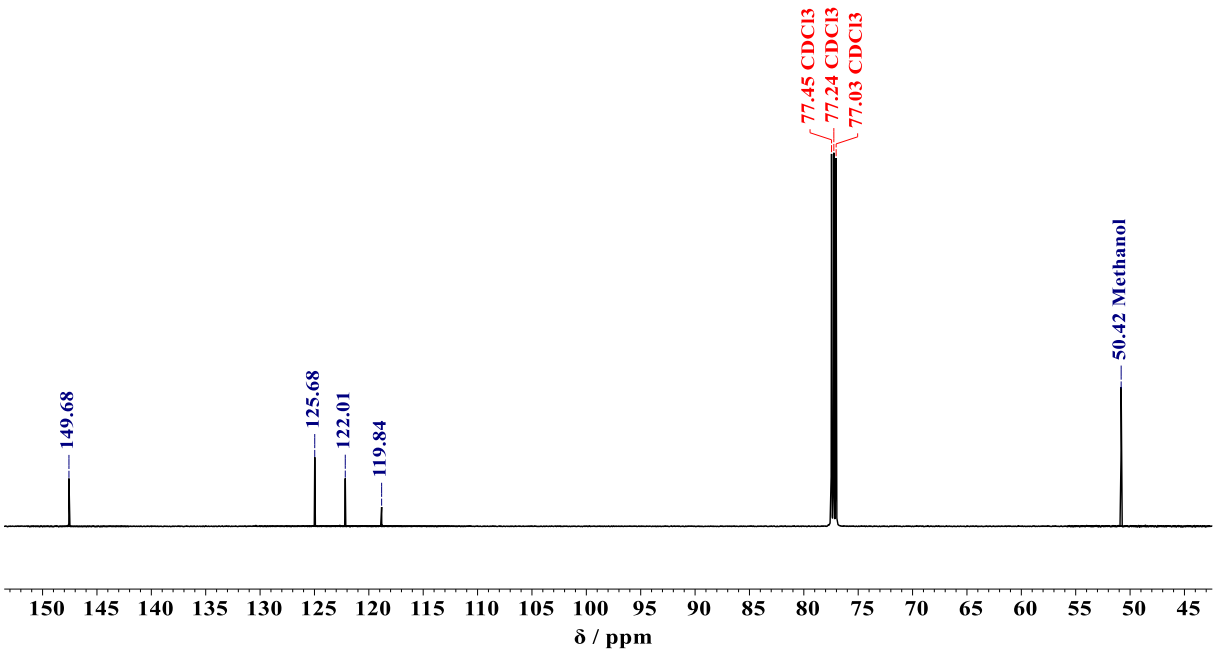

2.10 ^{1}H NMR: (HO)BSubPc($C_{12}H_{25}$)$_6$(H)$_6$

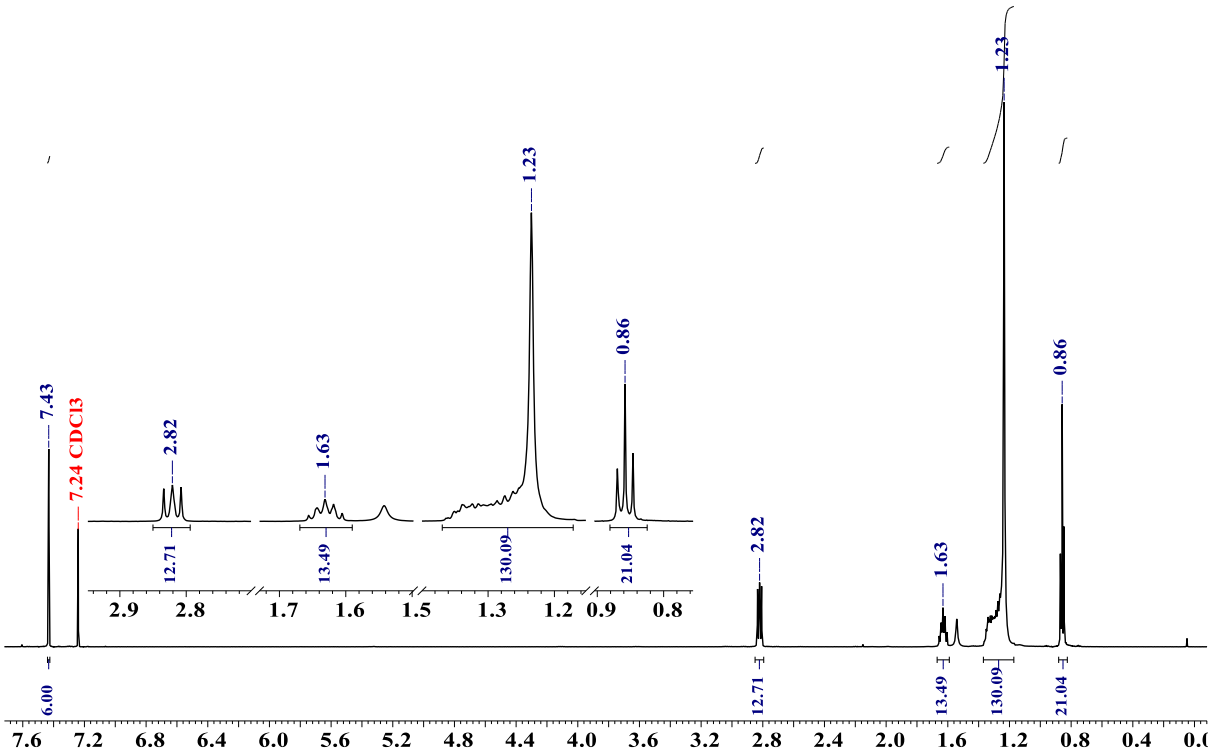

2.11 ^{11}B NMR: (HO)BSubPc($C_{12}H_{25}$)$_6$(H)$_6$

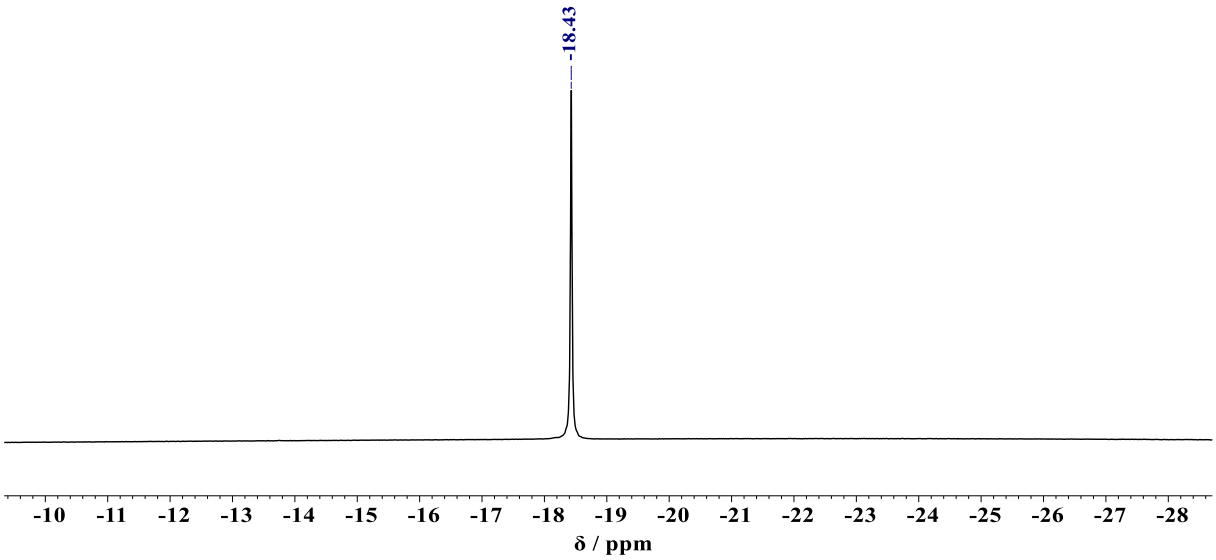

2.12 ^{13}C NMR: (HO)BSubPc($C_{12}H_{25}$)$_6$(H)$_6$

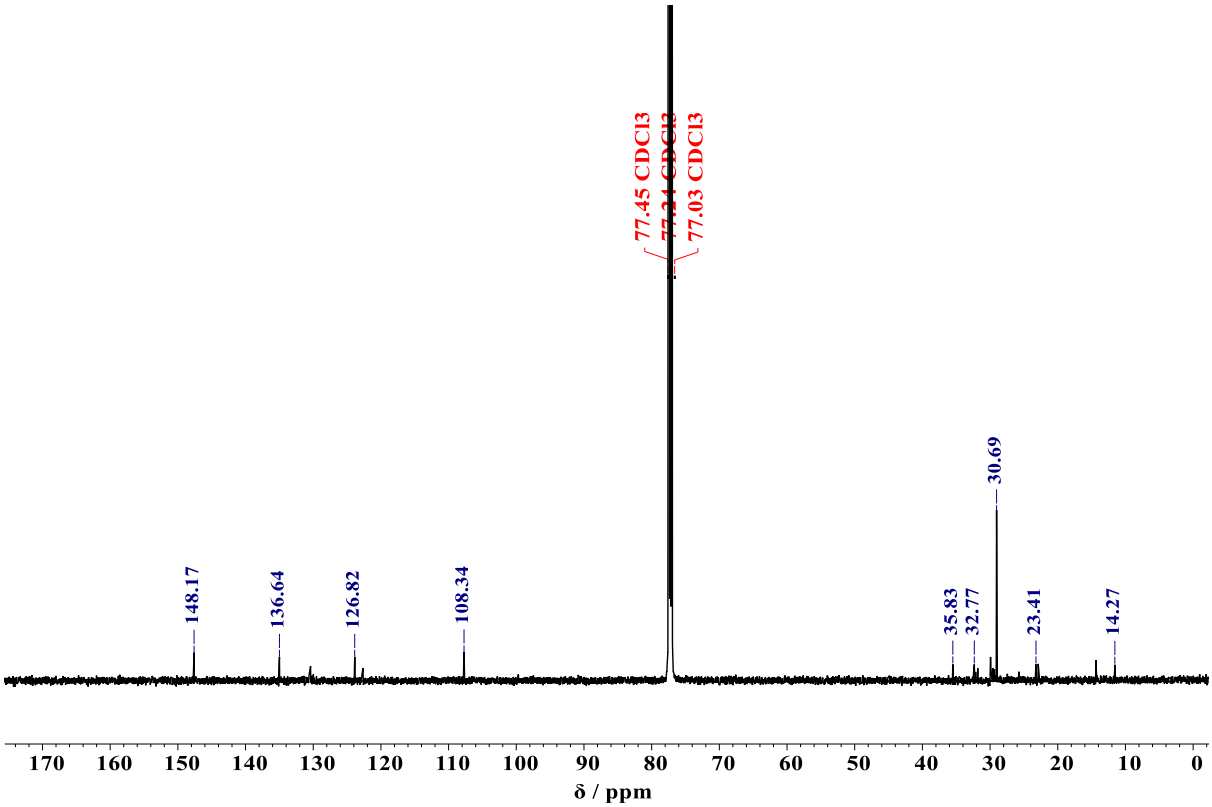

3 ATR-FTIR

3.1 ClBSubPc(F)$_{12}$

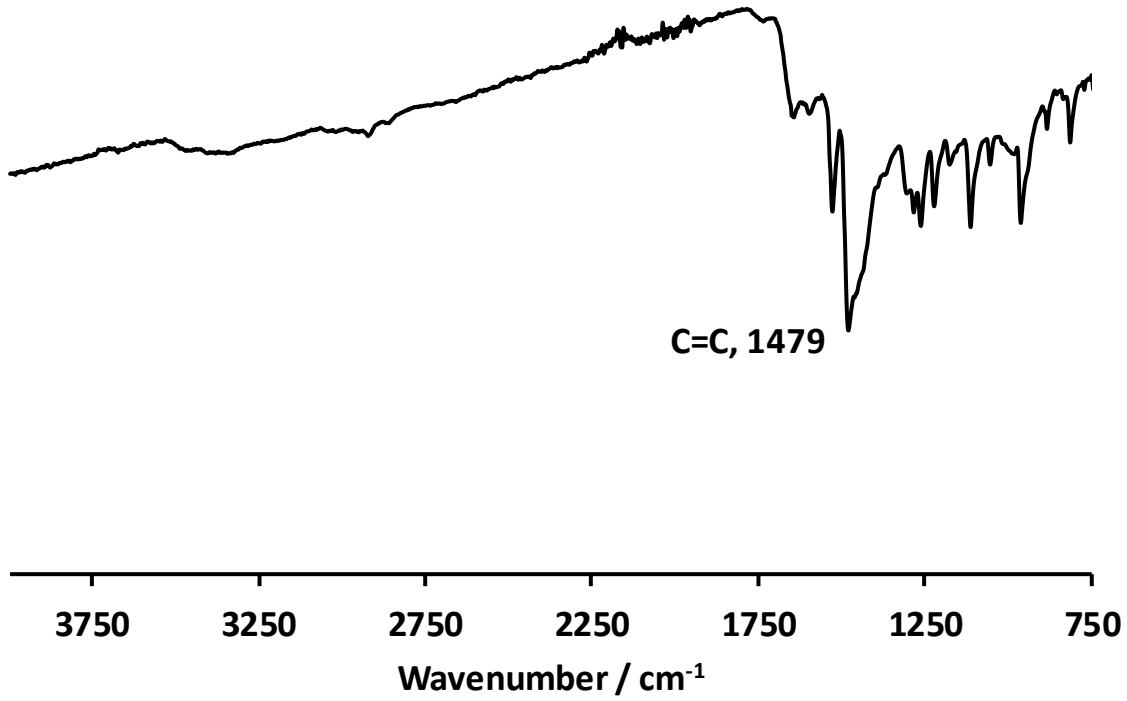

3.2 ClBSubPc(H)$_{12}$

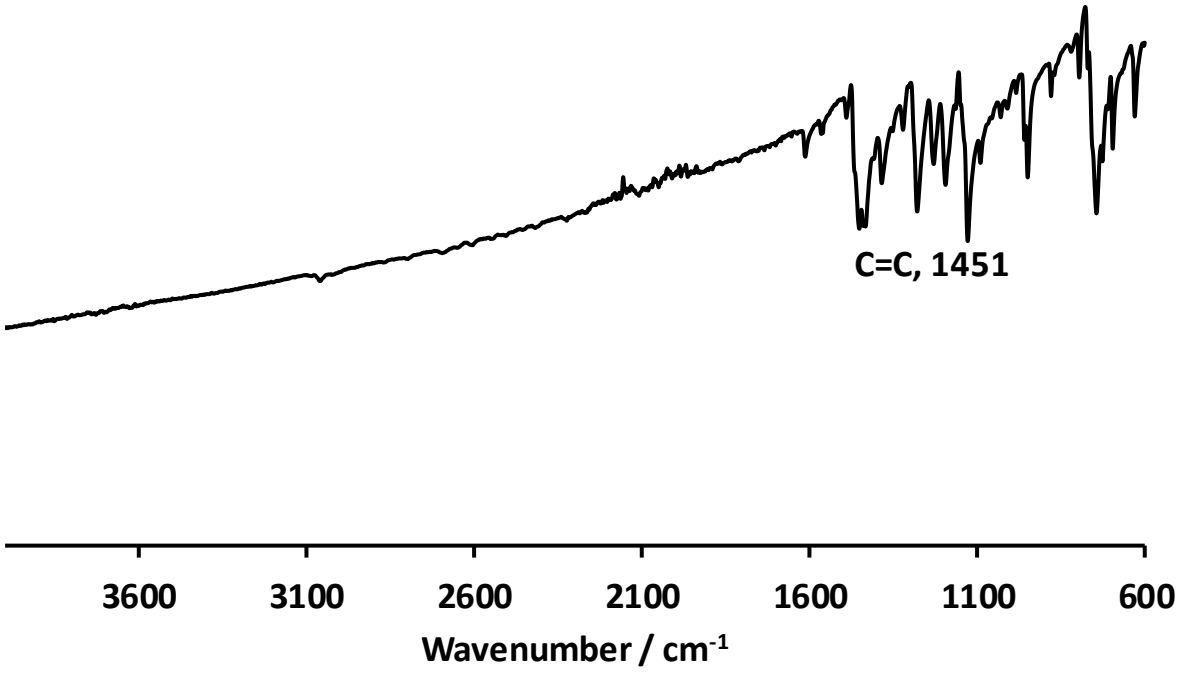

3.3 (HO)BSubPc($C_{12}H_{25}$)$_6$(H)$_6$

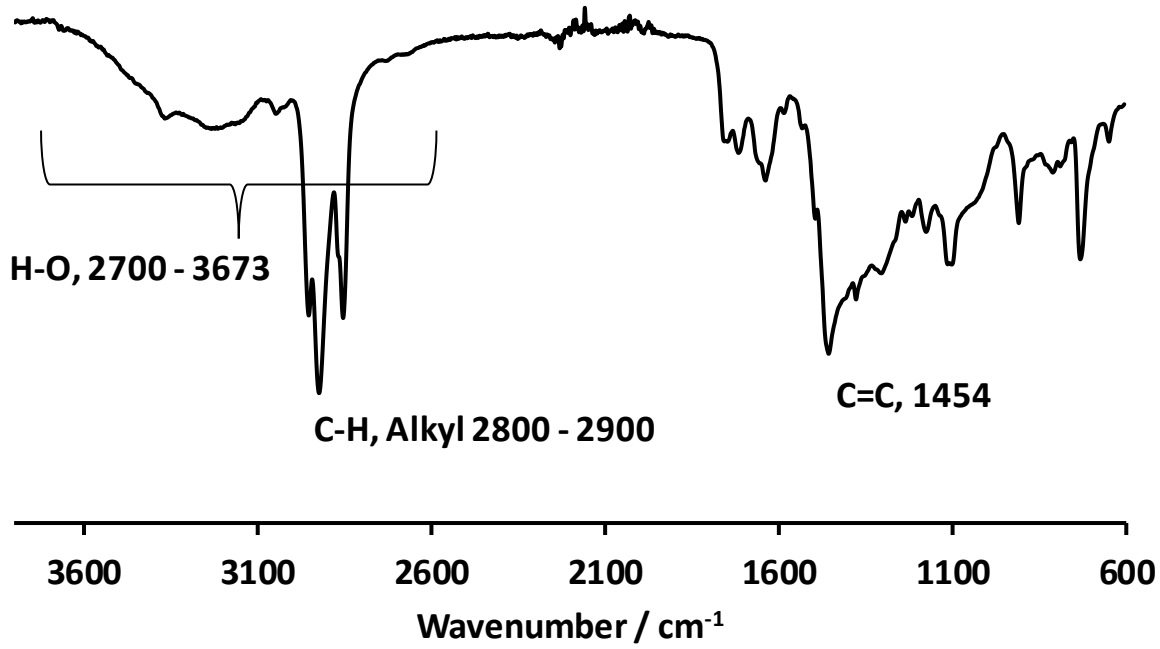

4 Electrochemistry

4.1 ClBSubPc(F)$_{12}$

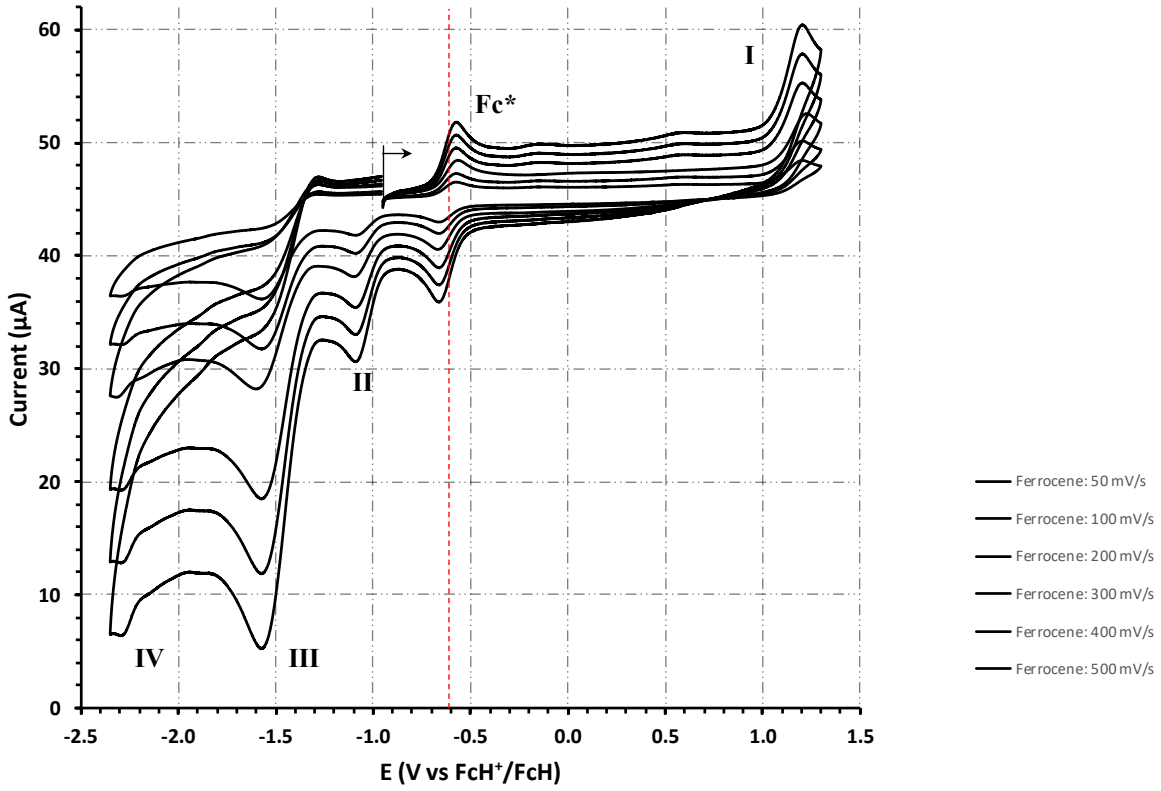

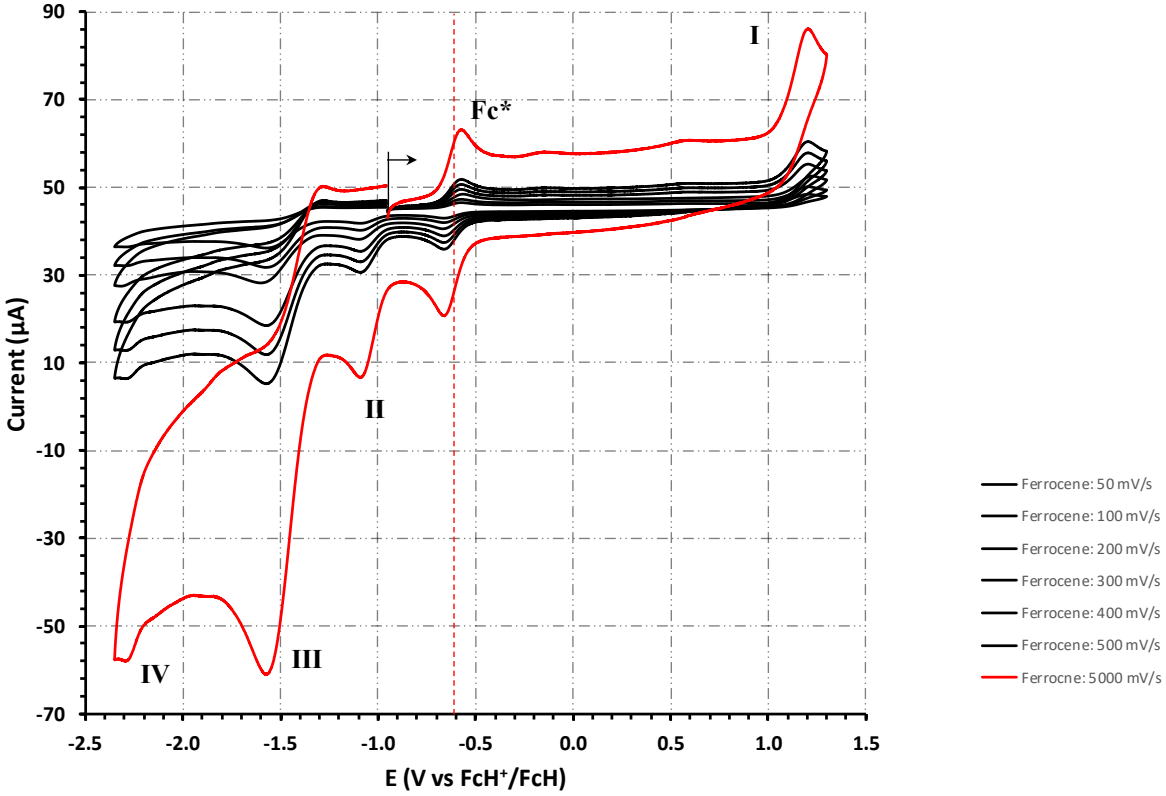

4.2 ClBSubPc(H)$_{12}$

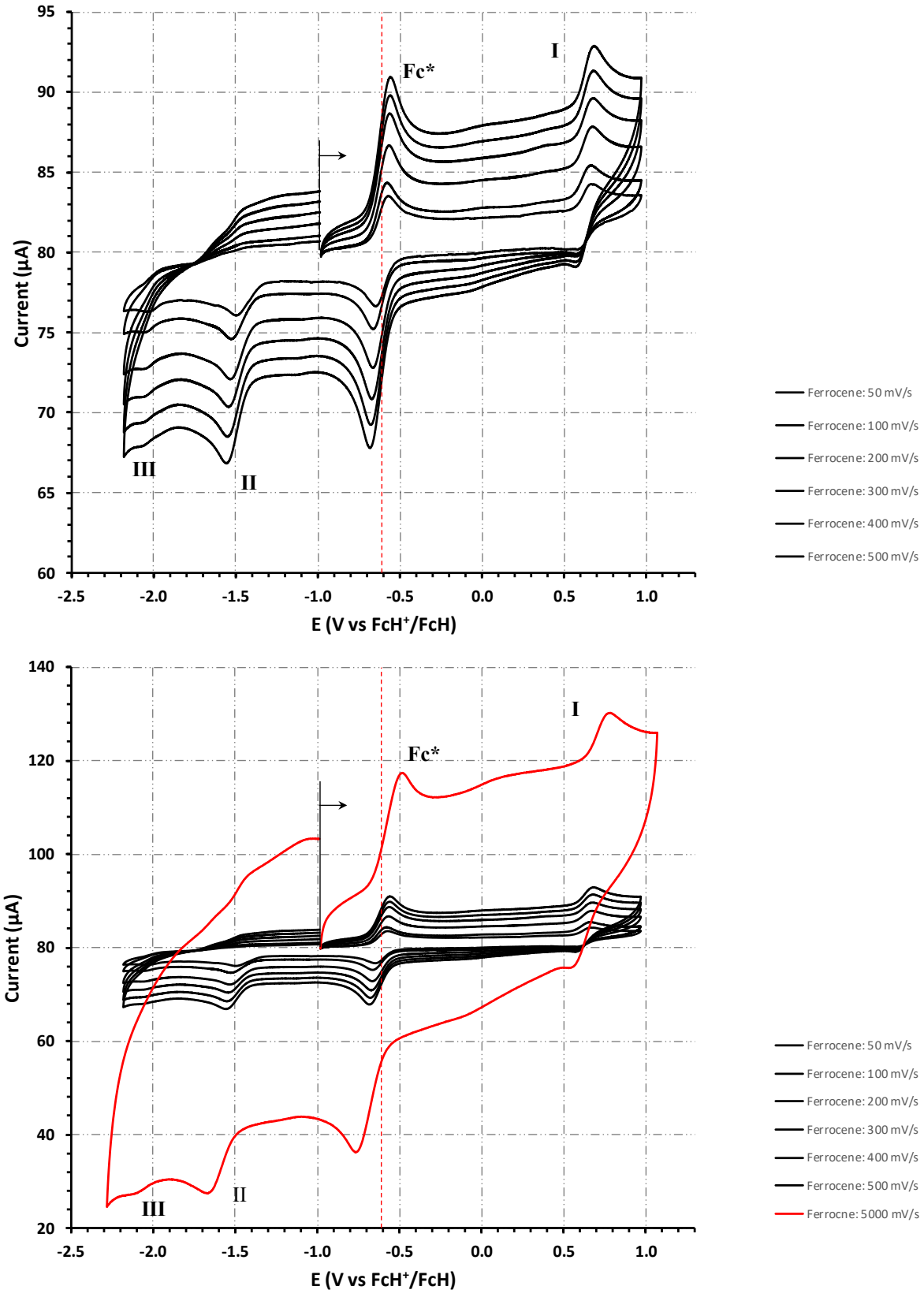

4.3 *(HO)BSubPc($C_{12}H_{25}$)$_6$(H)$_6$*

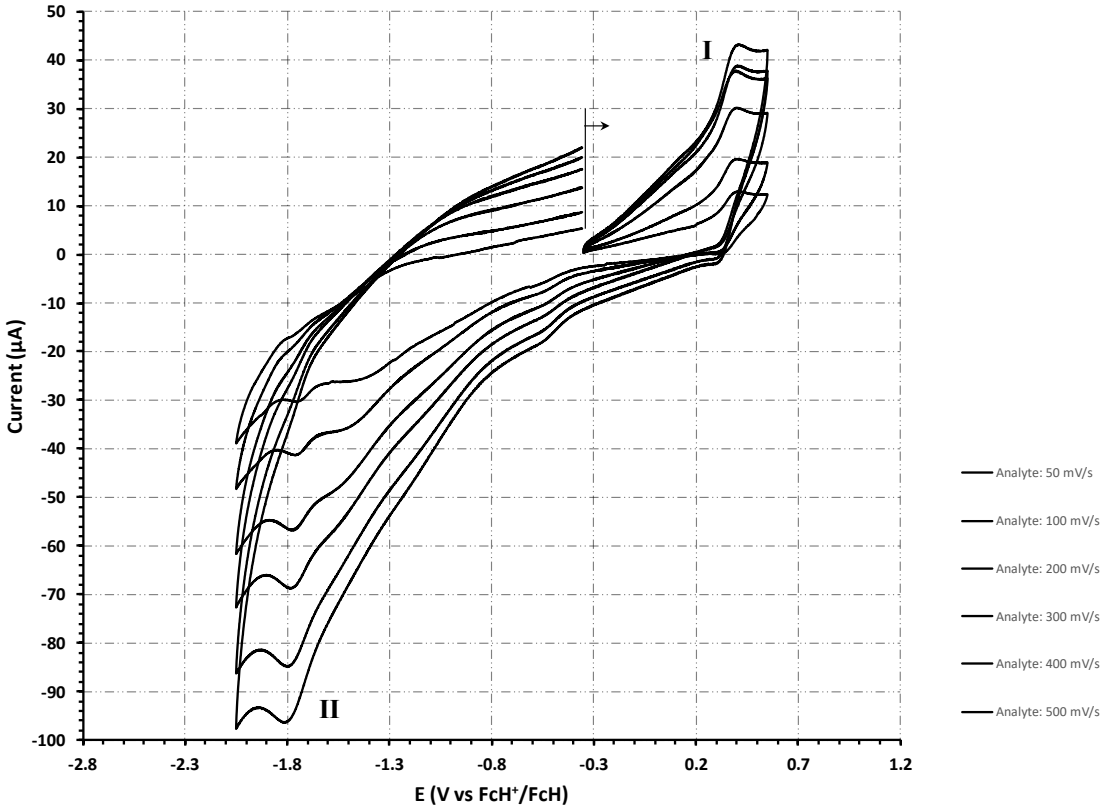

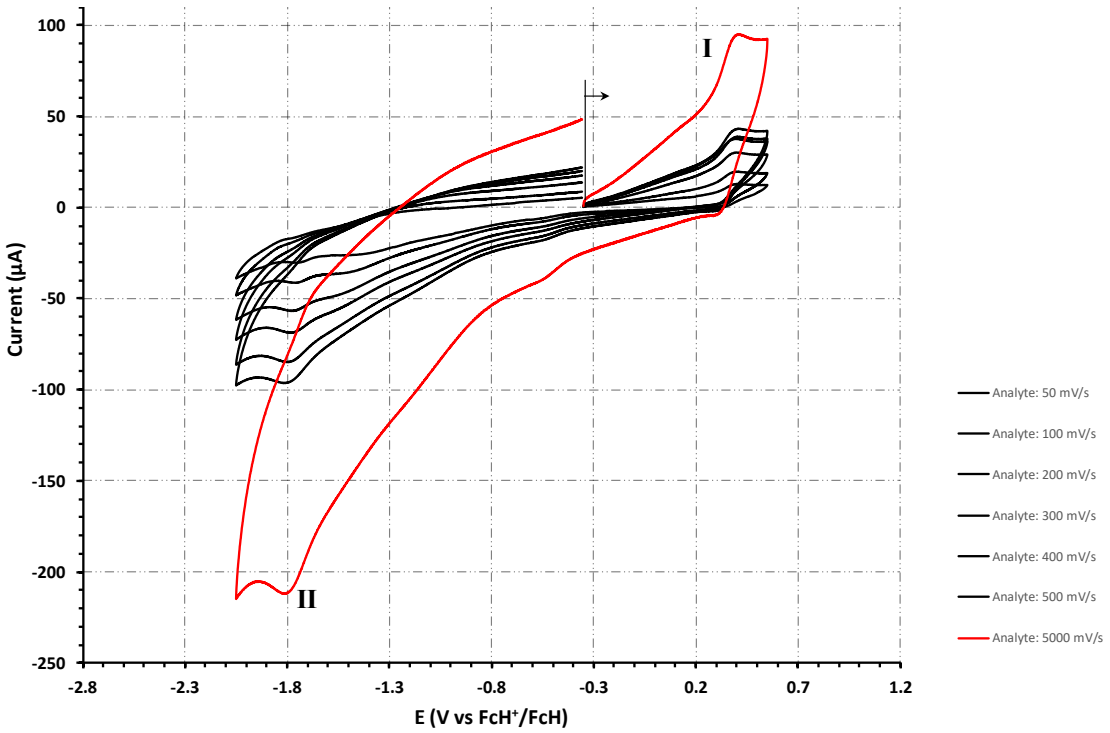

ClBSubPc(F)$_{12}$ – SubPc 1

	Fc*				Wave: I					Wave: II					Wave: III				
V (mV/s)	E_{pa} / V	ΔE_p / V	$E^{o'}$ / V	i_{pa} / µA	i_{pc}/i_{pa}	E_{pa} / V	ΔE_p / V	$E^{o'}$ / V	i_{pa} / µA	i_{pc}/i_{pa}	E_{pc} / V	ΔE_p / V	$E^{o'}$ / V	i_{pc} / µA	i_{pa}/i_{pc}	E_{pc} / V	ΔE_p / V	$E^{o'}$ / V	i_{pc} / µA	i_{pa}/i_{pc}
50	-0.570	0.079	-0.610	1.133	0.998	1.196	-	-	0.210	-	-1.093	-	-	1.338	-	-1.560	-	-	-	-
100	**-0.571**	**0.081**	**-0.610**	**1.565**	**0.992**	**1.196**	**-**	**-**	**0.216**	**-**	**-1.094**	**-**	**-**	**2.107**	**-**	**-1.562**	**-**	**-**	**-**	**-**
200	-0.572	0.083	-0.610	2.075	0.987	1.196	-	-	0.219	-	-1.098	-	-	3.161	-	-1.564	-	-	-	-
300	-0.572	0.086	-0.610	2.581	0.985	1.197	-	-	0.223	-	-1.101	-	-	4.742	-	-1.567	-	-	-	-
400	-0.572	0.092	-0.611	3.108	0.983	1.197	-	-	0.227	-	-1.108	-	-	6.322	-	-1.568	-	-	-	-
500	-0.573	0.095	-0.611	3.583	0.971	1.197	-	-	0.231	-	-1.110	-	-	7.903	-	-1.570	-	-	-	-
5000	-0.598	-	-	-	-	1.207	-	-	-	-	-1.119	-	-	-	-	-1.581	-	-	-	-

	Wave: IV				
V (mV/s)	E_{pa} / V	ΔE_p / V	$E^{o'}$ / V	i_{pc} / µA	i_{pa}/i_{pc}
50	-2.276	-	-	-	-
100	**-2.279**	-	-	-	-
200	-2.284	-	-	-	-
300	-2.288	-	-	-	-
400	-2.290	-	-	-	-
500	-2.292	-	-	-	-
5000	-2.311	-	-	-	-

ClBSubPc(H)$_{12}$ – SubPc 2

	Fc*					Wave: I					Wave: II					Wave: III				
V (mV/s)	E_{pa} / V	ΔE_p / V	$E^{o'}$ / V	i_{pc} / µA	i_{pc}/i_{pa}	E_{pa} / V	ΔE_p / V	$E^{o'}$ / V	i_{pa} / µA	i_{pc}/i_{pa}	E_{pc} / V	ΔE_p / V	$E^{o'}$ / V	i_{pc} / µA	i_{pa}/i_{pc}	E_{pc} / V	ΔE_p / V	$E^{o'}$ / V	i_{pc} / µA	i_{pa}/i_{pc}
50	-0.571	0.061	-0.609	1.693	0.994	0.673	0.087	0.627	0.061	0.064	-1.542	-	-	1.493	-	-2.050	-	-	1.354	-
100	**-0.572**	**0.076**	**-0.610**	**1.886**	**0.988**	**0.674**	**0.094**	**0.628**	**0.075**	**0.061**	**-1.543**	**-**	**-**	**1.728**	**-**	**-2.050**	**-**	**-**	**1.509**	**-**
200	-0.572	0.113	-0.610	2.075	0.982	0.679	0.098	0.628	0.113	0.060	-1.544	-	-	1.992	-	-2.051	-	-	1.886	-
300	-0.573	0.125	-0.610	2.264	0.980	0.680	0.105	0.628	0.132	0.058	-1.546	-	-	2.125	-	-2.051	-	-	2.264	-
400	-0.573	0.142	-0.610	2.453	0.977	0.687	0.111	0.629	0.151	0.057	-1.546	-	-	2.357	-	-2.051	-	-	1.642	-
500	-0.573	0.153	-0.610	3.018	0.975	0.692	0.120	0.629	0.169	0.053	-1.547	-	-	2.589	-	-2.051	-	-	3.018	-
5000	-0.588	-	-	-	-	0.707	-	-	-	-	-1.562	-	-	-	-	-2.055	-	-	-	-

(HO)BSubPc($C_{12}H_{25}$)$_6$(H)$_6$– SubPc 3

	Fc*					Wave: I					Wave: II				
V (mV/s)	E_{pa} / V	ΔE_p / V	$E^{o'}$ / V	i_{pc} / µA	i_{pc}/i_{pa}	E_{pa} / V	ΔE_p / V	$E^{o'}$ / V	i_{pa} / µA	i_{pc}/i_{pa}	E_{pc} / V	ΔE_p / V	$E^{o'}$ / V	i_{pc} / µA	i_{pa}/i_{pc}
50	-0.569	0.063	-0.610	1.762	0.992	0.398	0.059	0.365	1.698	0.332	-1.777	-	-	-	-
100	**-0.576**	**0.068**	**-0.611**	**1.803**	**0.989**	**0.398**	**0.061**	**0.365**	**1.761**	**0.355**	**-1.778**	**-**	**-**	**-**	**-**
200	-0.576	0.079	-0.611	2.386	0.982	0.399	0.063	0.365	1.822	0.407	-1.778	-	-	-	-
300	-0.574	0.087	-0.610	2.969	0.978	0.401	0.066	0.368	1.883	0.443	-1.779	-	-	-	-
400	-0.574	0.095	-0.610	3.553	0.975	0.402	0.069	0.369	1.943	0.601	-1.779	-	-	-	-
500	-0.571	0.104	-0.611	4.129	0.971	0.402	0.075	0.402	1.968	0.725	-1.780	-	-	-	-
5000	-0.584	-	-	-	-	0.411	-	-	-	-	-1.792	-	-	-	-

5 DFT

HOMO and LUMO of optimized SubPc **1** and **2** with calculations performed on the neutral molecules using the B3LYP functional

5.1 ClBSubPc(H)$_{12}$ - 1

HOMO	LUMO
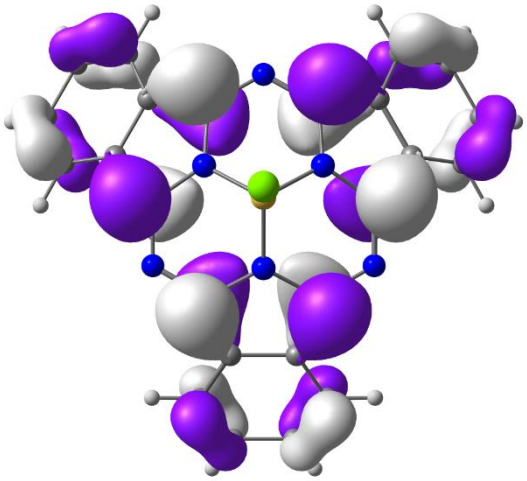	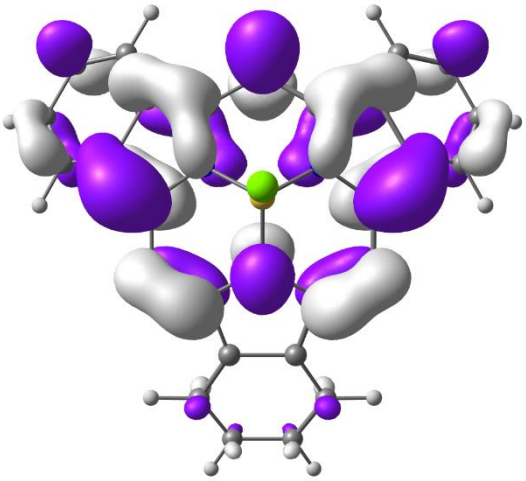

5.2 ClBSubPc(F)$_{12}$ - 2

HOMO	LUMO
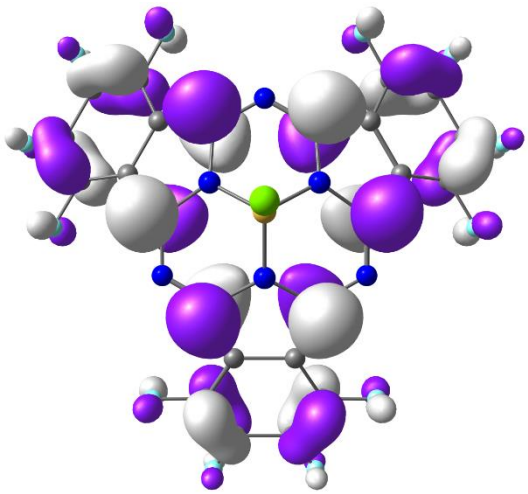	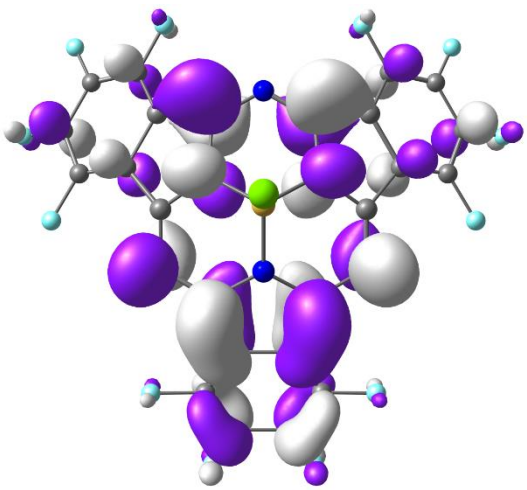

6 Optimised Coordinates

Only in electronic version

7 References

[1] J.C. Swarts, E.H.G. Langner, N. Krokeide-Hove, M.J. Cook, Synthesis and electrochemical characterisation of some long chain 1,4,8,11,15,18,22,25-octa-alkylated metal-free and zinc phthalocyanines possessing discotic liquid crystalline properties, J. Mater. Chem. 11 (2001) 434–443. doi:10.1039/b006123i.

Chapter 4

Redox and photophysical properties of four SubPcs containing ferrocenylcarboxylic acid dyads as axial ligands

Submitted to: Inorganic Chemistry

Manuscript number: ic-2020-00150d

Oxidation and reduction data of four SubPcs with axially coordinated ferrocenylcarboxylic acid dyads

To be submitted to: Data in brief (DIB)

Supporting information also included.

Author Contributions:

Pieter J. Swarts

1. Synthesis of compounds of compounds
2. Electrochemical studies and interpretation
3. Characterisation:
    a. ^{1}H NMR, ^{11}B NMR, ^{13}C NMR and ^{19}F NMR
    b. UV/vis
    c. DFT calculations
4. Writing of publication manuscript draft and revised publications under the supervision of Prof. Jeanet Conradie

Above mentioned work was done under the supervision of Prof. Jeanet Conradie.

Synopsis TOC

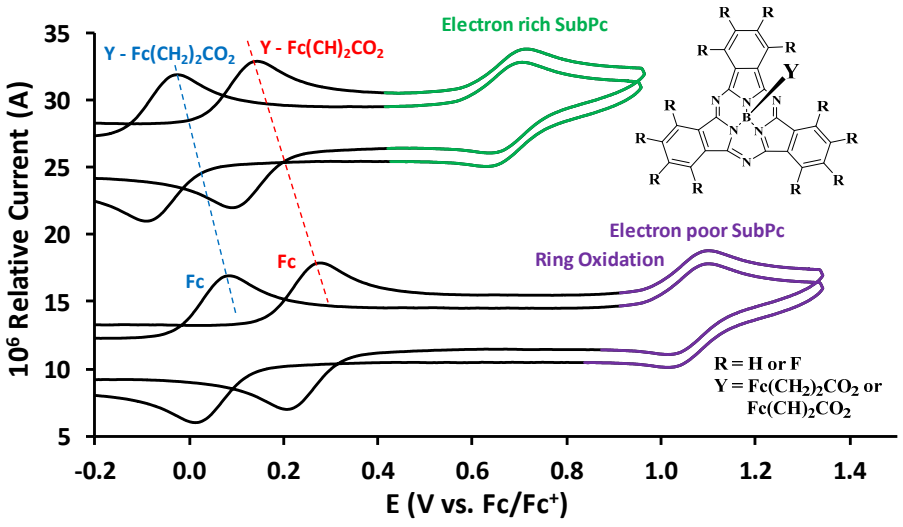

Redox and photophysical properties of four SubPcs containing ferrocenylcarboxylic acid dyads as axial ligands

Pieter J. Swarts and Jeanet Conradie*

Department of Chemistry, University of the Free State, P.O. Box 339, Bloemfontein, 9300, South Africa

Corresponding author: Jeanet Conradie, email conradj@ufs.ac.za

0000-0002-8120-6830 (J Conradie)

0000-0003-0157-8763 (PJ Swarts)

Synopsis TOC

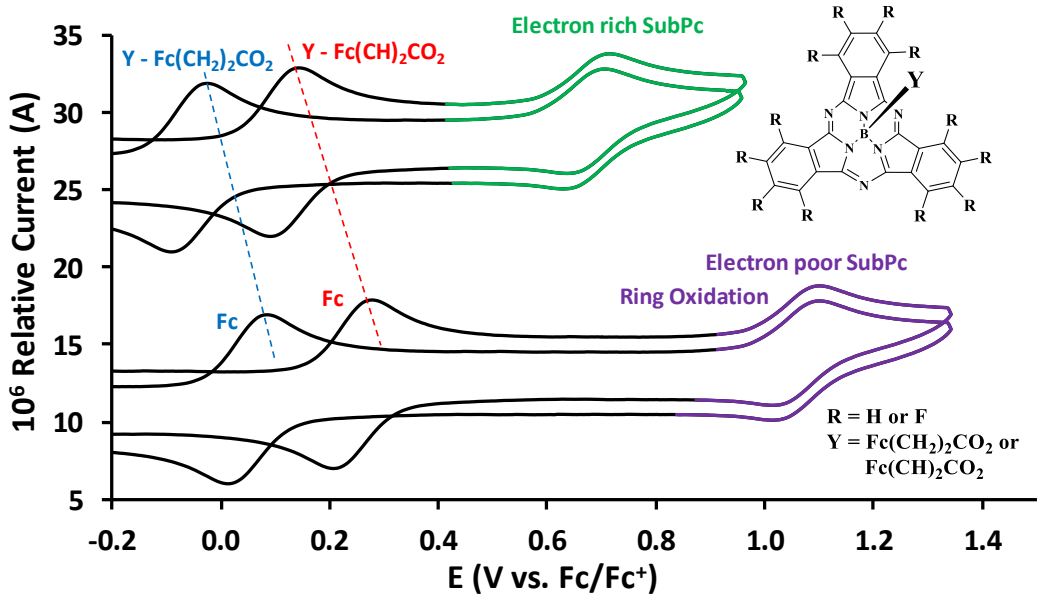

Synopsis Text

The effect of the electron-rich Y-BSubPc(H)$_{12}$ and electron-poor Y-BSubPc(F)$_{12}$ subphthalocyanines on the iron(II/III) oxidation potential of ferrocenylcarboxylic acid dyads Y in the axial position was determined by means of electrochemical analysis. Y = non π communicating (Fc-**CH$_2$-CH$_2$**-COO-) or a π communicating (Fc-**CH=CH**-COO-) ferrocenyl moiety.

Keywords

Subphthalocyanines; Ferrocene; redox potential; DFT; electron-donating; electron-withdrawing

Highlights

Four novel ferrocenylsubphthalocyanine dyads synthesised in 40% yield

^{1}H NMR ferrocenyl signals of axial ligand Y in fluorinated YSubPc(H$_{12}$) were ca 0.9 ppm downfield relative to related YSubPc(H$_{12}$).

Ferrocenyl oxidation of the axial ligand occurs before ring oxidation of the subphthalocyanine

Fluorine ring substituents shifted the ferrocenyl oxidation of the axial ligand with *ca.* 0.1 V more positive

Chemically reversible ring-based oxidation of the subphthalocyanine

DFT optimised cation species confirm the order of ferrocenyl and ring oxidation of the subphthalocyanine

Abstract

Four new ferrocenylsubphthalocyanine dyads YSubPc with ferrocenylcarboxylic acid dyads YH = (Fc-CH_2-CH_2-COOH, **1**) or (Fc-CH=CH-COOH, **2**) in the axially Y position, were synthesised in 60% yield. The axial ferrocenylcarboxylic acid moiety did not have a significant influence of the UV/vis of the ferrocenylsubphthalocyanine dyads or ^{1}H NMR position of the ring proton peaks of YSubPc(H_{12}) or the ^{19}F NMR peaks of YSubPc(F_{12}) relative to ClSubPc(H_{12}) **3**, and ClSubPc(F_{12}), **4**, respectively. However, the axial ferrocenylcarboxylic acid did influence the redox properties of the ferrocenylsubphthalocyanine dyads (Fc$(CH_2)_2$COO))BSubPc$(H)_{12}$, **5**, (Fc$(CH)_2$COO))BSubPc$(H)_{12}$, **6**, (Fc$(CH_2)_2$COO))BSubPc$(F)_{12}$, **7** and (Fc$(CH)_2$COO))BSubPc$(F)_{12}$, **8**. The Fe group of the ferrocenyl-containing axial ligand is involved in the first reversible oxidation process, followed by a second oxidation localised on the subphthalocyanine ligand. The fluorine ring substituents in SubPcs **7** and **8** caused the ferrocenyl oxidation to shift with *ca.* 0.1 V compared to SubPcs **5** and **6**. Density functional theory (DFT) calculations gave further insight into the redox properties of the novel dyads. The neutral species of SubPc **5** – **8** have LUMOs and HOMOs mainly π-ring and iron-d character, confirming ring-based reduction and Fe(II) to Fe(III) oxidation. Optimisation of the cation (oxidised) species was essential to verify the second ring-based oxidation.

Introduction

Ferrocene has been extensively researched, and numerous good reviews for both its organic and inorganic chemistry are available.[1–4] Ferrocene reacts in multiple different ways such as Friedel-Crafts acylation and alkylation; furthermore, it can be sulfonated, formylated and metallated with *n*-butyllithium.[5,6] Research into ferrocene-containing compounds thrives and is greatly stimulated by their successful applications, especially electrochemistry due to the ideal redox behaviour of the iron (II/III) couple.[7, 8]

The ClBSubPc$(H)_{12}$, **3**, shown in **Scheme 1**, was a fortunate discovery made in 1972 by Meller and Ossko during an attempt to synthesise a boron centred phthalocyanine.[9] The applications of SubPcs are varied and include light-emitting diodes,[10] dye-sensitised solar cells,[11] and photodynamic therapy [12] among others. The effective use of SubPcs for certain applications can be modified by substituting the axial ligand as well as by functionalising the peripheral and non-peripheral positions R, see **Scheme 1**.[13] It is observed that substitution of the electron-withdrawing axial chloride ligand with an electron-donating alkoxy group, shifts the first oxidation potential of the SubPc with ca 0.13 V to less positive potentials.[14] Ferrocenylsubphthalocyanine dyads with a direct ferrocene-boron or substituted ferrocene-boron bond in the axial position, have been investigated by Nemykin and co-workers.[15] They found that the first reversible oxidation process of these ferrocenylsubphthalocyanine dyads is ferrocene-centred, while the second ring-based oxidation was only partially reversible due to significant degradation of the subphthalocyanine core.[15,16]

In this paper, we report the synthesis, characterisation and electrochemical studies of four new ferrocenylsubphthalocyanine dyads shown in **Scheme 1**. Ferrocenylpropanoic acid **1** and ferrocenylpropenoic acid **2** are directly bound to the boron atom of SubPcs **3** and **4**, to form

the four novel compounds (Fc$(CH_2)_2$COO))BSubPc$(H)_{12}$, **5**, (Fc$(CH)_2$COO))BSubPc$(H)_{12}$, **6**, (Fc$(CH_2)_2$COO))BSubPc$(F)_{12}$, **7** and (Fc$(CH)_2$COO))BSubPc$(F)_{12}$, **8**, shown in **Scheme 1**. This study was designed to determine, through cyclic voltammetry, (i) the influence of electron-withdrawing F ring-substituents on the redox potentials of SubPcs of the type Y-BSubPc$(F)_{12}$ relative to Y-BSubPc$(H)_{12}$ with Y = (Fc-CH_2-CH_2-COO) or (Fc-CH=CH-COO), (ii) the influence of the axially ferrocenylcarboxylic acid dyads Y on the UV/vis maxima and the ring-based oxidations and reductions of the ferrocenylsubphthalocyanine dyads **5** - **8** and (iii) to improve the cyclic voltammetry experimental setup to get reversible ring-based oxidation for ferrocenylsubphthalocyanine dyads **5** - **8**. The two axial ligands Y are chosen to either have π-communication between the ferrocenyl and the carboxylic group (i.e. the (Fc-CH=CH-COO-) ferrocenylcarboxylic acid with a non-isolated ferrocenyl group) or to have no π-communication between the ferrocenyl and the carboxylic group (i.e. the (Fc-CH_2-CH_2-COO-) ferrocenyl dyad with an isolated ferrocenyl group).

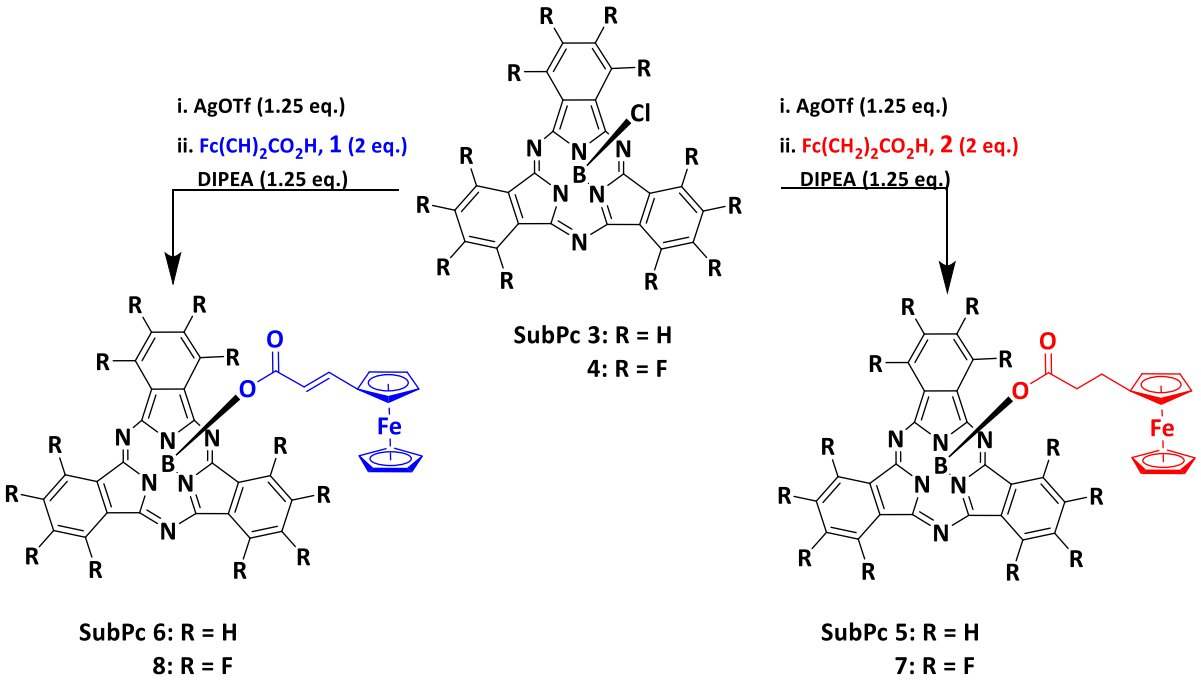

Scheme 1 Reaction scheme for the synthesis of $(Fc(CH_2)_2COO)BSubPc(H)_{12}$, **5**, $(Fc(CH)_2COO)BSubPc(H)_{12}$, **6**, $(Fc(CH_2)_2COO)BSubPc(F)_{12}$, **7**, and $(Fc(CH)_2COO)BSubPc(F)_{12}$, **8**, from SubPc's $ClBSubPc(H)_{12}$, **3,** and $ClBSubPc(F)_{12}$, **4**. Note: AgOTf = silver trifluoromethanesulfonate and DIPEA = *N*,*N*-Diisopropylethylamine.

Experimental Section

Reagents and Materials

Solid reagents (Sigma-Aldrich, Strem and Merck) were used as received. Liquid reagents (Sigma-Aldrich and Merck) were used without any further purification unless specified otherwise. Solvents were distilled, and water was double distilled. Organic solvents used in this study were dried according to published methods [17]. Melting points are uncorrected and were determined with an Olympus BX 51 microscope equipped with a Linkam THMS 600 hot stage.

Spectroscopy Measurements

^{1}H, ^{11}B, ^{13}C and ^{19}F NMR spectroscopic analysis were performed for all compounds in the study. ^{1}H, ^{13}C and ^{19}F NMR spectra were recorded at 25°C on a 600 MHz AVANCE II NMR spectrometer at 600.28 MHz, 150.95 MHz and 564.33 MHz respectively. ^{11}B NMR spectra were recorded at 25°C on a 400 MHz AVANCE III NMR spectrometer at 128.38 MHz. Hydrogen and carbon chemical shifts are relative to hydrogen and carbon in $CDCl_3$ at 7.24 ppm and 77.16 ppm, respectively. The following abbreviations are used to describe peak patterns: s = singlet, d = doublet, pt = pseudo-triplet, t = triplet, q = quartet and m = multiplet. UV/vis spectra were recorded on a Varian Cary 5000 UV/Vis-NIR Spectrophotometer. Melting points

are uncorrected and were determined with an Olympus BX 51 microscope equipped with a Linkam THMS 600 hot stage.

Preparation of novel SubPc's 1 – 4

$Fc(CH_2)_2COOH$, **1**, $Fc(CH)_2COOH$, **2**, $ClBSubPc(H)_{12}$, **3** and $ClBSubPc(F)_{12}$, **4**, were synthesised using slight modifications to literature methods (see the supporting information for the reaction scheme and the characterisation data),[7,8,18] as described in our previous publications.[14,19] Compounds **5** – **8** were characterised by NMR, UV/vis, elemental analysis and m.p.

Preparation of $(Fc(CH_2)_2COO)SubPc(H)_{12}$, (5).

To a solution of chlorosubphthalocyanine, **3**, (200 mg; 0.46 mmol) and dry toluene (3 cm^3), silver trifluoromethanesulfonate (150 mg, 0.58 mmol; 1.25 eq.) was added and the mixture stirred at 45°C, under argon atmosphere for 4 hours. Once the $(OTf)SubPc(H)_{12}$ specie was generated, ferrocenylpropanoic acid, **1**, (211 mg, 0.92 mmol, 2 eq.) and *N*,*N*-diisopropylethylamine (0.10 cm^3, 75 mg, 0.58 mmol, 1.25 eq.) was added. The mixture was stirred at 50 °C for 12 hours. The solvent was removed by evaporation under reduced pressure and the product was directly purified by chromatography using hexane: DCM (1:1) (R_f: 0.71) as eluent to give 122 mg (40 % based on, **3**). m.p.: 175-180°C, UV/vis: λ_{max} 563 nm, ε = 153630 $dm^3\ mol^{-1}\ cm^{-1}$ in THF. ^{1}H NMR: δH (600.28 MHz, CDCl3, 25 °C): δ 8.84 (6H, dd, SubPc), 7.85 (6H, dd, SubPc), 3.83 (5 H, s, Unsubstituted-Cp), 3.77 (2 H, pt, 2 x CH2: Substituted-Cp), 3.57 (2 H, pt, 2 x CH2: Substituted-Cp), 1.89 (2H, t, CH2), 1.50 (2H, t, CH2). ^{11}B NMR: δ_B (128.38

MHz, $CDCl_3$): δ -16.41 (1B). ^{13}C NMR: δ_C (150.95 MHz, $CDCl_3$, 25 °C): δ 179.37 (1C, Fc-$(CH_2)_2$-$\underline{C}O_2$), 151.60 (6C, SubPc: N-$\underline{C}$=N), 131.12 (6C, SubPc: C=C), 129.95 (6C, SubPc: non-peripheral), 122.39 (6C, SubPc: peripheral), 87.49 (1C, Substituted-Cp-ring), 68.89 (2C, Substituted-Cp-ring), 68.23 (5C, Unsubstituted-Cp-ring), 67.75 (2C, Substituted-Cp-ring), 35.53 (1C, Fc-CH_2-$\underline{C}H_2$-CO_2), 24.76 (1C, Fc-$\underline{C}H_2$-CH_2-CO_2).Elemental analysis calculated for $C_{37}H_{25}BFeN_6O_2$ (element, %): C, 68.13; H, 3.86; N, 12.88 obtained: C, 68.34; H, 3.97; N, 12.99.

Preparation of (Fc(CH)$_2$COO)SubPc(H)$_{12}$, (6).

To a solution of chlorosubphthalocyanine, **3**, (200 mg; 0.46 mmol) and dry toluene (3 cm^3), silver trifluoromethanesulfonate (150 mg, 0.58 mmol; 1.25 eq.) was added and the mixture stirred at 45°C, under argon atmosphere for 4 hours. Once the (OTf)SubPc(H)$_{12}$ was generated, ferrocenylpropenoic acid, **2**, (211 mg, 0.92 mmol, 2 eq.) and *N*,*N*-diisopropylethylamine (0.10 cm^3, 75 mg, 0.58 mmol, 1.25 eq.) was added. The mixture was stirred at 50 °C for 12 hours. The solvent was removed by evaporation under reduced pressure and the product was directly purified by chromatography using hexane: DCM (1:1) (R_f: 0.62) as eluent to give 114 mg (38 % based on, **3**). m.p.: 167-172°C, UV/vis: λ_{max} 563 nm, ε = 113729 $dm^3\ mol^{-1}\ cm^{-1}$ in THF. ^{1}H NMR: δH (600.28 MHz, CDCl3, 25 °C): δ 8.84 (6H, dd, SubPc), 7.85 (6H, dd, SubPc), 6.70 (1H, d, CH=CH), 4.95 (1H, d, CH=CH), 4.21 (2 H, pt, 2 x CH2: Substituted-Cp), 4.10 (2 H, pt, 2 x CH2: Substituted-Cp), 3.90 (5 H, s, Unsubstituted-Cp). ^{11}B NMR: δ_B (128.38 MHz, $CDCl_3$): δ -16.31 (1B). ^{13}C NMR: δ_C (150.95 MHz, $CDCl_3$, 25 °C): δ 172.29 (1C, Fc-$(CH)_2$-$\underline{C}O_2$), 153.60 (6C, SubPc: N-$\underline{C}$=N), 148.76 (6C, SubPc: C=C), 133.12 (1C, Fc-CH=$\underline{C}$H-CO_2), 131.95 (6C, SubPc: non-peripheral), 124.39 (6C, SubPc: peripheral), 113.87 (1C, Fc-$\underline{C}$H=CH-CO_2), 78.26 (1C, Substituted-Cp-ring), 71.44 (2C, Substituted-Cp-ring), 69.92 (5C,

Unsubstituted-Cp-ring), 69.05 (2C, Substituted-Cp-ring). Elemental analysis calculated for $C_{37}H_{23}BFeN_6O_2$ (element, %): C, 68.34; H, 3.57; N, 12.92 obtained: C, 68.28; H, 3.66; N, 13.02.

Preparation of $(Fc(CH_2)_2COO)SubPc(F)_{12}$, (7).

To a solution of chlorosubphthalocyanine, **4**, (200 mg; 0.46 mmol) and dry toluene (3 cm^3), silver trifluoromethanesulfonate (150 mg, 0.58 mmol; 1.25 eq.) was added and the mixture stirred at 45°C, under argon atmosphere for 4 hours. Once the $(OTf)SubPc(H)_{12}$ was generated, ferrocenylpropanoic acid, **1**, (211 mg, 0.92 mmol, 2 eq.) and *N*,*N*-diisopropylethylamine (0.10 cm^3, 75 mg, 0.58 mmol, 1.25 eq.) was added. The mixture was stirred at 50 °C for 12 hours. The solvent was removed by evaporation under reduced pressure and the product was directly purified by chromatography using hexane: DCM (1:1) (R_f: 0.68) as eluent to give 128 mg (48 % based on, **4**). m.p.: 153-159°C, UV/vis: λ_{max} 573 nm, ε = 174397 $dm^3\ mol^{-1}\ cm^{-1}$ in THF. ^{1}H NMR: δH (600.28 MHz, CDCl3, 25 °C): δ 4.71 (5 H, s, Unsubstituted-Cp-ring), 4.65 (2 H, pt, 2 x CH2: Substituted-Cp-ring), 4.45 (2 H, pt, 2 x CH2: Substituted-Cp-ring), 2.77 (2H, t, CH2), 2.38 (2H, t, CH2). ^{11}B NMR: δ_B (128.38 MHz, $CDCl_3$): δ -14.79 (1B). ^{13}C NMR: δ_C (150.95 MHz, $CDCl_3$, 25 °C): δ 187.15 (1C, Fc-$(CH_2)_2$-$\underline{C}O_2$), 173.93 (6C, SubPc: N-$\underline{C}$=N), 153.45 (6C, SubPc: C=C), 152.27 (6C, SubPc: non-peripheral), 144.72 (6C, SubPc: peripheral), 87.49 (1C, Substituted-Cp-ring), 68.89 (2C, Substituted-Cp-ring), 68.23 (5C, Unsubstituted-Cp-ring), 67.75 (2C, Substituted-Cp-ring), 35.53 (Fc-CH_2-$\underline{C}H_2$-CO_2), 24.76 (Fc-$\underline{C}H_2$-CH_2-CO_2). ^{19}F NMR: δ_C (564.33 MHz, $CDCl_3$, 25 °C): δ -134.37 (6F, q, non-peripheral F_6) and -146.82 (6F, q, peripheral F_6). Elemental analysis calculated for $C_{37}H_{13}BF_{12}FeN_6O_2$ (element, %): C, 51.99; H, 1.51; F, 22.26; N, 8.68; obtained: C, 52.14; H, 1.68; F, 22.31; N, 8.74.

Preparation of $(Fc(CH)_2COO)SubPc(F)_{12}$, (8).

To a solution of chlorosubphthalocyanine, **4**, (200 mg; 0.46 mmol) and dry toluene (3 cm^3), silver trifluoromethanesulfonate (150 mg, 0.58 mmol; 1.25 eq.) was added and the mixture stirred at 45°C, under argon atmosphere for 4 hours. Once the $(OTf)SubPc(H)_{12}$ was generated, ferrocenylpropenoic acid, **2**, (211 mg, 0.92 mmol, 2 eq.) and *N*,*N*-diisopropylethylamine (0.10 cm^3, 75 mg, 0.58 mmol, 1.25 eq.) was added. The mixture was stirred at 50 °C for 12 hours. The solvent was removed by evaporation under reduced pressure and the product was directly purified by chromatography using hexane: DCM (1:1) (R_f: 0.54) as eluent to give 113 mg (42 % based on, **4**). m.p.: 148-153°C, UV/vis: λ_{max} 573 nm, ε = 134952 $dm^3\ mol^{-1}\ cm^{-1}$ in THF. ^{1}H NMR: δH (600.28 MHz, CDCl3, 25 °C): δ 7.58 (1H, d, CH=CH), 5.83 (1H, d, CH=CH), 5.09 (2 H, pt, 2 x CH2: Substituted-Cp-ring), 4.98 (2 H, pt, 2 x CH2: Substituted-Cp-ring), 4.78 (5 H, s, Unsubstituted-Cp-ring). ^{11}B NMR: δ_B (128.38 MHz, $CDCl_3$): δ -14.51 (1B). ^{13}C NMR: δ_C (150.95 MHz, $CDCl_3$, 25 °C): δ 179.42 (1C, Fc-$(CH)_2$-$\underline{C}O_2$), 172.29 (6C, SubPc: N-$\underline{C}$=N), 158.94 (6C, SubPc: C=C), 157.76 (6C, SubPc: non-peripheral), 150.21 (6C, SubPc: peripheral), 148.76 (1C, Fc-CH=$\underline{C}$H-CO_2), 113.87 (1C, Fc-$\underline{C}$H=CH-CO_2), 78.26 (1C, Substituted-Cp-ring), 71.44 (2C, Substituted-Cp-ring), 69.92 (5C, Unsubstituted-Cp-ring), 69.05 (2C, Substituted-Cp-ring). ^{19}F NMR: δ_C (564.33 MHz, $CDCl_3$, 25 °C): δ -135.62 (6F, q, non-peripheral F_6) and -145.72 (6F, q, peripheral F_6). Elemental analysis calculated for $C_{37}H_{11}BF_{12}FeN_6O_2$ (element, %): C, 51.31; H, 1.38; F, 26.32; N, 9.50 obtained: C, 51.38; H, 1.46; F, 26.39; N, 9.53.

Cyclic Voltammetry

All the electrochemical experiments were performed in an M Bruan Lab Master SP glove box under a high purity argon atmosphere (H_2O and O_2 < 10 ppm). Cyclic voltammetry (CV)

measurements were performed utilising a Princeton Applied Research PARSTAT 2273 potentiostat, running Powersuite software (Version 2.58). A three-electrode cell was used. A glassy carbon electrode with a surface area 3.14 x 10^{-6} m^2 was chosen as working electrode, platinum wires were chosen as auxiliary and reference electrodes. The glassy carbon working electrode was polished and prepared before every experiment on a Buhler polishing mat first with 1-micron and then with ¼-micron diamond paste, rinsed with H_2O, acetone and dichloromethane (DCM), and dried before each experiment. Electrochemical analysis of the complexes was performed in DCM (anhydrous, ≥ 99.8%, contains 40-150 ppm amylene as a stabiliser) room temperature. Solutions were made in 0.001 dm^3 spectrochemical grade anhydrous DCM containing ca. 0.0005 M of an analyte, 0.0005 mol dm^{-3} of internal reference (decamethylferrocene, DmFc) and 0.1 mol dm^{-3} of supporting electrolyte tetrabutylammonium tetrakispentafluorophenylborate, $[N(^nBu)_4][B(C_6F_5)_4]$ in DCM. Experimental potential data was collected *vs.* the Pt wire reference electrode but is reported *vs.* the redox couple of ferrocene, Fc/Fc^+ at 0 V. $E°'$ (DmFc) = - 0.610 V *vs.* Fc/Fc^+ at 0 V in DCM/$[N(^nBu)_4][B(C_6F_5)_4]$. Scan rates were between 0.05 and 5.00 Vs^{-1}. Electrochemical reversibility (or Nernstian behaviour) of redox processes is indicated by a peak current ratio (i_{pc}/i_{pa} for oxidation and i_{pa}/i_{pc} for reduction) of 1 [20,21] and peak current separation $\Delta E = |E_{pa} - E_{pc}|$ = 0.059 V for a one-electron transfer process. [22] In this experiment, due to experimental cell imperfections and ohmic drop effects, ΔE_p slightly larger than 0.059 V was obtained, even for the known 1 e^- transfer processes of decamethylferrocene, $DmFc^+$/DmFc, namely 0.074 - 0.076 V.[23–25] The formal reduction potential is determined by $E°' = (E_{pa} - E_{pc})/2$ for an electrochemically reversible (and quasi reversible) process where E_{pa} (E_{pc}) = anodic (cathodic) peak potential and i_{pa} (i_{pc}) = anodic (cathodic) peak current.

DFT calculations

Density functional theory (DFT) optimisations were performed on the neutral and oxidised molecules in the gas phase using the hybrid PBE1PBE[26–28] exchange-correlation functional and the triple-ζ basis set 6-311G(d,p) basis set, as implemented in the Gaussian 16 package.[29] Single calculations using pure BP86[30–32] exchange-correlation were performed in DCM as the solvent, using the IEF-PCM model (polarisable continuum model (PCM)[33] which solved the non-homogeneous Poisson equation by applying the integral equation formalism variant).[34] The energy and plots of the highest occupied molecular orbital (E_{HOMO}) and the lowest unoccupied molecular orbital (E_{LUMO}) were obtained from the output files from the BP86-DCM calculations. Both the gas phase PBE1PBE/6-311G(d,p) and solvent phase BP86/6-311G(d,p) results gave the same molecular orbital (MO) insight into the observed experimental redox processes.

Results and Discussion

Synthesis

Ferrocenylpropanoic acid, **1**, and ferrocenylpropenoic acid, **2**, were synthesised in multigram quantities using slightly modified methods than previously published,[18] as described in our previous publication.[19] The synthesis of ferrocenylsubphthalocyanine dyads **5** – **8** from subphthalocyanines **3** and **4** (Scheme 1), was complex due to the moisture sensitivity of silver trifluoromethanesulfonate and the intermediate that forms (OTf)SubPcs, which is highly

reactive, see **Scheme 2**.[35,36] With moisture in the system AgOTf reacts with H_2O and forms AgOH and HOTf, and as a result, it is not possible to form the intermediate (OTf)SubPc.

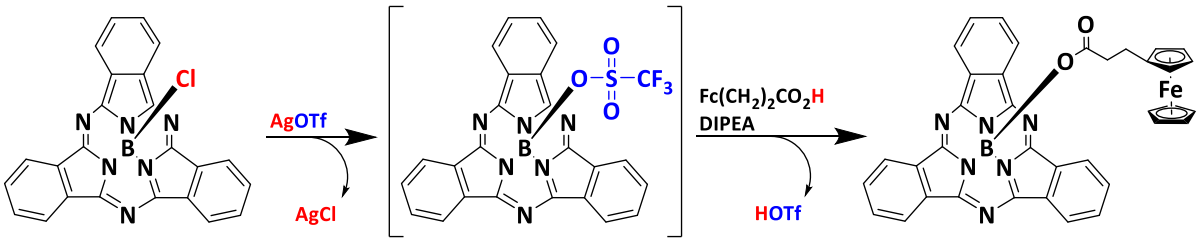

Scheme 2 Basic reaction steps with (OTf)SubPc intermediate formation.[35]

The weakly-coordinating triflate (OTf^-) anion activated the triflate-SubPc drastically increasing reactivity towards nucleophilic attack at the boron atom.[35] The success of the synthesis is drastically affected when not working under strict Schlenk conditions. When the reactions were performed in a glovebox with H_2O: < 0.5 ppm and O_2: < 10 ppm, it was possible to improve the yields of all ferrocenylsubphthalocyanine dyads by *ca.* 30% to 60%, in comparison to bench reactions. The purification of the ferrocenylsubphthalocyanine dyads was easily done utilising flash column chromatography on a short column. The yields of SubPc, **5** and **7** were higher than **6** and **8** due to the electron-donating effect of the ferrocene group being stronger on the OH group of the COOH moiety of **1** than **2**, increasing its reactivity.

The well-known conical structure of SubPcs[13] provides them with relatively strong solubility and a low tendency to aggregate. The ferrocenyl moieties in the axial position of complexes **5** – **8** significantly increased the solubility in common organic solvents compared to the parent macrocycles **3** and **4** with chlorine in the axial position. Complexes **5** – **8** are soluble in DCM,

chloroform, toluene and THF; however, they are poorly soluble in hexane and diethyl ether. The fluorinated SubPcs **4**, **7** and **8** were slightly more soluble than SubPcs **3**, **5** and **6**.

On ^{1}H NMR the peripheral and non-peripheral peaks shifted slightly upfield by 0.04-0.09 ppm for SubPc **5,** and **6** relative to ClBSubPc **3**. ^{19}F NMR showed a small shift in peripheral and non-peripheral peaks with a downfield shift of 1 - 2 ppm for SubPc **7** and **8** relative to ClBSubPc(F)$_{12}$, **4**. The most significant effect on ^{1}H NMR was observed for the substituted and unsubstituted-cyclopentadienyl (cp) ring peaks of **5** – **8**. The effect of the SubPc on the signals of ferrocenyl was similar for the two axial ligands (Fc-CH=CH-COO-) and (Fc-CH_2-CH_2-COO-). For example, in comparison to the free ferrocenylcarboxylic acid **1** ($C_5H_{5,Fc}$ at 4.12 ppm), the signals of the unsubstituted-cp ring are shifted upfield with 0.29 ppm for SubPc **5** (3.83 ppm) and downfield with 0.59 ppm for SubPc **7** (4.71 ppm). Similarly, the signals of the ferrocenyl moieties of the unsubstituted-cp ring of SubPc **6** and **7** were ca 0.3 downfield and 0.6 ppm upfield relative to that of **2** ($C_5H_{5,Fc}$ at 4.15 ppm). The effect on the signals of the ferrocenyl moieties of the substituted-cp ring $C_5H_{4,Fc}$ for SubPc **5** (3.77 and 3.57 ppm) and **7** (4.65 and 4.45 ppm) relative to **2** ($C_5H_{4,Fc}$ at 4.09 and 4.07 ppm), and that of SubPc **6** (4.21 and 4.20 ppm) and **8** (5.09 and 4.98 ppm) relative to **1** ($C_5H_{4,Fc}$ at 4.50 and 4.42 ppm), were similar. However, all ferrocenyl signals of the fluorinated SubPcs **7** and **8** were ca 0.9 ppm downfield relative to SubPc's **5** and **6**.

The UV/vis spectra of SubPcs **5** – **8** exhibited the expected two main transitions, the Soret band between 250 and 350 nm, and the Q-band between 450 and 620 nm, see **Figure 1**. The effect of substituting the axial chlorine atom in **3** with the ferrocenyl dyads **1** and **2** was negligible, with a blue shift of only 1 nm in the Q-band to 563 nm for SubPcs **5** and **6**. The similar Soret and Q-bands for **3** and the ferrocenylcarboxcylic acid subphthalocyanine dyads

SubPcs **5** and **6** (see **Table 1**), indicates that the Soret and Q-bands involve purely π-π* transitions, without any metal-to-ligand-charge-transfer (MLCT) transitions involved in the Q-bands. The MLCT transitions is expected in the near-IR (NIR) region.[16] Similarly, no shift in the Q-band maximum was observed for fluorinated SubPcs, **7** and **8** (573 nm) relative to **4** (573 nm). However, it has been reported that both donor and acceptor peripheral substituents shifted the Q band of SubPcs toward longer wavelengths, due to extension of the π conjugation of the macrocycle.[13] Here the electron-withdrawing fluorine ring substituents shifted the Q-bands with 10 nm from c.a. 563 nm (SubPcs **3**, **5** and **6**) to 573 nm (SubPcs **4**, **7** and **8**). SubPcs **5** to **8** showed no aggregation in the concentration range of 0.01 – 0.10 (x 10^{-3} M) and followed the Beer-Lambert law, see **Figure 1**.

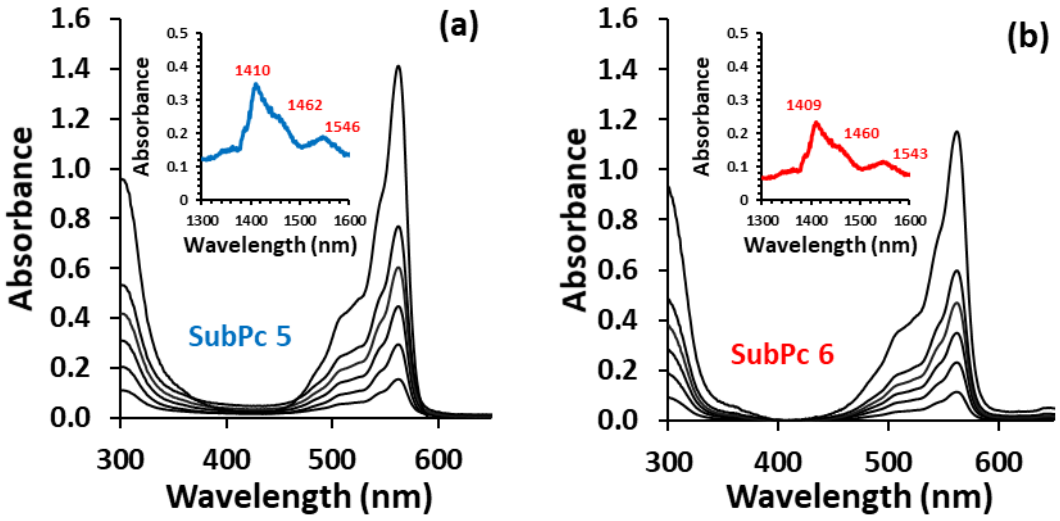

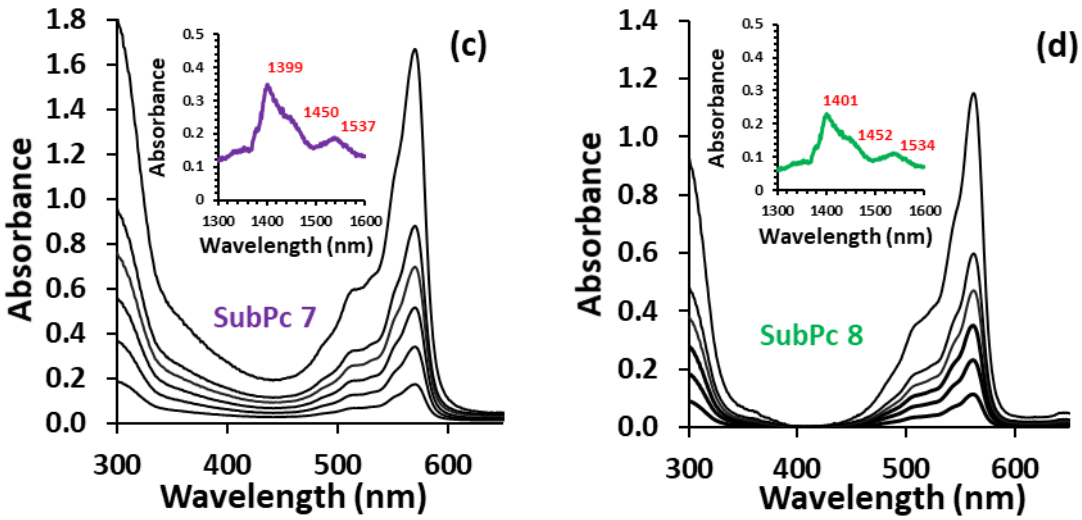

Figure 1 (a) – (d) The UV/vis spectra of SubPc **(5 – 8)** at concentrations 0.01, 0.02, 0.03, 0.04, 0.05 and 0.10 (x 10^{-3} M), obtained with a 1cm pathlength cuvette. The metal to ligand charge transfer (MLCT) of $(Fc(CH_2)_2COO)BSubPc(H)_{12}$, **5**; $(Fc(CH)_2COO)BSubPc(H)_{12}$, **6**; $(Fc(CH_2)_2COO)BSubPc(F)_{12}$, **7** and $(Fc(CH)_2COO)BSubPc(F)_{12}$, **8** was obtained at concentration 1 (x 10^{-3} M) with wavelengths indicated on spectra in nm. UV/vis spectra of SubPc (**4** – **8**) at concentration 0.01 x 10^{-3} M, from 250 – 650 nm, is provided in the Supplementary Information. The Beer-Lambert correlation between the absorbance A and concentration of SubPc (**5** – **8**) is provided in Supplementary Information.

Table 1 UV/vis data of SubPcs **3** – **8** in THF.

	Sorret Band	**Q Band**		
	Max	1st shoulder	2nd shoulder	Max
$ClBSubPc(H)_{12}$, **3**	308	525	532	564
$ClBSubPc(F)_{12}$, **4**	303	506	541	573
$(Fc(CH_2)_2COO)BSubPc(H)_{12}$, **5**	302	505	544	563
$(Fc(CH)_2COO)BSubPc(H)_{12}$, **6**	291	504	543	563
$(Fc(CH_2)_2COO)BSubPc(F)_{12}$, **7**	282	511	542	573
$(Fc(CH)_2COO)BSubPc(F)_{12}$, **8**	284	510	542	573

Cyclic Voltammetry

The redox properties of the novel ferrocenylsubphthalocyanine dyads SubPc **5** – **8** were examined using cyclic voltammetry (CVs) and linear sweep voltammetry (LSVs). The CVs and LSVs of SubPc **5** – **8** at 25°C in dichloromethane (DCM) at a scan rate of 0.100 Vs^{-1} are shown in **Figure 2** (also see the overlay CV in the Supplementary Information) with electrochemically

relevant data summarised in **Table 2**. The cyclic voltammetry showed chemically reversible results with peak ratios approaching 1 for the first oxidation process for **5** - **8** (assigned to as ferrocenyl oxidation), the second ring-based oxidation for **5** - **8** (wave I in **Figure 2**), the first ring-based reduction peak for **5** - **8** (wave II in **Figure 2**) and the second ring-based reduction peak for **7** - **8** (wave III in **Figure 2**), all with peak current separations ΔE_p between 0.074 and 0.090 V. The second ring-based reduction peak for **5** - **6** (wave III in **Figure 2**) and the third ring-based reduction peak for **7** - **8** (wave IV in **Figure 2**) were irreversible and did not show any re-oxidation peaks. Linear sweep voltammetry showed, as expected, 1 e^- redox couples for Fc oxidation and waves I to IV.

Ferrocenyl moiety oxidation

The oxidation of the Fe group of the ferrocenyl-containing axial ligand is the first observed redox process for all four SubPcs **5** – **8**. This assignment is in agreement with literature[15,16] and also supported by DFT calculations, see computational analysis below. SubPcs **5** and **6** have ferrocenyl oxidation potentials $E°'$ at -0.058 and 0.119 V, while SubPcs **7** and **8** have oxidation potentials at 0.050 and 0.243 V respectively, all with ΔE_p between 0.074 – 0.078 V, see **Table 2** and **Figure 2**, as well as the overlay CV in the Supplementary Information.

The fluorine ring substituents in SubPcs **7** and **8** causes the ferrocenyl oxidation to shift *ca.* with 0.1 V to a more positive potential compared to SubPcs **5** and **6** respectively. The electron-rich macrocycle of SubPc, Y-BSubPc(H)$_{12}$ (SubPcs **5** and **6**) had an electron-donating effect on the axial ligand Y, shifting the oxidation potential of ferrocenyl in the unsubstituted ferrocenylcarboxylic acid YH **1** (-0.015 V)[19] and **2** (0.170 V)[19] with c.a. 0.05 V more negative compared to the oxidation potential of ferrocenyl of the substituted ferrocenylcarboxylic acid

in SubPcs **5** (-0.058 V) and **6** (0.119 V) respectively. In contrary, the less electron-rich macrocycle of the fluorinated SubPc, Y-BSubPc$(F)_{12}$ (SubPcs **7** and **8**) had an electron-withdrawing effect on the axial ligand Y, shifting the oxidation potential of ferrocenyl in the unsubstituted ferrocenylcarboxylic acid YH **1** (-0.015 V) and **2** (0.170 V) with c.a. 0.07 V more positive compared to the oxidation potential of ferrocenyl of the substituted ferrocenylcarboxylic acid in SubPcs **7** (0.050 V) and **8** (0.243 V) respectively.

For the free ferrocenyl dyads **1** and **2** it was found that the formal reduction potential $E^{\circ\prime}$ of the ferrocene group of **2** that is not isolated from the electron-withdrawing effect of the carbonyl group (due to π-communication via the sp^2 hybridised carbon atoms in the -CH=CH- fragment), is 0.170 V more positive than free ferrocene at 0 V *vs.* Fc/Fc^+.[19] However, $E^{\circ\prime}$ of the ferrocene group of **1** that is more isolated from the electron-withdrawing effect of the carbonyl group (containing the sp^3 hybridised carbon atoms in the $-CH_2-CH_2-$ fragment) is much lower, at -0.015 *vs.* Fc/Fc^+.[19] The same trend was observed here, the oxidation potentials of ferrocenyl in SubPcs **5** (-0.058 V) and SubPcs **7** (0.050 V) containing ferrocenyl dyad **1** in the axial position, were nearly 0.2 V lower than the oxidation potentials of ferrocenyl in **6** (0.119 V) and **8** (0.243 V) respectively, containing ferrocenyl dyad **2** in the axial position.

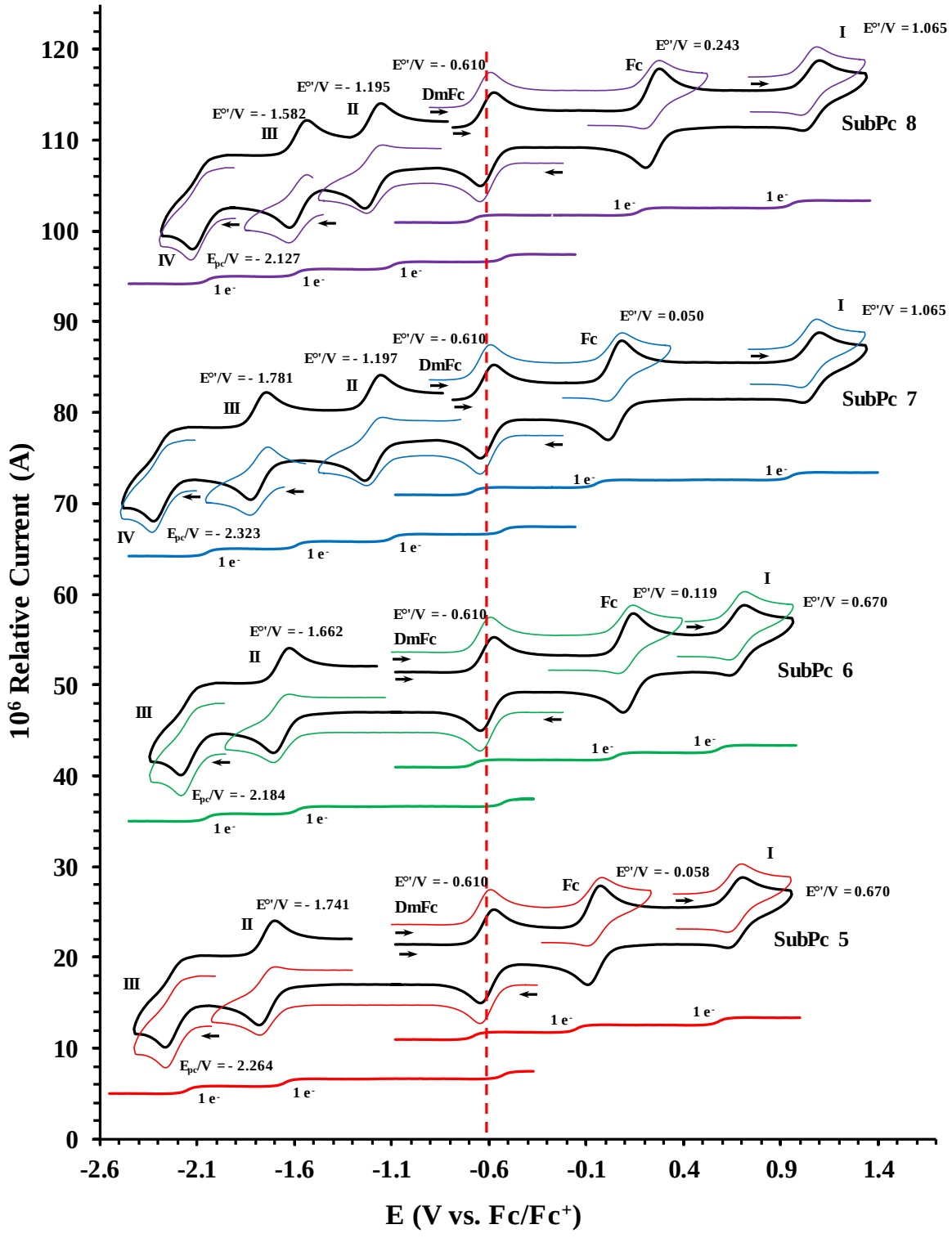

Figure 2 CV's and LSV's of SubPc, **5** - (red), **6** - (green), **7** - (blue) and **8** - (purple) in DCM / $[N(^{n}Bu)_4][B(C_6F_5)_4]$. Concentration of **5** – **8** = 0.0005 mol dm^{-3}. Scan rate for CVs is 0.100 V s^{-1} and LSVs at 0.001 V s^{-1}. Scan directions are indicated at starting point of each scan. Also see the overlay CV in the Supplementary Information.

Table 2 Cyclic voltammetry data of SubPcs **5** – **8** in DCM containing 0.1 mol dm^{-3} $[N(^nBu)_4][B(C_6F_5)_4]$ as supporting electrolyte at a scan rate of 0.100 V/s at 25°C.

	Description	E_p[a]	$E^{o'}$ (V), ΔE_p (V)	i_p (µA)[b], current ratio[c]
$Fc(CH_2)_2COOH$[d]	Fc	0.020	-0.015, 0.070	3.87, 0.99
$Fc(CH)_2COOH$[d]	Fc	0.210	0.170, 0.079	3.36, 0.99
SubPc **5**	DmFc	-0.573	-0.610,0.074	3.89, 0.99
	Fc	-0.021	-0.058, 0.074	3.66, 0.99
	Wave I	0.712	0.670, 0.084	3.31, 0.99
	Wave II	-1.783	-1.741, 0.084	3.42, 0.99
	Wave III	-2.264	- , -	- , -
SubPc **6**	DmFc	-0.573	-0.610, 0.074	3.93, 0.99
	Fc	0.156	0.119, 0.074	3.54, 0.99
	Wave I	0.711	0.670, 0.082	3.24, 0.99
	Wave II	-1.704	-1.662, 0.084	3.47, 0.99
	Wave III	-2.184	- , -	- , -
SubPc **7**	DmFc	-0.572	-0.610, 0.076	3.87, 0.99
	Fc	0.089	0.050, 0.078	3.71, 0.99
	Wave I	1.106	1.065, 0.082	3.41, 0.99
	Wave II	-1.240	-1.197, 0.086	3.58, 0.99
	Wave III	-1.825	-1.781, 0.088	4.01, 0.99
	Wave IV	-2.323	- , -	- , -
SubPc **8**	DmFc	-0.573	-0.610, 0.074	3.91. 0.99
	Fc	0.282	0.243, 0.078	3.64, 0.99
	Wave I	1.107	1.065,0.084	3.37, 0.99
	Wave II	-1.239	-1.195, 0.088	3.46, 0.99
	Wave III	-1.627	-1.582, 0.090	3.89, 0.99
	Wave IV	-2.127	- , -	- , -

[a] E_p is the peak anodic peak for oxidation (E_{ox}) and peak cathodic peak for reduction (E_{red}).
[b] i_p is the peak anodic peak for oxidation (i_{pa}) and peak cathodic peak for reduction (i_{pc}).
[c] peak current ratio = i_{pc}/i_{pa} for oxidation and i_{pa}/i_{pc} for reduction.
[d] Data from reference [19]

Ring-based Oxidation

The first ring-based oxidation of SubPc **5** and **6** (wave I in **Figure 2**) is the same, namely 0.670 V. Similarly, the first ring-based oxidation of SubPc **7** and **8** (wave I in **Figure 2**) is the same, namely 1.065 V. The first ring-based oxidations of SubPc **5** - **8** are thus mainly influenced by the ring substituents (H or F) and not by the oxidised axial ferroceniumcarboxcylic acid dyad. The different oxidised axial ferroceniumcarboxcylic acid dyads (Fc^+-CH_2-CH_2-COO) and (Fc^+-

CH=CH-COO) on SubPc **5** and **6** respectively, thus seem to have the same influence on the first ring-based oxidation of SubPc **5** and **6**, namely, substituting the axial chloride ligand of SubPc **3** with ferroceniumcarboxcylic acid dyads causes the first ring-oxidation (wave I in **Figure 2**) to shift with 0.042 V more positive from 0.628 V (SubPc **3**) to 0.670 V (SubPc **5** and **6**). The first ring-based oxidation of the fluorinated SubPcs **7** – **8** shifted opposite with 0.131 V more negative from 1.196 V (SubPc **4**) to 1.065 V (SubPc **7** and **8**). Here, for the first time, quasi reversible first ring-based oxidation is obtained for ferrocenylsubphthalocyanine dyads, namely for SubPcs **5** – **8** with peak ratios approaching 1 and ΔE_p ranging between 0.082 and 0.084 V (see **Table 2**). Generally the first ring-based oxidation of SubPc's show irreversible oxidation behaviour.[13] Previously published ring-based oxidation of ferrocenylsubphthalocyanine dyads was only partially reversible, ascribed to significant degradation of the subphthalocyanine core.[15,16]

Ring-based Reduction

The ring-based reductions of SubPc's **5** - **8**, redox waves II, III and IV in **Figure 2** and **Table 2**, generally follow the same trend than the ferrocene and ring-based oxidations, namely that the reduction of SubPc's **5** and **7** containing ferrocenyl dyad **1** as axial ligand, were lower or the same than the reduction of SubPc's **6** and **8** containing ferrocenyl dyad **2** as axial ligand, as illustrated in the overlay CV in the Supplementary Information. Only for SubPc **7** and **8**, in addition to reduction waves II and III, a third non-reversible reduction wave is observed (wave IV), see **Figure 2**. Wave IV, is observed for SubPc **7** and **8** and not for **5** and **6** because of the strong electron-withdrawing properties of the fluorinated SubPcs, moving the third reduction wave into the solvent window.

Computational Analysis

The SubPcs $(Fc(CH_2)_2COO)BSubPc(H)_{12}$, **5**, $(Fc(CH)_2COO)BSubPc(H)_{12}$, **6**, $(Fc(CH_2)_2COO)BSubPc(F)_{12}$, **7** and $(Fc(CH)_2COO)BSubPc(F)_{12}$, **8**, was optimised to gain further insight into the redox properties of the ferrocene dyads. On a molecular level, the highest occupied molecular orbital (HOMO) of these molecules, provide information of where the electrons are removed during the oxidation process of these molecules. As expected, the LUMOs and HOMOs of neutral SubPcs **5** – **8** are of mainly π-ring and iron-d character respectively, confirming ring-based reduction and Fe(II) to Fe(III) oxidation respectively, see **Figure 3**. Both HOMO and HOMO-1 were centred on the iron centre; however, experimentally the second oxidation of SubPcs **5** – **8** were assigned to be SubPc ring-based. Since it sometimes happens that orbitals can rearrange upon oxidation,[37–39] it is essential to optimise the cation (oxidised) species as well, to locate the locus of the second experimentally observed oxidation. The oxidised SubPcs **5** – **8** all showed that the LUMO is on the iron centre (first oxidation) and the HOMO and HOMO-1 are on the SubPc-ring (second and third oxidation), in agreement with the experimental assignment, see **Figure 4**. The molecular orbital (MO) energy level diagram in **Figure 4** show that the equi-energetic PBE1PBE/6-311G(d,p) ring-based HOMO and HOMO-1 of the oxidised fluorinated SubPc **7** (**7**$^+$) are 0.35 eV lower in energy than the HOMOs of oxidised SubPc **5** (**5**$^+$) implying that it will be more difficult (higher potential needed) for the second oxidation of SubPc **7**. It will be more difficult to remove an electron upon oxidation from the more stable, lower energy HOMO of SubPc **7**$^+$ ($E^{\circ\prime}$ = 1.065 V) than from the higher energy HOMO of SubPc **5**$^+$ ($E^{\circ\prime}$ = 0.670 V). However, the difference in energy between the HOMOs of SubPc **7**$^+$ and SubPc **8**$^+$ is only 0.04 eV, explaining

why the ring-based oxidation of SubPc **7**$^{+}$ and SubPc **8**$^{+}$ occurs at the same potential (1.065 V).

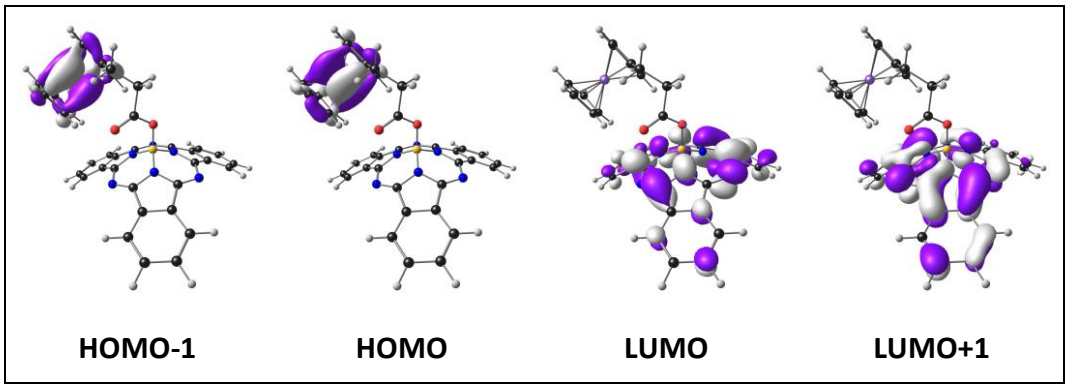

Figure 3 Selected PBE1PBE/6-311G(d,p) frontier MOs for neutral SubPcs **5** and **7**. A contour of 0.03 e/Å^3 was used for the orbital plots. Colour code of atoms (online version): Fe (purple), B (yellow), C (grey), O (red), H (white).

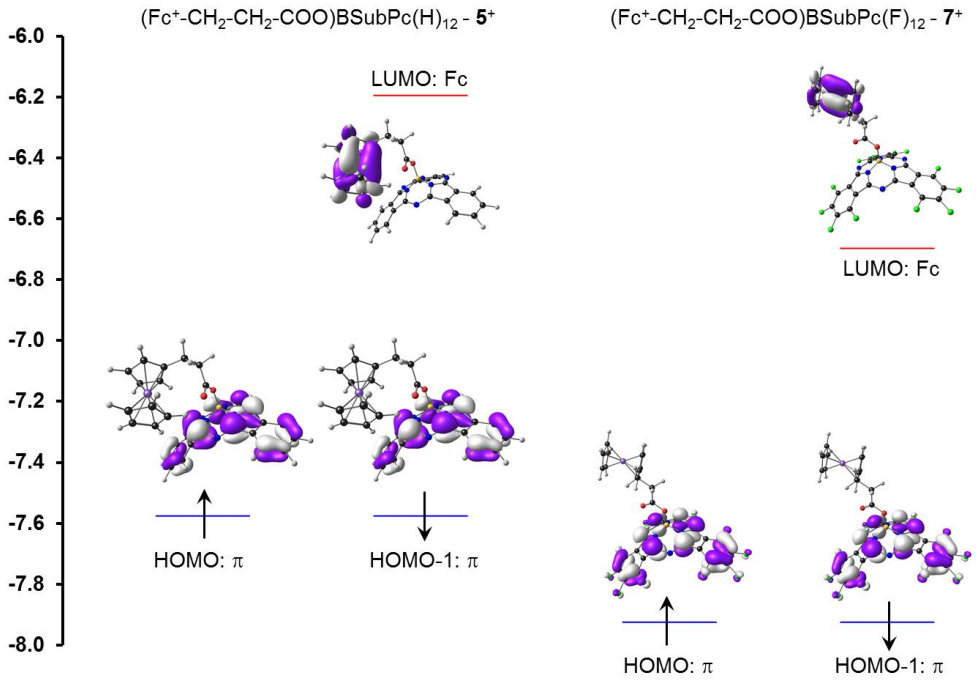

Figure 4 PBE1PBE/6-311G(d,p) MO energy level diagrams for the cations of SubPcs **5** and **7**. The y-axis show energies in eV. A contour of 0.03 e/Å^3 was used for the orbital plots. Colour code of atoms (online version): Fe (purple), B (yellow), C (grey), O (red), H (white). The energy levels of filled MOs are shown in blue and the energy levels of empty MOs in red. The arrows indicate the α-electrons (up spin) and β electrons (down spin).

Conclusions

Subphthalocyanines with ferrocenylcarboxylic acids in the axial position can be synthesised in a 60% yield when reactions are performed under extremely dry conditions (e.g. in a glovebox). The axial ferrocenylcarboxylic acids did not influence the UV/vis wavelength maxima of the Soret and Q-bands of the ferrocenylsubphthalocyanine dyads, that were similar to the wavelength maxima of the parent ClBSubPcs. The CVs of the ferrocenylsubphthalocyanine dyads revealed that the first reversible oxidation process is ferrocene-centred, while the second oxidation and all observed reduction processes were localised on the SubPc-ring. By performing the CV experiments in DCM with $[N(^{n}Bu)_4][B(C_6F_5)_4]$ as supporting electrolyte tetrabutylammonium, it was possible, for the first time, to obtain chemically reversible ring-based oxidation for ferrocenylsubphthalocyanine dyads. DFT optimisation of the oxidised SubPcs was necessary to confirm the locus of the second observed SubPc-ring-based oxidation.

Supplementary Information

The synthesis and characterisation, additional graphs, tables, and optimised coordinates are provided in the Supporting information.

Author Information

Name: Jeanet Conradie, Tel: +27-(51)-4012194, Fax: +27-4017295, email: conradj@ufs.ac.za

Notes

The authors declare no competing financial interest.

Acknowledgements

This work has received support the South African National Research Foundation (Grant numbers 113327 and 96111) and the Central Research Fund of the University of the Free State, Bloemfontein. The High-Performance Computing facility of the UFS, the CHPC of South Africa and the Norwegian Supercomputing Program (UNINETT Sigma2, Grant No. NN9684K) are acknowledged for computer time.

References

(1) Bublitz, D. E.Rinehart, K. L. *Inorganic Reactions*, 17th ed.; Eiley: New York, 1969.

(2) Deeming, J. *In Comprehensive Organometallic Chemistry*, 4th ed.; Pergamon, Ed.; Oxford, 1982.

(3) Watts, W . *In Comprhensive Organometallic Chemistry*, 8th ed.; Pergamon, Ed.; Oxford, 1982.

(4) Nesmeyanov, A. N.; Kochetkova, N. S. Applications of Ferrocene and Its Derivatives. *Russ. Chem. Rev.* **1974**, *5* (9), 710–715. https://doi.org/10.1143/JJAP.33.5533.

(5) Rosenblum, N. *Chemistry of The Iron Group Metallocenes: Ferrocene, Ruthenocene, Osmocene*; John Wiley & Sons, Ed.; John Wiley & Sons: New York, 1965.

(6) Rausch, M. D.; Fischer, E. O.; Grubert, H. The Aromatic Reactivity of Ferrocene, Ruthenocene and Osmocene 1,2. *J. Am. Chem. Soc.* **1960**, *82* (1), 76–82. https://doi.org/10.1021/ja01486a016.

(7) Nonjola, P. T. N.; Siegert, U.; Swarts, J. C. Synthesis, Electrochemistry and Cytotoxicity of Ferrocene-Containing Amides, Amines and Amino-Hydrochlorides. *J. Inorg. Organomet. Polym. Mater.* **2015**, *25* (3), 376–385. https://doi.org/10.1007/s10904-015-0195-4.

(8) Davis, W. L.; Shago, R. F.; Langner, E. H. G.; Swarts, J. C. Synthesis and Electrochemical Properties of a Series of Ferrocene-Containing Alcohols. *Polyhedron* **2005**, *24* (12), 1611–1616. https://doi.org/10.1016/j.poly.2005.04.022.

(9) Meller, A.; Ossko, A. Phthalocyaninartige Bor-Komplexe. *Monatshefte fur Chemie* **1972**, *155*, 150–151.

(10) Ma, Z.; Liu, S.; Hu, S.; Yu, J. Highly Efficient Tandem Organic Light-Emitting Diodes Based on SubPc:C60 Bulk Heterojunction as Charge Generation Layer. *J. Lumin.* **2016**, *169*, 29–34. https://doi.org/10.1016/j.jlumin.2015.08.040.

(11) Ince, M.; Medina, A.; Yum, J. H.; Yella, A.; Claessens, C. G.; Martínez-Díaz, M. V.; Grätzel, M.; Nazeeruddin, M. K.; Torres, T. Peripherally and Axially Carboxylic Acid Substituted Subphthalocyanines for Dye-Sensitized Solar Cells. *Chem. - A Eur. J.* **2014**, *20* (7), 2016–2021. https://doi.org/10.1002/chem.201303639.

(12) Van de Winckel, E.; Mascaraque, M.; Zamarrón, A.; Juarranz de la Fuente, Á.; Torres, T.; de la Escosura, A. Dual Role of Subphthalocyanine Dyes for Optical Imaging and Therapy of Cancer. *Adv. Funct. Mater.* **2018**, *28* (24), 1–10.

https://doi.org/10.1002/adfm.201705938.

(13) Claessens, C. G.; González-Rodríguez, D.; Rodríguez-Morgade, M. S.; Medina, A.; Torres, T. Subphthalocyanines, Subporphyrazines, and Subporphyrins: Singular Nonplanar Aromatic Systems. *Chem. Rev.* **2014**, *114* (4), 2192–2277. https://doi.org/10.1021/cr400088w.

(14) Swarts, P. J.; Conradie, J. Electrochemical Behaviour of Chloro- and Hydroxy-Subphthalocyanines. *Electrochim. Acta* **2020**, *329*, 135165. https://doi.org/10.1016/j.electacta.2019.135165.

(15) Maligaspe, E.; Hauwiller, M. R.; Zatsikha, Y. V.; Hinke, J. A.; Solntsev, P. V.; Blank, D. A.; Nemykin, V. N. Redox and Photoinduced Electron-Transfer Properties in Short Distance Organoboryl Ferrocene-Subphthalocyanine Dyads. *Inorg. Chem.* **2014**, *53* (17), 9336–9347. https://doi.org/10.1021/ic5014544.

(16) Solntsev, P. V.; Spurgin, K. L.; Sabin, J. R.; Heikal, A. A.; Nemykin, V. N. Photoinduced Charge Transfer in Short-Distance Ferrocenylsubphthalocyanine Dyads. *Inorg. Chem.* **2012**, *51* (12), 6537–6547. https://doi.org/10.1021/ic3000608.

(17) Williams, D. B. G.; Lawton, M. Drying of Organic Solvents: Quantitative Evaluation of the Efficiency of Several Desiccants. *J. Org. Chem.* **2010**, *75* (24), 8351–8354. https://doi.org/10.1021/jo101589h.

(18) Blom, N. F.; Neuse, E. W.; Thomas, H. G. Electrochemical Characterization of Some Ferrocenylcarboxylic Acids. *Transit. Met. Chem.* **1987**, *12* (4), 301–306. https://doi.org/10.1007/BF01024018.

(19) Swarts, P. J.; Conradie, J. Solvent and Substituent Effect on Electrochemistry of

519 Ferrocenylcarboxylic Acid Dyads. *J. Electroanal. Chem.*

520 (20) Elgrishi, N.; Rountree, K. J.; McCarthy, B. D.; Rountree, E. S.; Eisenhart, T. T.; Dempsey,
521 J. L. A Practical Beginner's Guide to Cyclic Voltammetry. *J. Chem. Educ.* **2018**, *95* (2),
522 197–206. https://doi.org/10.1021/acs.jchemed.7b00361.

523 (21) Kissinger, P. T.; Heineman, W. R. Cyclic Voltammetry. *J. Chem. Educ.* **1983**, *60*, 702–706.
524 https://doi.org/10.1021/ed060p702.

525 (22) Gericke, H. J.; Barnard, N. I.; Erasmus, E.; Swarts, J. C.; Cook, M. J.; Aquino, M. A. S.
526 Solvent and Electrolyte Effects in Enhancing the Identification of Intramolecular
527 Electronic Communication in a Multi Redox-Active Diruthenium Tetraferrocenoate
528 Complex, a Triple-Sandwiched Dicadmium Phthalocyanine and a Ruthenocene-
529 Containing β-Diketone. *Inorganica Chim. Acta* **2010**, *363* (10), 2222–2232.
530 https://doi.org/10.1016/j.ica.2010.03.031.

531 (23) Birke, R. L.; Kim, M.-H.; Strassfeld, M. Diagnosis of Reversible, Quasi-Reversible, and
532 Irreversible Electrode Processes with Differential Pulse Polarography. *Anal. Chem.*
533 **1981**, *53* (6), 852–856. https://doi.org/10.1021/ac00229a026.

534 (24) Mirkin, M. V.; Bard, A. J. Simple Analysis of Quasi-Reversible Steady-State
535 Voltammograms. *Anal. Chem.* **1992**, *64* (19), 2293–2302.
536 https://doi.org/10.1021/ac00043a020.

537 (25) Myland, J. C.; Oldham, K. B. Quasireversible Cyclic Voltammetry of a Surface Confined
538 Redox System: A Mathematical Treatment. *Electrochem. commun.* **2005**, *7* (3), 282–
539 287. https://doi.org/10.1016/j.elecom.2005.01.005.

540 (26) Perdew, J. P.; Burke, K.; Ernzerhof, M. Generalized Gradient Approximation Made

Simple. *Phys. Rev. Lett.* **1996**, *77* (18), 3865–3868. https://doi.org/10.1103/PhysRevLett.77.3865.

(27) Perdew, J. P.; Burke, K.; Ernzerhof, M. Generalized Gradient Approximation Made Simple (ERRATA). *Phys. Rev. Lett.* **1997**, *78* (1992), 1396–1396. https://doi.org/DOI 10.1103/PhysRevLett.78.1396.

(28) Adamo, C.; Barone, V. Toward Reliable Density Functional Methods without Adjustable Parameters: The PBE0 Model. *J. Chem. Phys.* **1999**, *110* (13), 6158–6170. https://doi.org/10.1063/1.478522.

(29) Frisch, M. J.; Trucks, G. W.; Schlegel, H. B.; Scuseria, G. E.; Robb, M. A.; Cheeseman, J. R.; Scalmani, G.; Barone, V.; Petersson, G. A.; Nakatsuji, H.; et al. Gaussian 16, Revision B.01. Gaussian, Inc., Wallingford CT 2016, p 2016.

(30) Becke, A. D. Density-Functional Exchange-Energy Approximation with Correct Asymptotic Behavior. *Phys. Rev. A* **1988**, *38* (6), 3098–3100. https://doi.org/10.1103/PhysRevA.38.3098.

(31) Perdew, J. P. Density-Functional Approximation for the Correlation Energy of the Inhomogeneous Electron Gas. *Phys. Rev. B* **1986**, *33* (12), 8822–8824. https://doi.org/10.1103/PhysRevB.33.8822.

(32) Perdew, J. P. Erratum: Density-Functional Approximation for the Correlation Energy of the Inhomogeneous Electron Gas (Physical Review B (1986) 34, 10 (7406)). *Phys. Rev. B* **1986**, *34* (10), 7406. https://doi.org/10.1103/PhysRevB.34.7406.

(33) Marenich, A. V; Cramer, C. J.; Truhlar, D. G. Universal Solvation Model Based on Solute Electron Density and on a Continuum Model of the Solvent Defined by the Bulk

563 Dielectric Constant and Atomic Surface Tensions. *J. Phys. Chem. B* **2009**, *113*, 6378–
564 6396.

565 (34) Skyner, R. E.; Mcdonagh, J. L.; Groom, C. R.; Mourik, T. Van. A Review of Methods for
566 the Calculation of Solution Free Energies and the Modelling of Systems in Solution.
567 *Phys. Chem. Chem. Phys.* **2015**, *17*, 6174–6191. https://doi.org/10.1039/C5CP00288E.

568 (35) Guilleme, J.; González-Rodríguez, D.; Torres, T. Triflate-Subphthalocyanines: Versatile,
569 Reactive Intermediates for Axial Functionalization at the Boron Atom. *Angew. Chemie*
570 *- Int. Ed.* **2011**, *50* (15), 3506–3509. https://doi.org/10.1002/anie.201007240.

571 (36) Kato, T.; Tham, F. S.; Boyd, P. D. W.; Reed, C. A. Synthesis and Structure of the
572 Coordinatively Unsaturated Boron Subphthalocyanine Cation, [B(SubPc)]+. *Heteroat.*
573 *Chem.* **2006**, *17* (3), 209–216. https://doi.org/10.1002/hc.20223.

574 (37) Ferrando-Soria, J.; Fabelo, O.; Castellano, M.; Cano, J.; Fordham, S.; Zhou, H. C.
575 Multielectron Oxidation in a Ferromagnetically Coupled Dinickel(II) Triple Mesocate.
576 *Chem. Commun.* **2015**, *51* (69), 13381–13384. https://doi.org/10.1039/c5cc03544a.

577 (38) Buitendach, B. E.; Conradie, J.; Malan, F. P.; Niemantsverdriet, J. W.; Swarts, J. C.
578 Synthesis, Spectroscopy and Electrochemistry in Relation to DFT Computed Energies of
579 Ferrocene- and Ruthenocene-Containing -Diketonato Iridium(III) Heteroleptic
580 Complexes. Structure of [(2-Pyridylphenyl)2Ir(RcCOCHCOCH3]. *Molecules* **2019**, *24*
581 (21), 3923. https://doi.org/10.3390/molecules24213923.

582 (39) Malan, F. P.; Singleton, E.; Conradie, J.; Landman, M. Electrochemistry of a Series of
583 Symmetric and Asymmetric CpNiBr(NHC) Complexes: Probing the Electrochemical
584 Environment Due to Push-Pull Effects. *J. Electroanal. Chem.* **2018**, *814* (December

585 2017), 66–76. https://doi.org/10.1016/j.jelechem.2018.02.043.

586

Data in brief (DIB)

Supporting information for publication: **Redox and photophysical properties of four SubPcs containing ferrocenylcarboxylic acid dyads as axial ligands**

Oxidation and reduction data of four SubPcs with axially coordinated ferrocenylcarboxylic acid dyads

Pieter J. Swarts and Jeanet Conradie

Department of Chemistry, PO Box 339, University of the Free State, Bloemfontein, 9300, South Africa

Corresponding author(s)
conradj@ufs.ac.za

Abstract
The data presented in this paper are related to the research article entitled "*Redox and photophysical properties of four SubPcs containing ferrocenylcarboxylic acid dyads as axial ligands*" Submitted to Inorganic Chemistry, manuscript: ic-2020-00150d.

Keywords

Ferrocenylsubphthalocyanine; cyclic voltammetry; oxidation

Specifications Table

Subject	Chemistry
Specific subject area	Electrochemistry
Type of data	Table Image Graph Figure
How data were acquired	Princeton Applied Research PARSTAT 2273 potentiostat running Powersuite software (Version 2.58).

Data format	Raw Analysed
Parameters for data collection	Samples was used as synthesized. All the electrochemical experiments were performed in an M Bruan Lab Master SP glove box under a high purity argon atmosphere (H_2O and O_2 < 10 ppm).
Description of data collection	All electrochemical experiments were done in a 2 ml electrochemical cell containing three-electrodes (a glassy carbon working electrode, a Pt auxiliary electrode and a Pt pseudo reference electrode), connected to a Princeton Applied Research PARSTAT 2273 electrochemical analyser. Data obtained were exported to excel for analysis and diagram preparation.
Data source location	Institution: University of the Free State City/Town/Region: Bloemfontein Country: South Africa
Data accessibility	With the article
Related research article	P.J. Swarts, J. Conradie, "Submitted to Inorganic Chemistry, manuscript: ic-2020-00150d".

Value of the Data

- This data provides cyclic voltammograms and detailed electrochemical data for four novel ferrocenylsubphthalocyanine dyads in DCM for scan rates over two orders of magnitude (0.05 – 5.0 Vs^{-1}).

- This data illustrates the effect of electron-rich and electron-poor macrocycles of Y-BSubPc(H)$_{12}$ and Y-BSubPc(F)$_{12}$ subphthalocyanines on the iron(II/III) oxidation potential of ferrocenylcarboxylic acid dyads Y in the axial position. Y = non π communicating (Fc-**CH_2-CH_2**-COO-) or a π communicating (Fc-**CH=CH**-COO-) ferrocenyl moiety.

- This data illustrates that chemical reversible first ring-based oxidation with peak current ratios of 1 and peak current separations, ΔE = 0.074 – 0.084 V can be obtained when electrochemical experiments are performed in a high purity argon atmosphere, while using DCM as the solvent and [N(^{n}Bu)$_4$][B(C_6F_5)$_4$] as supporting electrolyte.

Data Description

The electrochemical data of ferrocenylsubphthalocyanine dyads shown in Figure 1 are summarized in Table 1 - 4, with the CVs shown in Figure 2 - 5. Cyclic voltammograms of the fluorinated subphthalocyanines showed an iron based and ring-based oxidations as well as three ring-based reductions. Cyclic voltammograms of the non-fluorinated subphthalocyanines also showed an iron based and ring-based oxidations but only two ring-based reductions. Previous studies showed that the first oxidation in related ferrocenylsubphthalocyanine dyads is iron based [1,2]. Porphyrins, phthalocyanines and subphthalocyanines can show up to three ring-based oxidations and three ring-based reductions [3].

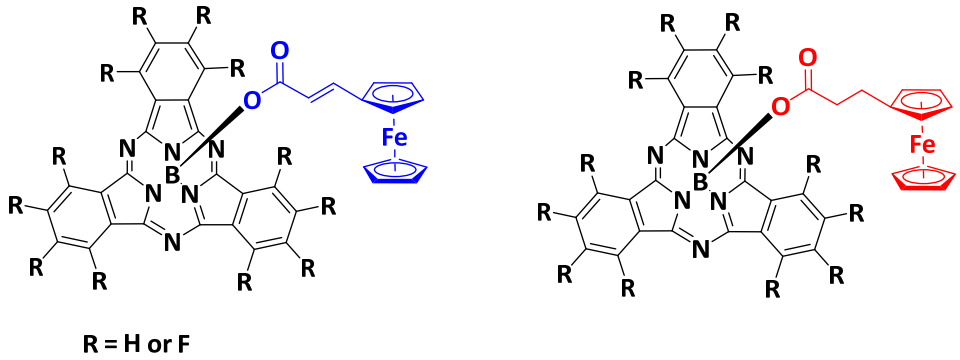

Figure 1. Structure of compounds in study.

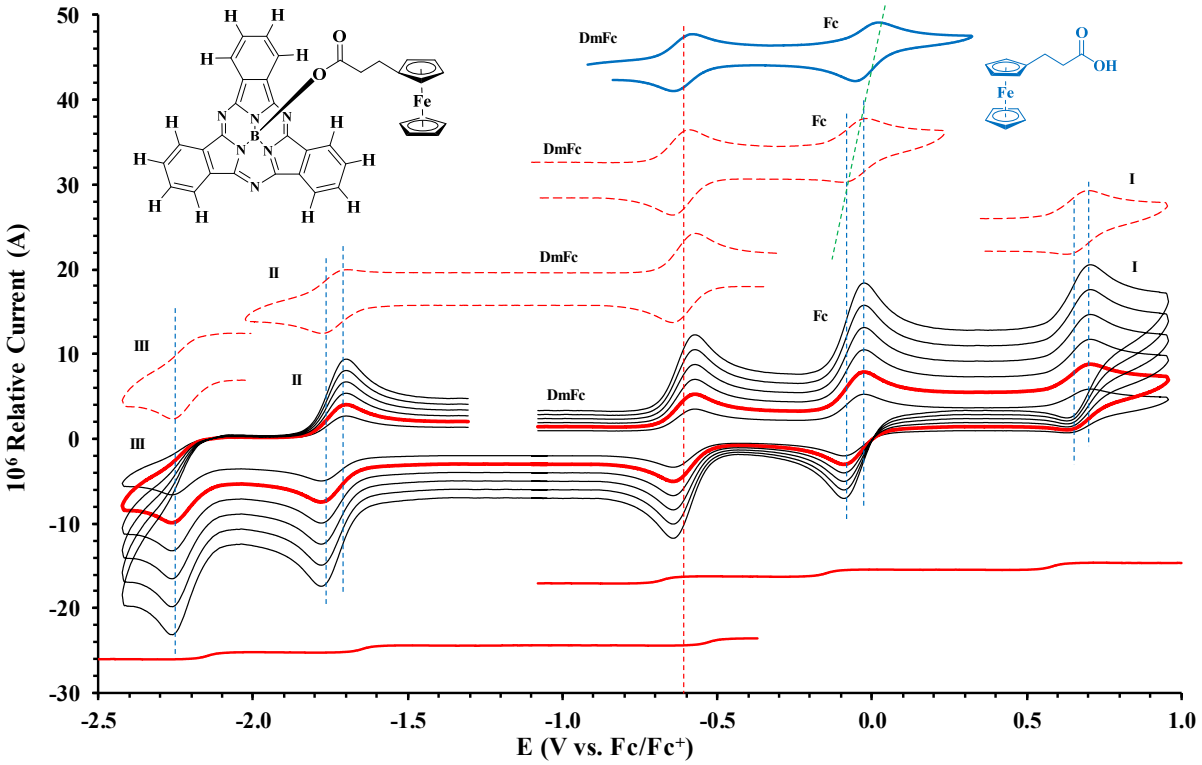

Figure 2. Cyclic voltammograms in DCM of $Fc(CH_2)_2CO_2BSubPc(H)_{12}$ at scan rates 0.050 (smallest peak currents), 0.100, 0.200, 0.300, 0.400 and 0.500 (largest peak currents).

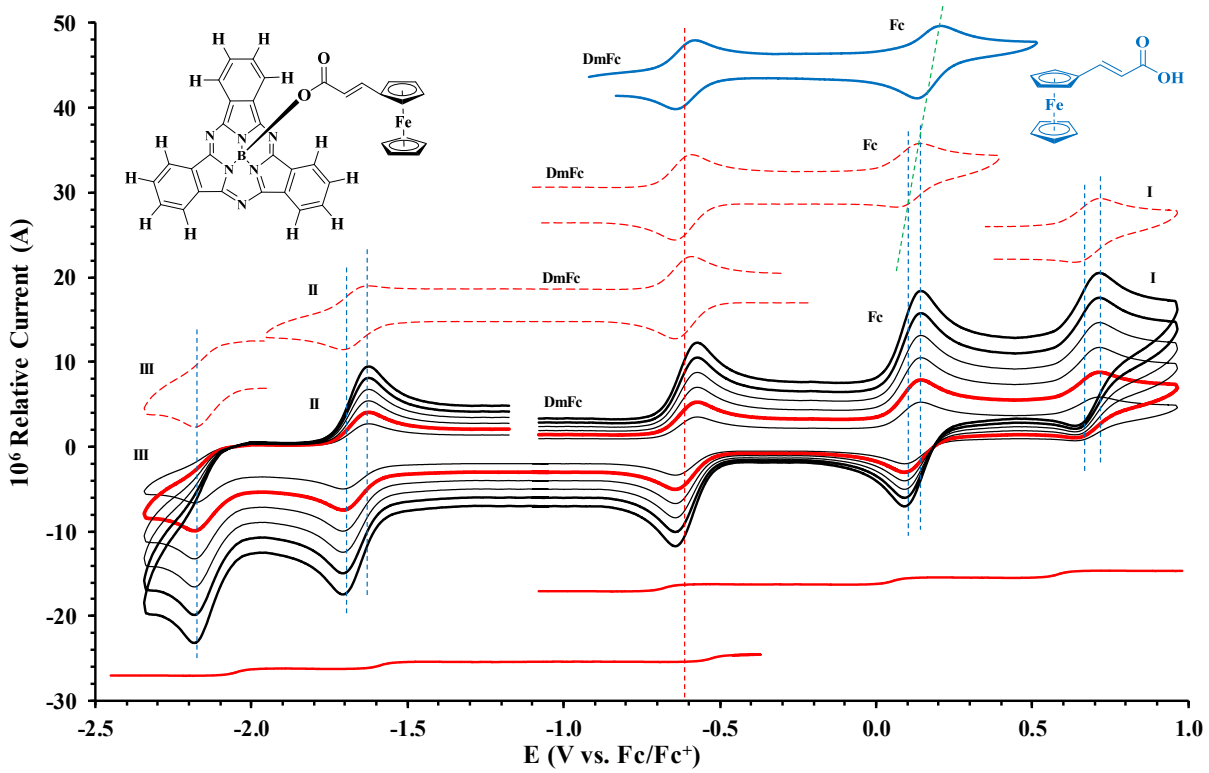

Figure 3. Cyclic voltammograms in DCM of $Fc(CH)_2CO_2BSubPc(H)_{12}$ at scan rates 0.050 (smallest peak currents), 0.100, 0.200, 0.300, 0.400 and 0.500 (largest peak currents).

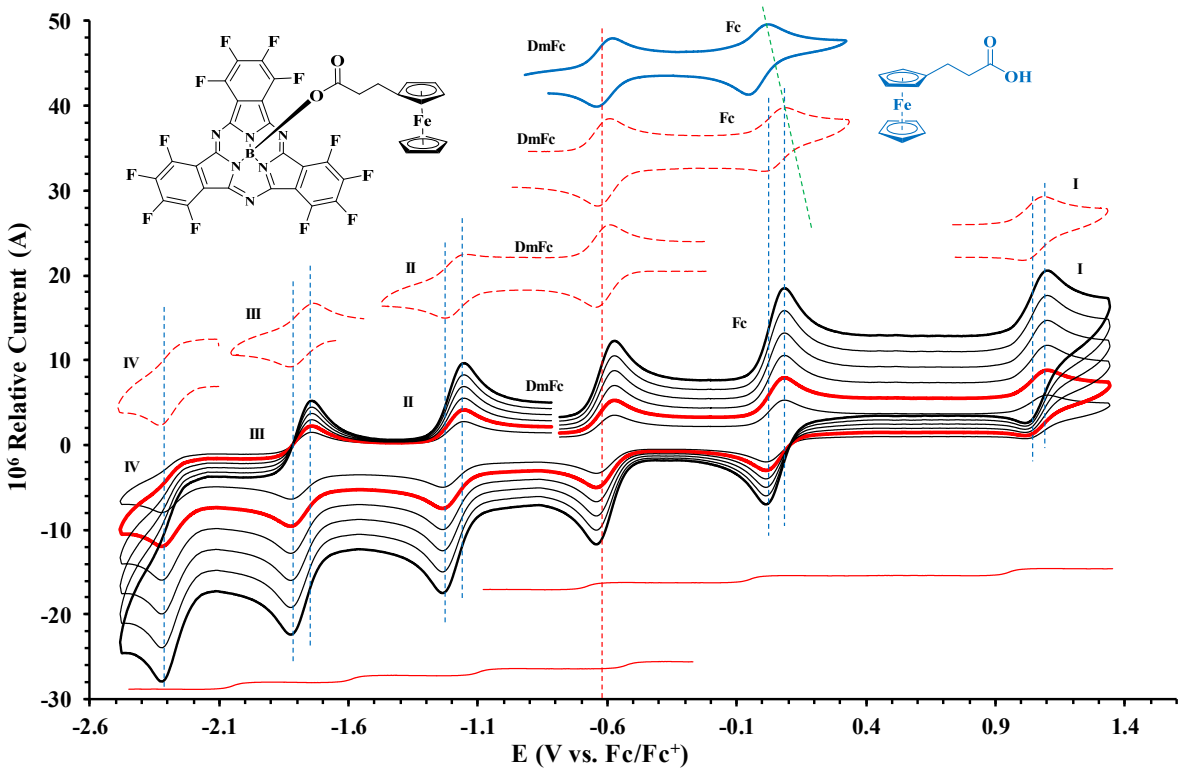

Figure 4. Cyclic voltammograms in DCM of $Fc(CH_2)_2CO_2BSubPc(F)_{12}$ at scan rates 0.050 (smallest peak currents), 0.100, 0.200, 0.300, 0.400 and 0.500 (largest peak currents).

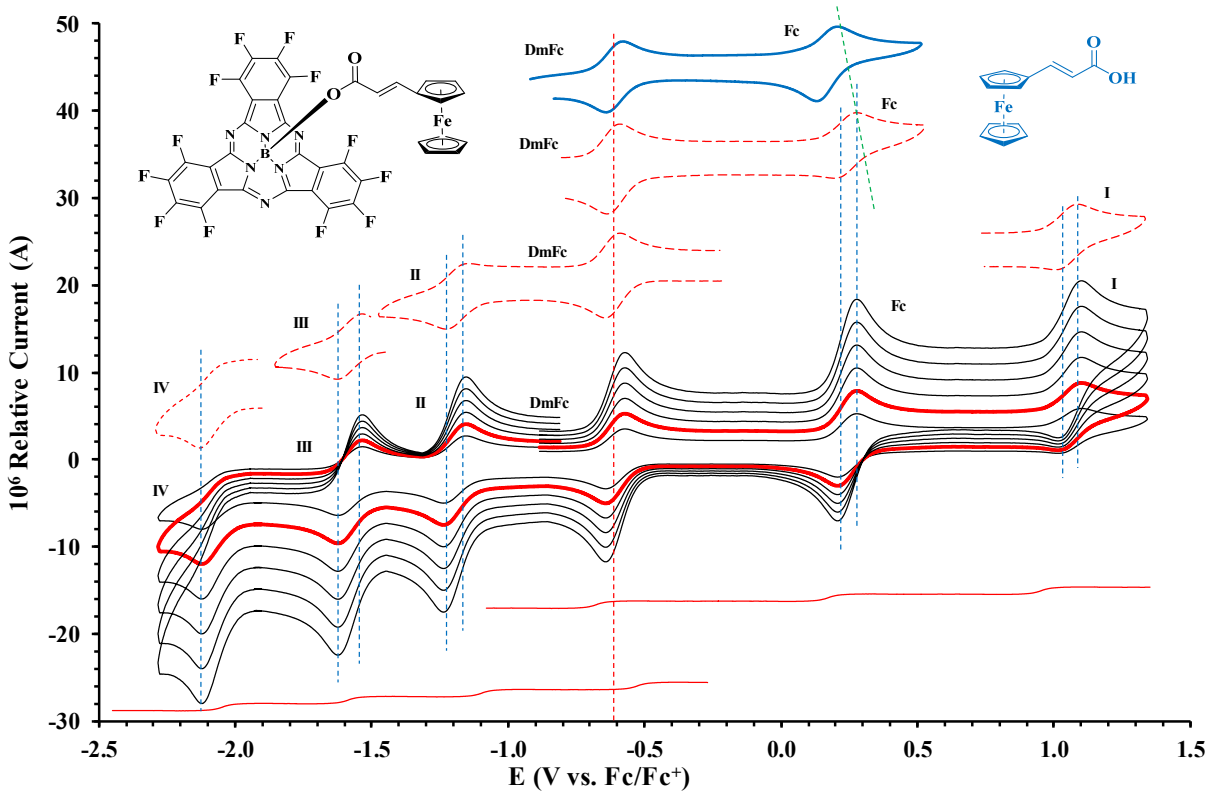

Figure 5. Cyclic voltammograms in DCM of $Fc(CH)_2CO_2BSubPc(F)_{12}$ at scan rates 0.050 (smallest peak currents), 0.100, 0.200, 0.300, 0.400 and 0.500 (largest peak currents).

Table 1. Electrochemical data (potential in V *vs* Fc/Fc^{+}) in DCM for *c.a.* 0.0005 mol dm^{-3} of $Fc(CH_2)_2CO_2BSubPc(H)_{12}$ at indicated scan rates (V in V/s).

V (V/s)	E_{pa} / V	ΔE_p / V	$E^{o'}$ / V	i_{pa} / μA	i_{pc}/i_{pa}
DmFc					
0.100	**-0.573**	**0.074**	**-0.610**	**3.89**	**0.99**
Fc					
0.050	-0.021	0.073	-0.058	2.61	0.99
0.100	**-0.021**	**0.074**	**-0.058**	**3.66**	**0.99**
0.200	-0.020	0.075	-0.058	5.12	0.99
0.300	-0.020	0.076	-0.058	5.86	0.99
0.400	-0.019	0.077	-0.058	8.42	0.99
0.500	-0.019	0.078	-0.058	9.15	0.99
5.000	-0.018	-	-	-	-
Wave I					
0.050	0.711	0.083	0.670	2.36	0.99
0.100	**0.712**	**0.084**	**0.670**	**3.31**	**0.99**
0.200	0.712	0.085	0.670	4.63	0.99
0.300	0.713	0.086	0.670	5.30	0.99
0.400	0.713	0.087	0.670	7.61	0.99
0.500	0.714	0.088	0.670	8.28	0.99
5.000	0.715	-	-	-	-
Wave II					
0.050	-1.782	0.083	-1.741	2.44	0.99
0.100	**-1.783**	**0.084**	**-1.741**	**3.42**	**0.99**
0.200	-1.783	0.085	-1.741	4.79	0.99
0.300	-1.784	0.086	-1.741	5.47	0.99
0.400	-1.784	0.087	-1.741	7.87	0.99
0.500	-1.785	0.088	-1.741	8.55	0.99
5.000	-1.786	-	-	-	-
Wave III					
0.050	-2.263	-	-	-	-
0.100	**-2.264**	-	-	-	-
0.200	-2.264	-	-	-	-
0.300	-2.265	-	-	-	-
0.400	-2.265	-	-	-	-
0.500	-2.266	-	-	-	-
5.000	-2.267	-	-	-	-

Table 2. Electrochemical data (potential in V *vs* Fc/Fc^{+}) in DCM for *c.a.* 0.0005 mol dm^{-3} of $Fc(CH)_2CO_2BSubPc(H)_{12}$ at indicated scan rates (V in V/s).

V (V/s)	E_{pa} / V	ΔE_p / V	$E^{o'}$ / V	i_{pa} / µA	i_{pc}/i_{pa}
DmFc					
0.100	**-0.573**	**0.074**	**-0.610**	**3.93**	**0.99**
Fc					
0.050	0.156	0.073	0.119	2.53	0.99
0.100	**0.156**	**0.074**	**0.119**	**3.54**	**0.99**
0.200	0.156	0.075	0.119	4.96	0.99
0.300	0.157	0.076	0.119	5.66	0.99
0.400	0.157	0.077	0.119	8.14	0.99
0.500	0.158	0.078	0.119	8.85	0.99
5.000	0.159	-	-	-	-
Wave I					
0.050	0.710	0.081	0.670	2.31	0.99
0.100	**0.711**	**0.082**	**0.670**	**3.24**	**0.99**
0.200	0.711	0.083	0.670	4.54	0.99
0.300	0.712	0.084	0.670	5.18	0.99
0.400	0.712	0.085	0.670	7.45	0.99
0.500	0.713	0.086	0.670	8.10	0.99
5.000	0.714	-	-	-	-
Wave II					
0.050	-1.703	0.083	-1.662	2.48	0.99
0.100	**-1.704**	**0.084**	**-1.662**	**3.47**	**0.99**
0.200	-1.704	0.085	-1.662	4.86	0.99
0.300	-1.705	0.086	-1.662	5.55	0.99
0.400	-1.705	0.087	-1.662	7.98	0.99
0.500	-1.706	0.088	-1.662	8.68	0.99
5.000	-1.707	-	-	-	-
Wave III					
0.050	-2.183	-	-	-	-
0.100	**-2.184**	-	-	-	-
0.200	-2.184	-	-	-	-
0.300	-2.185	-	-	-	-
0.400	-2.185	-	-	-	-
0.500	-2.186	-	-	-	-
5.000	-2.187	-	-	-	-

Table 3. Electrochemical data (potential in V *vs* Fc/Fc^{+}) in DCM for *c.a.* 0.0005 mol dm^{-3} of $Fc(CH_2)_2CO_2BSubPc(F)_{12}$ at indicated scan rates (V in V/s).

V (V/s)	E_{pa} / V	ΔE_p / V	$E^{o'}$ / V	i_{pa} / μA	i_{pc}/i_{pa}
DmFc					
0.100	**-0.572**	**0.076**	**-0.610**	**3.87**	**0.99**
Fc					
0.050	0.089	0.077	0.050	2.65	0.99
0.100	**0.089**	**0.078**	**0.050**	**3.71**	**0.99**
0.200	0.089	0.079	0.050	5.19	0.99
0.300	0.090	0.080	0.050	5.94	0.99
0.400	0.090	0.081	0.050	8.53	0.99
0.500	0.091	0.082	0.050	9.28	0.99
5.000	0.092	-	-	-	-
Wave I					
0.050	1.105	0.081	1.065	2.44	0.99
0.100	**1.106**	**0.082**	**1.065**	**3.41**	**0.99**
0.200	1.106	0.083	1.065	4.77	0.99
0.300	1.107	0.084	1.065	5.46	0.99
0.400	1.107	0.085	1.065	7.84	0.99
0.500	1.108	0.086	1.065	8.53	0.99
5.000	1.109	-	-	-	-
Wave II					
0.050	-1.239	0.085	-1.197	2.56	0.99
0.100	**-1.240**	**0.086**	**-1.197**	**3.58**	**0.99**
0.200	-1.240	0.087	-1.197	5.01	0.99
0.300	-1.241	0.088	-1.197	5.73	0.99
0.400	-1.241	0.089	-1.197	8.23	0.99
0.500	-1.242	0.090	-1.197	8.95	0.99
5.000	-1.243	-	-	-	-
Wave III					
0.050	-1.824	0.087	-1.781	2.86	0.99
0.100	**-1.825**	**0.088**	**-1.781**	**4.01**	**0.99**
0.200	-1.825	0.089	-1.781	5.61	0.99
0.300	-1.826	0.090	-1.781	6.42	0.99
0.400	-1.826	0.091	-1.781	9.22	0.99
0.500	-1.827	0.092	-1.781	10.03	0.99
5.000	-1.828	-	-	-	-
Wave IV					
0.050	-2.322	-	-	-	-
0.100	**-2.323**	-	-	-	-

0.200	-2.323	-	-	-	-
0.300	-2.324	-	-	-	-
0.400	-2.324	-	-	-	-
0.500	-2.325	-	-	-	-
5.000	-2.326	-	-	-	-

Table 4. Electrochemical data (potential in V *vs* Fc/Fc^{+}) in DCM for *c.a.* 0.0005 mol dm^{-3} of $Fc(CH)_2CO_2BSubPc(H)_{12}$ at indicated scan rates (V in V/s).

V (V/s)	E_{pa} / V	ΔE_p / V	$E^{o'}$ / V	i_{pa} / µA	i_{pc}/i_{pa}
DmFc					
0.100	**-0.573**	**0.074**	**-0.610**	**3.91**	**0.99**
Fc					
0.050	0.282	0.077	0.243	2.60	0.99
0.100	**0.282**	**0.078**	**0.243**	**3.64**	**0.99**
0.200	0.282	0.079	0.243	5.10	0.99
0.300	0.283	0.080	0.243	5.82	0.99
0.400	0.283	0.081	0.243	8.37	0.99
0.500	0.284	0.082	0.243	9.10	0.99
5.000	0.285	-	-	-	-
Wave I					
0.050	1.106	0.083	1.065	2.41	0.99
0.100	**1.107**	**0.084**	**1.065**	**3.37**	**0.99**
0.200	1.107	0.085	1.065	4.72	0.99
0.300	1.108	0.086	1.065	5.39	0.99
0.400	1.108	0.087	1.065	7.75	0.99
0.500	1.109	0.088	1.065	8.43	0.99
5.000	1.110	-	-	-	-
Wave II					
0.050	-1.238	0.087	-1.195	2.47	0.99
0.100	**-1.239**	**0.088**	**-1.195**	**3.46**	**0.99**
0.200	-1.239	0.089	-1.195	4.84	0.99
0.300	-1.240	0.090	-1.195	5.54	0.99
0.400	-1.240	0.091	-1.195	7.96	0.99
0.500	-1.241	0.092	-1.195	8.65	0.99
5.000	-1.242	-	-	-	-
Wave III					
0.050	-1.626	0.089	-1.582	2.78	0.99
0.100	**-1.627**	**0.090**	**-1.582**	**3.89**	**0.99**
0.200	-1.627	0.091	-1.582	5.45	0.99

0.300	-1.628	0.092	-1.582	6.22	0.99
0.400	-1.628	0.093	-1.582	8.95	0.99
0.500	-1.629	0.094	-1.582	9.73	0.99
5.000	-1.630	-	-	-	-
Wave IV					
0.050	-2.126	-	-	-	-
0.100	**-2.127**	-	-	-	-
0.200	-2.127	-	-	-	-
0.300	-2.128	-	-	-	-
0.400	-2.128	-	-	-	-
0.500	-2.129	-	-	-	-
5.000	-2.130	-	-	-	-

Experimental Design, Materials, and Methods

Electrochemical studies by means of cyclic voltammetry (CV) experiments were performed in an M Bruan Lab Master SP glove box under a high purity argon atmosphere (H_2O and O_2 < 10 ppm), utilizing a Princeton Applied Research PARSTAT 2273 potentiostat running Powersuite software (Version 2.58).

The cyclic voltammetry experimental setup consists of a cell with three electrodes, namely (i) a glassy carbon electrode as working electrode, (ii) a platinum wire auxiliary and (ii) a platinum wire as pseudo reference electrode. The glassy carbon working electrode was polished and prepared before every experiment on a Buhler polishing mat first with 1-micron and then with ¼-micron diamond paste, rinsed with H_2O, acetone and DCM, and dried before each experiment.

Electrochemical analysis in dichloromethane (DCM, anhydrous, ≥ 99.8%, contains 40-150 ppm amylene as stabilizer) as solvent was at RT. Solutions were made in 0.001 dm^3 spectrochemical

grade anhydrous DCM containing ca. 0.0005 M of analyte, 0.0005 mol dm^{-3} of internal reference (decamethylferrocene, DmFc) and 0.1 mol dm^{-3} of supporting electrolyte tetrabutylammonium tetrakispentafluorophenylborate, $[N(^{n}Bu)_4][B(C_6F_5)_4]$ in DCM.

Experimental potential data was measured vs. the redox couple of decamethyl ferrocene Fc* as internal standard and reported vs. the redox couple of ferrocene FcH, as suggested by IUPAC [4]. Experimental potential data was collected vs. the Pt wire reference electrode but is reported vs the redox couple of ferrocene, Fc/Fc^{+} at 0 V. E°`(DmFc) = - 0.610 V vs. Fc/Fc^{+} at 0 V in DCM/$[N(nBu)_4][B(C_6F_5)_4]$. Scan rates were between 0.05 and 5.00 Vs^{-1}.

Acknowledgments

This work has received support from the South African National Research Foundation (Grant numbers 113327 and 96111) and the Central Research Fund of the University of the Free State, Bloemfontein, South Africa.

Competing Interests

The authors declare that they have no known competing financial interests or personal relationships which have, or could be perceived to have, influenced the work reported in this article.

References

[1] E. Maligaspe, M.R. Hauwiller, Y. V. Zatsikha, J.A. Hinke, P. V. Solntsev, D.A. Blank, V.N. Nemykin, Redox and photoinduced electron-transfer properties in short distance organoboryl

ferrocene-subphthalocyanine dyads, Inorg. Chem. 53 (2014) 9336–9347. doi:10.1021/ic5014544.

[2] P. V. Solntsev, K.L. Spurgin, J.R. Sabin, A.A. Heikal, V.N. Nemykin, Photoinduced charge transfer in short-distance ferrocenylsubphthalocyanine dyads, Inorg. Chem. 51 (2012) 6537–6547. doi:10.1021/ic3000608.

[3] C.G. Claessens, D. González-Rodríguez, M.S. Rodríguez-Morgade, A. Medina, T. Torres, Subphthalocyanines, Subporphyrazines, and Subporphyrins: Singular Nonplanar Aromatic Systems, Chem. Rev. 114 (2014) 2192–2277. doi:10.1021/cr400088w.

[4] G. Gritzner, J. Kuta, Recommendations on reporting electrode potentials in nonaqueous solvents (Recommendations 1983), Pure Appl. Chem. 56 (1984) 461–466. doi:10.1351/pac198456040461.

Supporting Information

Additional supporting information for publication: **Redox and photophysical properties of four SubPcs containing ferrocenylcarboxylic acid dyads as axial ligands**

Redox and photophysical properties of four SubPcs containing ferrocenylcarboxylic acid dyads as axial ligands

Pieter J. Swarts and Jeanet Conradie*

Department of Chemistry, University of the Free State, P.O. Box 339, Bloemfontein, 9300, South Africa

Corresponding author: Jeanet Conradie, email conradj@ufs.ac.za

0000-0002-8120-6830 (J Conradie)

0000-0003-0157-8763 (PJ Swarts)

Supporting Information

Contents

1 Synthesis

The synthetic methods reported below were modified to improve yields and simplify the reaction setup.

Preparation of 2,5- didodecylthiophene: To a solution of thiophene (0.5 g, 0.0005 dm^3, 0.0059 mol) in anhydrous THF (dried over sodium; 0.01 dm^3), pre-cooled to -60°C in an isopropanol bath, was added under argon over 30 min *n*-butyllithium in hexanes (0.0063 dm^3 of a 2.0 mol dm^{-3} solution, 0.0125 mol, 2.1 eq.). After the addition was completed the reaction mixture was allowed to spontaneously heat up to room temperature, while stirring continued for 18 hours at room temperature. The dilithiated species that formed during this time was not isolated but treated *in situ* at -60°C under argon over 30 minutes with 1-bromdodecane (2.96 g, 0.0028 cm^3, 0.012 mol, 2 eq.). The stirred reaction mixture was then allowed to warm to room temperature. After 18 hours it was poured onto ice, the product extracted with diethyl ether (3 x 0.07 dm^3) and the organic extracts were washed with H_2O (2 x 0.07 dm^3) before it was dried with ($MgSO_4$) and filtered. Removal of solvents was followed recrystallisation of the residue from warm ethanol gave pure 2,5-dodecylthiophene (yield: 0.47 g, 94 %) as an off-white low-melting wax after solvent evaporation. MP: 56°C. ^{1}H NMR: δ_H (600.28 MHz, $CDCl_3$, 25 °C): δ 6.53 (2 H, s, C_4H_2), 2.71 (4 H, t, 2 x CH_2), 1.62 (4 H, m, 2 x CH_2), 1.24 (36 H, m, 18 x CH_2), 0.86 (6 H, t, 2 x CH_3).

Preparation of 2,5-didodecylthiophene-1,1-dioxide: To a 1L 2-neck flask, equipped with an efficient stirrer, a large condenser (Acetone cooled to – 40 °C with a cold finger) and charged with H_2O (0.4 dm^3), acetone (0.3 dm^3) and $NaHCO_3$ (200 g, 2.3 mol, 140 eq.) was added a solution of 2,5-dodecylthiophene (10 g, 0.017 mol) in dichloromethane (0.3 dm^3). The resulting heterogeneous mixture was cooled in an ice bath before solid oxone (350 g, 11 mol,66 eq.) was carefully added over 30 min under efficient stirring. Stirring continued at 0°C for 16 hours before water (2 dm^3) was added to dissolve most inorganics. The filtered aqueous layer and all remaining solids were extracted with

chloroform, the combined organic phases washed with water (0.2 – 0.3 cm^3) and dried ($MgSO_4$) before solvent removal and recrystallisation of the residue from warm ethanol gave pure off-white 2,5-didodecylthiophene-1,1-dioxide (yield: 9.12 g, 91 %). MP: 88°C. ^1H NMR: δ_H (600.28 MHz, $CDCl_3$): δ 6.24 (2 H, s, C_4H_2), 2.44 (4 H, t, 2 x CH_2), 1.63 (4 H, m, 2 x CH_2), 1.35 (4 H, m, 2 x CH_2), 1.24 (36 H, m, 18 x CH_2) and 0.86 (6 H, t, 2 x CH_3).

Preparation of 3,6-didodecylphthalonitrile: A minimum amount of chloroform (*ca.* 0.2 cm^3) was used to dissolve 2,5-didodecylthiophene-1,1-dioxide (2 g, 0.004 mol) and fumaronitrile (0.345 g, 0.004 mmol, 1 eq.). The stirred solution was sealed in a high-pressure glass vessel and heated to 160°C. After 24 hours the contents of the reactor vessel were dissolved in chloroform and the solvent evaporated under reduced pressure at 90°C. The oily residue was kept under reduced pressure until it no longer liberated gas anymore (*ca.* 1 hour). The remaining residue was chromatographed over silica with toluene as eluent. The second eluted band afforded after solvent removal and recrystallisation from ethanol 3,6-dodecylphthalonitrile (yield: 1.82 g, 91 %). MP: 82°C. ^1H NMR: δ_H (600.28 MHz, $CDCl_3$): δ 7.43 (2 H, s, C_4H_2), 2.82 (4 H, t, 2 x CH_2), 1.63 (4 H, m, 2 x CH_2), 1.35 (4 H, m, 2 x CH_2), 1.23 (36 H, m, 18 x CH_2) and 0.86 (6 H, t, 2 x CH_3).

Preparation of $Fc(CH)_2CO_2H$, 1:[1] Ferrocenecarboxaldehyde (1.5 g, 0.006 mol), malonic acid (1.785 g, 0.017 mol) and piperidine (0.56 cm^3) were dissolved in pyridine and heated in an oil bath at 110 °C for 2 hours under an argon atmosphere. The cooled solution was diluted with water and extracted with chloroform. The chloroform extracts were washed with 1 M HCl (2 x 100 cm^3) and water (2 x 100 cm^3) before the acrylic acid was extracted with ice-cooled 2 M NaOH (200 cm^3). While effectively cooling the solution with ice, the water phase was acidified with 1 M HCl and the precipitate filtered, washed with water and air-dried to yield 1.58 g (90 %) as a yellow powder. m.p.: 132 – 138 °C. NMR: δ_H (600.28 MHz, $CDCl_3$, 25 °C): δ 7.64 (1H, d, CH_2), 6.01 (1H, d, CH_2), 4.50 (2 H, pt, 2 x CH_2: Substituted-Cp), 4.42 (2 H, pt, 2 x CH_2: Substituted-Cp), 4.15 (5 H, s, Unsubstituted-

Cp). ^{13}C NMR: δ_C (150.95 MHz, $CDCl_3$, 25 °C): δ 172.29 (1C, C=O), 148.76 (1C,CH=CH), 113.73 (1C,CH=CH), 78.26 (1C, C-CO_2H), 71.44 (2C, Substituted-Cp), 69.92 (5C, Unsubstituted-Cp), 69.05 (2C, Substituted-Cp).

Preparation of $FcCH_2CO_2H$, 2: [2] To a solution of potassium hydroxide (1 g, 0.018 mol) in water (10 cm^3), a suspension of the ferrocene acetonitrile (0.2 g, 0.00074 mol) in ethanol (5 cm^3) was added and refluxed for 5 hours until the evolution of ammonia had ceased. Most (> 95 %) of the ethanol was removed under reduced pressure. The residual suspension was dissolved in water (50 cm^3), extracted with ether (2 x 50 cm^3) and filtered. The solution was acidified with 2 M HCl and the precipitate filtered, washed and air-dried to yield 0.110 g (51 %) as a white powder. m.p.: 159 – 165 °C. NMR: δ_H (600.28 MHz, $CDCl_3$, 25 °C): δ 4.21 (2 H, pt, 2 x CH_2: Substituted-Cp), 4.13 (5 H, s, Unsubstituted-Cp), 3.73 (2 H, pt, 2 x CH_2: Substituted-Cp), 3.38 (2H, s, CH_2). ^{13}C NMR: δ_C (150.95 MHz, $CDCl_3$, 25 °C): δ 172.34 (1C, C=O), 82.44 (1C, C-CO_2H), 69.19 (5C, Unsubstituted-Cp), 68.31 (2C, Substituted-Cp), 67.97 (2C, Substituted-Cp), 39.84 (1C, CH_2).

Preparation of $ClSubPc(H)_{12}$, 3:[3] BCl_3 (15 cm^3,1 M solution in p-xylene, 1.5 eq.) was added to dry phthalonitrile (1 g, 0.008 mol) in a glove box (H_2O: < 0.5 ppm and O_2: < 10 ppm) at room temperature in a high-pressure glass tube. The reaction mixture was stirred under reflux (137°C) for 30 minutes. The solvent was evaporated, and the solid was extracted with toluene (0.4 dm^3). The solution was evaporated, and the resultant purple solid was thoroughly washed with methanol (0.2 dm^3) and hexane (0.2 dm^3). Pure $ClSubPc(H)_{12}$ was obtained as a purple solid, yield: 94 % (0.94 g). MP: 375 – 380°C. ^{1}H NMR: δ_H (600.28 MHz, $CDCl_3$): δ 8.88 (6H, q, non-peripheral H_6) and 7.94 (6H, q, peripheral H_6). ^{11}B NMR: δ_B (128.38 MHz, $CDCl_3$): δ -16.22 (1B). ^{13}C NMR: δ_C (150.95 MHz, $CDCl_3$, 25 °C): δ 149.68 (6C, C=N: inner core carbons), 125.68 (6C, C=C: iminoisoindoline unit), 122.01 (6C, non-

peripheral C_6), 119.84 (6C, peripheral C_6). IR: υ/cm^{-1}: 1451 (C=C, Stretch). Elemental analysis calculated C, 66.94; H, 2.81; N, 19.51, obtained: C, 66.42; H, 2.68; N, 18.31.

Preparation of ClSubPc(F)$_{12}$, 4: [3] BCl_3 (6 cm^3,1 M solution in p-xylene, 1.5 eq.) was added to dry phthalonitrile (0.4 g, 1.9 mmol) in a glove box (H_2O: < 0.5 ppm and O_2: < 10 ppm) at room temperature in a high-pressure glass tube. The reaction mixture was stirred under reflux (137°C) for 30 minutes. The solvent was evaporated, and the solid was extracted with toluene (0.1 dm^3). The solution was evaporated, and the resultant purple solid was purified with by silica gel column chromatography using hexane: ethyl acetate (3:1, v:v, R_f: 0.68). Pure ClSubPc(F)$_{12}$ was obtained as a purple solid, yield: 92 % (0.368 g). MP: 355 – 360°C. ^{11}B NMR: δ_B (128.38 MHz, $CDCl_3$): δ -14.89 (1B). ^{13}C NMR: δ_C (150.95 MHz, $CDCl_3$, 25 °C): δ 149.23 (6C, C=N: inner core carbons), 144.92 (6C, C=C: iminoisoindoline unit), 140.75 (6C, non-peripheral C_6), 108.33 (6C, peripheral C_6). ^{19}F NMR: δ_C (564.33 MHz, $CDCl_3$, 25 °C): δ -136.27 (6H, q, non-peripheral H_6) and -146.81 (6H, q, peripheral H_6).

IR: υ/cm^{-1}: 1479 (C=C, Stretch). Elemental analysis calculated C, 44.59; F, 35.26; N, 13.00, obtained: C, 46.99; F, 34.89; N, 12.74.

2 NMR

2.1 Fc(CH$_2$)$_2$CO$_2$BSubPc(H)$_{12}$, 5

^{1}H NMR

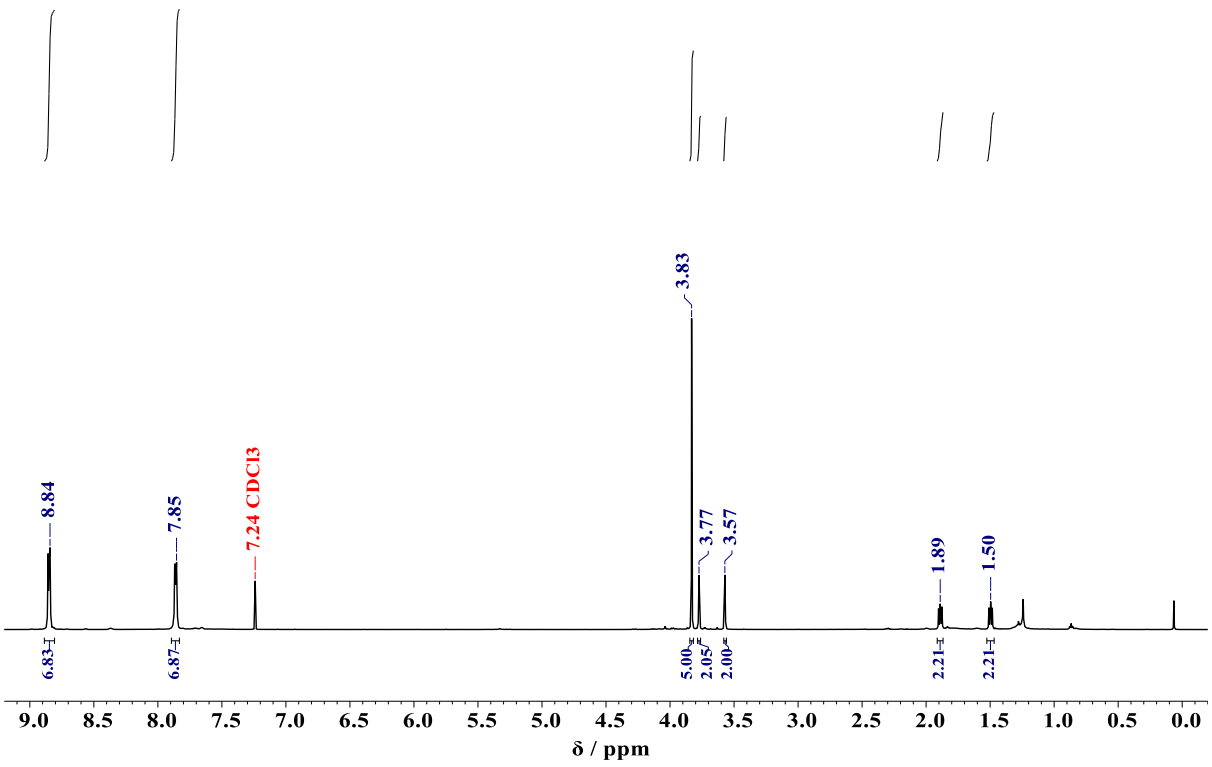
8.84
7.85
7.24 CDCl3
3.83
3.77
3.57
1.89
1.50
6.83
6.87
5.00
2.05
2.00
2.21
2.21
9.0 8.5 8.0 7.5 7.0 6.5 6.0 5.5 5.0 4.5 4.0 3.5 3.0 2.5 2.0 1.5 1.0 0.5 0.0
δ / ppm

^{11}B NMR

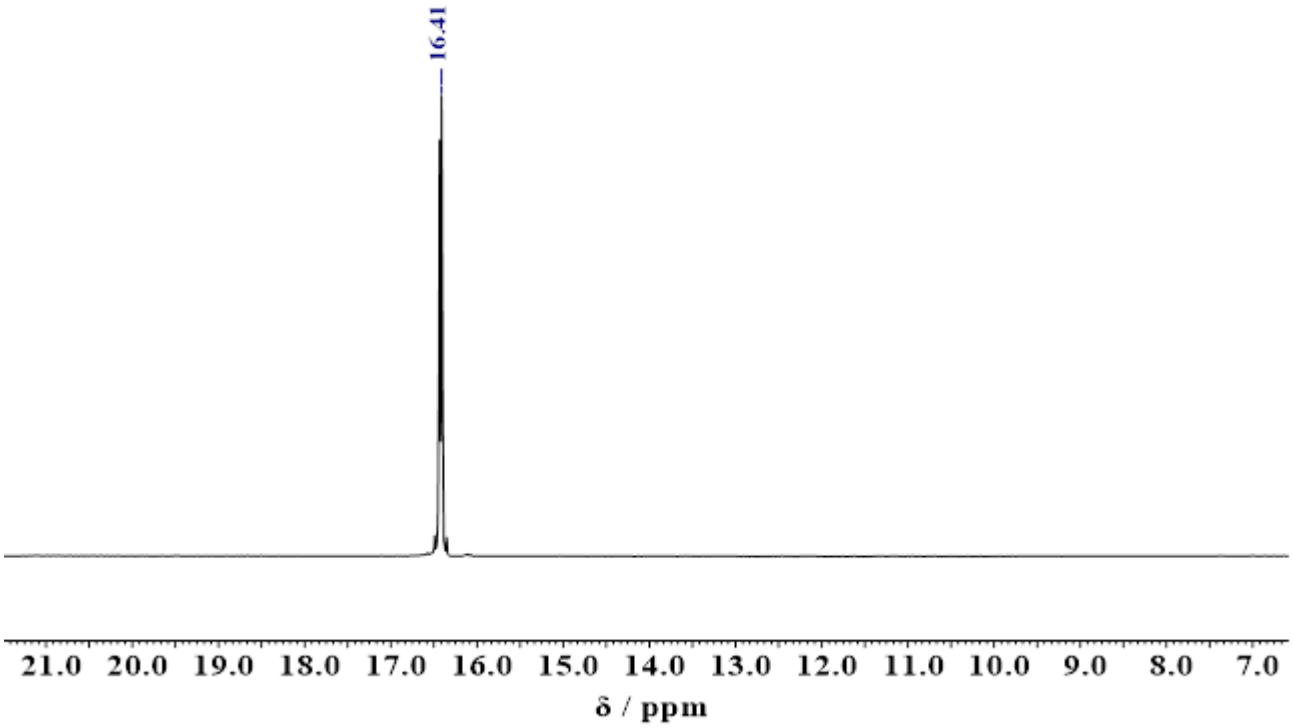
16.41
21.0 20.0 19.0 18.0 17.0 16.0 15.0 14.0 13.0 12.0 11.0 10.0 9.0 8.0 7.0
δ / ppm

^{13}C NMR

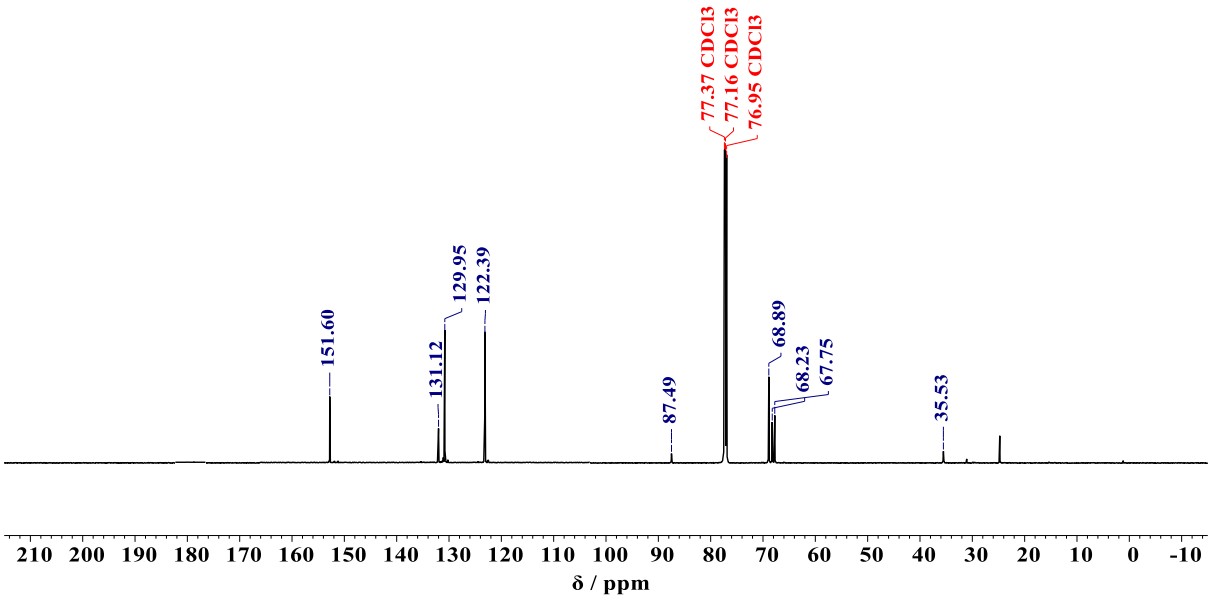

2.2 $Fc(CH)_2CO_2BSubPc(H)_{12}$, 6

^{1}H NMR

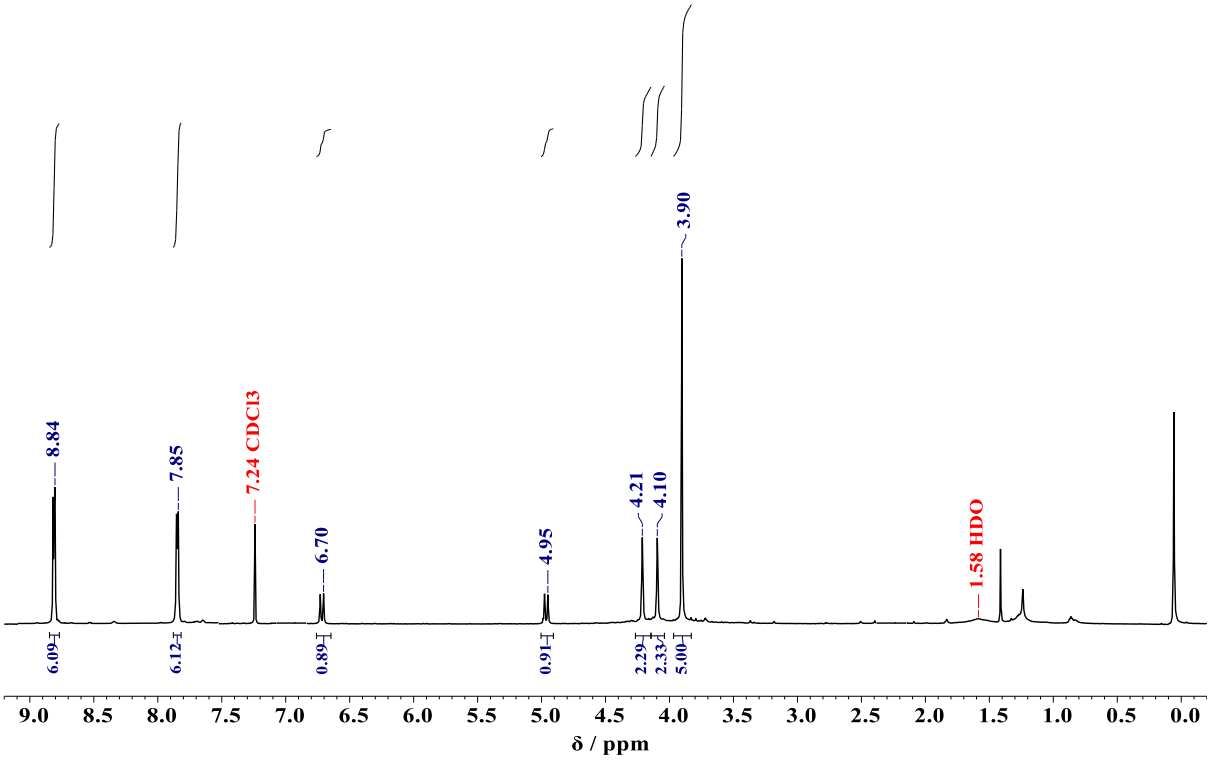
8.84
7.85
7.24 CDCl3
6.70
4.95
4.21
4.10
3.90
1.58 HDO
6.09
6.12
0.89
0.91
2.29
2.33
5.00
9.0 8.5 8.0 7.5 7.0 6.5 6.0 5.5 5.0 4.5 4.0 3.5 3.0 2.5 2.0 1.5 1.0 0.5 0.0
δ / ppm

^{11}B NMR

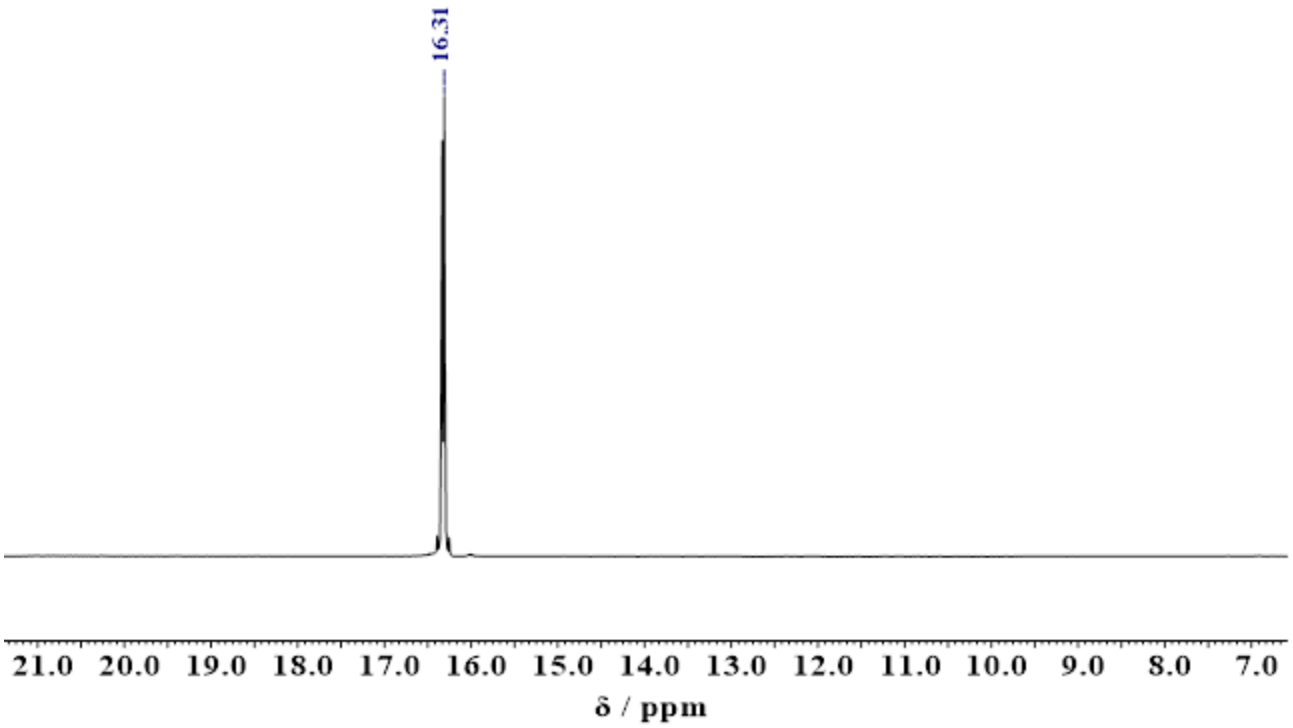
16.31
21.0 20.0 19.0 18.0 17.0 16.0 15.0 14.0 13.0 12.0 11.0 10.0 9.0 8.0 7.0
δ / ppm

^{13}C NMR

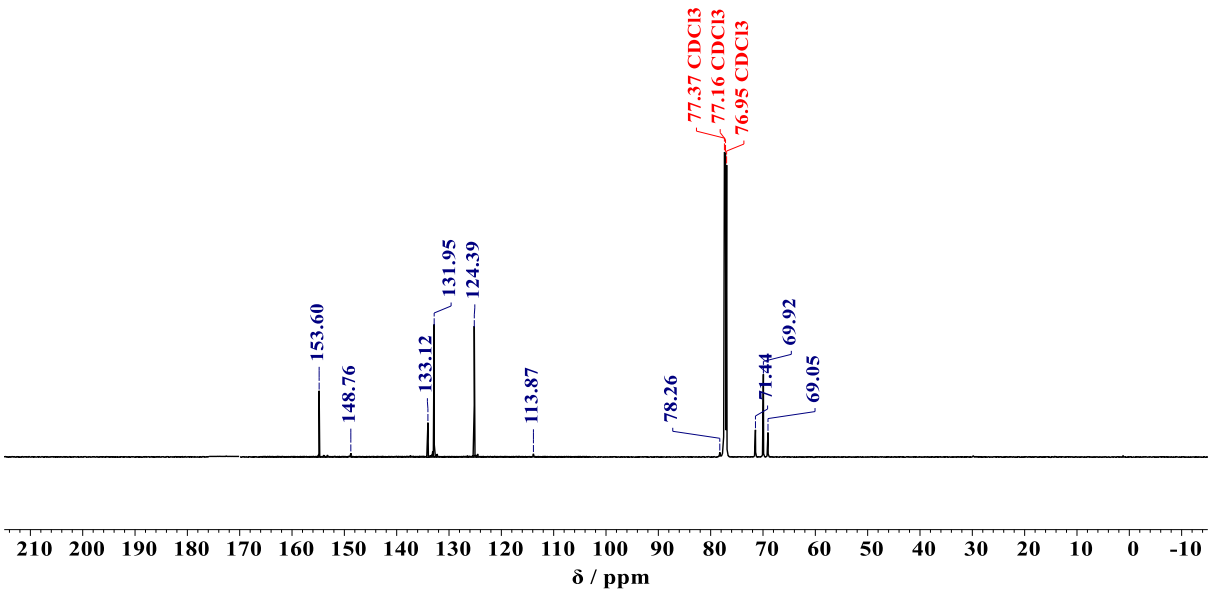
77.37 CDCl3
77.16 CDCl3
76.95 CDCl3
153.60
148.76
133.12
131.95
124.39
113.87
78.26
71.44
69.92
69.05
210 200 190 180 170 160 150 140 130 120 110 100 90 80 70 60 50 40 30 20 10 0 -10
δ / ppm

2.3 *Fc(CH$_2$)$_2$CO$_2$BSubPc(F)$_{12}$, 7*

^{1}H NMR

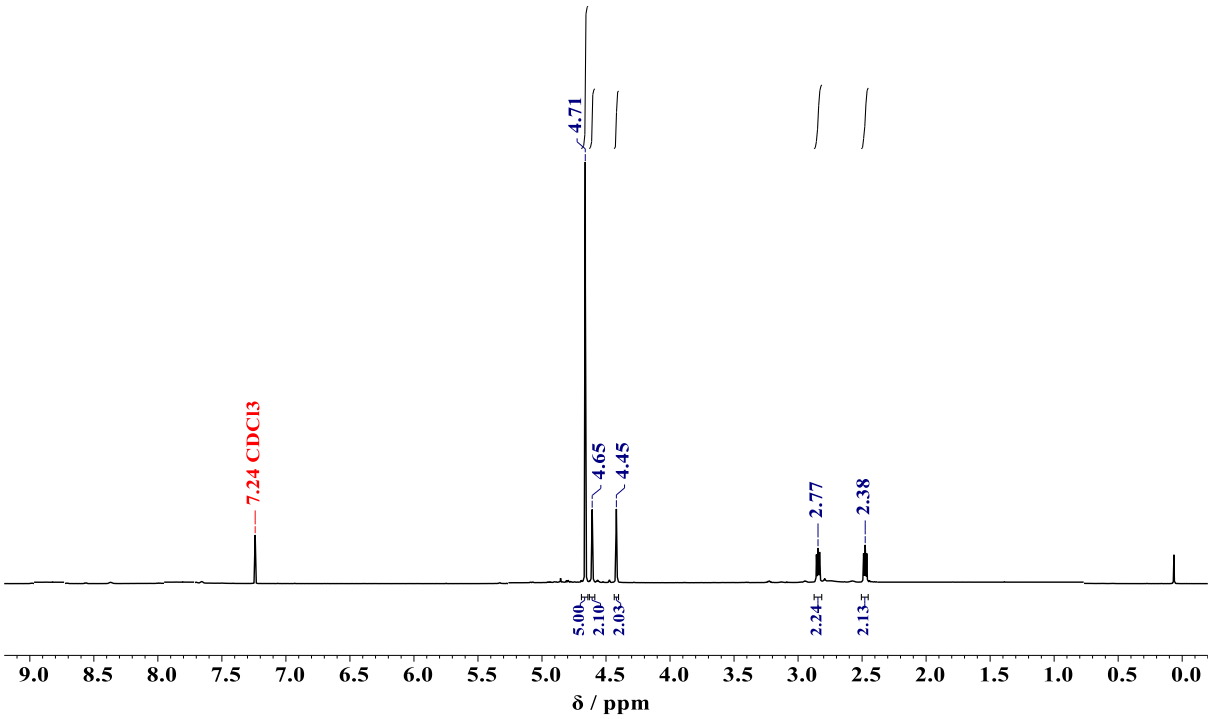

^{11}B NMR

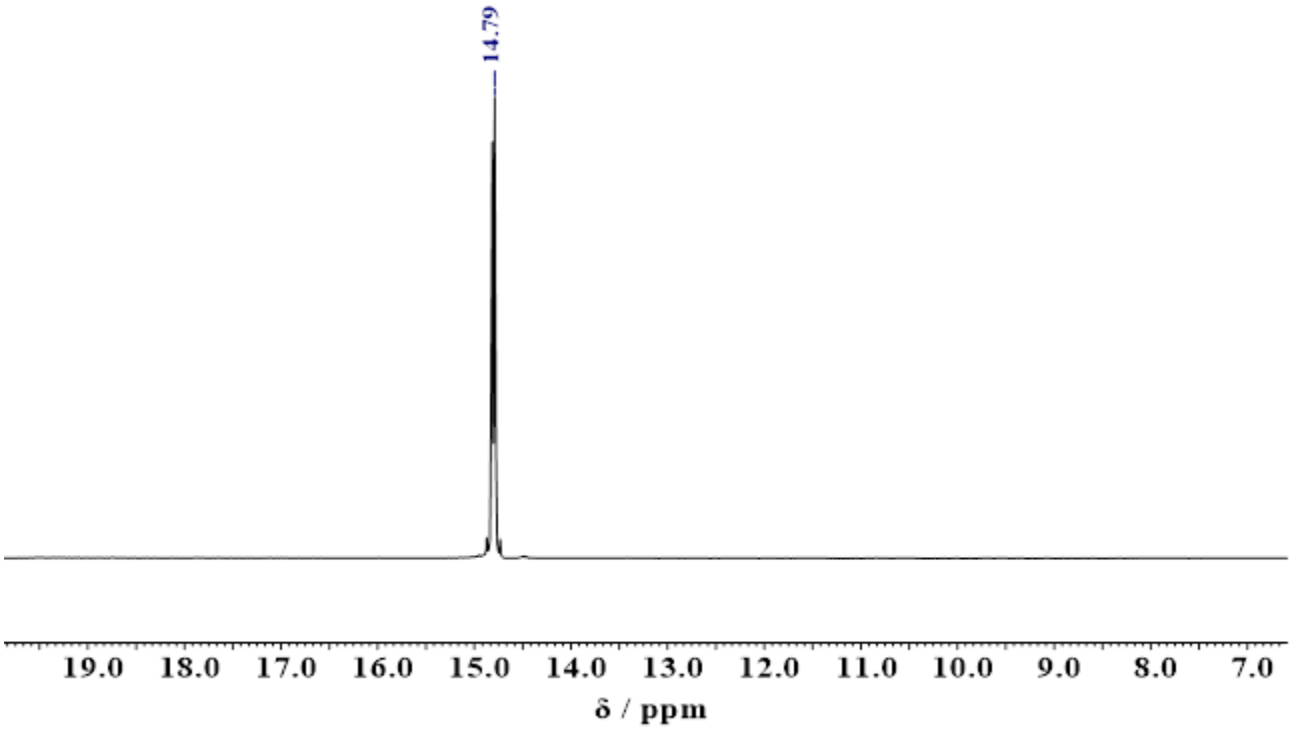

^{13}C NMR

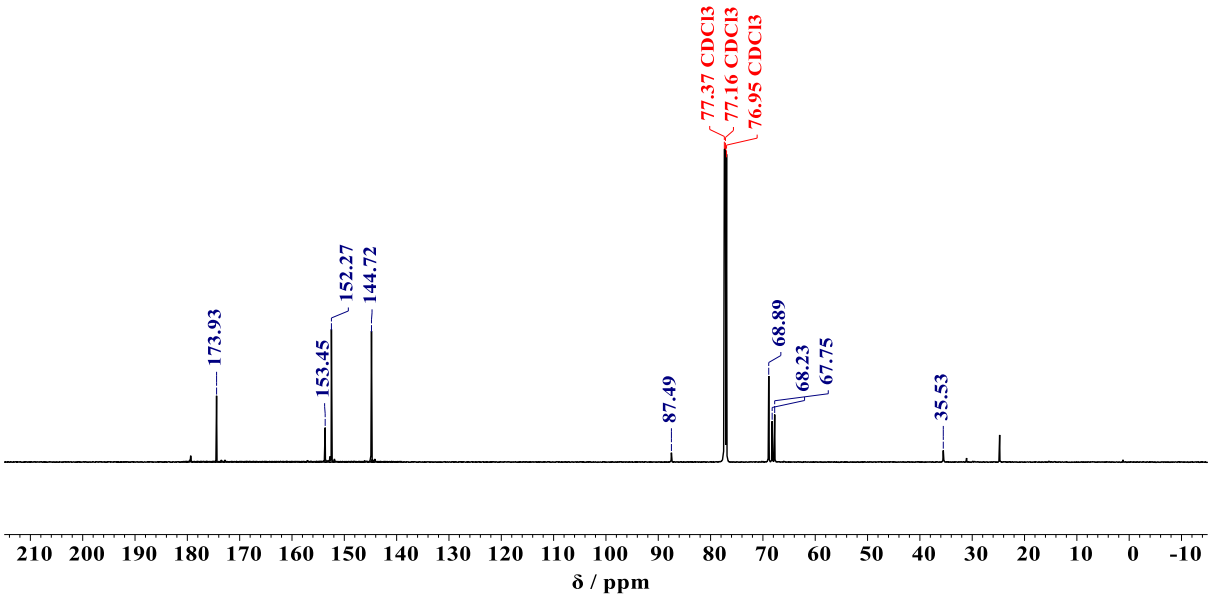

^{19}F NMR

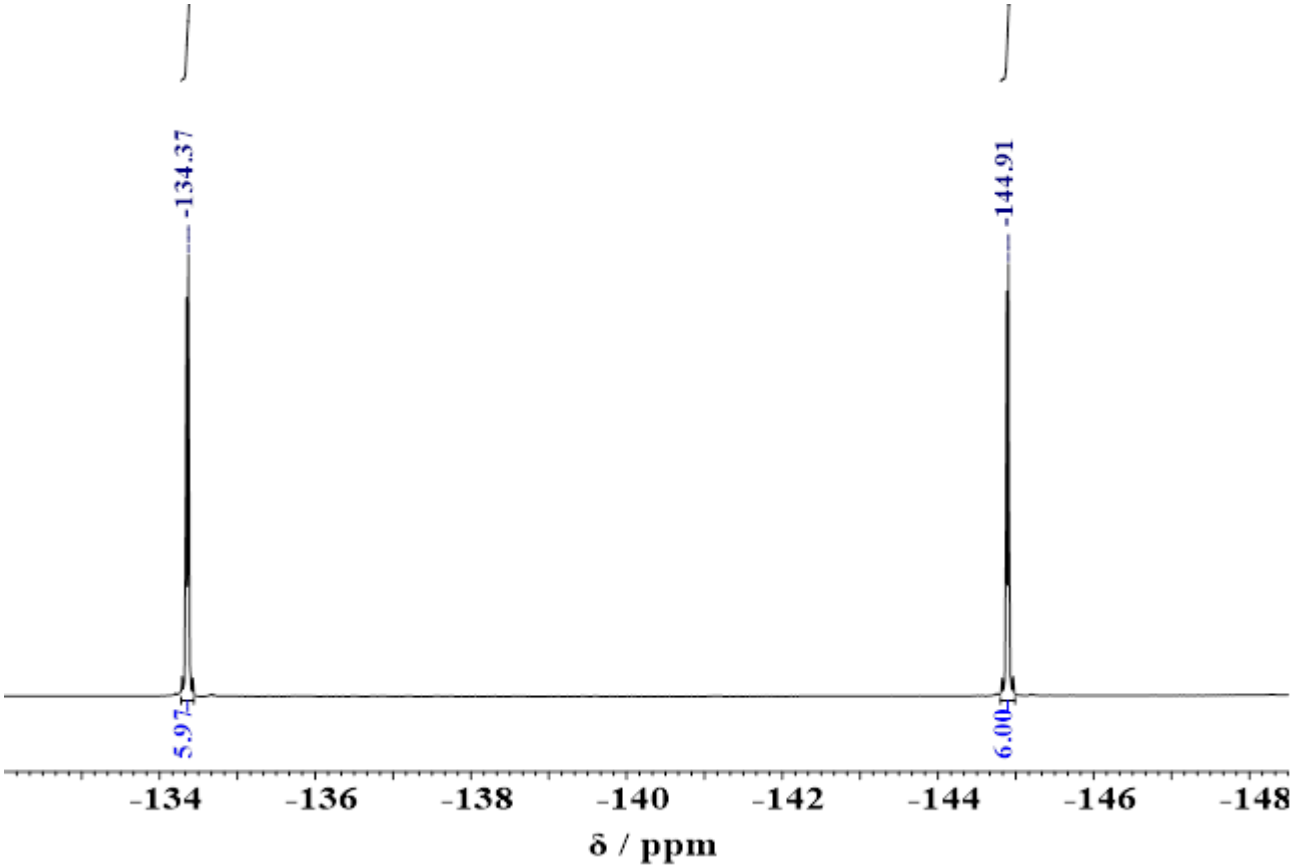

2.4 *$Fc(CH)_2CO_2BSubPc(F)_{12}$, 8*

^{1}H NMR

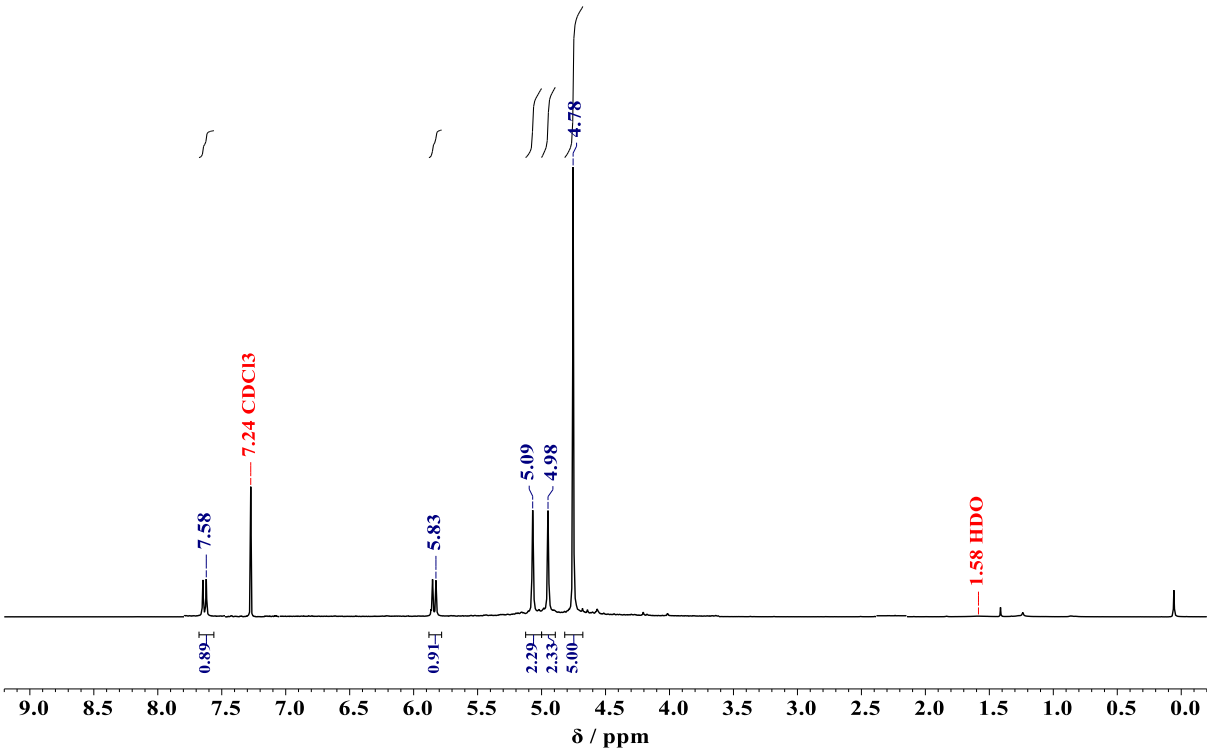

^{11}B NMR

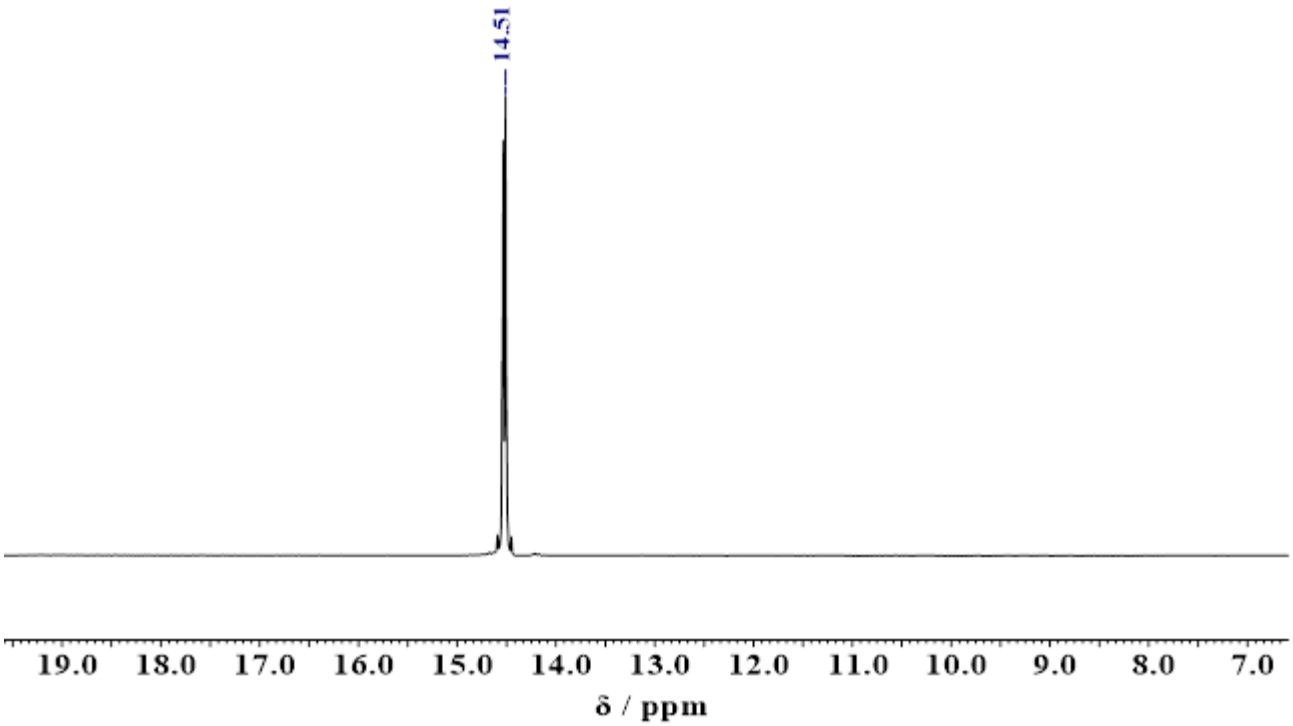

^{13}C NMR

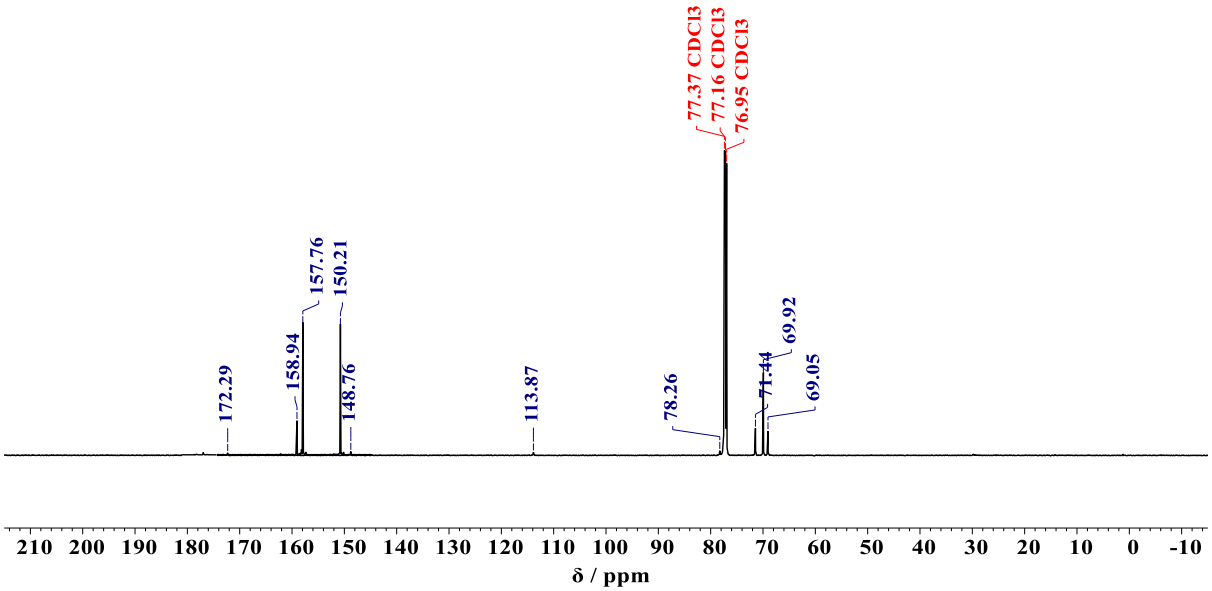

^{19}F NMR

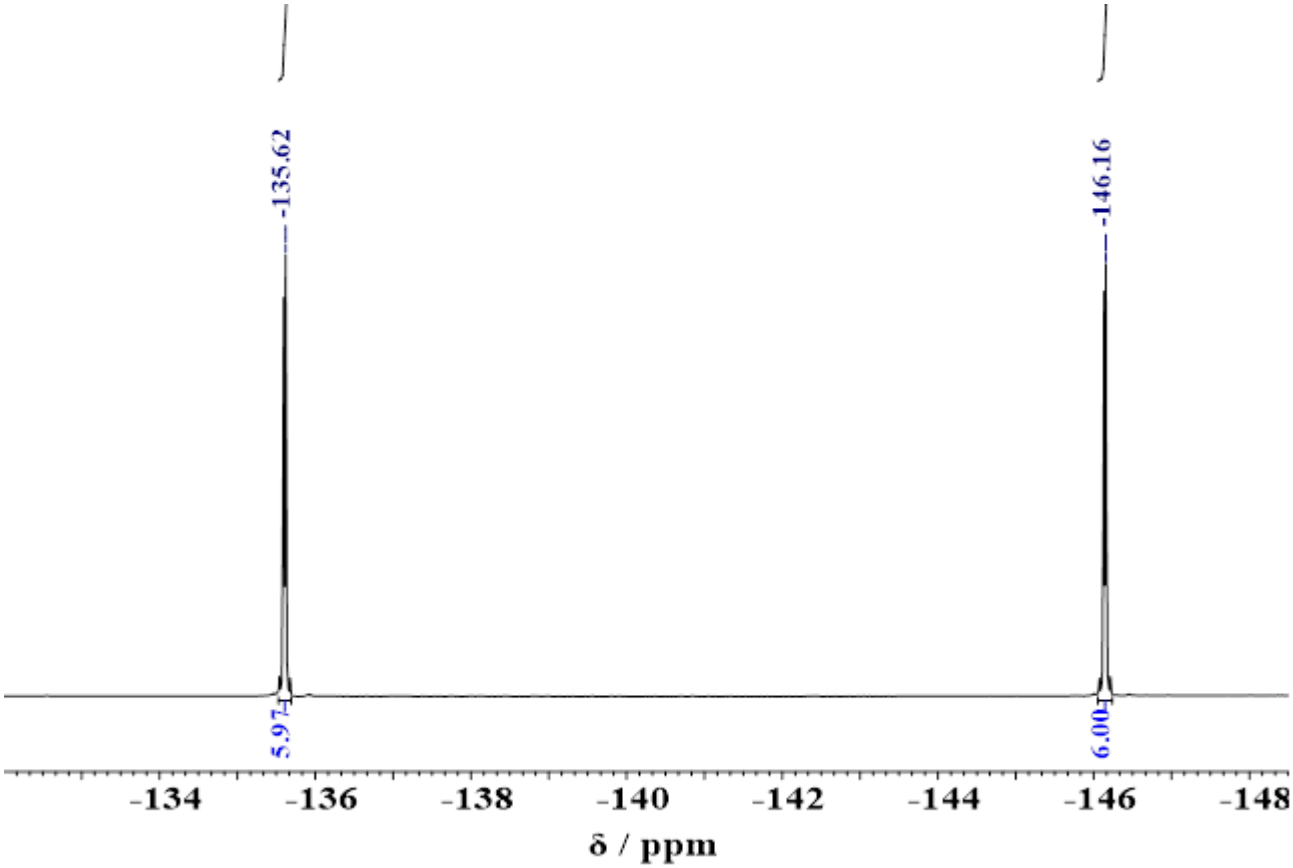

3 UV-vis

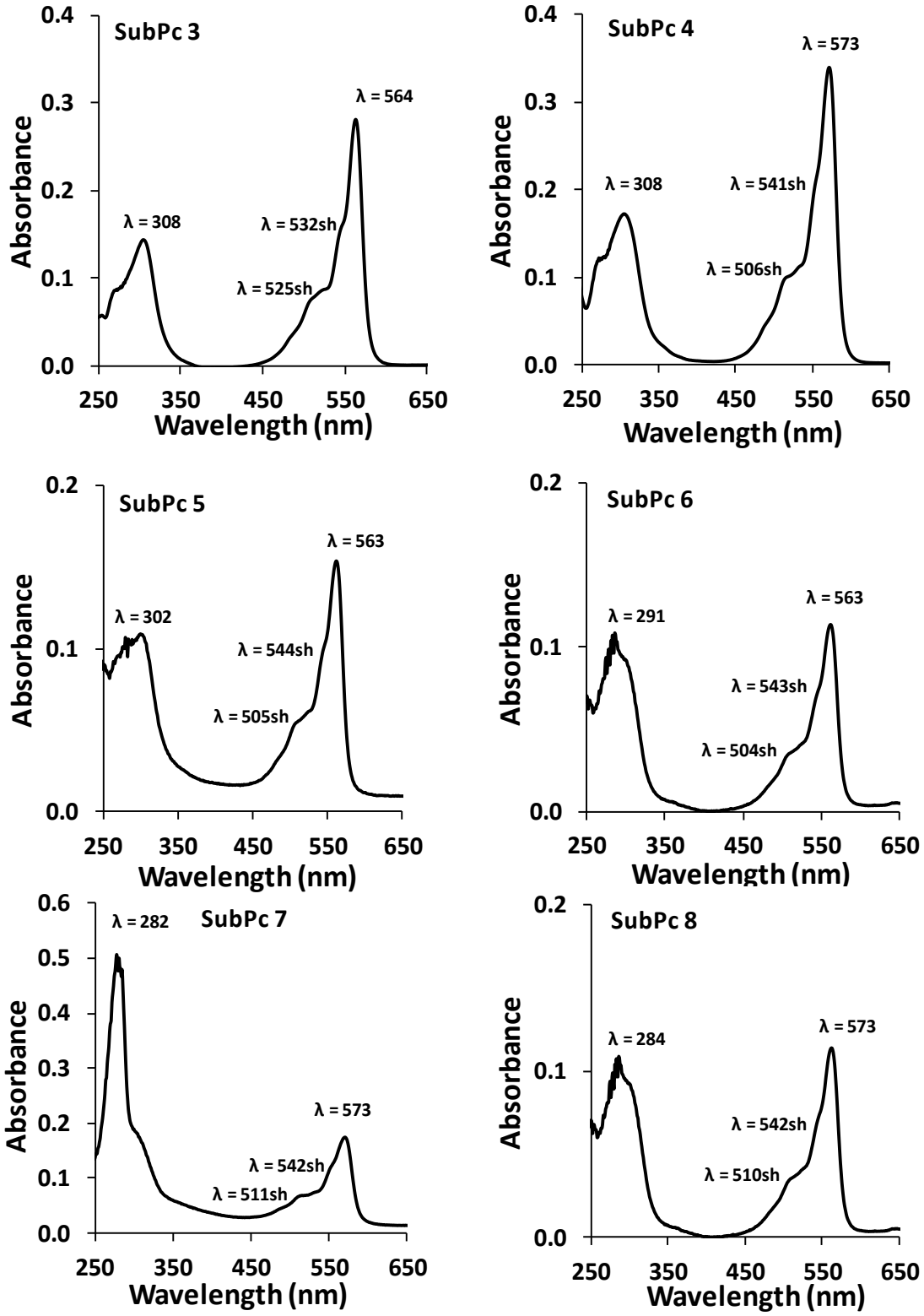

The UV-vis spectra showing Sorret and Q-bands of SubPc (4 – 8) at concentration 0.01 (x 10^{-3} M), obtained with a 1cm pathlength cuvette with THF as solvent.

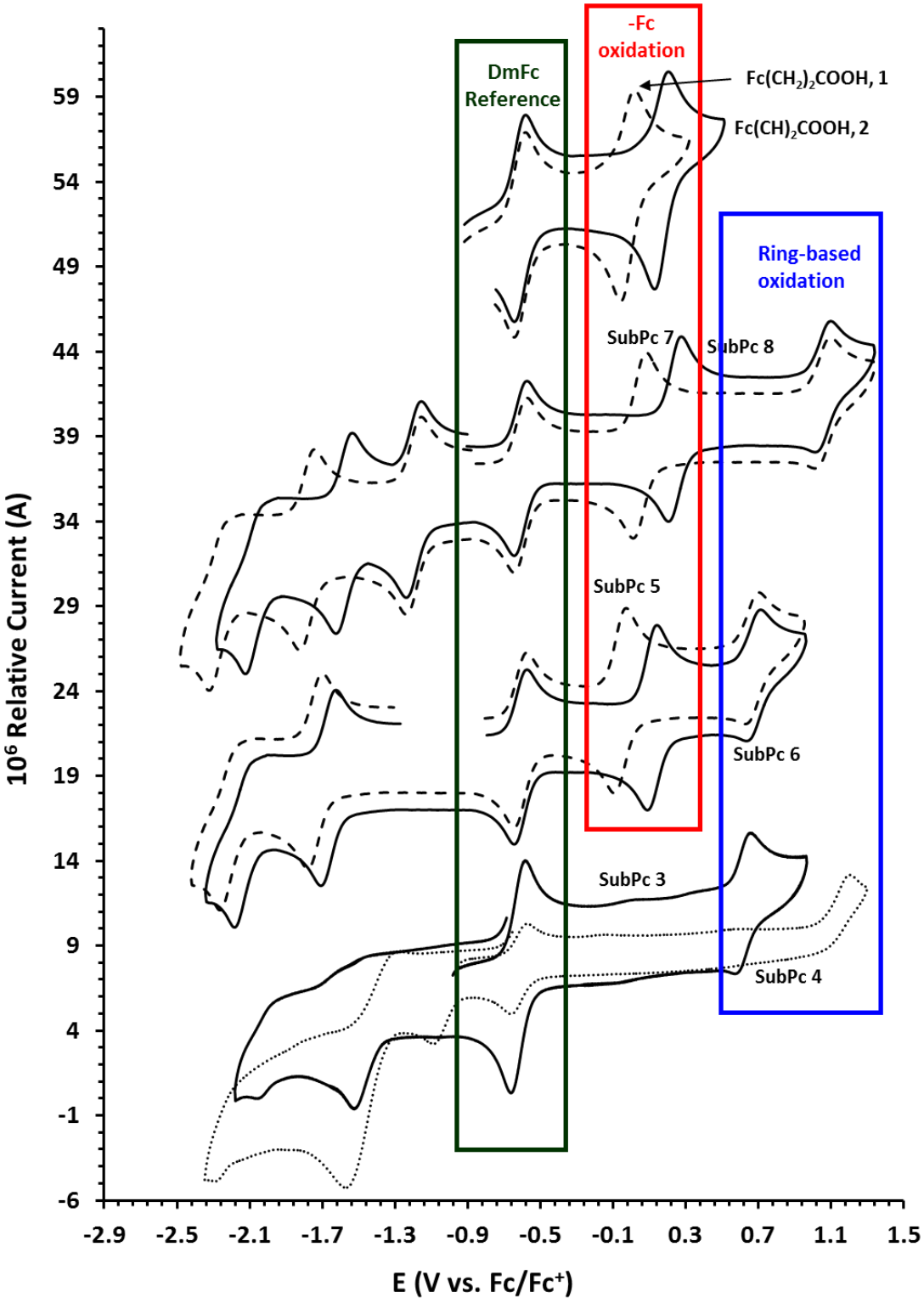

Comparative CV's of ferrocenyl dyads 1 and 2 and SubPc 3 - 8 in DCM / $[N(^{n}Bu)_4][B(C_6F_5)_4]$. Concentration = 0.0005 mol dm^{-3}. Scan rate for CVs is 0.100 V s^{-1}. Data of SubPc 3 - 4 is from reference [3].

5 DFT

PBE1PBE/6-311G(d,p) optimized coordinates for SubPcs **5** – **8** and oxidized **5** – **8.**

Only in electronic version

6 References

(1) Broadhead, G. D.; Osgerby, J. M.; Pauson, P. L. Broadhead, Osgerby, and Pauson : 127. Ferrocene Derivatives. Part V. * Perrocenealdehyde.. *J. Chem. Soc.* **1958**, No. 650, 650–656.

(2) Blom, N. F.; Neuse, E. W.; Thomas, H. G. Electrochemical Characterization of Some Ferrocenylcarboxylic Acids. *Transit. Met. Chem.* **1987**, *12* (4), 301–306. https://doi.org/10.1007/BF01024018.

(3) Swarts, P. J.; Conradie, J. Electrochemical Behaviour of Chloro- and Hydroxy-Subphthalocyanines. *Electrochim. Acta* **2020**, *329*, 135165. https://doi.org/10.1016/j.electacta.2019.135165.

Chapter 5

Synthesis, Spectroscopy, Electrochemistry and DFT of Electron-rich ferrocenylsubphthalocyanine dyads

To be submitted to: Molecules

Redox effect on ferrocenyl moiety of electron-rich ferrocenylsubphthalocyanine dyads

To be submitted to: Data in brief (DIB)

Supporting information also included.

Author Contributions:

Pieter J. Swarts

1. Synthesis of compounds of compounds
2. Electrochemical studies and interpretation
3. Characterisation:
    a. ^{1}H NMR, ^{11}B NMR, ^{13}C NMR and ^{19}F NMR
    b. UV/vis
    c. DFT calculations
4. Writing of publication manuscript draft and revised publications under the supervision of Prof. Jeanet Conradie

Above mentioned work was done under the supervision of Prof. Jeanet Conradie.

Synopsis TOC

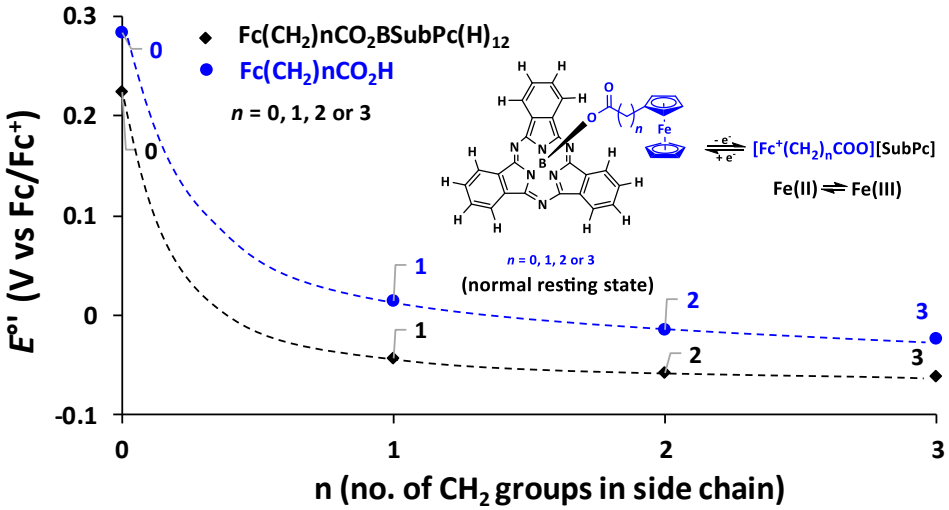

molecules
Article

Synthesis, Spectroscopy, Electrochemistry and DFT of Electron-rich ferrocenylsubphthalocyanine dyads

Pieter J. Swarts[1] and Jeanet Conradie[1]*

[1] Affiliation 1; Department of Chemistry, University of the Free State, Bloemfontein 9300, South Africa; swarts.pieter@gmail.com (P.J.S.)
* Correspondence: conradj@ufs.ac.za; Tel.: +27-(51)-4012194, Fax: +27-4017295

0000-0002-8120-6830 (J Conradie)
0000-0003-0157-8763 (PJ Swarts)

Received: date; Accepted: date; Published: date

Abstract: A series of novel ferrocenylsubphthalocyanine dyads Y-BSubPc(H)$_{12}$ with ferrocenylcarboxylic acid dyads Y-H = (FcCH$_2$CO$_2$-H), (Fc(CH$_2$)$_3$CO$_2$-H) or (FcCO(CH$_2$)$_2$CO$_2$-H) in axial position, were synthesized from the parent Cl-BSubPc(H)$_{12}$ via an activated triflate-SubPc intermediate. UV/vis data revealed that the axial ferrocenyl-containing ligand did not influence the Q-band maxima compared to Cl-BSubPc(H)$_{12}$. A combined electrochemical and density functional theory (DFT) study showed that Fe group of the ferrocenyl-containing axial ligand is involved in the first reversible oxidation process, followed by a second oxidation localized on the macrocycle of the subphthalocyanine. Both observed reductions were ring-based. It was found that the novel Fc(CH$_2$)$_3$CO$_2$BSubPc(H)$_{12}$ exhibited the lowest first macrocycle-based reduction potential (-1.871 V *vs.* Fc/Fc$^+$) reported for SubPcs till date. The oxidation and reduction values of Fc(CH$_2$)$_n$CO$_2$BSubPc(H)$_{12}$ (n = 0 – 3), FcCO(CH$_2$)$_2$CO$_2$BSubPc(H)$_{12}$, and Cl-BSubPc(H)$_{12}$ illustrated the electronic influence of the carboxyl group, the different alkyl chains and the ferrocenyl group in the axial ligand on the ring-based oxidation and reduction values of the SubPcs.

Keywords: Subphthalocyanines; Ferrocene; redox potentials; DFT; electron rich.

1. Introduction

The discovery of ferrocene (1951) [1] unlocked an entirely new research field and over the years. Ferrocene has been extensively researched with numerous good reviews in organic and inorganic chemistry [2–5]. The research of ferrocene-containing compounds thrives, and new research keeps on growing due to their varying successful applications. This includes asymmetric catalysis [6–8], non-linear optics [8], antineoplastic properties [9,10] antimalarial activity [11] and especially electrochemistry due to the ideal redox behavior of the $Fe^{II/III}$ couple [8,12]. For a series of four ferrocenyl carboxylic acid dyads $Fc(CH_2)_nCO_2H$ with n = 0 (**1**), 1 (**2**), 2 (**3**) or 3 (**4**) (Figure 1), it was found that the length of the alkyl chain separating the ferrocene moiety and electron-withdrawing carboxy group decreases, the formal reduction potential of Fe of the ferrocenyl group also decreases [13,14]. The electron-withdrawing carboxy group directly bound to ferrocene in **1** and $FcCO(CH_2)_2CO_2H$ (**5**), led to an increase in the formal reduction potential of the ferrocene moiety compared to free ferrocene [13,14].

Subphthalocyanines such as $ClBSubPc(H)_{12}$, **6**, have been used in research for almost 50 years [15] due to their diverse applications including light-emitting diodes [16], dye-sensitized solar cells [17], sensors [18] and photodynamic therapy [19]. The uses and reactivity of SubPcs can be modified by substituting the axial ligand as well as by functionalizing the ring substituents [18]. Redox data of the ring-based oxidation and reduction processes of SubPcs showed that axial or peripheral substitution has a smaller influence on the shift of the oxidation and reduction potential of the SubPc (ca 0.1 V shift) than non-peripheral substitution (ca 0.3 V shift) [20]. Ferrocenylsubphthalocyanine dyads with a direct ferrocene-boron or substituted ferrocene-boron bond have been investigated by V. Nemykin and co-workers [21,22]. They found that the first oxidation process in these ferrocenylsubphthalocyanine dyads is ferrocene based, while second oxidation and the first reduction processes are centered at the macrocyclic ligand of the SubPc [21,22].

In this paper, we report the synthesis, characterisation and electrochemical studies of three novel (**8**, **10** and **11**) ferrocenylsubphthalocyanine dyads. The appropriate ferrocenyl carboxylic acid **2**, **4** and **5** was directly bound to the boron atom in the axial position of SubPc, **6**, to form the three

new ferrocenylsubphthalocyanine dyads, $FcCH_2CO_2BSubPc(H)_{12}$, **8**, $Fc(CH_2)_3CO_2BSubPc(H)_{12}$, **10**, and $FcCO(CH_2)_2CO_2BSubPc(H)_{12}$, **11**, see Scheme 1 and Figure 1. For comparative purposes, the two known ferrocenylsubphthalocyanine dyads **7** [21] and **9** [23] were included in this study to systematically evaluate (i) the effect of the electron rich macrocycle of SubPcs **7** - **11** on the formal reduction potential of Fe of the ferrocenyl group of the ferrocenylcarboxylic acid moieties of **7** – **11**, and (ii) the influence of the axially ferrocenylcarboxylic acid dyads **1** - **5** on the UV/vis maxima and the ring-based oxidations and reductions of the ferrocenylsubphthalocyanine dyads **7** – **11**.

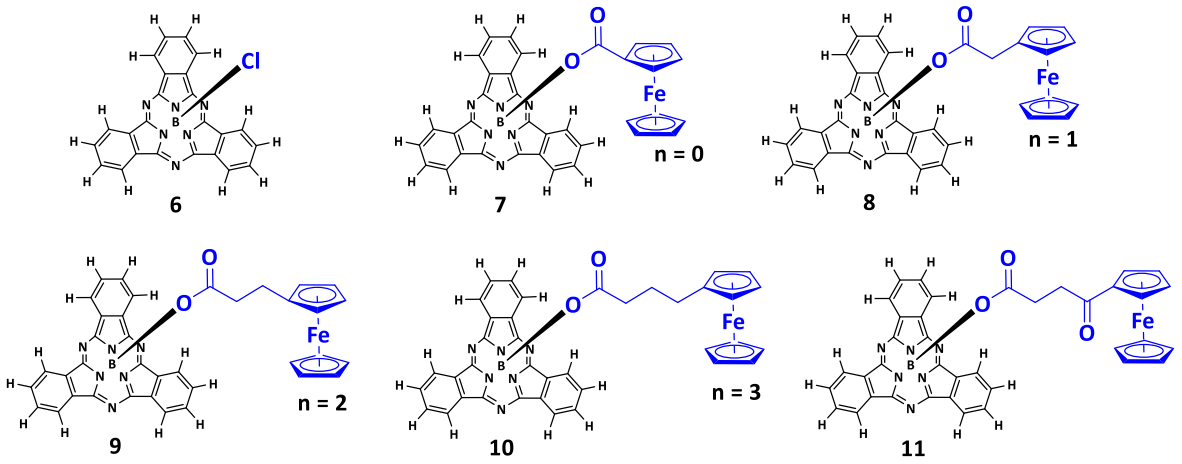

Figure 1 Structures of $FcCO_2BSubPc(H)_{12}$, **7** [21], $FcCH_2CO_2BSubPc(H)_{12}$, **8** (novel), $Fc(CH_2)_2CO_2BSubPc(H)_{12}$, **9** [23], $Fc(CH_2)_3CO_2BSubPc(H)_{12}$, **10** (novel) and $FcCO(CH_2)_2CO_2BSubPc(H)_{12}$, **11** (novel), containing the ferrocenylcarboxylic acids $FcCO_2H$ (**1**), $FcCH_2CO_2H$ (**2**), $Fc(CH_2)_2CO_2H$ (**3**), $Fc(CH_2)_3CO_2H$ (**4**) and $FcCO(CH_2)_2CO_2H$ (**5**) in the axial position. n = number of alkyl groups in the axial ligand.

2. Results and Discussion

2.1. Synthesis

The free ferrocenylcarboxylic acids **1** – **5**, were synthesized using slightly modified methods than previously published [13], as described in our previous publication [14]. The synthesis of ferrocenylsubphthalocyanine dyads **7** – **11**, was complex due to the moisture sensitivity of the reactions. In the first step any of the two well-known halophiles, such as Me_3Si groups or Ag^+ ions are used to irreversibly substitute the axial chloride in the axial position [23,24]. We found that using Me_3SiOTf did not give desirable yields. Using AgOTf, however, enabled us to increase our yields by more than 30 % compared to previous studies [21]. Once the activated triflate species was formed the

activated SubPc showed considerable reactivity toward the different ferrocenyl acids **1** – **5**, see Scheme 1. The success of the synthesis is drastically affected when not working under strict Schlenk conditions. SubPcs **7** – **11** were soluble in common organic solvents such as DCM, chloroform and THF.

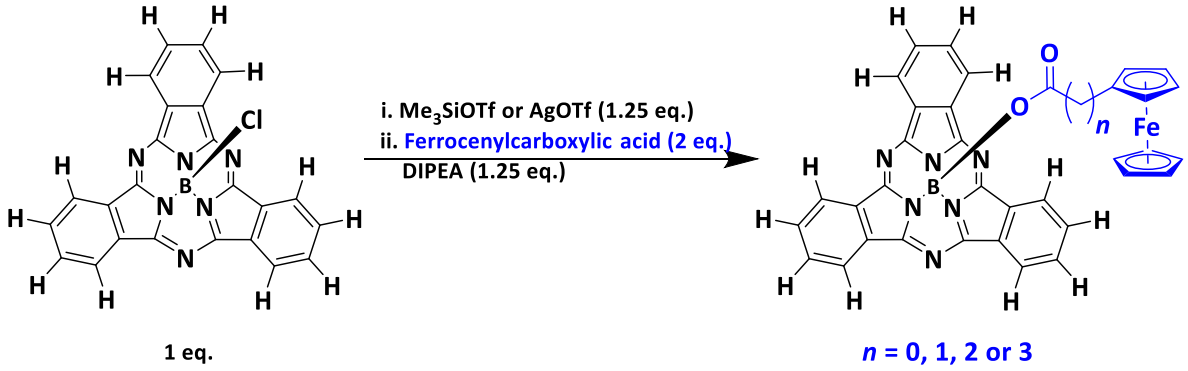

Scheme 1 Reaction scheme for $FcCO_2BSubPc(H)_{12}$, **7**, $FcCH_2CO_2BSubPc(H)_{12}$, **8**, $Fc(CH_2)_2CO_2BSubPc(H)_{12}$, **9**, $Fc(CH_2)_3CO_2BSubPc(H)_{12}$, **10**, and $FcCO(CH_2)_2CO_2BSubPc(H)_{12}$, **11**. **Note:** AgOTf = silver trifluoromethanesulfonate, Me_3SiOTf = Trimethylsilyl trifluoromethanesulfonate and DIPEA = *N*,*N*-Diisopropylethylamine.

2.3. ^1H NMR

The ^1H NMR results showed that signals of the SubPc ring protons (H) shifted upfield by *ca.* 0.04 – 0.07 ppm for SubPcs 7 – **11** relative to the signals of the parent ring protons $ClBSubPc(H)_{12}$, **6**. The most significant effect on ^1H NMR was observed for the signals of the ferrocenyl axial ligands peaks. Ferrocenyl of SubPc **7** (signals of the protons of substituted-Cp = 3.96 and 3.95, un-substituted-Cp = 3.63) is the closest to the electron rich macrocycle of SubPc and as a result the signals of the protons of the substituted and un-substituted-Cp rings shift the furthest upfield with ppm shifts between 0.50 and 0.88 ppm compared to ferrocenyl acid **1** (substituted-Cp = 4.84 and 4.45, un-substituted-Cp = 4.24). With the increase of $(CH_2)n$ linker groups the distance between the ferrocenyl moiety and SubPc increases and as a result the ferrocene peaks shift less upfield as the chain lengths increase.

2.3. UV/vis

As usually found for SubPcs, the UV/vis spectra of SubPcs **7** – **11** exhibited the two main transitions, the Soret band between 250 and 350 nm, and the Q-band between 450 and 620 nm, see Figure 2. The substitution of the parent macrocycles axial chloride with the different ferrocenylcarboxylic acid groups, had a negligible effect on the Q-bands position, see Table 1. In a similar fashion there was no shift when comparing the Q-bands of SubPcs **7** – **11** to **6**. The similar Soret and Q-bands for **6** and SubPcs **7** – **11** indicates that the Soret and Q-bands involve π-π* transitions. SubPcs **7** to **11** followed the Beer-Lambert law and no aggregation in the concentration range of 0.01 – 0.10 (x 10^{-3} M) was observed, see Figure 2.

Table 1 UV/vis data of SubPcs **6** – **11** in THF.

	Sorret Band	**Q Band**		
	Max	1st shoulder	2nd shoulder	Max
ClBSubPc(H)$_{12}$, **6**, [20]	308	525	532	564
FcCO$_2$BSubPc(H)$_{12}$, **7**	299	515	530	563
FcCH$_2$CO$_2$BSubPc$_{12}$, **8**	300	518	534	563
Fc(CH$_2$)$_2$CO$_2$BSubPc(H)$_{12}$, **9**, [23]	302	505	544	563
Fc(CH$_2$)$_3$CO$_2$BSubPc(H)$_{12}$, **10**	328	521	539	563
FcCO(CH$_2$)$_2$CO$_2$BSubPc(F)$_{12}$, **11**	327	523	542	563

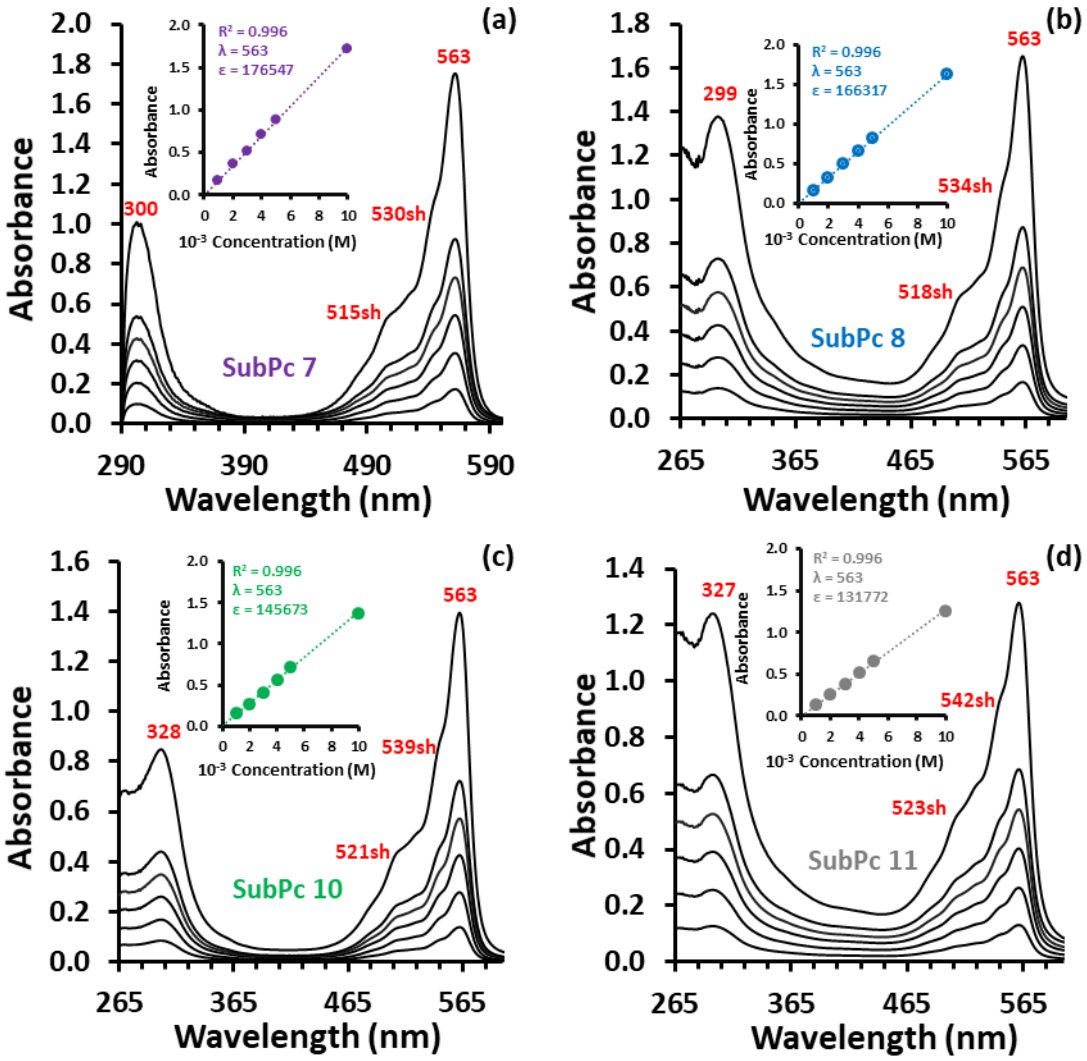

Figure 2 (a) – (d) The UV/vis spectra of SubPc (**7**, **8**, **10** and **11**) at concentrations 0.01, 0.02, 0.03, 0.04, 0.05 and 0.10 (x 10^{-3} M), obtained with a 1 cm pathlength cuvette with THF as solvent. UV/vis spectra of SubPc **9** can be found in reference [23]. Insert: The Beer-Lambert correlation between the absorbance A and concentration of $FcCO_2BSubPc(H)_{12}$, **7** (ε = 176547 dm^3 mol^{-1} cm^{-1}); $Fc(CH_2CO_2BSubPc(H)_{12}$, **8** (ε = 166317 dm^3 mol^{-1} cm^{-1}), $Fc(CH_2)_2CO_2BSubPc(H)_{12}$, **9** (ε = 153630 dm^3 mol^{-1} cm^{-1} [23]), $Fc(CH_2)_3CO_2BSubPc(H)_{12}$, **10** (ε = 145673 dm^3 mol^{-1} cm^{-1}) and $FcCO(CH_2)_2CO_2BSubPc(H)_{12}$, **11** (ε = 131772 dm^3 mol^{-1} cm^{-1}) at indicated wavelength in nm.

2.4. Cyclic Voltammetry

The redox properties of the ferrocenylsubphthalocyanine dyads, SubPc **7**, **8**, **10** and **11** were examined utilizing cyclic voltammetry (CVs) and linear sweep voltammetry (LSV). The CVs and the LSVs of SubPc **7**, **8**, **10** and **11**, performed at 25 °C in dichloromethane (DCM) at a scan rate of 0.100 Vs^{-1} are shown in Figure 3 with the relevant electrochemical data summarised in Table 2. Data of the free ferrocenylcarboxylic acids **1** – **5** [12] and SubPcs **6** [20] and **9** [21] are added for comparative

reasons in Table 2. The CVs of SubPc **7**, **8**, **10** and **11** (Figure 3) showed two oxidation and two reduction peaks in the experimental solvent window of DCM. The oxidation of the Fe group ($Fe^{II/III}$) of the ferrocenyl moiety on the axial ligand is the first observed redox process for all five SubPc **7** – **11**. The assignment that the Fe group is oxidised first, is supported by DFT calculations (see computational analysis below) and is in agreement with literature [21,22]. Both oxidation and the first reduction peaks are chemically reversible with peak ratios approaching 1 and peak current separations, ΔE_P, of 0.074-0.076 (ferrocenyl oxidation), 0.080-0.084 V (wave I in Figure 3) and 0.082-0.086 V (wave II in Figure 3) respectively. The second ring-based reduction (wave III in Figure 3) were irreversible and did not show any re-oxidation peaks. The linear sweep voltammetry showed, as expected, 1 e^- redox couples for Fc and waves I to III. The reaction scheme for the redox signals of SubPc **7** – **10** (similar for **11**) is given in Scheme 2.

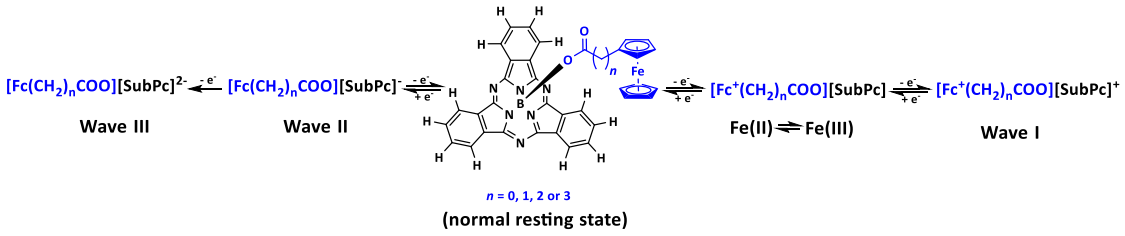

Scheme 2 The reaction scheme of the redox signals of SubPcs **7** to **10** in DCM as solvent, see Figure 3. Reactions scheme for **11** is similar.

2.4.1. *Effect of SubPc on ferrocenyl moiety oxidation*

The oxidation potentials, $E°'$, of the Fe group ($Fe^{II/III}$) of the ferrocenyl moiety on the axial ligand of SubPcs **7** – **11** range between -0.062 and 0.262 V and with ΔE_p between 0.074 and 0.076 V (Figure 3 and Table 2). Comparing $E°'$ (of the first process) of the Fc moiety of SubPcs **7** – **11** with the $E°'$ of the free ferrocenyl acids **1** – **5** (obtained under the experimental same conditions [14] as the SubPcs **7** – **11**) it is clear that the aromatic SubPc ring acts as an electron-donating specie in the complex, decreasing (lower oxidation potential) $E°'$ of the Fe group of SubPcs **7** – **11** with 0.060 – 0.038 V relative to $E°'$ of the Fe group of the free ferrocenylcarboxylic acids **1** – **5**. The largest electron-donating effect was, as expected, on the ferrocenyl moiety closest to the ring, with a

decrease of 0.060 V between **7** (0.224 V) and **1** (0.284 V). As the chain length increases with $(CH_2)_n$ groups the effect of the SubPc on ferrocenyl oxidation becomes less. The Fe group in SubPc **10** with three (CH_2) groups separating the ferrocenyl moiety from the SubPc, is more shielded from the electron-donating effect of the SubPc and as a result *E*°' of Fe shifts with only 0.038 V between **10** (-0.062 V) and **4** (-0.024 V). With an additional carbonyl group as well as the (CH_2) groups in SubPc **11** *E*°' of the Fe group of SubPc **11** shifted the least in the range namely, with only a 0.033 V between **11** (0.262 V) and **5** (0.295 V).

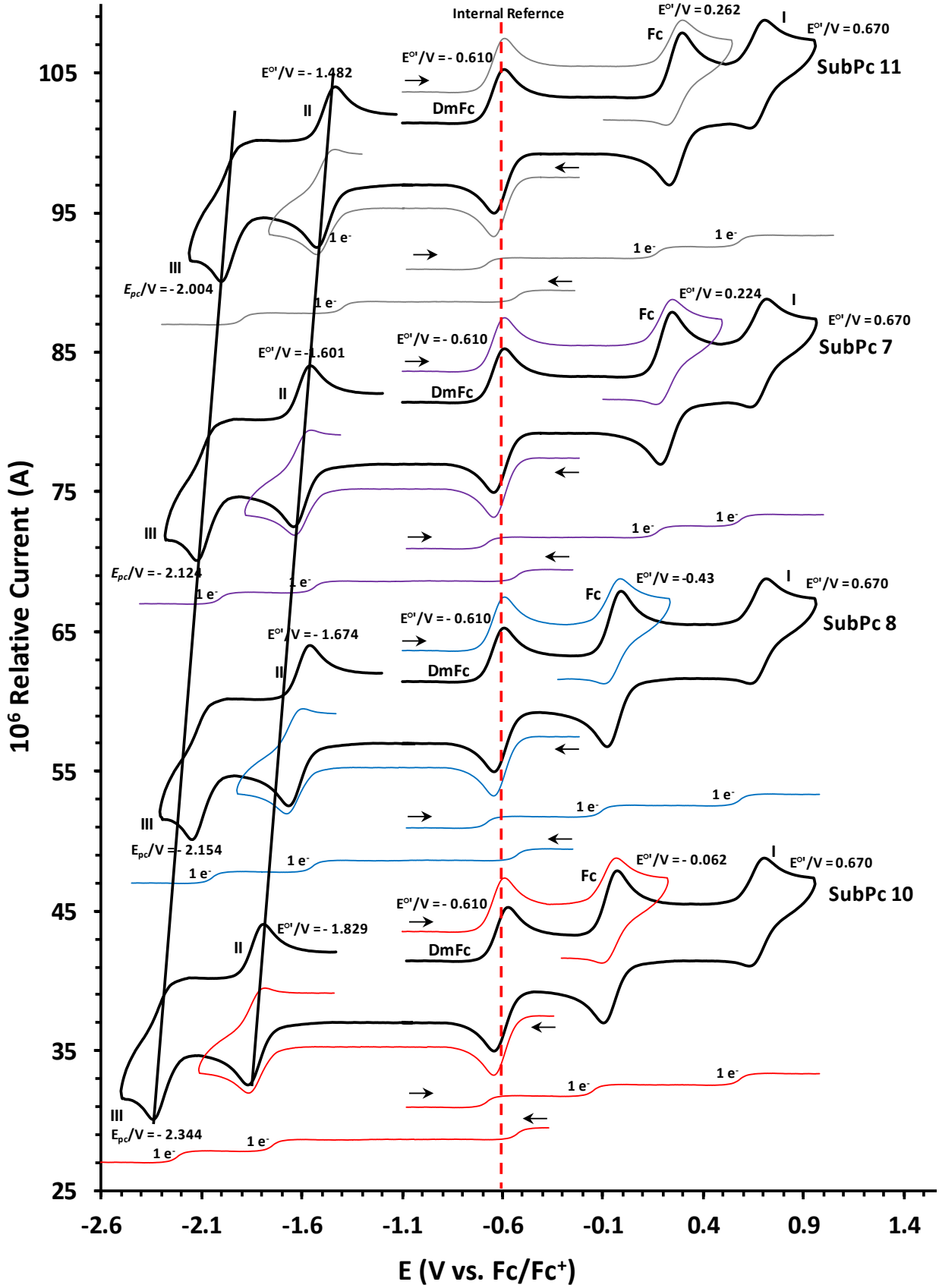

Figure 3 CVs and LSVs of SubPc, **7** - (purple), **8** - (blue), **10** – (red) and **11** - (grey) in DCM. Concentration of **7** – **11** = 0.0005 mol dm^{-3}. Scan rate for CVs is 0.100 V s^{-1} and LSVs at 0.001 V s^{-1}. Scan directions are indicated at starting point of each scan. DmFc was used as internal reference with $E^{\circ\prime}$ (DmFc) = -0.610 *vs.* free Fc/Fc$^+$ at 0 V.

2.4.2. *Effect of chain length on ferrocenyl moiety oxidation*

The formal reduction potential $E^{\circ'}$ of Fe in the axial ligand of SubPc **7** is at 0.224 V compared to free ferrocene 0 V. With one additional CH_2 spacer group between ferrocene and the SubPc, $E^{\circ'}$ of Fe is significantly shifted by 0.264 V to – 0.043 V in SubPc **8**, SubPcs **9** and **10** had two and three additional CH_2 spacer groups respectively, with $E^{\circ'}$ of the ferrocene group decreasing to -0.058 V and -0.062 V respectively. There was an exponential decrease to lower oxidation potential with an increase in $(CH_2)_n$ chain lengths for SubPc **7** – **10**, see Figure 4 a. This is because Fe of the ferrocene group is increasingly shielded from the electron donating effect of the SubPc and electron-withdrawing effect of the carboxy group as the $(CH_2)_n$ chain length increases. This trend was similar as observed for the free ferrocenylcarboxylic acids **1** – **5** [14], see Figure 4 a.

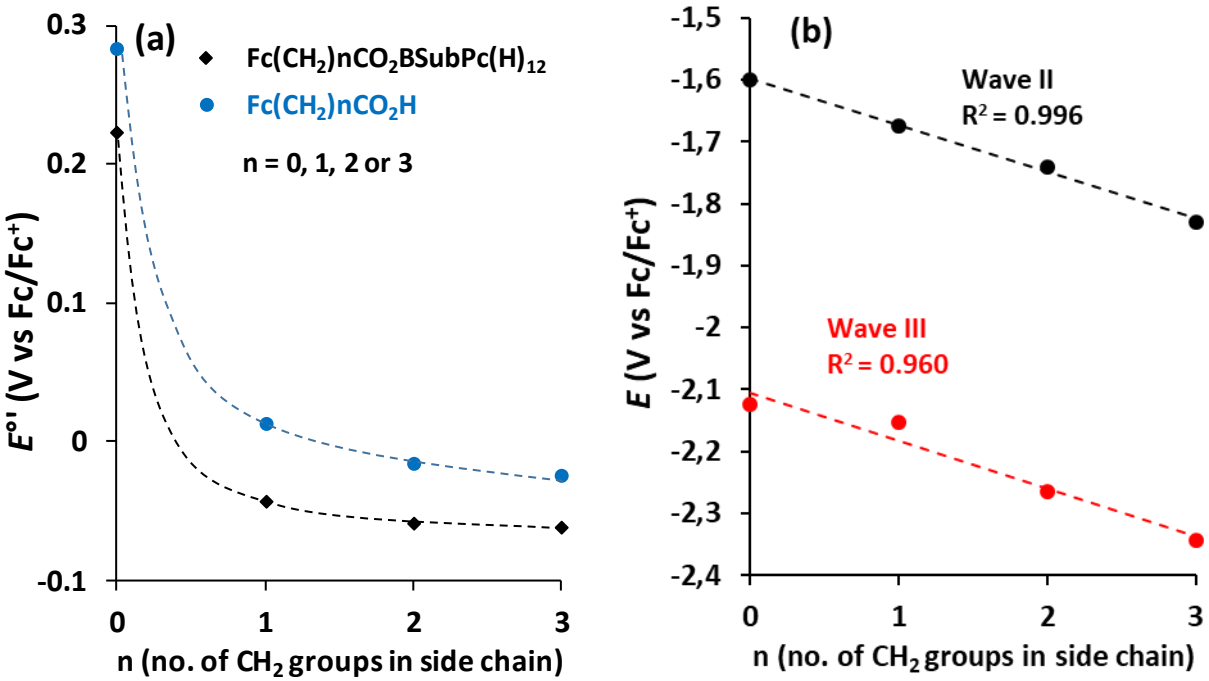

Figure 4 (a) Relationship between $E^{\circ'}$ of the Fe group and the number n of CH_2 groups in the side chain of $Fc–(CH_2)_n–CO_2$ for ferrocenyl carboxylic acids **1** – **5** and ferrocenylsubphthalocyanine dyads **7** – **11**. Data of **1** – **5** from reference [14]. (b) Relationship between $E^{\circ'}$(wave II) and E_{pc} (wave III) and n, of the first and second ring-based reductions respectively, of ferrocenylsubphthalocyanine dyads **7** – **11**.

2.4.3. *Effect of carboxyl and carbonyl group on ferrocenyl moiety oxidation*

The formal reduction potential $E°'$ of the Fe group of SubPc **7**, separated by a carboxyl group from the electron donating SubPc, is at 0.224 V compared to free ferrocene 0 V, implying that the electron withdrawing effect of the carboxyl group is larger than the electron donating effect of the SubPc on the $E°'$ of the Fe group. The additional electron withdrawing carbonyl group bound next to the ferrocenyl moiety in SubPc **11** resulted in the highest oxidation potential of the Fe group with $E°'$ at 0.262 V, Figure 3. With the two electron withdrawing CO groups in SubPc **11** the oxidation potential was 0.038 V higher than $E°'$ of Fe in SubPc **7** (0.224 V) containing only one electron withdrawing CO group.

Table 2 Cyclic voltammetry data of SubPcs **7** – **11** in DCM containing 0.1 mol dm^{-3} $[N(^{n}Bu)_4][B(C_6F_5)_4]$ as supporting electrolyte at a scan rate of 0.100 V/s at 25°C.

	Description	E_p[a]	$E°'$ (V), ΔE_p (V)	i_p (μA)[b], current ratio[c]
FcCOOH[d] **1**	Fc	0.321	0.284, 0.074	3.60, 0.99
$FcCH_2COOH$[d] **2**	Fc	0.047	0.014, 0.066	3.79, 0.99
$Fc(CH_2)_2COOH$[d] **3**	Fc	0.020	-0.015, 0.070	3.87, 0.99
$Fc(CH_2)_3COOH$[d] **4**	Fc	0.011	-0.024, 0.070	3.98, 0.99
$FcCO(CH_2)_2COOH$[d] **5**	Fc	0.330	0.295, 0.070	3.66, 0.99
SubPc 6 -	DmFc	-0.647	-0.610, 0.076	3.89, 0.99
$ClBSubPc(H)_{12}$[e]	Wave I	0.674	0.628, 0.086	3.08, 0.99
	Wave II	-1.519	- , -	3.63, -
	Wave III	-2.050	- , -	- , -
SubPc **7** -	DmFc	-0.647	-0.610, 0.074	3.91, 0.99
Fc$CO_2SubPc(H)_{12}$	Fc	0.262	0.224, 0.076	3.61, 0.99
	Wave I	0.711	0.670, 0.082	3.34, 0.99
	Wave II	-1.643	-1.601, 0.084	3.47, 0.99
	Wave III	-2.124	- , -	- , -
SubPc **8** -	DmFc	-0.647	-0.610, 0.075	3.84, 0.99
Fc$CH_2CO_2SubPc(H)_{12}$	Fc	-0.005	-0.043, 0.076	3.61, 0.99
	Wave I	0.710	0.670, 0.080	3.38, 0.99
	Wave II	-1.715	-1.674, 0.082	3.49,0.99
	Wave III	-2.154	- , -	- , -
SubPc **9** -	DmFc	-0.647	-0.610,0.074	3.89, 0.99
Fc$(CH_2)_2CO_2SubPc(H)_{12}$[f]	Fc	-0.021	-0.058, 0.074	3.66, 0.99

	Wave I	0.712	0.670, 0.084	3.31, 0.99
	Wave II	-1.783	-1.741, 0.084	3.42, 0.99
	Wave III	-2.264	- , -	- , -
SubPc **10** -	DmFc	-0.647	-0.610, 0.075	3.97, 0.99
Fc$(CH_2)_3CO_2$SubPc$(H)_{12}$	Fc	-0.024	-0.062, 0.076	3.58, 0.99
	Wave I	0.711	0.670, 0.082	3.27, 0.99
	Wave II	-1.871	-1.829, 0.084	3.39, 0.99
	Wave III	-2.344	- , -	- , -
SubPc **11** -	DmFc	-0.647	-0.610, 0.074	3.84, 0.99
Fc$CO(CH_2)_2CO_2$SubPc$(H)_{12}$	Fc	0.300	0.262, 0.076	3.57, 0.99
	Wave I	0.711	0.670, 0.082	3.35, 0.99
	Wave II	-1.525	-1.482, 0.086	3.41, 0.99
	Wave III	-2.004	- , -	- , -

[a] E_p is the peak anodic peak for oxidation (E_{ox}) and peak cathodic peak for reduction (E_{red}).
[b] i_p is the peak anodic peak for oxidation (i_{pa}) and peak cathodic peak for reduction (i_{pc}).
[c] peak current ratio = i_{pc}/i_{pa} for oxidation and i_{pa}/i_{pc} for reduction.
[d] Data from reference [14]
[e]. Data from reference [20]
[f]. Data from reference [23]

2.4.4. *Ring Based Reductions*

The first (wave II) and second (wave III) ring-based reductions of SubPcs 7 – 11 are lower than that of SubPc **6**. The axial ferrocenylcarboxylic ligands of SubPcs **7** – **11** thus have a nett electron donating effect on the aromatic ring electrons of SubPcs **7** – **11** compared to Cl in SubPc **6**. Both ring-based reductions of SubPcs **7** – **11**, redox waves II and III in Figure 3 and Table 2, followed the same trend, namely the reduction value decreases near linear as the number of (CH_2) groups, n, in the different axially bonded ferrocenyl carboxylic acid moieties (Fc-$(CH_2)_n$-CO_2) increases in SubPcs **7** – **10**, with the reduction values of SubPc **11** higher than that of SubPc **7**, see Figure 4 (b). The charge on Fc in **7** – **10** is isolated from the rest of the molecules, and the aromatic ring electron density of the SubPcs systematically increased as n of the alkyl group in –$OCO(CH_2)_n$- increases. SubPc **10** exhibited the lowest first ring-based reduction potential (-1.872 V), reported to date [18,21,22,25], due to the carboxyl-alkyl ($OOC(CH_2)_3$), group's electron-donating effect being isolated from ferrocenium moiety. The donating effect is the most prominent on SubPc **10** containing the longest

alkyl chain. Propyl (n = 3) is more electron donating than ethyl (n = 2) that is more electron donating then methyl (n = 1).

2.4.5. *Ring Based Oxidation*

$E°'$ of the first ring-based oxidation of SubPcs **7** – **11** (wave I in Figure 3) is exactly the same, with $E°'$ = 0.670 V for all five complexes **7** – **11**. This is because the charge located on the ferrocenium group (Fc^+) in the different oxidised ferrocenyl carboxylic acid moieties (Fc^+-$(CH_2)_n$-CO_2) and (Fc^+-$CO(CH_2)_2$-CO_2) for SubPcs **7** – **11**, is isolated from the rest of the molecule. The Fc^+ group is highly electronegative [26], withdrawing any available electron density from the alkyl groups bonded to it. The first ring-based oxidation of SubPcs **7** – **11** is consequently only influenced by the electron withdrawing carboxyl group attached directly to boron in the axial position, shifting the first ring-based oxidation of SubPcs **7** – **11** with exactly the same value namely 0.042 V more positive than $E°'$ of the first ring-based oxidation of SubPcs **6** at 0.628 V. The electron withdrawing effect of the carboxyl group in **7** – **11** is thus larger than the electron withdrawing effect of Cl in **6**, on the aromatic ring electron density of the SubPcs. It was possible to get chemically reversible ring-based oxidation with peak current ratios approaching 1 and peak current separation ΔE_p between 0.080 and 0.084 V, see Table 2.

2.5. Computational Analysis

The ferrocenylcarboxylic-containing SubPc dyads **7** – **11**, were optimised using density functional theory (DFT) to gain further insight into the redox properties of the ferrocene dyads. In agreement with previous studies on related SubPcs, the HOMOs of the neutral species are of iron-d character while the LUMOs have π-ring character [21,23]. This confirm Fe(II) to Fe(III) oxidation and ring-based reduction respectively. However, since the top three HOMOs of **7** – **11** are all iron-d based, and Fe(III) to Fe(IV) oxidation is not expected, it was essential to also optimise the cation (oxidised) species, to locate the locus of the second experimentally observed oxidation. It is known that orbitals can rearrange upon oxidation [27–29]. The DFT results of oxidised SubPcs **7** – **11** all

showed that the LUMO is of iron-d character (the first oxidation, see Figure 5) and the HOMO is on the SubPc ring (the second oxidation, see Figure 5). HOMO-1, also on the SubPc ring, will be the second ring oxidation, however, it is out of the solvent window in cyclic voltammetry scans and not experimentally observed.

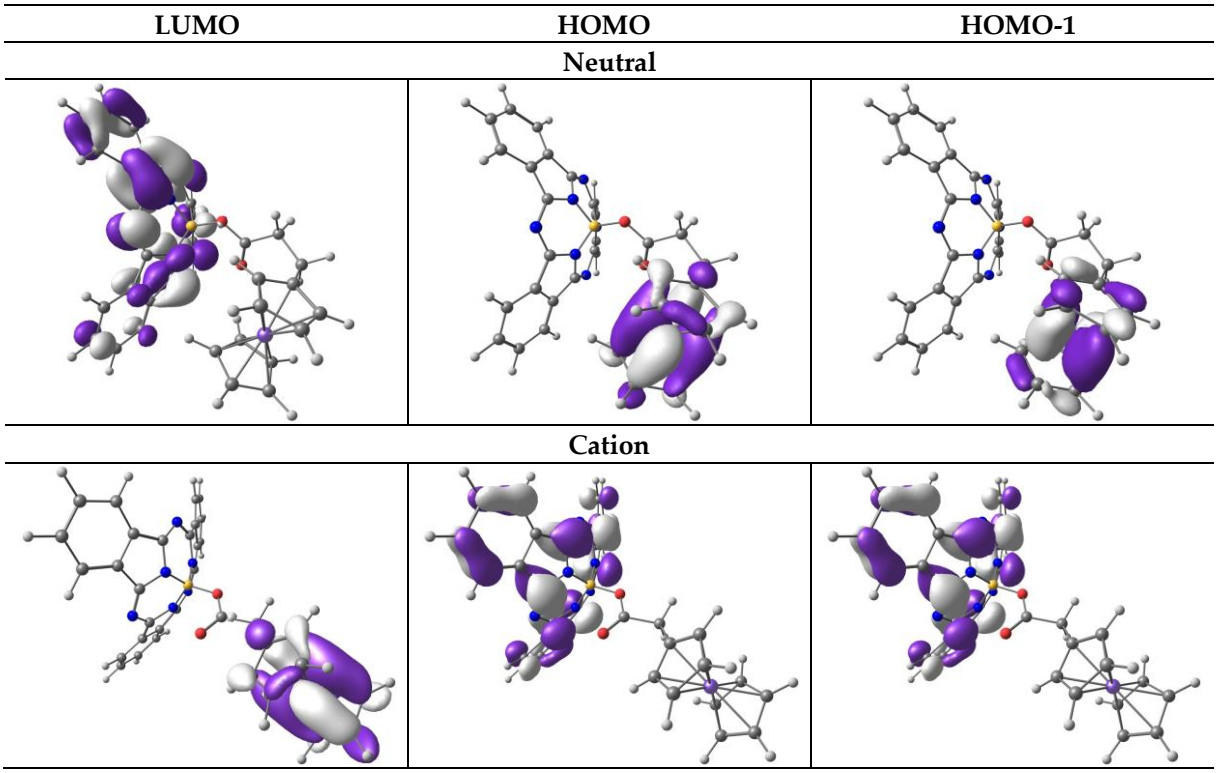

Figure 5 Selected PBE1PBE/6-311G(d,p) frontier MOs for cation SubPc, **8**. A contour of 0.03 e/Å^3 was used for the orbital plots. Colour code of atoms (online version): Fe (purple), B (yellow), C (grey), O (red), H (white).

3. Materials and Methods

Solid reagents (Sigma-Aldrich, Strem and Merck) were used as received. Liquid reagents (Sigma-Aldrich and Merck) were used without any further purification unless specified otherwise. Solvents were distilled, and water was double distilled. Organic solvents used in this study were dried according to published methods [30]. Melting points are uncorrected and were determined with an Olympus BX 51 microscope equipped with a Linkam THMS 600 hot stage.

3.1. Spectroscopy Measurements

^{1}H, ^{11}B and ^{13}C spectroscopic analysis were performed for all compounds in the study. ^{1}H and ^{13}C spectra were recorded at 25°C on a 600 MHz AVANCE II NMR spectrometer at 600.28 MHz and 150.95 MHz respectively. ^{11}B NMR spectra were recorded at 25°C on a 400 MHz AVANCE III NMR spectrometer at 128.38 MHz. Hydrogen and carbon chemical shifts are relative to hydrogen and carbon in $CDCl_3$ at 7.24 ppm and 77.16 ppm, respectively. The following abbreviations are used to describe peak patterns: s = singlet, d = doublet, t = triplet, q = quartet and m = multiplet. UV/vis spectra were recorded on a Varian Cary 5000 UV-Vis-NIR Spectrophotometer. Melting points are uncorrected and were determined with an Olympus BX 51 microscope equipped with a Linkam THMS 600 hot stage.

3.2. Cyclic Voltammetry

All the electrochemical experiments were performed in an M Bruan Lab Master SP glove box under a high purity argon atmosphere (H_2O and O_2 < 10 ppm). Cyclic voltammetry (CV) measurements were performed utilising a Princeton Applied Research PARSTAT 2273 potentiostat, running Powersuite software (Version 2.58). A three-electrode cell was used. A glassy carbon electrode with a surface area 3.14 x 10^{-6} m^2 was chosen as working electrode, platinum wires were chosen as auxiliary and reference electrodes. The glassy carbon working electrode was polished and prepared before every experiment on a Buhler polishing mat first with 1-micron and then with ¼-micron diamond paste, rinsed with H_2O, acetone and dichloromethane (DCM), and dried before each experiment. Electrochemical analysis of the complexes was performed in DCM (anhydrous, ≥ 99.8%, contains 40-150 ppm amylene as a stabiliser) at room temperature. Solutions were made in 0.001 dm^3 spectrochemical grade anhydrous DCM containing *ca.* 0.0005 M of an analyte, 0.0005 mol dm^{-3} of internal reference (decamethylferrocene, DmFc) and 0.1 mol dm^{-3} of supporting electrolyte tetrabutylammonium tetrakispentafluorophenylborate, $[N(^{n}Bu)_4][B(C_6F_5)_4]$ in DCM. Experimental potential data was collected *vs.* the Pt wire reference electrode but is reported *vs.* the redox couple of ferrocene, Fc/Fc^+ at 0 V. $E°'$ (DmFc) = - 0.610 V *vs.* Fc/Fc^+ at 0 V in DCM/$[N(^{n}Bu)_4][B(C_6F_5)_4]$. Scan rates were between 0.05 and 5.00 Vs^{-1}. Electrochemical reversibility (or Nernstian behaviour) of redox

processes is indicated by a peak current ratio (i_{pc}/i_{pa} for oxidation and i_{pa}/i_{pc} for reduction) of 1 [31,32] and peak current separation $\Delta E = |E_{pa} - E_{pc}| = 0.059$ V for a one-electron transfer process [33]. In this experiment, due to experimental cell imperfections and ohmic drop effects, ΔE_p slightly larger than 0.059 V was obtained, even for the known 1 e^- transfer processes of decamethylferrocene, $DmFc^+$/DmFc, namely 0.074 - 0.076 V [34–36]. The formal reduction potential is determined by $E^{\circ\prime} = (E_{pa} - E_{pc})/2$ for an electrochemically reversible (and quasi reversible) process where E_{pa} (E_{pc}) = anodic (cathodic) peak potential and i_{pa} (i_{pc}) = anodic (cathodic) peak current.

3.3.DFT Calculations

Density functional theory (DFT) optimisations were performed on the neutral and oxidised molecules in the gas phase using the hybrid PBE1PBE [37–39] exchange-correlation functional and the triple-ζ basis set 6-311G(d,p) basis set, as implemented in the Gaussian 16 package [40]. Single point calculations using pure BP86 [41–43] exchange-correlation were performed in DCM as the solvent, using the IEF-PCM model (polarisable continuum model (PCM) [44] which solved the non-homogeneous Poisson equation by applying the integral equation formalism variant) [45]. Both the gas phase PBE1PBE/6-311G(d,p) and solvent phase BP86/6-311G(d,p) results gave the same molecular orbital (MO) insight into the observed experimental redox processes.

*3.4. Preparationof SubPcs **7** - **11***

$FcCO_2H$, **1**, $FcCH_2CO_2H$, **2**, $Fc(CH_2)_2CO_2H$, **3**, $Fc(CH_2)_3CO_2H$, **4**, $ClBSubPc(H)_{12}$, **5**, and $Fc(CH_2)_2CO_2BSubPc(H)_{12}$, **9**, were synthesised using slight modifications to literature methods (see the supporting information) [8,12,13,23]. Compounds **7** – **11** were characterised by NMR, UV/vis, elemental analysis and m.p.

3.4.1. Preparation of $FcCO_2SubPc(H)_{12}$, **7**.

To a solution of chlorosubphthalocyanine, **6**, (200 mg; 0.46 mmol) and dry toluene (3 cm^3), silver trifluoromethanesulfonate (150 mg, 0.58 mmol; 1.25 eq.) was added and the mixture stirred at 45°C,

under argon atmosphere for 4 hours. Once the (OTf)SubPc(H)$_{12}$ was generated, ferrocenylcarboxylic acid, **1**, (212 mg, 0.92 mmol, 2 eq.) and *N*,*N*-diisopropylethylamine (0.10 cm^3, 75 mg, 0.58 mmol, 1.25 eq.) was added. The mixture was stirred at 50 °C for 12 hours. The solvent was removed by evaporation under reduced pressure and the product was directly purified by flash chromatography using hexane: DCM (1:1) (R$_f$: 0.82) as eluent to give 184 mg (92%). m.p.: 172-182°C, UV/vis: λ_{max} 563 nm, ε = 176547 dm^3 mol^{-1} cm^{-1} in THF. NMR: δ_H (600.28 MHz, $CDCl_3$, 25 °C): δ 8.84 (6H, dd, SubPc), 7.90 (6H, dd, SubPc), 3.96 (2 H, pt, 2 x CH_2: Substituted-Cp), 3.95 (2 H, pt, 2 x CH_2: Substituted-Cp), 3.63 (5 H, s, Unsubstituted-Cp). ^{11}B NMR: δ_B (128.38 MHz, $CDCl_3$): δ 16.82 (1B). ^{13}C NMR: δ_C (150.95 MHz, $CDCl_3$, 25 °C): δ 151.64 (6C, N=C), 130.00 (6C, SubPc - C=C), 122.49 (6C, SubPc-Ph), 71.02 (1C, C-CO_2H), 70.01 (2C, Substituted-Cp), 69.58 (5C, Unsubstituted-Cp). Elemental analysis calculated for $C_{35}H_{21}BFeN_6O_2$ (element, %): C, 67.34; H, 3.39; N, 13.46. Obtained: C, 67.73; H, 3.47; N, 13.58.

3.4.2. Preparation of $FcCH_2CO_2SubPc(H)_{12}$, **8**.

To a solution of chlorosubphthalocyanine, **6**, (200 mg; 0.46 mmol) and dry toluene (3 cm^3), silver trifluoromethanesulfonate (150 mg, 0.58 mmol; 1.25 eq.) was added and the mixture stirred at 45°C, under argon atmosphere for 4 hours. Once the (OTf)SubPc(H)$_{12}$ was generated, ferrocenylmethanoic acid, **2**, (225 mg, 0.92 mmol, 2 eq.) and *N*,*N*-diisopropylethylamine (0.10 cm^3, 75 mg, 0.58 mmol, 1.25 eq.) was added. The mixture was stirred at 50 °C for 12 hours. The solvent was removed by evaporation under reduced pressure and the product was directly purified by flash chromatography using hexane: DCM (1:1) (R$_f$: 0.78) as eluent to give 140 mg (79%). m.p.: 175 – 183°C, UV/vis: λ_{max} 563 nm, ε = 166317 dm^3 mol^{-1} cm^{-1} in THF. NMR: δ_H (600.28 MHz, $CDCl_3$, 25 °C): δ 8.86 (6H, dd, SubPc), 7.89 (6H, dd, SubPc), 3.79 (2 H, pt, 2 x CH_2: Substituted-Cp), 3.67 (5 H, s, Unsubstituted-Cp), 3.53 (2 H, pt, 2 x CH_2: Substituted-Cp), 2.28 (2H, t, CH_2). ^{11}B NMR: δ_B (128.38 MHz, $CDCl_3$): δ 16.76 (1B). ^{13}C NMR: δ_C (150.95 MHz, $CDCl_3$, 25 °C): δ 151.68 (6C, N=C), 130.04 (6C, SubPc - C=C), 122.45 (6C, SubPc-Ph), 69.10 (1C, C-CO_2H), 68.41 (2C, Substituted-Cp), 67.48 (5C, Unsubstituted-Cp), 30.48 (2C, CH2). Elemental analysis calculated for $C_{36}H_{23}BFeN_6O_2$ (element, %): C, 67.74; H, 3.63; N, 13.17. Obtained: C, 67.90; H, 3.82; N, 13.72.

3.4.3. Preparation of $Fc(CH_2)_3CO_2SubPc(H)_{12}$, **10**.

To a solution of chlorosubphthalocyanine, **6**, (200 mg; 0.46 mmol) and dry toluene (3 cm^3), silver trifluoromethanesulfonate (150 mg, 0.58 mmol; 1.25 eq.) was added and the mixture stirred at 45°C, under argon atmosphere for 4 hours. Once the $(OTf)SubPc(H)_{12}$ was generated, ferrocenylethanoic acid, **4**, (250 mg, 0.92 mmol, 2 eq.) and *N*,*N*-diisopropylethylamine (0.10 cm^3, 75 mg, 0.58 mmol, 1.25 eq.) was added. The mixture was stirred at 50 °C for 12 hours. The solvent was removed by evaporation under reduced pressure and the product was directly purified by flash chromatography using hexane: DCM (1:1) (R_f: 0.73) as eluent to give 104 mg (52%). m.p.: 182-190°C, UV/vis: λ_{max} 563 nm, ε = 145673 $dm^3\ mol^{-1}\ cm^{-1}$ in THF. NMR: δ_H (600.28 MHz, $CDCl_3$, 25 °C): δ 8.86 (6H, dd, SubPc), 7.88 (6H, dd, SubPc), 3.89 (5 H, s, Unsubstituted-Cp), 3.84 (2 H, pt, 2 x CH_2: Substituted-Cp), 3.70 (2 H, pt, 2 x CH_2: Substituted-Cp), 1.76 (2H, t, CH_2), 1.26 (2H, t, CH_2), 1.06 (2H, q, CH_2). ^{11}B NMR: δ_B (128.38 MHz, $CDCl_3$): δ 16.32 (1B). ^{13}C NMR: δ_C (150.95 MHz, $CDCl_3$, 25 °C): δ 151.64 (6C, N=C), 129.99 (6C, SubPc - C=C), 122.43 (6C, SubPc-Ph), 68.48 (1C, C-CO_2H), 68.01 (2C, Substituted-Cp), 67.01 (5C, Unsubstituted-Cp), 28.42 (2C, CH_2), 25.39 (2C, CH_2). Elemental analysis calculated for $C_{38}H_{27}BFeN_6O_2$ (element, %): C, 68.50; H, 4.08; N, 12.61. Obtained: C, 68.61; H, 4.16; N, 12.74.

3.4.4. Preparation of $FcCO(CH_2)_2CO_2SubPc(H)_{12}$, **11**.

To a solution of chlorosubphthalocyanine, **6**, (200 mg; 0.46 mmol) and dry toluene (3 cm^3), silver trifluoromethanesulfonate (150 mg, 0.58 mmol; 1.25 eq.) was added and the mixture stirred at 45°C, under argon atmosphere for 4 hours. Once the $(OTf)SubPc(H)_{12}$ was generated, ferrocenyloxobutanoic acid, **4**, (263 mg, 0.92 mmol, 2 eq.) and *N*,*N*-diisopropylethylamine (0.10 cm^3, 75 mg, 0.58 mmol, 1.25 eq.) was added. The mixture was stirred at 50 °C for 12 hours. The solvent was removed by evaporation under reduced pressure and the product was directly purified by flash chromatography using hexane: DCM (1:1) (R_f: 0.62) as eluent to give 114 mg (57%). m.p.: 201-207°C, UV/vis: λ_{max} 563 nm, ε = 113729 $dm^3\ mol^{-1}\ cm^{-1}$ in THF. NMR: δ_H (600.28 MHz, $CDCl_3$, 25 °C): δ 8.85 (6H, dd, SubPc), 7.88 (6H, dd, SubPc), 4.49 (2 H, pt, 2 x CH_2: Substituted-Cp), 4.31 (2 H, pt, 2 x CH_2:

Substituted-Cp), 3.98 (5 H, s, Unsubstituted-Cp), 2.23 (2H, t, CH_2), 1.66 (2H, t, CH_2).^{11}B NMR: δ_B (128.38 MHz, $CDCl_3$): δ 16.79 (1B). ^{13}C NMR: δ_C (150.95 MHz, $CDCl_3$, 25 °C): δ 156.51 (6C, N=C), 144.73 (6C, SubPc - C=C), 130.42 (6C, SubPc-Ph), 72.55 (1C, C-CO_2H), 70.14 (2C, Substituted-Cp), 69.41 (5C, Unsubstituted-Cp),34.23 (2C, CH_2). Elemental analysis calculated for $C_{38}H_{25}BFeN_6O_3$ (element, %): C, 67.09; H, 3.70; N, 12.35. Obtained: C, 67.09; H, 3.82; N, 12.35.

4. Conclusions

Subphthalocyanines with ferrocenylcarboxylic acids in the axial position can be synthesized in 90% yields when reactions are performed under strict Schlenk conditions, in this case a glovebox. The axial ferrocenyl moiety did not influence the UV/vis wavelength maxima of the Soret or Q-bands comparing SubPcs **7** – **11** with parent macrocycle, **6**. The cyclic voltammetry data revealed that the first reversible oxidation process is ferrocene-centered, with the second oxidation and all observed reduction processes are SubPc ring-based. DFT optimization of the oxidized (cation) SubPc was necessary to confirm the locus of the second observed SubPc ring-based oxidation.

The oxidation potential of Fe of the axial ferrocenyl moiety was affected by the subphthalocyanine, shifting $Fe^{II/III}$ oxidation potentials with 0.03 – 0.06 V to a lower oxidation potential compared to $Fe^{II/III}$ oxidation potentials of the free ferrocenyl acids. The oxidized axial electron withdrawing ferrocenium moiety, withdraws charge from the alkyl chains bonded to it, and consequently the first ring-based oxidation of all ferrocenylsubphthalocyanine dyads Y-BSubPc(H)$_{12}$ is only influenced by the electron withdrawing carboxyl group in the axial position, shifting the first ring-based oxidation for all ferrocenylsubphthalocyanine dyads with exactly the same value of 0.042 V more positive compared to the first ring-based oxidation of Cl-BSubPc(H)$_{12}$. Both the carboxyl and alkyl groups in the axial position influenced the ring electron density of the neutral SubPc, leading to a systematic decrease in the two observed ring-based reductions of the ferrocenylsubphthalocyanine dyads as the number of alkyl groups n in the different axially bonded ferrocenyl carboxylic acid moieties (Fc-$(CH_2)_n$-CO_2) increases. Fc$(CH_2)_3$BSubPc(H)$_{12}$, SubPc **10**, has the lowest first ring-based

reduction potential reported to date, due to the strong electron withdrawing effect of the axial carboxyl-alkyl group ($OOC(CH_2)_3$), being isolated from the ferrocenium moiety.

Supplementary Materials: The following are available online at www.mdpi.com/xxx/s1, synthesis and characterisation, additional graphs, tables, and optimised coordinates are provided in the Supporting information.

Funding: This research was funded by South African National Research Foundation (Grant numbers 113327 and 96111) and the Central Research Fund of the University of the Free State, Bloemfontein. The High-Performance Computing facility of the UFS, the CHPC of South Africa and the Norwegian Supercomputing Program (UNINETT Sigma2, Grant No. NN9684K) are acknowledged for computer time.

Conflicts of Interest: The authors declare no competing financial interest.

References

1. Dagani, R. Fifty Years of Ferrocene Chemistry. *Chem. Eng. News* **2001**, *79*, 37–38.
2. Bublitz, D. E.Rinehart, K.L. *Inorganic Reactions*; 17th ed.; Eiley: New York, 1969;
3. Deeming, J. *In Comprehensive Organometallic Chemistry*; Pergamon, Ed.; 4th ed.; Oxford, 1982;
4. Watts, W.. *In Comprhensive Organometallic Chemistry*; Pergamon, Ed.; 8th ed.; Oxford, 1982;
5. Nesmeyanov, A.N.; Kochetkova, N.S. Applications of Ferrocene and Its Derivatives. *Russ. Chem. Rev.* **1974**, *5*, 710–715.
6. Conradie, J.; Lamprecht, G.J.; Roodt, A.; Swarts, J.C. Kinetic study of the oxidative addition reaction between methyl iodide and [Rh(FcCOCHCOCF3)(CO)(PPh3)]: Structure of [Rh(FcCOCHCOCF3)(CO)(PPh3)(CH3)(I)]. *Polyhedron* **2007**, *26*, 5075–5087.
7. Shen, Q.; Shekhar, S.; Stambuli, J.P.; Hartwig, J.F. Highly reactive, general, and long-lived catalysts for coupling heteroaryl and aryl chlorides with primary nitrogen nucleophiles. *Angew. Chemie - Int. Ed.* **2005**, *44*, 1371–1375.
8. Nonjola, P.T.N.; Siegert, U.; Swarts, J.C. Synthesis, Electrochemistry and Cytotoxicity of Ferrocene-Containing Amides, Amines and Amino-Hydrochlorides. *J. Inorg. Organomet. Polym. Mater.* **2015**, *25*, 376–385.
9. Swarts, J.C.; Vosloo, T.G.; Cronje, S.J.; Du Plessis, W.C.; Van Rensburg, C.E.J.; Kreft, E.; Van Lier, J.E. Cytotoxicity of a series of ferrocene-containing β-diketones. *Anticancer Res.* **2008**, *28*, 2781–2784.
10. Shago, R.F.; Swarts, J.C.; Kreft, E.; Van Rensburg, C.E.J. Antineoplastic activity of a series of ferrocene-containing alcohols. *Anticancer Res.* **2007**, *27*, 3431–3433.
11. Peter, S.; Aderibigbe, B.A. Ferrocene-Based Compounds with Antimalaria/Anticancer Activity. *Molecules* **2019**, *24*, 3604.

12. Davis, W.L.; Shago, R.F.; Langner, E.H.G.; Swarts, J.C. Synthesis and electrochemical properties of a series of ferrocene-containing alcohols. *Polyhedron* **2005**, *24*, 1611–1616.
13. Blom, N.F.; Neuse, E.W.; Thomas, H.G. Electrochemical characterization of some ferrocenylcarboxylic acids. *Transit. Met. Chem.* **1987**, *12*, 301–306.
14. Swarts, P.J.; Conradie, J. Solvent and Substituent Effect on Electrochemistry of Ferrocenylcarboxylic Acid Dyads. *J. Electroanal. Chem.*
15. A, M.; A, O. Phthalocyaninartige Bor-Komplexe. *Monatshefte fur Chemie* **1972**, *103*, 150–155.
16. Ma, Z.; Liu, S.; Hu, S.; Yu, J. Highly efficient tandem organic light-emitting diodes based on SubPc:C60 bulk heterojunction as charge generation layer. *J. Lumin.* **2016**, *169*, 29–34.
17. Ince, M.; Medina, A.; Yum, J.H.; Yella, A.; Claessens, C.G.; Martínez-Díaz, M.V.; Grätzel, M.; Nazeeruddin, M.K.; Torres, T. Peripherally and axially carboxylic acid substituted subphthalocyanines for dye-sensitized solar cells. *Chem. - A Eur. J.* **2014**, *20*, 2016–2021.
18. Claessens, C.G.; González-Rodríguez, D.; Rodríguez-Morgade, M.S.; Medina, A.; Torres, T. Subphthalocyanines, subporphyrazines, and subporphyrins: Singular nonplanar aromatic systems. *Chem. Rev.* 2014, *114*, 2192–2277.
19. van de Winckel, E.; Mascaraque, M.; Zamarrón, A.; Juarranz de la Fuente, Á.; Torres, T.; de la Escosura, A. Dual Role of Subphthalocyanine Dyes for Optical Imaging and Therapy of Cancer. *Adv. Funct. Mater.* **2018**, *28*.
20. Swarts, P.J.; Conradie, J. Electrochemical behaviour of chloro- and hydroxy-subphthalocyanines. *Electrochim. Acta* **2020**, *329*, 135165.
21. Solntsev, P. V.; Spurgin, K.L.; Sabin, J.R.; Heikal, A.A.; Nemykin, V.N. Photoinduced charge transfer in short-distance ferrocenylsubphthalocyanine dyads. *Inorg. Chem.* **2012**, *51*, 6537–6547.
22. Maligaspe, E.; Hauwiller, M.R.; Zatsikha, Y. V.; Hinke, J.A.; Solntsev, P. V.; Blank, D.A.; Nemykin, V.N. Redox and photoinduced electron-transfer properties in short distance organoboryl ferrocene-subphthalocyanine dyads. *Inorg. Chem.* **2014**, *53*, 9336–9347.
23. Swarts, P.J.; Conradie, J. Redox and photophysical properties of four SubPcs containing ferrocenylcarboxylic acid dyads as axial ligands. *Inorg. Chem*.
24. Guilleme, J.; González-Rodríguez, D.; Torres, T. Triflate-subphthalocyanines: Versatile, reactive intermediates for axial functionalization at the boron atom. *Angew. Chemie - Int. Ed.* **2011**, *50*, 3506–3509.
25. Sampson, K.L.; Josey, D.S.; Li, Y.; Virdo, J.D.; Lu, Z.H.; Bender, T.P. Ability to Fine-Tune the Electronic Properties and Open-Circuit Voltage of Phenoxy-Boron Subphthalocyanines through Meta-Fluorination of the Axial Substituent. *J. Phys. Chem. C* **2018**, *122*, 1091–1102.
26. du Plessis, W.; Erasmus, J.J.; Lamprecht, G.J.; Conradie, J.; Cameron, T.S.; Aquino, M.A.; Swarts, J.C. Cyclic voltammetry of ferrocene-containing β-diketones as a tool to obtain group electronegativities. The structure of 3-ferrocenoyl-1,1,1-trifluoro-2-hydroxyprop-2-ene. *Can. J. Chem.* **2011**, *77*, 378–386.
27. Ferrando-Soria, J.; Fabelo, O.; Castellano, M.; Cano, J.; Fordham, S.; Zhou, H.C. Multielectron oxidation in a ferromagnetically coupled dinickel(II) triple mesocate. *Chem. Commun.* **2015**, *51*, 13381–13384.
28. Buitendach, B.E.; Conradie, J.; Malan, F.P.; Niemantsverdriet, J.W.; Swarts, J.C. Synthesis, Spectroscopy and Electrochemistry in Relation to DFT Computed Energies of Ferrocene- and

Ruthenocene-Containing -Diketonato Iridium(III) Heteroleptic Complexes. Structure of [(2-Pyridylphenyl)2Ir(RcCOCHCOCH3]. *Molecules* **2019**, *24*, 3923.

29. Malan, F.P.; Singleton, E.; Conradie, J.; Landman, M. Electrochemistry of a series of symmetric and asymmetric CpNiBr(NHC) complexes: Probing the electrochemical environment due to push-pull effects. *J. Electroanal. Chem.* **2018**, *814*, 66–76.
30. Williams, D.B.G.; Lawton, M. Drying of organic solvents: Quantitative evaluation of the efficiency of several desiccants. *J. Org. Chem.* **2010**, *75*, 8351–8354.
31. Elgrishi, N.; Rountree, K.J.; McCarthy, B.D.; Rountree, E.S.; Eisenhart, T.T.; Dempsey, J.L. A Practical Beginner's Guide to Cyclic Voltammetry. *J. Chem. Educ.* **2018**, *95*, 197–206.
32. Kissinger, P.T.; Heineman, W.R. Cyclic voltammetry. *J. Chem. Educ.* **1983**, *60*, 702–706.
33. Gericke, H.J.; Barnard, N.I.; Erasmus, E.; Swarts, J.C.; Cook, M.J.; Aquino, M.A.S. Solvent and electrolyte effects in enhancing the identification of intramolecular electronic communication in a multi redox-active diruthenium tetraferrocenoate complex, a triple-sandwiched dicadmium phthalocyanine and a ruthenocene-containing β-diketone. *Inorganica Chim. Acta* **2010**, *363*, 2222–2232.
34. Blrke, R.L.; Kim, M.H.; Strassfeld, M. Diagnosis of Reversible, Quasi-Reversible, and Irreversible Electrode Processes with Differential Pulse Polarography. *Anal. Chem.* **1981**, *53*, 852–856.
35. Mirkin, M. V.; Bard, A.J. Simple Analysis of Quasi-Reversible Steady-State Voltammograms. *Anal. Chem.* **1992**, *64*, 2293–2302.
36. Myland, J.C.; Oldham, K.B. Quasireversible cyclic voltammetry of a surface confined redox system: A mathematical treatment. *Electrochem. commun.* **2005**, *7*, 282–287.
37. Perdew, J.P.; Burke, K.; Ernzerhof, M. Generalized gradient approximation made simple. *Phys. Rev. Lett.* **1996**, *77*, 3865–3868.
38. Perdew, J.P.; Burke, K.; Ernzerhof, M. Generalized Gradient Approximation Made Simple (ERRATA). *Phys. Rev. Lett.* **1997**, *78*, 1396–1396.
39. Adamo, C.; Barone, V. Toward reliable density functional methods without adjustable parameters: The PBE0 model. *J. Chem. Phys.* **1999**, *110*, 6158–6170.
40. Frisch, M.J.; Trucks, G.W.; Schlegel, H.B.; Scuseria, G.E.; Robb, M.A.; Cheeseman, J.R.; Scalmani, G.; Barone, V.; Petersson, G.A.; Nakatsuji, H.; et al. Gaussian 16, Revision B.01 2016, 2016.
41. Becke, A.D. Density-functional exchange-energy approximation with correct asymptotic behavior. *Phys. Rev. A* **1988**, *38*, 3098–3100.
42. Perdew, J.P. Density-functional approximation for the correlation energy of the inhomogeneous electron gas. *Phys. Rev. B* **1986**, *33*, 8822–8824.
43. Perdew, J.P. Erratum: Density-functional approximation for the correlation energy of the inhomogeneous electron gas (Physical Review B (1986) 34, 10 (7406)). *Phys. Rev. B* **1986**, *34*, 7406.
44. Marenich, A. V; Cramer, C.J.; Truhlar, D.G. Universal Solvation Model Based on Solute Electron Density and on a Continuum Model of the Solvent Defined by the Bulk Dielectric Constant and Atomic Surface Tensions. *J. Phys. Chem. B* **2009**, *113*, 6378–6396.
45. Skyner, R.E.; Mcdonagh, J.L.; Groom, C.R.; Mourik, T. Van A review of methods for the calculation of solution free energies and the modelling of systems in solution. *Phys. Chem.*

Chem. Phys. **2018**, *17*, 6174–6191.

Data in brief (DIB)

Supporting information for publication: **Synthesis, Spectroscopy, Electrochemistry and DFT of Electron-rich ferrocenylsubphthalocyanine dyads**

Redox effect on ferrocenyl moiety of electron-rich ferrocenylsubphthalocyanine dyads

Pieter J. Swarts and Jeanet Conradie

Department of Chemistry, PO Box 339, University of the Free State, Bloemfontein, 9300, South Africa

Corresponding author(s)
conradj@ufs.ac.za

Abstract
The data presented in this paper are related to the research article entitled "*Synthesis, Spectroscopy, Electrochemistry and DFT of Electron-rich ferrocenylsubphthalocyanine dyads*", to be submitted to Molecules.

Keywords

Ferrocenylsubphthalocyanine; cyclic voltammetry; oxidation

Specifications Table

Subject	Chemistry
Specific subject area	Electrochemistry
Type of data	Table Image Graph Figure
How data were acquired	Princeton Applied Research PARSTAT 2273 potentiostat running Powersuite software (Version 2.58).

Data format	Raw Analysed
Parameters for data collection	Samples was used as synthesized. All the electrochemical experiments were performed in an M Bruan Lab Master SP glove box under a high purity argon atmosphere (H_2O and O_2 < 10 ppm).
Description of data collection	All electrochemical experiments were done in a 2 ml electrochemical cell containing three-electrodes (a glassy carbon working electrode, a Pt auxiliary electrode and a Pt pseudo reference electrode), connected to a Princeton Applied Research PARSTAT 2273 electrochemical analyser. Data obtained were exported to excel for analysis and diagram preparation.
Data source location	Institution: University of the Free State City/Town/Region: Bloemfontein Country: South Africa
Data accessibility	With the article
Related research article	P.J. Swarts, J. Conradie, To be submitted at Molecules

Value of the Data

- This data provides detailed redox data for four ferrocenylsubphthalocyanine dyads in DCM. Cyclic voltammograms for scan rates over two orders of magnitude (0.05 – 5.0 Vs^{-1}) are provided.
- This data illustrates the effect on the redox potentials of the electron rich macrocycle of Y-BSubPc(H)$_{12}$ on the iron(II/III) oxidation potential of ferrocenylcarboxylic acid moieties with varying alkyl chain lengths with Y = $Fc(CH_2)_nCO_2H$ and n = 0, 1, 2 or 3.
- This data illustrates the effect of the axial ferrocenylcarboxylic acid moieties on the ring-based oxidation and reductions of the ferrocenylsubphthalocyanine dyads.
- This data illustrate that chemical reversible first ring-based oxidation with peak current ratios of 1 and peak current separations, ΔE = 0.076 – 0.082 V can be obtained when electrochemical experiments are performed in a high purity argon atmosphere, while using DCM as the solvent and $[N(^nBu)_4][B(C_6F_5)_4]$ as supporting electrolyte.

Data Description

The electrochemical data of four ferrocenylsubphthalocyanine dyads, $FcCO_2BSubPc(H)_{12}$, $FcCH_2CO_2BSubPc(H)_{12}$, $Fc(CH_2)_3CO_2BSubPc(H)_{12}$ and $FcCO(CH_2)_2CO_2BSubPc(H)_{12}$ shown in Figure 1 are reported in Table 1 – 4 and Figures 2 – 5. The cyclic voltammetry results shows one iron based and one ring-based oxidations and two ring-based reductions for the three SubPcs, in agreement to previous studies [1,2]. The trend of the first iron based redox couple are similar to the trend of the oxidation of iron in the free ferrocenylcarboxylic acid dyads [3].

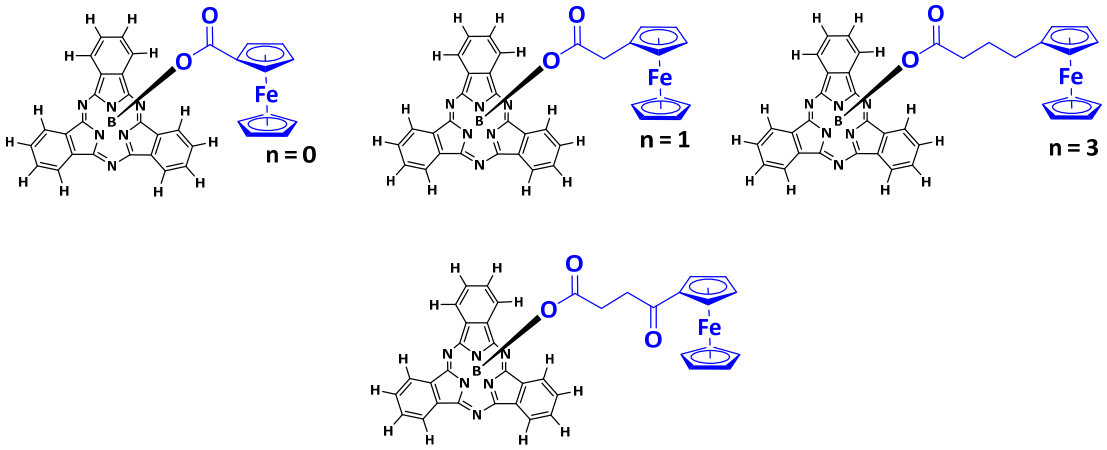

Figure 1. Structure of compounds in study used for DFT.

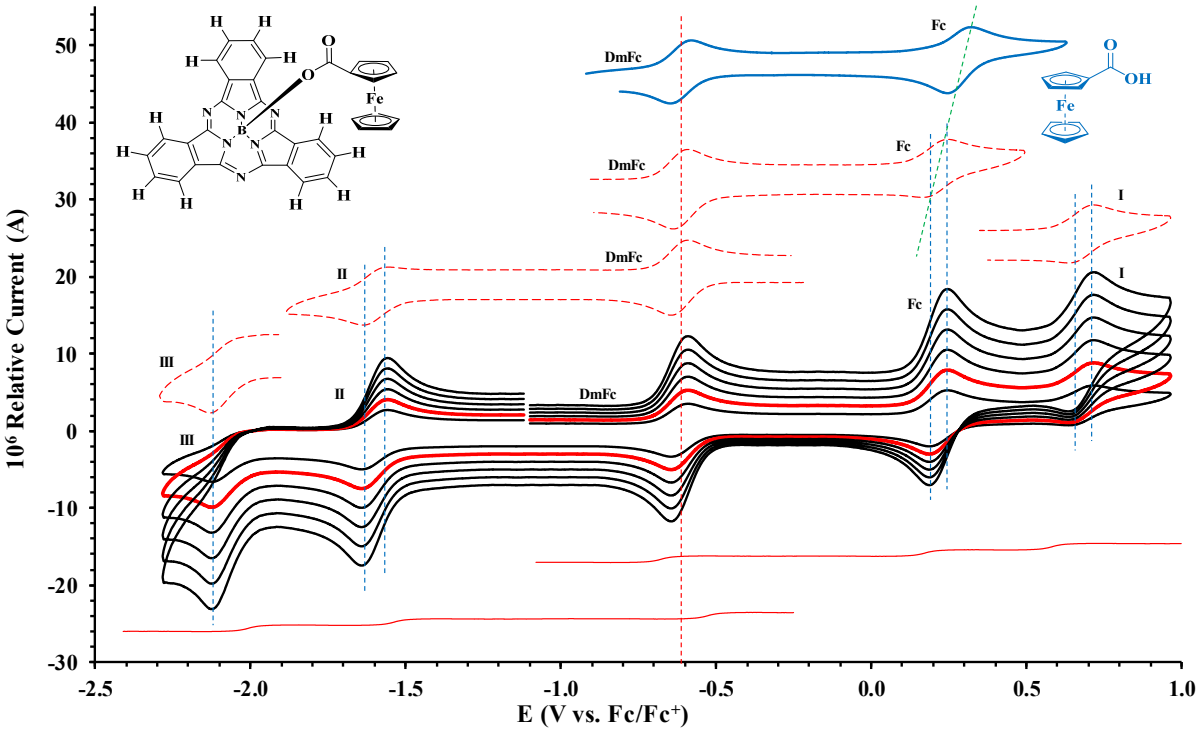

Figure 2. Cyclic voltammograms in DCM of $FcCO_2BSubPc(H)_{12}$ at scan rates 0.050 (smallest peak currents), 0.100, 0.200, 0.300, 0.400 and 0.500 (largest peak currents).

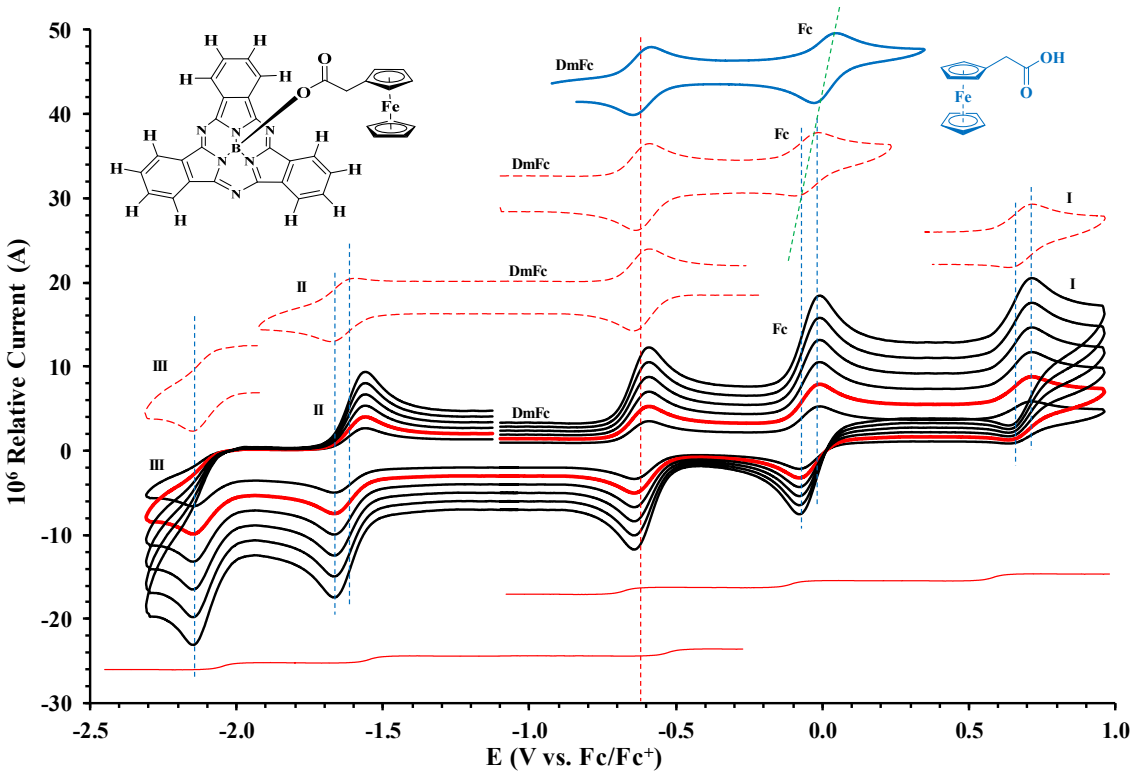

Figure 3. Cyclic voltammograms in DCM of $FcCH_2CO_2BSubPc(H)_{12}$ at scan rates 0.050 (smallest peak currents), 0.100, 0.200, 0.300, 0.400 and 0.500 (largest peak currents).

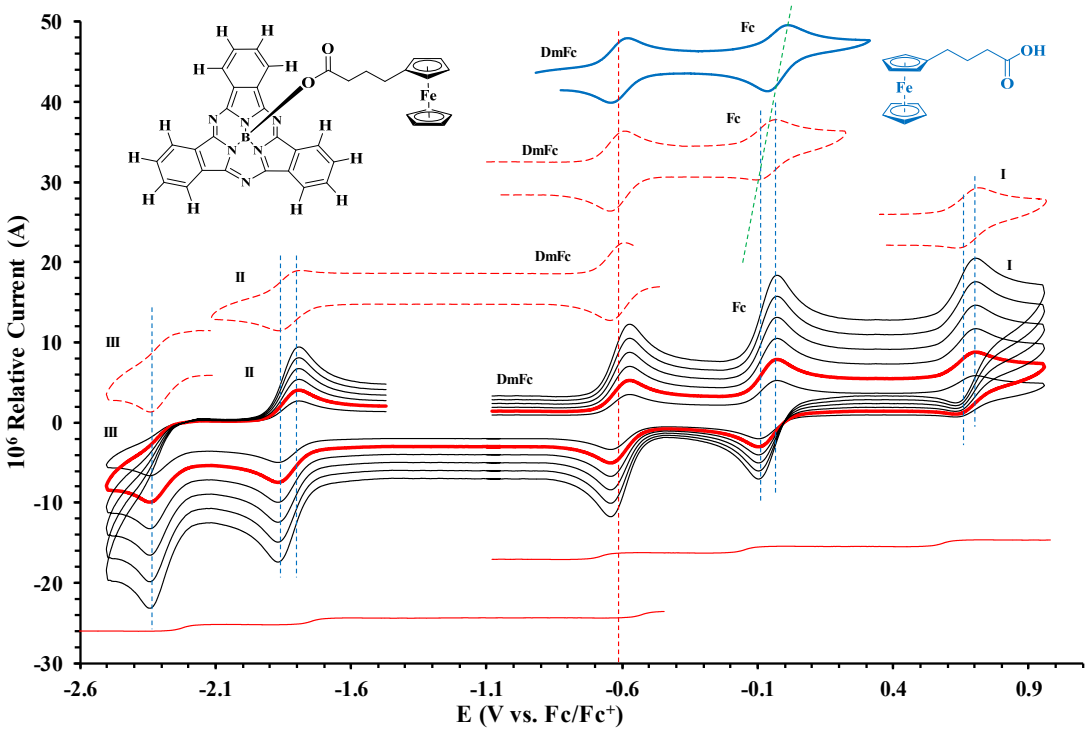

Figure 4. Cyclic voltammograms in DCM of $Fc(CH_2)_3CO_2BSubPc(H)_{12}$ at scan rates 0.050 (smallest peak currents), 0.100, 0.200, 0.300, 0.400 and 0.500 (largest peak currents).

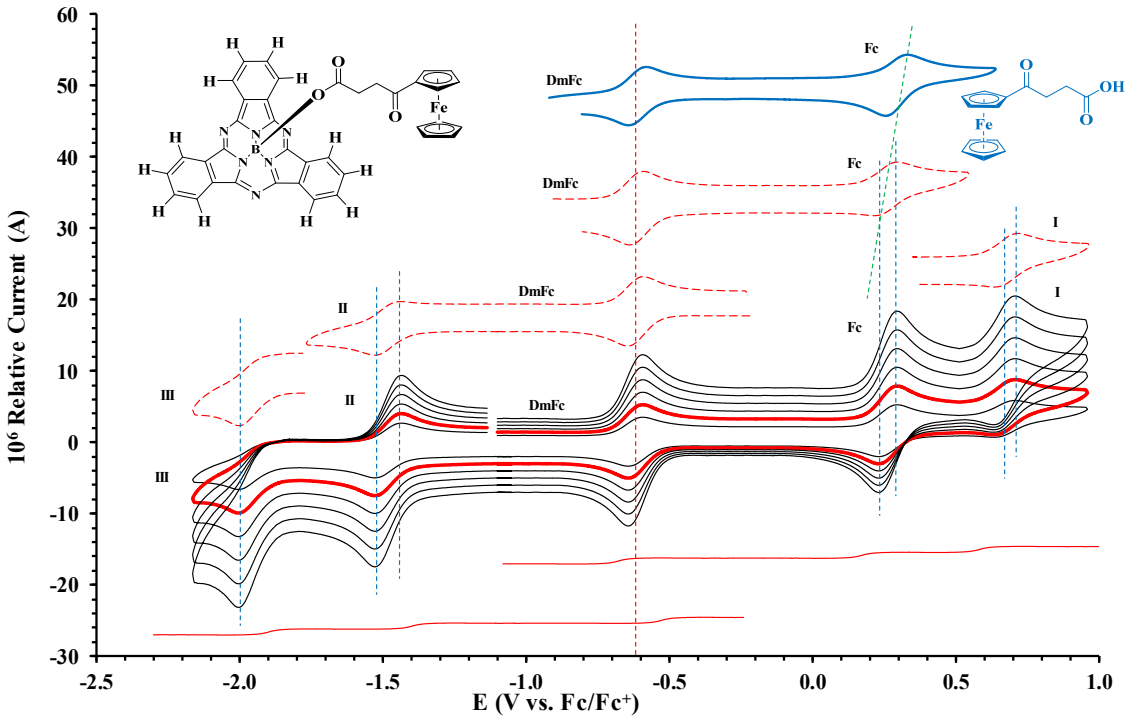

Figure 5. Cyclic voltammograms in DCM of $FcCO(CH_2)_2CO_2BSubPc(F)_{12}$ at scan rates 0.050 (smallest peak currents), 0.100, 0.200, 0.300, 0.400 and 0.500 (largest peak currents).

Table 1. Electrochemical data (potential in V *vs* Fc/Fc^+) in DCM for *c.a.* 0.0005 mol dm^{-3} of $FcCO_2BSubPc(H)_{12}$ at indicated scan rates (V in V/s).

V (V/s)	E_{pa} / V	ΔE_p / V	$E^{o'}$ / V	i_{pa} / µA	i_{pc}/i_{pa}
DmFc					
0.100	**-0.647**	**0.074**	**-0.610**	**0.39**	**0.99**
Fc					
0.050	0.262	0.075	0.224	2.58	0.99
0.100	**0.262**	**0.076**	**0.224**	**3.61**	**0.99**
0.200	0.262	0.077	0.224	5.05	0.99
0.300	0.263	0.078	0.224	5.78	0.99
0.400	0.263	0.079	0.224	8.30	0.99
0.500	0.264	0.080	0.224	9.03	0.99
5.000	0.265	-	-	-	-
Wave I					
0.050	0.710	0.081	0.670	2.39	0.99
0.100	**0.711**	**0.082**	**0.670**	**3.34**	**0.99**
0.200	0.711	0.083	0.670	4.68	0.99
0.300	0.712	0.084	0.670	5.34	0.99
0.400	0.712	0.085	0.670	7.68	0.99

0.500	0.713	0.086	0.670	8.35	0.99
5.000	0.714	-	-	-	-
Wave II					
0.050	-1.642	0.083	-1.601	2.48	0.99
0.100	**-1.643**	**0.084**	**-1.601**	**3.47**	**0.99**
0.200	-1.643	0.085	-1.601	4.86	0.99
0.300	-1.644	0.086	-1.601	5.55	0.99
0.400	-1.644	0.087	-1.601	7.98	0.99
0.500	-1.645	0.088	-1.601	8.68	0.99
5.000	-1.646	-	-	-	-
Wave III					
0.050	-2.123	-	-	-	-
0.100	**-2.124**	-	-	-	-
0.200	-2.124	-	-	-	-
0.300	-2.125	-	-	-	-
0.400	-2.125	-	-	-	-
0.500	-2.126	-	-	-	-
5.000	-2.127	-	-	-	-

Table 2. Electrochemical data (potential in V *vs* Fc/Fc^{+}) in DCM for *c.a.* 0.0005 mol dm^{-3} of $FcCH_2CO_2BSubPc(H)_{12}$ at indicated scan rates (V in V/s).

V (V/s)	E_{pa} / V	ΔE_p / V	$E^{o'}$ / V	i_{pa} / µA	i_{pc}/i_{pa}
DmFc					
0.100	**-0.647**	**0.075**	**-0.610**	**3.89**	**0.99**
Fc					
0.050	-0.005	0.075	-0.043	2.58	0.99
0.100	**-0.005**	**0.076**	**-0.043**	**3.61**	**0.99**
0.200	-0.004	0.077	-0.043	5.05	0.99
0.300	-0.004	0.078	-0.043	5.78	0.99
0.400	-0.003	0.079	-0.043	8.30	0.99
0.500	-0.003	0.080	-0.043	9.03	0.99
5.000	-0.002	-	-	-	-
Wave I					
0.050	0.709	0.079	0.670	2.41	0.99
0.100	**0.710**	**0.080**	**0.670**	**3.38**	**0.99**
0.200	0.710	0.081	0.670	4.73	0.99
0.300	0.711	0.082	0.670	5.41	0.99
0.400	0.711	0.083	0.670	7.77	0.99
0.500	0.712	0.084	0.670	8.45	0.99

5.000	0.713	-	-	-	-
Wave II					
0.050	-1.642	0.081	-1.674	2.49	0.99
0.100	**-1.643**	**0.082**	**-1.674**	**3.49**	**0.99**
0.200	-1.643	0.083	-1.674	4.89	0.99
0.300	-1.644	0.084	-1.674	5.58	0.99
0.400	-1.644	0.085	-1.674	8.03	0.99
0.500	-1.645	0.086	-1.674	8.73	0.99
5.000	-1.646	-	-	-	-
Wave III					
0.050	-2.153	-	-	-	-
0.100	**-2.154**	-	-	-	-
0.200	-2.154	-	-	-	-
0.300	-2.155	-	-	-	-
0.400	-2.155	-	-	-	-
0.500	-2.156	-	-	-	-
5.000	-2.157	-	-	-	-

Table 3. Electrochemical data (potential in V *vs* Fc/Fc^{+}) in DCM for *c.a.* 0.0005 mol dm^{-3} of $Fc(CH_2)_3CO_2BSubPc(H)_{12}$ at indicated scan rates (V in V/s).

V (V/s)	E_{pa} / V	ΔE_p / V	$E^{o'}$ / V	i_{pa} / μA	i_{pc}/i_{pa}
DmFc					
0.100	**-0.647**	**0.075**	**-0.610**	**3.97**	**0.99**
Fc					
0.050	-0.024	0.075	-0.062	2.56	0.99
0.100	**-0.024**	**0.076**	**-0.062**	**3.58**	**0.99**
0.200	-0.023	0.077	-0.062	5.01	0.99
0.300	-0.023	0.078	-0.062	5.73	0.99
0.400	-0.022	0.079	-0.062	8.23	0.99
0.500	-0.022	0.080	-0.062	8.95	0.99
5.000	-0.021	-	-	-	-
Wave I					
0.050	0.710	0.081	0.670	2.34	0.99
0.100	**0.711**	**0.082**	**0.670**	**3.27**	**0.99**
0.200	0.711	0.083	0.670	4.58	0.99
0.300	0.712	0.084	0.670	5.23	0.99
0.400	0.712	0.085	0.670	7.52	0.99
0.500	0.713	0.086	0.670	8.18	0.99
5.000	0.714	-	-	-	-
Wave II					

0.050	-1.870	0.083	-1.829	2.42	0.99
0.100	**-1.871**	**0.084**	**-1.829**	**3.39**	**0.99**
0.200	-1.871	0.085	-1.829	4.75	0.99
0.300	-1.872	0.086	-1.829	5.42	0.99
0.400	-1.872	0.087	-1.829	7.80	0.99
0.500	-1.873	0.088	-1.829	8.48	0.99
5.000	-1.874	-	-	-	-
Wave III					
0.050	-2.343	-	-	-	-
0.100	**-2.344**	-	-	-	-
0.200	-2.344	-	-	-	-
0.300	-2.345	-	-	-	-
0.400	-2.345	-	-	-	-
0.500	-2.346	-	-	-	-
5.000	-2.347	-	-	-	-

Table 4. Electrochemical data (potential in V *vs* Fc/Fc^{+}) in DCM for *c.a.* 0.0005 mol dm^{-3} of $FcCO(CH_2)_2CO_2BSubPc(H)_{12}$ at indicated scan rates (V in V/s).

V (V/s)	E_{pa} / V	ΔE_p / V	$E^{o'}$ / V	i_{pa} / µA	i_{pc}/i_{pa}
DmFc					
0.100	**-0.647**	**0.074**	**-0.610**	**3.84**	**0.99**
Fc					
0.050	0.300	0.075	0.262	2.55	0.99
0.100	**0.300**	**0.076**	**0.262**	**3.57**	**0.99**
0.200	0.300	0.077	0.262	5.00	0.99
0.300	0.301	0.078	0.262	5.71	0.99
0.400	0.301	0.079	0.262	8.21	0.99
0.500	0.302	0.080	0.262	8.93	0.99
5.000	0.303	-	-	-	-
Wave I					
0.050	0.710	0.081	0.670	2.39	0.99
0.100	**0.711**	**0.082**	**0.670**	**3.35**	**0.99**
0.200	0.711	0.083	0.670	4.69	0.99
0.300	0.712	0.084	0.670	5.36	0.99
0.400	0.712	0.085	0.670	7.71	0.99
0.500	0.713	0.086	0.670	8.38	0.99
5.000	0.714	-	-	-	-
Wave II					
0.050	-1.524	0.085	-1.482	2.44	0.99
0.100	**-1.525**	**0.086**	**-1.482**	**3.41**	**0.99**

0.200	-1.525	0.087	-1.482	4.77	0.99
0.300	-1.526	0.088	-1.482	5.46	0.99
0.400	-1.526	0.089	-1.482	7.84	0.99
0.500	-1.527	0.090	-1.482	8.53	0.99
5.000	-1.528	-	-	-	-
Wave III					
0.050	-2.003	-	-	-	-
0.100	**-2.004**	-	-	-	-
0.200	-2.004	-	-	-	-
0.300	-2.005	-	-	-	-
0.400	-2.005	-	-	-	-
0.500	-2.006	-	-	-	-
5.000	-2.007	-	-	-	-

Experimental Design, Materials, and Methods

Electrochemical studies by means of cyclic voltammetry (CV) experiments were performed in an M Bruan Lab Master SP glove box under a high purity argon atmosphere (H_2O and O_2 < 10 ppm), utilizing a Princeton Applied Research PARSTAT 2273 potentiostat running Powersuite software (Version 2.58).

The cyclic voltammetry experimental setup consists of a cell with three electrodes, namely (i) a glassy carbon electrode as working electrode, (ii) a platinum wire auxiliary and (ii) a platinum wire as pseudo reference electrode. The glassy carbon working electrode was polished and prepared before every experiment on a Buhler polishing mat first with 1-micron and then with ¼-micron diamond paste, rinsed with H_2O, acetone and DCM, and dried before each experiment.

Electrochemical analysis in dichloromethane (DCM, anhydrous, ≥ 99.8%, contains 40-150 ppm amylene as stabilizer) as solvent was at RT. Solutions were made in 0.001 dm^3 spectrochemical grade anhydrous DCM containing ca. 0.0005 M of analyte, 0.0005 mol dm^{-3} of internal reference (decamethylferrocene, DmFc) and 0.1 mol dm^{-3} of supporting electrolyte tetrabutylammonium tetrakispentafluorophenylborate, $[N(^nBu)_4][B(C_6F_5)_4]$ in DCM.

Experimental potential data was measured vs. the redox couple of decamethyl ferrocene Fc* as internal standard and reported vs. the redox couple of ferrocene FcH, as suggested by IUPAC. Experimental potential data was collected vs. the Pt wire reference electrode but is reported vs the redox couple of ferrocene, Fc/Fc^+ at 0 V. $E°`(DmFc) = - 0.610$ V vs. Fc/Fc^+ at 0 V in $DCM/[N(nBu)_4][B(C_6F_5)_4]$. Scan rates were between 0.05 and 5.00 Vs^{-1}.

Acknowledgments

This work has received support from the South African National Research Foundation (Grant numbers 113327 and 96111) and the Central Research Fund of the University of the Free State, Bloemfontein, South Africa.

Competing Interests

The authors declare that they have no known competing financial interests or personal relationships which have, or could be perceived to have, influenced the work reported in this article.

References

[1] P. V. Solntsev, K.L. Spurgin, J.R. Sabin, A.A. Heikal, V.N. Nemykin, Photoinduced charge transfer in short-distance ferrocenylsubphthalocyanine dyads, Inorg. Chem. 51 (2012) 6537–6547. https://doi.org/10.1021/ic3000608.

[2] E. Maligaspe, M.R. Hauwiller, Y. V. Zatsikha, J.A. Hinke, P. V. Solntsev, D.A. Blank, V.N. Nemykin, Redox and photoinduced electron-transfer properties in short distance organoboryl ferrocene-subphthalocyanine dyads, Inorg. Chem. 53 (2014) 9336–9347. https://doi.org/10.1021/ic5014544.

[3] P.J. Swarts, J. Conradie, Solvent and Substituent Effect on Electrochemistry of Ferrocenylcarboxylic Acid Dyads, J. Electroanal. Chem. (n.d.).

Supporting Information

Additional supporting information for publication: **Synthesis, Spectroscopy, Electrochemistry and DFT of Electron-rich ferrocenylsubphthalocyanine dyads**

molecules

MDPI

Supporting Information

Redox effect on ferrocenyl moiety of electron-rich ferrocenylsubphthalocyanine dyads

Pieter J. Swarts[1] and Jeanet Conradie[2]*

[1] Affiliation 1; swarts.pieter@gmail.com

[2] Affiliation 2; conradj@ufs.ac.za

* Correspondence: conradj@ufs.ac.za; Tel.: +27-(51)-4012194, Fax: +27-4017295

Received: date; Accepted: date; Published: date

Supporting Information

Contents

Keywords: Synthesis; NMR; Cyclic Voltammetry; DFT

1. Synthesis

Free ferrocenylcarboxylic acids **1** – **5**, were synthesized in multigram quantities using slightly modified methods than previously published [1], as described in our previous publication [2]. The parent macrocycle SubPc **6** was synthesized using previously published methods [3], see Scheme 1.

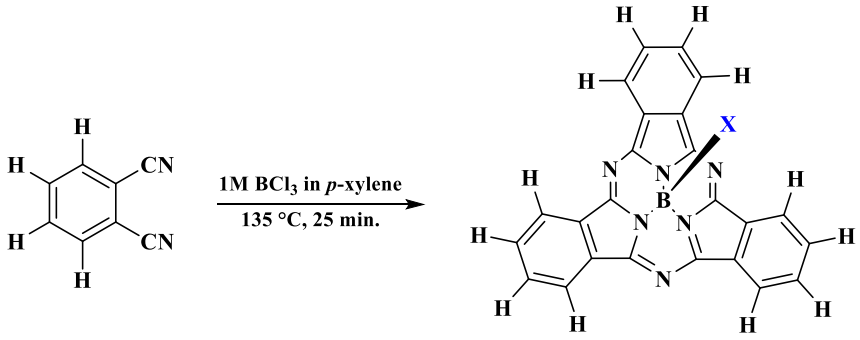

Scheme 1 Reaction scheme of **parent macrocycle SubPc, 6**.

*1.1. Preparation of $FcCO_2H$, **1** [4]:*

2-Chlorobenzoyl ferrocene (1.75 g, 0.005 mol) was added to a mixture of potassium tertiary butoxide (13 g, 0.115 mol) and water (0.61 cm3, 0.034 mol) in dimethoxyethane (0.1 dm3) under an argon atmosphere. The mixture produced a yellow slurry which was refluxed for 24 hours. After cooling the mixture, ice water (0.3 dm3) was added, and the resulting solution was washed with ether (3 x 0.1 dm3). The aqueous phases were combined and acidified with concentrated hydrochloric acid. The residue was collected by filtration, washed thoroughly with water and air-dried, yielding 1.01 g (80 %) of as light-yellow crystals. m.p.: 156 – 162 °C. NMR: δH (600.28 MHz, CDCl3, 25 °C): δ 4.84 (2 H, pt, 2 x CH2: Substituted-Cp), 4.45 (2 H, pt, 2 x CH2: Substituted-Cp), 4.24 (5 H, s, Unsubstituted-Cp). 13C NMR: δC (150.95 MHz, CDCl3, 25 °C): δ 168.24 (1C, C=O), 70.23 (1C, C-CO2H), 69.72 (5C, Unsubstituted-Cp), 68.42 (2C, Substituted-Cp), 66.24 (2C, Substituted-Cp).

*1.2. Preparation of $FcCH_2CO_2H$, **2** [4]:*

To a solution of potassium hydroxide (1 g, 0.018 mol) in water (10 cm^3), a suspension of the ferrocene acetonitrile (0.2 g, 0.00074 mol) in ethanol (5 cm^3) was added and refluxed for 5 hours until the evolution of ammonia had ceased. Most (> 95 %) of the ethanol was removed under reduced pressure. The residual suspension was dissolved in water (50 cm^3), extracted with ether (2 x 50 cm^3) and filtered. The solution was acidified with 2 M HCl and the precipitate filtered, washed and air-dried to yield 0.110 g (51 %) as a white powder. m.p.: 159 – 165 °C. NMR: δ_H (600.28 MHz, $CDCl_3$, 25 °C): δ 4.21 (2 H, pt, 2 x CH_2: Substituted-Cp), 4.13 (5 H, s, Unsubstituted-Cp), 3.73 (2 H, pt, 2 x CH_2: Substituted-Cp), 3.38 (2H, s, CH_2). ^{13}C NMR: δ_C (150.95 MHz, $CDCl_3$, 25 °C): δ 172.34 (1C, C=O), 82.44 (1C, C-CO_2H), 69.19 (5C, Unsubstituted-Cp), 68.31 (2C, Substituted-Cp), 67.97 (2C, Substituted-Cp), 39.84 (1C, CH_2).

*1.3. Preparation of $Fc(CH_2)_2CO_2H$, **3** [4]:*

3-Ferrocenylacrylic acid (0.250 g, 0.00082 mol) and H_2/Pd (0.030 g) was suspended in absolute ethanol (50 cm^3). The suspension was stirred under a 10-bar hydrogen atmosphere for 20 hours before the reaction mixture was filtered through 2 cm of silica gel. Equal volumes of water and ice were added to the yellow ethanolic mixture. The solution was extracted with diethyl ether (2 x 250 cm^3) and the combined ether extracts were thoroughly washed with water to remove the excess ethanol. The solution was dried over $MgSO_4$ and evaporated under reduced pressure to yield 0.177 g (71%) an off-white powder. m.p.: 124 – 138 °C. NMR: δ_H (600.28 MHz, $CDCl_3$, 25 °C): δ 4.12 (5 H, s, Unsubstituted-Cp), 4.09 (2 H, pt, 2 x CH_2: Substituted-Cp), 4.07 (2 H, pt, 2 x CH_2: Substituted-Cp), 2.66 (2H, d, CH_2), 2.59 (2H, d, CH_2). ^{13}C NMR: δ_C (150.95 MHz, $CDCl_3$, 25 °C): δ 179.37 (1C, C=O), 87.49 (1C, C-CO_2H), 68.89 (5C, Unsubstituted-Cp), 68.23 (2C, Substituted-Cp), 67.75 (2C, Substituted-Cp), 35.53 (2C, CH2-CH_2).

*1.4. Preparation of Preparation of $Fc(CH_2)_3CO_2H$, **4** [4]:*

The ester (0.150 g, 0.00045 mol) was dissolved in ethanol (25 cm^3) followed by the addition of sodium hydroxide solution (25 cm^3, 2 M). The solution was stirred for 1 hour at room temperature followed by the addition of ice (25 m^3) and washed with cold diethyl ether (3 x 50 cm^3). While cooling the solution by adding fresh ice chunks, the water phase was acidified with 1 M HCl and the precipitate filtered, washed and air-dried to liberate 0.132 g (93 %) as an off-white powder. m.p.: 120 – 124 °C. NMR: δ_H (600.28 MHz, $CDCl_3$, 25 °C): δ 4.12 (5 H, s, Unsubstituted-Cp), 4.09 (2 H, pt, 2 x CH_2: Substituted-Cp), 4.07 (2 H, pt, 2 x CH_2: Substituted-Cp), 2.38 (2H, d, CH_2), 1.84 (2H, d, CH_2), 0.86 (2H, m, CH_2). ^{13}C NMR: δ_C (150.95 MHz, $CDCl_3$, 25 °C): δ 179.42 (1C, C=O), 82.44 (1C, C-CO_2H), 68.31 (2C, Substituted-Cp), 67.48 (5C, Unsubstituted-Cp), 66.24 (2C, Substituted-Cp), 33.45 (2C, CH_2-CH_2-CH_2), 28.88 (1C, CH_2-CH_2-CH_2).

*1.5. Preparation of $FcCO(CH_2)_2CO_2H$, **5** [5]:*

Succinic anhydride (0.250 g, 0.00215 mol) dissolved in dichloromethane (25 cm^3) was added to a mixture of ferrocene (0.250 g, 0.0215 mol) and aluminium chloride (0.76 g, 0.0056 mol) in dichloromethane (25 cm^3) under a nitrogen atmosphere. The reaction mixture was refluxed for 24 hours. After cooling, ice-cold water (40 cm^3) was added and the aqueous layer extracted twice with dichloromethane. The combined dichloromethane extracts were thoroughly washed with water. The organic phase was then extracted twice with equal amounts of 2 M NaOH. While cooling the solution with ice, the water phase was acidified with 1 M HCl and the precipitate filtered, washed with water and air-dried to liberate 1.1 g (74 %) as orange crystals. m.p.: 134 – 148 °C. NMR: δ_H (600.28 MHz, $CDCl_3$, 25 °C): δ 4.80 (2 H, pt, 2 x CH_2: Substituted-Cp), 4.51 (2 H, pt, 2 x CH_2: Substituted-Cp), 4.22 (5 H, s, Unsubstituted-Cp), 3.07 (2H, d, CH_2), 2.75 (2H, d, CH_2), 0.86 (2H, m, CH_2). ^{13}C NMR: δ_C (150.95 MHz, $CDCl_3$, 25 °C): δ 202.54 (1C, C=O), 171.21 (1C, CO_2H), 80.38 (1C, C-CO_2H), 72.55 (2C, Substituted-Cp), 70.14 (5C, Unsubstituted-Cp), 69.41 (2C, Substituted-Cp), 34.23 (2C, CH_2-CH_2).

1.6. Preparation of ***ClSubPc(H)$_{12}$, 6*** [3], *Scheme 1:*

BCl_3 (15 cm^3,1 M solution in p-xylene, 1.5 eq.) was added to dry phthalonitrile (1 g, 0.008 mol) in a glove box (H_2O: < 0.5 ppm and O_2: < 10 ppm) at room temperature in a high-pressure glass tube. The reaction mixture was stirred under reflux (137°C) for 30 minutes. The solvent was evaporated and the solid was extracted with toluene (0.4 dm^3). The solution was evaporated, and the resultant purple solid was thoroughly washed with methanol (0.2 dm^3) and hexane (0.2 dm^3). Pure ClSubPc(H)$_{12}$ was obtained as a purple solid, yield: 94 % (0.94 g). MP: 375 – 380°C. ^{1}H NMR: δ_H (600.28 MHz, $CDCl_3$): δ 8.88 (6H, q, non-peripheral H_6) and 7.94 (6H, q, peripheral H_6). ^{11}B NMR: δ_B (128.38 MHz, $CDCl_3$): δ -16.22 (1B). ^{13}C NMR: δ_C (150.95 MHz, $CDCl_3$, 25 °C): δ 149.68 (6C, C=N: inner core carbons), 125.68 (6C, C=C: iminoisoindoline unit), 122.01 (6C, non-peripheral C_6), 119.84 (6C, peripheral C_6). IR: υ/cm^{-1}: 1451 (C=C, Stretch). Elemental analysis calculated C, 66.94; H, 2.81; N, 19.51, obtained: C, 66.42; H, 2.68; N, 18.31.

2. NMR

2.1. ^{1}H NMR of $FcCO_2BSubPc(H)_{12}$, ***7****:*

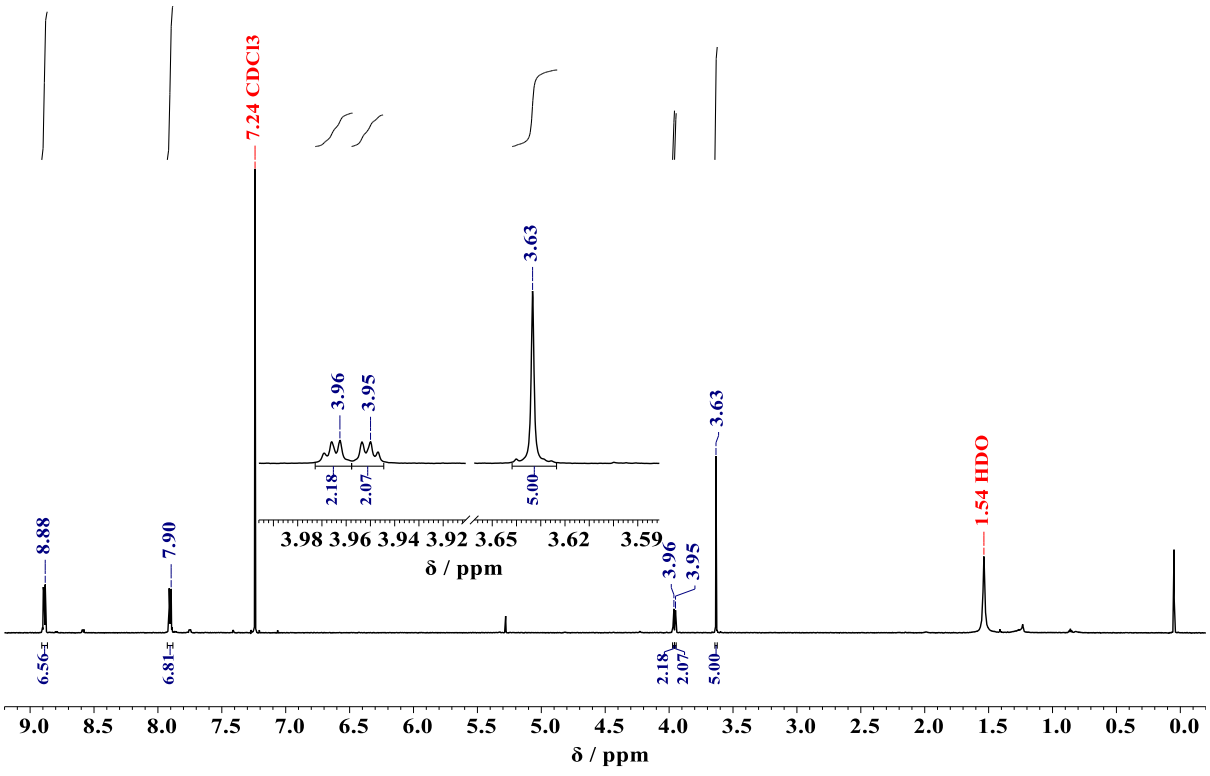

*2.2. ^{11}B NMR of $FcCO_2BSubPc(H)_{12}$, **7**:*

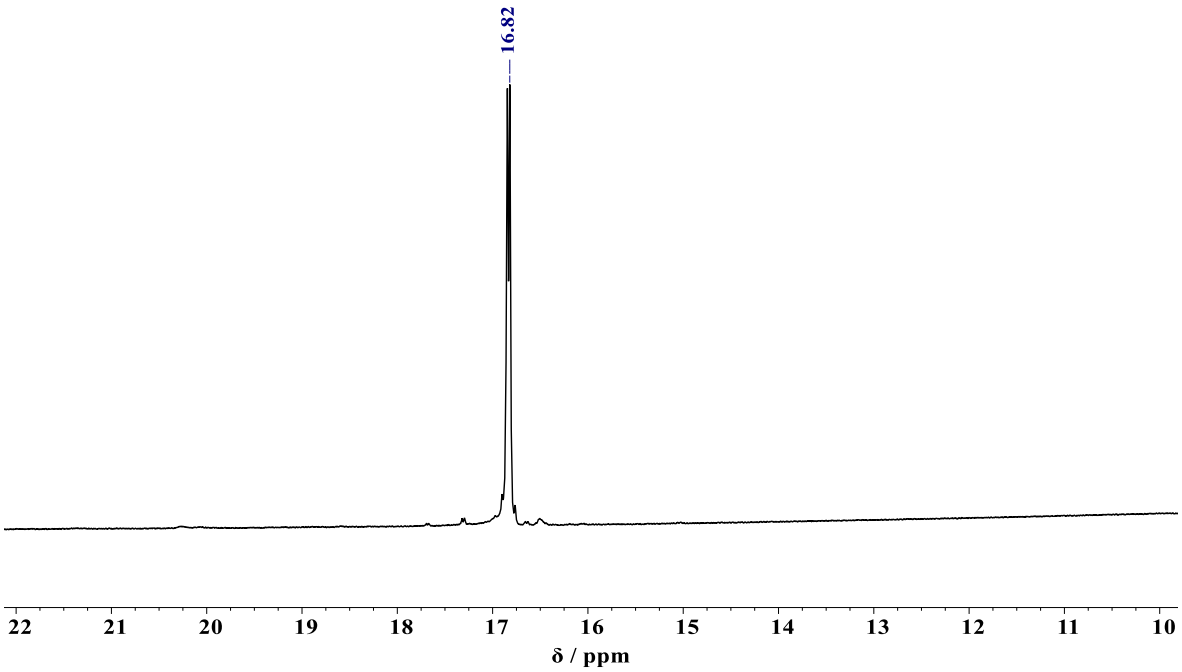

*2.3. ^{13}C NMR of $FcCO_2BSubPc(H)_{12}$, **7**:*

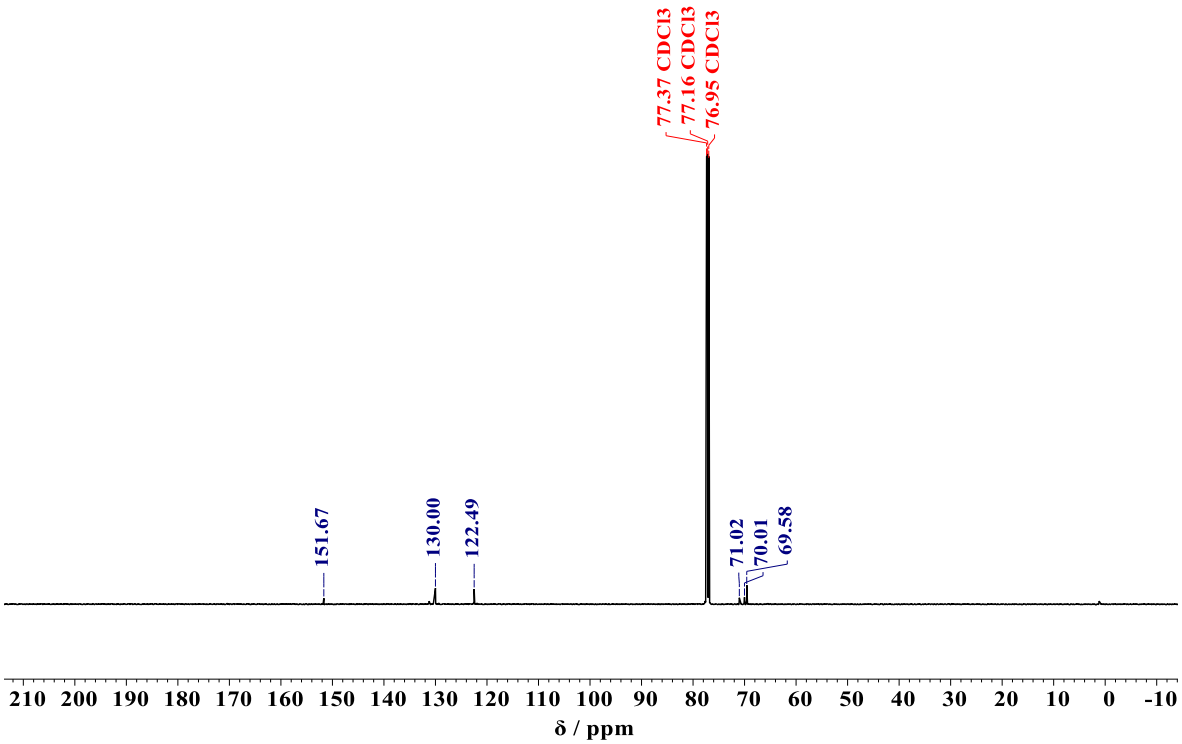

*2.4. ^{1}H NMR of Fc $CH_2CO_2BSubPc(H)_{12}$, **8**:*

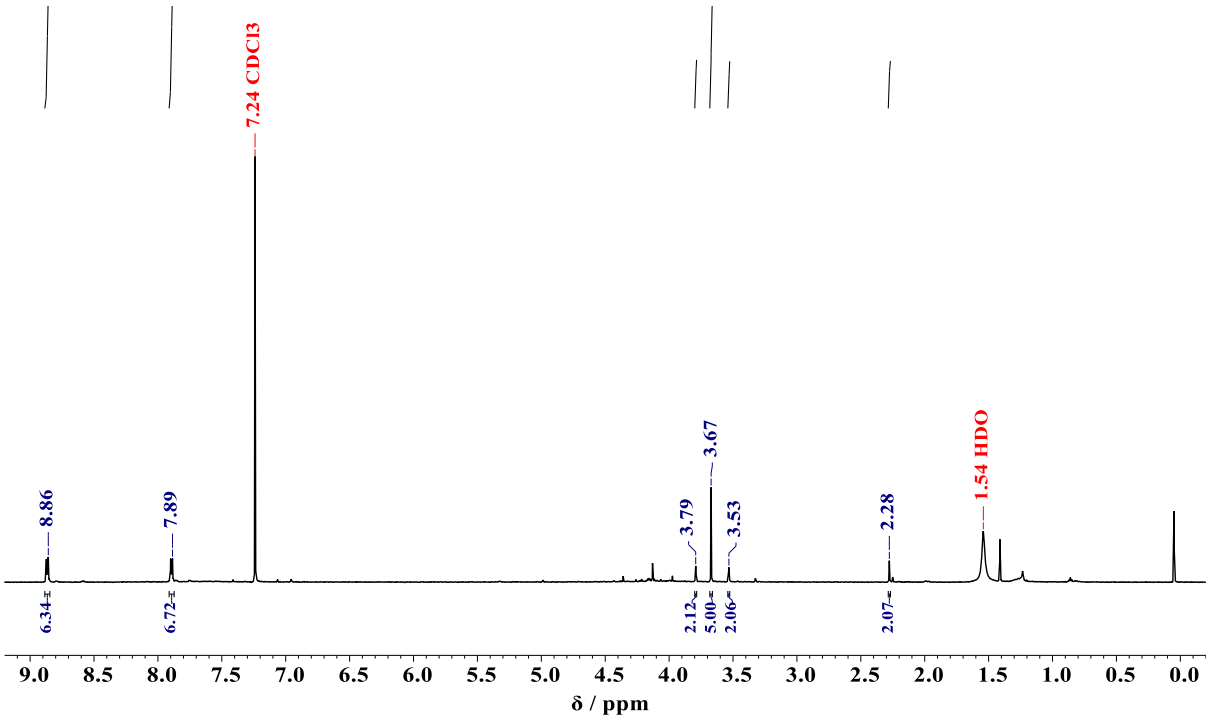

*2.5. ^{11}B NMR of Fc $CH_2CO_2BSubPc(H)_{12}$, **8**:*

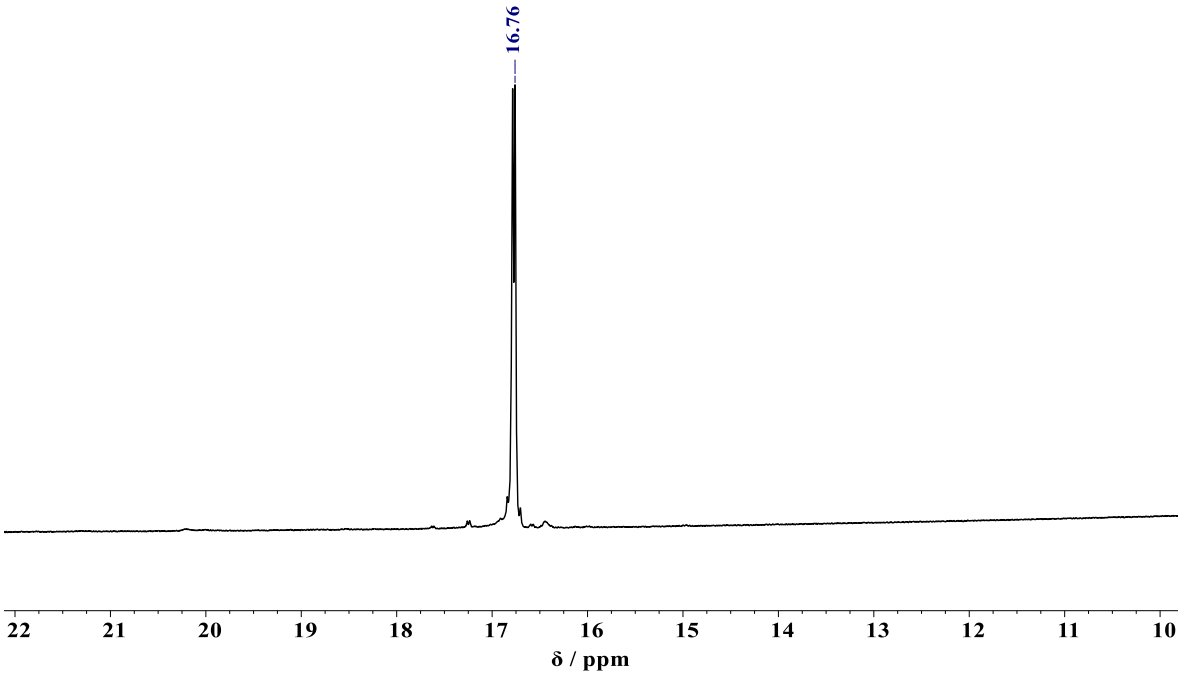

*2.6. ^{13}C NMR of Fc $CH_2CO_2BSubPc(H)_{12}$, **8**:*

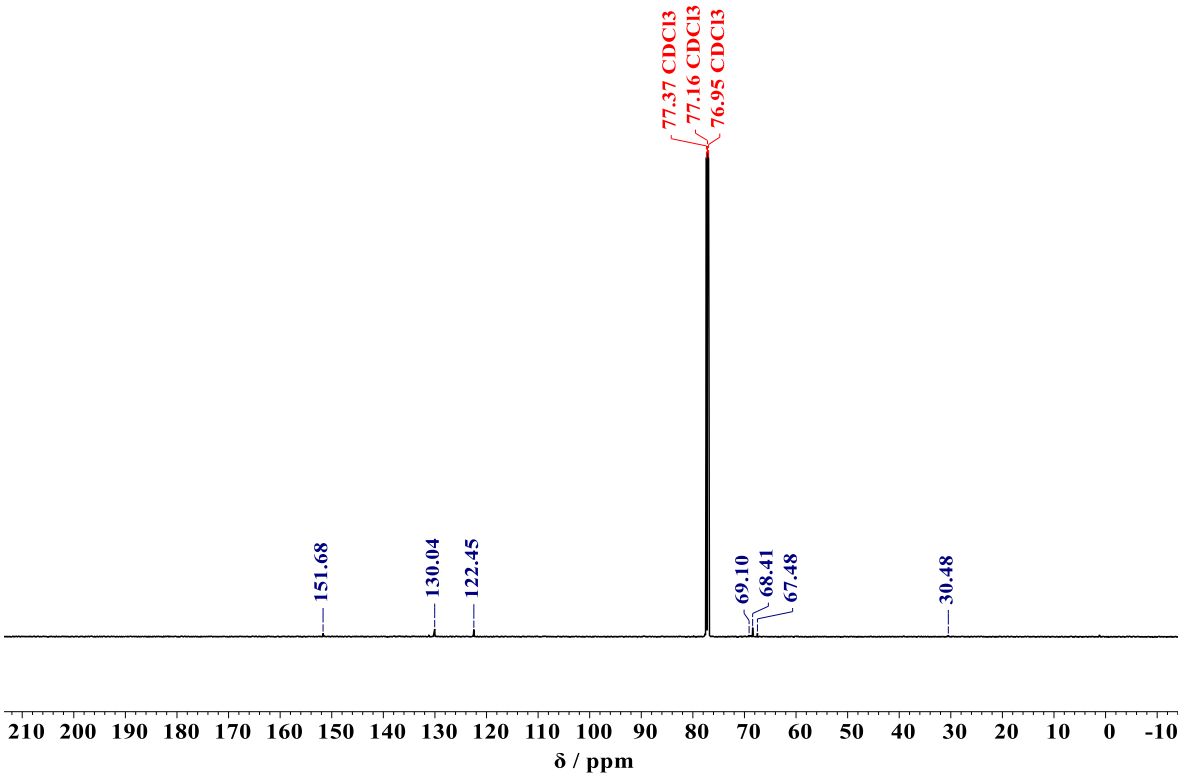

2.7. ^{1}H NMR of $Fc(CH_2)_3CO_2BSubPc(H)_{12}$, ***10****:*

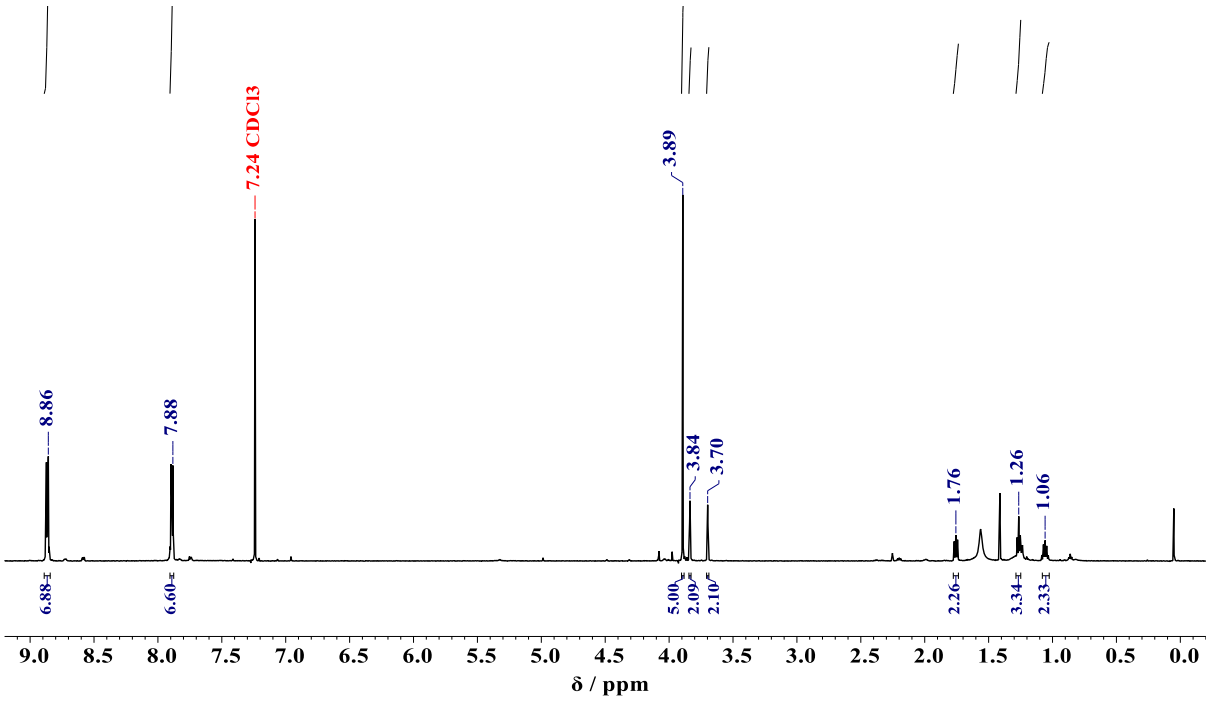

2.8. ^{11}B NMR of $Fc(CH_2)_3CO_2BSubPc(H)_{12}$, ***10****:*

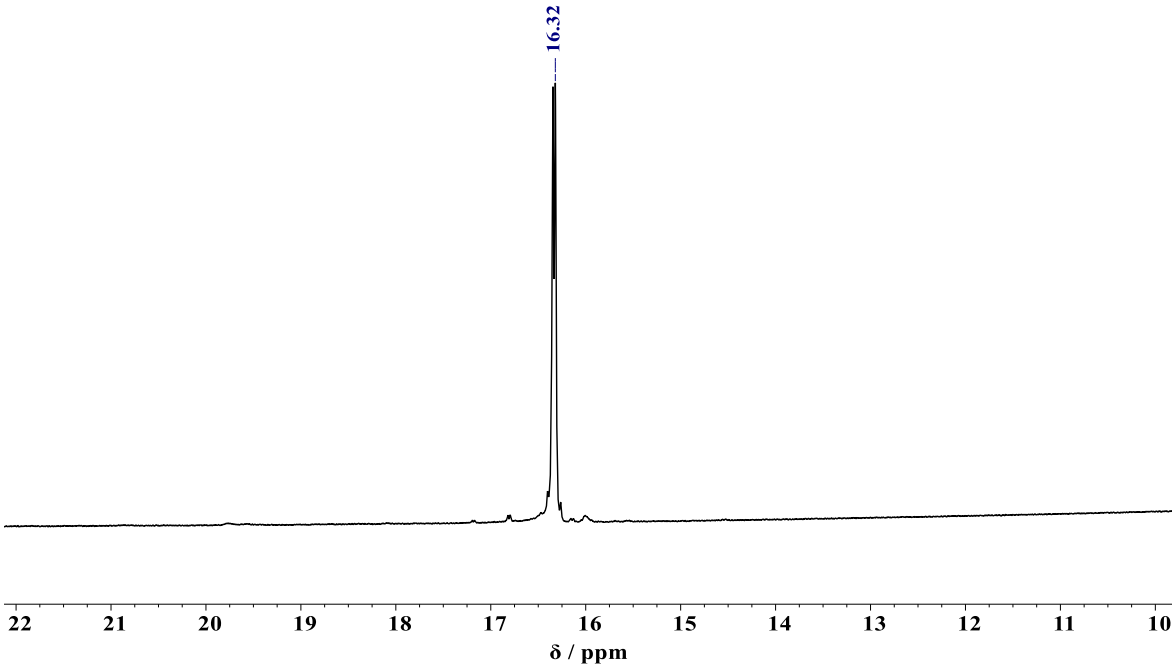

2.9. ^{13}C NMR of $Fc(CH_2)_3CO_2BSubPc(H)_{12}$, ***10****:*

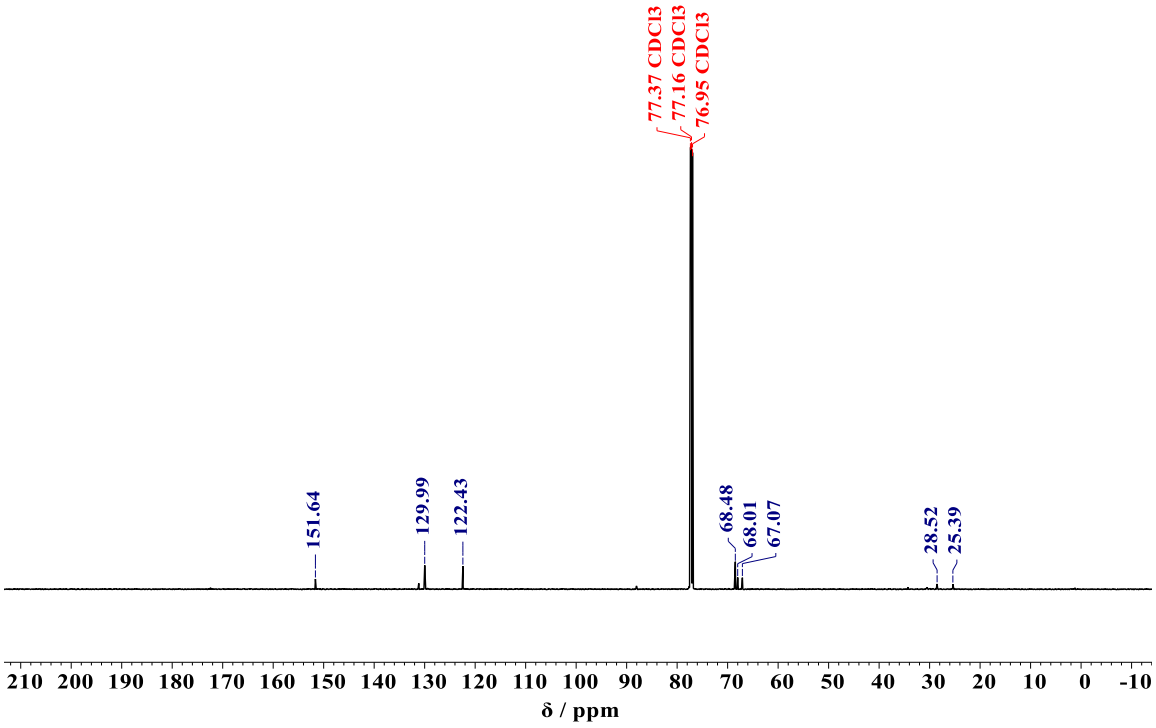

2.10. ^{1}H NMR of $FcCO(CH_2)_2CO_2BSubPc(H)_{12}$, ***11****:*

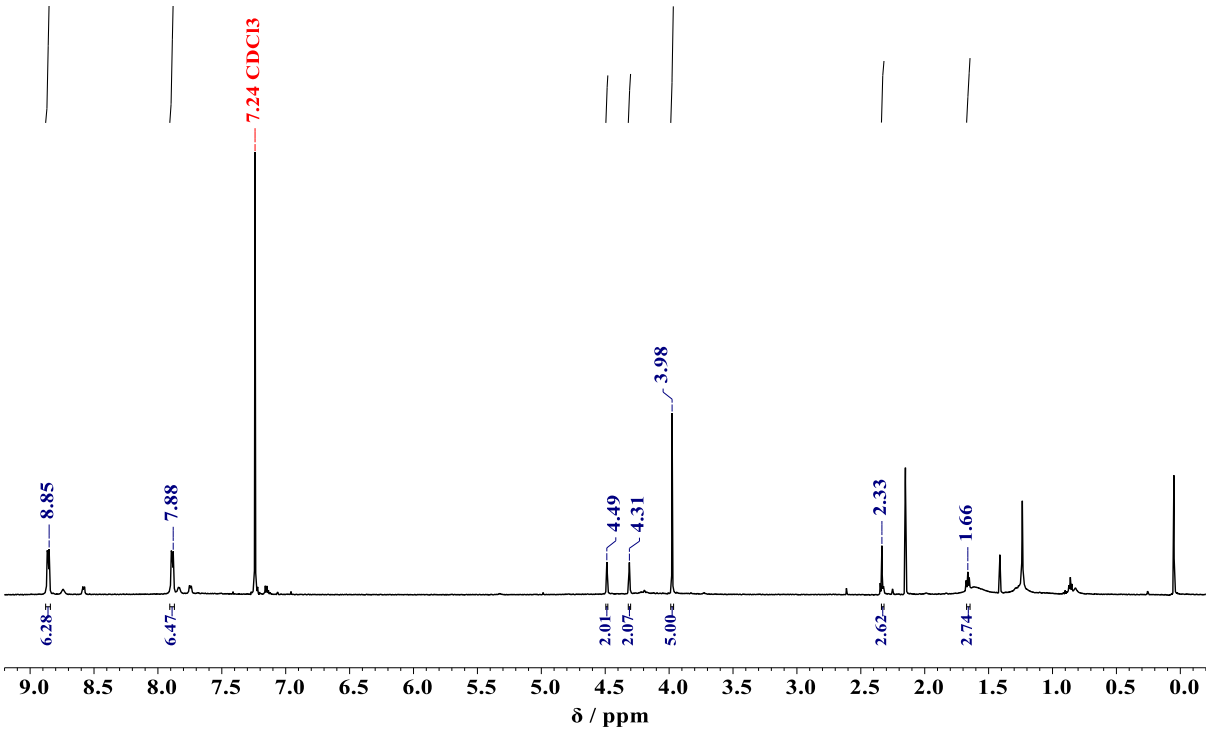

2.11. ^{11}B NMR of FcCO(CH$_2$)$_2$CO$_2$BSubPc(H)$_{12}$, ***11****:*

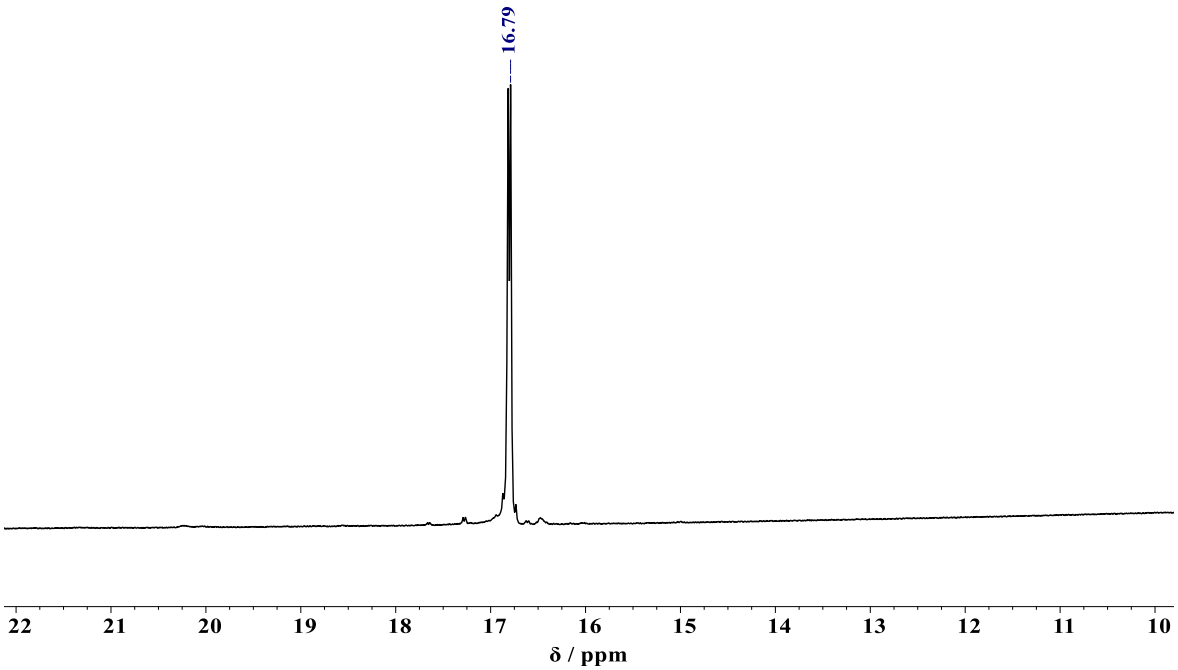

2.12. ^{13}C NMR of FcCO(CH$_2$)$_2$CO$_2$BSubPc(H)$_{12}$, ***11****:*

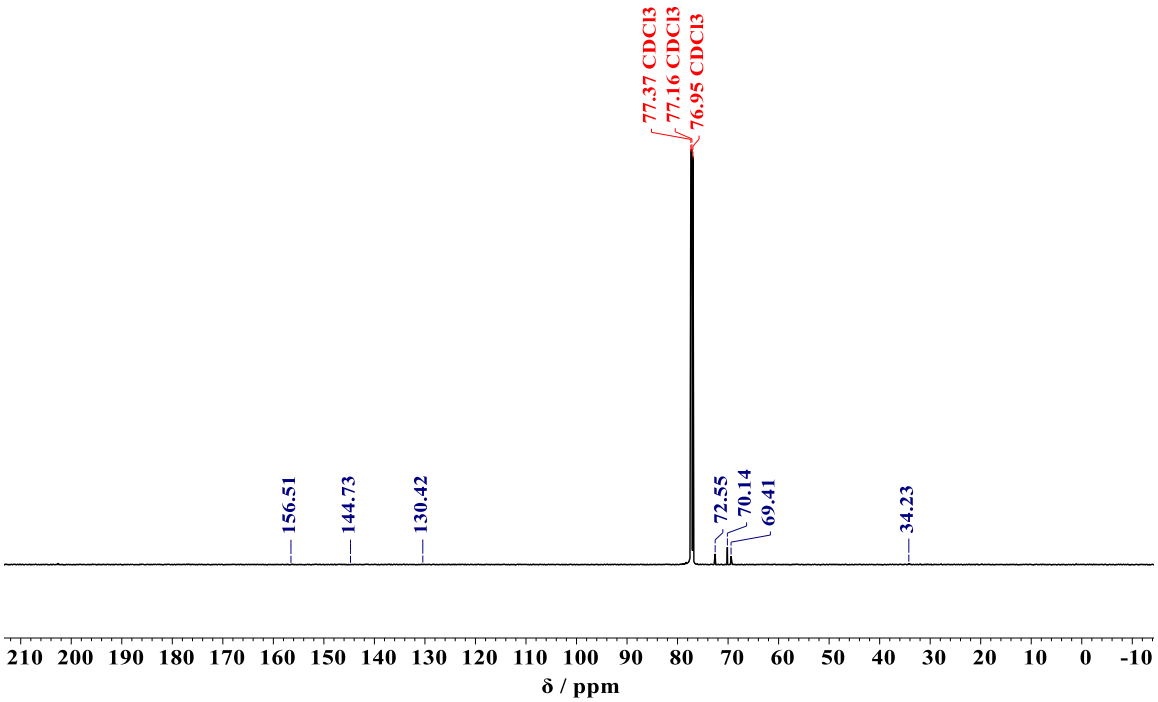

3. Cyclic Voltammetry (CV)

Please see Data in Brief.

4. DFT

LUMO and HOMO of optimized cation species pf SubPc **7**, **10** and **11**.

$FcCO_2BSubPc(H)_{12}$, ***7***:

LUMO	HOMO
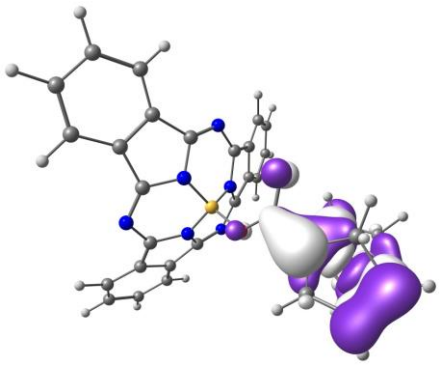	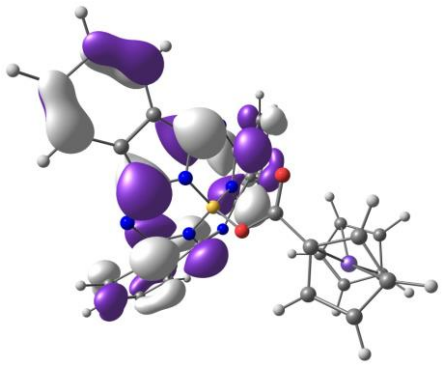

A contour of 0.03 e/Å^3 was used for the orbital plots. Colour code of atoms (online version): Fe (purple), B (yellow), C (grey), O (red), H (white).

$Fc(CH_2)_3CO_2BSubPc(H)_{12}$, ***10***:

LUMO	HOMO

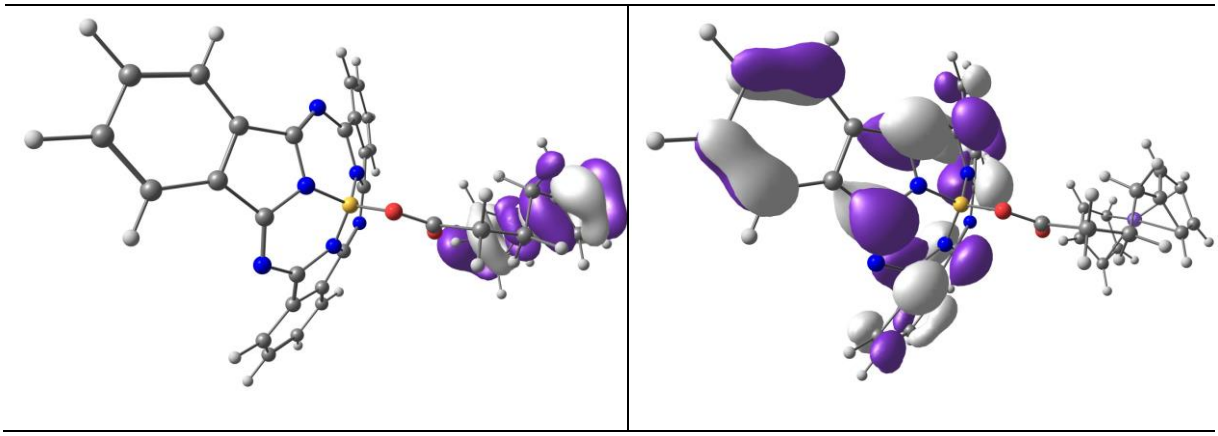

A contour of 0.03 e/Å^3 was used for the orbital plots. Colour code of atoms (online version): Fe (purple), B (yellow), C (grey), O (red), H (white).

FcCO(CH$_2$)$_2$CO$_2$BSubPc(H)$_{12}$, ***11***:

LUMO	**HOMO**
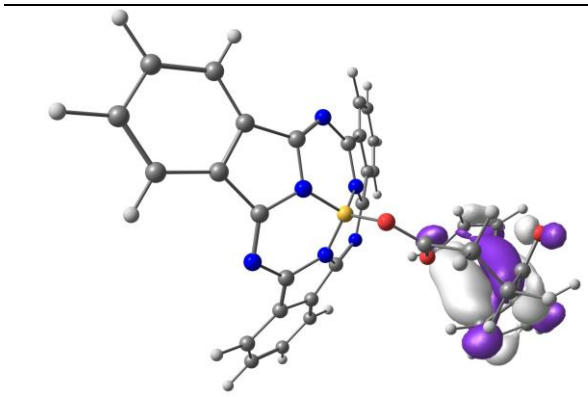	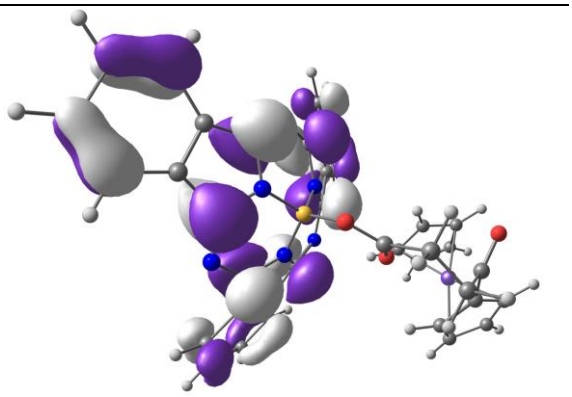

A contour of 0.03 e/Å^3 was used for the orbital plots. Colour code of atoms (online version): Fe (purple), B (yellow), C (grey), O (red), H (white).

Only in electronic version

5. References

1. Blom, N.F.; Neuse, E.W.; Thomas, H.G. Electrochemical characterization of some ferrocenylcarboxylic acids. *Transit. Met. Chem.* **1987**, *12*, 301–306.
2. Swarts, P.J.; Conradie, J. Solvent and Substituent Effect on Electrochemistry of Ferrocenylcarboxylic Acid Dyads. *J. Electroanal. Chem.*
3. Swarts, P.J.; Conradie, J. Electrochemical behaviour of chloro- and hydroxy-subphthalocyanines. *Electrochim. Acta* **2020**, *329*, 135165.
4. Blom, N.F.; Neuse, E.W.; Thomas, H.G. Electrochemical characterization of some ferrocenylcarboxylic acids. *Transit. Met. Chem.* **1987**, *12*, 301–306.
5. Davis, W.L.; Shago, R.F.; Langner, E.H.G.; Swarts, J.C. Synthesis and electrochemical properties of a series of ferrocene-containing alcohols. *Polyhedron* **2005**, *24*, 1611–1616.

Chapter 6
Conclusion

Subphthalocyanines with ferrocenylcarboxylic acids in the axial position, ClBSubPc$(F)_{12}$ and the mother compound ClBSubPc$(H)_{12}$ can be synthesised in 90% yields when working under strict Schlenk conditions (Glove Box). Only OHBSubPc$(C_{12}H_{25})_6(H)_6$ could not be obtained in high yields due to the large alkyl $C_{12}H_{25}$ non-peripheral chains causing steric hindrance The axial ferrocenylcarboxylic acids did not influence the UV/vis wavelength maxima of the Q-bands of the ferrocenylsubphthalocyanine dyads, that were similar to the wavelength maxima of the parent ClBSubPc$(H)_{12}$. Electron donating or withdrawing ring substituents did shift the UV/vis wavelength maxima of the Q-bands toward longer wavelengths

The experimental conditions used to perform cyclic voltammetry experiments made it possible for the first time to experimentally observe chemically reversible ring-based oxidation with peak current ratios approaching 1 and peak current separation $\Delta E_p < 0.086$ V for SubPcs. To improve the reversibility of CV curves, electrochemical experiments should be performed in dry oxygen-free conditions, for example in an M Bruan Lab Master SP glove box under a high purity argon atmosphere (H_2O and $O_2 < 10$ ppm). DCE as solvent increase the solubility while both DCE and DCM as solvent with $[N(^nBu)_4][B(C_6F_5)_4]$ as supporting electrolyte minimises ionic interactions between cationic species and the electrolyte.

Cyclic voltammetry results showed that the experimental formal reduction potential of Fe in the six ferrocenyl carboxylic acid dyads is *ca* 0.1 V higher in dichloromethane than in acetonitrile. The electron-withdrawing effect of the carboxy group on the reduction potential of the ferrocenyl group became exponentially smaller as the length of the alkyl chain separating the two groups increases. The formal reduction potential of Fe is also affected by the electron-

withdrawing carbonyl group depending on whether the carbonyl group is directly bonded to ferrocenyl or is isolated from ferrocenyl by an sp^3 hybridised carbon atom backbone or by an sp^2 hybridised carbon atom backbone. The CVs of the ferrocenylsubphthalocyanine dyads revealed that the first reversible oxidation process is ferrocene-centred, while the second oxidation and all observed reduction processes were localised on the SubPc-ring. Cyclic voltammetry results of the formal reduction potential of Fe(II/III) of the axial ferrocenyl moiety of the eight ferrocenylcarboxylic acid-containing SubPc dyads followed a similar trend than obtained for the free ferrocenylcarboxylic acid dyads, though shifted to a lower oxidation potential compared to free ferrocenylcarboxylic acid dyads. SubPc (HOBSubPc($C_{12}H_{25}$)$_6$(H)$_6$) contains the most electron-rich macrocycle of all reported SubPcs till date with an oxidation potential in DCM of 0.398 V vs Fc/Fc^+. SubPc (Fc(CH_2)$_3$$CO_2$BSubPc(H)$_{12}$) has the lowest first ring-based reduction potential reported till date.

Density functional theory (DFT) calculations gave further insight into the redox properties of the dyads and SubPcs. A linear relationship between the formal reduction potential of the ferrocenyl carboxylic acid dyads and DFT calculated HOMO (highest occupied molecular orbital) energies were obtained. The DFT study also provided linear relationships between the first oxidation potential and HOMO energies, as well as between the first reduction potential and LUMO (lowest unoccupied molecular orbital) energies for a series of non-ferrocene-containing SubPcs with peripheral and non-peripheral substituents = H, F or ($C_{12}H_{25}$) and axial substituent = Cl or an alkoxy group. These relationships can be used to determine HOMO and LUMO energies from experimental first oxidation and the first reduction potential of related compounds (and *vice versa*). The neutral ferrocenylcarboxylic acid subphthalocyanines dyads have LUMOs and HOMOs of mainly π-ring and iron-d character respectively, confirming ring-based reduction and Fe(II) to Fe(III) oxidation. Optimisation of the cation (oxidised) species

was essential to verify the locus of the second ring-based oxidation since the frontier orbitals rearranged upon oxidation.

There is still much research that can be performed on this topic. However, it would have increased the volume of work beyond the scope of an Ph.D. study. Topics that can emanate from this study in follow-up research projects include synthesis of ferrocene alcohols with varying alkyl chain lengths in the axial position of both electron-rich and poor SubPcs can be synthesised and characterised spectroscopically and with computational methods. These compounds will be very interesting especially from an electrochemical point of view.

Photodynamic transfer studies results could improve the effectiveness of photodynamic therapy (PDT). With the combination of subphthalocyanines and ferrocene moieties, antineoplastic studies could advance the effectiveness of photodynamic therapy. The research performed by the author may have opened up new interesting research avenues worthwhile pursuing.

Appendix - A

Author Copyright Permission

All copyright permissions of articles for th use in this thesis/dissertation was requested from Copyright Clearence Center.

Electrochemical behaviour of chloro- and hydroxy- subphthalocyanines

Author: Pieter J. Swarts,Jeanet Conradie

Publication: Electrochimica Acta

Publisher: Elsevier

Date: 1 January 2020

Oxidation and reduction data of subphthalocyanines

Author: Pieter J. Swarts,Jeanet Conradie

Publication: Data in Brief

Publisher: Elsevier

Date: February 2020

Appendix - B

Author Instructions

Journal of Electroanalyical Chemistry

Chapter 2

JOURNAL OF ELECTROANALYTICAL CHEMISTRY

An International Journal also devoted to All Physicochemical Aspects of Fundamental and Applied Electrochemistry.

AUTHOR INFORMATION PACK

TABLE OF CONTENTS

ISSN: 1572-6657

DESCRIPTION

The *Journal of Electroanalytical Chemistry* is the foremost international journal devoted to the interdisciplinary subject of **electrochemistry** in all its aspects, theoretical as well as applied.

Electrochemistry is a wide ranging area that is in a state of continuous evolution. Rather than compiling a long list of topics covered by the Journal, the editors would like to draw particular attention to the key issues of novelty, topicality and quality. Papers should present new and interesting **electrochemical science** in a way that is accessible to the reader. The presentation and discussion should be at a level that is consistent with the international status of the Journal. Reports describing the application of well-established techniques to problems that are essentially technical will not be accepted. Similarly, papers that report observations but fail to provide adequate interpretation will be rejected by the Editors. Papers dealing with technical electrochemistry should be submitted to other specialist journals unless the authors can show that their work provides substantially new insights into **electrochemical processes**.

Benefits to authors
We also provide many author benefits, such as free PDFs, a liberal copyright policy, special discounts on Elsevier publications and much more. Please click here for more information on our author services.

Please see our Guide for Authors for information on article submission. If you require any further information or help, please visit our Support Center

AUDIENCE

Electrochemists and those in many other disciplines who use the electrochemical approach

IMPACT FACTOR

2018: 3.218 © Clarivate Analytics Journal Citation Reports 2019

ABSTRACTING AND INDEXING

Chemical Abstracts
Current Contents
Engineering Index
INSPEC
Metals Abstracts
World Aluminum Abstracts
Scopus

EDITORIAL BOARD

GUIDE FOR AUTHORS

Your Paper Your Way

We now differentiate between the requirements for new and revised submissions. You may choose to submit your manuscript as a single Word or PDF file to be used in the refereeing process. Only when your paper is at the revision stage, will you be requested to put your paper in to a 'correct format' for acceptance and provide the items required for the publication of your article.
To find out more, please visit the Preparation section below.

INTRODUCTION

The Journal of Electroanalytical Chemistry is the foremost international journal devoted to the interdisciplinary subject of electrochemical science in all its aspects, theoretical as well as applied. Electrochemistry is a wide-ranging area that is in a state of continuous evolution. Rather than compiling a long list of topics covered by the Journal, the Editors would like to draw particular attention to the key issues of novelty, topicality and quality. Papers should present new and interesting electrochemical science in a way that is accessible to the reader. The presentation and discussion should be at a level that is consistent with the international status of the Journal. Reports describing the application of well-established techniques to problems that are essentially technical will not be accepted. Similarly, papers that report observations, but fail to provide adequate interpretation, will be rejected by the Editors. Papers dealing with technical electrochemistry should be submitted to other specialist journals unless the Authors can show that their work provides substantially new insights into electrochemical processes.

Types of paper
(a) Regular papers reporting original research work not previously published in other periodicals.
(b) Reviews on recent developments in various fields of interest.
(c) Short communications.

Reviews should cover a part of the subject of active current interest. A Short communication is a concise, but complete, description of a limited investigation, which will not be included in a later article. Short communications should be as completely documented, both by reference to the literature and description of the experimental procedures employed, as a regular article.

Submission checklist

You can use this list to carry out a final check of your submission before you send it to the journal for review. Please check the relevant section in this Guide for Authors for more details.

Ensure that the following items are present:

One author has been designated as the corresponding author with contact details:
• E-mail address
• Full postal address

All necessary files have been uploaded:
Manuscript:
• Include keywords
• All figures (include relevant captions)
• All tables (including titles, description, footnotes)
• Ensure all figure and table citations in the text match the files provided
• Indicate clearly if color should be used for any figures in print
Graphical Abstracts / Highlights files (where applicable)
Supplemental files (where applicable)

Further considerations
• Manuscript has been 'spell checked' and 'grammar checked'
• All references mentioned in the Reference List are cited in the text, and vice versa
• Permission has been obtained for use of copyrighted material from other sources (including the Internet)
• A competing interests statement is provided, even if the authors have no competing interests to declare
• Journal policies detailed in this guide have been reviewed

• Referee suggestions and contact details provided, based on journal requirements

For further information, visit our Support Center.

BEFORE YOU BEGIN

Ethics in publishing

Please see our information pages on Ethics in publishing and Ethical guidelines for journal publication.

Declaration of interest

All authors must disclose any financial and personal relationships with other people or organizations that could inappropriately influence (bias) their work. Examples of potential conflicts of interest include employment, consultancies, stock ownership, honoraria, paid expert testimony, patent applications/ registrations, and grants or other funding. Authors should complete the declaration of interest statement using this template and upload to the submission system at the Attach/Upload Files step. If there are no interests to declare, please choose: 'Declarations of interest: none' in the template. This statement will be published within the article if accepted. More information.

Submission declaration and verification

Submission of an article implies that the work described has not been published previously (except in the form of an abstract, a published lecture or academic thesis, see 'Multiple, redundant or concurrent publication' for more information), that it is not under consideration for publication elsewhere, that its publication is approved by all authors and tacitly or explicitly by the responsible authorities where the work was carried out, and that, if accepted, it will not be published elsewhere in the same form, in English or in any other language, including electronically without the written consent of the copyright-holder. To verify originality, your article may be checked by the originality detection service Crossref Similarity Check.

Preprints

Please note that preprints can be shared anywhere at any time, in line with Elsevier's sharing policy. Sharing your preprints e.g. on a preprint server will not count as prior publication (see 'Multiple, redundant or concurrent publication' for more information).

Use of inclusive language

Inclusive language acknowledges diversity, conveys respect to all people, is sensitive to differences, and promotes equal opportunities. Articles should make no assumptions about the beliefs or commitments of any reader, should contain nothing which might imply that one individual is superior to another on the grounds of race, sex, culture or any other characteristic, and should use inclusive language throughout. Authors should ensure that writing is free from bias, for instance by using 'he or she', 'his/her' instead of 'he' or 'his', and by making use of job titles that are free of stereotyping (e.g. 'chairperson' instead of 'chairman' and 'flight attendant' instead of 'stewardess').

Author contributions

For transparency, we encourage authors to submit an author statement file outlining their individual contributions to the paper using the relevant CRediT roles: Conceptualization; Data curation; Formal analysis; Funding acquisition; Investigation; Methodology; Project administration; Resources; Software; Supervision; Validation; Visualization; Roles/Writing - original draft; Writing - review & editing. Authorship statements should be formatted with the names of authors first and CRediT role(s) following. More details and an example

Changes to authorship

Authors are expected to consider carefully the list and order of authors **before** submitting their manuscript and provide the definitive list of authors at the time of the original submission. Any addition, deletion or rearrangement of author names in the authorship list should be made only **before** the manuscript has been accepted and only if approved by the journal Editor. To request such a change, the Editor must receive the following from the **corresponding author**: (a) the reason for the change in author list and (b) written confirmation (e-mail, letter) from all authors that they agree with the addition, removal or rearrangement. In the case of addition or removal of authors, this includes confirmation from the author being added or removed.

Only in exceptional circumstances will the Editor consider the addition, deletion or rearrangement of authors **after** the manuscript has been accepted. While the Editor considers the request, publication of the manuscript will be suspended. If the manuscript has already been published in an online issue, any requests approved by the Editor will result in a corrigendum.

Article transfer service
This journal is part of our Article Transfer Service. This means that if the Editor feels your article is more suitable in one of our other participating journals, then you may be asked to consider transferring the article to one of those. If you agree, your article will be transferred automatically on your behalf with no need to reformat. Please note that your article will be reviewed again by the new journal. More information.

Copyright

Upon acceptance of an article, authors will be asked to complete a 'Journal Publishing Agreement' (see more information on this). An e-mail will be sent to the corresponding author confirming receipt of the manuscript together with a 'Journal Publishing Agreement' form or a link to the online version of this agreement.

Subscribers may reproduce tables of contents or prepare lists of articles including abstracts for internal circulation within their institutions. Permission of the Publisher is required for resale or distribution outside the institution and for all other derivative works, including compilations and translations. If excerpts from other copyrighted works are included, the author(s) must obtain written permission from the copyright owners and credit the source(s) in the article. Elsevier has preprinted forms for use by authors in these cases.

For gold open access articles: Upon acceptance of an article, authors will be asked to complete an 'Exclusive License Agreement' (more information). Permitted third party reuse of gold open access articles is determined by the author's choice of user license.

Author rights

As an author you (or your employer or institution) have certain rights to reuse your work. More information.

Elsevier supports responsible sharing
Find out how you can share your research published in Elsevier journals.

Role of the funding source

You are requested to identify who provided financial support for the conduct of the research and/or preparation of the article and to briefly describe the role of the sponsor(s), if any, in study design; in the collection, analysis and interpretation of data; in the writing of the report; and in the decision to submit the article for publication. If the funding source(s) had no such involvement then this should be stated.

Open access

Please visit our Open Access page from the Journal Homepage for more information.

Elsevier Researcher Academy
Researcher Academy is a free e-learning platform designed to support early and mid-career researchers throughout their research journey. The "Learn" environment at Researcher Academy offers several interactive modules, webinars, downloadable guides and resources to guide you through the process of writing for research and going through peer review. Feel free to use these free resources to improve your submission and navigate the publication process with ease.

Language (usage and editing services)
Please write your text in good English (American or British usage is accepted, but not a mixture of these). Authors who feel their English language manuscript may require editing to eliminate possible grammatical or spelling errors and to conform to correct scientific English may wish to use the English Language Editing service available from Elsevier's Author Services.

Submission

Our online submission system guides you stepwise through the process of entering your article details and uploading your files. The system converts your article files to a single PDF file used in the peer-review process. Editable files (e.g., Word, LaTeX) are required to typeset your article for final publication. All correspondence, including notification of the Editor's decision and requests for revision, is sent by e-mail.

Upon manuscript submissions please suggest 3 international experts as potential reviewers and include their affiliation, e-mail address and a link to their professional web page. Please also note that the suggested referees should not be from the same institution and/or country of the authors. Note

that the editor retains the sole right to decide whether or not the suggested reviewers are used. The final choice of Referees used will be made by the Editors. Manuscripts that are judged by the Editors to fall within the scope of the Journal will be considered independently by at least two Referees.
The Referees' reports provide advice for Editors to assist them in reaching a decision on a submitted paper. The final decision concerning a manuscript is the responsibility of the Editors. If there is a notable disagreement between the reports of two Referees, or if a disagreement between the Authors and the Referees cannot be resolved with the Editor's help, a third Referee may be consulted for advice.
The anonymity of Referees is strictly preserved. Referees should not communicate directly with Authors or pass confidential information to third parties. An exception is the case where a polemical contribution is concerned. In this case a Referee may ask an Editor for permission to enter into a dialogue with Authors.
All manuscripts and supplementary material are treated as confidential by the Editors. They will be disclosed only to Referees. Referees are expected to respect the confidential nature of submitted manuscripts.
Revised papers should normally be resubmitted within 12 weeks of the date of rejection. In exceptional circumstances, the Editors may extend this period if requested to do so. The dates of receipt of the original and final revised versions will both appear in the publication.

Editorial Policy
The Editors wish to ensure that the *Journal of Electroanalytical Chemistry* continues to serve the world scientific community by publishing, as rapidly as possible, papers of a high scientific quality. Authors and Referees are asked to pay particular attention to the criteria for acceptance that are outlined in the description of the Journal. In summary, papers should present new experimental or theoretical results or present new interpretations of existing results, leading to significant advances in knowledge and understanding.
The Editors regard it as their duty to assist Authors to achieve clarity and brevity in accepted papers. They will provide advice to Authors in addition to the comments made by Referees. Authors are asked to pay careful attention to the information about the preparation of articles and figures given below. The Editors are bound to perform their duties in accordance with the highest ethical standards. Referees and Authors also have a clear obligation to act in accordance with these standards.
Electrochemistry is an evolving discipline that is important in many contexts. In recognition of the dynamic nature of the subject, the Editors welcome contributions from scientists working in areas in which the contribution of Electrochemistry is beginning to emerge.
Although Short Communications are accepted for publication, the Editors wish to discourage fragmentation of a substantial body of work into a number of short publications. Authors who wish to communicate novel work of urgent interest should submit short papers to *Electrochemistry Communications*. The Editors may invite Authors to submit articles on particular topics. Such papers will be subject to the same rigorous refereeing as all other submitted papers.
The Editors may appoint a Guest Editor for a special issue of the Journal. One of the Editors will provide advice and support in the preparation of the special issue. Papers for special issues will be refereed in the normal way, in accordance with the Journal's policy.

PREPARATION

NEW SUBMISSIONS

Submission to this journal proceeds totally online and you will be guided stepwise through the creation and uploading of your files. The system automatically converts your files to a single PDF file, which is used in the peer-review process.
As part of the Your Paper Your Way service, you may choose to submit your manuscript as a single file to be used in the refereeing process. This can be a PDF file or a Word document, in any format or lay-out that can be used by referees to evaluate your manuscript. It should contain high enough quality figures for refereeing. If you prefer to do so, you may still provide all or some of the source files at the initial submission. Please note that individual figure files larger than 10 MB must be uploaded separately.

References
There are no strict requirements on reference formatting at submission. References can be in any style or format as long as the style is consistent. Where applicable, author(s) name(s), journal title/ book title, chapter title/article title, year of publication, volume number/book chapter and the article

number or pagination must be present. Use of DOI is highly encouraged. The reference style used by the journal will be applied to the accepted article by Elsevier at the proof stage. Note that missing data will be highlighted at proof stage for the author to correct.

Formatting requirements
There are no strict formatting requirements but all manuscripts must contain the essential elements needed to convey your manuscript, for example Abstract, Keywords, Introduction, Materials and Methods, Results, Conclusions, Artwork and Tables with Captions.
If your article includes any Videos and/or other Supplementary material, this should be included in your initial submission for peer review purposes.
Divide the article into clearly defined sections.

Figures and tables embedded in text
Please ensure the figures and the tables are embedded in the text, rather than at the bottom or the top of the file.

Peer review

This journal operates a single blind review process. All contributions will be initially assessed by the editor for suitability for the journal. Papers deemed suitable are then typically sent to a minimum of two independent expert reviewers to assess the scientific quality of the paper. The Editor is responsible for the final decision regarding acceptance or rejection of articles. The Editor's decision is final. More information on types of peer review.

REVISED SUBMISSIONS

Use of word processing software
Regardless of the file format of the original submission, at revision you must provide us with an editable file of the entire article. Keep the layout of the text as simple as possible. Most formatting codes will be removed and replaced on processing the article. The electronic text should be prepared in a way very similar to that of conventional manuscripts (see also the Guide to Publishing with Elsevier). See also the section on Electronic artwork.
To avoid unnecessary errors you are strongly advised to use the 'spell-check' and 'grammar-check' functions of your word processor.

Article structure

Subdivision - numbered sections
Divide your article into clearly defined and numbered sections. Subsections should be numbered 1.1 (then 1.1.1, 1.1.2, ...), 1.2, etc. (the abstract is not included in section numbering). Use this numbering also for internal cross-referencing: do not just refer to 'the text'. Any subsection may be given a brief heading. Each heading should appear on its own separate line.

Introduction
State the objectives of the work and provide an adequate background, avoiding a detailed literature survey or a summary of the results.

Material and methods
Provide sufficient details to allow the work to be reproduced by an independent researcher. Methods that are already published should be summarized, and indicated by a reference. If quoting directly from a previously published method, use quotation marks and also cite the source. Any modifications to existing methods should also be described.

Theory/calculation
A Theory section should extend, not repeat, the background to the article already dealt with in the Introduction and lay the foundation for further work. In contrast, a Calculation section represents a practical development from a theoretical basis.

Results
Results should be clear and concise.

Discussion
This should explore the significance of the results of the work, not repeat them. A combined Results and Discussion section is often appropriate. Avoid extensive citations and discussion of published literature.

Conclusions
The main conclusions of the study may be presented in a short Conclusions section, which may stand alone or form a subsection of a Discussion or Results and Discussion section.

Appendices
If there is more than one appendix, they should be identified as A, B, etc. Formulae and equations in appendices should be given separate numbering: Eq. (A.1), Eq. (A.2), etc.; in a subsequent appendix, Eq. (B.1) and so on. Similarly for tables and figures: Table A.1; Fig. A.1, etc.

Essential title page information

• ***Title.*** Concise and informative. Titles are often used in information-retrieval systems. Avoid abbreviations and formulae where possible.
• ***Author names and affiliations.*** Please clearly indicate the given name(s) and family name(s) of each author and check that all names are accurately spelled. Present the authors' affiliation addresses (where the actual work was done) below the names. Indicate all affiliations with a lower-case superscript letter immediately after the author's name and in front of the appropriate address. Provide the full postal address of each affiliation, including the country name and it is mandatory to mention the e-mail address of each author.
• ***Corresponding author.*** Clearly indicate who will handle correspondence at all stages of refereeing and publication, also post-publication. **Ensure that the e-mail address is given and that contact details are kept up to date by the corresponding author.**
• ***Present/permanent address.*** If an author has moved since the work described in the article was done, or was visiting at the time, a 'Present address' (or 'Permanent address') may be indicated as a footnote to that author's name. The address at which the author actually did the work must be retained as the main, affiliation address. Superscript Arabic numerals are used for such footnotes.

Highlights

Highlights are mandatory for this journal as they help increase the discoverability of your article via search engines. They consist of a short collection of bullet points that capture the novel results of your research as well as new methods that were used during the study (if any). Please have a look at the examples here: example Highlights.

Highlights should be submitted in a separate editable file in the online submission system. Please use 'Highlights' in the file name and include 3 to 5 bullet points (maximum 85 characters, including spaces, per bullet point).

Abstract

A concise and factual abstract is required. The abstract should state briefly the purpose of the research, the principal results and major conclusions. An abstract is often presented separately from the article, so it must be able to stand alone. For this reason, References should be avoided, but if essential, then cite the author(s) and year(s). Also, non-standard or uncommon abbreviations should be avoided, but if essential they must be defined at their first mention in the abstract itself.

Graphical abstract
Although a graphical abstract is optional, its use is encouraged as it draws more attention to the online article. The graphical abstract should summarize the contents of the article in a concise, pictorial form designed to capture the attention of a wide readership. Graphical abstracts should be submitted as a separate file in the online submission system. Image size: Please provide an image with a minimum of 531 × 1328 pixels (h × w) or proportionally more. The image should be readable at a size of 5 × 13 cm using a regular screen resolution of 96 dpi. Preferred file types: TIFF, EPS, PDF or MS Office files. You can view Example Graphical Abstracts on our information site.
Authors can make use of Elsevier's Illustration Services to ensure the best presentation of their images and in accordance with all technical requirements.

Keywords

Immediately after the abstract, provide a maximum of 6 keywords, using American spelling and avoiding general and plural terms and multiple concepts (avoid, for example, 'and', 'of'). Be sparing with abbreviations: only abbreviations firmly established in the field may be eligible. These keywords will be used for indexing purposes.

Abbreviations
Define abbreviations that are not standard in this field in a footnote to be placed on the first page of the article. Such abbreviations that are unavoidable in the abstract must be defined at their first mention there, as well as in the footnote. Ensure consistency of abbreviations throughout the article.

Acknowledgements
Collate acknowledgements in a separate section at the end of the article before the references and do not, therefore, include them on the title page, as a footnote to the title or otherwise. List here those individuals who provided help during the research (e.g., providing language help, writing assistance or proof reading the article, etc.).

Formatting of funding sources
List funding sources in this standard way to facilitate compliance to funder's requirements:

Funding: This work was supported by the National Institutes of Health [grant numbers xxxx, yyyy]; the Bill & Melinda Gates Foundation, Seattle, WA [grant number zzzz]; and the United States Institutes of Peace [grant number aaaa].

It is not necessary to include detailed descriptions on the program or type of grants and awards. When funding is from a block grant or other resources available to a university, college, or other research institution, submit the name of the institute or organization that provided the funding.

If no funding has been provided for the research, please include the following sentence:

This research did not receive any specific grant from funding agencies in the public, commercial, or not-for-profit sectors.

Math formulae
Please submit math equations as editable text and not as images. Present simple formulae in line with normal text where possible and use the solidus (/) instead of a horizontal line for small fractional terms, e.g., X/Y. In principle, variables are to be presented in italics. Powers of e are often more conveniently denoted by exp. Number consecutively any equations that have to be displayed separately from the text (if referred to explicitly in the text).

Footnotes
Footnotes should be used sparingly. Number them consecutively throughout the article. Many word processors build footnotes into the text, and this feature may be used. Should this not be the case, indicate the position of footnotes in the text and present the footnotes themselves separately at the end of the article.

Image manipulation
Whilst it is accepted that authors sometimes need to manipulate images for clarity, manipulation for purposes of deception or fraud will be seen as scientific ethical abuse and will be dealt with accordingly. For graphical images, this journal is applying the following policy: no specific feature within an image may be enhanced, obscured, moved, removed, or introduced. Adjustments of brightness, contrast, or color balance are acceptable if and as long as they do not obscure or eliminate any information present in the original. Nonlinear adjustments (e.g. changes to gamma settings) must be disclosed in the figure legend.

Electronic artwork
General points
• Make sure you use uniform lettering and sizing of your original artwork.
• Preferred fonts: Arial (or Helvetica), Times New Roman (or Times), Symbol, Courier.
• Number the illustrations according to their sequence in the text.
• Use a logical naming convention for your artwork files.
• Indicate per figure if it is a single, 1.5 or 2-column fitting image.
• For Word submissions only, you may still provide figures and their captions, and tables within a single file at the revision stage.
• Please note that individual figure files larger than 10 MB must be provided in separate source files.

A detailed guide on electronic artwork is available.
You are urged to visit this site; some excerpts from the detailed information are given here.
Formats
Regardless of the application used, when your electronic artwork is finalized, please 'save as' or convert the images to one of the following formats (note the resolution requirements for line drawings, halftones, and line/halftone combinations given below):
EPS (or PDF): Vector drawings. Embed the font or save the text as 'graphics'.
TIFF (or JPG): Color or grayscale photographs (halftones): always use a minimum of 300 dpi.

TIFF (or JPG): Bitmapped line drawings: use a minimum of 1000 dpi.
TIFF (or JPG): Combinations bitmapped line/half-tone (color or grayscale): a minimum of 500 dpi is required.
Please do not:
• Supply files that are optimized for screen use (e.g., GIF, BMP, PICT, WPG); the resolution is too low.
• Supply files that are too low in resolution.
• Submit graphics that are disproportionately large for the content.

Color artwork
Please make sure that artwork files are in an acceptable format (TIFF (or JPEG), EPS (or PDF) or MS Office files) and with the correct resolution. If, together with your accepted article, you submit usable color figures then Elsevier will ensure, at no additional charge, that these figures will appear in color online (e.g., ScienceDirect and other sites) in addition to color reproduction in print. Further information on the preparation of electronic artwork.

Figure captions
Ensure that each illustration has a caption. A caption should comprise a brief title (**not** on the figure itself) and a description of the illustration. Keep text in the illustrations themselves to a minimum but explain all symbols and abbreviations used.

Tables
Please submit tables as editable text and not as images. Tables can be placed either next to the relevant text in the article, or on separate page(s) at the end. Number tables consecutively in accordance with their appearance in the text and place any table notes below the table body. Be sparing in the use of tables and ensure that the data presented in them do not duplicate results described elsewhere in the article. Please avoid using vertical rules and shading in table cells.

References
Citation in text
Please ensure that every reference cited in the text is also present in the reference list (and vice versa). Any references cited in the abstract must be given in full. Unpublished results and personal communications are not recommended in the reference list, but may be mentioned in the text. If these references are included in the reference list they should follow the standard reference style of the journal and should include a substitution of the publication date with either 'Unpublished results' or 'Personal communication'. Citation of a reference as 'in press' implies that the item has been accepted for publication.

Reference links
Increased discoverability of research and high quality peer review are ensured by online links to the sources cited. In order to allow us to create links to abstracting and indexing services, such as Scopus, CrossRef and PubMed, please ensure that data provided in the references are correct. Please note that incorrect surnames, journal/book titles, publication year and pagination may prevent link creation. When copying references, please be careful as they may already contain errors. Use of the DOI is highly encouraged.

A DOI is guaranteed never to change, so you can use it as a permanent link to any electronic article. An example of a citation using DOI for an article not yet in an issue is: VanDecar J.C., Russo R.M., James D.E., Ambeh W.B., Franke M. (2003). Aseismic continuation of the Lesser Antilles slab beneath northeastern Venezuela. Journal of Geophysical Research, https://doi.org/10.1029/2001JB000884. Please note the format of such citations should be in the same style as all other references in the paper.

Web references
As a minimum, the full URL should be given and the date when the reference was last accessed. Any further information, if known (DOI, author names, dates, reference to a source publication, etc.), should also be given. Web references can be listed separately (e.g., after the reference list) under a different heading if desired, or can be included in the reference list.

Data references
This journal encourages you to cite underlying or relevant datasets in your manuscript by citing them in your text and including a data reference in your Reference List. Data references should include the following elements: author name(s), dataset title, data repository, version (where available), year, and global persistent identifier. Add [dataset] immediately before the reference so we can properly identify it as a data reference. The [dataset] identifier will not appear in your published article.

References in a special issue
Please ensure that the words 'this issue' are added to any references in the list (and any citations in the text) to other articles in the same Special Issue.

Reference management software
Most Elsevier journals have their reference template available in many of the most popular reference management software products. These include all products that support Citation Style Language styles, such as Mendeley. Using citation plug-ins from these products, authors only need to select the appropriate journal template when preparing their article, after which citations and bibliographies will be automatically formatted in the journal's style. If no template is yet available for this journal, please follow the format of the sample references and citations as shown in this Guide. If you use reference management software, please ensure that you remove all field codes before submitting the electronic manuscript. More information on how to remove field codes from different reference management software.

Users of Mendeley Desktop can easily install the reference style for this journal by clicking the following link:
http://open.mendeley.com/use-citation-style/journal-of-electroanalytical-chemistry
When preparing your manuscript, you will then be able to select this style using the Mendeley plug-ins for Microsoft Word or LibreOffice.

Reference formatting
There are no strict requirements on reference formatting at submission. References can be in any style or format as long as the style is consistent. Where applicable, author(s) name(s), journal title/book title, chapter title/article title, year of publication, volume number/book chapter and the article number or pagination must be present. Use of DOI is highly encouraged. The reference style used by the journal will be applied to the accepted article by Elsevier at the proof stage. Note that missing data will be highlighted at proof stage for the author to correct. If you do wish to format the references yourself they should be arranged according to the following examples:

Reference style
Text: Indicate references by number(s) in square brackets in line with the text. The actual authors can be referred to, but the reference number(s) must always be given.
Example: '..... as demonstrated [3,6]. Barnaby and Jones [8] obtained a different result ....'
List: Number the references (numbers in square brackets) in the list in the order in which they appear in the text.
Examples:
Reference to a journal publication:
[1] J. van der Geer, J.A.J. Hanraads, R.A. Lupton, The art of writing a scientific article, J. Sci. Commun. 163 (2010) 51–59. https://doi.org/10.1016/j.Sc.2010.00372.
Reference to a journal publication with an article number:
[2] J. van der Geer, J.A.J. Hanraads, R.A. Lupton, 2018. The art of writing a scientific article. Heliyon. 19, e00205. https://doi.org/10.1016/j.heliyon.2018.e00205.
Reference to a book:
[3] W. Strunk Jr., E.B. White, The Elements of Style, fourth ed., Longman, New York, 2000.
Reference to a chapter in an edited book:
[4] G.R. Mettam, L.B. Adams, How to prepare an electronic version of your article, in: B.S. Jones, R.Z. Smith (Eds.), Introduction to the Electronic Age, E-Publishing Inc., New York, 2009, pp. 281–304.
Reference to a website:
[5] Cancer Research UK, Cancer statistics reports for the UK. http://www.cancerresearchuk.org/aboutcancer/statistics/cancerstatsreport/, 2003 (accessed 13 March 2003).
Reference to a dataset:
[dataset] [6] M. Oguro, S. Imahiro, S. Saito, T. Nakashizuka, Mortality data for Japanese oak wilt disease and surrounding forest compositions, Mendeley Data, v1, 2015. https://doi.org/10.17632/xwj98nb39r.1.

Journal abbreviations source
Journal names should be abbreviated according to the List of Title Word Abbreviations.

Video
Elsevier accepts video material and animation sequences to support and enhance your scientific research. Authors who have video or animation files that they wish to submit with their article are strongly encouraged to include links to these within the body of the article. This can be done in the

same way as a figure or table by referring to the video or animation content and noting in the body text where it should be placed. All submitted files should be properly labeled so that they directly relate to the video file's content. In order to ensure that your video or animation material is directly usable, please provide the file in one of our recommended file formats with a preferred maximum size of 150 MB per file, 1 GB in total. Video and animation files supplied will be published online in the electronic version of your article in Elsevier Web products, including ScienceDirect. Please supply 'stills' with your files: you can choose any frame from the video or animation or make a separate image. These will be used instead of standard icons and will personalize the link to your video data. For more detailed instructions please visit our video instruction pages. Note: since video and animation cannot be embedded in the print version of the journal, please provide text for both the electronic and the print version for the portions of the article that refer to this content.

Data visualization

Include interactive data visualizations in your publication and let your readers interact and engage more closely with your research. Follow the instructions here to find out about available data visualization options and how to include them with your article.

Supplementary material

Supplementary material such as applications, images and sound clips, can be published with your article to enhance it. Submitted supplementary items are published exactly as they are received (Excel or PowerPoint files will appear as such online). Please submit your material together with the article and supply a concise, descriptive caption for each supplementary file. If you wish to make changes to supplementary material during any stage of the process, please make sure to provide an updated file. Do not annotate any corrections on a previous version. Please switch off the 'Track Changes' option in Microsoft Office files as these will appear in the published version.

Research data

This journal encourages and enables you to share data that supports your research publication where appropriate, and enables you to interlink the data with your published articles. Research data refers to the results of observations or experimentation that validate research findings. To facilitate reproducibility and data reuse, this journal also encourages you to share your software, code, models, algorithms, protocols, methods and other useful materials related to the project.

Below are a number of ways in which you can associate data with your article or make a statement about the availability of your data when submitting your manuscript. If you are sharing data in one of these ways, you are encouraged to cite the data in your manuscript and reference list. Please refer to the "References" section for more information about data citation. For more information on depositing, sharing and using research data and other relevant research materials, visit the research data page.

Data linking

If you have made your research data available in a data repository, you can link your article directly to the dataset. Elsevier collaborates with a number of repositories to link articles on ScienceDirect with relevant repositories, giving readers access to underlying data that gives them a better understanding of the research described.

There are different ways to link your datasets to your article. When available, you can directly link your dataset to your article by providing the relevant information in the submission system. For more information, visit the database linking page.

For supported data repositories a repository banner will automatically appear next to your published article on ScienceDirect.

In addition, you can link to relevant data or entities through identifiers within the text of your manuscript, using the following format: Database: xxxx (e.g., TAIR: AT1G01020; CCDC: 734053; PDB: 1XFN).

Mendeley Data

This journal supports Mendeley Data, enabling you to deposit any research data (including raw and processed data, video, code, software, algorithms, protocols, and methods) associated with your manuscript in a free-to-use, open access repository. During the submission process, after uploading your manuscript, you will have the opportunity to upload your relevant datasets directly to *Mendeley Data*. The datasets will be listed and directly accessible to readers next to your published article online.

For more information, visit the Mendeley Data for journals page.

Data in Brief
You have the option of converting any or all parts of your supplementary or additional raw data into one or multiple data articles, a new kind of article that houses and describes your data. Data articles ensure that your data is actively reviewed, curated, formatted, indexed, given a DOI and publicly available to all upon publication. You are encouraged to submit your article for *Data in Brief* as an additional item directly alongside the revised version of your manuscript. If your research article is accepted, your data article will automatically be transferred over to *Data in Brief* where it will be editorially reviewed and published in the open access data journal, *Data in Brief*. Please note an open access fee of 600 USD is payable for publication in *Data in Brief*. Full details can be found on the Data in Brief website. Please use this template to write your Data in Brief.

MethodsX
You have the option of converting relevant protocols and methods into one or multiple MethodsX articles, a new kind of article that describes the details of customized research methods. Many researchers spend a significant amount of time on developing methods to fit their specific needs or setting, but often without getting credit for this part of their work. MethodsX, an open access journal, now publishes this information in order to make it searchable, peer reviewed, citable and reproducible. Authors are encouraged to submit their MethodsX article as an additional item directly alongside the revised version of their manuscript. If your research article is accepted, your methods article will automatically be transferred over to MethodsX where it will be editorially reviewed. Please note an open access fee is payable for publication in MethodsX. Full details can be found on the MethodsX website. Please use this template to prepare your MethodsX article.

Data statement
To foster transparency, we encourage you to state the availability of your data in your submission. This may be a requirement of your funding body or institution. If your data is unavailable to access or unsuitable to post, you will have the opportunity to indicate why during the submission process, for example by stating that the research data is confidential. The statement will appear with your published article on ScienceDirect. For more information, visit the Data Statement page.

AFTER ACCEPTANCE

Online Proof Correction
Corresponding authors will receive an e-mail with a link to our ProofCentral system, allowing annotation and correction of proofs online. The environment is similar to MS Word: in addition to editing text, you can also comment on figures/tables and answer questions from the Copy Editor. Web-based proofing provides a faster and less error-prone process by allowing you to directly type your corrections, eliminating the potential introduction of errors.
If preferred, you can still choose to annotate and upload your edits on the PDF version. All instructions for proofing will be given in the e-mail we send to authors, including alternative methods to the online version and PDF. We will do everything possible to get your article published quickly and accurately - please upload all of your corrections within 48 hours. It is important to ensure that all corrections are sent back to us in one communication. Please check carefully before replying, as inclusion of any subsequent corrections cannot be guaranteed. Proofreading is solely your responsibility. Note that Elsevier may proceed with the publication of your article if no response is received.

Offprints
The corresponding author will, at no cost, receive a customized Share Link providing 50 days free access to the final published version of the article on ScienceDirect. The Share Link can be used for sharing the article via any communication channel, including email and social media. For an extra charge, paper offprints can be ordered via the offprint order form which is sent once the article is accepted for publication. Both corresponding and co-authors may order offprints at any time via Elsevier's Author Services. Corresponding authors who have published their article gold open access do not receive a Share Link as their final published version of the article is available open access on ScienceDirect and can be shared through the article DOI link.

AUTHOR INQUIRIES

Visit the Elsevier Support Center to find the answers you need. Here you will find everything from Frequently Asked Questions to ways to get in touch.
You can also check the status of your submitted article or find out when your accepted article will be published.

Appendix - C

Author Instructions

Inorganic Chemistry

Chapter 4

ACS Publications
Most Trusted. Most Cited. Most Read.

Inorganic Chemistry

Last updated: December 12, 2019 View the latest guidelines online

Manuscript Submission Requirements Checklist

1. The names of all coauthors of a manuscript must be entered into Paragon Plus upon submission.
2. If relevant, authors are required to (a) check the quality of their CIFs through the checkCIF website *prior to submission of their manuscript*, (b) submit CIFs and structure factor tables for inorganic or metal organics to the Cambridge Crystallographic Data Centre (CCDC) prior to submission and provide the CCDC access code(s) upon submission, (c) provide the checkCIF output file (as a PDF uploaded as Supporting Information for Review Only), and (d) address any A and/or B level alerts in the checkCIF PDF and consider inserting their comments directly into CIFs. **Note that while checkCIFs are required, uploading CIF files into ACS Paragon Plus for compounds accommodated by CCDC is no longer required.**
3. Communications must not exceed 2200 words, including titles/footnotes/captions and approximately five graphics (each typically 2 inches long in a single column); one of the graphics includes the TOC graphic. References and the TOC synopsis are not included in the word count. Authors no longer need to fit the manuscript to the strict pages by the template measure, but communications exceeding the word count limit must be shortened before acceptance (See Manuscript Types).
4. The Table of Contents graphic AND the synopsis must be on a separate page at the end of the submitted manuscript file. The synopsis can contain up to 75 words.
5. References must include titles along with the appropriate citation information.
6. Authors must emphasize any unexpected, new, and/or significant hazards or risks associated with the reported work, and clearly describe how to mitigate them.

Scope of the Journal

Inorganic Chemistry publishes fundamental studies, both experimental and theoretical, on all topics of inorganic chemistry from across the periodic table, including but not limited to coordination chemistry, main-group chemistry, bioinorganic chemistry, organometallic chemistry, solid- state/materials/nanoscale chemistry, energy and photochemistry, catalysis, and theory/computation.

The journal places emphasis on scientifically rigorous studies of the synthesis and mechanisms, structure, thermodynamics, kinetics, reactivity, spectroscopy, bonding, and functional properties of new and significant known compounds. Only those manuscript submissions that sufficiently emphasize inorganic chemistry aspects will be considered. Illustrative examples of manuscripts that will not be considered include ones that describe poorly defined or characterized compounds or materials, or that are deemed to emphasize morphological, nanoscale, or larger scale attributes of materials, biological phenomena, analytical methods, speculative or predominantly technical aspects of theory, or technological applications. Reports of routine research describing incremental additions to the scientific literature are discouraged. More detailed discussion (organized by topic) of submissions that will be considered are presented below.

Coordination and Organometallic Chemistry: Fundamental studies of the design and synthesis of new coordination and organometallic complexes incorporating main group, transition metal, and/or lanthanide/actinide elements with tailored reactivity and/or functional electronic, optical, and

magnetic properties are welcome. These studies should include details of coordination environment, electronic structure, bonding, magnetic properties, and/or reactivity probed through experimental and/or computational methods and involving spectroscopy, electrochemistry, and other characterization means. The added value to general knowledge in inorganic chemistry should be clearly visible, for example in the description of uncommon structures, bonding, reactivity, and/or proven potential for new molecular or materials applications (such as catalysis, sensing, and optics). Articles that focus solely on solid-state structures or synthetic organic applications are discouraged.

Bioinorganic Chemistry: Studies in the area of bioinorganic chemistry should emphasize new inorganic structures, solution chemistry, detailed mechanisms of biological efficacy or reactions, or spectroscopic properties. The inorganic chemistry must be central and contribute new perspectives to the field, for example in areas of biomimetic and bioinspired coordination chemistry, metalloproteins and metallodrugs, and metal-based probes. Manuscripts with a focus on biology that lack in-depth studies of inorganic chemistry aspects will not be considered.

Solid State, Materials, and Nanoscale Chemistry: *Inorganic Chemistry* encourages submissions that contribute significant new synthetic, mechanistic, or structural insight on well-characterized molecular, nanostructured, or extended inorganic compounds (clusters and supramolecular compounds) and push the frontiers of functional inorganic chemistry-dependent materials properties, characterization techniques, or theoretical description. Manuscripts that emphasize technological applications or that describe routine syntheses and characterization, incremental advances for well-known families of compounds, routine formulations of known components, or phenomenological work that does not provide new inorganic chemistry insight will not be considered.

Energy and Photochemistry: Studies in the area of energy and photochemistry should emphasize new inorganic structures or coordination compounds with properties and functions related but not limited to electrical, redox, luminescence, excited states, photoredox sensitization, and energy-transfer chemistry or to applications in solar-energy conversion and storage. Contributions that focus on applications, including analytical techniques and photophysics, or on speculative theoretical aspects, will not be considered.

Catalysis: Studies on heterogeneous and homogeneous catalysis using inorganic or organometallic compounds and/or inorganic-organic hybrid compounds and materials as well as metallosupramolecules are welcome. The focus should be on inorganic chemistry aspects, in particular new complexes with interesting structures, bonding, coordination numbers, or electron configurations, rather than applications to organic synthesis or industrial process development with well-known compounds, for example.

Theory and Computation: *Inorganic Chemistry* welcomes studies that use state-of-the art theoretical/computational methods to contribute to conceptual advances in all areas of inorganic chemistry, especially those that combine experiment and theory. Studies that focus on technical aspects, for example the choice of density functionals and/or basis sets, or are largely speculative, that is, make predictions that cannot reasonably be subjected to experimental testing, will not be considered.

Manuscript Types

Inorganic Chemistry publishes Articles, Communications, invited Viewpoint Articles, and invited Forum Articles.

Articles represent complete studies and are not restricted in length. However, authors are urged to be as concise as possible, presenting experimental results clearly and carefully in a separate section and placing material in the Supporting Information file that, while of importance for practitioners on the topic, is of significantly less interest to the general reader.

Communications are reports of unusual urgency, significance, and interest originating in all areas

of inorganic chemistry. A statement from the authors describing why their manuscript meets these criteria is required in the cover letter. Communications must convey the scientific findings concisely in 2,200 words or less, which includes the abstract, main text, and figure captions, plus approximately four graphics (each typically 2 inches long in a single column) and the TOC graphic. References and the TOC synopsis are not included in the word count. Authors no longer need to fit their manuscript into the three-page template, but communications will have to be under the word count limit before acceptance. *Complete* experimental work should appear in the Supporting Information; additional documentation in the Supporting Information is encouraged. Communications that contain X-ray crystallographic information must be accompanied by full documentation to be used as Supporting Information in the editorial and review process.

Viewpoints are personalized discussions of a developing subject or field, firmly based in science, with the intent of inspiring future research efforts. In each Viewpoint, authors introduce the topic, provide insight and critical assessment of recent advances, and discuss new directions and future outlook for the field. The manuscript length should fit within 5–10 final published journal pages. While Viewpoints are typically invited by the Editor-in-Chief, proposals for Viewpoint submissions are welcome.

Forums are published several times annually and consist of a set of thematically linked invited research Articles and Communications from leading scientists on a multidisciplinary topic of growing interest. The article format is neither a review nor a typical research publication. As such, more leeway is available in the article introduction to frame the importance of the work within the field and in the discussion section to integrate how the research results are broadly impactful in the topic area. Thus, the research account should identify the important questions on the subject and the authors' contribution to addressing its key challenges, with additional attention given to providing educational value for undergraduate and graduate students.

Inorganic Chemistry does not publish comprehensive reviews or book reviews. Commentaries on prior work published in the journal or elsewhere will be considered if significant new results or insights are presented.

In all types of submissions, authors should present their material as clearly and concisely as possible. Introductions should contain sufficient background material to show why the work was done and how it relates to the subject. However, extensive reviews of the literature and/or numerous general references are inappropriate. **The description of experimental work must be presented accurately and in sufficient detail to allow the work to be duplicated in other laboratories.**

ACS Publishing Center

While this document will provide basic information on how to prepare and submit the manuscript as well as other critical information about publishing, we also encourage authors to visit the ACS Publishing Center for additional information on everything that is needed to prepare (and review) manuscripts for ACS journals and partner journals, such as

- Mastering the Art of Scientific Publication, which shares editor tips about a variety of topics including making your paper scientifically effective, preparing excellent graphics, and writing cover letters.
- Resources on how to prepare and submit a manuscript to ACS Paragon Plus, ACS Publications' manuscript submission and peer review environment.
- Sharing your research with the public through the ACS Publications open access program.
- ACS Reviewer Lab, a free online course covering best practices for peer review and related ethical considerations.

Manuscript Preparation

Review Ready Submission

All ACS journals and partner journals have simplified their formatting requirements in favor of a streamlined and standardized review-ready format for an initial manuscript submission. Read more about the requirements and the benefits these serves authors and reviewers here.

Manuscripts submitted for initial consideration must adhere to these standards:

- Submissions must be complete with clearly identified standard sections used to report original research, free of annotations or highlights, and include all numbered and labeled components.
- Figures, charts, tables, schemes, and equations should be embedded in the text at the point of relevance. Separate graphics can be supplied later at revision, if necessary.
- A two-column manuscript template is available and can be used for manuscripts submitted to any ACS journal or partner journal. Templates are not required but may be useful to approximate how an article will compose. For manuscripts with word count limits, authors are not required to fit content into a page limit based on the template.
- References can be provided in any style, but they must be complete, including titles.
- Supporting Information should be submitted as a separate file(s).
- Author names and affiliations on the manuscript must match what is entered into ACS.

Document Templates and Format

The templates facilitate the peer review process by allowing authors to place artwork and tables close to the point where they are discussed within the text. Learn more about document templates here.

General information on the preparation of manuscripts may also be found in the ACS Guide to Scholarly Communication.

Acceptable Software, File Designations, and TeX/LaTeX

See the list of Acceptable Software and appropriate File Designations to be sure your file types are compatible with ACS Paragon Plus. Information for manuscripts generated from TeX/LaTeX is also available.

Cover Letter

A cover letter must accompany every manuscript submission. During the submission process, you may type it or paste it into the submission system, or you may attach it as a file.

Authors must explain clearly and convincingly in their cover letter how their manuscript is original, significant, and novel and why it will be of interest to the readers of *Inorganic Chemistry*.

Manuscript Text Components

Manuscripts of full Articles should include:

1. Title page
2. Abstract
3. Introduction
4. Experimental Section
5. Results
6. Discussion

7. Footnotes (including explanatory notes and literature references)
8. Tables
9. Schemes
10. Charts
11. Captions for Figures
12. Figures
13. Table of Contents Synopsis
14. Table of Contents Graphic

The abstract of each manuscript should not exceed 300 words for an article and 150 words for a communication.

For all categories of papers, authors must submit a TOC graphic and synopsis, which can contain up to 75 words.

Supporting Information

This information is provided to the reviewers during the peer-review process (for Review Only) and is available to readers of the published work (for Publication). Supporting Information must be submitted at the same time as the manuscript. See the list of Acceptable Software by File Designation and confirm that your Supporting Information is viewable.

If the manuscript is accompanied by any supporting information files for publication, these files will be made available free of charge to readers. A brief description of each file is required, and the paragraph and descriptions should be placed at the end of the manuscript before the list of references. The appropriate format is as follows:

Supporting Information. Brief descriptions in nonsentence format listing the contents of the files supplied as Supporting Information.

When including supporting information for review only, include copies of references that are unpublished or in-press. These files are available only to editors and reviewers.

Data Requirements

Characterization of New Compounds

The Journal upholds a high standard for compound characterization to ensure that substances being added to the chemical literature have been correctly identified and can be synthesized in known yield and purity by the reported preparation and isolation methods.

For all **new** compounds, evidence adequate to establish both *identity* and *degree of purity* (homogeneity) must be provided. For known compounds prepared by a new or modified synthetic procedure, the types of physical and spectroscopic data that were found to match *cited* literature data should be identified, and purity documentation should be provided.

Single-crystal X-ray diffraction results are not, in general, acceptable as the *only* means of characterization of new compounds. Compounds *must* also be characterized by spectroscopic and analytical methods appropriate for the particular sample or compound. Methods may include elemental analyses to demonstrate bulk composition, NMR spectroscopy, mass spectrometry, infrared spectroscopy, and electronic spectroscopy.

Structure Reports

(A) Crystal Structure Studies

A checklist for authors derived from recommendations of the Commission on Crystallographic Data of the International Union of Crystallography (*Acta Crystallogr.* **1967**, *22*, 445) is available from the *Inorganic Chemistry* website. Authors should consult this checklist (revised 2001) before preparing manuscripts for submission. Not all data requested for review will be shown in the printed text.

This applies both to reports in which the structure study is the main thrust of the work (full structure report) and to those in which such a study plays only a supporting role (abbreviated structure report). Single-crystal X-ray diffraction results are not, in general, acceptable as the only means of characterization of new compounds. See the statement under Characterization of New Compounds given above. If electronic spectral data are employed to relate the bulk and crystallographic samples, extinction coefficients should be provided. It is possible that syntheses will occasionally produce a material that cannot be reliably analyzed, gives uninformative IR and electronic spectra, and presents no definitive NMR data because of paramagnetism or dynamic exchange processes. Cases of this sort may be acceptable if and only if the author clearly delineates the limitations of the available data.

(1) Structure Reports in Articles.

(a) Experimental Section. Every effort should be made to minimize the quantity of tabular material appearing in the published text. The collection of data and refinement of the structure are usually routine, and a concise description can be accomplished with a brief written description and a table containing crystallographic parameters and data collection and refinement information described below.

(b) Tabular Material. An abbreviated table containing unit cell constants, space group information, Z, data collection and refinement parameters, and final agreement factors may be helpful to readers and may be included in either the text or Supporting Information. In addition, important bond lengths and angles (with esd's) should be supplied for the published text when they are significant to the overall discussion. *Inorganic Chemistry* does not publish refined positional parameters in the published text except in cases where such information is essential to the clarity of the manuscript. This information can be accessed easily from the web page displaying the final published article, which links to the data deposited at the CCDC via the Accession Codes box. Note that a list of the Accession Codes will also be published in the PDF version of the final article. If relevant, other information such as least-squares planes and atomic deviations therefrom, closest intermolecular contacts (e.g., details of intermolecular hydrogen-bonding or other packing interactions), and unit cell and packing diagrams (optional if no unusual intermolecular contacts exist), stylized to emphasize packing information and drawn with right- handed axes, should be deposited in PDF format as Supporting Information. A statement should appear at the end of the printed manuscript text enumerating the contents of the Supporting Information.

(c) Figures. Drawings of crystal or molecular structures should be made with the noncrystallographer in mind. **For structures refined anisotropically, plots showing thermal ellipsoids are required rather than ball-and-stick drawings.** Stereoscopic pairs of perspective drawings and unit cell and packing diagrams should be deposited as Supporting Information unless they contribute directly to the discussion.

(d) Deposited Data. Prior to manuscript submission, authors are **required** to check the quality of their CIFs (for single-crystal data collections) through the checkCIF website of the International Union of Crystallography (checkcif.iucr.org) and to upload the checkCIF output files (combined into one PDF file) as Supporting Information for Review Only. Any A and/or B level alerts must be addressed prior to submission or otherwise explained in the checkCIF PDF, and authors are further encouraged to insert their comments directly into CIFs.

CIFs, structure factor tables, and CheckCIF reports must be submitted to the Cambridge Crystallographic Data Centre (CCDC) **prior to manuscript submission**. The CCDC deposition number(s) should be entered into the ACS Paragon Plus Environment during submission**.** See Requirements for Depositing X-Ray Crystallographic Data for complete details on submission of CIFs. Any subsequent revisions to the CIFs or structure factor tables should be deposited directly with the CCDC before uploading a revised manuscript to ACS Paragon Plus.

Reviewers will have access via the CCDC to an electronic copy of the CIF(s) associated with a manuscript. For many reviewers, an electronic CIF greatly simplifies the review process. Thus, the lack of availability of an electronic CIF may result in significant delays in the review process. If the manuscript is accepted and published, the CIF(s) will be made available to readers via the ACS

Publications Web site.

CCDC will accept organic, metal-organic, and inorganic compounds, including extended molecular solids and powder data where a constrained refinement has been used. Structural data for inorganic compounds will be transferred by CCDC to the Inorganic Crystal Structure Database (ICSD) after publication and will maintain the original deposition number(s). For all other crystallographic data that are not accommodated by the CCDC, authors are encouraged to deposit into a database according to instructions in the Requirements for Depositing X-Ray Crystallographic Data, in addition to uploading the data in ACS Paragon Plus during manuscript submission as Supporting Information. Please indicate whether the other crystallographic data is intended for publication or for review only.

If restraints or constraints on non-hydrogen atoms or adjustments to the structure factors are used in the refinement of a crystal structure, these should be described in detail in the experimental section and their application justified. Data from complementary experiments should be made available to resolve any ambiguities arising from problems with a refinement.

(2) Abbreviated Structure Reports in Communications and Articles. In a Communication or in the case where a structural study plays a supporting role in a full paper devoted to another principal objective, a good molecular or unit cell diagram should appear as a figure. A brief summary of unit cell constants and data collection and refinement information should be given in a footnote, while selected distances and angles should be placed in the figure caption or a short table. The corresponding CIF should still be deposited with the CCDC as described above.

(B) Powder Diffraction Data

The structural determination of new materials by powder diffraction methods (laboratory X-ray, synchrotron, and/or neutron diffraction) is encouraged. Authors must include a table with the information shown below, as well as a figure showing the observed, calculated, and difference diffraction patterns and tick marks indicating the positions of the reflections for the refined phase and impurity phase(s). Authors are encouraged but not required to supply a CIF for a structure determined from powder diffraction. If a CIF file is provided for a powder diffraction structure, a checkCIF file is not required.

Crystallographic Data (Powder)

- Source (laboratory X-ray, synchrotron, neutron time of flight (TOF), neutron constant wavelength)
- Chemical formula
- Formula weight
- Temperature
- Pressure (if not ambient)
- Wavelength for constant wavelength or TOF
- Crystal system
- Space group (No.)
- *a*, *b*, *c*, , ,
- *V* (A3)
- *Z*
- *d*-space range
- 2
- *R*p
- *R*wp
- Definition of *R* factors

(C) Corrections

Errors discovered in published structure reports should be communicated directly to the corresponding author of the work. The Editor should be kept informed by a copy of such correspondence. Upon verifying the error, the author or authors should submit a suitable

correction to the Editor without delay, carrying an acknowledgment of the colleagues who brought the matter to their attention.

Computational Reports

With great advances in computational facilities and the availability of electronic structure codes (particularly DFT), there has been a significant increase in the number of computational papers being submitted to *Inorganic Chemistry*. In addition to computational competence (level of theory, basis sets, etc.), **for a manuscript to be appropriate for publication in *Inorganic Chemistry*, it must be strongly correlated to experimental data, address problems of broad interest to the inorganic community, and provide significant chemical insight**.

Comparison of methods, studies of various levels of theory, basis set effects, etc., are considered to be technically oriented computational papers and are not encouraged. In addition, studies simply confirming results already present in the literature or which are entirely speculative should be directed toward more specialized journals.

Authors should supply enough Supporting Information to reproduce the calculations or to make the results utilizable without repeating the calculations. Computational manuscripts should include at least the following Supporting Information:

1. Description of specific programs and the release or version. If the author's own or a modified version of a commercially available program is used, it is encouraged that the program/code/modification be made available to the scientific community (QCPE, publication in a computational journal, commercially, etc.), if the license permits. A clear exposition of any nonstandard equations and algorithms used and, where feasible, tests of the codes in various limiting cases should also be provided.
2. Details of the calculations including input coordinates along with input keywords. The choice of basis sets must be explicitly discussed including any deviation from standard basis sets. Convergence criteria, integration parameters, active space definition in multireference calculations, and, for open-shell systems, the way in which spin states are handled should be mentioned explicitly. The exact definition of any applied numerical or symmetry constraint should be indicated.
3. Certain data of the output files such as absolute energies, gross orbital populations, atomic spin densities, etc. Where feasible, critical checkpoint/restart files should be saved and made available upon request. If the paper discusses a reaction mechanism in terms of its potential energy surface, optimized molecular structures should be provided in Cartesian atomic coordinates for each calculated molecule, intermediate, transition state, etc., as separate plain-text files in standard .xyz file format. More information about the .xyz file format is available at http://openbabel.sourceforge.net/wiki/XYZ.

Magnetic measurements

Fits of magnetic data such as (T), $^{-1}$(T), T(T), (T), M(H), etc., to an analytical expression must include both the Hamiltonian from which the analytical expression is derived and the final analytical expression and fitting parameters. When the value of an exchange coupling constant, J, is given in the abstract, the form of the Hamiltonian must also be included. The expressions may be included in the manuscript or, if long and complex, as Supporting Information; if the latter method is used, it should be noted as such in the "Supporting Information Available" paragraph at the end of the manuscript. In addition, how the sample was measured (in a gelatin capsule, Teflon capsule, etc.) and the diamagnetic correction for the sample holder, as well as the diamagnetic correction for the material, must be provided and the manner in which it was calculated (Pascal's constants) or measured stated.

NMR Spectra

Please follow the specific guidelines for presenting NMR spectroscopic data (as text and as spectra).

Language and Editing Services

A well-written paper helps share your results most clearly. ACS Publications' English Editing Service is designed to help scientists communicate their research effectively. Our subject-matter expert editors will edit your manuscript for grammar, spelling, and other language errors so your ideas are presented at their best.

Preparing Graphics

The quality of illustrations in ACS journals and partner journals depends on the quality of the original files provided by the authors. Figures are not modified or enhanced by journal production staff. All graphics must be prepared and submitted in digital format.

Graphics should be inserted into the main body whenever possible. Please see Appendix 2 for additional information.

Any graphic (figure chart, scheme, or equation) that has appeared in an earlier publication should include a credit line citing the original source. Authors are responsible for obtaining written permission to re-use this material.

Figure and Illustration Services

The impact of your research is not limited to what you can express with words. Tables and figures such as graphs, photographs, illustrations, diagrams, and other visuals can play a significant role in effectively communicating your findings. Our Figures service generates publication-ready figures that conform to your chosen journal's specifications. This includes changes to file type, resolution, color space, font, scale, line weights, and layout (to improve readability and professional appearance).

Preparing for Submission

Manuscripts, graphics, supporting information, and required forms, as well as manuscript revisions, must all be submitted in digital format through ACS Paragon Plus, which requires an ACS ID to log in. Registering for an ACS ID is fast, free, and does not require an ACS membership. Please refer to Appendix 1 for additional information on preparing your submission

Prior Publication Policy

Inorganic Chemistry authors are allowed to deposit an initial draft of their manuscript in a preprint service such as ChemRxiv, bioRxiv, and arXiv prior to submission to the journal. Please note any use of a preprint server in the cover letter and include a link to the preprint, and as appropriate, state how the manuscript has been adjusted/updated between deposition and submission. The preprint should be cited as a reference in the manuscript. Authors are discouraged from posting a revised version of the preprint, or for depositing the initial version of manuscript as a preprint, after the manuscript has been submitted and a decision is pending. All other prior/redundant publication is forbidden.

Upon publication in *Inorganic Chemistry*, authors are advised to add a link from the preprint to the published paper via the Digital Object Identifier (DOI). Some services, such as ChemRxiv and bioRxiv, add this link for authors automatically after publication.

For the ACS Publications policy on theses and dissertations, click the American Chemical Society's Policy on Theses and Dissertations [PDF].

Providing Potential Reviewer Names

Please suggest four reviewers. Authors are encouraged to avoid suggesting reviewers from the authors' institutions. Do not suggest reviewers who may have a real or perceived conflict of interest. Whenever possible, suggest academic email addresses rather than personal email addresses.

Manuscript Transfer

If your submission is declined for publication by this journal, the editors might deem your work to be better suited for another ACS Publications journal or partner journal and suggest that the authors consider transferring the submission. Manuscript Transfer simplifies and shortens the process of submitting to another ACS journal or partner journal, as all the coauthors, suggested reviewers, manuscript files, and responses to submission questions are copied by ACS Paragon Plus to the new draft submission. Authors are free to accept or decline the transfer offer.

Note that each journal is editorially independent. Transferring a manuscript is not a guarantee that the manuscript will be accepted, as the final publication decision will belong to the editor of the next journal.

PRODUCTION AND PUBLICATION

Proofs via ACS Direct Correct

Correction of the galley proofs is the responsibility of the Corresponding Author. The Corresponding Author of an accepted manuscript will receive e-mail notification and complete instructions when page proofs are available for review via ACS Direct Correct. Extensive or important changes on page proofs, including changes to the title or list of authors, are subject to review by the editor.

It is the responsibility of the Corresponding Author to ensure that all authors listed on the manuscript agree with the changes made on the proofs. Galley proofs should be returned within 48 hours in order to ensure timely publication of the manuscript.

Publication Date and Patent Dates

Accepted manuscripts will be published on the ACS Publications Web site as soon as page proofs are corrected and all author concerns are resolved. The first date on which the document is published on the Web is considered the publication date.

Publication of manuscripts on the Web may occur weeks in advance of the cover date of the issue of publication. Authors should take this into account when planning their patent and intellectual property activities related to a document and should ensure that all patent information is available at the time of first publication, whether ASAP or issue publication.

All articles published ahead of print receive a unique Digital Object Identifier (DOI) number, which is used to cite the manuscript before and after the paper appears in an issue. Additionally, any supplemental information submitted along with the manuscript will automatically be assigned a DOI and hosted on Figshare to promote open data discoverability and use of your research outputs.

ASAP Publication

Manuscripts will be published on the “Articles ASAP” page on the Web as soon as page proofs are corrected and all author concerns are resolved. ASAP publication usually occurs within a few working days of receipt of page proof corrections, which can be several weeks in advance of the cover date of the issue.

Post-Publication Policies

The American Chemical Society follows guidance from the Committee on Publication Ethics (COPE) when considering any ethical concerns regarding a published article, Retractions, and Expressions of Concern.

Additions and Corrections

Additions and Corrections may be requested by the author(s) or initiated by the Editor to address important issues or correct errors and omissions of consequence that arise after publication of an article. All Additions and Corrections are subject to approval by the Editor, and should bring new and directly relevant information and corrections that fix scientific facts. Minor corrections and additions will not be published. Readers who detect errors of consequence in the work of others should contact the corresponding author of that work.

Additions and Corrections must be submitted as new manuscripts via ACS Paragon Plus by the Corresponding Author for publication in the “Addition/Correction” section of the Journal. The corresponding author should obtain approval from all coauthors prior to submitting or provide evidence that such approval has been solicited. The manuscript should include the original article title and author list, citation including DOI, and details of the correction.

Retractions

Articles may be retracted for scientific or ethical reasons and may be requested by the article author(s) or by the journal Editor(s), but are ultimately published at the discretion of the Editor. Articles that contain seriously flawed or erroneous data such that their findings and conclusions cannot be relied upon may be retracted in order to correct the scientific record. When an article is retracted, a notice of Retraction will be published containing information about the reason for the Retraction. The originally published article will remain online except in extraordinary circumstances (e.g. where deemed legally necessary, or if the availability of the published content poses public health risks).

Expressions of Concern

Expressions of Concern may be issued at the discretion of the Editor if:

- there is inconclusive evidence of research or publication misconduct by the authors;
- there is evidence that the findings are unreliable but the authors’ institution will not investigate the case;
- an investigation into alleged misconduct related to the publication either has not been, or would not be, fair and impartial or conclusive;
- an investigation is underway but a judgment will not be available for a considerable time.
- Upon completion of any related investigation, and when a final determination is made about the outcome of the article, the Expression of Concern may be replaced with a Retraction notice or Correction.

Sharing Your Published Article

At ACS Publications, we know it is important for you to be able to share your peer reviewed, published work with colleagues in the global community of scientists. As sharing on sites known as scholarly collaboration networks (SCNs) is becoming increasingly prevalent in today’s scholarly research ecosystem, we would like to remind you of the many ways in which you, a valued ACS author, can share your published work.

Publishing open access makes it easy to share your work with friends, colleagues, and family members. In addition, ACS Publications makes it easy to share your newly published research with ACS Articles on Request (see below). Don't forget to promote your research and related data on social media, at conferences, and through scholarly communication networks. Increase the impact of your research using the following resources: Altmetrics, Figshare, ACS Certified Deposit

E-Prints

When your article is published in an ACS journal or partner journal, corresponding authors are provided with a link that offers up to 50 free digital prints of the final published work. This link is valid for the first 12 months following online publication, and can be shared via email or an author's website. After one year, the access restrictions to your article will be lifted, and you can share the Articles on Request URL on social media and other channels. To access all your Articles on Request links, log in to your ACS Publishing Center account and visit the "My Published Manuscripts" page.

Reprints

Article, journal, and commercial reprints are available to order.

Appendix 1: PREPARING FOR SUBMISSION

We've developed ACS' publishing and editorial policies in consultation with the research communities that we serve, including authors and librarians. Browse our policies below to learn more.

Ethical Guidelines

ACS editors have provided Ethical Guidelines for persons engaged in the publication of chemical research—specifically, for editors, authors, and reviewers. Each journal also has a specific policy on prior publication.

Safety Considerations

Authors must emphasize any unexpected, new, and/or significant hazards or risks associated with the reported work. This information should be in the Experimental Section of the full article and included in the main text of a letter.

Conflict of Interest Disclosure

A statement describing any financial conflicts of interest or lack thereof is published in each ACS journal and partner journal article.

During the submission process, the Corresponding Author must provide a statement on behalf of all authors of the manuscript, describing all potential sources of bias, including affiliations, funding sources, and financial or management relationships, that may constitute conflicts of interest. If the manuscript is accepted, the statement will be published in the final article.

If the manuscript is accepted and no conflict of interest has been declared, the following statement will be published in the final article: "The authors declare no competing financial interest."

Plagiarism

In publishing only original research, ACS is committed to deterring plagiarism, including self-plagiarism. ACS Publications uses CrossCheck's iThenticate software to screen submitted

manuscripts for similarity to published material. Note that your manuscript may be screened during the submission process.

Further information about plagiarism can be found in Part B of the Ethical Guidelines to Publication of Chemical Research. See also the press release regarding ACS' participation in the CrossCheck initiative.

Author List and Coauthor Notification

Authors are required to obtain the consent of all their coauthors prior to submitting a manuscript. The submitting author accepts the responsibility of notifying all coauthors that the manuscript is being submitted.

If any change in authorship is necessary after a manuscript has been submitted, the Corresponding Author must e-mail a signed letter to the Editor-in-Chief confirming that all of the original coauthors have been notified and have agreed to the change. If the change involves the removal of a coauthor's name, the Corresponding Author must, in addition, arrange for the coauthor involved to e-mail a separate signed letter to the Editor-in-Chief consenting to the change. No changes in the author list will be permitted after a manuscript has been accepted.

During manuscript submission, the submitting author must provide contact information (full name, email address, institutional affiliation, and mailing address) for all of the coauthors. Because all of the author names are automatically imported into the electronic Journal Publishing Agreement, the names must be entered into ACS Paragon Plus in the same sequence as they appear on the first page of the manuscript. (Note that coauthors are not required to register in ACS Paragon Plus.)

Patent Activities and Intellectual Property

Authors are responsible for ensuring that all patent activities and intellectual property issues are satisfactorily resolved prior to first publication (Just Accepted, ASAP, or in issue). Acceptance and publication will not be delayed for pending or unresolved issues of this nature.

Open Researcher and Contributor ID (ORCID)

Authors submitting manuscript revisions are required to provide their own personal, validated ORCID iD before completing the submission, if an ORCID iD is not already associated with their ACS Paragon Plus user profiles. This ID may be provided during original manuscript submission or when submitting the manuscript revision. All authors are strongly encouraged to register for an ORCID iD, a unique researcher identifier. The ORCID iD will be displayed in the published article for any author on a manuscript who has a validated ORCID iD associated with ACS when the manuscript is accepted.

ORCID iDs should not be typed into the manuscript. ACS publishes only those ORCID iDs that have been properly verified and linked **before the manuscript is accepted**. After your ORCID iD is linked, it will be displayed automatically in all subsequently accepted manuscripts for any/all ACS journals. We do not publish ORCID iDs provided during proof review or via other communications after a manuscript is accepted for publication.

With an ORCID iD, you can create a profile of your research activities to distinguish yourself from other researchers with similar names, and make it easier for your colleagues to find your publications. If you do not yet have an ORCID iD, or you wish to associate your existing ORCID iD with your ACS Paragon Plus account, you may do so by clicking on "Edit Your Profile" from your ACS Paragon Plus account homepage and following the ORCID-related links. Learn more at www.orcid.org.

Copyright and Permissions

To obtain forms and guidelines for copyright transfer, obtaining permissions from copyright owners, and to explore a Copyright Learning Module for chemists, click here.

Funder Reporting Requirement

Authors are required to report funding sources and grant/award numbers. Enter **ALL** sources of funding for **ALL** authors in **BOTH** the Funder Registry Tool in ACS Paragon Plus and in your manuscript to meet this requirement.

Open Access Compliance

ACS offers options by which authors can fulfill the requirements of manuscript deposit for research funded by the National Institutes of Health, the Wellcome Trust, and the Austrian Science Fund. ACS offers options by which authors can fulfill the requirements for open access and deposition into repositories for funded research. Read more about Open Access Compliance and ACS Open Access initiatives.

Appendix 2: Preparing Graphics

Resolution

Digital graphics pasted into manuscripts should have the following minimum resolutions:

- Black and white line art, 1200 dpi
- Grayscale art, 600 dpi
- Color art, 300 dpi

Size

Graphics must fit a one- or two-column format. Single-column graphics can be sized up to 240 points wide (3.33 in.) and double-column graphics must be sized between 300 and 504 points (4.167 in. and 7 in.). The maximum depth for all graphics is 660 points (9.167 in.) including the caption (allow 12 pts. For each line of caption text). Lettering should be no smaller than 4.5 points in the final published format. The text should be legible when the graphic is viewed full-size. Helvetica or Arial fonts work well for lettering. Lines should be no thinner than 0.5 point.

Color

Color may be used to enhance the clarity of complex structures, figures, spectra, and schemes, etc., and color reproduction of graphics is provided at no cost to the author. Graphics intended to appear in black and white or grayscale should not be submitted in color.

Type of Graphics

Table of Contents (TOC)/Abstract Graphic

Consult the Guidelines for Table of Contents/Abstract Graphics for specifications.

Figures

A caption giving the figure number and a brief description must be included below each figure. The caption should be understandable without reference to the text. It is preferable to place any key to symbols used in the artwork itself, not in the caption. Ensure that any symbols and abbreviations used in the text agree with those in the artwork.

Charts

Charts (groups of structures that do not show reactions) may have a brief caption describing their contents.

Tables

Each table must have a brief (one phrase or sentence) title that describes the contents. The title should be understandable without reference to the text. Details should be put in footnotes, not in the title. Tables should be used when the data cannot be presented clearly in the narrative, when many numbers must be presented, or when more meaningful inter-relationships can be conveyed by the tabular format. Tables should supplement, not duplicate, information presented in the text and figures. Tables should be simple and concise.

Schemes

Each scheme (sequences of reactions) may have a brief caption describing its contents.

Chemical Structures

Chemical structures should be produced with the use of a drawing program such as ChemDraw.

Cover Art

The Editor-in-Chief's office will contact selected authors to invite submission of front cover artwork and provide specifications for preparing the cover. However, volunteer front cover suggestions will be considered. The journal is looking for aesthetically pleasing covers that are scientifically interesting and exhibit simplicity, clarity, and eye-catching color graphics. Caption/Tagline: Authors must submit a 3-4 sentence caption that describes the art and corresponding chemistry, and a 5-7 word tagline for the cover, which may be omitted by the EIC office if the artwork is self-explanatory. In so far as possible, please ensure that the authors or the image designer are the copyright holder of any content used for the cover; if not, additional steps may be necessary to prepare the cover for publication.

Inorganic Chemistry also offers authors to promote their work through Supplementary Covers. Submit your cover idea, artwork, and caption when submitting your manuscript revision in ACS Paragon Plus. If your article is accepted for publication, your suggestion may be selected for use on one of the journal's supplementary covers.

Web Enhanced Objects (WEO)

The Web editions of ACS journals allow readers to view multimedia attachments such as animations and movies that complement understanding of the research being reported.

WEOs should be uploaded in ACS Paragon Plus with ‘Web Enhanced Object’ selected as the file designation. Consult the list of compatible WEO formats.

Appendix - D

Author Instructions

Molecules

Chapter 5

molecules

MDPI

Type of the Paper (Article, Review, Communication, etc.)

Title

Firstname Lastname [1], Firstname Lastname [2] and Firstname Lastname [2,*]

[1] Affiliation 1; e-mail@e-mail.com
[2] Affiliation 2; e-mail@e-mail.com
* Correspondence: e-mail@e-mail.com; Tel.: (optional; include country code; if there are multiple corresponding authors, add author initials) +xx-xxxx-xxx-xxxx (F.L.)

Received: date; Accepted: date; Published: date

Abstract: A single paragraph of about 200 words maximum. For research articles, abstracts should give a pertinent overview of the work. We strongly encourage authors to use the following style of structured abstracts, but without headings: (1) Background: Place the question addressed in a broad context and highlight the purpose of the study; (2) Methods: Describe briefly the main methods or treatments applied; (3) Results: Summarize the article's main findings; and (4) Conclusions: Indicate the main conclusions or interpretations. The abstract should be an objective representation of the article, it must not contain results which are not presented and substantiated in the main text and should not exaggerate the main conclusions.

Keywords: keyword 1; keyword 2; keyword 3. List three to ten pertinent keywords specific to the article; yet reasonably common within the subject discipline.

0. How to Use This Template

The template details the sections that can be used in a manuscript. Note that each section has a corresponding style, which can be found in the 'Styles' menu of Word. Sections that are not mandatory are listed as such. The section titles given are for Articles. Review papers and other article types have a more flexible structure.

Remove this paragraph and start section numbering with 1. For any questions, please contact the editorial office of the journal or support@mdpi.com.

1. Introduction

The introduction should briefly place the study in a broad context and highlight why it is important. It should define the purpose of the work and its significance. The current state of the research field should be reviewed carefully and key publications cited. Please highlight controversial and diverging hypotheses when necessary. Finally, briefly mention the main aim of the work and highlight the principal conclusions. As far as possible, please keep the introduction comprehensible to scientists outside your particular field of research. References should be numbered in order of appearance and indicated by a numeral or numerals in square brackets, e.g., [1] or [2,3], or [4–6]. See the end of the document for further details on references.

2. Results

This section may be divided by subheadings. It should provide a concise and precise description of the experimental results, their interpretation as well as the experimental conclusions that can be drawn.

2.1. Subsection

2.1.1. Subsubsection

Bulleted lists look like this:

- First bullet
- Second bullet
- Third bullet

Numbered lists can be added as follows:

1. First item
2. Second item
3. Third item

The text continues here.

2.2. Figures, Tables and Schemes

All figures and tables should be cited in the main text as Figure 1, Table 1, etc.

(**a**) (**b**)

Figure 1. This is a figure, Schemes follow the same formatting. If there are multiple panels, they should be listed as: (**a**) Description of what is contained in the first panel; (**b**) Description of what is contained in the second panel. Figures should be placed in the main text near to the first time they are cited. A caption on a single line should be centered.

Table 1. This is a table. Tables should be placed in the main text near to the first time they are cited.

Title 1	Title 2	Title 3
entry 1	data	data
entry 2	data	data [1]

[1] Tables may have a footer.

2.3. Formatting of Chemical Structures

The chemical structures should be drawn with a professional program. For ChemDraw users, document settings from the template "ACS Document 1996" is recommended. Authors not using ChemDraw should adapt the setting parameters in Table 2. When a paper contains multiple structures, they should all be scaled to the same size.

Table 2. Parameters for chemical structures.

Item	Parameter
Drawing Settings	
chain angle	120 degrees
bond spacing	18% of length
fixed length	14.4 pt (0.2 in.)
bold width	2.0 pt (0.0278 in.)
line width	0.6 pt (0.0083 in.)
margin width	1.6 pt (0.0222 in.)
hash spacing	2.5 pt (0.0345 in.)
Text Settings	
page setup	US/Letter/Paper
scale	100%
font	Helvetica (Mac), Arial (PC)
size	10 pt
Preferences	
units	points
tolerances	3 pixels

2.4. Formatting of Mathematical Components

This is an example of an equation:

$$a = 1, \tag{1}$$

the text following an equation need not be a new paragraph. Please punctuate equations as regular text.

Theorem-type environments (including propositions, lemmas, corollaries etc.) can be formatted as follows:

Theorem 1. *Example text of a theorem. Theorems, propositions, lemmas,* etc. *should be numbered sequentially (i.e., Proposition 2 follows Theorem 1). Examples or Remarks use the same formatting, but should be numbered separately, so a document may contain Theorem 1, Remark 1 and Example 1.*

The text continues here. Proofs must be formatted as follows:

Proof of Theorem 1. Text of the proof. Note that the phrase 'of Theorem 1' is optional if it is clear which theorem is being referred to. Always finish a proof with the following symbol. □

The text continues here.

3. Discussion

Authors should discuss the results and how they can be interpreted in perspective of previous studies and of the working hypotheses. The findings and their implications should be discussed in the broadest context possible. Future research directions may also be highlighted.

4. Materials and Methods

Materials and Methods should be described with sufficient details to allow others to replicate and build on published results. Please note that publication of your manuscript implicates that you must make all materials, data, computer code, and protocols associated with the publication available to readers. Please disclose at the submission stage any restrictions on the availability of materials or information. New methods and protocols should be described in detail while well-established methods can be briefly described and appropriately cited.

Research manuscripts reporting large datasets that are deposited in a publicly available database should specify where the data have been deposited and provide the relevant accession numbers. If the accession numbers have not yet been obtained at the time of submission, please state that they will be provided during review. They must be provided prior to publication.

Interventionary studies involving animals or humans, and other studies require ethical approval must list the authority that provided approval and the corresponding ethical approval code.

5. Conclusions

This section is not mandatory, but can be added to the manuscript if the discussion is unusually long or complex.

6. Patents

This section is not mandatory, but may be added if there are patents resulting from the work reported in this manuscript.

Supplementary Materials: The following are available online at www.mdpi.com/xxx/s1, Figure S1: title, Table S1: title, Video S1: title.

Author Contributions: For research articles with several authors, a short paragraph specifying their individual contributions must be provided. The following statements should be used "Conceptualization, X.X. and Y.Y.; methodology, X.X.; software, X.X.; validation, X.X., Y.Y. and Z.Z.; formal analysis, X.X.; investigation, X.X.; resources, X.X.; data curation, X.X.; writing—original draft preparation, X.X.; writing—review and editing, X.X.; visualization, X.X.; supervision, X.X.; project administration, X.X.; funding acquisition, Y.Y. All authors have read and agreed to the published version of the manuscript.", please turn to the CRediT taxonomy for the term explanation. Authorship must be limited to those who have contributed substantially to the work reported.

Funding: Please add: "This research received no external funding" or "This research was funded by NAME OF FUNDER, grant number XXX" and "The APC was funded by XXX". Check carefully that the details given are accurate and use the standard spelling of funding agency names at https://search.crossref.org/funding, any errors may affect your future funding.

Acknowledgments: In this section you can acknowledge any support given which is not covered by the author contribution or funding sections. This may include administrative and technical support, or donations in kind (e.g., materials used for experiments).

Conflicts of Interest: Declare conflicts of interest or state "The authors declare no conflict of interest." Authors must identify and declare any personal circumstances or interest that may be perceived as inappropriately influencing the representation or interpretation of reported research results. Any role of the funders in the design of the study; in the collection, analyses or interpretation of data; in the writing of the manuscript, or in the decision to publish the results must be declared in this section. If there is no role, please state "The funders had no role in the design of the study; in the collection, analyses, or interpretation of data; in the writing of the manuscript, or in the decision to publish the results".

Appendix A

The appendix is an optional section that can contain details and data supplemental to the main text. For example, explanations of experimental details that would disrupt the flow of the main text, but nonetheless remain crucial to understanding and reproducing the research shown; figures of replicates for experiments of which representative data is shown in the main text can be added here if brief, or as Supplementary data. Mathematical proofs of results not central to the paper can be added as an appendix.

Appendix B

All appendix sections must be cited in the main text. In the appendixes, Figures, Tables, etc. should be labeled starting with 'A', e.g., Figure A1, Figure A2, etc.

References

References must be numbered in order of appearance in the text (including citations in tables and legends) and listed individually at the end of the manuscript. We recommend preparing the references with a bibliography software package, such as EndNote, ReferenceManager or Zotero to avoid typing mistakes and duplicated references. Include the digital object identifier (DOI) for all references where available.

Citations and References in Supplementary files are permitted provided that they also appear in the reference list here.

In the text, reference numbers should be placed in square brackets [ ], and placed before the punctuation; for example [1], [1–3] or [1,3]. For embedded citations in the text with pagination, use both parentheses and brackets to indicate the reference number and page numbers; for example [5] (p. 10), or [6] (pp. 101–105).

1. Author 1, A.B.; Author 2, C.D. Title of the article. *Abbreviated Journal Name* **Year**, *Volume*, page range.
2. Author 1, A.; Author 2, B. Title of the chapter. In *Book Title*, 2nd ed.; Editor 1, A., Editor 2, B., Eds.; Publisher: Publisher Location, Country, 2007; Volume 3, pp. 154–196.
3. Author 1, A.; Author 2, B. *Book Title*, 3rd ed.; Publisher: Publisher Location, Country, 2008; pp. 154–196.
4. Author 1, A.B.; Author 2, C. Title of Unpublished Work. *Abbreviated Journal Name* stage of publication (under review; accepted; in press).
5. Author 1, A.B. (University, City, State, Country); Author 2, C. (Institute, City, State, Country). Personal communication, 2012.
6. Author 1, A.B.; Author 2, C.D.; Author 3, E.F. Title of Presentation. In Title of the Collected Work (if available), Proceedings of the Name of the Conference, Location of Conference, Country, Date of Conference; Editor 1, Editor 2, Eds. (if available); Publisher: City, Country, Year (if available); Abstract Number (optional), Pagination (optional).
7. Author 1, A.B. Title of Thesis. Level of Thesis, Degree-Granting University, Location of University, Date of Completion.
8. Title of Site. Available online: URL (accessed on Day Month Year).

Sample Availability: Samples of the compounds ..... are available from the authors.

Appendix - E

Optimised Coordinates

Only in electronic version

Optimised Coordinates

Chapter 3: Electrochemical behavior of chloro- and hydroxy-subphthalocyanines

ClBSubPc$(F)_{12}$ – 1

Cl	0.000751000	3.576541000	0.000000000
N	0.681933000	1.107405000	1.181048000
N	-1.363701000	1.107981000	0.000000000
N	2.664162000	0.556956000	0.000000000
N	-1.332175000	0.557927000	2.307302000
C	1.983889000	0.691874000	1.141783000
C	2.255356000	0.175805000	2.473934000
C	1.014569000	0.176135000	3.190304000
C	-0.003188000	0.692371000	2.289030000
C	3.400408000	-0.349067000	3.060691000
C	3.322210000	-0.849672000	4.353778000
C	2.108792000	-0.849297000	5.054367000
C	0.950022000	-0.348384000	4.475464000
C	-1.980820000	0.692867000	1.147241000
C	-3.270266000	0.176852000	0.716374000
C	-4.350701000	-0.348389000	1.414750000
C	-5.431082000	-0.849881000	0.700573000

B	0.000217000	1.709297000	0.000000000
N	0.681933000	1.107405000	-1.181048000
N	-1.332175000	0.557927000	-2.307302000
C	1.983889000	0.691874000	-1.141783000
C	2.255356000	0.175805000	-2.473934000
C	1.014569000	0.176135000	-3.190304000
C	-0.003188000	0.692371000	-2.289030000
C	3.400408000	-0.349067000	-3.060691000
C	3.322210000	-0.849672000	-4.353778000
C	2.108792000	-0.849297000	-5.054367000
C	0.950022000	-0.348384000	-4.475464000
C	-1.980820000	0.692867000	-1.147241000
C	-3.270266000	0.176852000	-0.716374000
C	-4.350701000	-0.348389000	-1.414750000
C	-5.431082000	-0.849881000	-0.700573000
F	-0.187881000	-0.373283000	-5.167307000
F	2.081515000	-1.337479000	-6.294017000
F	4.409200000	-1.338238000	-4.950080000
F	4.568476000	-0.374560000	-2.421118000
F	4.568476000	-0.374560000	2.421118000
F	4.409200000	-1.338238000	4.950080000
F	2.081515000	-1.337479000	6.294017000
F	-0.187881000	-0.373283000	5.167307000
F	-4.380871000	-0.373628000	2.746118000
F	-6.490659000	-1.339003000	1.343896000

F	-6.490659000	-1.339003000	-1.343896000
F	-4.380871000	-0.373628000	-2.746118000

ClBSubPc$(H)_{12}$ – 2

Cl	0.000000000	-0.000298000	3.226731000
N	-1.181360000	-0.682055000	0.751305000
N	0.000000000	1.364003000	0.751441000
N	0.000000000	-2.663008000	0.194586000
N	-2.306293000	1.331597000	0.195197000
C	-1.144918000	-1.983307000	0.329372000
C	-2.473058000	-2.252799000	-0.201884000
C	-3.187571000	-1.015174000	-0.201863000
C	-2.290268000	0.000229000	0.329634000
C	-3.048705000	-3.403196000	-0.740697000
H	-2.498660000	-4.336202000	-0.755879000
C	-4.339332000	-3.316793000	-1.247760000
H	-4.813691000	-4.201754000	-1.655971000
C	-5.042275000	-2.099267000	-1.247698000
H	-6.045859000	-2.067570000	-1.655932000
C	-4.471719000	-0.938409000	-0.740601000
H	-5.004684000	0.004445000	-0.755491000
C	-1.145262000	1.983275000	0.329948000
C	-0.714510000	3.268189000	-0.201434000

C	-1.423054000	4.341705000	-0.740553000
H	-2.506093000	4.331802000	-0.755627000
C	-0.702941000	5.415995000	-1.248137000
H	-1.232149000	6.269089000	-1.656763000
B	0.000000000	-0.000097000	1.344753000
N	1.181360000	-0.682055000	0.751305000
N	2.306293000	1.331597000	0.195197000
C	1.144918000	-1.983307000	0.329372000
C	2.473058000	-2.252799000	-0.201884000
C	3.187571000	-1.015174000	-0.201863000
C	2.290268000	0.000229000	0.329634000
C	3.048705000	-3.403196000	-0.740697000
H	2.498660000	-4.336202000	-0.755879000
C	4.339332000	-3.316793000	-1.247760000
H	4.813691000	-4.201754000	-1.655971000
C	5.042275000	-2.099267000	-1.247698000
H	6.045859000	-2.067570000	-1.655932000
C	4.471719000	-0.938409000	-0.740601000
H	5.004684000	0.004445000	-0.755491000
C	1.145262000	1.983275000	0.329948000
C	0.714510000	3.268189000	-0.201434000
C	1.423054000	4.341705000	-0.740553000
H	2.506093000	4.331802000	-0.755627000
C	0.702941000	5.415995000	-1.248137000
H	1.232149000	6.269089000	-1.656763000

ClBSubPc$(F)_3(H)_9$

Cl	0.000375000	0.000196000	3.400735000
N	-0.300117000	-1.330465000	0.926806000
N	-1.002165000	0.925286000	0.926787000
N	1.955915000	-1.806639000	0.368666000
N	-2.542598000	-0.790544000	0.369162000
C	0.680009000	-2.186483000	0.503235000
C	-0.022913000	-3.343213000	-0.028356000
C	-1.417066000	-3.028993000	-0.026527000
C	-1.553746000	-1.681002000	0.505779000
C	0.430139000	-4.545911000	-0.572254000
H	1.487704000	-4.777559000	-0.590977000
C	-0.503067000	-5.436625000	-1.082208000
H	-0.206824000	-6.390182000	-1.500595000
C	-1.863301000	-5.104649000	-1.067037000
C	-2.351648000	-3.912418000	-0.564220000
H	-3.410384000	-3.690550000	-0.589301000
C	-2.233627000	0.504376000	0.503526000
C	-2.884099000	1.691406000	-0.028020000
C	-4.152382000	1.900345000	-0.571511000
H	-4.881867000	1.100361000	-0.589675000
C	-4.457290000	3.153788000	-1.081613000
H	-5.431388000	3.373995000	-1.499607000

B	0.000122000	0.000110000	1.522496000
N	1.302408000	0.405360000	0.926523000
N	0.586610000	2.597117000	0.368109000
C	2.232718000	-0.505059000	0.505398000
C	3.331789000	0.287315000	-0.026859000
C	2.906898000	1.651822000	-0.028563000
C	1.553590000	1.682158000	0.502802000
C	4.564188000	-0.080331000	-0.564478000
H	4.901376000	-1.108169000	-0.589639000
C	5.352707000	0.938766000	-1.066893000
C	4.960193000	2.282782000	-1.081852000
H	5.638027000	3.016160000	-1.499914000
C	3.722113000	2.645581000	-0.572120000
H	3.394032000	3.677314000	-0.590677000
C	-0.678947000	2.186016000	0.505147000
C	-1.914822000	2.741586000	-0.026852000
C	-2.212704000	3.992549000	-0.564779000
H	-1.491151000	4.798455000	-0.590300000
C	-3.489581000	4.165730000	-1.067094000
F	6.561732000	0.629515000	-1.578006000
F	-3.826320000	5.367244000	-1.578551000
F	-2.735613000	-5.996950000	-1.578394000

ClBSubPc$(F)_6(H)_6$

Cl	0.000724000	3.548356000	0.000000000
N	0.681996000	1.075193000	1.181103000
N	-1.363734000	1.075727000	0.000000000
N	2.661969000	0.514424000	0.000000000
N	-1.331035000	0.515362000	2.305373000
C	1.982298000	0.651455000	1.143800000
C	2.250382000	0.118991000	2.470343000
C	1.013979000	0.119301000	3.184164000
C	-0.000603000	0.651935000	2.288626000
C	3.403392000	-0.425114000	3.037712000
H	4.349075000	-0.453142000	2.512309000
C	3.304535000	-0.932105000	4.317148000
C	2.085838000	-0.931741000	5.020757000
C	0.928596000	-0.424457000	4.466504000
H	0.000717000	-0.452014000	5.022763000
C	-1.981724000	0.652405000	1.144826000
C	-3.264620000	0.119990000	0.713836000
C	-4.332265000	-0.424362000	1.428825000
H	-4.350021000	-0.452235000	2.510515000
C	-5.390611000	-0.932017000	0.703614000
B	0.000237000	1.673129000	0.000000000
N	0.681996000	1.075193000	-1.181103000
N	-1.331035000	0.515362000	-2.305373000
C	1.982298000	0.651455000	-1.143800000
C	2.250382000	0.118991000	-2.470343000

C	1.013979000	0.119301000	-3.184164000
C	-0.000603000	0.651935000	-2.288626000
C	3.403392000	-0.425114000	-3.037712000
H	4.349075000	-0.453142000	-2.512309000
C	3.304535000	-0.932105000	-4.317148000
C	2.085838000	-0.931741000	-5.020757000
C	0.928596000	-0.424457000	-4.466504000
H	0.000717000	-0.452014000	-5.022763000
C	-1.981724000	0.652405000	-1.144826000
C	-3.264620000	0.119990000	-0.713836000
C	-4.332265000	-0.424362000	-1.428825000
H	-4.350021000	-0.452235000	-2.510515000
C	-5.390611000	-0.932017000	-0.703614000
F	4.381478000	-1.450219000	-4.924495000
F	-6.454800000	-1.450488000	-1.332739000
F	2.073072000	-1.449465000	6.257243000
F	2.073072000	-1.449465000	-6.257243000
F	-6.454800000	-1.450488000	1.332739000
F	4.381478000	-1.450219000	4.924495000

(HO)BSubPc($C_{12}H_{25}$)$_6$(H)$_6$ – 3

Cl	-0.647687000	-0.048152000	1.441959000
N	-1.538953000	0.529048000	-1.178065000
N	0.806486000	0.591644000	-0.896259000
N	-2.543180000	-1.531116000	-1.772396000

N	-0.349398000	2.525133000	-1.623876000
C	-2.575519000	-0.191825000	-1.700067000
C	-3.437389000	0.783168000	-2.358468000
C	-2.764598000	2.051956000	-2.295095000
C	-1.492159000	1.822804000	-1.615561000
C	-4.646911000	0.629841000	-3.053304000
C	-5.150903000	1.778584000	-3.664837000
C	-4.505063000	3.016384000	-3.588662000
C	-3.301748000	3.195379000	-2.904120000
C	0.794668000	1.880956000	-1.348260000
C	2.174799000	2.180130000	-1.712804000
C	2.768887000	3.348927000	-2.216106000
C	4.115180000	3.249354000	-2.566197000
B	-0.420784000	-0.103449000	-0.432959000
N	-0.318663000	-1.484003000	-0.969700000
N	2.034246000	-1.406443000	-1.221113000
C	-1.392008000	-2.155728000	-1.482255000
C	-0.878709000	-3.462808000	-1.884851000
C	0.549078000	-3.417398000	-1.723655000
C	0.880747000	-2.091068000	-1.215461000
C	-1.517493000	-4.587081000	-2.427870000
C	-0.683556000	-5.636926000	-2.816548000
C	0.705976000	-5.588839000	-2.668703000
C	1.364605000	-4.489524000	-2.116254000
C	1.977312000	-0.068174000	-1.144995000

C	2.918104000	0.958764000	-1.580557000
C	4.273502000	0.886693000	-1.938121000
C	4.842487000	2.061462000	-2.428269000
C	5.105341000	-0.359990000	-1.756561000
H	4.493109000	-1.244284000	-1.946139000
H	5.909512000	-0.351427000	-2.498034000
C	5.704739000	-0.461490000	-0.337146000
H	4.883941000	-0.453834000	0.387149000
H	6.295987000	0.437826000	-0.132835000
C	6.553291000	-1.721309000	-0.102424000
H	6.820236000	-1.762259000	0.959312000
H	5.927941000	-2.603041000	-0.284374000
C	7.829519000	-1.845837000	-0.954383000
H	8.297662000	-2.810332000	-0.728550000
H	7.557603000	-1.898367000	-2.014645000
C	8.865815000	-0.721813000	-0.775546000
H	8.423477000	0.233624000	-1.080005000
H	9.687298000	-0.898083000	-1.479063000
C	9.436037000	-0.556313000	0.644546000
H	10.108502000	0.308493000	0.645972000
H	8.625661000	-0.294908000	1.334061000
C	10.176808000	-1.779854000	1.214084000
H	10.488892000	-1.544579000	2.239050000
H	9.477362000	-2.618558000	1.303754000
C	11.407953000	-2.250559000	0.421627000

H	11.112413000	-2.536007000	-0.595225000
H	11.785332000	-3.168354000	0.888814000
C	12.552469000	-1.231748000	0.347393000
H	12.214236000	-0.325072000	-0.167939000
H	12.822835000	-0.919731000	1.364899000
C	13.799121000	-1.771385000	-0.363282000
H	13.528032000	-2.091049000	-1.378094000
H	14.148839000	-2.674082000	0.154508000
C	14.948770000	-0.760593000	-0.444753000
H	14.600976000	0.139893000	-0.965499000
H	15.218435000	-0.439403000	0.568692000
C	16.190525000	-1.310722000	-1.152255000
H	15.960730000	-1.608498000	-2.180179000
H	16.990473000	-0.566359000	-1.193639000
C	2.011743000	4.648730000	-2.353150000
H	1.020365000	4.440607000	-2.761311000
H	2.530397000	5.283611000	-3.077396000
C	1.829149000	5.412318000	-1.020129000
H	1.145047000	6.247919000	-1.200812000
H	1.315012000	4.755089000	-0.312418000
C	3.122449000	5.927451000	-0.367847000
H	2.872505000	6.314004000	0.626113000
H	3.796529000	5.081782000	-0.192700000
C	3.888285000	7.006963000	-1.154369000
H	4.198597000	6.602763000	-2.124689000

H	4.820784000	7.221524000	-0.620527000
C	3.129527000	8.322813000	-1.404482000
H	3.757493000	8.968070000	-2.028586000
H	2.235747000	8.119985000	-2.005234000
C	2.697484000	9.095567000	-0.145009000
H	2.127336000	9.977178000	-0.463102000
H	1.996892000	8.483998000	0.434178000
C	3.833403000	9.555184000	0.784632000
H	4.391943000	8.685907000	1.152057000
H	3.383684000	10.015008000	1.673019000
C	4.811485000	10.555710000	0.155780000
H	5.315190000	10.097728000	-0.703608000
H	4.246423000	11.408727000	-0.242860000
C	5.872167000	11.067345000	1.137797000
H	6.431696000	10.214040000	1.542672000
H	5.373858000	11.536785000	1.995841000
C	6.854920000	12.065789000	0.516117000
H	7.355900000	11.595916000	-0.340420000
H	6.295942000	12.918529000	0.109020000
C	7.914044000	12.580972000	1.497460000
H	8.472895000	11.729422000	1.904320000
H	7.414129000	13.051664000	2.352709000
C	-2.654961000	4.562785000	-2.825519000
H	-2.483791000	4.924288000	-3.846233000
H	-1.673401000	4.476342000	-2.360579000

C	-3.513742000	5.611654000	-2.081085000
H	-3.025965000	6.586783000	-2.186099000
H	-4.478416000	5.705720000	-2.591536000
C	-3.774413000	5.310595000	-0.595860000
H	-4.542278000	6.003410000	-0.234601000
H	-4.215371000	4.311457000	-0.509090000
C	-2.545199000	5.385405000	0.327210000
H	-1.781280000	4.683163000	-0.022086000
H	-2.839989000	5.023107000	1.318064000
C	-1.898538000	6.775411000	0.466219000
H	-1.005573000	6.675152000	1.092532000
H	-1.529611000	7.107128000	-0.511183000
C	-2.801492000	7.883042000	1.039446000
H	-2.228808000	8.818733000	1.053804000
H	-3.639053000	8.060503000	0.355288000
C	-3.365002000	7.630070000	2.447923000
H	-3.984886000	6.725505000	2.445600000
H	-4.044085000	8.454309000	2.698451000
C	-2.306524000	7.512902000	3.552025000
H	-1.648068000	6.660075000	3.350295000
H	-1.665091000	8.404071000	3.532006000
C	-2.908241000	7.354698000	4.953426000
H	-3.555877000	6.468561000	4.970092000
H	-3.561376000	8.211264000	5.165407000
C	-1.858781000	7.232634000	6.063818000

H	-1.207253000	6.374502000	5.853763000
H	-1.208988000	8.117518000	6.047419000
C	-2.460366000	7.076149000	7.465134000
H	-3.109086000	6.191991000	7.481702000
H	-3.111066000	7.933652000	7.675901000
C	2.863721000	-4.480916000	-1.931821000
H	3.256690000	-3.514497000	-2.255692000
H	3.302658000	-5.240922000	-2.584774000
C	3.318128000	-4.714204000	-0.471700000
H	4.402011000	-4.563484000	-0.429104000
H	2.884091000	-3.929814000	0.155216000
C	2.958702000	-6.083907000	0.126180000
H	3.202137000	-6.063587000	1.193964000
H	1.873261000	-6.223005000	0.075279000
C	3.637343000	-7.302257000	-0.525906000
H	3.338933000	-7.368769000	-1.578368000
H	3.237557000	-8.207567000	-0.055587000
C	5.175153000	-7.330748000	-0.461122000
H	5.525320000	-8.214508000	-1.005721000
H	5.579579000	-6.473103000	-1.010555000
C	5.785193000	-7.327239000	0.952326000
H	6.877551000	-7.304125000	0.853851000
H	5.514689000	-6.396003000	1.462307000
C	5.398472000	-8.510876000	1.855001000
H	4.312092000	-8.529307000	2.003503000

H	5.829985000	-8.338781000	2.848531000
C	5.862800000	-9.882792000	1.349512000
H	5.401171000	-10.100893000	0.379262000
H	6.945783000	-9.852491000	1.170491000
C	5.542998000	-11.026144000	2.319844000
H	4.460991000	-11.052357000	2.503366000
H	6.009415000	-10.816688000	3.291197000
C	6.004120000	-12.401377000	1.824516000
H	5.536511000	-12.612928000	0.853951000
H	7.086058000	-12.375887000	1.639847000
C	5.686332000	-13.544228000	2.795611000
H	4.605402000	-13.570585000	2.979614000
H	6.153570000	-13.333423000	3.765238000
H	-4.958345000	3.869462000	-4.082976000
H	-6.079704000	1.707771000	-4.221083000
H	-1.128745000	-6.527055000	-3.248927000
H	1.295418000	-6.439445000	-2.994536000
H	4.616769000	4.125270000	-2.963977000
H	5.888727000	2.052415000	-2.717302000
C	-5.380982000	-0.688145000	-3.126132000
H	-4.660293000	-1.485893000	-3.319021000
H	-6.066843000	-0.661943000	-3.977947000
C	-6.156799000	-1.047500000	-1.837035000
H	-6.526356000	-2.072953000	-1.940801000
H	-5.449605000	-1.069550000	-1.002549000

C	-7.318484000	-0.107400000	-1.476509000
H	-7.685364000	-0.385376000	-0.482526000
H	-6.934205000	0.913283000	-1.372501000
C	-8.498699000	-0.085279000	-2.464806000
H	-8.150940000	0.263489000	-3.443885000
H	-9.212912000	0.673515000	-2.125990000
C	-9.233626000	-1.422731000	-2.666544000
H	-10.006079000	-1.277861000	-3.429823000
H	-8.541731000	-2.159157000	-3.090774000
C	-9.870770000	-2.033069000	-1.405002000
H	-10.322915000	-2.993864000	-1.680550000
H	-9.084406000	-2.273509000	-0.681016000
C	-10.935480000	-1.171835000	-0.704911000
H	-10.493478000	-0.223080000	-0.377594000
H	-11.243134000	-1.687151000	0.213080000
C	-12.184267000	-0.882892000	-1.547718000
H	-11.907229000	-0.321187000	-2.447598000
H	-12.607777000	-1.832461000	-1.900959000
C	-13.261593000	-0.101188000	-0.786566000
H	-12.835169000	0.843946000	-0.426009000
H	-13.550720000	-0.664067000	0.110377000
C	-14.512293000	0.195845000	-1.621325000
H	-14.224230000	0.760663000	-2.517660000
H	-14.939256000	-0.748650000	-1.983219000
C	-15.590067000	0.976139000	-0.859980000

H	-15.163806000	1.919784000	-0.498318000
H	-15.879022000	0.411660000	0.034889000
C	-3.020644000	-4.699956000	-2.577456000
H	-3.250080000	-4.892301000	-3.632101000
H	-3.484829000	-3.745722000	-2.330327000
C	-3.643418000	-5.836853000	-1.734081000
H	-4.701310000	-5.920977000	-2.005254000
H	-3.185270000	-6.787458000	-2.027988000
C	-3.501647000	-5.676007000	-0.211378000
H	-3.792611000	-6.619812000	0.262557000
H	-2.442657000	-5.538277000	0.033200000
C	-4.303806000	-4.521840000	0.415667000
H	-4.008123000	-3.575570000	-0.049059000
H	-4.009164000	-4.432639000	1.466916000
C	-5.835384000	-4.648490000	0.326137000
H	-6.278243000	-3.737121000	0.742017000
H	-6.140721000	-4.663217000	-0.726488000
C	-6.450406000	-5.876909000	1.021499000
H	-7.533731000	-5.861731000	0.848720000
H	-6.087291000	-6.789939000	0.536169000
C	-6.195825000	-5.991623000	2.533948000
H	-5.118591000	-6.058221000	2.727973000
H	-6.619061000	-6.942054000	2.881553000
C	-6.789962000	-4.853375000	3.373320000
H	-6.340514000	-3.897704000	3.079628000

H	-7.862312000	-4.765773000	3.153301000
C	-6.598042000	-5.049057000	4.881933000
H	-5.526444000	-5.143958000	5.100095000
H	-7.054204000	-6.000794000	5.184145000
C	-7.186309000	-3.915340000	5.729213000
H	-6.728603000	-2.963794000	5.429085000
H	-8.257952000	-3.818198000	5.510919000
C	-6.995956000	-4.111223000	7.237685000
H	-5.925470000	-4.207358000	7.455977000
H	-7.453299000	-5.061805000	7.538302000
C	-16.835281000	1.268945000	-1.701886000
H	-17.304629000	0.343058000	-2.049055000
H	-17.583078000	1.825669000	-1.130424000
H	-16.583979000	1.862650000	-2.586462000
C	-7.586585000	-2.973823000	8.075904000
H	-7.123562000	-2.014888000	7.822934000
H	-8.663353000	-2.874961000	7.905598000
H	-7.434187000	-3.143731000	9.145347000
C	6.151306000	-14.913973000	2.292953000
H	5.674170000	-15.168947000	1.341402000
H	7.234040000	-14.929931000	2.133223000
H	5.909894000	-15.705706000	3.007507000
C	8.891123000	13.577252000	0.866738000
H	9.632255000	13.924816000	1.591745000
H	9.432351000	13.124537000	0.029939000

H	8.365538000	14.456831000	0.481799000
C	-1.404759000	6.954102000	8.567824000
H	-1.865955000	6.843971000	9.553206000
H	-0.760671000	6.084518000	8.403782000
H	-0.761605000	7.839294000	8.599357000
H	16.583158000	-2.191334000	-0.634196000

(EtO)BSubPc(H)$_{12}$

B	0.012161000	0.000000000	1.233138000
O	0.006901000	0.000000000	2.653077000
C	1.180105000	0.000000000	3.454025000
H	1.795944000	0.884227000	3.239426000
H	1.795944000	-0.884227000	3.239426000
C	0.769621000	0.000000000	4.917413000
H	0.169739000	-0.884577000	5.143858000
H	0.169739000	0.884576000	5.143858000
H	1.650957000	-0.000001000	5.565454000
N	-0.708081000	1.180401000	0.611393000
N	1.341489000	-0.000001000	0.519140000
N	-2.713099000	0.000002000	0.151853000
N	1.270720000	2.305321000	-0.052508000
C	-2.024142000	1.143630000	0.252842000
C	-2.325263000	2.470517000	-0.271716000
C	-1.091188000	3.185876000	-0.334634000

C	-0.052014000	2.287051000	0.152592000
C	-3.500710000	3.041573000	-0.756911000
H	-4.432056000	2.489253000	-0.726186000
C	-3.441736000	4.330988000	-1.273065000
H	-4.346275000	4.801975000	-1.640457000
C	-2.227202000	5.035063000	-1.334978000
H	-2.216231000	6.036746000	-1.749132000
C	-1.042007000	4.467027000	-0.882220000
H	-0.101345000	5.000315000	-0.947054000
C	1.929106000	1.142986000	0.048190000
C	3.172291000	0.714326000	-0.575470000
C	4.202515000	1.422646000	-1.194953000
H	4.189819000	2.505686000	-1.211896000
C	5.236092000	0.703184000	-1.781002000
H	6.055620000	1.232469000	-2.253474000
N	-0.708082000	-1.180400000	0.611393000
N	1.270717000	-2.305323000	-0.052508000
C	-2.024144000	-1.143627000	0.252842000
C	-2.325267000	-2.470514000	-0.271716000
C	-1.091193000	-3.185874000	-0.334634000
C	-0.052018000	-2.287051000	0.152592000
C	-3.500714000	-3.041568000	-0.756911000
H	-4.432059000	-2.489247000	-0.726186000
C	-3.441742000	-4.330983000	-1.273065000
H	-4.346282000	-4.801968000	-1.640457000

C	-2.227210000	-5.035060000	-1.334978000
H	-2.216239000	-6.036743000	-1.749132000
C	-1.042014000	-4.467026000	-0.882220000
H	-0.101353000	-5.000315000	-0.947054000
C	1.929105000	-1.142989000	0.048190000
C	3.172290000	-0.714331000	-0.575470000
C	4.202513000	-1.422652000	-1.194953000
H	4.189815000	-2.505692000	-1.211896000
C	5.236091000	-0.703192000	-1.781002000
H	6.055618000	-1.232478000	-2.253474000

(MeO)BSubPc(H)$_{12}$

B	0.001190000	0.000000000	1.419526000
O	-0.040442000	0.000000000	2.838104000
C	1.115101000	0.000002000	3.654035000
H	1.737326000	0.889589000	3.493501000
H	1.737328000	-0.889583000	3.493501000
H	0.783788000	0.000001000	4.694478000
N	-0.702722000	1.180442000	0.779382000
N	1.348812000	0.000000000	0.740854000
N	-2.695074000	0.000000000	0.268011000
N	1.292651000	2.305298000	0.167131000
C	-2.008986000	1.143625000	0.386911000
C	-2.296453000	2.470538000	-0.145388000

C	-1.061162000	3.185886000	-0.176338000
C	-0.034953000	2.287039000	0.337747000
C	-3.458916000	3.041559000	-0.660856000
H	-4.390765000	2.489272000	-0.654170000
C	-3.386601000	4.330971000	-1.175388000
H	-4.281339000	4.801931000	-1.566071000
C	-2.170886000	5.035009000	-1.205879000
H	-2.149150000	6.036675000	-1.619645000
C	-0.997805000	4.466972000	-0.722532000
H	-0.055787000	5.000276000	-0.763010000
C	1.948446000	1.143079000	0.285228000
C	3.207349000	0.714356000	-0.305939000
C	4.253293000	1.422656000	-0.898617000
H	4.241031000	2.505699000	-0.915892000
C	5.301619000	0.703207000	-1.457778000
H	6.133070000	1.232481000	-1.908949000
N	-0.702723000	-1.180442000	0.779382000
N	1.292650000	-2.305298000	0.167131000
C	-2.008987000	-1.143624000	0.386911000
C	-2.296454000	-2.470537000	-0.145388000
C	-1.061163000	-3.185886000	-0.176338000
C	-0.034954000	-2.287040000	0.337747000
C	-3.458917000	-3.041558000	-0.660855000
H	-4.390766000	-2.489271000	-0.654170000
C	-3.386603000	-4.330970000	-1.175388000

H	-4.281341000	-4.801929000	-1.566070000
C	-2.170888000	-5.035008000	-1.205878000
H	-2.149152000	-6.036675000	-1.619645000
C	-0.997806000	-4.466972000	-0.722532000
H	-0.055789000	-5.000276000	-0.763009000
C	1.948446000	-1.143080000	0.285228000
C	3.207349000	-0.714358000	-0.305939000
C	4.253293000	-1.422658000	-0.898617000
H	4.241030000	-2.505701000	-0.915892000
C	5.301619000	-0.703209000	-1.457777000
H	6.133069000	-1.232484000	-1.908949000

(PhO)BSubPc(F)$_{12}$

B	0.011112000	0.000002000	1.267416000
C	-0.141949000	-2.289643000	0.222413000
C	0.773752000	-3.188121000	-0.463707000
C	0.621279000	-4.468507000	-0.981805000
C	1.677826000	-5.040361000	-1.678270000
C	2.872777000	-4.336946000	-1.879630000
C	3.033643000	-3.048436000	-1.388018000
C	1.994074000	-2.469490000	-0.670227000
C	1.809601000	-1.142369000	-0.105186000
C	1.809781000	1.142058000	-0.105207000
C	1.994452000	2.469132000	-0.670295000

C	3.034108000	3.047895000	-1.388105000
C	2.873435000	4.336411000	-1.879768000
C	1.678588000	5.040009000	-1.678443000
C	0.621952000	4.468337000	-0.981961000
C	0.774236000	3.187951000	-0.463811000
C	-0.141601000	2.289639000	0.222347000
C	-2.096259000	1.144467000	0.498089000
C	-3.448862000	0.716401000	0.171795000
C	-4.593777000	1.414573000	-0.191037000
C	-5.736027000	0.700758000	-0.530230000
C	-5.736135000	-0.699930000	-0.530210000
C	-4.593994000	-1.413910000	-0.190996000
C	-3.448972000	-0.715904000	0.171818000
C	-2.096435000	-1.144168000	0.498132000
F	-0.503528000	-5.163605000	-0.818059000
F	1.568917000	-6.276478000	-2.165476000
F	3.861661000	-4.926773000	-2.551691000
F	4.180118000	-2.405108000	-1.606723000
F	4.180489000	2.404390000	-1.606783000
F	3.862411000	4.926064000	-2.551847000
F	1.569862000	6.276123000	-2.165697000
F	-0.502751000	5.163608000	-0.818247000
F	-4.627806000	2.746480000	-0.211672000
F	-6.855913000	1.344937000	-0.859499000
F	-6.856120000	-1.343947000	-0.859458000

F	-4.628229000	-2.745814000	-0.211587000
N	0.603414000	-1.184902000	0.536930000
N	0.603595000	1.184799000	0.536909000
N	-1.425233000	0.000107000	0.811157000
N	2.455764000	-0.000206000	-0.359083000
N	-1.475639000	2.307621000	0.279347000
N	-1.475992000	-2.307418000	0.279423000
O	0.034644000	0.000001000	2.692960000
C	1.071051000	0.000021000	3.581332000
C	0.716422000	0.000105000	4.935546000
C	2.422848000	-0.000034000	3.226729000
C	1.698275000	0.000125000	5.917461000
C	3.400385000	-0.000004000	4.222641000
C	3.049277000	0.000073000	5.568030000
H	-0.336380000	0.000148000	5.190533000
H	2.730913000	-0.000096000	2.190490000
H	1.406695000	0.000188000	6.961862000
H	4.445349000	-0.000045000	3.933001000
H	3.814851000	0.000094000	6.334662000

$(F_5C_6O)BSubPc(F)_{12}$

B	-0.046984000	-0.000063000	0.689076000
C	0.372636000	2.293564000	-0.249152000
C	-0.312498000	3.188161000	-1.167186000

C	-0.018459000	4.467287000	-1.624938000
C	-0.830515000	5.033276000	-2.598360000
C	-1.915876000	4.325364000	-3.132915000
C	-2.209587000	3.038295000	-2.703660000
C	-1.419930000	2.465254000	-1.713177000
C	-1.404119000	1.140466000	-1.117500000
C	-1.404315000	-1.139779000	-1.117866000
C	-1.420350000	-2.464374000	-1.713967000
C	-2.210104000	-3.036963000	-2.704634000
C	-1.916609000	-4.323944000	-3.134304000
C	-0.831367000	-5.032210000	-2.599978000
C	-0.019215000	-4.466671000	-1.626375000
C	-0.313039000	-3.187643000	-1.168210000
C	0.372247000	-2.293457000	-0.249890000
C	2.185023000	-1.145513000	0.527503000
C	3.573940000	-0.716850000	0.589325000
C	4.774847000	-1.414943000	0.561386000
C	5.966248000	-0.701004000	0.554967000
C	5.966367000	0.699903000	0.555193000
C	4.775088000	1.414043000	0.561842000
C	3.574061000	0.716145000	0.589556000
C	2.185217000	1.145064000	0.527872000
F	1.010124000	5.165531000	-1.146349000
F	-0.588604000	6.267642000	-3.038590000
F	-2.669084000	4.910212000	-4.063903000

F	-3.241881000	2.390876000	-3.241207000
F	-3.242290000	-2.389198000	-3.241971000
F	-2.669917000	-4.908365000	-4.065480000
F	-0.589663000	-6.266475000	-3.040607000
F	1.009251000	-5.165242000	-1.148011000
F	4.812731000	-2.746574000	0.550976000
F	7.133163000	-1.344904000	0.551204000
F	7.133391000	1.343606000	0.551638000
F	4.813198000	2.745671000	0.551862000
N	-0.437242000	1.189203000	-0.146152000
N	-0.437444000	-1.188993000	-0.146534000
N	1.454321000	-0.000179000	0.631587000
N	-1.937295000	0.000459000	-1.556673000
N	1.642109000	-2.310167000	0.160835000
N	1.642500000	2.309928000	0.161578000
O	-0.393123000	-0.000269000	2.096957000
C	-1.505297000	-0.000382000	2.842521000
C	-1.330827000	-0.000802000	4.235989000
C	-2.820174000	-0.000113000	2.373671000
C	-2.410602000	-0.000942000	5.106012000
C	-3.910137000	-0.000253000	3.237369000
C	-3.710111000	-0.000668000	4.609633000
F	-3.056407000	0.000298000	1.047758000
F	-5.150375000	0.000018000	2.739173000
F	-4.752545000	-0.000804000	5.445997000

F	-2.205000000	-0.001345000	6.426240000
F	-0.090980000	-0.001075000	4.737058000

$(F_5C_6O)SubPc(H)_{12}$

B	-0.173917000	-0.281814000	-0.000234000
C	-1.067334000	0.222066000	-2.294820000
C	-1.079111000	1.372828000	-3.184526000
C	-1.605482000	1.561108000	-4.462880000
C	-1.536688000	2.831289000	-5.020371000
C	-0.981684000	3.910668000	-4.309487000
C	-0.482422000	3.745112000	-3.024218000
C	-0.516911000	2.468114000	-2.462875000
C	-0.160889000	1.975561000	-1.142224000
C	-0.160608000	1.974192000	1.144455000
C	-0.516314000	2.465163000	2.465779000
C	-0.481698000	3.741489000	3.028640000
C	-0.980658000	3.905506000	4.314224000
C	-1.535491000	2.825277000	5.023948000
C	-1.604412000	1.555763000	4.464956000
C	-1.078341000	1.369013000	3.186254000
C	-1.066776000	0.219317000	2.295169000
C	-2.059035000	-1.490741000	1.142624000
C	-3.147983000	-2.357401000	0.713519000
C	-4.136917000	-3.039316000	1.421564000

C	-5.099672000	-3.735811000	0.701081000
C	-5.099842000	-3.734968000	-0.704495000
C	-4.137262000	-3.037610000	-1.424376000
C	-3.148157000	-2.356545000	-0.715754000
C	-2.059313000	-1.489371000	-1.144083000
H	-2.050659000	0.732804000	-5.000416000
H	-1.922377000	2.998349000	-6.019391000
H	-0.950045000	4.889508000	-4.773712000
H	-0.072299000	4.578234000	-2.466642000
H	-0.071710000	4.575279000	2.471964000
H	-0.948914000	4.883791000	4.779610000
H	-1.920946000	2.991142000	6.023257000
H	-2.049459000	0.726816000	5.001606000
H	-4.145024000	-3.025007000	2.504625000
H	-5.868416000	-4.287030000	1.230089000
H	-5.868715000	-4.285553000	-1.233977000
H	-4.145631000	-3.022003000	-2.507417000
N	-0.352279000	0.616806000	-1.188959000
N	-0.351987000	0.615381000	1.189609000
N	-1.403438000	-1.138982000	-0.000600000
N	0.005820000	2.644282000	0.001495000
N	-1.840910000	-0.870910000	2.308772000
N	-1.841471000	-0.868144000	-2.309542000
O	0.958065000	-1.208161000	-0.000924000
C	2.289994000	-1.137365000	-0.000905000

C	2.987952000	-2.358135000	-0.001497000
C	3.067436000	0.024216000	-0.000377000
C	4.373142000	-2.410724000	-0.001557000
C	4.457647000	-0.018574000	-0.000428000
C	5.118974000	-1.236873000	-0.001018000
F	2.470737000	1.230326000	0.000196000
F	5.155640000	1.123470000	0.000093000
F	6.456784000	-1.284297000	-0.001071000
F	4.998371000	-3.593802000	-0.002131000
F	2.295829000	-3.503529000	-0.002019000

Chapter 4: Redox and photophysical properties of four SubPcs containing ferrocenylcarboxylic acid dyads as axial ligands

SubPc 5, (Fc(CH2)2COO)BSubPc(H)12

N	2.264162000	-1.165775000	-0.580717000

N	4.040330000	0.173371000	-1.375561000
N	2.089365000	1.182191000	-0.490887000
N	0.876751000	2.124320000	1.309416000
N	0.612998000	-0.161416000	0.764128000
N	1.151778000	-2.446668000	1.063764000
C	2.087311000	-2.316823000	0.120815000
C	3.263766000	-3.119195000	-0.153068000
C	4.157379000	-2.308591000	-0.908156000
C	3.517093000	-1.019929000	-1.087418000
C	3.640041000	-4.394767000	0.257581000
H	2.964354000	-5.002068000	0.849117000
C	4.890996000	-4.858791000	-0.114404000
H	5.200728000	-5.856197000	0.178828000
C	5.771781000	-4.059749000	-0.858563000
H	6.746033000	-4.454310000	-1.126689000
C	5.422830000	-2.777344000	-1.248788000
H	6.108166000	-2.149814000	-1.807189000
C	3.355413000	1.250071000	-0.993474000

C	3.824798000	2.587075000	-0.682110000
C	2.845186000	3.189339000	0.153518000
C	1.785593000	2.216444000	0.342098000
C	5.015198000	3.247923000	-0.969139000
H	5.769032000	2.776688000	-1.589562000
C	5.200175000	4.516697000	-0.444276000
H	6.111797000	5.060536000	-0.667820000
C	4.233116000	5.111451000	0.379352000
H	4.414773000	6.104206000	0.777037000
C	3.057517000	4.451663000	0.698831000
H	2.315663000	4.898897000	1.350562000
C	0.359296000	0.922073000	1.548777000
C	-0.248631000	0.391771000	2.754797000
C	-0.168418000	-1.025898000	2.677223000
C	0.491870000	-1.347527000	1.425769000
C	-0.764907000	1.012139000	3.887904000
H	-0.813381000	2.093307000	3.947076000
C	-1.222628000	0.209240000	4.920001000

H	-1.649953000	0.667806000	5.805207000
C	-1.141578000	-1.188897000	4.844829000
H	-1.505198000	-1.785323000	5.674793000
C	-0.602042000	-1.819357000	3.735032000
H	-0.520969000	-2.899101000	3.681025000
B	1.266911000	-0.059287000	-0.572244000
Fe	-4.521928000	-0.156162000	-0.571459000
C	-3.664566000	-0.277938000	-2.436544000
C	-3.213620000	-1.341531000	-1.600924000
H	-2.187965000	-1.536003000	-1.318661000
C	-4.343189000	-2.092288000	-1.171391000
H	-4.322191000	-2.942972000	-0.505271000
C	-5.502537000	-1.499973000	-1.740193000
H	-6.523263000	-1.818987000	-1.583828000
C	-5.084819000	-0.382563000	-2.514213000
H	-5.733724000	0.292172000	-3.056182000
C	-3.618140000	1.328866000	0.502556000
H	-2.660779000	1.756776000	0.239891000

C	-3.829891000	0.183540000	1.318991000
H	-3.060048000	-0.393993000	1.811119000
C	-5.225053000	-0.091091000	1.341393000
H	-5.702201000	-0.917610000	1.848754000
C	-5.877724000	0.884223000	0.538167000
H	-6.937146000	0.929602000	0.329132000
C	-4.883576000	1.761206000	0.021559000
H	-5.056871000	2.590830000	-0.649396000
C	-2.824592000	0.733421000	-3.169217000
C	-1.343485000	0.380186000	-3.238848000
C	-0.588084000	0.673919000	-1.965901000
O	-0.817738000	1.619314000	-1.248846000
O	0.390307000	-0.199647000	-1.737969000
H	-2.924606000	1.724299000	-2.715692000
H	-3.208333000	0.814769000	-4.191647000
H	-1.187578000	-0.662574000	-3.522714000
H	-0.860299000	0.992237000	-4.010604000

SubPc 6, (Fc(CH)2COO)BSubPc(H)12.

N	1.567735000	-0.398687000	1.313363000
N	2.664283000	-2.455570000	0.928257000
N	2.344526000	-0.922931000	-0.847523000
N	3.097488000	0.860641000	-2.206463000
N	1.746570000	1.294592000	-0.313959000
N	1.495778000	1.870058000	1.968758000
C	1.516634000	0.568980000	2.266477000
C	1.816654000	-0.104119000	3.515223000
C	2.178422000	-1.442707000	3.193176000
C	2.095170000	-1.572150000	1.751375000
C	1.888531000	0.352196000	4.828414000
H	1.632059000	1.378215000	5.066988000
C	2.291013000	-0.538787000	5.809490000
H	2.339132000	-0.211520000	6.842654000
C	2.647477000	-1.858153000	5.492076000
H	2.964412000	-2.526300000	6.285782000

C	2.609956000	-2.317797000	4.186058000
H	2.904004000	-3.330447000	3.934141000
C	2.854700000	-2.078671000	-0.334792000
C	3.841755000	-2.528805000	-1.298792000
C	3.978034000	-1.498101000	-2.267678000
C	3.070721000	-0.430733000	-1.888517000
C	4.656735000	-3.655515000	-1.342707000
H	4.563879000	-4.429987000	-0.589815000
C	5.577628000	-3.755259000	-2.373229000
H	6.212366000	-4.632425000	-2.440619000
C	5.711355000	-2.738682000	-3.330034000
H	6.446806000	-2.848530000	-4.119865000
C	4.927713000	-1.597075000	-3.279383000
H	5.039984000	-0.799811000	-4.005264000
C	2.494528000	1.705641000	-1.374400000
C	2.731852000	3.120598000	-1.156488000
C	2.231814000	3.436019000	0.136000000
C	1.697325000	2.208744000	0.696431000

C	3.396139000	4.080370000	-1.913443000
H	3.791706000	3.829476000	-2.891061000
C	3.527981000	5.353780000	-1.383494000
H	4.026015000	6.125154000	-1.961192000
C	3.035659000	5.664694000	-0.107604000
H	3.162368000	6.670746000	0.277975000
C	2.399015000	4.710213000	0.669252000
H	2.034955000	4.941274000	1.663926000
B	1.307909000	-0.121761000	-0.129382000
Fe	-5.706459000	-0.225097000	-0.256863000
C	-4.155219000	-1.395683000	-0.887898000
C	-4.897992000	-2.045461000	0.150479000
H	-4.497276000	-2.348224000	1.107924000
C	-6.237527000	-2.199178000	-0.284947000
H	-7.046056000	-2.631672000	0.286716000
C	-6.341294000	-1.641089000	-1.588951000
H	-7.244476000	-1.571636000	-2.178311000
C	-5.067685000	-1.141466000	-1.960382000

H	-4.833520000	-0.628536000	-2.882086000
C	-5.060061000	1.195965000	1.054536000
H	-4.144009000	1.134133000	1.624527000
C	-6.329899000	0.697401000	1.453233000
H	-6.550230000	0.189513000	2.381246000
C	-7.248824000	0.941500000	0.395737000
H	-8.290045000	0.652600000	0.380190000
C	-6.546364000	1.591004000	-0.656055000
H	-6.959741000	1.879712000	-1.611831000
C	-5.193582000	1.747542000	-0.249653000
H	-4.394929000	2.170523000	-0.842329000
C	-2.751027000	-1.045654000	-0.802000000
C	-1.987172000	-0.603320000	-1.810186000
C	-0.567420000	-0.256880000	-1.664508000
O	0.105320000	0.147199000	-2.587599000
O	-0.085990000	-0.425010000	-0.426637000
H	-2.281706000	-1.168085000	0.170999000
H	-2.373098000	-0.473258000	-2.815384000

SubPc 7, (Fc(CH2)2COO)BSubPc(F)12

N	2.052907000	-0.808362000	-1.005903000
N	3.394732000	1.056910000	-1.552473000
N	1.384904000	1.348425000	-0.336069000
N	0.199320000	1.549246000	1.701077000
N	0.379510000	-0.551840000	0.631054000
N	1.430535000	-2.651438000	0.333797000
C	2.202436000	-2.095155000	-0.598771000
C	3.480082000	-2.515781000	-1.136954000
C	4.088913000	-1.366161000	-1.722144000
C	3.175975000	-0.257130000	-1.534100000
C	4.165809000	-3.720360000	-1.085781000
C	5.436421000	-3.786241000	-1.631819000
C	6.033222000	-2.659208000	-2.205596000
C	5.371328000	-1.443793000	-2.244736000

C	2.538929000	1.823225000	-0.882290000
C	2.729000000	3.133130000	-0.291492000
C	1.738904000	3.282899000	0.722159000
C	0.952372000	2.065479000	0.736205000
C	3.693522000	4.111504000	-0.477989000
C	3.657936000	5.240848000	0.322858000
C	2.686580000	5.387957000	1.317453000
C	1.730718000	4.408728000	1.531577000
C	-0.015509000	0.239070000	1.664847000
C	-0.361372000	-0.676993000	2.734042000
C	0.016681000	-1.982969000	2.308265000
C	0.593487000	-1.849356000	0.985088000
C	-0.862213000	-0.475008000	4.010967000
C	-1.006909000	-1.568677000	4.848623000
C	-0.635682000	-2.849859000	4.430700000
C	-0.111977000	-3.064032000	3.166440000
B	0.840085000	-0.001133000	-0.680686000
Fe	-6.281630000	-0.143770000	-1.423575000

C	-4.325184000	-0.231240000	-1.995272000
C	-4.433894000	-0.277368000	-0.573937000
H	-4.004657000	0.448344000	0.101805000
C	-5.225074000	-1.404154000	-0.220492000
H	-5.519878000	-1.684430000	0.780923000
C	-5.607395000	-2.066505000	-1.419011000
H	-6.241882000	-2.938580000	-1.489644000
C	-5.050737000	-1.346494000	-2.511095000
H	-5.187859000	-1.577267000	-3.559071000
C	-6.957898000	1.781310000	-1.426114000
H	-6.328170000	2.657093000	-1.359315000
C	-7.508846000	1.064578000	-0.328727000
H	-7.367834000	1.298824000	0.716686000
C	-8.237261000	-0.040651000	-0.847059000
H	-8.747644000	-0.794042000	-0.264173000
C	-8.136132000	-0.008339000	-2.264630000
H	-8.557756000	-0.731510000	-2.948039000
C	-7.345606000	1.118310000	-2.622697000

H	-7.065781000	1.403952000	-3.626804000
C	-3.552506000	0.766188000	-2.801339000
C	-2.088195000	0.369641000	-2.975039000
C	-1.265793000	0.566491000	-1.729738000
O	-1.591817000	1.247125000	-0.787658000
O	-0.095698000	-0.077899000	-1.789704000
H	-3.597389000	1.747672000	-2.321783000
H	-4.011673000	0.865107000	-3.789515000
H	-1.985830000	-0.670551000	-3.296667000
H	-1.611558000	0.976918000	-3.755212000
F	3.636344000	-4.803539000	-0.542279000
F	6.108423000	-4.926782000	-1.620848000
F	7.248827000	-2.773090000	-2.717373000
F	5.970051000	-0.396051000	-2.786182000
F	4.632995000	4.001266000	-1.402450000
F	4.548671000	6.205478000	0.154220000
F	2.692355000	6.486461000	2.056046000
F	0.834904000	4.576482000	2.489015000

F	0.238266000	-4.287910000	2.808526000
F	-0.795651000	-3.864158000	5.266117000
F	-1.504993000	-1.414619000	6.065460000
F	-1.213324000	0.723625000	4.444336000

SubPc 8, (Fc(CH)2COO)BSubPc(F)12

N	0.675968000	-0.914126000	0.935572000
N	1.891815000	-2.598599000	-0.188825000
N	1.619770000	-0.463956000	-1.174348000
N	2.370324000	1.738941000	-1.595106000
N	0.878294000	1.309890000	0.188992000
N	0.441826000	0.864609000	2.472290000
C	0.508587000	-0.437423000	2.195886000
C	0.745416000	-1.572576000	3.064018000
C	1.195179000	-2.646105000	2.239069000
C	1.227373000	-2.153440000	0.877229000
C	0.697925000	-1.722798000	4.442280000

C	1.072936000	-2.936178000	4.992870000
C	1.513904000	-3.988597000	4.184154000
C	1.588434000	-3.848174000	2.809055000
C	2.144529000	-1.720544000	-1.154624000
C	3.203368000	-1.707276000	-2.145119000
C	3.354661000	-0.358361000	-2.577233000
C	2.383309000	0.435818000	-1.850327000
C	4.064775000	-2.690841000	-2.605523000
C	5.054394000	-2.337883000	-3.508072000
C	5.203062000	-1.014427000	-3.932165000
C	4.365026000	-0.016233000	-3.462719000
C	1.670759000	2.140434000	-0.540000000
C	1.808885000	3.338810000	0.264474000
C	1.205107000	3.070421000	1.526577000
C	0.709958000	1.708512000	1.480332000
C	2.459606000	4.542672000	0.041850000
C	2.488002000	5.480855000	1.060612000
C	1.895477000	5.217310000	2.298826000

C	1.262432000	4.010092000	2.544102000
B	0.491631000	-0.059657000	-0.276777000
Fe	-6.474074000	-0.202187000	-1.097168000
C	-4.815647000	-0.973963000	-2.002681000
C	-5.605010000	-2.012427000	-1.408583000
H	-5.269287000	-2.686012000	-0.632418000
C	-6.891780000	-1.988933000	-1.999954000
H	-7.719811000	-2.634377000	-1.744565000
C	-6.918339000	-0.934231000	-2.953872000
H	-7.772436000	-0.636850000	-3.545353000
C	-5.648903000	-0.304062000	-2.954882000
H	-5.368519000	0.552795000	-3.550353000
C	-6.031745000	0.561310000	0.742877000
H	-5.165423000	0.291923000	1.330036000
C	-7.295136000	-0.088118000	0.769788000
H	-7.558731000	-0.940124000	1.379909000
C	-8.137000000	0.550126000	-0.181621000
H	-9.152532000	0.268606000	-0.420689000

C	-7.393479000	1.595065000	-0.794937000
H	-7.744324000	2.244645000	-1.584036000
C	-6.091700000	1.601173000	-0.225702000
H	-5.276990000	2.253464000	-0.506286000
C	-3.446678000	-0.672131000	-1.640723000
C	-2.627827000	0.170210000	-2.288166000
C	-1.249151000	0.439583000	-1.876519000
O	-0.517698000	1.203995000	-2.466865000
O	-0.853962000	-0.234139000	-0.781294000
H	-3.053373000	-1.192068000	-0.770681000
H	-2.937218000	0.710704000	-3.175781000
F	0.294724000	-0.746004000	5.238218000
F	1.015886000	-3.120330000	6.302966000
F	1.858624000	-5.131261000	4.757698000
F	2.019362000	-4.861360000	2.075857000
F	3.960121000	-3.951232000	-2.218103000
F	5.877828000	-3.257328000	-3.987047000
F	6.162822000	-0.726512000	-4.797422000

F	4.543407000	1.226345000	-3.876485000
F	3.041229000	4.822081000	-1.111713000
F	3.079715000	6.650313000	0.873357000
F	1.945890000	6.146559000	3.240584000
F	0.721446000	3.790980000	3.731229000

SubPc 5+, (Fc+(CH2)2COO)BSubPc(H)12

N	2.564225000	-0.898849000	-0.742660000
N	3.979867000	0.920954000	-1.250852000
N	1.830238000	1.305059000	-0.334836000
N	0.398478000	1.665969000	1.513147000
N	0.700814000	-0.519944000	0.650565000
N	1.771028000	-2.635152000	0.646771000
C	2.659328000	-2.154856000	-0.219800000
C	3.996726000	-2.609613000	-0.553610000
C	4.680851000	-1.507197000	-1.137545000
C	3.754949000	-0.389997000	-1.157217000

C	4.659934000	-3.808316000	-0.313762000
H	4.143845000	-4.640865000	0.150364000
C	5.991139000	-3.902533000	-0.688366000
H	6.526905000	-4.831670000	-0.527793000
C	6.664773000	-2.816356000	-1.264085000
H	7.708339000	-2.926104000	-1.537796000
C	6.025108000	-1.606059000	-1.480524000
H	6.548754000	-0.757976000	-1.906466000
C	3.053111000	1.739604000	-0.755062000
C	3.181448000	3.091329000	-0.244683000
C	2.070792000	3.323643000	0.612084000
C	1.272639000	2.111942000	0.617020000
C	4.187711000	4.042470000	-0.378882000
H	5.043877000	3.852164000	-1.015778000
C	4.057344000	5.230865000	0.321640000
H	4.818870000	5.996549000	0.222536000
C	2.963067000	5.460136000	1.167806000
H	2.900076000	6.398794000	1.707384000

C	1.970129000	4.507967000	1.334986000
H	1.136174000	4.674479000	2.007101000
C	0.188172000	0.349364000	1.567431000
C	-0.274961000	-0.477243000	2.662152000
C	0.140480000	-1.813153000	2.388233000
C	0.861653000	-1.787143000	1.133314000
C	-0.900503000	-0.164305000	3.869393000
H	-1.177190000	0.859762000	4.095443000
C	-1.139044000	-1.190313000	4.768149000
H	-1.629565000	-0.973174000	5.710919000
C	-0.732677000	-2.506974000	4.495403000
H	-0.921576000	-3.281319000	5.230942000
C	-0.076854000	-2.827429000	3.319273000
H	0.267339000	-3.836339000	3.121760000
B	1.344194000	-0.069199000	-0.610436000
Fe	-4.554920000	-0.134664000	-0.530684000
C	-3.698008000	-0.455736000	-2.498213000
C	-3.342796000	-1.482001000	-1.582426000

H	-2.336039000	-1.752084000	-1.294810000
C	-4.531683000	-2.096601000	-1.095159000
H	-4.579056000	-2.919133000	-0.395609000
C	-5.637027000	-1.427662000	-1.689167000
H	-6.683016000	-1.643885000	-1.522816000
C	-5.118508000	-0.406323000	-2.530499000
H	-5.704811000	0.296352000	-3.107757000
C	-3.604470000	1.392919000	0.562584000
H	-2.642599000	1.792069000	0.271505000
C	-3.802835000	0.279199000	1.412064000
H	-3.018948000	-0.286352000	1.899424000
C	-5.189998000	-0.002405000	1.460787000
H	-5.653522000	-0.816250000	2.001244000
C	-5.860713000	0.940495000	0.635410000
H	-6.926209000	0.986366000	0.458904000
C	-4.874653000	1.805041000	0.075936000
H	-5.059864000	2.628257000	-0.599607000
C	-2.786668000	0.414432000	-3.311953000

C	-1.320035000	0.016058000	-3.283015000
C	-0.638295000	0.360865000	-1.978821000
O	-1.127650000	1.120267000	-1.168293000
O	0.517777000	-0.242850000	-1.836697000
H	-2.881143000	1.454857000	-2.986265000
H	-3.151242000	0.377556000	-4.343880000
H	-1.173593000	-1.046300000	-3.497512000
H	-0.780183000	0.551215000	-4.071766000

SubPc 6+, (Fc+(CH)2COO)BSubPc(H)12.

N	1.618598000	-0.378065000	1.325654000
N	2.729828000	-2.430413000	0.950665000
N	2.362033000	-0.930448000	-0.843926000
N	3.074698000	0.838805000	-2.244352000
N	1.755216000	1.294138000	-0.332760000
N	1.543505000	1.901434000	1.946753000
C	1.580710000	0.606195000	2.266386000

C	1.910484000	-0.046125000	3.518003000
C	2.277970000	-1.386826000	3.209201000
C	2.169315000	-1.540437000	1.772152000
C	2.011905000	0.433584000	4.820985000
H	1.757625000	1.462315000	5.049663000
C	2.447836000	-0.437826000	5.805625000
H	2.523425000	-0.092082000	6.830840000
C	2.808874000	-1.758859000	5.501351000
H	3.155840000	-2.408826000	6.297209000
C	2.743673000	-2.241421000	4.204552000
H	3.046086000	-3.253884000	3.962478000
C	2.896002000	-2.073700000	-0.320993000
C	3.866390000	-2.530329000	-1.298106000
C	3.975106000	-1.514165000	-2.286272000
C	3.068347000	-0.447322000	-1.907095000
C	4.692022000	-3.649088000	-1.336799000
H	4.623502000	-4.411405000	-0.569257000
C	5.595443000	-3.755534000	-2.382534000

H	6.239535000	-4.625776000	-2.446055000
C	5.701880000	-2.753904000	-3.357743000
H	6.426001000	-2.868766000	-4.156860000
C	4.907932000	-1.618802000	-3.312737000
H	5.002249000	-0.832192000	-4.052454000
C	2.484884000	1.694580000	-1.413767000
C	2.715742000	3.112952000	-1.220531000
C	2.237781000	3.445003000	0.076981000
C	1.721481000	2.224757000	0.666848000
C	3.366112000	4.062556000	-2.002328000
H	3.748504000	3.799260000	-2.981799000
C	3.505505000	5.342807000	-1.491014000
H	3.995299000	6.106074000	-2.085729000
C	3.036257000	5.669926000	-0.210575000
H	3.173200000	6.679841000	0.160427000
C	2.414431000	4.725994000	0.591017000
H	2.073920000	4.970208000	1.590785000
B	1.358535000	-0.119312000	-0.110707000

Fe	-5.794049000	-0.247330000	-0.231593000
C	-4.119892000	-1.481613000	-0.763154000
C	-4.870492000	-2.043027000	0.309743000
H	-4.476919000	-2.265655000	1.292466000
C	-6.206228000	-2.250589000	-0.122969000
H	-7.005978000	-2.677520000	0.465580000
C	-6.300407000	-1.795295000	-1.468556000
H	-7.186169000	-1.810499000	-2.087956000
C	-5.025537000	-1.301181000	-1.851491000
H	-4.782661000	-0.859357000	-2.807723000
C	-5.129624000	1.672464000	0.382460000
H	-4.089473000	1.966707000	0.426398000
C	-5.858417000	1.047523000	1.421738000
H	-5.478136000	0.806213000	2.404695000
C	-7.162105000	0.758243000	0.935686000
H	-7.956436000	0.281627000	1.492525000
C	-7.232186000	1.204963000	-0.415257000
H	-8.091110000	1.133320000	-1.067359000

C	-5.969335000	1.767751000	-0.752788000
H	-5.690737000	2.177697000	-1.713575000
C	-2.721770000	-1.097595000	-0.684856000
C	-1.989468000	-0.682477000	-1.724289000
C	-0.554692000	-0.308133000	-1.616650000
O	0.054223000	0.081952000	-2.583850000
O	-0.065460000	-0.440575000	-0.397574000
H	-2.236938000	-1.186359000	0.283341000
H	-2.390871000	-0.593272000	-2.728877000

SubPc 7+, (Fc+(CH2)2COO)BSubPc(F)12

N	2.227474000	-0.432399000	-1.138129000
N	3.099594000	1.759043000	-1.261870000
N	1.097859000	1.338931000	-0.068154000
N	-0.070675000	0.854680000	1.931484000
N	0.570627000	-0.897514000	0.474353000
N	2.074453000	-2.596981000	-0.206629000

C	2.678398000	-1.707990000	-0.990570000
C	4.004950000	-1.709082000	-1.572401000
C	4.323301000	-0.357462000	-1.898566000
C	3.187642000	0.454916000	-1.513109000
C	4.947385000	-2.711196000	-1.744573000
C	6.189478000	-2.374287000	-2.259054000
C	6.501636000	-1.049127000	-2.578855000
C	5.578156000	-0.032794000	-2.390929000
C	2.106504000	2.162218000	-0.473858000
C	2.001646000	3.334764000	0.369467000
C	1.017287000	3.053141000	1.361515000
C	0.529634000	1.712309000	1.114165000
C	2.719726000	4.520742000	0.411000000
C	2.442307000	5.430221000	1.418877000
C	1.475603000	5.154494000	2.391628000
C	0.767334000	3.964022000	2.376655000
C	0.024631000	-0.438120000	1.636106000
C	-0.073218000	-1.600737000	2.493026000

C	0.591765000	-2.673347000	1.828640000
C	1.090258000	-2.155017000	0.572681000
C	-0.573755000	-1.776475000	3.775069000
C	-0.431718000	-3.012842000	4.381790000
C	0.222654000	-4.064575000	3.730481000
C	0.746685000	-3.899823000	2.459181000
B	0.884959000	-0.003134000	-0.672169000
Fe	-6.369229000	-0.177483000	-1.426513000
C	-4.385031000	-0.416603000	-2.189323000
C	-4.445367000	-0.694657000	-0.795202000
H	-3.875698000	-0.160770000	-0.047058000
C	-5.369166000	-1.753935000	-0.582452000
H	-5.629658000	-2.186360000	0.373622000
C	-5.904121000	-2.127875000	-1.847504000
H	-6.641751000	-2.896812000	-2.030226000
C	-5.300971000	-1.295425000	-2.830199000
H	-5.517731000	-1.307025000	-3.890372000
C	-6.834849000	1.775003000	-0.969414000

H	-6.098820000	2.541064000	-0.769797000
C	-7.436844000	0.925193000	-0.001724000
H	-7.220884000	0.915442000	1.057688000
C	-8.341171000	0.066383000	-0.672209000
H	-8.922612000	-0.722807000	-0.215312000
C	-8.299594000	0.372088000	-2.052925000
H	-8.855857000	-0.133912000	-2.829936000
C	-7.370224000	1.430378000	-2.243331000
H	-7.116193000	1.889385000	-3.188411000
C	-3.536737000	0.614162000	-2.866093000
C	-2.073791000	0.181736000	-2.988151000
C	-1.313907000	0.300353000	-1.686774000
O	-1.816033000	0.698249000	-0.657860000
O	-0.055233000	-0.062232000	-1.813182000
H	-3.570342000	1.550058000	-2.302462000
H	-3.938221000	0.806688000	-3.864246000
H	-1.976047000	-0.844683000	-3.355911000
H	-1.561032000	0.809033000	-3.724008000

F	4.688604000	-3.970854000	-1.443574000
F	7.100735000	-3.308576000	-2.458017000
F	7.696993000	-0.777399000	-3.068778000
F	5.908433000	1.209289000	-2.693415000
F	3.644385000	4.807793000	-0.486669000
F	3.088861000	6.580274000	1.472821000
F	1.242376000	6.054138000	3.330333000
F	-0.133378000	3.731972000	3.316171000
F	1.364548000	-4.910382000	1.874972000
F	0.328454000	-5.227212000	4.348603000
F	-0.921740000	-3.220082000	5.591700000
F	-1.193189000	-0.802519000	4.421321000

SubPc 8+, (Fc+(CH)2COO)BSubPc(F)12

N	0.706112000	-0.901954000	0.944787000
N	1.927999000	-2.597353000	-0.158896000
N	1.645283000	-0.478517000	-1.177359000

N	2.390193000	1.721450000	-1.629011000
N	0.902970000	1.315600000	0.166209000
N	0.468981000	0.899293000	2.456689000
C	0.539866000	-0.406818000	2.201467000
C	0.781739000	-1.529126000	3.082431000
C	1.236060000	-2.612610000	2.271601000
C	1.265497000	-2.141203000	0.903716000
C	0.740160000	-1.659136000	4.463285000
C	1.126533000	-2.861488000	5.030819000
C	1.572555000	-3.923583000	4.235946000
C	1.640421000	-3.803666000	2.858046000
C	2.177875000	-1.735062000	-1.138525000
C	3.232481000	-1.730974000	-2.131656000
C	3.379081000	-0.387386000	-2.583894000
C	2.409814000	0.415527000	-1.866905000
C	4.098147000	-2.718262000	-2.576143000
C	5.087789000	-2.374310000	-3.483481000
C	5.231790000	-1.056042000	-3.927329000

C	4.388993000	-0.053554000	-3.473335000
C	1.696858000	2.138435000	-0.575408000
C	1.832883000	3.345514000	0.212805000
C	1.229636000	3.093857000	1.479794000
C	0.736348000	1.732458000	1.455507000
C	2.487217000	4.545051000	-0.025964000
C	2.519693000	5.495823000	0.981588000
C	1.927242000	5.248950000	2.224458000
C	1.290678000	4.046490000	2.485481000
B	0.546240000	-0.060936000	-0.267960000
Fe	-6.587666000	-0.231337000	-1.083193000
C	-4.795772000	-1.030132000	-1.959885000
C	-5.590259000	-2.051394000	-1.363852000
H	-5.264754000	-2.705843000	-0.566247000
C	-6.867312000	-2.058952000	-1.982230000
H	-7.681736000	-2.730655000	-1.749641000
C	-6.883181000	-1.020362000	-2.954926000
H	-7.713815000	-0.756076000	-3.594405000

C	-5.619638000	-0.374007000	-2.922821000
H	-5.332251000	0.477334000	-3.524109000
C	-6.298351000	0.567392000	0.791167000
H	-5.470258000	0.311535000	1.437175000
C	-7.566597000	-0.075567000	0.761015000
H	-7.866831000	-0.920795000	1.364799000
C	-8.360240000	0.564835000	-0.220895000
H	-9.362582000	0.279996000	-0.510707000
C	-7.588760000	1.595901000	-0.808805000
H	-7.907170000	2.243088000	-1.614494000
C	-6.313032000	1.604695000	-0.184186000
H	-5.495080000	2.272147000	-0.417175000
C	-3.430600000	-0.710392000	-1.578485000
C	-2.632045000	0.118657000	-2.258684000
C	-1.227965000	0.410184000	-1.868837000
O	-0.555093000	1.180663000	-2.508972000
O	-0.829775000	-0.239082000	-0.786502000
H	-3.028822000	-1.215074000	-0.704429000

H	-2.949964000	0.634584000	-3.159173000
F	0.329806000	-0.673506000	5.243153000
F	1.074036000	-3.025765000	6.340695000
F	1.925911000	-5.052548000	4.823689000
F	2.073163000	-4.822609000	2.137178000
F	3.995813000	-3.970958000	-2.169852000
F	5.912443000	-3.295541000	-3.946615000
F	6.188145000	-0.777424000	-4.793814000
F	4.559964000	1.182392000	-3.903740000
F	3.065252000	4.806105000	-1.183457000
F	3.112211000	6.658515000	0.779368000
F	1.979590000	6.187555000	3.152302000
F	0.747658000	3.842502000	3.673403000

Chapter 5: Synthesis, Spectroscopy, Electrochemistry and DFT of Electron-rich ferrocenylsubphthalocyanine dyads

Optimized cation coordinates of $FcCO_2BSubPc(H)_{12}$, **7**:

Fe	4.097544000	-0.060142000	-1.082864000
O	0.421510000	0.028743000	-1.294316000
O	0.991721000	-2.137841000	-1.032484000
N	-1.906289000	-0.843176000	-0.789395000
N	-1.547142000	-2.494904000	0.868678000
N	-0.435734000	-0.412149000	1.008685000
N	-0.229187000	1.812239000	1.797597000
N	-1.291875000	1.374964000	-0.266953000
N	-3.158202000	0.972357000	-1.655135000
C	-2.972211000	-0.333232000	-1.476795000
C	-3.906055000	-1.434646000	-1.615439000
C	-3.406454000	-2.509837000	-0.831017000
C	-2.170342000	-2.058541000	-0.220250000
C	-5.139807000	-1.531481000	-2.250446000
H	-5.528445000	-0.701967000	-2.829797000
C	-5.846410000	-2.716495000	-2.120216000
H	-6.803146000	-2.825898000	-2.618925000

C	-5.353647000	-3.777146000	-1.346907000
H	-5.939001000	-4.686163000	-1.262693000
C	-4.141046000	-3.681549000	-0.682754000
H	-3.767772000	-4.491679000	-0.067061000
C	-0.747956000	-1.641889000	1.508195000
C	-0.311870000	-1.614691000	2.888905000
C	0.104499000	-0.282110000	3.176814000
C	-0.085960000	0.495109000	1.968850000
C	-0.342158000	-2.580639000	3.892170000
H	-0.682625000	-3.586612000	3.674993000
C	0.068875000	-2.215329000	5.162740000
H	0.065513000	-2.951854000	5.958734000
C	0.475279000	-0.902228000	5.447615000
H	0.776290000	-0.650187000	6.458623000
C	0.482783000	0.077206000	4.469023000
H	0.767820000	1.098303000	4.696080000
C	-0.909738000	2.226976000	0.726718000
C	-1.653843000	3.448334000	0.488671000

C	-2.563536000	3.185591000	-0.575915000
C	-2.365324000	1.807950000	-0.980826000
C	-1.677168000	4.671368000	1.153067000
H	-1.003298000	4.862391000	1.980445000
C	-2.583813000	5.628274000	0.727247000
H	-2.612192000	6.594230000	1.219472000
C	-3.477610000	5.369892000	-0.322431000
H	-4.178697000	6.141150000	-0.621793000
C	-3.488584000	4.146889000	-0.972630000
H	-4.193708000	3.936166000	-1.768463000
C	1.194044000	-1.020582000	-1.437584000
C	2.466754000	-0.678415000	-2.142791000
C	2.882859000	0.596036000	-2.631561000
H	2.293272000	1.500864000	-2.592508000
C	4.198124000	0.456236000	-3.136894000
H	4.810639000	1.250302000	-3.542539000
C	4.600083000	-0.891804000	-2.965314000
H	5.570040000	-1.298147000	-3.218479000

C	3.536718000	-1.597666000	-2.352912000
H	3.519403000	-2.640028000	-2.066518000
C	3.592728000	0.864357000	0.757792000
H	2.652638000	1.365028000	0.952699000
C	4.753199000	1.453689000	0.198509000
H	4.859014000	2.490299000	-0.090149000
C	5.737837000	0.437464000	0.049786000
H	6.733757000	0.569210000	-0.349171000
C	5.173171000	-0.784552000	0.517591000
H	5.659571000	-1.749837000	0.529693000
C	3.847886000	-0.514107000	0.952233000
H	3.133953000	-1.241888000	1.315430000
B	-0.764771000	-0.000623000	-0.374602000

Optimized cation coordinates of $FcCH_2CO_2BSubPc(H)_{12}$, **8**:

Fe	-5.638214000	-0.003938000	-0.444545000

N	2.287587000	0.491683000	-1.283334000
N	2.653924000	2.625992000	-0.339463000
N	1.538397000	0.948198000	0.907439000
N	1.553165000	-0.834221000	2.465130000
N	1.677382000	-1.284707000	0.144958000
N	2.924862000	-1.718393000	-1.821753000
C	2.948125000	-0.407342000	-2.064551000
C	3.837669000	0.383826000	-2.891718000
C	3.753575000	1.729023000	-2.433051000
C	2.813480000	1.747505000	-1.329733000
C	4.739463000	0.030809000	-3.891433000
H	4.817447000	-0.998070000	-4.223638000
C	5.525418000	1.029195000	-4.442907000
H	6.225480000	0.783200000	-5.233866000
C	5.442653000	2.354562000	-3.990933000
H	6.080399000	3.107359000	-4.441271000
C	4.571786000	2.715407000	-2.976023000
H	4.522045000	3.734494000	-2.609928000

C	2.101457000	2.188063000	0.791068000
C	2.247989000	2.673457000	2.148627000
C	1.910548000	1.598792000	3.017824000
C	1.557213000	0.466748000	2.185053000
C	2.729943000	3.875227000	2.660352000
H	3.010506000	4.683405000	1.994605000
C	2.839095000	4.001156000	4.035189000
H	3.198670000	4.931946000	4.460216000
C	2.506269000	2.941406000	4.892576000
H	2.615490000	3.073835000	5.963489000
C	2.055876000	1.729488000	4.396254000
H	1.822264000	0.900355000	5.054311000
C	1.690152000	-1.683964000	1.450748000
C	2.196675000	-3.041874000	1.433406000
C	2.619010000	-3.317755000	0.103387000
C	2.369912000	-2.124578000	-0.680934000
C	2.404598000	-3.969559000	2.450090000
H	2.103729000	-3.746697000	3.467348000

C	3.003328000	-5.174360000	2.120885000
H	3.163909000	-5.920334000	2.891621000
C	3.419881000	-5.446226000	0.809060000
H	3.894012000	-6.397053000	0.591328000
C	3.248282000	-4.520102000	-0.206438000
H	3.591111000	-4.717567000	-1.215650000
C	-3.579526000	-0.580734000	-0.565948000
C	-4.057941000	-0.682775000	0.766938000
H	-3.639630000	-0.158849000	1.613684000
C	-5.161127000	-1.576655000	0.785517000
H	-5.734845000	-1.856304000	1.658060000
C	-5.382287000	-2.027120000	-0.546354000
H	-6.149747000	-2.715150000	-0.871958000
C	-4.410855000	-1.400816000	-1.376363000
H	-4.318448000	-1.518048000	-2.447869000
C	-6.120336000	1.606635000	-1.652715000
H	-5.543498000	1.916358000	-2.512963000
C	-5.919074000	2.028460000	-0.307644000

H	-5.168388000	2.724567000	0.039325000
C	-6.887317000	1.371752000	0.501978000
H	-6.986821000	1.461421000	1.574740000
C	-7.683199000	0.556518000	-0.340545000
H	-8.479937000	-0.100155000	-0.018878000
C	-7.210965000	0.697982000	-1.666050000
H	-7.590917000	0.174110000	-2.532347000
B	1.290929000	0.083652000	-0.269727000
C	-1.155266000	-0.074507000	-0.201265000
O	-0.074413000	0.208442000	-0.879421000
O	-1.209245000	-0.474132000	0.935661000
C	-2.411165000	0.219966000	-1.027342000
H	-2.202190000	0.045902000	-2.083569000
H	-2.589718000	1.295388000	-0.912792000

Optimized cation coordinates of $Fc(CH_2)_3CO_2BSubPc(H)_{12}$, **10**:

Fe	5.213439000	0.013784000	-0.271772000
N	-3.096825000	-0.591163000	-0.878862000
N	-2.803519000	-2.605705000	0.317931000
N	-1.250533000	-0.834113000	0.565828000
N	-0.454006000	1.101260000	1.673628000
N	-1.864218000	1.307150000	-0.215761000
N	-4.006258000	1.564797000	-1.193096000
C	-4.111296000	0.237132000	-1.247326000
C	-5.281708000	-0.612963000	-1.360802000
C	-4.909263000	-1.904550000	-0.894308000
C	-3.514846000	-1.831198000	-0.499314000
C	-6.596099000	-0.342225000	-1.726793000
H	-6.881332000	0.648078000	-2.062742000
C	-7.518735000	-1.373510000	-1.651504000
H	-8.546651000	-1.193963000	-1.946887000
C	-7.151966000	-2.646132000	-1.191640000
H	-7.903421000	-3.426410000	-1.140174000
C	-5.852961000	-2.921610000	-0.794945000

H	-5.572084000	-3.899106000	-0.420049000
C	-1.733807000	-2.064942000	0.903235000
C	-1.083392000	-2.403960000	2.152599000
C	-0.360166000	-1.252494000	2.575402000
C	-0.571373000	-0.223162000	1.578231000
C	-1.154275000	-3.534093000	2.963629000
H	-1.727964000	-4.399072000	2.650753000
C	-0.478767000	-3.515129000	4.172159000
H	-0.509549000	-4.387223000	4.816183000
C	0.230755000	-2.378954000	4.591970000
H	0.730077000	-2.394052000	5.554847000
C	0.283715000	-1.236297000	3.811266000
H	0.797685000	-0.343716000	4.150967000
C	-1.163511000	1.843074000	0.826510000
C	-1.644307000	3.205274000	0.955021000
C	-2.743746000	3.348918000	0.064189000
C	-2.927201000	2.072401000	-0.598260000
C	-1.290586000	4.241322000	1.814534000

H	-0.470672000	4.121134000	2.513458000
C	-2.016216000	5.419656000	1.750277000
H	-1.751679000	6.247265000	2.399463000
C	-3.098726000	5.561295000	0.869601000
H	-3.648877000	6.495752000	0.853622000
C	-3.483791000	4.527086000	0.032393000
H	-4.334999000	4.624015000	-0.631699000
C	4.536574000	-1.209609000	-1.911408000
C	5.440203000	-0.205329000	-2.347728000
H	5.218264000	0.565274000	-3.072755000
C	6.673727000	-0.361946000	-1.655736000
H	7.555909000	0.249204000	-1.784504000
C	6.533669000	-1.465599000	-0.768402000
H	7.289113000	-1.847074000	-0.095961000
C	5.212557000	-1.969651000	-0.916529000
H	4.780659000	-2.790551000	-0.359576000
C	3.600001000	1.122171000	0.565263000
H	2.600557000	1.120810000	0.143685000

C	4.657360000	1.994926000	0.218340000
H	4.596745000	2.806302000	-0.494170000
C	5.823807000	1.591757000	0.919368000
H	6.797054000	2.058119000	0.856574000
C	5.486330000	0.453363000	1.706087000
H	6.153840000	-0.089617000	2.360184000
C	4.108980000	0.164757000	1.478376000
H	3.544419000	-0.647618000	1.915151000
B	-1.716335000	-0.107101000	-0.643083000
C	0.363354000	-0.053905000	-1.919259000
O	-0.915922000	-0.334671000	-1.876662000
O	0.988000000	0.431360000	-0.994735000
C	1.003157000	-0.390672000	-3.247380000
C	2.519821000	-0.296970000	-3.187229000
C	3.126392000	-1.425562000	-2.355661000
H	2.511035000	-1.604606000	-1.468460000
H	3.106898000	-2.360899000	-2.930467000
H	2.933112000	-0.313636000	-4.200256000

H	2.778296000	0.669307000	-2.742950000
H	0.658811000	-1.382552000	-3.557355000
H	0.595922000	0.306860000	-3.987257000

Optimized cation coordinates of $FcCO(CH_2)_2CO_2BSubPc(H)_{12}$, **11**:

Fe	4.589882000	0.013034000	-0.048853000
N	-3.080022000	-0.046051000	-0.899637000
N	-3.123079000	-2.381370000	-0.562184000
N	-1.245343000	-1.111858000	0.128159000
N	-0.033349000	0.104155000	1.758165000
N	-1.477675000	1.233117000	0.263535000
N	-3.573752000	2.182553000	-0.298840000
C	-3.933823000	1.011283000	-0.820877000
C	-5.249601000	0.467133000	-1.102536000
C	-5.110010000	-0.946203000	-1.184960000
C	-3.710281000	-1.252049000	-0.952433000
C	-6.502826000	1.063064000	-1.192537000

H	-6.609231000	2.138553000	-1.109802000
C	-7.600876000	0.241562000	-1.394768000
H	-8.587859000	0.681512000	-1.486059000
C	-7.463320000	-1.150952000	-1.476110000
H	-8.346567000	-1.761349000	-1.628831000
C	-6.223985000	-1.760461000	-1.357384000
H	-6.117835000	-2.838282000	-1.400551000
C	-1.942906000	-2.282573000	0.050537000
C	-1.313407000	-3.170546000	1.005694000
C	-0.360093000	-2.401248000	1.731430000
C	-0.412960000	-1.050976000	1.206867000
C	-1.568424000	-4.495518000	1.349063000
H	-2.311991000	-5.069280000	0.807911000
C	-0.849174000	-5.049086000	2.394605000
H	-1.018861000	-6.083388000	2.672820000
C	0.086383000	-4.291126000	3.115149000
H	0.618539000	-4.753854000	3.939180000
C	0.327810000	-2.963335000	2.804981000

H	1.026228000	-2.371130000	3.385729000
C	-0.632855000	1.217557000	1.334039000
C	-0.835597000	2.486116000	2.005664000
C	-1.931662000	3.129356000	1.364697000
C	-2.390181000	2.246537000	0.311444000
C	-0.252614000	3.049176000	3.138292000
H	0.558761000	2.544742000	3.650912000
C	-0.743391000	4.261583000	3.593682000
H	-0.297715000	4.725864000	4.466704000
C	-1.820445000	4.896680000	2.957338000
H	-2.183998000	5.840559000	3.348361000
C	-2.434832000	4.332303000	1.852061000
H	-3.284631000	4.805951000	1.374090000
C	4.178187000	0.868704000	-1.914369000
C	3.899117000	1.836052000	-0.915709000
H	2.918217000	2.238647000	-0.704141000
C	5.078521000	2.052989000	-0.166778000
H	5.169549000	2.704034000	0.691928000

C	6.108232000	1.233268000	-0.709163000
H	7.130057000	1.181670000	-0.360197000
C	5.550363000	0.492739000	-1.788024000
H	6.054929000	-0.228857000	-2.414982000
C	3.242841000	-0.678701000	1.427014000
H	2.393580000	-0.113939000	1.795412000
C	4.557165000	-0.682326000	1.950711000
H	4.902669000	-0.110469000	2.801378000
C	5.363734000	-1.508604000	1.125588000
H	6.421109000	-1.694178000	1.254556000
C	4.540021000	-2.022974000	0.083000000
H	4.852337000	-2.671977000	-0.722735000
C	3.228600000	-1.502550000	0.272411000
H	2.379056000	-1.649298000	-0.378249000
B	-1.622734000	0.084586000	-0.666260000
C	0.345110000	0.406841000	-2.093288000
O	-0.945325000	0.226574000	-1.982897000
O	1.120266000	0.467153000	-1.153009000

C	0.818887000	0.520744000	-3.520452000
C	2.214540000	1.124352000	-3.576130000
C	3.231438000	0.239751000	-2.895590000
H	2.534910000	1.211350000	-4.620991000
H	2.222462000	2.130296000	-3.151097000
H	0.826014000	-0.487569000	-3.948938000
H	0.100672000	1.103399000	-4.100548000
O	3.354151000	-0.932477000	-3.159559000

Additional Indormation

Supervisors Note TurnItIn Report

Enclosed herewith a copy of Originality Report (Turnitin Report) of PhD thesis of Petrus J Swarts.

Petrus J Swarts, Student Number: 2008042273 has submitted a Philosophia Doctor thesis under my supervision. The student's thesis is article based i.e. he has included the publications he authored, submitted or intend to submit as a major part of his thesis.

The student wrote an Abstract, Introduction and Conclusion together with his one published paper, two submitted manuscripts and one manuscript to be submitted to Molecules. We ran two TurnItIn Reports, namely on (1) the Abstract, Introduction and Conclusion and (2) the publication to be submitted to Molecules.

Comments on the similarity report

(1) Abstract, Introduction and Conclusion is 14% similarity of which 9% is to his own published article "Electrochemical behaviour of chloro- and hydroxy- subphthalocyanines", in Electrochimica Acta, 329 (2020) 135165, that is own work than forms part of this thesis. This left us with an acceptable 5% similarity.

(2) Publication to be submitted to Molecules is 14% similarity. The similarity consist of fourteen times 1% similarity from different sources that is acceptable. Most similarity refers to technical aspects that need to be reported in the Experimental section.

Detail of the two similarity reports are included in the electronic version of the thesis as an Appendix.

05 February 2020

Prof J.Conradie Date

Publication 3

by Petrus Swarts

Submission date: 05-Feb-2020 02:40PM (UTC+0200)
Submission ID: 1251912211
File name: 1._Publication_3_-_Normal_Space.docx (2.15M)
Word count: 6531
Character count: 35622

molecules

MDPI

Article

Synthesis, Spectroscopy, Electrochemistry and DFT of Electron-rich ferrocenylsubphthalocyanine dyads

Pieter J. Swarts[1] and Jeanet Conradie[1]*

[1] Affiliation 1; Department of Chemistry, University of the Free State, Bloemfontein 9300, South Africa; swarts.pieter@gmail.com (P.J.S.)

* Correspondence: conradj@ufs.ac.za; Tel.: +27-(51)-4012194, Fax: +27-4017295

0000-0002-8120-6830 (J Conradie)

0000-0003-0157-8763 (PJ Swarts)

Received: date; Accepted: date; Published: date

Abstract: A series of novel ferrocenylsubphthalocyanine dyads Y-BSubPc(H)$_{12}$ with ferrocenylcarboxylic acid dyads Y-H = (FcCH$_2$CO$_2$-H), (Fc(CH$_2$)$_3$CO$_2$-H) or (FcCO(CH$_2$)$_2$CO$_2$-H) in axial position, were synthesized from the parent Cl-BSubPc(H)$_{12}$ via an activated triflate-SubPc intermediate. UV/vis data revealed that the axial ferrocenyl-containing ligand did not influence the Q-band maxima compared to Cl-BSubPc(H)$_{12}$. A combined electrochemical and density functional theory (DFT) study showed that Fe group of the ferrocenyl-containing axial ligand is involved in the first reversible oxidation process, followed by a second oxidation localized on the macrocycle of the subphthalocyanine. Both observed reductions were ring-based. It was found that the novel Fc(CH$_2$)$_3$CO$_2$BSubPc(H)$_{12}$ exhibited the lowest first macrocycle-based reduction potential (-1.871 V *vs*. Fc/Fc$^+$) reported for SubPcs till date. The oxidation and reduction values of Fc(CH$_2$)$_n$CO$_2$BSubPc(H)$_{12}$ (n = 0 – 3), FcCO(CH$_2$)$_2$CO$_2$BSubPc(H)$_{12}$, and Cl-BSubPc(H)$_{12}$ illustrated the electronic influence of the carboxyl group, the different alkyl chains and the ferrocenyl group in the axial ligand on the ring-based oxidation and reduction values of the SubPcs.

Keywords: Subphthalocyanines; Ferrocene; redox potentials; DFT; electron rich.

1. Introduction

The discovery of ferrocene (1951) [1] unlocked an entirely new research field and over the years. Ferrocene has been extensively researched with numerous good reviews in organic and inorganic chemistry [2–5]. The research of ferrocene-containing compounds thrives, and new research keeps on growing due to their varying successful applications. This includes asymmetric catalysis [6–8], non-linear optics [8], antineoplastic properties [9,10] antimalarial activity [11] and especially electrochemistry due to the ideal redox behavior of the $Fe^{II/III}$ couple [8,12]. For a series of four ferrocenyl carboxylic acid dyads $Fc(CH_2)_nCO_2H$ with n = 0 (**1**), 1 (**2**), 2 (**3**) or 3 (**4**) (Figure 1), it was found that the as the length of the alkyl chain separating the ferrocene moiety and electron-withdrawing carboxy group decreases, the formal reduction potential of Fe of the ferrocenyl group also decreases [13,14]. The electron-withdrawing carboxy group directly bound to ferrocene in **1** and $FcCO(CH_2)_2CO_2H$ (**5**), led to an increase in the formal reduction potential of the ferrocene moiety compared to free ferrocene [13,14].

Subphthalocyanines such as $ClBSubPc(H)_{12}$, **6**, have been used in research for almost 50 years [15] due to their diverse applications including light-emitting diodes [16], dye-sensitized solar cells [17], sensors [18] and photodynamic therapy [19]. The uses and reactivity of SubPcs can be modified by substituting the axial ligand as well as by functionalizing the ring substituents [18]. Redox data of the ring-based oxidation and reduction processes of SubPcs showed that axial or peripheral substitution has a smaller influence on the shift of the oxidation and reduction potential of the SubPc (ca 0.1 V shift) than non-peripheral substitution (ca 0.3 V shift) [20]. Ferrocenylsubphthalocyanine dyads with a direct ferrocene-boron or substituted ferrocene-boron bond have been investigated by V. Nemykin and co-workers [21,22]. They found that the first oxidation process in these ferrocenylsubphthalocyanine dyads is ferrocene based, while second oxidation and the first reduction processes are centered at the macrocyclic ligand of the SubPc [21,22].

In this paper, we report the synthesis, characterisation and electrochemical studies of three novel (**8**, **10** and **11**) ferrocenylsubphthalocyanine dyads. The appropriate ferrocenyl carboxylic acid **2**, **4** and **5** was directly bound to the boron atom in the axial position of SubPc, **6**, to form the three

new ferrocenylsubphthalocyanine dyads, $FcCH_2CO_2BSubPc(H)_{12}$, **8**, $Fc(CH_2)_3CO_2BSubPc(H)_{12}$, **10**, and $FcCO(CH_2)_2CO_2BSubPc(H)_{12}$, **11**, see Scheme 1 and Figure 1. For comparative purposes, the two known ferrocenylsubphthalocyanine dyads **7** [21] and **9** [23] were included in this study to systematically evaluate (i) the effect of the electron rich macrocycle of SubPcs **7** - **11** on the formal reduction potential of Fe of the ferrocenyl group of the ferrocenylcarboxylic acid moieties of **7** – **11**, and (ii) the influence of the axially ferrocenylcarboxylic acid dyads **1** - **5** on the UV/vis maxima and the ring-based oxidations and reductions of the ferrocenylsubphthalocyanine dyads **7** – **11**.

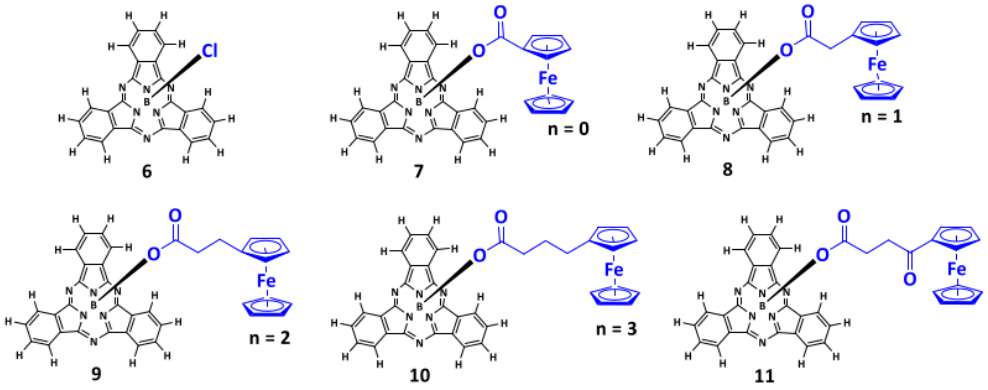

Figure 1 Structures of $FcCO_2BSubPc(H)_{12}$, **7** [21], $FcCH_2CO_2BSubPc(H)_{12}$, **8** (novel), $Fc(CH_2)_2CO_2BSubPc(H)_{12}$, **9** [23], $Fc(CH_2)_3CO_2BSubPc(H)_{12}$, **10** (novel) and $FcCO(CH_2)_2CO_2BSubPc(H)_{12}$, **11** (novel), containing the ferrocenylcarboxylic acids $FcCO_2H$ (**1**), $FcCH_2CO_2H$ (**2**), $Fc(CH_2)_2CO_2H$ (**3**), $Fc(CH_2)_3CO_2H$ (**4**) and $FcCO(CH_2)_2CO_2H$ (**5**) in the axial position. n = number of alkyl groups in the axial ligand.

2. Results and Discussion

2.1. Synthesis

The free ferrocenylcarboxylic acids **1** – **5**, were synthesized using slightly modified methods than previously published [13], as described in our previous publication [14]. The synthesis of ferrocenylsubphthalocyanine dyads **7** – **11**, was complex due to the moisture sensitivity of the reactions. In the first step any of the two well-known halophiles, such as Me_3Si groups or Ag^+ ions are used to irreversibly substitute the axial chloride in the axial position [23,24]. We found that using Me_3SiOTf did not give desirable yields. Using AgOTf, however, enabled us to increase our yields by more than 30 % compared to previous studies [21]. Once the activated triflate species was formed the

activated SubPc showed considerable reactivity toward the different ferrocenyl acids **1** – **5**, see Scheme 1. The success of the synthesis is drastically affected when not working under strict Schlenk conditions. SubPcs **7** – **11** were soluble in common organic solvents such as DCM, chloroform and THF.

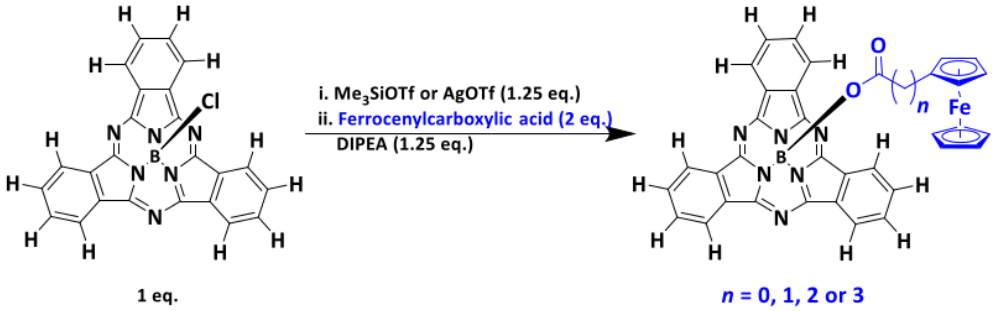

Scheme 1 Reaction scheme for $FcCO_2BSubPc(H)_{12}$, **7**, $FcCH_2CO_2BSubPc(H)_{12}$, **8**, $Fc(CH_2)_2CO_2BSubPc(H)_{12}$, **9**, $Fc(CH_2)_3CO_2BSubPc(H)_{12}$, **10**, and $FcCO(CH_2)_2CO_2BSubPc(H)_{12}$, **11**. **Note:** AgOTf = silver trifluoromethanesulfonate, Me_3SiOTf = Trimethylsilyl trifluoromethanesulfonate and DIPEA = *N*,*N*-Diisopropylethylamine.

2.3. ^1H NMR

The ^1H NMR results showed that signals of the SubPc ring protons (H) shifted upfield by *ca.* 0.04 – 0.07 ppm for SubPcs 7 – **11** relative to the signals of the parent ring protons $ClBSubPc(H)_{12}$, **6**. The most significant effect on ^1H NMR was observed for the signals of the ferrocenyl axial ligands peaks. Ferrocenyl of SubPc **7** (signals of the protons of substituted-Cp = 3.96 and 3.95, un-substituted-Cp = 3.63) is the closest to the electron rich macrocycle of SubPc and as a result the signals of the protons of the substituted and un-substituted-Cp rings shift the furthest upfield with ppm shifts between 0.50 and 0.88 ppm compared to ferrocenyl acid **1** (substituted-Cp = 4.84 and 4.45, un-substituted-Cp = 4.24). With the increase of $(CH_2)n$ linker groups the distance between the ferrocenyl moiety and SubPc increases and as a result the ferrocene peaks shift less upfield as the chain lengths increase.

2.3. UV/vis

As usually found for SubPcs, the UV/vis spectra of SubPcs **7** – **11** exhibited the two main transitions, the Soret band between 250 and 350 nm, and the Q-band between 450 and 620 nm, see Figure 2. The substitution of the parent macrocycles axial chloride with the different ferrocenylcarboxylic acid groups, had a negligible effect on the Q-bands position, see Table 1. In a similar fashion there was no shift when comparing the Q-bands of SubPcs **7** – **11** to **6**. The similar Soret and Q-bands for **6** and SubPcs **7** – **11** indicates that the Soret and Q-bands involve π-π* transitions. SubPcs **7** to **11** followed the Beer-Lambert law and no aggregation in the concentration range of 0.01 – 0.10 (x 10^{-3} M) was observed, see Figure 2.

Table 1 UV/vis data of SubPcs **6** – **11** in THF.

	Sorret Band	**Q Band**		
	Max	1st shoulder	2nd shoulder	Max
ClBSubPc(H)$_{12}$, **6**, [20]	308	525	532	564
FcCO$_2$BSubPc(H)$_{12}$, **7**	299	515	530	563
FcCH$_2$CO$_2$BSubPc$_{12}$, **8**	300	518	534	563
Fc(CH$_2$)$_2$CO$_2$BSubPc(H)$_{12}$, **9**, [23]	302	505	544	563
Fc(CH$_2$)$_3$CO$_2$BSubPc(H)$_{12}$, **10**	328	521	539	563
FcCO(CH$_2$)$_2$CO$_2$BSubPc(F)$_{12}$, **11**	327	523	542	563

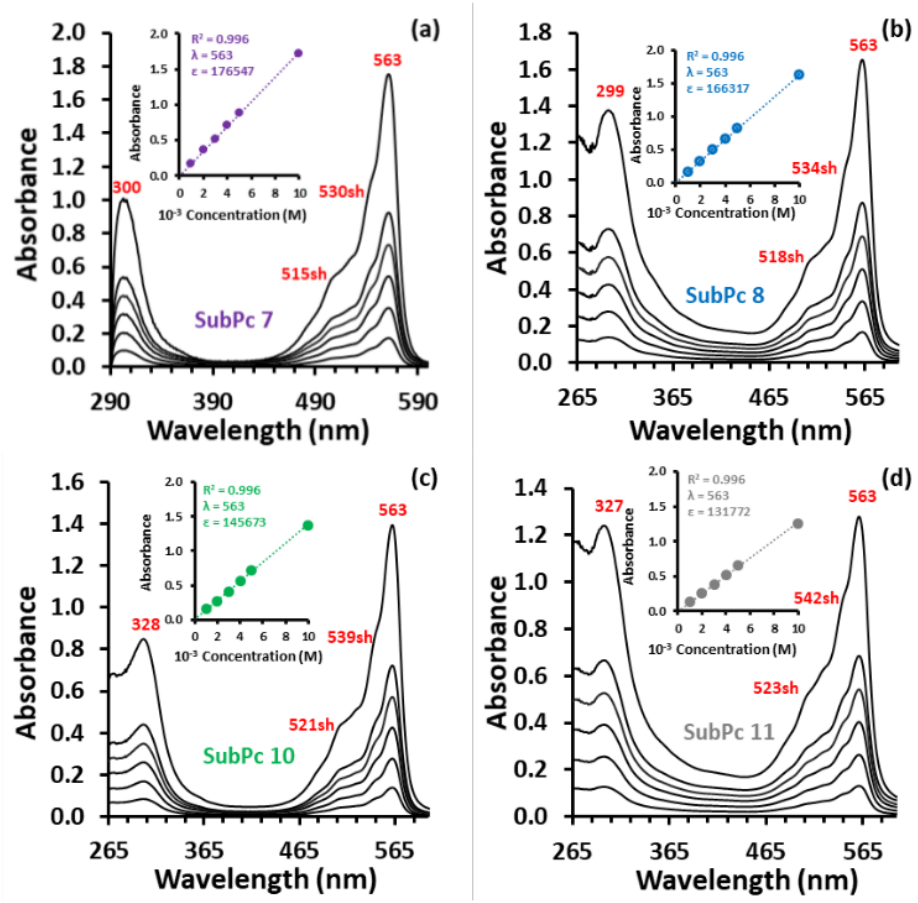

Figure 2 (a) – (d) The UV/vis spectra of SubPc (**7**, **8**, **10** and **11**) at concentrations 0.01, 0.02, 0.03, 0.04, 0.05 and 0.10 (x 10^{-3} M), obtained with a 1 cm pathlength cuvette with THF as solvent. UV/vis spectra of SubPc **9** can be found in reference [23]. Insert: The Beer-Lambert correlation between the absorbance A and concentration of $FcCO_2BSubPc(H)_{12}$, **7** (ε = 176547 dm^3 mol^{-1} cm^{-1}); $Fc(CH_2CO_2BSubPc(H)_{12}$, **8** (ε = 166317 dm^3 mol^{-1} cm^{-1}), $Fc(CH_2)_2CO_2BSubPc(H)_{12}$, **9** (ε = 153630 dm^3 mol^{-1} cm^{-1} [23]), $Fc(CH_2)_3CO_2BSubPc(H)_{12}$, **10** (ε = 145673 dm^3 mol^{-1} cm^{-1}) and $FcCO(CH_2)_2CO_2BSubPc(H)_{12}$, **11** (ε = 131772 dm^3 mol^{-1} cm^{-1}) at indicated wavelength in nm.

2.4. Cyclic Voltammetry

The redox properties of the ferrocenylsubphthalocyanine dyads, SubPc **7**, **8**, **10** and **11** were examined utilizing cyclic voltammetry (CVs) and linear sweep voltammetry (LSV). The CVs and the LSVs of SubPc **7**, **8**, **10** and **11**, performed at 25 °C in dichloromethane (DCM) at a scan rate of 0.100 Vs^{-1} are shown in Figure 3 with the relevant electrochemical data summarised in Table 2. Data of the free ferrocenylcarboxylic acids **1** – **5** [12] and SubPcs **6** [20] and **9** [21] are added for comparative

reasons in Table 2. The CVs of SubPc **7**, **8**, **10** and **11** (Figure 3) showed two oxidation and two reduction peaks in the experimental solvent window of DCM. The oxidation of the Fe group ($Fe^{II/III}$) of the ferrocenyl moiety on the axial ligand is the first observed redox process for all five SubPc **7** – **11**. The assignment that the Fe group is oxidised first, is supported by DFT calculations (see computational analysis below) and is in agreement with literature [21,22]. Both oxidation and the first reduction peaks are chemically reversible with peak ratios approaching 1 and peak current separations, ΔE_P, of 0.074-0.076 (ferrocenyl oxidation), 0.080-0.084 V (wave I in Figure 3) and 0.082-0.086 V (wave II in Figure 3) respectively. The second ring-based reduction (wave III in Figure 3) were irreversible and did not show any re-oxidation peaks. The linear sweep voltammetry showed, as expected, 1 e^- redox couples for Fc and waves I to III. The reaction scheme for the redox signals of SubPc **7** – **10** (similar for **11**) is given in Scheme 2.

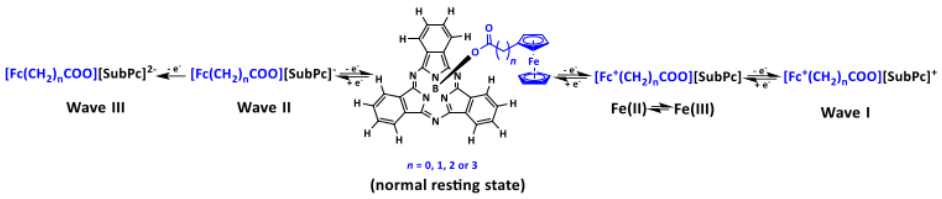

Scheme 2 The reaction scheme of the redox signals of SubPcs **7** to **10** in DCM as solvent, see Figure 3. Reactions scheme for **11** is similar.

2.4.1. *Effect of SubPc on ferrocenyl moiety oxidation*

The oxidation potentials, $E°'$, of the Fe group ($Fe^{II/III}$) of the ferrocenyl moiety on the axial ligand of SubPcs **7** – **11** range between -0.062 and 0.262 V and with ΔE_P between 0.074 and 0.076 V (Figure 3 and Table 2). Comparing $E°'$ (of the first process) of the Fc moiety of SubPcs **7** – **11** with the $E°'$ of the free ferrocenyl acids **1** – **5** (obtained under the experimental same conditions [14] as the SubPcs **7** – **11**) it is clear that the aromatic SubPc ring acts as an electron-donating specie in the complex, decreasing (lower oxidation potential) $E°'$ of the Fe group of SubPcs **7** – **11** with 0.060 – 0.038 V relative to $E°'$ of the Fe group of the free ferrocenylcarboxylic acids **1** – **5**. The largest electron-donating effect was, as expected, on the ferrocenyl moiety closest to the ring, with a

decrease of 0.060 V between **7** (0.224 V) and **1** (0.284 V). As the chain length increases with $(CH_2)_n$ groups the effect of the SubPc on ferrocenyl oxidation becomes less. The Fe group in SubPc **10** with three (CH_2) groups separating the ferrocenyl moiety from the SubPc, is more shielded from the electron-donating effect of the SubPc and as a result $E^{\circ\prime}$ of Fe only shifts with only 0.038 V between **10** (-0.062 V) and **4** (-0.024 V). With an additional carbonyl group as well as the (CH_2) groups in SubPc **11** $E^{\circ\prime}$ of the Fe group of SubPc **11** shifted the least in the range namely, with only a 0.033 V between **11** (0.262 V) and **5** (0.295 V).

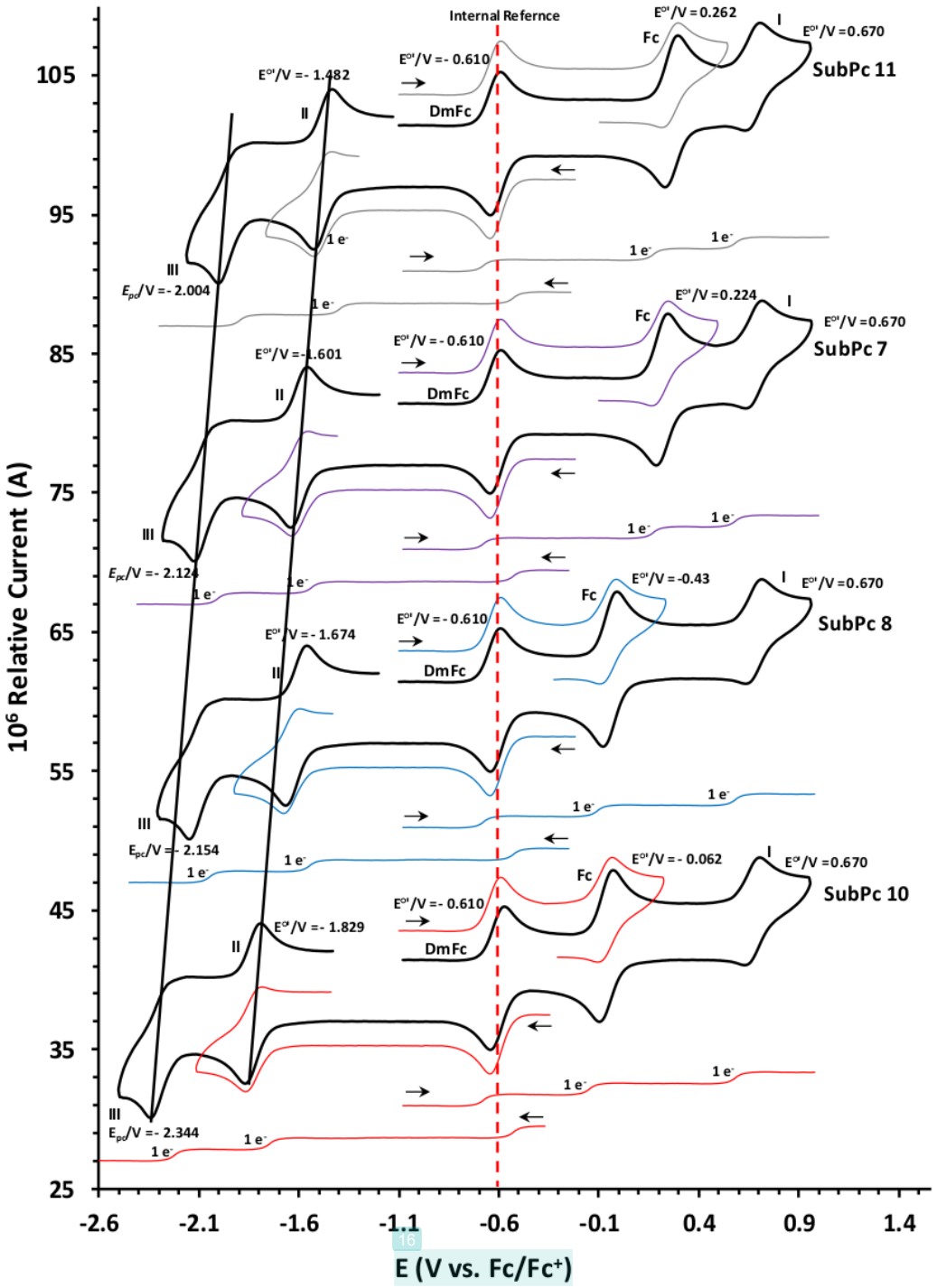

Figure 3 CVs and LSVs of SubPc, **7** - (purple), **8** - (blue), **10** – (red) and **11** - (grey) in DCM. Concentration of **7** – **11** = 0.0005 mol dm^{-3}. Scan rate for CVs is 0.100 V s^{-1} and LSVs at 0.001 V s^{-1}. Scan directions are indicated at starting point of each scan. DmFc was used ass internal reference with $E^{\circ\prime}$ (DmFc) = -0.610 *vs.* free Fc/Fc^{+} at 0 V.

2.4.2. *Effect of chain length on ferrocenyl moiety oxidation*

The formal reduction potential $E^{\circ\prime}$ of Fe in the axial ligand of SubPc **7** is at 0.224 V compared to free ferrocene 0 V. With one additional CH_2 spacer group between ferrocene and the SubPc, $E^{\circ\prime}$ of Fe is significantly shifted by 0.264 V to – 0.043 V in SubPc **8**, SubPcs **9** and **10** had two and three additional CH_2 spacer groups respectively, with $E^{\circ\prime}$ of the ferrocene group decreasing to -0.058 V and -0.062 V respectively. There was an exponential decrease to lower oxidation potential with an increase in $(CH_2)_n$ chain lengths for SubPc **7** – **10**, see Figure 4 a. This is because Fe of the ferrocene group is increasingly shielded from the electron donating effect of the SubPc and electron-withdrawing effect of the carboxy group as the $(CH_2)_n$ chain length increases. This trend was similar as observed for the free ferrocenylcarboxylic acids **1** – **5** [14], see Figure 4 a.

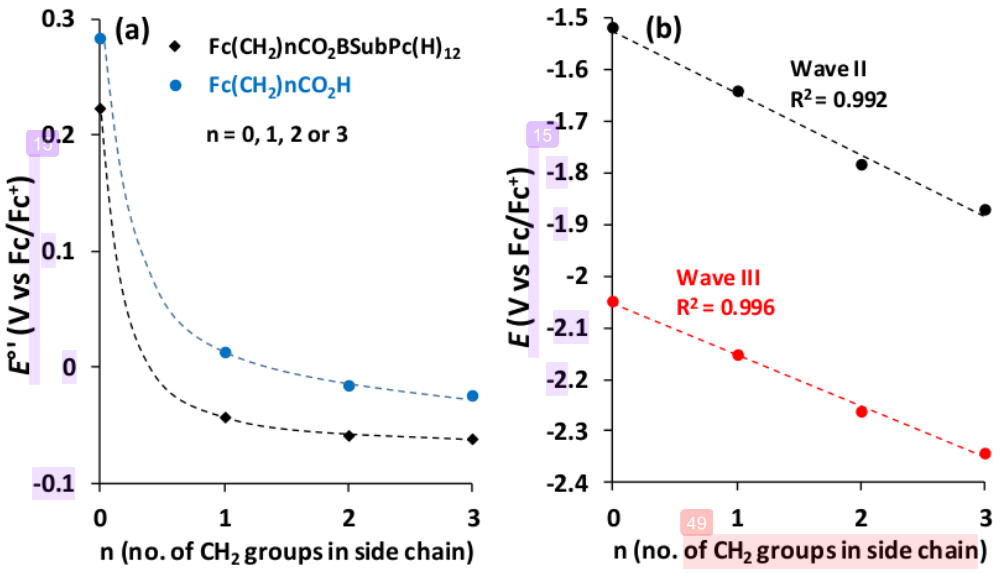

Figure 4 (a) Relationship between $E^{\circ\prime}$ of the Fe group and the number n of CH_2 groups in the side chain of Fc–$(CH_2)_n$–CO_2 for ferrocenyl carboxylic acids **1** – **5** and ferrocenylsubphthalocyanine dyads **7** – **11**. Data of **1** – **5** from reference [14]. (b) Relationship between $E^{\circ\prime}$(wave II) and E_{pc} (wave III) and n, of the first and second ring-based reductions respectively, of ferrocenylsubphthalocyanine dyads **7** – **11**.

2.4.3. *Effect of carboxyl and carbonyl group on ferrocenyl moiety oxidation*

The formal reduction potential $E^{o'}$ of the Fe group of SubPc **7**, separated by a carboxyl group from the electron donating SubPc, is at 0.224 V compared to free ferrocene 0 V, implying that the electron withdrawing effect of the carboxyl group is larger than the electron donating effect of the SubPc on the $E^{o'}$ of the Fe group. The additional electron withdrawing carbonyl group bound next to the ferrocenyl moiety in SubPc **11** resulted in the highest oxidation potential of the Fe group with $E^{o'}$ at 0.262 V, Figure 3. With the two electron withdrawing CO groups in SubPc **11** the oxidation potential was 0.038 V higher than $E^{o'}$ of Fe in SubPc **7** (0.224 V) containing only one electron withdrawing CO group.

Table 2 Cyclic voltammetry data of SubPcs **7** – **11** in DCM containing 0.1 mol dm^{-3} $[N(^{n}Bu)_4][B(C_6F_5)_4]$ as supporting electrolyte at a scan rate of 0.100 V/s at 25°C.

	Description	E_p[a]	$E^{o'}$ (V), ΔE_p (V)	i_p (μA)[b], current ratio[c]
FcCOOH[d] **1**	Fc	0.321	0.284, 0.074	3.60, 0.99
$FcCH_2COOH$[d] **2**	Fc	0.047	0.014, 0.066	3.79, 0.99
$Fc(CH_2)_2COOH$[d] **3**	Fc	0.020	-0.015, 0.070	3.87, 0.99
$Fc(CH_2)_3COOH$[d] **4**	Fc	0.011	-0.024, 0.070	3.98, 0.99
$FcCO(CH_2)_2COOH$[d] **5**	Fc	0.330	0.295, 0.070	3.66, 0.99
SubPc **6** -	DmFc	-0.647	-0.610, 0.076	3.89, 0.99
$ClBSubPc(H)_{12}$[e]	Wave I	0.674	0.628, 0.086	3.08, 0.99
	Wave II	-1.519	- , -	3.63, -
	Wave III	-2.050	- , -	- , -
SubPc **7** -	DmFc	-0.647	-0.610, 0.074	3.91, 0.99
Fc$CO_2SubPc(H)_{12}$	Fc	0.262	0.224, 0.076	3.61, 0.99
	Wave I	0.711	0.670, 0.082	3.34, 0.99
	Wave II	-1.643	-1.601, 0.084	3.47, 0.99
	Wave III	-2.124	- , -	- , -
SubPc **8** -	DmFc	-0.647	-0.610, 0.075	3.84, 0.99
Fc$CH_2CO_2SubPc(H)_{12}$	Fc	-0.005	-0.043, 0.076	3.61, 0.99
	Wave I	0.710	0.670, 0.080	3.38, 0.99
	Wave II	-1.643	-1.674, 0.082	3.49,0.99
	Wave III	-2.154	- , -	- , -
SubPc **9** -	DmFc	-0.647	-0.610,0.074	3.89, 0.99
Fc$(CH_2)_2CO_2SubPc(H)_{12}$[f]	Fc	-0.021	-0.058, 0.074	3.66, 0.99

	Wave I	0.712	0.670, 0.084	3.31, 0.99
	Wave II	-1.783	-1.741, 0.084	3.42, 0.99
	Wave III	-2.264	- , -	- , -
SubPc **10** - **Fc**$(CH_2)_3CO_2$SubPc(H)$_{12}$	DmFc	-0.647	-0.610, 0.075	3.97, 0.99
	Fc	-0.024	-0.062, 0.076	3.58, 0.99
	Wave I	0.711	0.670, 0.082	3.27, 0.99
	Wave II	-1.871	-1.829, 0.084	3.39, 0.99
	Wave III	-2.344	- , -	- , -
SubPc **11** - **Fc**$CO(CH_2)_2CO_2$SubPc(H)$_{12}$	DmFc	-0.647	-0.610, 0.074	3.84, 0.99
	Fc	0.300	0.262, 0.076	3.57, 0.99
	Wave I	0.711	0.670, 0.082	3.35, 0.99
	Wave II	-1.525	-1.482, 0.086	3.41, 0.99
	Wave III	-2.004	- , -	- , -

[a] E_P is the peak anodic peak for oxidation (E_{ox}) and peak cathodic peak for reduction (E_{red}).
[b] i_P is the peak anodic peak for oxidation (i_{Pa}) and peak cathodic peak for reduction (i_{Pc}).
[c] peak current ratio = i_{Pc}/i_{Pa} for oxidation and i_{Pa}/i_{Pc} for reduction.
[d] Data from reference [14]
[e]. Data from reference [20]
[f]. Data from reference [23]

2.4.4. *Ring Based Reductions*

The first (wave II) and second (wave III) ring-based reductions of SubPcs 7 – 11 are lower than that of SubPc **6**. The axial ferrocenylcarboxylic ligands of SubPcs **7** – **11** thus have a nett electron donating effect on the aromatic ring electrons of SubPcs **7** – **11** compared to Cl in SubPc **6**. Both ring-based reductions of SubPcs **7** – **11**, redox waves II and II in Figure 3 and Table 2, followed the same trend, namely the reduction value decreases near linear as the number of (CH_2) groups, n, in the different axially bonded ferrocenyl carboxylic acid moieties (Fc-$(CH_2)_n$-CO_2) increases in SubPcs **7** – **10**, with the reduction values of SubPc **11** higher than that of SubPc **7**, see Figure 4 (b). The charge on Fc in **7** – **10** is isolated from the rest of the molecules, and the aromatic ring electron density of the SubPcs systematically increased as n of the alkyl group in –OCO$(CH_2)_n$- increases. SubPc **10** exhibited the lowest first ring-based reduction potential (-1.872 V), reported to date [18,21,22,25], due to the carboxyl-alkyl (OOC$(CH_2)_3$), group's electron-withdrawing effect being isolated from ferrocenium moiety. The withdrawing effect is the most prominent on SubPc **10** containing the

longest alkyl chain. Propyl (n = 3) is more electron donating than ethyl (n = 2) that is more electron donating then methyl (n = 1).

2.4.5. *Ring Based Oxidation*

$E^{\circ\prime}$ of the first ring-based oxidation of SubPcs **7** – **11** (wave I in Figure 3) is exactly the same, with $E^{\circ\prime}$ = 0.670 V for all five complexes **7** – **11**. This is because the charge located on the ferrocenium group (Fc^+) in the different oxidised ferrocenyl carboxylic acid moieties (Fc^+-$(CH_2)_n$-CO_2) and (Fc^+-$CO(CH_2)_2$-CO_2) for SubPcs **7** – **11**, is isolated from and the rest of the molecule. The Fc^+ group is highly electronegative [26], withdrawing any available electron density from the alkyl groups bonded to it. The first ring-based oxidation of SubPcs **7** – **11** is consequently only influenced by the electron withdrawing carboxyl group attached directly to boron in the axial position, shifting the first ring-based oxidation of SubPcs **7** – **11** with exactly the same value namely 0.042 V more positive than $E^{\circ\prime}$ of the first ring-based oxidation of SubPcs **6** at 0.628 V. The electron withdrawing effect of the carboxyl group in **7** – **11** is thus larger than the electron withdrawing effect of Cl in **6**, on the aromatic ring electron density of the SubPcs. It was possible to get chemically reversible ring-based oxidation with peak current ratios approaching 1 and peak current separation ΔE_p between 0.080 and 0.084 V, see Table 2.

2.5. Computational Analysis

The ferrocenylcarboxylic-containing SubPc dyads **7** – **11**, were optimised using density functional theory (DFT) to gain further insight into the redox properties of the ferrocene dyads. In agreement with previous studies on related SubPcs, the HOMOs of the neutral species are of iron-d character while the LUMOs have π-ring character [21,23]. This confirm Fe(II) to Fe(III) oxidation and ring-based reduction respectively. However, since the top three HOMOs of **7** – **11** are all iron-d based, and Fe(III) to Fe(IV) oxidation is not expected, it was essential to also optimise the cation (oxidised) species, to locate the locus of the second experimentally observed oxidation. It is known that orbitals can rearrange upon oxidation [27–29]. The DFT results of oxidised SubPcs **7** – **11** all

showed that the LUMO is of iron-d character (the first oxidation, see Figure 5) and the HOMO is on the SubPc ring (the second oxidation, see Figure 5). HOMO-1, also on the SubPc ring, will be the second ring oxidation, however, it is out of the solvent window in cyclic voltammetry scans and not experimentally observed.

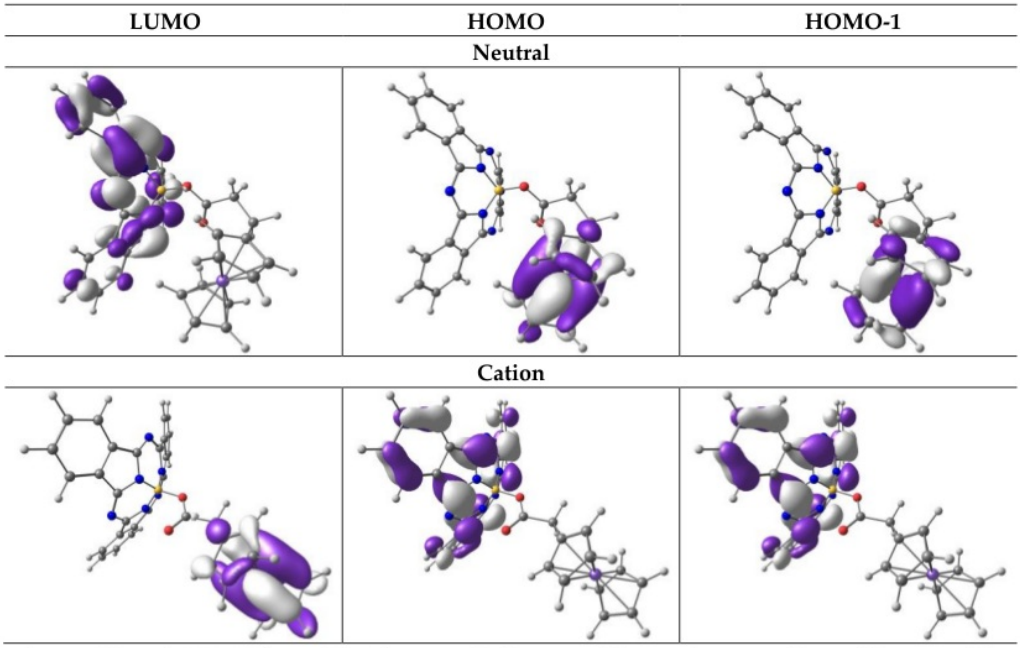

Figure 5 Selected PBE1PBE/6-311G(d,p) frontier MOs for cation SubPc, **8**. A contour of 0.03 e/Å^3 was used for the orbital plots. Colour code of atoms (online version): Fe (purple), B (yellow), C (grey), O (red), H (white).

3. Materials and Methods

Solid reagents (Sigma-Aldrich, Strem and Merck) were used as received. Liquid reagents (Sigma-Aldrich and Merck) were used without any further purification unless specified otherwise. Solvents were distilled, and water was double distilled. Organic solvents used in this study were dried according to published methods [30]. Melting points are uncorrected and were determined with an Olympus BX 51 microscope equipped with a Linkam THMS 600 hot stage.

3.1. Spectroscopy Measurements

^{1}H, ^{11}B and ^{13}C spectroscopic analysis were performed for all compounds in the study. ^{1}H and ^{13}C spectra were recorded at 25°C on a 600 MHz AVANCE II NMR spectrometer at 600.28 MHz and 150.95 MHz respectively. ^{11}B NMR spectra were recorded at 25°C on a 400 MHz AVANCE III NMR spectrometer at 128.38 MHz. Hydrogen and carbon chemical shifts are relative to hydrogen and carbon in $CDCl_3$ at 7.24 ppm and 77.16 ppm, respectively. The following abbreviations are used to describe peak patterns: s = singlet, d = doublet, t = triplet, q = quartet and m = multiplet. UV/vis spectra were recorded on a Varian Cary 5000 UV-Vis-NIR Spectrophotometer. Melting points are uncorrected and were determined with an Olympus BX 51 microscope equipped with a Linkam THMS 600 hot stage.

3.2. *Cyclic Voltammetry*

All the electrochemical experiments were performed in an M Bruan Lab Master SP glove box under a high purity argon atmosphere (H_2O and O_2 < 10 ppm). Cyclic voltammetry (CV) measurements were performed utilising a Princeton Applied Research PARSTAT 2273 potentiostat, running Powersuite software (Version 2.58). A three-electrode cell was used. A glassy carbon electrode with a surface area 3.14 x 10^{-6} m^2 was chosen as working electrode, platinum wires were chosen as auxiliary and reference electrodes. The glassy carbon working electrode was polished and prepared before every experiment on a Buhler polishing mat first with 1-micron and then with ¼-micron diamond paste, rinsed with H_2O, acetone and dichloromethane (DCM), and dried before each experiment. Electrochemical analysis of the complexes was performed in DCM (anhydrous, ≥ 99.8%, contains 40-150 ppm amylene as a stabiliser) at room temperature. Solutions were made in 0.001 dm^3 spectrochemical grade anhydrous DCM containing *ca.* 0.0005 M of an analyte, 0.0005 mol dm^{-3} of internal reference (decamethylferrocene, DmFc) and 0.1 mol dm^{-3} of supporting electrolyte tetrabutylammonium tetrakispentafluorophenylborate, $[N(^{n}Bu)_4][B(C_6F_5)_4]$ in DCM. Experimental potential data was collected *vs.* the Pt wire reference electrode but is reported *vs.* the redox couple of ferrocene, Fc/Fc^{+} at 0 V. $E^{o'}$ (DmFc) = - 0.610 V *vs.* Fc/Fc^{+} at 0 V in DCM/$[N(^{n}Bu)_4][B(C_6F_5)_4]$. Scan rates were between 0.05 and 5.00 Vs^{-1}. Electrochemical reversibility (or Nernstian behaviour) of redox

processes is indicated by a peak current ratio (i_{pc}/i_{pa} for oxidation and i_{pa}/i_{pc} for reduction) of 1 [31,32] and peak current separation $\Delta E = |E_{pa} - E_{pc}| = 0.059$ V for a one-electron transfer process [33]. In this experiment, due to experimental cell imperfections and ohmic drop effects, ΔE_P slightly larger than 0.059 V was obtained, even for the known 1 e- transfer processes of decamethylferrocene, $DmFc^+/DmFc$, namely 0.074 - 0.076 V [34–36]. The formal reduction potential is determined by $E^{o'} = (E_{pa} - E_{pc})/2$ for an electrochemically reversible (and quasi reversible) process where E_{pa} (E_{pc}) = anodic (cathodic) peak potential and i_{pa} (i_{pc}) = anodic (cathodic) peak current.

3.3.DFT Calculations

Density functional theory (DFT) optimisations were performed on the neutral and oxidised molecules in the gas phase using the hybrid PBE1PBE [37–39] exchange-correlation functional and the triple-ζ basis set 6-311G(d,p) basis set, as implemented in the Gaussian 16 package [40]. Single point calculations using pure BP86 [41–43] exchange-correlation were performed in DCM as the solvent, using the IEF-PCM model (polarisable continuum model (PCM) [44] which solved the non-homogeneous Poisson equation by applying the integral equation formalism variant) [45]. Both the gas phase PBE1PBE/6-311G(d,p) and solvent phase BP86/6-311G(d,p) results gave the same molecular orbital (MO) insight into the observed experimental redox processes.

3.4. Preparationof SubPcs ***7*** *-* ***11***

$FcCO_2H$, **1**, $FcCH_2CO_2H$, **2**, $Fc(CH_2)_2CO_2H$, **3**, $Fc(CH_2)_3CO_2H$, **4**, $ClBSubPc(H)_{12}$, **5**, and $Fc(CH_2)_2CO_2BSubPc(H)_{12}$, **9**, were synthesised using slight modifications to literature methods (see the supporting information) [8,12,13,23]. Compounds **7** – **11** were characterised by NMR, UV/vis, elemental analysis and m.p.

3.4.1. Preparation of $FcCO_2SubPc(H)_{12}$, **7**.

To a solution of chlorosubphthalocyanine, **6**, (200 mg; 0.46 mmol) and dry toluene (3 cm^3), silver trifluoromethanesulfonate (150 mg, 0.58 mmol; 1.25 eq.) was added and the mixture stirred at 45°C,

under argon atmosphere for 4 hours. Once the (OTf)SubPc(H)$_{12}$ was generated, ferrocenylcarboxylic acid, **1**, (212 mg, 0.92 mmol, 2 eq.) and *N*,*N*-diisopropylethylamine (0.10 cm^3, 75 mg, 0.58 mmol, 1.25 eq.) was added. The mixture was stirred at 50 °C for 12 hours. The solvent was removed by evaporation under reduced pressure and the product was directly purified by flash chromatography using hexane: DCM (1:1) (R_f: 0.82) as eluent to give 184 mg (92%). m.p.: 172-182°C, UV/vis: λ_{max} 563 nm, ε = 176547 dm^3 mol^{-1} cm^{-1} in THF. NMR: δ_H (600.28 MHz, $CDCl_3$, 25 °C): δ 8.84 (6H, dd, SubPc), 7.90 (6H, dd, SubPc), 3.96 (2 H, pt, 2 x CH_2: Substituted-Cp), 3.95 (2 H, pt, 2 x CH_2: Substituted-Cp), 3.63 (5 H, s, Unsubstituted-Cp). ^{11}B NMR: δ_B (128.38 MHz, $CDCl_3$): δ 16.82 (1B). ^{13}C NMR: δ_C (150.95 MHz, $CDCl_3$, 25 °C): δ 151.64 (6C, N=C), 130.00 (6C, SubPc - C=C), 122.49 (6C, SubPc-Ph), 71.02 (1C, C-CO_2H), 70.01 (2C, Substituted-Cp), 69.58 (5C, Unsubstituted-Cp). Elemental analysis calculated for $C_{35}H_{21}BFeN_6O_2$ (element, %): C, 67.34; H, 3.39; N, 13.46. Obtained: C, 67.73; H, 3.47; N, 13.58.

3.4.2. Preparation of FcCH_2CO_2SubPc(H)$_{12}$, **8**.

To a solution of chlorosubphthalocyanine, **6**, (200 mg; 0.46 mmol) and dry toluene (3 cm^3), silver trifluoromethanesulfonate (150 mg, 0.58 mmol; 1.25 eq.) was added and the mixture stirred at 45°C, under argon atmosphere for 4 hours. Once the (OTf)SubPc(H)$_{12}$ was generated, ferrocenylmethanoic acid, **2**, (225 mg, 0.92 mmol, 2 eq.) and *N*,*N*-diisopropylethylamine (0.10 cm^3, 75 mg, 0.58 mmol, 1.25 eq.) was added. The mixture was stirred at 50 °C for 12 hours. The solvent was removed by evaporation under reduced pressure and the product was directly purified by flash chromatography using hexane: DCM (1:1) (R_f: 0.78) as eluent to give 140 mg (79%). m.p.: 175 – 183°C, UV/vis: λ_{max} 563 nm, ε = 166317 dm^3 mol^{-1} cm^{-1} in THF. NMR: δ_H (600.28 MHz, $CDCl_3$, 25 °C): δ 8.86 (6H, dd, SubPc), 7.89 (6H, dd, SubPc), 3.79 (2 H, pt, 2 x CH_2: Substituted-Cp), 3.67 (5 H, s, Unsubstituted-Cp), 3.53 (2 H, pt, 2 x CH_2: Substituted-Cp), 2.28 (2H, t, CH_2). ^{11}B NMR: δ_B (128.38 MHz, $CDCl_3$): δ 16.76 (1B). ^{13}C NMR: δ_C (150.95 MHz, $CDCl_3$, 25 °C): δ 151.68 (6C, N=C), 130.04 (6C, SubPc - C=C), 122.45 (6C, SubPc-Ph), 69.10 (1C, C-CO_2H), 68.41 (2C, Substituted-Cp), 67.48 (5C, Unsubstituted-Cp), 30.48 (2C, CH2). Elemental analysis calculated for $C_{36}H_{23}BFeN_6O_2$ (element, %): C, 67.74; H, 3.63; N, 13.17. Obtained: C, 67.90; H, 3.82; N, 13.72.

3.4.3. Preparation of $Fc(CH_2)_3CO_2SubPc(H)_{12}$, **10**.

To a solution of chlorosubphthalocyanine, **6**, (200 mg; 0.46 mmol) and dry toluene (3 cm^3), silver trifluoromethanesulfonate (150 mg, 0.58 mmol; 1.25 eq.) was added and the mixture stirred at 45°C, under argon atmosphere for 4 hours. Once the $(OTf)SubPc(H)_{12}$ was generated, ferrocenylethanoic acid, **4**, (250 mg, 0.92 mmol, 2 eq.) and *N*,*N*-diisopropylethylamine (0.10 cm^3, 75 mg, 0.58 mmol, 1.25 eq.) was added. The mixture was stirred at 50 °C for 12 hours. The solvent was removed by evaporation under reduced pressure and the product was directly purified by flash chromatography using hexane: DCM (1:1) (R_f: 0.73) as eluent to give 104 mg (52%). m.p.: 182-190°C, UV/vis: λ_{max} 563 nm, ε = 145673 dm^3 mol^{-1} cm^{-1} in THF. NMR: δ_H (600.28 MHz, $CDCl_3$, 25 °C): δ 8.86 (6H, dd, SubPc), 7.88 (6H, dd, SubPc), 3.89 (5 H, s, Unsubstituted-Cp), 3.84 (2 H, pt, 2 x CH_2: Substituted-Cp), 3.70 (2 H, pt, 2 x CH_2: Substituted-Cp), 1.76 (2H, t, CH_2), 1.26 (2H, t, CH_2), 1.06 (2H, q, CH_2). ^{11}B NMR: δ_B (128.38 MHz, $CDCl_3$): δ 16.32 (1B). ^{13}C NMR: δ_C (150.95 MHz, $CDCl_3$, 25 °C): δ 151.64 (6C, N=C), 129.99 (6C, SubPc - C=C), 122.43 (6C, SubPc-Ph), 68.48 (1C, C-CO_2H), 68.01 (2C, Substituted-Cp), 67.01 (5C, Unsubstituted-Cp), 28.42 (2C, CH_2), 25.39 (2C, CH_2). Elemental analysis calculated for $C_{38}H_{27}BFeN_6O_2$ (element, %): C, 68.50; H, 4.08; N, 12.61. Obtained: C, 68.61; H, 4.16; N, 12.74.

3.4.4. Preparation of $FcCO(CH_2)_2CO_2SubPc(H)_{12}$, **11**.

To a solution of chlorosubphthalocyanine, **6**, (200 mg; 0.46 mmol) and dry toluene (3 cm^3), silver trifluoromethanesulfonate (150 mg, 0.58 mmol; 1.25 eq.) was added and the mixture stirred at 45°C, under argon atmosphere for 4 hours. Once the $(OTf)SubPc(H)_{12}$ was generated, ferrocenyloxobutanoic acid, **4**, (263 mg, 0.92 mmol, 2 eq.) and *N*,*N*-diisopropylethylamine (0.10 cm^3, 75 mg, 0.58 mmol, 1.25 eq.) was added. The mixture was stirred at 50 °C for 12 hours. The solvent was removed by evaporation under reduced pressure and the product was directly purified by flash chromatography using hexane: DCM (1:1) (R_f: 0.62) as eluent to give 114 mg (57%). m.p.: 201-207°C, UV/vis: λ_{max} 563 nm, ε = 113729 dm^3 mol^{-1} cm^{-1} in THF. NMR: δ_H (600.28 MHz, $CDCl_3$, 25 °C): δ 8.85 (6H, dd, SubPc), 7.88 (6H, dd, SubPc), 4.49 (2 H, pt, 2 x CH_2: Substituted-Cp), 4.31 (2 H, pt, 2 x CH_2:

Substituted-Cp), 3.98 (5 H, s, Unsubstituted-Cp), 2.23 (2H, t, CH_2), 1.66 (2H, t, CH_2).^{11}B NMR: δ_B (128.38 MHz, $CDCl_3$): δ 16.79 (1B). ^{13}C NMR: δ_C (150.95 MHz, $CDCl_3$, 25 °C): δ 156.51 (6C, N=C), 144.73 (6C, SubPc - C=C), 130.42 (6C, SubPc-Ph), 72.55 (1C, C-CO_2H), 70.14 (2C, Substituted-Cp), 69.41 (5C, Unsubstituted-Cp),34.23 (2C, CH_2). Elemental analysis calculated for $C_{38}H_{25}BFeN_6O_3$ (element, %): C, 67.09; H, 3.70; N, 12.35. Obtained: C, 67.09; H, 3.82; N, 12.35.

4. Conclusions

Subphthalocyanines with ferrocenylcarboxylic acids in the axial position can be synthesized in 90% yields when reactions are performed under strict Schlenk conditions, in this case a glovebox. The axial ferrocenyl moiety did not influence the UV/vis wavelength maxima of the Soret or Q-bands comparing SubPcs **7** – **11** with parent macrocycle, **6**. The cyclic voltammetry data revealed that the first reversible oxidation process is ferrocene-centered, with the second oxidation and all observed reduction processes are SubPc ring-based. DFT optimization of the oxidized (cation) SubPc was necessary to confirm the locus of the second observed SubPc ring-based oxidation.

The oxidation potential of Fe of the axial ferrocenyl moiety was affected by the subphthalocyanine, shifting $Fe^{II/III}$ oxidation potentials with 0.03 – 0.06 V to a lower oxidation potential compared to $Fe^{II/III}$ oxidation potentials of the free ferrocenyl acids. The oxidized axial electron withdrawing ferrocenium moiety, withdraws charge from the alkyl chains bonded to it, and consequently the first ring-based oxidation of all ferrocenylsubphthalocyanine dyads Y-BSubPc(H)$_{12}$ is only influenced by the electron withdrawing carboxyl group in the axial position, shifting the first ring-based oxidation for all ferrocenylsubphthalocyanine dyads with exactly the same value of 0.042 V more positive compared to the first ring-based oxidation of Cl-BSubPc(H)$_{12}$. Both the carboxyl and alkyl groups in the axial position influenced the ring electron density of the neutral SubPc, leading to a systematic decrease in the two observed ring-based reductions of the ferrocenylsubphthalocyanine dyads as the number of alkyl groups n in the different axially bonded ferrocenyl carboxylic acid moieties (Fc-$(CH_2)_n$-CO_2) increases. Fc$(CH_2)_3$BSubPc(H)$_{12}$, SubPc **10**, has the lowest first ring-based

reduction potential reported to date, due to the strong electron withdrawing effect of the axial carboxyl-alkyl group ($OOC(CH_2)_3$), being isolated from the ferrocenium moiety.

Supplementary Materials: The following are available online at www.mdpi.com/xxx/s1, synthesis and characterisation, additional graphs, tables, and optimised coordinates are provided in the Supporting information.

Funding: This research was funded by South African National Research Foundation (Grant numbers 113327 and 96111) and the Central Research Fund of the University of the Free State, Bloemfontein. The High-Performance Computing facility of the UFS, the CHPC of South Africa and the Norwegian Supercomputing Program (UNINETT Sigma2, Grant No. NN9684K) are acknowledged for computer time.

Conflicts of Interest: The authors declare no competing financial interest.

References

1. Dagani, R. Fifty Years of Ferrocene Chemistry. *Chem. Eng. News* **2001**, *79*, 37–38.
2. Bublitz, D. E.Rinehart, K.L. *Inorganic Reactions*; 17th ed.; Eiley: New York, 1969;
3. Deeming, J. *In Comprehensive Organometallic Chemistry*; Pergamon, Ed.; 4th ed.; Oxford, 1982;
4. Watts, W.. *In Comprhensive Organometallic Chemistry*; Pergamon, Ed.; 8th ed.; Oxford, 1982;
5. Nesmeyanov, A.N.; Kochetkova, N.S. Applications of Ferrocene and Its Derivatives. *Russ. Chem. Rev.* **1974**, *5*, 710–715.
6. Conradie, J.; Lamprecht, G.J.; Roodt, A.; Swarts, J.C. Kinetic study of the oxidative addition reaction between methyl iodide and [Rh(FcCOCHCOCF3)(CO)(PPh3)]: Structure of [Rh(FcCOCHCOCF3)(CO)(PPh3)(CH3)(I)]. *Polyhedron* **2007**, *26*, 5075–5087.
7. Shen, Q.; Shekhar, S.; Stambuli, J.P.; Hartwig, J.F. Highly reactive, general, and long-lived catalysts for coupling heteroaryl and aryl chlorides with primary nitrogen nucleophiles. *Angew. Chemie - Int. Ed.* **2005**, *44*, 1371–1375.
8. Nonjola, P.T.N.; Siegert, U.; Swarts, J.C. Synthesis, Electrochemistry and Cytotoxicity of Ferrocene-Containing Amides, Amines and Amino-Hydrochlorides. *J. Inorg. Organomet. Polym. Mater.* **2015**, *25*, 376–385.
9. Swarts, J.C.; Vosloo, T.G.; Cronje, S.J.; Du Plessis, W.C.; Van Rensburg, C.E.J.; Kreft, E.; Van Lier, J.E. Cytotoxicity of a series of ferrocene-containing β-diketones. *Anticancer Res.* **2008**, *28*, 2781–2784.
10. Shago, R.F.; Swarts, J.C.; Kreft, E.; Van Rensburg, C.E.J. Antineoplastic activity of a series of ferrocene-containing alcohols. *Anticancer Res.* **2007**, *27*, 3431–3433.
11. Peter, S.; Aderibigbe, B.A. Ferrocene-Based Compounds with Antimalaria/Anticancer Activity. *Molecules* **2019**, *24*, 3604.

12. Davis, W.L.; Shago, R.F.; Langner, E.H.G.; Swarts, J.C. Synthesis and electrochemical properties of a series of ferrocene-containing alcohols. *Polyhedron* **2005**, *24*, 1611–1616.
13. Blom, N.F.; Neuse, E.W.; Thomas, H.G. Electrochemical characterization of some ferrocenylcarboxylic acids. *Transit. Met. Chem.* **1987**, *12*, 301–306.
14. Swarts, P.J.; Conradie, J. Solvent and Substituent Effect on Electrochemistry of Ferrocenylcarboxylic Acid Dyads. *J. Electroanal. Chem.*
15. A, M.; A, O. Phthalocyaninartige Bor-Komplexe. *Monatshefte fur Chemie* **1972**, *103*, 150–155.
16. Ma, Z.; Liu, S.; Hu, S.; Yu, J. Highly efficient tandem organic light-emitting diodes based on SubPc:C60 bulk heterojunction as charge generation layer. *J. Lumin.* **2016**, *169*, 29–34.
17. Ince, M.; Medina, A.; Yum, J.H.; Yella, A.; Claessens, C.G.; Martínez-Díaz, M.V.; Grätzel, M.; Nazeeruddin, M.K.; Torres, T. Peripherally and axially carboxylic acid substituted subphthalocyanines for dye-sensitized solar cells. *Chem. - A Eur. J.* **2014**, *20*, 2016–2021.
18. Claessens, C.G.; González-Rodríguez, D.; Rodríguez-Morgade, M.S.; Medina, A.; Torres, T. Subphthalocyanines, subporphyrazines, and subporphyrins: Singular nonplanar aromatic systems. *Chem. Rev.* 2014, *114*, 2192–2277.
19. van de Winckel, E.; Mascaraque, M.; Zamarrón, A.; Juarranz de la Fuente, Á.; Torres, T.; de la Escosura, A. Dual Role of Subphthalocyanine Dyes for Optical Imaging and Therapy of Cancer. *Adv. Funct. Mater.* **2018**, *28*.
20. Swarts, P.J.; Conradie, J. Electrochemical behaviour of chloro- and hydroxy-subphthalocyanines. *Electrochim. Acta* **2020**, *329*, 135165.
21. Solntsev, P. V.; Spurgin, K.L.; Sabin, J.R.; Heikal, A.A.; Nemykin, V.N. Photoinduced charge transfer in short-distance ferrocenylsubphthalocyanine dyads. *Inorg. Chem.* **2012**, *51*, 6537–6547.
22. Maligaspe, E.; Hauwiller, M.R.; Zatsikha, Y. V.; Hinke, J.A.; Solntsev, P. V.; Blank, D.A.; Nemykin, V.N. Redox and photoinduced electron-transfer properties in short distance organoboryl ferrocene-subphthalocyanine dyads. *Inorg. Chem.* **2014**, *53*, 9336–9347.
23. Swarts, P.J.; Conradie, J. Redox and photophysical properties of four SubPcs containing ferrocenylcarboxylic acid dyads as axial ligands. *Inorg. Chem.*
24. Guilleme, J.; González-Rodríguez, D.; Torres, T. Triflate-subphthalocyanines: Versatile, reactive intermediates for axial functionalization at the boron atom. *Angew. Chemie - Int. Ed.* **2011**, *50*, 3506–3509.
25. Sampson, K.L.; Josey, D.S.; Li, Y.; Virdo, J.D.; Lu, Z.H.; Bender, T.P. Ability to Fine-Tune the Electronic Properties and Open-Circuit Voltage of Phenoxy-Boron Subphthalocyanines through Meta-Fluorination of the Axial Substituent. *J. Phys. Chem. C* **2018**, *122*, 1091–1102.
26. du Plessis, W.; Erasmus, J.J.; Lamprecht, G.J.; Conradie, J.; Cameron, T.S.; Aquino, M.A.; Swarts, J.C. Cyclic voltammetry of ferrocene-containing β-diketones as a tool to obtain group electronegativities. The structure of 3-ferrocenoyl-1,1,1-trifluoro-2-hydroxyprop-2-ene. *Can. J. Chem.* **2011**, *77*, 378–386.
27. Ferrando-Soria, J.; Fabelo, O.; Castellano, M.; Cano, J.; Fordham, S.; Zhou, H.C. Multielectron oxidation in a ferromagnetically coupled dinickel(II) triple mesocate. *Chem. Commun.* **2015**, *51*, 13381–13384.
28. Buitendach, B.E.; Conradie, J.; Malan, F.P.; Niemantsverdriet, J.W.; Swarts, J.C. Synthesis, Spectroscopy and Electrochemistry in Relation to DFT Computed Energies of Ferrocene- and

Ruthenocene-Containing -Diketonato Iridium(III) Heteroleptic Complexes. Structure of [(2-Pyridylphenyl)2Ir(RcCOCHCOCH3]. *Molecules* **2019**, *24*, 3923.

29. Malan, F.P.; Singleton, E.; Conradie, J.; Landman, M. Electrochemistry of a series of symmetric and asymmetric CpNiBr(NHC) complexes: Probing the electrochemical environment due to push-pull effects. *J. Electroanal. Chem.* **2018**, *814*, 66–76.
30. Williams, D.B.G.; Lawton, M. Drying of organic solvents: Quantitative evaluation of the efficiency of several desiccants. *J. Org. Chem.* **2010**, *75*, 8351–8354.
31. Elgrishi, N.; Rountree, K.J.; McCarthy, B.D.; Rountree, E.S.; Eisenhart, T.T.; Dempsey, J.L. A Practical Beginner's Guide to Cyclic Voltammetry. *J. Chem. Educ.* **2018**, *95*, 197–206.
32. Kissinger, P.T.; Heineman, W.R. Cyclic voltammetry. *J. Chem. Educ.* **1983**, *60*, 702–706.
33. Gericke, H.J.; Barnard, N.I.; Erasmus, E.; Swarts, J.C.; Cook, M.J.; Aquino, M.A.S. Solvent and electrolyte effects in enhancing the identification of intramolecular electronic communication in a multi redox-active diruthenium tetraferrocenoate complex, a triple-sandwiched dicadmium phthalocyanine and a ruthenocene-containing β-diketone. *Inorganica Chim. Acta* **2010**, *363*, 2222–2232.
34. Blrke, R.L.; Kim, M.H.; Strassfeld, M. Diagnosis of Reversible, Quasi-Reversible, and Irreversible Electrode Processes with Differential Pulse Polarography. *Anal. Chem.* **1981**, *53*, 852–856.
35. Mirkin, M. V.; Bard, A.J. Simple Analysis of Quasi-Reversible Steady-State Voltammograms. *Anal. Chem.* **1992**, *64*, 2293–2302.
36. Myland, J.C.; Oldham, K.B. Quasireversible cyclic voltammetry of a surface confined redox system: A mathematical treatment. *Electrochem. commun.* **2005**, *7*, 282–287.
37. Perdew, J.P.; Burke, K.; Ernzerhof, M. Generalized gradient approximation made simple. *Phys. Rev. Lett.* **1996**, *77*, 3865–3868.
38. Perdew, J.P.; Burke, K.; Ernzerhof, M. Generalized Gradient Approximation Made Simple (ERRATA). *Phys. Rev. Lett.* **1997**, *78*, 1396–1396.
39. Adamo, C.; Barone, V. Toward reliable density functional methods without adjustable parameters: The PBE0 model. *J. Chem. Phys.* **1999**, *110*, 6158–6170.
40. Frisch, M.J.; Trucks, G.W.; Schlegel, H.B.; Scuseria, G.E.; Robb, M.A.; Cheeseman, J.R.; Scalmani, G.; Barone, V.; Petersson, G.A.; Nakatsuji, H.; et al. Gaussian 16, Revision B.01 2016, 2016.
41. Becke, A.D. Density-functional exchange-energy approximation with correct asymptotic behavior. *Phys. Rev. A* **1988**, *38*, 3098–3100.
42. Perdew, J.P. Density-functional approximation for the correlation energy of the inhomogeneous electron gas. *Phys. Rev. B* **1986**, *33*, 8822–8824.
43. Perdew, J.P. Erratum: Density-functional approximation for the correlation energy of the inhomogeneous electron gas (Physical Review B (1986) 34, 10 (7406)). *Phys. Rev. B* **1986**, *34*, 7406.
44. Marenich, A. V; Cramer, C.J.; Truhlar, D.G. Universal Solvation Model Based on Solute Electron Density and on a Continuum Model of the Solvent Defined by the Bulk Dielectric Constant and Atomic Surface Tensions. *J. Phys. Chem. B* **2009**, *113*, 6378–6396.
45. Skyner, R.E.; Mcdonagh, J.L.; Groom, C.R.; Mourik, T. Van A review of methods for the calculation of solution free energies and the modelling of systems in solution. *Phys. Chem.*

Chem. Phys. **2018**, *17*, 6174–6191.

Publication 3

ORIGINALITY REPORT

15%	8%	10%	9%
SIMILARITY INDEX	INTERNET SOURCES	PUBLICATIONS	STUDENT PAPERS

PRIMARY SOURCES

1	Li-Cheng Song, Fei-Xian Luo, Hao Tan, Xiao-Jing Sun, Zhao-Jun Xie, Hai-Bin Song. "Synthesis, Structures, and Properties of Diiron Azadithiolate Complexes Containing a Subphthalocyanine Moiety as Biomimetic Models for [FeFe]-Hydrogenases", European Journal of Inorganic Chemistry, 2013 Publication	1%
2	Submitted to University of Basel Student Paper	1%
3	Pavlo V. Solntsev, Katelynn L. Spurgin, Jared R. Sabin, Ahmed A. Heikal, Victor N. Nemykin. "Photoinduced Charge Transfer in Short-Distance Ferrocenylsubphthalocyanine Dyads", Inorganic Chemistry, 2012 Publication	1%
4	www.mdpi.com Internet Source	1%
5	conservancy.umn.edu Internet Source	1%

6	Submitted to University of Durham Student Paper	1%
7	Mohamed E. El-Khouly, Sun Hee Shim, Yasuyuki Araki, Osamu Ito, Kwang-Yol Kay. "Effect of Dual Fullerenes on Lifetimes of Charge-Separated States of Subphthalocyanine−Triphenylamine−Fullerene Molecular Systems", The Journal of Physical Chemistry B, 2008 Publication	1%
8	Submitted to University of Hong Kong Student Paper	1%
9	repository.up.ac.za Internet Source	<1%
10	Daniela I. Bezuidenhout, Israel Fernández, Belinda van der Westhuizen, Pieter J. Swarts, Jannie C. Swarts. "Electrochemical and Computational Study of Tungsten(0) Ferrocene Complexes: Observation of the Mono-Oxidized Tungsten(0) Ferrocenium Species and Intramolecular Electronic Interactions", Organometallics, 2013 Publication	<1%
11	J.-L Bister, B Noël, B Perrad, S.N.M Mandiki, J Mbayahaga, R Paquay. "Control of ovarian follicles activity in the ewe", Domestic Animal	<1%

Endocrinology, 1999
Publication

12	etd.uovs.ac.za Internet Source	<1%
13	Submitted to Higher Education Commission Pakistan Student Paper	<1%
14	Tae-Hyuk Kwon. "New Approach Toward Fast Response Light-Emitting Electrochemical Cells Based on Neutral Iridium Complexes via Cation Transport", Advanced Functional Materials, 03/10/2009 Publication	<1%
15	Submitted to Nanyang Technological University, Singapore Student Paper	<1%
16	ir.soken.ac.jp Internet Source	<1%
17	Submitted to Indian Institute of Technology, Madras Student Paper	<1%
18	Teixeira, Róbson Ricardo, Wagner Luiz Pereira, Deborah Campos Tomaz, Fabrício Marques de Oliveira, Samuele Giberti, and Giuseppe Forlani. "Synthetic Analogues of the Natural Compound Cryphonectric Acid Interfere with	<1%

Photosynthetic Machinery through Two Different Mechanisms", Journal of Agricultural and Food Chemistry, 2013.
Publication

19	Bottari, Giovanni, Gema de la Torre, Dirk M. Guldi, and Tomás Torres. "Covalent and Noncovalent Phthalocyanine−Carbon Nanostructure Systems: Synthesis, Photoinduced Electron Transfer, and Application to Molecular Photovoltaics", Chemical Reviews, 2010. Publication	<1%
20	res.mdpi.com Internet Source	<1%
21	www.jove.com Internet Source	<1%
22	Romolo Francesconi, Adriana Bigi, Katia Rubini, Fabio Comelli. "Excess Enthalpies, Heat Capacities, Densities, Viscosities and Refractive Indices of Dimethyl Sulfoxide + Three Aryl Alcohols at 308.15 K and Atmospheric Pressure", Journal of Chemical & Engineering Data, 2005 Publication	<1%
23	Submitted to University of Strathclyde Student Paper	<1%

24	Submitted to Universiti Teknologi Malaysia Student Paper	<1%
25	link.springer.com Internet Source	<1%
26	Submitted to University of Newcastle upon Tyne Student Paper	<1%
27	Prithwish Mahapatra, Soumavo Ghosh, Sanjib Giri, Vinayak Rane, Ramakant Kadam, Michael G. B. Drew, Ashutosh Ghosh. " Subtle Structural Changes in (Cu L) Mn Complexes To Induce Heterometallic Cooperative Catalytic Oxidase Activities on Phenolic Substrates (H L = Salen Type Unsymmetrical Schiff Base) ", Inorganic Chemistry, 2017 Publication	<1%
28	scholarworks.sjsu.edu Internet Source	<1%
29	d-nb.info Internet Source	<1%
30	Raphael F. Ribeiro, Aleksandr V. Marenich, Christopher J. Cramer, Donald G. Truhlar. "Prediction of SAMPL2 aqueous solvation free energies and tautomeric ratios using the SM8, SM8AD, and SMD solvation models", Journal of Computer-Aided Molecular Design, 2010 Publication	<1%

31	digitalcommons.wku.edu Internet Source	<1%
32	Quartarone, Eliana, Valentina Dall'Asta, Alessandro Resmini, Cristina Tealdi, Ilenia Giuseppina Tredici, Umberto Anselmi Tamburini, and Piercarlo Mustarelli. "Graphite-coated ZnO nanosheets as high-capacity, highly stable, and binder-free anodes for lithium-ion batteries", Journal of Power Sources, 2016. Publication	<1%
33	onlinelibrary.wiley.com Internet Source	<1%
34	Electrochemistry in Ionic Liquids, 2015. Publication	<1%
35	Submitted to University of Ulsan Student Paper	<1%
36	Abdel-Hafez, A.A.. "5-(4-Chlorophenyl)-5,6-dihydro-1,3-oxazepin-7(4H)-one derivatives as lipophilic cyclic analogues of baclofen: Design, synthesis, and neuropharmacological evaluation", Bioorganic & Medicinal Chemistry, 20080901 Publication	<1%
37	Submitted to University Of Tasmania Student Paper	<1%

38	epdf.pub Internet Source	<1%
39	Xiang, Debo, Jerome Noel, Huibo Shao, Georges Dupas, Nabyl Merbouh, and Hua-Zhong Yu. "Unique Intramolecular Electronic Communications in Mono-ferrocenylpyrimidine Derivatives: Correlation between Redox Properties and Structural Nature", Electrochimica Acta, 2015. Publication	<1%
40	Submitted to University of Warwick Student Paper	<1%
41	academicjournals.org Internet Source	<1%
42	Christian G. Claessens, David González-Rodríguez, Tomás Torres. "Subphthalocyanines: Singular Nonplanar Aromatic CompoundsSynthesis, Reactivity, and Physical Properties", Chemical Reviews, 2002 Publication	<1%
43	summit.sfu.ca Internet Source	<1%
44	Dietrich, S.. "Alkynyl Ti-M complexes with M = Cd and Hg: Synthesis, characterization, and reaction chemistry", Journal of Organometallic Chemistry, 20110701	<1%

Publication

45	Yang, H.. "Bridged 1,2-azaborolyl zirconium complexes: Heterocyclic analogs of the ansa-zirconocene olefin polymerization catalysts", Polyhedron, 20050804 Publication	<1%
46	Submitted to Imperial College of Science, Technology and Medicine Student Paper	<1%
47	Submitted to University of California, Los Angeles Student Paper	<1%
48	Submitted to Manchester Metropolitan University Student Paper	<1%
49	Joachim M. Mayer. "Structural Factors Affecting the Basicity of ω-Pyridylalkanols, ω-Pyridylalkanamides and ω-Pyridylalkylamines", Helvetica Chimica Acta, 09/22/1982 Publication	<1%
50	Submitted to University of Sydney Student Paper	<1%
51	Richard L. Marchese Robinson, Dawn Geatches, Chris Morris, Rebecca Mackenzie et al. "Evaluation of Force-Field Calculations of Lattice Energies on a Large Public Dataset,	<1%

Assessment of Pharmaceutical Relevance, and Comparison to Density Functional Theory", Journal of Chemical Information and Modeling, 2019
Publication

---

52 Ladurée, Daniel, Christine Fossey, Zoica Delbederi, Elena Sugeac, Sylvie Schmidt, Geraldine Laumond, and Anne-Marie Aubertin. "Synthesis and antiviral activity of aryl phosphoramidate derivatives of β-D- and β-L-C-5-Substituted 2',3'-didehydro-2',3'-dideoxy-uridine bearing linker arms", Journal of Enzyme Inhibition and Medicinal Chemistry, 2005.
Publication

<1%

---

53 "Handbook of Computational Chemistry", Springer Nature, 2017
Publication

<1%

---

54 Jacopo Tomasi, Benedetta Mennucci, Roberto Cammi. "Quantum Mechanical Continuum Solvation Models", Chemical Reviews, 2005
Publication

<1%

Exclude quotes	Off	Exclude matches	Off
Exclude bibliography	On		